Methods in Molecular Biology 1124

Springer Protocols

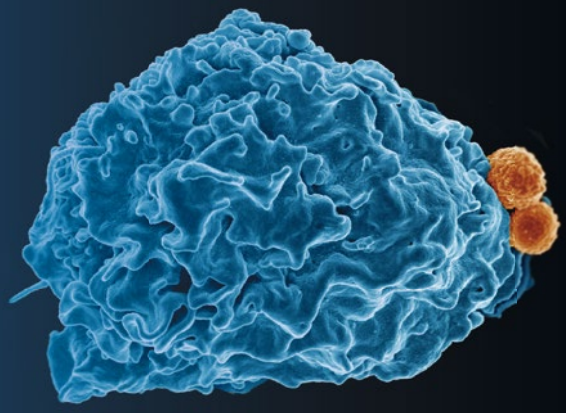

Mark T. Quinn
Frank R. DeLeo *Editors*

Neutrophil Methods and Protocols

Second Edition

Humana Press

METHODS IN MOLECULAR BIOLOGY

Series Editor
John M. Walker
School of Life Sciences
University of Hertfordshire
Hatfield, Hertfordshire, AL10 9AB, UK

For further volumes:
http://www.springer.com/series/7651

Neutrophil Methods and Protocols

Second Edition

Edited by

Mark T. Quinn

Department of Microbiology and Immunology, Montana State University, Bozeman, MT, USA

Frank R. DeLeo

Laboratory of Human Bacterial Pathogenesis, Rocky Mountain Laboratories,
National Institute of Allergy and Infectious Diseases, National Institutes of Health, Hamilton, MT, USA

Humana Press

Editors
Mark T. Quinn
Department of Microbiology and Immunology
Montana State University
Bozeman, MT, USA

Frank R. DeLeo
Laboratory of Human Bacterial Pathogenesis
Rocky Mountain Laboratories
National Institute of Allergy and Infectious Diseases
National Institutes of Health
Hamilton, MT, USA

ISSN 1064-3745 ISSN 1940-6029 (electronic)
ISBN 978-1-62703-844-7 ISBN 978-1-62703-845-4 (eBook)
DOI 10.1007/978-1-62703-845-4
Springer New York Heidelberg Dordrecht London

Library of Congress Control Number: 2014930433

Printed on acid-free paper

Humana Press is a brand of Springer
Springer is part of Springer Science+Business Media (www.springer.com)

Dedication

This volume is dedicated to Dr. Gary M. Bokoch (1954–2010) in recognition of his extensive contributions to neutrophil biology and GTPase signaling. Gary was a good friend and coeditor of the first edition of this volume. This volume is also dedicated to our families, who are quite patient with all of the time we spend studying neutrophils.

Preface

Neutrophils [also known as polymorphonuclear leukocytes (PMNs) or granulocytes] are the most abundant white cell in humans. Granulocytes and/or granulocyte precursors normally comprise ~60 % of the nucleated cells in bone marrow and blood. Mature neutrophils have a typical circulating half-life of 6–8 h in the blood and then migrate through tissues for ~2–3 days. Their relatively short life-span is devoted largely to surveillance for invading microorganisms. During infection, the neutrophil life-span is extended, granulopoiesis increases, and large numbers of neutrophils are rapidly recruited to the site(s) of infection. Following recognition (binding) and phagocytosis of microorganisms, neutrophils utilize an extraordinary array of oxygen-dependent and oxygen-independent microbicidal weapons to destroy infectious agents. Oxygen-dependent mechanisms involve the production of reactive oxygen species (ROS), while oxygen-independent mechanisms include degranulation and release of lytic enzymes and bactericidal peptides. Inasmuch as these processes are highly effective at killing most ingested microbes, neutrophils serve as the primary cellular defense against infection.

The aim of *Neutrophils: Methods and Protocols, Second Edition* is to provide (1) a set of protocols to assess most basic neutrophil functions, (2) protocols for investigating specialized areas in neutrophil research, and (3) step-by-step diagnostic assays for common neutrophil disorders. A wide variety of methods have been developed to assess neutrophil function, and these methods have been instrumental in advancing our understanding of the role of neutrophils in host defense and inflammatory disease. For those researchers and clinicians interested in the study of neutrophils, the availability of a comprehensive source of protocols describing the most modern methodological advances in neutrophil biology is invaluable, as many publications do not provide information on the finer details critical to success of a given method. As such, we have compiled a series of protocols written by leading researchers in the field that provide detailed guidelines for establishing and performing the most common neutrophil function assays. Hints of the best way to perform these methods as well as guidance in detecting associated problems are included, so novice investigators will also be able to effectively utilize these assays. While the volume provides current protocols for evaluation of most basic neutrophil functions and certain specialized functions, a section is dedicated to diagnostic assays for common neutrophil disorders. Thus, this volume is designed for the basic researcher involved in the study of neutrophil function and clinical investigators interested in medical aspects of neutrophil function in health and disease.

In the second edition of *Neutrophils: Methods and Protocols* all of the chapters have been updated, including many new approaches. In addition, the *Second Edition* contains a number of new chapters that were not included in the *First Edition*. Part I is an overview of neutrophils and their role in host defense and inflammation. Part II describes the most commonly used methods to isolate neutrophils from humans and other animal species and procedures for subcellular fractionation of human neutrophils. This section also contains a chapter that details collection and analysis of in vivo-transmigrated neutrophils.

Part III encompasses protocols addressing neutrophil biochemistry, electrophysiology, signal transduction, and apoptosis. New chapters covering neutrophil microinjection and generation of mature neutrophils from induced pluripotent stem cells are now included. Part IV details methods for investigating adhesion and chemotaxis, with new chapters on evaluation of neutrophil migration through extracellular matrix and characterization of outside-in signaling via integrins. Part V provides protocols for assessing neutrophil phagocytosis and bactericidal activity, including new chapters that describe how to measure phagocytosis by flow cytometry and analyze formation and function of extracellular traps. Part VI provides an extensive set of assays for evaluating NADPH oxidase priming and activation, production of reactive oxygen species, and new chapters describing analysis of $p47^{phox}$ phosphorylation and flavocytochrome *b* conformational changes during neutrophil activation. Part VII includes protocols to measure gene expression in neutrophils and a new chapter on high-purity neutrophil isolation from saliva for transcriptome analysis. Finally, Part VIII provides assays for diagnosis of the most common neutrophil disorders, including an updated section on assays for myeloperoxidase and myeloperoxidase deficiency. In addition to the step-by-step protocols, the *Notes* section of each chapter provides an outstanding depot of useful and interesting information not typically published in the Methods sections of standard journal articles.

We thank John M. Walker, Series Editor, and Humana Press for the opportunity to assemble an outstanding collection of articles and for help with the publication of the volume. We also thank the Montana State University COBRE Center for Zoonotic and Emerging Infectious Diseases (NIH P20 GM103500) and the Intramural Research Program of the NIH, National Institutes of Allergy and Infectious Diseases, for sponsoring this volume. Finally, we thank the authors for taking time to write outstanding chapters.

Bozeman, MT, USA ***Mark T. Quinn***
Hamilton, MT, USA ***Frank R. DeLeo***

Contents

Contributors

Maha Al-Jumaa • *Neutrophil Signalling Group, School of Medicine, Cardiff University, Cardiff, UK*

Lee-Ann H. Allen • *Inflammation Program and the Departments of Medicine and Microbiology, University of Iowa and the VA Medical Center, Iowa City, IA, USA*

Stuart M. Altman • *Department of Biomedical Engineering, University of California, Davis, CA, USA*

Bart W. Bardoel • *Department of Cellular Microbiology, Max Planck Institute for Infection Biology, Berlin, Germany*

Flavia Bazzoni • *Section of General Pathology, Department of Pathology and Diagnostic, University of Verona, Verona, Italy*

Sahra Amel Belambri • *Département de Biologie, Faculté des Sciences, Université Ferhat Abbas, Sétif, Algeria*

Lena Björkman • *The Phagocyte Research Group, Department of Rheumatology and Inflammation Research, University of Gothenburg, Gothenburg, Sweden*

Halla Björnsdottir • *The Phagocyte Research Group, Department of Rheumatology and Inflammation Research, University of Gothenburg, Gothenburg, Sweden*

Niels Borregaard • *The Granulocyte Research Laboratory, Department of Hematology, Rigshospitalet, Copenhagen University, Copenhagen, Denmark*

Johan Bylund • *The Phagocyte Research Group, Department of Rheumatology and Inflammation Research, University of Gothenburg, Gothenburg, Sweden*

Marco A. Cassatella • *Section of General Pathology, Department of Pathology and Diagnostic, University of Verona, Verona, Italy*

Uimook Choi • *Laboratory of Host Defenses, National Institute of Allergy and Infectious Diseases, National Institutes of Health, Bethesda, MD, USA*

Karin Christenson • *Department of Rheumatology and Inflammation Research, University of Gothenburg, Gothenburg, Sweden*

Stine Novrup Clemmensen • *The Granulocyte Research Laboratory, Department of Hematology, Rigshospitalet, Copenhagen University, Copenhagen, Denmark*

Claes Dahlgren • *The Phagocyte Research Group, Department of Rheumatology and Inflammation Research, University of Gothenburg, Gothenburg, Sweden*

Pham My-Chan Dang • *Faculté de Medecine, Centre de Recherche Biomédicale Bichat Beaujon, INSERM U773, Paris, France*

Lisa Davidsson • *The Phagocyte Research Group, Department of Rheumatology and Inflammation Research, University of Gothenburg, Gothenburg, Sweden*

Thomas E. DeCoursey • *Department of Molecular Biophysics and Physiology, Rush University Medical Center, Chicago, IL, USA*

Frank R. DeLeo • *Laboratory of Human Bacterial Pathogenesis, Rocky Mountain Laboratories, National Institute of Allergy and Infectious Diseases, National Institutes of Health, Hamilton, MT, USA*

Sharon Dewitt • *Neutrophil Signalling Group, School of Medicine, Cardiff University, Cardiff, UK*
Mary C. Dinauer • *Departments of Pediatrics (Hematology/Oncology) and Pathology & Immunology, Washington University School of Medicine, St. Louis Children's Hospital, St. Louis, MO, USA*
Neha Dixit • *Department of Biomedical Engineering, University of California, Davis, CA, USA*
David A. Dorward • *MRC Centre for Inflammation Research, Queen's Medical Research Institute, University of Edinburgh, Edinburgh, UK*
Ian Dransfield • *MRC Centre for Inflammation Research, Queen's Medical Research Institute, University of Edinburgh, Edinburgh, UK*
Jamel El-Benna • *Faculté de Medecine, Centre de Recherche Biomédicale Bichat Beaujon, INSERM U773, Paris, France*
Houda Zghal Elloumi • *Laboratory of Clinical Infectious Diseases, National Institute of Allergy and Infectious Diseases, National Institutes of Health, Bethesda, MD, USA*
Robert S. Fischer • *Cell Biology and Physiology Center, National Heart, Lung, and Blood Institute, National Institutes of Health, Bethesda, MD, USA*
Per Follin • *Department of Communicable Disease Control and Prevention, Västra Götaland Region, Gothenburg, Sweden*
Michael Glogauer • *Department of Periodontology and Matrix Dynamics Group, Faculty of Dentistry, University of Toronto, Toronto, ON, Canada*
Alejandro Sanchez Gonzalez • *Department of Cellular Microbiology, Max Planck Institute for Infection Biology, Berlin, Germany*
Marie-Anne Gougerot-Pocidalo • *Centre de Recherche Biomédicale Bichat Beaujon, INSERM U773, Paris, France*
Jessie N. Green • *Free Radical Research Group, Department of Pathology, Christchurch School of Medicine, Christchurch, New Zealand*
Sergio Grinstein • *Cell Biology Programme, Hospital for Sick Children, Toronto, ON, Canada*
Maurice B. Hallett • *Neutrophil Signalling Group, School of Medicine, Cardiff University, Cardiff, UK*
Mark B. Hampton • *Free Radical Research Group, Department of Pathology, Christchurch School of Medicine, Christchurch, New Zealand*
Christopher J. Harbort • *Department of Cellular Microbiology, Max Planck Institute for Infection Biology, Berlin, Germany*
Steven M. Holland • *Laboratory of Clinical Infectious Diseases, National Institute of Allergy and Infectious Diseases, National Institutes of Health, Bethesda, MD, USA*
Margarita Hurtado-Nedelec • *Centre de Recherche Biomédicale Bichat Beaujon, INSERM U773, Paris, France*
Anna Huttenlocher • *Departments of Pediatrics and Pharmacology, University of Wisconsin Medical School, Madison, WI, USA*
Richard T. Jennings • *Conway Institute, University College Dublin, Dublin, Ireland*
Algirdas J. Jesaitis • *Department of Microbiology, Montana State University, Bozeman, MT, USA*
Anna Karlsson • *The Phagocyte Research Group, Department of Rheumatology and Inflammation Research, University of Gothenburg, Gothenburg, Sweden*
Liliya N. Kirpotina • *Department of Immunology and Infectious Diseases, Montana State University, Bozeman, MT, USA*

Ulla G. Knaus • *Conway Institute, University College Dublin, Dublin, Ireland*
Scott D. Kobayashi • *Department of Microbiology, Molecular Biology, and Biochemistry, University of Idaho, Moscow, ID, USA*
Douglas B. Kuhns • *Neutrophil Monitoring Lab, Applied/Developmental Research Directorate, Frederick National Laboratory on Cancer Research, Frederick, MD, USA*
Iraj Laffafian • *Neutrophil Signalling Group, School of Medicine, Cardiff University, Cardiff, UK*
Flavia S. Lakschevitz • *Matrix Dynamics Group, Faculty of Dentistry, University of Toronto, Toronto, ON, Canada*
Pui-ying Lam • *Program in Cellular and Molecular Biology, University of Wisconsin-Madison, Madison, WI, USA*
Benfang Lei • *Department of Immunology and Infectious Diseases, Montana State University, Bozeman, MT, USA*
Kimberly J. Lewis • *Neutrophil Signalling Group, School of Medicine, Cardiff University, Cardiff, UK*
Christopher D. Lucas • *MRC Centre for Inflammation Research, Queen's Medical Research Institute, University of Edinburgh, Edinburgh, UK*
Marco A.O. Magalhaes • *Cell Biology Programme, Hospital for Sick Children, Toronto, ON, Canada*
Nicholas J. Magon • *Free Radical Research Group, Department of Pathology, Christchurch School of Medicine, Christchurch, New Zealand*
Karama Makni-Maalej • *Centre de Recherche Biomédicale Bichat Beaujon, INSERM U773, Paris, France*
Natalia Malachowa • *Laboratory of Human Bacterial Pathogenesis, Rocky Mountain Laboratories, National Institute of Allergy and Infectious Diseases, National Institutes of Health, Hamilton, MT, USA*
Harry L. Malech • *Laboratory of Host Defenses, National Institute of Allergy and Infectious Diseases, National Institutes of Health, Bethesda, MD, USA*
K. Benjamin Masterman • *Neutrophil Signalling Group, School of Medicine, Cardiff University, Cardiff, UK*
Patrick P. McDonald • *Department of Pharmacology, University of Illinois, Chicago, IL, USA*
Linda C. McPhail • *Department of Biochemistry, Wake Forest University School of Medicine, Winston-Salem, NC, USA*
Randall K. Merling • *Laboratory of Host Defenses, National Institute of Allergy and Infectious Diseases, National Institutes of Health, Bethesda, MD, USA*
Deri Morgan • *Department of Molecular Biophysics and Physiology, Rush University Medical Center, Chicago, IL, USA*
William M. Nauseef • *Inflammation Program and Department of Medicine, Roy J. and Lucille A. Carver College of Medicine, University of Iowa, Coralville, IA, USA*
Pontus Nordenfelt • *Department of Biological Chemistry and Molecular Pharmacology, Harvard Medical School, Harvard University, Boston, MA, USA*
Heather A. Parker • *Free Radical Research Group, Department of Pathology, Christchurch School of Medicine, Christchurch, New Zealand*
Edgar Pick • *The Julius Friedrich Cohnheim-Minerva Center for Phagocyte Research and the Ela Kodesz Institute of Host Defense against Infectious Diseases, Sackler School of Medicine, Tel Aviv University, Tel Aviv, Israel*

Debra Long Priel • *Neutrophil Monitoring Lab, Applied/Developmental Research Directorate, Frederick National Laboratory on Cancer Research, Frederick, MD, USA*
Mark T. Quinn • *Department of Microbiology and Immunology, Montana State University, Bozeman, MT, USA*
Marcia Riesselman • *Department of Microbiology, Montana State University, Bozeman, MT, USA*
Adriano G. Rossi • *MRC Centre for Inflammation Research, Queen's Medical Research Institute, University of Edinburgh, Edinburgh, UK*
Igor A. Schepetkin • *Department of Immunology and Infectious Diseases, Montana State University, Bozeman, MT, USA*
Susan Sergeant • *Department of Biochemistry, Wake Forest University School of Medicine, Winston-Salem, NC, USA*
William D. Shin • *Cell Biology and Physiology Center, National Heart, Lung, and Blood Institute, National Institutes of Health, Bethesda, MD, USA*
Daniel W. Siemsen • *Department of Immunology and Infectious Diseases, Montana State University, Bozeman, MT, USA*
Scott I. Simon • *Department of Biomedical Engineering, University of California, Davis, CA, USA*
Benjamin E. Steinberg • *Cell Biology Programme, Hospital for Sick Children, Toronto, ON, Canada*
Daniel E. Sturdevant • *Genomics Unit, Rocky Mountain Laboratories, National Institute of Allergy and Infectious Diseases, National Institutes of Health, Hamilton, MT, USA*
Martina Sundqvist • *The Phagocyte Research Group, Department of Rheumatology and Inflammation Research, University of Gothenburg, Gothenburg, Sweden*
Colin L. Sweeney • *Laboratory of Host Defenses, National Institute of Allergy and Infectious Diseases, National Institutes of Health, Bethesda, MD, USA*
Nicola Tamassia • *Section of General Pathology, Department of Pathology and Diagnostic, University of Verona, Verona, Italy*
Lene Udby • *The Granulocyte Research Laboratory, Department of Hematology, Rigshospitalet, Copenhagen University, Copenhagen, Denmark*
Hongmei Wang • *Laboratory of Host Defenses, National Institute of Allergy and Infectious Diseases, National Institutes of Health, Bethesda, MD, USA*
Clare M. Waterman • *Cell Biology and Physiology Center, National Heart, Lung, and Blood Institute, National Institutes of Health, Bethesda, MD, USA*
Adeline R. Whitney • *Laboratory of Human Bacterial Pathogenesis, Rocky Mountain Laboratories, National Institute of Allergy and Infectious Diseases, National Institutes of Health, Hamilton, MT, USA*
Christine C. Winterbourn • *Free Radical Research Group, Department of Pathology, Christchurch School of Medicine, Christchurch, New Zealand*
Richard D. Ye • *Department of Pharmacology, University of Illinois, Chicago, IL, USA*
Arturo Zychlinsky • *Department of Cellular Microbiology, Max Planck Institute for Infection Biology, Berlin, Germany*

Part I

Neutrophils: An Overview

Chapter 1

The Role of Neutrophils in the Immune System: An Overview

Harry L. Malech, Frank R. DeLeo, and Mark T. Quinn

Abstract

Neutrophils, also known as polymorphonuclear leukocytes (PMNs), have long been considered as the short-lived, nonspecific white cells that form pus—and also happen to kill invading microbes. Indeed, neutrophils were often neglected (and largely not considered) as immune cells. This historic view of neutrophils has changed considerably over the past several decades, and we know now that, in addition to playing the predominant role in the clearance of bacteria and fungi, they play a major role in shaping the host response to infection and immune system homeostasis. The change in our view of the role of neutrophils in the immune system has been due in large part to the study of these cells in vitro. Such work has been made possible by new and/or improved methods and approaches used to investigate neutrophils. These methods are the focus of this volume.

Key words Polymorphonuclear leukocyte, Granulocyte, Neutrophil methods

1 Introduction

This valuable and unique book contains a compendium of methods and reviews that does much more than allow one to study the biology of neutrophils. What makes this collection of contributions so special is that it highlights and facilitates using the neutrophil as a simple, pure, single primary cell suspension model to study a remarkable array of generalized cellular functions (priming, chemotaxis and transmigration, adhesion, phagocytosis, degranulation, oxygen radical production, apoptosis, extracellular trap formation), biochemical pathways (GTPase activation, phospholipid metabolism, calcium transients, ion channel regulation, phosphorylation events, adhesion molecule regulation), as well as specialized functions and molecules important to host defense against infection, the mediation and resolution of inflammation, and cytokine/chemokine modulation of immunity (*see* Fig. 1). Consideration of the array of chapter topics evokes some of the past history of inquiry into how neutrophils function and how we

Mark T. Quinn and Frank R. DeLeo (eds.), *Neutrophil Methods and Protocols*, Methods in Molecular Biology, vol. 1124,
DOI 10.1007/978-1-62703-845-4_1,

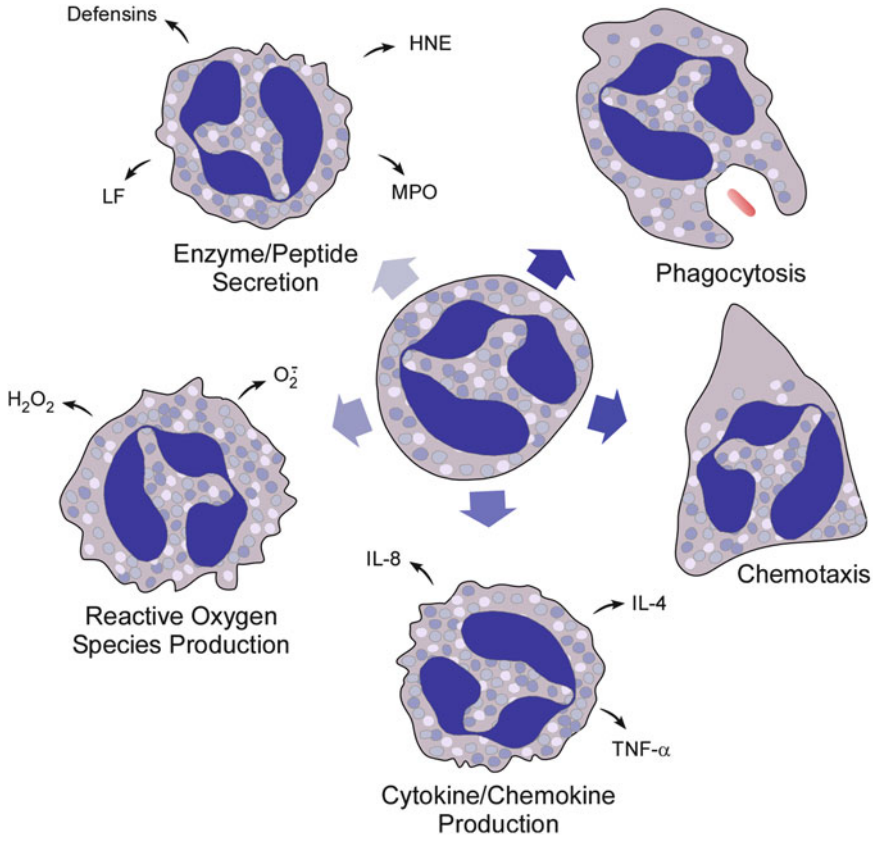

Fig. 1 Illustration of key neutrophil functions. Note that, for production reactive oxygen species, secretion of granule components, and production of cytokines and chemokines, only a few representative molecules are shown. *HNE* human neutrophil elastase, *IL-8* interleukin-8, *IL-4* interleukin-4, *LF* lactoferrin, *MPO* myeloperoxidase, *TNF-α* tumor nectosis factor-α

evolved into the current widespread use of the neutrophil as a convenient model system for studying so many types of cellular processes and biochemical pathways.

2 Historical Overview

Only a few decades ago, in the 1970s and even the early 1980s, the biology and pathophysiology of the neutrophil was a boutique area of study involving a relatively small number of laboratories and investigators internationally. These investigators all tended to know each other and most of the active investigators in the field of neutrophil biology could easily meet together at the biannual Gordon Research Conference on Phagocytes. Even as recently as the early 1980s, "real" immunologists were investigators who delineated the subtypes and life cycle of lymphocytes, and within this scheme

the only phagocytes of significance for lymphocyte immunologists were the monocytes. This was because only monocytes, which are long-lived, and not neutrophils, which are short-lived, were thought to be capable of antigen presentation, differentiation into tissue macrophages and other fixed tissue cell types, or capable of any significant protein synthesis, including production of potent immune modulating factors. The relatively recently coined phase, "innate immunity" encompasses in part the recent growing appreciation of the special role of neutrophils in host defense, immune regulation, and regulation of inflammation, reflecting a vast body of new knowledge about how the neutrophil functions and affects the classic lymphocyte-oriented area of immunity encompassed by the term "acquired immunity" (reviewed in ref. 1).

Although the rapid ameboid migration of neutrophils to sites of inflammation and their unique capacity to surround and engulf foreign bodies have been known since the early twentieth century, it was only in the 1960s that it was generally appreciated that neutrophils produced microbicidal activated oxygen products or contained other nonoxidative potently microbicidal substances (e.g., *see* refs. 2–4). It was only in the late 1960s and early 1970s that a more detailed understanding of the different types of granules was delineated (e.g., *see* refs. 5, 6) and in the 1980s and 1990s that studies delineated the biochemistry of a large array of specialized cationic microbicidal proteins and a more complete understanding of the many proteolytic enzymes that were contained in those granules (reviewed in ref. 7). Only in the late 1980s and early 1990s were the biochemical details of the phagocyte oxidase delineated in fine detail (reviewed in refs. 8–10). Although investigators studying the biochemistry of non-muscle actin in cell motility performed much of the critical early research in lower eukaryotic organisms, translation of this work to mammalian tissues was largely performed in the 1980s and 1990s in neutrophils and monocytes (e.g., *see* refs. 11, 12).

Since the human tritium tracer studies of the 1960s, it has been appreciated that, when neutrophils emerge from bone marrow to peripheral blood, the half-life in blood is only 6–10 h and even shorter in infected patients and that the lifespan in tissues is 3 days or less (e.g., *see* refs. 5, 13, 14). This provided a basis for considering neutrophils as end-stage cells only minimally more capable of anabolic processes than erythrocytes. This impression was further engendered by the observations that neutrophils, as compared to other cell types, produce energy for survival primarily through anaerobic metabolism, reserving most use of oxygen for production of superoxide in the context of the stimulated microbicidal respiratory burst [15]. There is a paucity of mitochondria and ribosomes in neutrophils compared, for example, to monocytes, and most investigators in the 1970s assumed that mature neutrophils in blood or tissues were devoid of significant protein synthetic capacity,

functioning entirely on the store of enzymes and other proteins that were contained within their granules, membranes, and cytoplasm as these cells emerged from the bone marrow. It was not that investigators viewed the neutrophil as inactive, since, after all, these are cells capable of remarkably rapid amoeboid migration, rapid engulfment of microorganisms, a prodigious respiratory burst-induced production of superoxide, and extremely rapid degranulation into phagosomes (reviewed in ref. 16). However, more recent studies have demonstrated unequivocally that neutrophils are capable of significant stimulated production of new proteins (e.g., *see* refs. 17–19); of note is production of a number of chemokines, in particular the production of large amounts of interleukin 8 [20]. This provides one important area of evidence for the important interface between the neutrophil component of innate immunity and the classic area of acquired immunity (e.g., *see* ref. 1).

One of the specialized motile properties of neutrophils is chemotaxis, and the delineation in the 1970s of bacteria-derived formyl peptides as chemotactic for neutrophils [21], in particular the discovery of the simple formylated tripeptide, formyl-methionyl-leucinyl-phenyalanine (fMLF), as a potent chemoattractant, began the process of making the neutrophil, in the 1980s, a model of choice for investigators interested in delineating a large array of biochemical signaling pathways whose diverse enzymes and regulatory proteins are still being worked out (e.g., *see* refs. 22, 23). Formylated peptides were shown to induce chemotaxis, but they also induced degranulation, which was associated metabolically with an ionized calcium transient, changes in electric potential similar to neural signaling, phosphorylations, metabolism of GTP, and metabolism of certain membrane phospholipids (e.g., *see* refs. 24–26). This was the beginning of the use of the neutrophil as the model system of choice for an increasing number of investigators delineating many types of newly identified biochemical signaling pathways, including the G-protein-coupled signaling pathway and the large array of small GTPases of the Ras and Rho families that regulate so many cell functions (e.g., *see* refs. 27–30).

Although it was appreciated that neutrophils have a relatively short lifespan following release from the bone marrow, the final fate of "old" neutrophils remained a mystery until the emergence of the new paradigm of apoptosis defined the process of regulated cell death as a final stage in the differentiation of cells and delineated it from trauma, toxin-induced, or immune-induced cell necrosis [17, 31–33]. The recent application of the apoptosis paradigm to neutrophils has been used to explain how some processes lead to resolution of infection or inflammation without tissue damage by allowing neutrophil apoptosis to occur. The apoptotic process prevents release of the cytotoxic and proteolytic contents of the neutrophil by facilitating phagocytosis of apoptotic neutrophils by

macrophages and dendritic cells through engagement of "death receptors" [32, 33]. Not only does this facilitate "cleanup" and resolution of infection and inflammation without tissue damage, but it also probably comprises an important interface of innate with acquired immunity in that the engagement of death receptors modulates the function of antigen presenting cells, and the contents of the phagocytosed apoptotic neutrophils include components of killed microorganisms, which are processed by antigen presenting cells. Thus, it is appropriate that there is a chapter in this volume on neutrophil apoptosis. Apoptosis of neutrophils can be replaced prematurely by necrosis and release of the potent proteolytic enzymatic contents of neutrophils by microorganisms that contain toxins that lyse the neutrophil (reviewed in ref. 34), by autoimmune processes such as antibodies to neutrophils or their contents that induce lysis or phagocytosis of neutrophils before normal apoptotic processes can occur or by other causes of cytolysis. One such cytolytic process can result in the extracellular extrusion of the nucleus to form weblike DNA structures called neutrophil extracellular traps (NETs), which are coated with histones and cationic granule proteins [35]. These interesting structures ensnare bacteria and fungi—and some reports suggest they kill bacteria—and can thereby contribute to host defense. The idea that DNA released from neutrophils can contribute to innate immunity was unheard of until NET discovery in 2004 [35].

Neutrophils are the primary mediators of the rapid innate host defense against most bacterial and fungal pathogens that occurs before the complex humoral and lymphocyte cellular processes of acquired immunity can be brought to bear on an infection. The importance of the neutrophil in this process is highlighted by the fact that iatrogenic neutropenia from cancer chemotherapy or reactions to cytotoxic drugs is the most common severe immune deficiency associated with significant morbidity encountered in medical practice [36–39]. Inherited forms of neutropenias are also associated with significant risk of infection from bacteria and fungi. As discussed in this volume, there are a number of single gene disorders affecting primarily specific neutrophil functions such as defects in the phagocyte oxidase responsible for the group of diseases with a common phenotype called chronic granulomatous disease (CGD) or defects in the CD18 β integrin responsible for leukocyte adhesion deficiency (LAD). The groups of bacterial and fungal organisms typically infecting patients with severe neutropenia, CGD, or LAD overlap a little, but in general are different and distinct, suggesting strongly that there are an array of microbicidal defense systems and molecules used by the neutrophil in host defense and that different systems have evolved to provide specific defense against different organisms. Also of note is that CGD patients have excessive inflammation and a tendency to develop a variety of autoimmune disorders including inflammatory bowel

disease and poor wound healing, suggesting that the superoxide or hydrogen peroxide products of the respiratory burst may play an important role in the resolution of inflammation and in wound healing [40]. LAD patients have large nonhealing ulcers, also suggesting a role for neutrophils in wound healing, since LAD neutrophils have trouble migrating into tissues [41].

3 Future Prospects

Despite strong evidence in a variety of model systems of inflammation that superoxide dismutase, which catabolizes superoxide; catalase, which catabolizes hydrogen peroxide; or dimethylsulfoxide (DSMO), which scavenges hydroxyl radical, protect against tissue injury from neutrophil-mediated tissue damage, there remains considerable controversy regarding the role of neutrophil products of oxidative metabolism in mediating any of the tissue damage syndromes associated with autoimmune disease or septic shock (e.g., *see* refs. 42–45). Stronger evidence exists for actual clinical benefit accruing from blocking the activity a number of the proteolytic enzymes derived from neutrophils in a variety of autoimmune or other disease processes (reviewed in ref. 46). Because of this, discovery and development of antiproteolytic small molecules active against specific proteases found in neutrophils are part of the anti-inflammatory drug development programs of a number of pharmaceutical companies (e.g., *see* refs. 47, 48). Neutrophils are also a source of a number of small potent antimicrobial proteins and peptides that could be developed into new classes of antibiotics, and this is another area of interest to pharmaceutical development (reviewed in ref. 49). Finally, recent advances in the area of induced pluripotent stem cells (iPSCs), which are embryonic-like stem cells that can be reprogrammed into many types of cells, including neutrophils, present an opportunity for long-term treatment of neutrophil disorders. Thus, the chapters in this series are likely to be of utility not only broadly to investigators interested in using the neutrophil as a model system, to investigators specifically interested in neutrophil function, or to investigators studying the interface between innate and acquired immunity but will also be important to investigators developing new classes of natural biologicals as antibiotics or developing new classes of anti-inflammatory agents.

References

1. Hoebe K, Janssen E, Beutler B (2004) The interface between innate and adaptive immunity. Nat Immunol 5:971–974
2. Babior BM, Kipnes RS, Curnutte JT (1973) Biological defense mechanisms: production by leukocytes of superoxide, a potential bactericidal agent. J Clin Invest 52:741–744
3. Klebanoff SJ (1967) Iodination of bacteria: a bactericidal mechanism. J Exp Med 126: 1063–1078
4. Lehrer RI, Hanifin J, Cline MJ (1969) Defective bactericidal activity in myeloperoxidase-deficient human neutrophils. Nature 223:78–79

5. Bainton DF, Ullyot JL, Farquhar MG (1971) The development of neutrophilic polymorphonuclear leukocytes in human bone marrow. J Exp Med 134:907–934
6. Bainton DF, Farquhar MG (1968) Differences in enzyme content of azurophil and specific granules of polymorphonuclear leukocytes. I. Histochemical staining of bone marrow smears. J Cell Biol 39:286–298
7. Borregaard N, Cowland JB (1997) Granules of the human neutrophilic polymorphonuclear leukocyte. Blood 89:3503–3521
8. Segal AW, Abo A (1993) The biochemical basis of the NADPH oxidase of phagocytes. Trends Biochem Sci 18:43–47
9. Babior BM (1999) NADPH oxidase: an update. Blood 93:1464–1476
10. Clark RA (1990) The human neutrophil respiratory burst oxidase. J Infect Dis 161:1140–1147
11. Zigmond SH (1978) Chemotaxis by polymorphonuclear leukocytes. J Cell Biol 77:269–287
12. Southwick FS, Stossel TP (1983) Contractile proteins in leukocyte function. Semin Hematol 20:305–321
13. Fliedner TM, Cronkite EP, Robertson JS (1964) Granulocytopoiesis. I. Senescence and random loss of neutrophilic granulocytes in human beings. Blood 24:402–414
14. Athens JW, Haab OP, Raab SO et al (1961) Leukokinetic studies. IV. The total blood, circulating and marginal granulocyte pools and the granulocyte turnover rate in normal subjects. J Clin Invest 40:989–995
15. Rossi F, Zatti M (1964) Changes in the metabolic pattern of polymorphonuclear leukocytes during phagocytosis. Br J Exp Pathol 45:548–559
16. Nauseef WM, Clark RA (2000) Granulocytic phagocytes. In: Mandell GL, Bennett JP, Dolin R (eds) Basic principles in the diagnosis and management of infectious diseases, 5th edn. Churchill Livingstone, New York, pp 89–112
17. Kobayashi SD, Voyich JM, Buhl CL, Stahl RM, DeLeo FR (2002) Global changes in gene expression by human polymorphonuclear leukocytes during receptor-mediated phagocytosis: cell fate is regulated at the level of gene expression. Proc Natl Acad Sci U S A 99:6901–6906
18. Theilgaard-Mönch K, Knudsen S, Follin P, Borregaard N (2004) The transcriptional activation program of human neutrophils in skin lesions supports their important role in wound healing. J Immunol 172:7684–7693
19. Zhang XQ, Kluger Y, Nakayama Y et al (2004) Gene expression in mature neutrophils: early responses to inflammatory stimuli. J Leukoc Biol 75:358–372
20. Strieter RM, Kasahara K, Allen RM et al (1992) Cytokine-induced neutrophil-derived interleukin-8. Am J Pathol 141:397–407
21. Schiffmann E, Corcoran BA, Wahl SM (1975) *N*-formylmethionyl peptides as chemoattractants for leucocytes. Proc Natl Acad Sci U S A 72:1059–1062
22. Snyderman R, Goetzl EJ (1981) Molecular and cellular mechanisms of leukocyte chemotaxis. Science 213:830–835
23. Allen RA, Jesaitis AJ, Cochrane CG (1990) The N-formyl peptide receptor. In: Cochrane CG, Gimbrone MA (eds) Cellular and molecular mechanisms of inflammation: receptors of inflammatory cells, structure–-function relationships. Academic, San Diego, pp 83–112
24. O'Flaherty JT, Showell HJ, Ward PA (1977) Influence of extracellular Ca^{2+} and Mg^{2+} on chemotactic factor-induced neutrophil aggregation. Inflammation 2:265–276
25. Serhan CN, Broekman MJ, Korchak HM, Smolen JE, Marcus AJ, Weissmann G (1983) Changes in phosphatidylinositol and phosphatidic acid in stimulated human neutrophils. Relationship to calcium mobilization, aggregation and superoxide radical generation. Biochim Biophys Acta 762:420–428
26. McPhail LC, Clayton CC, Snyderman R (1984) A potential second messenger role for unsaturated fatty acids: activation of Ca^{++}-dependent protein kinase. Science 224:622–625
27. Aharoni I, Pick E (1990) Activation of the superoxide-generating NADPH oxidase of macrophages by sodium dodecyl sulfate in a soluble cell-free system: evidence for involvement of a G protein. J Leukoc Biol 48: 107–115
28. Quinn MT, Parkos CA, Walker L, Orkin SH, Dinauer MC, Jesaitis AJ (1989) Association of a ras-related protein with cytochrome b of human neutrophils. Nature 342:198–200
29. Abo A, Pick E, Hall A, Totty N, Teahan CG, Segal AW (1991) Activation of the NADPH oxidase involves the small GTP-binding protein $p21^{rac1}$. Nature 353:668–670
30. Knaus UG, Heyworth PG, Evans T, Curnutte JT, Bokoch GM (1991) Regulation of phagocyte oxygen radical production by the GTP-binding protein Rac2. Science 254:1512–1515
31. Serhan CN, Savill J (2005) Resolution of inflammation: the beginning programs the end. Nat Immunol 6:1191–1197
32. Savill JS, Wyllie AH, Henson JE, Walport MJ, Henson PM, Haslett C (1989) Macrophage phagocytosis of aging neutrophils in inflammation. Programmed cell death in the neutrophil leads to its recognition by macrophages. J Clin Invest 83:865–875

33. Whyte MK, Meagher LC, MacDermot J, Haslett C (1993) Impairment of function in aging neutrophils is associated with apoptosis. J Immunol 150:5124–5134
34. DeLeo FR (2004) Modulation of phagocyte apoptosis by bacterial pathogens. Apoptosis 9:399–413
35. Brinkmann V, Reichard U, Goosmann C, Fauler B, Uhlemann Y, Weiss DS, Weinrauch Y, Zychlinsky A (2004) Neutrophil extracellular traps kill bacteria. Science 303:1532–1535
36. Tobias JD, Schleien C (1991) Granulocyte transfusions – a review for the intensive care physician. Anaesth Intensive Care 19: 512–520
37. Froland SS (1984) Bacterial infections in the compromised host. Scand J Infect Dis Suppl 43:7–16
38. Bodey GP, Buckley M, Sathe YS, Freireich EJ (1966) Quantitative relationships between circulating leukocytes and infection in patients with acute leukemia. Ann Intern Med 64:328–340
39. Dale DC, Guerry D, Wewerka JR, Bull JM, Chusid MJ (1979) Chronic neutropenia. Medicine (Baltimore) 58:128–144
40. Kobayashi SD, Voyich JM, Braughton KR et al (2004) Gene expression profiling provides insight into the pathophysiology of chronic granulomatous disease. J Immunol 172:636–643
41. Bunting M, Harris ES, McIntyre TM, Prescott SM, Zimmerman GA (2002) Leukocyte adhesion deficiency syndromes: adhesion and tethering defects involving beta 2 integrins and selectin ligands. Curr Opin Hematol 9:30–35
42. Finkel T, Holbrook NJ (2000) Oxidants, oxidative stress and the biology of ageing. Nature 408:239–247
43. Rahman I, Biswas SK, Kode A (2006) Oxidant and antioxidant balance in the airways and airway diseases. Eur J Pharmacol 533:222–239
44. Temple MD, Perrone GG, Dawes IW (2005) Complex cellular responses to reactive oxygen species. Trends Cell Biol 15:319–326
45. Weiss SJ (1989) Tissue destruction by neutrophils. N Engl J Med 320:365–376
46. Altieri DC (1995) Proteases and protease receptors in modulation of leukocyte effector functions. J Leukoc Biol 58:120–127
47. Zaidi SH, You XM, Ciura S, Husain M, Rabinovitch M (2002) Overexpression of the serine elastase inhibitor elafin protects transgenic mice from hypoxic pulmonary hypertension. Circulation 105:516–521
48. Zeiher BG, Matsuoka S, Kawabata K, Repine JE (2002) Neutrophil elastase and acute lung injury: prospects for sivelestat and other neutrophil elastase inhibitors as therapeutics. Crit Care Med 30:S281–S287
49. Ganz T (2004) Antimicrobial polypeptides. J Leukoc Biol 75:34–38

Part II

Neutrophil Isolation and Subcellular Fractionation

Chapter 2

Isolation of Human Neutrophils from Venous Blood

William M. Nauseef

Abstract

Venous blood provides a ready source of large numbers of unstimulated granulocytes and mononuclear cells. Exploiting the differences in the relative densities of the leukocytes circulating in venous blood, one can separate leukocytes from erythrocytes as well as isolate the individual leukocyte populations in high purity for use in ex vivo studies.

Key words Granulocytes, Mononuclear cells, Ficoll-Hypaque, Dextran sedimentation

1 Introduction

Under normal conditions, there are ~7.4 K/mm^3 (4.5–11.0) white blood cells in circulation, approximately 59 % are PMN, 2.7 % eosinophils, and 4 % monocytes. The different densities of the circulating hematopoietic cells are exploited in order to separate erythrocytes from leukocytes and then to isolate the individual leukocyte populations. Although a variety of methods for rapid, one-step isolation of PMN have been developed recently and used successfully, we routinely use one of two variants of a method first described by Bőyum in 1968 [1]. PMN isolated in this way do not consume oxygen and maintain their secretory vesicles intracellularly, two features that suggest that the PMN are bona fide resting cells and thus not activated by the isolation procedure.

Two major steps are involved, each using specific conditions to separate cells based on their intrinsic density: sedimentation in dextran at $1 \times g$ and differential sedimentation in a discontinuous density gradient of Ficoll-Hypaque. In dextran, erythrocytes form rouleaux and thus sediment more rapidly than do granulocytes in suspension. In the Ficoll-Hypaque, granulocytes and erythrocytes pellet to the bottom, whereas mononuclear cells (i.e., lymphocytes and monocytes), basophils, and platelets remain at the interphase between plasma/buffer and the Ficoll-Hypaque. Because we routinely process relatively large quantities of blood (e.g., ≥200 ml)

Mark T. Quinn and Frank R. DeLeo (eds.), *Neutrophil Methods and Protocols*, Methods in Molecular Biology, vol. 1124,
DOI 10.1007/978-1-62703-845-4_2,

and are primarily interested in recovering PMN (not monocytes), we generally perform dextran sedimentation first, followed by Ficoll-Hypaque sedimentation. When smaller volumes of blood are processed or when monocytes are the targeted cell of interest, the sedimentation in Ficoll-Hypaque can be performed first. Both approaches are described below.

2 Materials

1. Anticoagulant: The preferred anticoagulant is preservative-free sodium heparin (1,000 units/mL). Lithium heparin, EDTA, or citrate are also acceptable.
2. Dextran: 3 % (w/v) Dextran-500 (average molecular weight 200,000–500,000) in endotoxin-free, sterile 0.9 % NaCl. Dissolving 30 g/L of dextran in sterile saline (*see* **Note 1**). Heat the solution if necessary to promote dissolution of the dextran and handle the solution using sterile technique.
3. Ficoll-Hypaque solution: originally prepared by mixing Ficoll 400 and isopaque to create a solution with a density of 1.077 g/mL [1]. Currently premixed, sterilely prepared Ficoll-Hypaque plus can be purchased. Each 100 mL contains 5.7 g Ficoll 400 and 9.0 g diatrizoate solution with .0231 g of disodium calcium EDTA in endotoxin-free water. Protected from light, the solution is stable for 3 years when stored at 4–30 °C. The appearance of yellow color or particulate material indicates deterioration.
4. Endotoxin-free, sterile water.
5. 1.8 % (w/v) NaCl solution.
6. Sterile, endotoxin-free, Hanks' balanced salt solution (HBSS) without Ca^{2+} or Mg^{2+}.

3 Methods (*See* Note 2)

3.1 Dextran Sedimentation Followed by Ficoll-Hypaque Density Centrifugation

1. Draw blood into a syringe containing sufficient preservative-free heparin to have a final concentration of 20 U/mL in the blood sample.
2. In a 50 mL conical tube containing the blood, add an equal volume of 3 % dextran.
3. Mix tubes by repeated inversion (ten times), and set tubes upright for 18–20 min at room temperature (*see* **Note 3**).
4. Aspirate the straw-colored, leukocyte-rich, erythrocyte-poor upper layer with a sterile plastic pipette or a 10–15 mL sterile syringe and transfer the aspirate to a sterile 50 mL conical tube (*see* **Note 4**).

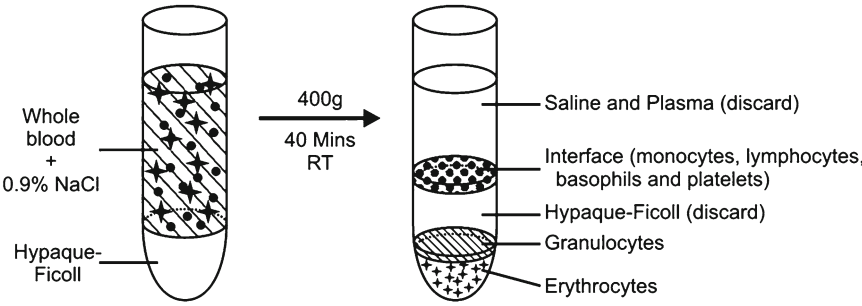

Fig. 1 Ficoll-Hypaque gradient separation of granulocytes and peripheral blood mononuclear cells. Ficoll-Hypaque gradient before (*left side*) and after (*right side*) centrifugation. Reproduced from ref. 4 by permission of Humana Press©2007

5. Pellet leukocytes by centrifugation at 500 × *g* for 10 min at 4 °C; aspirate and discard the supernatant.
6. Resuspend pellets in 10 mL, shake well but *do not* vortex. Three resuspended pellets can be pooled into a single conical tube to achieve a final volume of 35 mL. Top off with sterile saline if needed to reach 35 mL.
7. Carefully underlay the leukocyte suspension with 10 mL of Ficoll-Hypaque using a sterile, plastic 10-mL pipette (Fig. 1).
8. Centrifuge at 400 × *g* for 40 min at room temperature (*see* **Note 5**).
9. After centrifugation, two bands should be apparent in the conical tube (Fig. 1). The lighter band contains mononuclear cells, whereas the denser band has both granulocytes and erythrocytes. If monocytes are desired, aspirate the less dense band using a sterile plastic pipette and mix with an equal volume of cold sterile saline in a separate conical tube.
10. Aspirate and discard supernatant above the PMN-erythrocyte layer, taking care not to lose any of the PMN-rich pellet.
11. Resuspend each pellet in sterile water and mix well (but *do not* vortex) for 28 s. Promptly restore tonicity by adding an equal volume of 1.8 % saline and mixing (*see* **Note 6**).
12. Centrifuge 500 × *g* for 5 min at 4 °C. Discard supernatant and repeat **step 11** *if* more lysis is needed, but repeat **step 11** only *once* (*see* **Note 6**).
13. Resuspend cells in HBSS without Ca^{2+} and Mg^{2+} at $\leq 3 \times 10^7$ cells/mL.
14. Determine the cell concentration by manually counting using a hemocytometer. The differential of leukocytes can be assessed by examining a stained slide microscopically (*see* **Note 7**).

3.2 Ficoll-Hypaque Density Centrifugation-Mononuclear Cell Recovery

1. Draw blood into a syringe as above and dilute with 1 volume of 0.9 % NaCl at room temperature to a total volume of 40 mL in a sterile 50 mL conical plastic tube (*see* **Note 8**).
2. Carefully underlay the diluted blood with 10 mL of Ficoll-Hypaque.
3. Centrifuge at 400 × *g* for 40 min at room temperature.
4. After centrifugation, remove the HBSS and plasma above the mononuclear band at the interface (*see* Fig. 1) and discard.
5. Recover the fraction containing mononuclear cells, combining bands from no more than two gradients into a separate 50 mL conical tube.
6. Bring each of the pooled fractions to 50 mL with sterile HBSS without Ca^{2+} and Mg^{2+} to dilute the Ficoll-Hypaque (*see* **Note 9**).
7. Pellet mononuclear cells at 600 × *g* for 10 min at 4 °C.
8. Discard supernatant, pool, and wash pellets twice more with HBSS without Ca^{2+} and Mg^{2+}.
9. Resuspend final pellet in 5 mL of HBSS without Ca^{2+} and Mg^{2+} and count.

3.3 Ficoll-Hypaque Density Centrifugation First-PMN Recovery

1. After **step 5** in Subheading 3.2, when the supernatant and the mononuclear band have been removed, aspirate and discard the remaining gradient above the PMN-erythrocyte pellet (*see* Fig. 1).
2. Resuspend the pellet in a volume up to 25 mL with HBSS without Ca^{2+} and Mg^{2+}.
3. Add 25 mL of 3 % dextran, mix by inverting the tube ten times, and let stand upright at room temperature for 18–20 min.
4. Aspirate the straw-colored, leukocyte-rich, erythrocyte-poor upper layer with a sterile plastic pipette or a 10–15 mL sterile syringe and transfer the aspirate to a sterile 50 mL conical tube (*see* **Note 4**).
5. Pellet leukocytes by centrifugation at 500 × *g* for 10 min at 4 °C; aspirate and discard the supernatant.
6. Resuspend each pellet in sterile water and mix well (but *do not* vortex) for 28 s. Promptly restore tonicity by adding an equal volume of 1.8 % saline and mixing (*see* **Note 6**).
7. Resuspend cells in HBSS without Ca^{2+} and Mg^{2+} at $\leq 3 \times 10^7$ cells/mL.
8. Determine the cell concentration by manually counting using a hemacytometer. The differential of leukocytes can be assessed by examining a stained slide microscopically.

4 Notes

1. The concentration and the molecular weight range of the dextran is a critical determinant in the speed with which cells sediment [2]. The preparation of 3 % in the 200,000–500,000 weight range provides excellent sedimentation of erythrocytes within 18–20 min, with rates slower using either the lower molecular weight dextrans (<20,000) or the high molecular weight (>7,000,000) preparations. Given the range in size of the components in the dextran being used, one can anticipate corresponding variation in the rate of sedimentation (reflected as differences in the number of cells recovered). For example, we currently allow sedimentation to occur for 30 min at room temperature to obtain maximal number of granulocytes. Be prepared to modify the time allotted for sedimentation accordingly. The volume of the dextran–blood mixture has no effect on the efficiency of sedimentation. In the event that sedimentation has proceeded for longer than the intended time, the sample can be mixed again and the sedimentation repeated with no adverse effect on yield or purity. Whenever alternative agents are used for sedimentation, it is important to determine if the recovered PMN are primed, as occurs with gelatin [3].
2. In general, always use polypropylene tubes, as glass and polyethylene may activate the PMN during isolation. Pipettes should be sterile and buffers should be prepared with sterile, endotoxin-free reagents, as endotoxin will prime PMN. Cell suspensions should never be vortexed.
3. Adequate mixing of the sample is essential for reproducible sedimentation, presumably to distribute the erythrocytes throughout the suspension and provide maximal opportunities for rouleaux formation. When directly examined, ten mixing inversions were sufficient to guarantee reproducible and maximum sedimentation; fewer inversions compromised the reproducibility in yield.
4. Once the leukocyte-rich supernatant from the dextran sedimentation has been centrifuged, proceed as quickly as possible with the isolation procedure. Do not leave cell pellets at intermediate steps. Aspirates and cell pellets are biohazard waste and should be handled accordingly.
5. The centrifugation of the Ficoll-Hypaque gradient should be at 20 °C and with no brake on the centrifuge. When performed at 4 °C, there is more PMN contamination of the mononuclear band than seen when centrifugation is at 20 °C (2.3 vs 0.1 %, respectively), and more lymphocyte and mononuclear contamination of the PMN pellet (6.9 and 0.6 % vs 1.4 and 0.1 %).

It is best to have a dedicated room-temperature centrifuge for this use; alternatively, have the refrigeration in the centrifuge turned off overnight before running the gradient the following morning.

6. The hypotonic lysis of erythrocytes exploits the relative resistance of leukocytes to osmotic stress. This difference is relative and prolonged or repeated hypotonic lysis will damage PMN. Attention to limiting the time of exposure to hypotonicity to 18–20 s should be strictly maintained. More than two cycles of hypotonic lysis must be avoided, as they will not lyse additional erythrocytes but will begin to damage PMN.
7. When counting the PMN suspension, one can directly count the PMN by diluting the cell suspension 1:20 in 3 % acetic acid and observe under 40X objective. In the acetic acid solution, the nuclear morphology of PMN is clearly identified, allowing direct counting of the PMN in suspension. Alternatively, PMN suspension can be diluted 1:20 in HBSS and counted to determine the leukocyte concentration. A separate sample (e.g., 10 μL) can be diluted 1:5 in HBSS or saline and placed on a slide (either using a cytospin or simply maneuver the slide to obtain a thin layer) and allowed to air-dry. The slide can then be stained with Wright stain (or an equivalent) and a differential performed. With the total number of leukocytes and the percent of PMN on differential staining, the number of PMN isolated can be calculated. In general, the yield should be 2–4 million PMN/mL blood drawn and the suspension should be ~98 % PMN with a few contaminating eosinophils.
8. Efficient separation is achieved by 1:1 dilution of blood with saline prior to centrifugation in the Ficoll-Hypaque gradient. The tendency of lymphocytes to be trapped in erythrocyte-granulocyte aggregates decreases the yield of lymphocytes while simultaneously contaminating the granulocyte pellet with lymphocytes. Dilution of whole blood at the start of the isolation will decrease both problems.
9. Neither mononuclear cells nor granulocytes tolerate long incubation in Ficoll-Hypaque, so it is best to dilute the gradient matrix in the isolated cell fractions as soon as feasible.

References

1. Böyum A (1968) Isolation of mononuclear cells and granulocytes from human blood: isolation of mononuclear cells by one centrifugation, and of granulocytes by combining centrifugation and sedimentation at 1 g. Scand J Clin Lab Invest Suppl 97:77–89
2. Skoog WA, Beck WS (1956) Studies on the fibrinogen, dextran, and phytohemagglutinin methods of isolating leukocytes. Blood 11:436–454
3. Stie J, Jesaitis AJ (2007) Reorganization of the human neutrophil plasma membrane is associated with functional priming: implications for neutrophil preparations. J Leukoc Biol 81:672–685
4. Nauseef WN (2007) Isolation of human neutrophils from venous blood. Methods Mol Biol 412:15–20

Chapter 3

Neutrophil Isolation from Nonhuman Species

Daniel W. Siemsen, Natalia Malachowa, Igor A. Schepetkin, Adeline R. Whitney, Liliya N. Kirpotina, Benfang Lei, Frank R. DeLeo, and Mark T. Quinn

Abstract

The development of new advances in the understanding of neutrophil biochemistry requires effective procedures for isolating purified neutrophil populations. Although methods for human neutrophil isolation are now standard, similar procedures for isolating neutrophils from many of the nonhuman species used to model human diseases are not as well developed. Since neutrophils are reactive cells, the method of isolation is extremely important to avoid isolation technique-induced alterations in cell function. We present methods here for reproducibly isolating highly purified neutrophils from large animals (bovine, equine, ovine), small animals (murine and rabbit), and nonhuman primates (cynomolgus macaques), and describe optimized details for obtaining the highest cell purity, yield, and viability. We also describe methods to verify phagocytic capacity in the purified cell populations using a flow cytometry-based phagocytosis assay.

Key words Inflammation, Phagocytosis, Large animal model, Granulocyte, Polymorphonuclear leukocyte, Cell isolation, Flow cytometry, Blood, Bone marrow

1 Introduction

Over the years, various animal models have been developed for investigation of the pathogenesis of human inflammation and infectious diseases (reviewed in ref. 1). Although small animal models, such as rodents, are easier to handle, breed easily, require much less in the way of housing facilities, and are generally less expensive, they often do not provide an accurate reflection of human physiology [2]. Thus, nonhuman primates and larger animal models, such as bovine and sheep, are often desirable as models for human disease pathogenesis [2]. In these models, it is important to characterize neutrophil function, which requires efficient methods for purification of these phagocytic cells.

Mark T. Quinn and Frank R. DeLeo (eds.), *Neutrophil Methods and Protocols*, Methods in Molecular Biology, vol. 1124,
DOI 10.1007/978-1-62703-845-4_3,

Currently, much of our understanding of neutrophil biology is based on studies using human cells, whereas much less is known regarding the biology of these cells in nonhuman species. It is clear, however, that neutrophils from other species differ from their human counterpart in a number of important functional characteristics [3], and one cannot assume that the basic features of human neutrophil biochemistry and function are representative of neutrophils in all other species. Many species are used as models to understand human pathophysiology; thus, it is essential that we gain a thorough understanding of neutrophil functions in these models. It is also important to characterize neutrophil biology in various nonhuman species in order to determine immune status and host defense mechanisms in these organisms. Additionally, comparison of conserved features between neutrophils from different species can contribute to our understanding of neutrophil biochemistry in general.

One of the major challenges associated with neutrophil studies is the isolation of highly purified cell preparations that are morphologically and functionally similar to cells found in the blood in vivo. Neutrophils are temperamental cells that can be easily altered by improper handling [4]. Thus, the method of cell isolation is extremely important to avoid isolation technique-induced alterations in neutrophil function [4]. For instance, neutrophils can be primed during isolation, resulting in altered neutrophil responses to subsequent stimuli and changes in surface antigen expression [5–7]. Furthermore, some neutrophil function, such as chemotaxis, can actually be inhibited by isolation procedures [4]. To completely eliminate any isolation artifacts, methods have been developed for analysis of neutrophils in whole blood (e.g., *see* refs. 5, 8). Conversely, the use of whole blood can be impractical for many biochemical studies, which require purified cells in the absence of other contaminating cells and serum proteins.

Although effective methods for isolation of human neutrophils have been extensively developed (*see* Chapter 2 in this volume), these methods do not work in many nonhuman species. We present methods here for neutrophil isolation from a range of large (bovine, equine, nonhuman primate, ovine) and small (murine, rabbit) animals and describe optimized details for obtaining the highest cell purity, yield, and viability. We also verify functional phagocytic capacity in the purified cell populations using a flow cytometry-based phagocytosis assay. Importantly, all of these isolation methods are relatively inexpensive, utilize commonly available reagents, and do not require the acquisition of specialized equipment. Thus, they can be easily implemented in any lab.

2 Materials

1. Fifteen-mL Vacutainer tubes (Becton Dickinson) containing 150 μL of 500-mM disodium ethylenediaminetetraacetic acid (EDTA), pH 7.4, prepared in sterile H_2O and filtered (*see* **Note 1**).
2. Sterile endotoxin-free disposable plastic pipettes, polypropylene centrifuge tubes, and disposable polyethylene transfer pipettes (Fisher Scientific) (*see* **Note 2**).
3. CD66abce MicroBead Kit (Miltenyi Biotec).
4. MACS LS separation columns and MACS magnetic stand (Miltenyi Biotec) (*see* **Note 3**).
5. Sodium heparin 1,000 U/mL.

2.1 Buffers

1. Sterile injection-grade H_2O and 0.9 % NaCl solution (Baxter Healthcare Corporation) (*see* **Note 4**).
2. Phosphate-buffered saline (PBS): 140-mM NaCl, 2.7-mM KCl, 8-mM Na_2HPO_4, and 1.5-mM KH_2PO_4 dissolved in sterile water. Adjust pH to 7.2 and sterile filtered. Store at 4 °C.
3. Dulbecco's Modified Eagle Medium (DMEM), Dulbecco's Phosphate Buffered Saline (DPBS), 10× Hanks' balanced salt solution (10× HBSS) (without Ca^{2+}, Mg^{2+}, and phenol red), RPMI Medium 1640 without phenol red (RPMI) all from Gibco/Life Technologies.
4. HBSS: Dilute 10× HBSS in sterile H_2O, adjust pH to 7.4, and sterile filter. Store at 4 °C (*see* **Notes 4** and **5**).
5. RPMI/HEPES: RPMI supplemented with 10-mM HEPES buffer.
6. Hetastarch solution containing 6 % hetastarch in 0.9 % NaCl (Abbott Laboratories).
7. Solutions of 9 % (w/v) and 10 % (w/v) NaCl in sterile H_2O. Prepare fresh and sterile filter (*see* **Notes 4** and **5**).
8. Acid citrate dextrose (ACD): 65-mM citric acid, 85-mM sodium citrate, and 2 % dextrose dissolved in sterile H_2O and sterile filtered. Store at 4 °C (*see* **Notes 4** and **5**).
9. Murine neutrophil buffer: HBSS containing 0.1 % (w/v) bovine serum albumin, 1 % (w/v) glucose. Prepare fresh and sterile filter (*see* **Notes 4** and **5**).
10. Rabbit neutrophil buffer: 138-mM NaCl, 27-mM KCl, 8.1-mM Na_2HPO_4, 1.5-mM KH_2PO_4, and 5.5-mM glucose dissolved in sterile H_2O and sterile filtered. Store at 4 °C (*see* **Notes 4** and **5**).

11. Dextran solution: 6 % (w/v) non-pyrogenic dextran 500 (Amersham Biosciences) dissolved in sterile 0.9 % NaCl solution and sterile filtered. Store at 4 °C (*see* **Notes 4–6**).
12. 10× PBS/EDTA buffer: Dissolve 100-mM KH_2PO_4, 9 % (w/v) NaCl, 2-mg/L EDTA in sterile H_2O, adjust pH to 7.4, and sterile filter (*see* **Notes 4** and **5**).
13. PBS/EDTA buffer: Dilute 10× PBS/EDTA 1:10 in sterile H_2O, readjust pH to 7.4 if needed, and sterile filter (*see* **Notes 4** and **5**).
14. MACS erythrocyte lysis buffer: 155-mM NH_4Cl, 10-mM $KHCO_3$, and 0.1-mM EDTA dissolved in sterile water. Adjust pH to 7.3 and sterile filtered. Store at 4 °C (NHP protocol).
15. MACS neutrophil buffer: PBS (pH 7.2), 0.5 % human serum albumin, 2-mM EDTA. Sterile filtered and stored at 4 °C (*see* **Note 7**).

2.2 Density Gradient Solutions

1. Percoll, Histopaque 1077, and Histopaque 1119 (Sigma-Aldrich).
2. Histopaque 1077/1119 solution: Mix equal volumes of Histopaque 1077 and Histopaque 1119.
3. Percoll stock solution (100 % Percoll): Percoll and 10× HBSS, pH 7.4 mixed at a ratio of 9:1 (v/v) (*see* **Note 8**).
4. Percoll solutions: Mix 100 % Percoll stock with the appropriate volumes of 1× HBSS to obtain 85, 81, 70, 65, 62, 55, 50, and 45 % (v/v) Percoll solutions (*see* **Note 8**).
5. Percoll/EDTA stock solution (100 % Percoll/EDTA): Percoll and 10× PBS/EDTA, pH 7.4 mixed at a ratio of 9:1 (v/v) (*see* **Note 8**).
6. Percoll/EDTA solution: Mix 100 % Percoll/EDTA stock with the appropriate volume of 1× PBS/EDTA to obtain 65 % (v/v) Percoll/EDTA solution (*see* **Note 8**).

2.3 Cell Analysis Reagents

1. Acetic acid (2 %) prepared in sterile H_2O.
2. Trypan blue solution (0.4 %) (Sigma-Aldrich).
3. Vybrant phagocytosis assay kit (Molecular Probes).

3 Methods

In the methods described below, we outline the steps to obtain highly purified and functionally active neutrophils from bovine, equine, nonhuman primates, ovine, and rabbit blood, as well as murine bone marrow. Note that some of the methods detailed here have been adapted with modifications from previously published methods for isolation of equine [9], murine [10], ovine [11],

and rabbit neutrophils [12, 13]. Additionally, the method for isolation of neutrophils from nonhuman primates utilizes positive selection, which requires labeling of neutrophils with primary and secondary antibodies conjugated to MicroBeads and was adapted from the Miltenyi MicroBead Kit protocol (Miltenyi Biotec Inc., Auburn, CA, USA). Importantly, the presence of these antibodies on the surface of nonhuman primate neutrophils should be considered in the experimental design.

In addition to the basic neutrophil isolation procedures, we also provide details for quantifying cell yield, evaluating cell purity and viability, and measuring phagocytic function of the purified cells from several species. These parameters are compared with human neutrophils purified by a standard method. Although neutrophil isolation from all species except nonhuman primates is based on density gradient separation techniques, the gradient media and composition vary widely because of slight differences in neutrophil density between species. In addition, differences in red blood cell reactivity to aggregating reagents between species are reflected in the methods described below. Overall, these methods are efficient, easy to perform, and reproducibly generate high-quality neutrophil populations for biochemical and functional studies.

3.1 Bovine Neutrophil Isolation

1. Collect bovine blood into Vacutainer tubes containing EDTA. For the method outlined here, we collected 50 mL of blood. If different volumes of blood are required, adjust the indicated volumes proportionally.
2. Pool 50 mL of blood into a conical 50-mL polypropylene centrifuge tube and centrifuge at 740 × *g* for 10 min at room temperature with low brake.
3. Remove the upper plasma layer and buffy coat found at the plasma–red blood cell interface with a plastic transfer pipette. Transfer the remaining red blood cell layer into a conical 250-mL polypropylene tube.
4. Lyse red blood cells by adding 50 mL of sterile H_2O. Mix by gently inverting the tube for 20 s at room temperature (*see* **Note 9**).
5. Immediately add 5 mL of 10 % NaCl solution, and mix well by gently inverting the tube.
6. Centrifuge at 585 × *g* for 10 min at room temperature with low brake.
7. Remove the supernatant using a plastic transfer pipette, and resuspend the cell pellet in 50 mL of HBSS.
8. Lyse any remaining red blood cells by repeating **steps 4** through **6**.
9. Resuspend the leukocyte pellet in 10 mL of HBSS.

10. Prepare Histopaque gradients by first pipetting 15 mL of Histopaque 1077 into the bottom of a conical 50-mL centrifuge tube. Place a borosilicate glass Pasteur pipette into the tube so the pipette tip rests on the bottom of the tube. Use this pipette as a funnel to carefully underlay 15 mL of Histopaque 1077/1119 solution.
11. Layer the 10-mL leukocyte suspension on top of the Histopaque gradient using a plastic transfer pipette. This must be done carefully to avoid mixing the cell suspension with the Histopaque.
12. Centrifuge the gradient at 440 × *g* for 25 min at room temperature with no brake.
13. Remove the supernatant with a plastic transfer pipette and discard (*see* **Note 10**).
14. Wash the neutrophil pellet by resuspending the cells in 50 mL of HBSS and centrifuging at 585 × *g* for 10 min at room temperature.
15. Resuspend purified cells in the desired assay buffer.

3.2 Equine Neutrophil Isolation

1. Collect equine blood into Vacutainer tubes containing EDTA. For the method outlined here, we collected 24 mL of blood. If different volumes of blood are required, adjust the indicated volumes proportionally.
2. Prepare Percoll gradients by underlaying 2.5 mL of 85 % Percoll solution below 2.5 mL of 70 % Percoll solution in a conical 15-mL polypropylene centrifuge tube. Use a borosilicate glass Pasteur pipette as a funnel to underlay the Percoll solution (*see* **step 11** of Subheading 3.1).
3. Carefully layer 3 mL of blood on top of each gradient using a plastic transfer pipette.
4. Centrifuge the gradients for 20 min at 400 × *g* with no brake at room temperature.
5. The neutrophil band sediments at the interface between 70 and 85 % Percoll solutions. Carefully remove all of the supernatant above the neutrophil band with a plastic transfer pipette and discard (*see* **Note 10**).
6. Collect the neutrophil band with a clean plastic transfer pipette.
7. Wash the cells by resuspending them in 50 mL of HBSS and centrifuging at 200 × *g* for 10 min at room temperature.
8. Wash the cells twice more by repeating **step 7** above.
9. Resuspend purified cells in the desired assay buffer.

3.3 Human Neutrophil Isolation

1. Collect human blood into Vacutainer tubes containing EDTA. For the method outlined here, we collected 30 mL of blood. If different volumes of blood are required, adjust the indicated volumes proportionally.

2. Combine 6.7 mL of dextran solution with 30 mL of blood in a conical 50-mL polypropylene centrifuge tube. Mix by gently inverting the tube.
3. Allow the blood–dextran mixture to sediment for 45 min at room temperature. Dextran causes the red blood cells to form aggregates, which sediment to the bottom of the tube. This leaves a clear, red blood cell-depleted layer above the red blood cell-rich lower layer.
4. Transfer the upper cell layer to a clean conical 50-mL polypropylene centrifuge tube with a plastic transfer pipette.
5. Centrifuge the tube at 740 × *g* for 10 min with low brake at room temperature.
6. Remove the supernatant using a plastic transfer pipette and discard.
7. Resuspend the white blood cell pellet in 7 mL of sterile 0.9 % NaCl solution.
8. Place 7 mL of Histopaque 1077 into a conical 50-mL polypropylene centrifuge, and carefully layer the white blood cell suspension on top of the Histopaque. This must be done carefully to avoid mixing the cell suspension with the Histopaque.
9. Centrifuge at 700 × *g* for 15 min with no brake at room temperature.
10. Remove the supernatant using a plastic transfer pipette and discard (*see* **Note 10**).
11. Resuspend the neutrophil pellet in 6 mL of sterile 0.9 % NaCl solution.
12. Lyse contaminating red blood cells by adding 20 mL of sterile H_2O. Mix by gently inverting tubes for 20 s at room temperature (*see* **Note 9**).
13. Immediately add 1.8 mL of 10 % NaCl solution, and mix well by gently inverting tubes.
14. Centrifuge at 740 × *g* for 10 min at room temperature with low brake.
15. Remove the supernatant using a plastic transfer pipette and discard.
16. Resuspend the neutrophil pellet in 6 mL of sterile 0.9 % NaCl solution.
17. Lyse any remaining red blood cells by repeating **steps 12** through **15** above.
18. Remove the supernatant with a plastic transfer pipette.
19. Wash the neutrophil pellet by resuspending the cells in 50 mL of 0.9 % NaCl solution and centrifuging at 740 × *g* for 10 min at room temperature.
20. Resuspend purified cells in the desired assay buffer.

3.4 Murine Neutrophil Isolation

1. Dissect femurs and tibias from 8- to 12-week-old male mice. BALB/c mice were used here, but this procedure should also work for other strains of mice.
2. Clip the ends of each tibia and femur with dissecting scissors to expose the marrow.
3. Flush bone marrow cells from the tibias and femurs with murine neutrophil buffer using a syringe with 27-G needle. Use two 1-mL volumes of buffer for tibias and three 1-mL volumes of buffer for femurs.
4. Resuspend the pooled bone marrow eluates by gentle pipetting, followed by filtration through a 70-μm nylon cell strainer (Becton Dickinson) to remove cell clumps and bone particles.
5. Centrifuge pooled bone marrow cells at 600 × *g* for 10 min at 4 °C with low brake.
6. Remove the supernatant with a plastic transfer pipette and discard.
7. Resuspend the cell pellet in 3 mL of 45 % Percoll solution.
8. Prepare Percoll gradients by layering 2 mL each of the 62, 55, and 50 % Percoll solutions successively on top of 3 mL of 81 % Percoll solution in a conical 15-mL polypropylene tube.
9. Carefully layer the bone marrow cell suspension on top of the gradient.
10. Centrifuge at 1,600 × *g* for 30 min with no brake at 10 °C.
11. Remove the supernatant down to the 62 % Percoll layer using a plastic transfer pipette and discard (*see* **Note 10**).
12. Collect the cell band located between the 81 and 62 % Percoll layer.
13. Wash the collected cells by resuspending them in 10 mL of murine neutrophil buffer and centrifuging at 600 × *g* for 10 min at 10 °C.
14. Wash the cells again by repeating **step 13** above, and resuspend the final pellet in 3 mL of murine neutrophil buffer.
15. Carefully layer the cell suspension on top of 3 mL of Histopaque 1119 in conical 15-mL polypropylene tubes.
16. Centrifuge the gradients at 1,600 × *g* for 30 min at 10 °C and no brake to remove contaminating red blood cells.
17. Remove the supernatant using a plastic transfer pipette and discard (*see* **Note 10**).
18. Collect the cell layer between the Histopaque and buffer layers with a plastic transfer pipette.
19. Wash the cells by resuspending them in 10 mL of murine neutrophil buffer and centrifuging at 600 × *g* for 10 min at 10 °C.

20. Wash the cells again by repeating **step 19** above.
21. Resuspend purified cells in the desired assay buffer.

3.5 Nonhuman Primate Neutrophil Isolation

1. Collect blood from cynomolgus macaques (*Macaca fascicularis*) into syringes containing 100–150 μL of heparin (1,000 U/mL) per 10 mL of blood (*see* **Note 11**).
2. Transfer blood to a fresh tube and mix gently with 5–10 volumes of MACS erythrocyte lysis buffer (*see* **Note 12**).
3. Rotate tube continuously at low settings on a rotation mixer for slow and gentle rotation of cells (e.g., Rotamix, ATR, Laurel, MD) for 10 min at room temperature or rotate tubes by hand several times during the incubation.
4. Pellet cells by centrifugation at 300 × *g* for 10 min at room temperature.
5. Aspirate supernatant and wash cells once with 10 mL of MACS neutrophil buffer (*see* **Note 13**).
6. Pellet cells by centrifugation at 200 × *g* for 10 min at room temperature.
7. Remove supernatant and resuspend cell in 0.5 mL of MACS neutrophil buffer.

3.5.1 Magnetic Labeling

1. Count cells using a hemacytometer or estimate based on the known number of neutrophils per mL of blood.
2. If it is necessary to concentrate cells, centrifuge the cell suspension at 200 × *g* for 10 min at room temperature.
3. Aspirate supernatant and resuspend cell pellet in MACS neutrophil buffer (40-μL buffer per 10^7 cells).
4. Add CD66abce-Biotin-labeled antibody to cell suspension (10-μL antibody solution per 10^7 cells). Mix and incubate for 10 min at 2–8 °C.
5. Add MACS neutrophil buffer (30-μL buffer per 10^7 cells).
6. Add 20 μL of Anti-Biotin MicroBeads to the cell suspension. Mix and incubate for 15 min at 2–8 °C.
7. Wash cells by adding 1–2 mL of MACS neutrophil buffer per 10^7 cells and centrifuge at 300 × *g* for 10 min at 4 °C. Aspirate supernatant.
8. Resuspend cells in 500-μL MACS neutrophil buffer (up to 10^8 cells for every 500 μL of buffer).

3.5.2 Magnetic Separation

1. Place an LS column in the magnetic field of the MACS separator (*see* **Note 3**).
2. Rinse the LS column with 3 mL of MACS neutrophil buffer.
3. Transfer cell suspension to the LS column.

4. Collect cells that pass through the column (these will be unlabeled cells) and wash column three times with 3 mL of MACS neutrophil buffer. The total effluent should be collected (i.e., the unlabeled cell fraction) (*see* **Note 14**).
5. Transfer the column from the MACS separator to the top of an appropriate collection tube.
6. Pipette 5-mL MACS buffer onto the LS column. Flush out the magnetically labeled cells by depressing the plunger into the column.
7. Pellet cells by centrifugation at 300 × *g* for 10 min at 4 °C.
8. Resuspend cell pellet in 500-μL RPMI/HEPES.
9. Count cells and dilute to desired concentration.

3.6 Ovine Neutrophil Isolation

1. Collect ovine blood into Vacutainer tubes containing EDTA. For the method outlined here, we collected 50 mL of blood. If different volumes of blood are required, adjust the indicated volumes proportionally.
2. Transfer 50 mL of blood into a conical 50-mL polypropylene tube and centrifuge at 400 × *g* for 20 min with low brake at room temperature.
3. Remove the upper plasma layer and buffy coat found at the plasma–red blood cell interface with a plastic transfer pipette.
4. Dilute the red blood cell layer up to the starting blood volume (50 mL in this case) with PBS/EDTA buffer.
5. Pipette 25 mL of the diluted cells into each of two conical 250-mL polypropylene tubes.
6. Lyse red blood cells by adding 150 mL of sterile H_2O into each tube. Mix by gently inverting tubes for 20 s at room temperature (*see* **Note 9**).
7. Immediately add 15 mL of 9 % NaCl solution, and mix well by gently inverting tubes.
8. Centrifuge at 250 × *g* for 5 min at room temperature with low brake.
9. Remove the supernatant using a plastic transfer pipette, and resuspend the cell pellet in 50 mL of PBS/EDTA buffer.
10. Centrifuge at 250 × *g* for 5 min at room temperature.
11. Resuspend the leukocyte pellet in 9 mL of PBS/EDTA buffer.
12. Carefully layer 3 mL of the white blood cell suspension on top of 5 mL of 65 % Percoll/EDTA solution using a plastic transfer pipette.
13. Centrifuge the gradients at 400 × *g* for 20 min at room temperature with no brake.

14. Remove supernatant using a plastic transfer pipette and discard (*see* **Note 10**).
15. Wash the cells by resuspending them in 50 mL of PBS/EDTA buffer and centrifuging at 400× *g* for 10 min at room temperature.
16. Wash the cells again by repeating **step 15**.
17. Resuspend purified cells in the desired assay buffer.

3.7 Rabbit Neutrophil Isolation

1. Collect rabbit blood into a conical 50-mL polypropylene tube containing ACD so that a 4:1 (v/v) ratio of blood:ACD is achieved. For the method outlined here, we collected 24 mL of blood into a tube containing 6 mL of ACD. If different volumes of blood are required, adjust the indicated volumes proportionally.
2. Transfer 30 mL of blood into a conical 250-mL conical centrifuge tube and add 5 volumes of hetastarch to each tube (150 mL in this case). Mix by gently inverting the tube.
3. Allow the blood–hetastarch mixture to sediment for 40 min at room temperature. Hetastarch causes the red blood cells to form aggregates, which sediment to the bottom of the tube. This leaves a clear, red blood cell-depleted layer above the red blood cell-rich lower layer (*see* **Note 15**).
4. Transfer the upper red blood cell-depleted layer to a clean conical 250-mL polypropylene tube with a plastic transfer pipette.
5. Centrifuge the solutions at 585 × *g* for 10 min with low brake at room temperature.
6. Remove the supernatant using a plastic transfer pipette and discard.
7. Resuspend the white blood cell pellet in 10 mL of rabbit neutrophil buffer.
8. Lyse red blood cells by adding 100 mL of sterile H_2O. Mix by gently inverting tubes for 20 s at room temperature (*see* **Note 9**).
9. Immediately add 10 mL of 10 % NaCl solution, and mix well by gently inverting tubes.
10. Centrifuge at 585 × *g* for 10 min with low brake at room temperature.
11. Remove the supernatant using a plastic transfer pipette and discard.
12. Resuspend the cell pellet in 10 mL of rabbit neutrophil buffer.
13. Lyse any remaining red blood cells by repeating **steps 8–10** above.
14. Resuspend the leukocyte pellet in 5 mL of rabbit neutrophil buffer.

Table 1
Average neutrophil purity, yield, and cell viability using the described methods

Species	Total neutrophils[a]	Neutrophil purity (%)	Yield (per mL blood)[b]	Viability (%)
Bovine	9.79×10^7	93.7	6.94×10^5	>99
Equine	3.9×10^7	97.8	1.63×10^6	>99
Human	2.53×10^7	99.1	8.42×10^5	>99
Murine	5.12×10^6	85.9	1.71×10^6	>99
Nonhuman primate[c]	1.74×10^7	97.4	2.4×10^6	≥98
Ovine	1.8×10^7	93.6	4.89×10^5	>99
Rabbit	1.83×10^6	90.7	7.62×10^4	>99

[a]Number of neutrophils obtained from the described method
[b]Murine neutrophil yield is presented as cells per mouse
[c]Cynomolgus macaques. The data represent the average from at least three separate neutrophil preparations per species

15. Carefully layer cell suspension on top of 7 mL of Histopaque 1077 in a conical 50-mL polypropylene tube.
16. Centrifuge the gradients at $475 \times g$ for 25 min with no brake at room temperature.
17. Remove the supernatant using a plastic transfer pipette and discard (*see* **Note 10**).
18. Wash the neutrophil pellet by resuspending the cells in 50 mL of rabbit neutrophil buffer and centrifuging at $585 \times g$ for 10 min at room temperature.
19. Resuspend purified cells in the desired assay buffer.

3.8 Quantifying Cell Number and Viability

1. Resuspend the final neutrophil pellet into the desired volume of assay buffer to achieve the appropriate cell concentration (usually 2 to 5 mL) and remove an aliquot for counting.
2. To quantify cell number, dilute 10 µL of the final cell suspension in 190 µL of 2 % acetic acid. Pipette a few microliters onto a hemacytometer, and count the cells contained in the 25 squares inside the central double lines. Count only neutrophils, which are easily identified by their characteristic multilobed nuclei. Divide the neutrophil count by 25 to obtain the average per square. Multiply the average per square by 5×10^6 and then by the volume (in ml) of the final cell suspension to determine the total number of isolated neutrophils. A summary of the neutrophil recovery data determined for all species is shown in Table 1.
3. Cell viability is determined by mixing equal aliquots of neutrophil suspension and trypan blue, pipetting the mixture onto microscope slides, and viewing the cells under a microscope.

Cells that exclude the trypan blue and appear transparent are counted as viable, whereas cells that turn blue are counted as dead cells. A summary of the cell viability data determined for all species is shown in Table 1.

3.9 Analysis of Cell Purity

1. Purity can be evaluated with the hemacytometer (*see* **step 2** of Subheading 3.8) by differential counting of neutrophils versus non-neutrophils.
2. Analysis of cell purity can also be performed by flow cytometric analysis, which provides an effective approach to evaluate the cells present and their level of activation.
3. Collect 10,000 events for each sample using a flow cytometer with linear amplification of forward- and side-scatter channels.
4. Create a forward-scatter versus side-scatter dot plot, and gate out any cellular debris. Set a gate around the neutrophil population to obtain gate statistics, such as percent of total events (a measure of purity) and relative size and granularity. Figure 1a shows a representative dot plot, where the neutrophils form a relatively uniform profile (*see* **Note 16**). Likewise, Fig. 2 shows a comparison of representative dot plot of neutrophils isolated from human and nonhuman primate blood using positive selection on MicroBeads.
5. A summary of the neutrophil purity data obtained for all species is shown in Table 1.

3.10 Phagocytosis Assay

1. Phagocytosis assays were performed using a Vybrant phagocytosis assay kit with modifications for use with flow cytometry.
2. Thaw one vial each of fluorescent *Escherichia coli* K-12 bioparticles and concentrated HBSS.
3. To prepare stock bioparticles, pipette concentrated HBSS into the vial containing the bioparticles and sonicate. Transfer the solution into a clean glass test tube, add 4.5 mL of sterile H_2O, and sonicate again until the beads are completely dispersed.
4. Thaw one vial of trypan blue solution, transfer the trypan blue solution to a polycarbonate test tube, dilute with 4 mL of sterile H_2O, and sonicate.
5. Dilute isolated neutrophils from any species to a final concentration of 1×10^6 cells/mL in DMEM.
6. Dilute stock bioparticles by mixing 1 mL of bioparticles and 0.5 mL of DMEM.
7. Aliquot 150-μL DMEM, 100-μL neutrophils, and 10 μL of diluted bioparticles into 1.5-mL microcentrifuge tubes. For control samples, substitute 10-μL DMEM instead of bioparticles. This dilution gives a final bioparticle to neutrophil ratio of 20:1 (*see* **Note 17**).

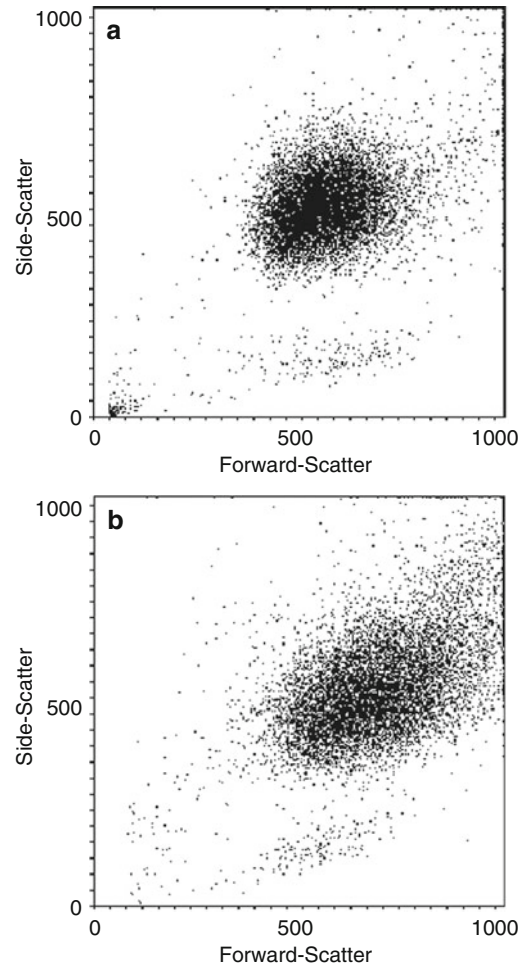

Fig. 1 Analysis of neutrophil Purity by flow cytometry. A *forward-scatter* versus *side-scatter dot* plot was used to evaluate neutrophil purity (equine cells shown here as an example). Resting (panel **a**) and mildly activated neutrophils (panel **b**) are shown (*see* **Note 17**). Neutrophils from all species showed similar forward-scatter versus side-scatter profiles. Reproduced by permission of Humana Press©2007 [15]

8. Incubate triplicate samples for 2, 5, 10, and 15 min at 37 °C. We normally incubate controls samples of neutrophils alone and neutrophils with trypan blue quench controls for 15 min to evaluate any effects resulting from the extended incubation time.
9. After each incubation time, the neutrophils are pelleted by centrifuging at 3,000 × *g* for 30 s in a microfuge at room temperature.
10. The pellet is very small and easy to lose, so carefully aspirate the supernatant.

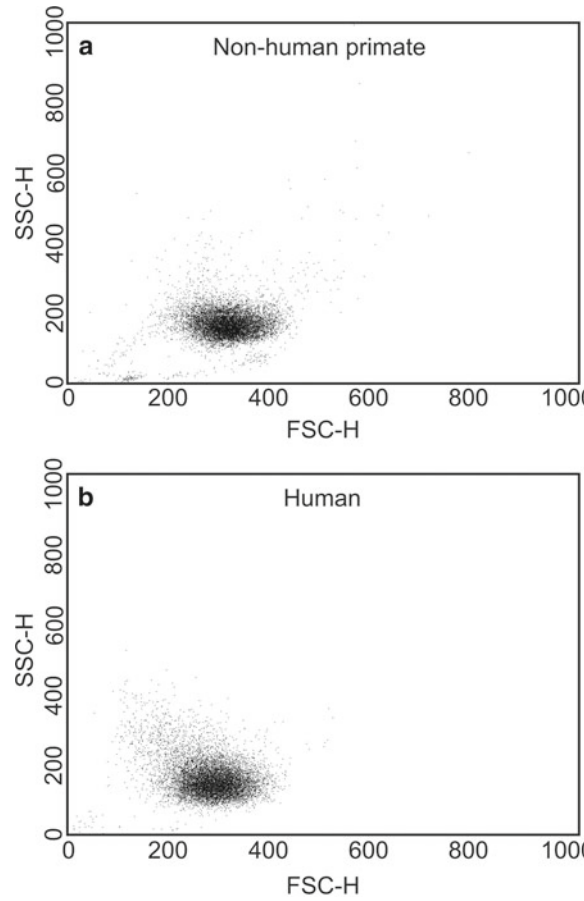

Fig. 2 Analysis of neutrophils from nonhuman primates (*Macaca fascicularis*) and humans by flow cytometry. Neutrophils were obtained from venous blood of nonhuman primates (**a**) or humans (**b**) using the positive selection methods described and then analyzed by flow cytometry to determine forward (FSC-H)- and side (SSC-H)-angle light scatter

11. To quench free bioparticles and neutrophil surface-associated bioparticles, add 100 μL of the trypan blue solution and mix well.
12. Incubate for 1 min at room temperature, and centrifuge at 3,000 × *g* for 30 s in a microfuge at room temperature.
13. Carefully aspirate the supernatant. Again, use care because the neutrophil pellet is very small and easily lost.
14. Resuspend each pellet in 250-μL DPBS, and transfer the samples to flow cytometer tubes.
15. Collect 10,000 events for each sample using a flow cytometer with linear amplification of forward-scatter and side-scatter channels and logarithmic amplification for the FL1 channel (*see* **Note 18**). Analyze the data using flow cytometry software (e.g., CellQuest software) to determine the percent of neutrophils

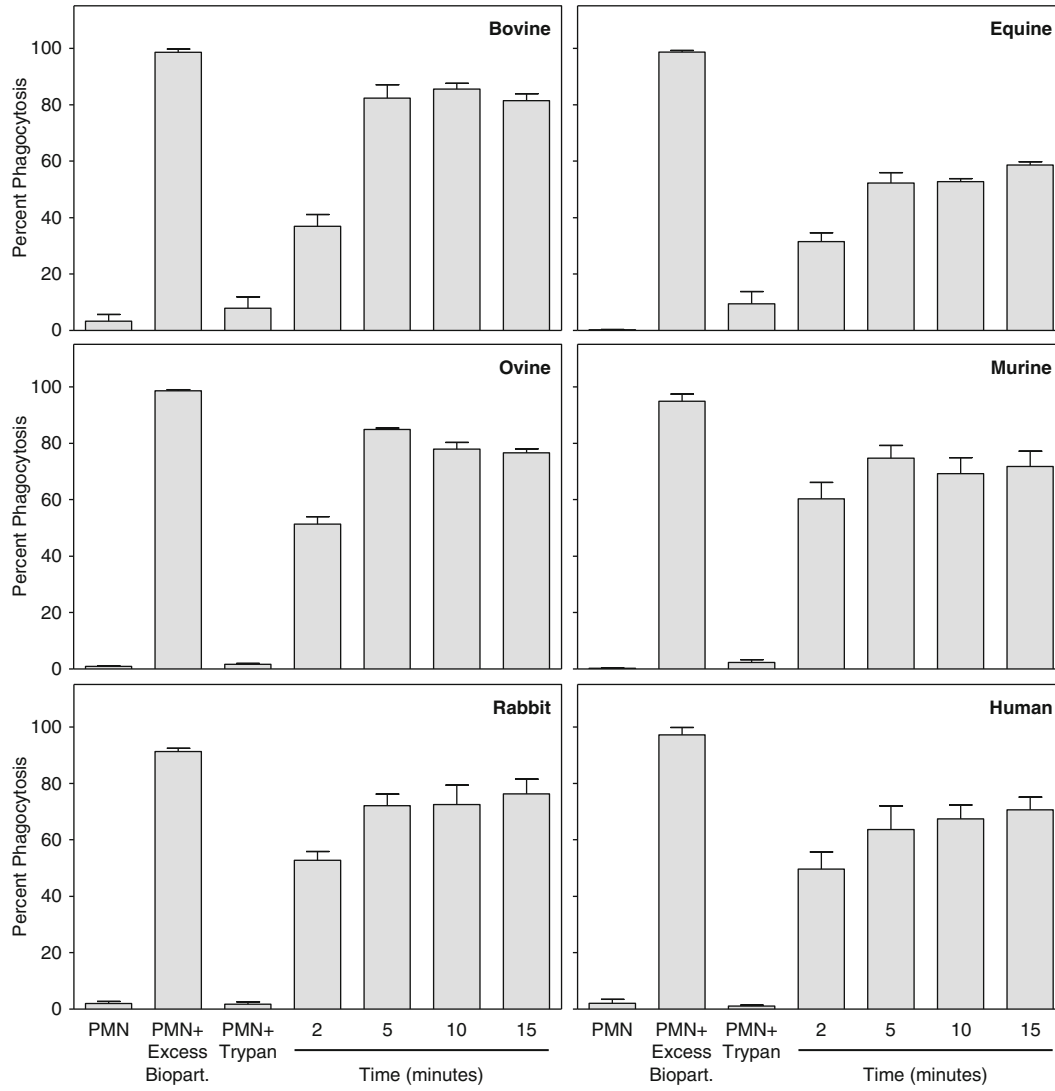

Fig. 3 Functional analysis of purified neutrophils. Neutrophils purified from the indicated species were analyzed for their ability to phagocytose fluorescent bioparticles, as described. Cells were incubated with bioparticles (1:20 ratio) for 2, 5, 10, and 15 min at 37 °C. Control samples include neutrophils alone (negative control), neutrophils incubated with trypan blue (trypan control), and neutrophils incubated with excess (1:200 ratio) bioparticles (positive control). In each panel, the results are presented as the mean ± SD of triplicate samples. Representative of at least three experiments for each panel. Reproduced from ref. 15 with permission from Humana Press

containing fluorescent bioparticles. A summary of the neutrophil phagocytosis data obtained for all species is shown in Fig. 3 (*see* **Note 19**).

4 Notes

1. EDTA was added to Vacutainer tubes by injection with a 1-mL syringe and 27-G needle.
2. It is essential that the blood and subsequently isolated neutrophils do not ever come into contact with glass, which leads to

cell activation. Thus, plasticware should be used throughout all procedures, with exception of the Vacutainer tubes, which are silicone coated.

3. An adequate-sized column should be selected based on its maximum cell capacity. The volumes provided here are for LS columns. Check the Miltenyi instructions on the package insert for appropriate volumes for use with other columns.
4. Neutrophils are highly susceptible to priming and/or activation by endotoxin or lipopolysaccharide (LPS) (e.g., *see* ref. 14), which is often a contaminant in biological reagents. Thus, all plasticware must be endotoxin-free. In addition, all buffers and reagents are prepared in sterile H_2O or saline and sterile filtered to avoid endotoxin contamination.
5. All buffers should be sterile filtered through 0.2-μm filter units (Fisher Scientific).
6. To avoid possible contamination, which is a common problem with dextran, 30 g of dextran 500 is weighed directly into a sterile plastic 500-mL Nalgene container and dissolved in sterile 0.9 % NaCl solution, followed by sterile filtering.
7. As suggested by manufacturer, human serum albumin (HSA) can be substituted with bovine serum albumin, fetal bovine serum, or human serum.
8. Use extreme care and accuracy when preparing Percoll mixtures, as small variations in the final density of Percoll mixtures affects the purity and yield of neutrophil preparation.
9. Do not extend this incubation longer than 20 s, as longer incubation in hypotonic solution can alter and/or damage the neutrophils.
10. After the supernatant has been removed from the gradients, cotton applicators may be used to wipe the walls of the centrifuge tube to remove any adherent debris, which may contaminate the preparation. Be sure to avoid touching the neutrophil band or pellet with the applicator.
11. Sodium heparin can be replaced by other anticoagulants such as EDTA or sodium citrate. Alternatively, blood can be collected into Vacutainer tubes (Becton Dickinson) as described for the other neutrophil isolation methods.
12. Typically we use 35 mL of lysis buffer per 5 mL of heparinized blood (7:1 ratio).
13. Handle neutrophils as gently as possible, e.g., have a pipette on the lowest settings.
14. Both purified neutrophil fraction and effluent (unlabeled) fraction should be analyzed to determine purification efficiency.
15. As an alternative, rabbit red blood cells can also be aggregated with 6 % dextran (100,000–200,000 molecular weight) for

30–40 min [13]; however, hetastarch seems to be more efficient. For some reason, rabbit red blood cells do not lyse as readily as those from other species. Even after two rounds of H_2O lysis, some red blood cells may still be present. If this is the case, remaining red blood cells may be removed by very gently washing the surface of the neutrophil pellet.

16. Note that neutrophil priming or activation causes an increase in cell size and granularity, which can also be evaluated with these dot plots (*see* Fig. 1b).
17. The relative amount of bioparticles and DMEM can be adjusted up or down to achieve different neutrophil:bioparticle ratios. However, we found that increased bioparticle concentrations resulted in close to 100 % phagocytosis at the 2-min time point, making it difficult to distinguish differences in rates of phagocytosis between samples.
18. Forward-scatter versus side-scatter plots yield different profiles due to varying lots of trypan blue used to quench external fluorescence.
19. Most phagocytosis experiments showed a decrease in the percent of positive cells after 5 min, which has been reported to be a result of acidification of the phagosomal compartments over time, resulting in quenching of the bioparticle fluorescence [12].

Acknowledgements

This work was supported in part by an Institutional Development Award (IDeA) from the National Institute of General Medical Sciences, National Institutes of Health under grant number GM103500 (D.S., I.A.S., L.K.N., B.L., M.Q.), the Intramural Research Program of the National Institute of Allergy and Infectious Diseases, National Institutes of Health (N.M., A.R.W., F.R.D.), and the Montana State University Agricultural Experimental Station.

References

1. Wiles S, Hanage WP, Frankel G et al (2006) Modelling infectious disease – time to think outside the box? Nat Rev Microbiol 4: 307–312
2. Casal M, Haskins M (2006) Large animal models and gene therapy. Eur J Hum Genet 14:266–272
3. Styrt B (1989) Species variation in neutrophil biochemistry and function. J Leukoc Biol 46: 63–74
4. Glasser L, Fiederlein RL (1990) The effect of various cell separation procedures on assays of neutrophil function. A critical appraisal. Am J Clin Pathol 93:662–669
5. Watson F, Robinson JJ, Edwards SW (1992) Neutrophil function in whole blood and after purification – changes in receptor expression, oxidase activity and responsiveness to cytokines. Biosci Rep 12:123–133
6. Forsyth KD, Levinsky RJ (1990) Preparative procedures of cooling and re-warming increase leukocyte integrin expression and function on neutrophils. J Immunol Methods 128: 159–163

7. Macey MG, Jiang XP, Veys P et al (1992) Expression of functional antigens on neutrophils. Effects of preparation. J Immunol Methods 149:37–42
8. Alvarez-Larrán A, Toll T, Rives S et al (2005) Assessment of neutrophil activation in whole blood by flow cytometry. Clin Lab Haematol 27:41–46
9. Pycock JF, Allen WE, Morris TH (1987) Rapid, single-step isolation of equine neutrophils on a discontinuous Percoll density gradient. Res Vet Sci 42:411–412
10. Lowell CA, Fumagalli L, Berton G (1996) Deficiency of Src family kinases p59/61hck and p58c-fgr results in defective adhesion-dependent neutrophil functions. J Cell Biol 133:895–910
11. Woldehiwet Z, Scaife H, Hart CA et al (2003) Purification of ovine neutrophils and eosinophils: anaplasma phagocytophilum affects neutrophil density. J Comp Pathol 128:277–282
12. White-Owen C, Alexander JW, Sramkoski RM et al (1992) Rapid whole-blood microassay using flow cytometry for measuring neutrophil phagocytosis. J Clin Microbiol 30: 2071–2076
13. Doerschuk CM, Allard MF, Martin BA et al (1987) Marginated pool of neutrophils in rabbit lungs. J Appl Physiol 63:1806–1815
14. DeLeo FR, Renee J, Mccormick S et al (1998) Neutrophils exposed to bacterial lipopolysaccharide upregulate NADPH oxidase assembly. J Clin Invest 101:455–463
15. Siemsen DW, Schepetkin IA, Kirpotina LN, Lei B, Quinn MT (2007) Neutrophil isolation from non-human species. Methods Mol Biol 412:21–34

Chapter 4

Collection of In Vivo Transmigrated Neutrophils from Human Skin

Karin Christenson, Lena Björkman, Lisa Davidsson, Anna Karlsson, Per Follin, Claes Dahlgren, and Johan Bylund

Abstract

A wealth of knowledge on the life and death of human neutrophils has been obtained by the in vitro study of isolated cells derived from peripheral blood. However, neutrophils are of main importance, physiologically as well as pathologically, after they have left circulation and transmigrated to extravascular tissues. The journey from blood to tissue is complex and eventful, and tissue neutrophils are in many aspects distinct from the cells left in circulation. Here we describe how to obtain human tissue neutrophils in a controlled experimental setting from aseptic skin lesions created by the application of negative pressure. One protocol enables the direct analysis of the blister content, infiltrating leukocytes as well as exudate fluid, and is a simple method to follow multiple parameters of aseptic inflammation in vivo. Also described is the skin chamber technique, a method based on denuded skin blisters which are subsequently covered by collection chambers filled with autologous serum. Although slightly more artificial as compared to analysis of the blister content directly, the cellular yield of this skin chamber method is sufficient to perform a large number of functional analyses of in vivo transmigrated cells.

Key words Chemotaxis, In vivo transmigration, Phagocyte, Subcellular granules, Trafficking, Innate immunity, Granulocytes

1 Introduction

As evidenced by the variety of techniques described in this volume, human neutrophils are rather well studied. The lion's share of in vitro work with human neutrophils is performed on neutrophils isolated from peripheral blood, which is due to the fact that standardized protocols are in use that enables purification of high numbers of neutrophils from limited volumes of peripheral blood. However, many vital neutrophil processes take place in extravascular tissues and knowledge on the behavior of neutrophils that have left circulation and transmigrated to tissues is limited. The journey from circulation to tissue is typically associated with a number of cellular changes, most notably represented by alterations

Mark T. Quinn and Frank R. DeLeo (eds.), *Neutrophil Methods and Protocols*, Methods in Molecular Biology, vol. 1124,
DOI 10.1007/978-1-62703-845-4_4,

in the flora of cell surface receptors [1]. The change in receptor expression occurs mainly as a result of granule mobilization whereby granule-localized receptors become exposed and ready to react to external stimuli. Hence, tissue neutrophils are primed, or hyperresponsive, and in many aspects distinct from the cells left in circulation [2].

Preparation and investigation of tissue neutrophils have been reported from numerous natural (often infected) sites, e.g., pus [3], saliva [4], cerebrospinal fluid [5], or BAL fluid [6]. Analysis of such samples can however be complicated by the presence of microbes (an abundant normal microbial flora, and/or the infection that triggered the inflammatory response). Also the study of in vivo transmigrated neutrophils from aseptic sites, e.g., synovial fluid from rheumatic patients [7], can be problematic since it is often impossible to determine when the acute inflammation was initiated; information that may be crucial for proper study of, e.g., short-lived neutrophils.

Controlled means of collecting tissue neutrophils typically involve the skin, and a standardized procedure for skin blistering using negative pressure was introduced in the 1960s [8] (*see* **Note 1**). When healthy skin is subjected to relatively low negative pressure, the epidermis separates from the dermis inducing the accumulation of fluid and the formation of a cleft between the basal membrane and the basal lamina [9–11]. Without damaging capillaries or causing bleeding, dermal papillae are thus exposed on the blister floor. Blister formation per se triggers an acute inflammatory response, and although the resulting exudate fluid volume (and thereby the number of infiltrating cells) is relatively low, the availability of modern micro-assays developed for small samples makes it possible to follow the arrival of neutrophils and other leukocytes [12, 37] as well as to monitor the kinetics of soluble inflammatory mediators in the exudate fluid. A detailed protocol for the generation and direct analysis of such skin blisters is given below (Subheadings 3.1–3.2).

Whereas the relatively low blister fluid volume limits the number of infiltrating cells, it is also possible to apply separate collection chambers (with much larger volumes), filled with a source of chemoattractant, to the denuded skin blisters. This skin chamber method underlies the bulk of our knowledge on in vivo transmigrated neutrophils and can be used with variations in terms of the time allowed for infiltration to occur and with a variety of attractants [13]. Described in detail below (Subheading 3.3) is the skin chamber method using autologous serum as a source of chemoattractants, with the chambers left on for 24 h. This setup leads to an impressive accumulation of a relatively pure neutrophil population and has been used for a wide variety of functional in vitro studies [14–18].

2 Materials

2.1 Creation of Skin Blisters

1. Cylindrical acrylic suction chambers with a diameter of 40 mm and a height of 18 mm. The skin chambers contain three wells with a diameter of 5 mm, situated 8 mm apart in a triangular shape, and can be connected to a vacuum pump (Fig. 1a). The suction chambers described here are custom-made, but similar chambers are commercially available, e.g., at Electronic Diversities (http://www.electdiv.com) (*see* **Note 2**).
2. Vacuum pump (Mityvac II, Mityvac, St. Louis, MO) (*see* **Note 3**).
3. Surgical tape (hypoallergenic) to fix the suction chambers.
4. Latex-free self-adherent wrap (100 mm, Coban LF; 3 M Health Care, St Paul, MN) (*see* **Note 4**).

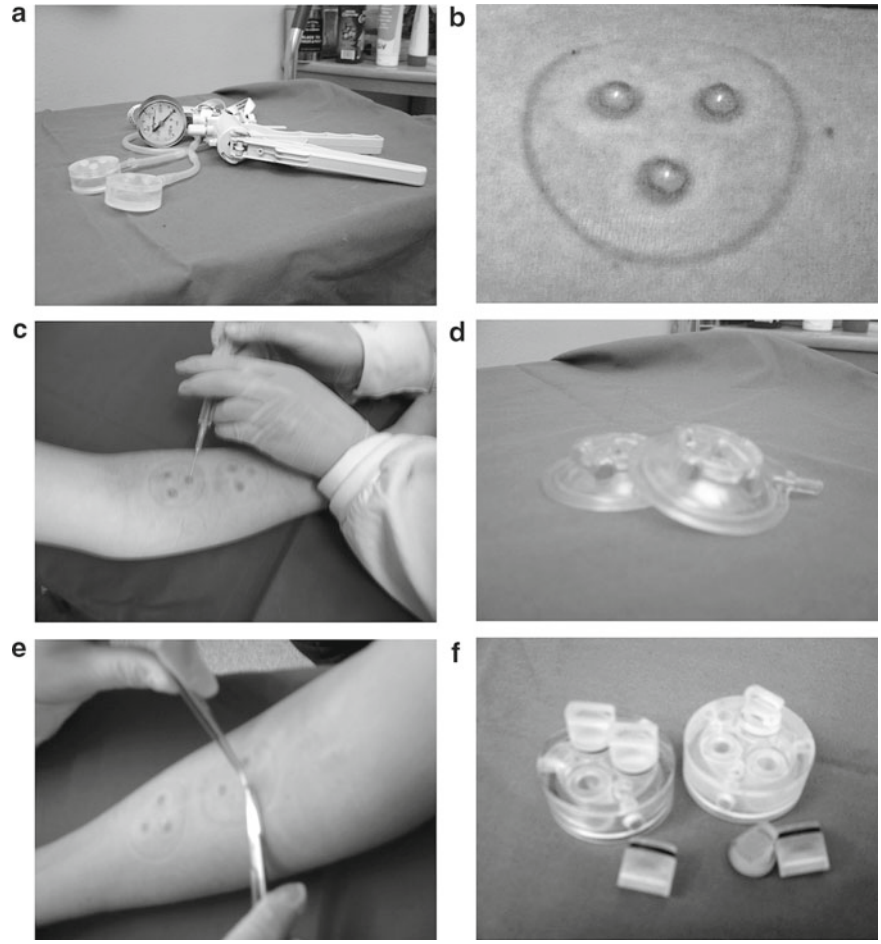

Fig. 1 Skin chamber equipment. (**a**) Suction chambers connected to a portable vacuum pump. (**b**) Typical appearance of blisters formed by negative pressure (300–400 mmHg) for 2 h. (**c**) The blister fluid is aspirated with a syringe. (**d**) Plastic covers used to prevent accidental blister damage. (**e**) Before collection chambers are mounted, blister roofs are removed to expose the lesions. (**f**) Collection chambers with stoppers

2.2 Direct Collection of Blister Fluid

1. Sterile needles (23 G).
2. Pipette with sterilized tips (20 μL).
3. Nonsticky Eppendorf tubes (1.5 mL, Protein LoBind Tube; Sigma) (*see* **Note 5**).
4. Plastic covers to protect the blisters (*see* **Note 6** and Fig. 1d).
5. Peripheral blood cells from the same subject to serve as control cells. Blood is collected in heparin tubes (9 mL, LH Lithium Heparin tubes, Vacuette; Greiner Bio-One, Austria), neutrophils isolated according to Boyum et al. [19, 20] and stored on melting ice until use.

2.3 Use of Collection Chambers

1. Scissors and tweezers (sterile).
2. Sterile collection chambers (cylindrical; Fig. 1f) with a diameter of 40 mm and three holes placed in a triangle similar to the suction chambers. The holes, however, have a slightly increased diameter of 7 mm to completely cover the lesions. To improve the contact to the skin, a rubber gasket is present in a trench on the lower side of the chambers (*see* **Note 7**).
3. Acrylic stoppers to seal each well in the chambers.
4. Serum tubes (9 mL) for collection of autologous serum (*see* Subheading 3.3.1).
5. Surgical tape (hypoallergenic) to fix the suction chambers.
6. Latex-free self-adherent wrap (10 mm, Coban LF; 3 M Health Care, St Paul, MN) (*see* **Note 8**).
7. Eppendorf tubes, 1.5 mL.
8. Krebs-Ringer phosphate buffer (KRG): 120 mM NaCl, 4.9 mM KCl, 1.7 mM KH_2PO_4, 8.3 mM Na_2HPO_4, 1.2 mM $MgSO_4$, 10 mM glucose, and 1 mM $CaCl_2$, in dH_2O, pH 7.3.
9. Peripheral blood cells from the same subject to serve as control cells. Blood is collected in heparin tubes (9 mL, LH Lithium Heparin tubes, Vacuette; Greiner Bio-One, Austria), neutrophils isolated according to Boyum et al. [19, 20] and stored on melting ice until use.

3 Methods

Both methods described are based on the generation of aseptic skin blisters by negative pressure (Subheading 3.1). After blisters have formed, they may either be left untouched for different time points until the blister content is analyzed directly (Subheading 3.2) or blisters may be denuded and the lesions covered with collection chambers for subsequent collection and analyses of chamber fluid (Subheading 3.3).

3.1 Creation of Skin Blisters

1. Connect the suction chambers to the vacuum pump.
2. Place the suction chambers on the volar part of the forearm, right below the elbow fold (*see* **Notes 9** and **10**).
3. Press the chambers gently against the forearm while removing the air from the chambers by pumping. As negative pressure builds up, manual pressure on the chambers can be gradually released. Fix the chambers with surgical tape in a crosswise fashion, cover them with a self-adhering wrap, and ensure that the arm with the chambers are kept warm, e.g., by a warm long-sleeved sweater (*see* **Note 11**).
4. A negative pressure of around 300–400 mmHg creates blisters within 1.5–2 h (*see* **Notes 12** and **13**, Fig 1b).
5. The blister formation is painless but generates a local itching during the last hour of the process as the epidermis detaches from the underlying dermis.
6. After 2 h, release the pressure, remove the wrap and tape, and carefully remove the chambers without harming the skin blisters (*see* **Note 14**).

At this time point, blister fluid is virtually free from infiltrating leukocytes (Fig. 2a) and is a good starting point (T0) to compare with blisters left untouched for specified time points (Subheading 3.2) (*see* **Note 15**). Alternatively, the blister roofs can be removed at this stage, and lesions covered with collection chambers (Subheading 3.3).

3.2 Collection and Direct Analysis of Skin Blister Fluid

Newly created skin blisters (T0) are filled with fluid, and it is possible to collect around 20 μL from each blister after removal of the suction chambers (*see* **Note 16**). The blister fluid at T0 contains a variety of cytokines (*see* **Notes 17** and **18**), but hardly any leukocytes (Fig. 2a). However, if blisters are left undisturbed, leukocytes will appear with neutrophils being the most abundant cell type in early blisters (T4–T8), after which monocytes and lymphocytes dominate (Fig. 2a) [12]. The number of leukocytes that can be recovered from the blisters varies considerably up to T8 and is then relatively stable with approximately 2,000 leukocytes/μL at T24. Despite this relatively low cellular yield, it is possible to perform a variety of analyses on the collected cells (*see* **Note 19**).

1. Puncture blisters with a sterile needle (*see* **Note 20** and Fig. 1c).
2. Aspirate blister fluid with a sterile pipette and transfer to non-sticky Eppendorf tubes on melting ice (*see* **Notes 5** and **21**).
3. If possible, perform subsequent cellular analyses directly on the cell-rich blister fluid, as washing steps inevitably lead to loss of cells (*see* **Note 22**).
4. For subsequent analyses of soluble substances, e.g., cytokines in the blister fluid, samples are frozen at −80 °C (*see* **Notes 17** and **18**).

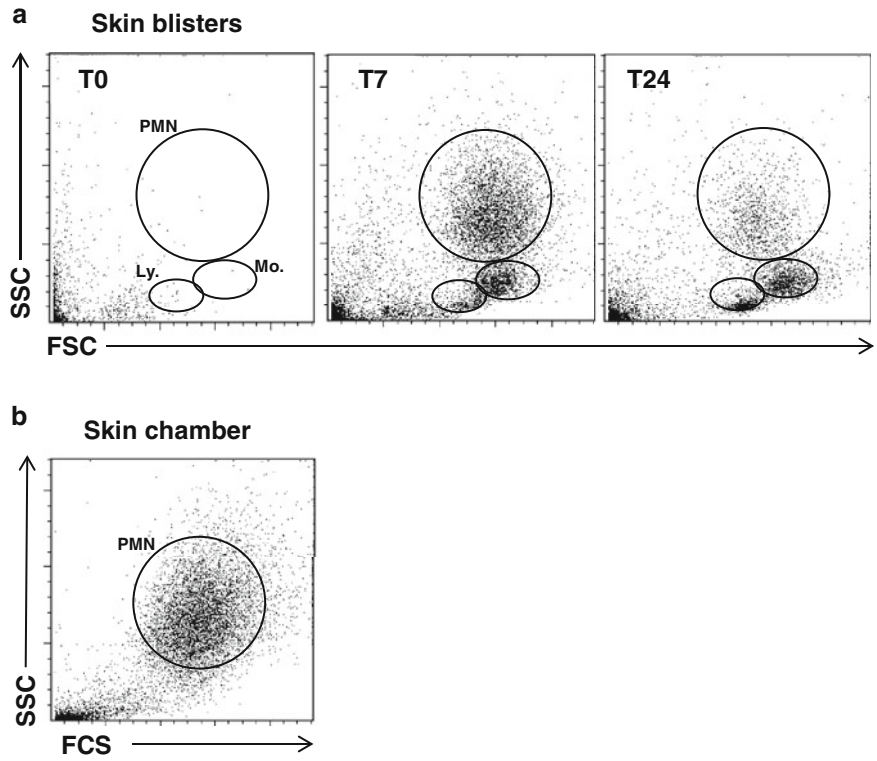

Fig. 2 Leukocyte content in blister fluid and skin chamber fluid. (**a**) Evaluation of leukocytes in skin blisters over time. Blister fluid aspirated directly after removal of the vacuum (T0, *left*) are virtually free of leukocytes. Leukocyte migration to blister fluid can be followed over time; in 7-h-old blisters (T7, *middle*), neutrophils (PMN) are the predominating cell type, while monocytes (Mo.) and lymphocytes (Ly.) dominate after 24 h (T24, *right*). The cell types are defined and gated on the basis of size (FSC) and granularity (SSC). (**b**) The cells collected from serum filled collection chambers after 24 h, comprising a rather pure neutrophil population, is shown for comparison

5. If any blisters are to be kept undisturbed for later time points, a plastic cover (*see* **Note 6** and Fig. 1d) fixed with tape is used to protect blisters from external pressure/trauma.

3.3 Application of Collection Chambers

Collection of blister fluid is a useful method to obtain in vivo transmigrated leukocytes from a controlled local, acute inflammation in otherwise healthy persons. However, the minor cell count is a limiting factor, and as it is difficult to purify one special cell type from the mixed leukocyte population, results from bulk assays may be difficult to interpret. Covering the lesions with collection chambers filled with autologous serum potently increases the cell yield and typically leads to the accumulation of a rather pure neutrophil population (Fig. 2b) that can be used for a wide variety of functional assays (*see* **Notes 23** and **24**).

3.3.1 Preparation of Serum

1. Aspirate blood in two serum tubes (with clot activators) from the individual wearing the skin chambers (*see* **Note 25**).
2. Keep the serum in room temperature until 30 min before removal of the suction chambers, then incubate at 4 °C for 20 min, and centrifuge at 430×*g* for 10 min in 4 °C (*see* **Note 26**).

3.3.2 Removal of Blister Roofs and Filling of Collection Chambers

1. Puncture the blisters with a sterile needle and aspirate the blister fluid with a sterile syringe or a pipette if blister fluid is of interest (described in Subheading 3.2).
2. Use sterile tweezers to lift the blister roof and remove it with a pair of scissors (*see* **Note 27** and Fig. 1e).
3. Fit a collection chamber with the wells placed over the non-bleeding, denuded skin lesions and hold it tight in place with the hand (*see* **Note 28**).
4. Fill each well with 600 μL autologous serum (from Subheading 3.3.1). Serum is frequently used in these types of studies and results in a high yield of transmigrated neutrophils. Also other types of attracting medium have been used with good results (*see* **Note 29**).
5. Seal the chambers with the tightly fitting stoppers. Fix the first chamber to the forearm by applying surgical tape in a crosswise fashion before the next chamber is filled and fixed in a similar manner (*see* **Note 30**).
6. Secure the chambers on the arm with a self-adhering wrap and leave it for 24 h (*see* **Note 31**).

3.3.3 Removal of Collection Chambers

1. After 24 h, carefully remove the wrapping from the forearm.
2. Cut the surgical tape that holds the chambers in place, but keep the chambers fixed to the arm with your hands. Turn the volar part of the chamber-bearing arm facing downwards and remove the chamber with the stoppers, still in place, facing down. Detach both chambers in a similar manner, one after the other (*see* **Note 32**).
3. Collect the chamber fluid from the wells by a pipette and transfer it to Eppendorf tubes (*see* **Note 33**).
4. Wash the chamber wells with KRG, 600 μL per well, and move to Eppendorf tubes.
5. Centrifuge the Eppendorf tubes for 7 s, up to 9,300×*g*, save the cell-free supernatants for analyses of soluble factors, and resuspend the cells in suitable buffer or medium.
6. Pool the cells, dilute them to suitable concentration, and put them on melting ice until use (*see* **Note 34**).

3.3.4 Analysis of Cell-Rich Skin Chamber Fluid

Even though the ability to obtain in vivo transmigrated leukocytes directly from skin blisters (as described above) is a very attractive model to study aseptic inflammation in a controlled manner, the poor cellular yield is a drawback. Even though the skin chamber method described below is slightly more artificial (due to the use of plastic collection chambers and serum as a source of chemoattractants) compared to the skin blisters, it has the benefits of providing an abundant population of relatively pure neutrophils (Fig. 2b) that have undergone in vivo transmigration from peripheral blood, via the skin lesions into the chambers. Neutrophils collected by the skin chamber methodology has been used for a wide variety of functional studies (*see* **Note 24**), clearly demonstrating that, during in vivo transmigration, neutrophils are functionally altered in many ways as compared to cells isolated in parallel from peripheral blood. Also the cell-free exudate fluid constitutes a rich source of possibilities to study pro- and anti-inflammatory cytokines and other soluble mediators [14, 21, 22] (*see* **Note 17**).

4 Notes

1. Alternative, controlled means of generating skin blisters exists, most notably by the application of Spanish fly venom, cantharidin, to intact skin [23].
2. Skin chambers in various materials have been used in a diversity of studies, e.g., different types of plastic [14, 15, 18, 24], siliconized glass [25], and siliconized rubber [26, 27]. No comparable studies have been performed to decide which chamber material that yields the best result, but one important thing regarding the choice of chamber material is that it should tolerate sterilization.
3. A portable, handheld vacuum pump is preferable, as the person wearing the chambers is then mobile which minimizes the inconvenience.
4. Self-adherent wrap fixes the chambers in place which ensures a sustained vacuum with minimal leakage of pressure.
5. Nonsticky tubes are preferable as activated cells may adhere to plastic surfaces. Some types of plastic are therefore more suitable than others, e.g., polypropylene. If washing steps or dilution is needed for specific blister cell assays, e.g., staining of surface markers, the addition of EDTA (100 μM, final concentration) further prevents adhesion to the plastic. However, as EDTA is a calcium chelator, it should not be used in assays where calcium ions are of importance for leukocyte functions, e.g., phagocytosis and degranulation.
6. The blisters are slightly delicate and need to be protected from unintentional damage. We use plastic covers (Fig. 1d), attached

by surgical tape, to minimize the risk of blister damage, but any type of cover that protects the blisters without disturbing them should suffice.

7. A preferable method to sterilize the chambers is by gas sterilization (ethylene oxide), but as few companies perform this type of sterilization, autoclaving is another option. When using autoclaving, it is however important to secure that the material in the chambers are not affected by the high temperatures and humidity connected to this method.
8. The self-adherent wrap functions very well in fixing the chambers enough to prevent leakage of serum while at the same time providing minimal inconvenience when chambers are worn overnight.
9. We usually place two identical suction chambers, coupled to the same vacuum pump, on the nondominant arm, as it is most convenient for the person wearing the chambers.
10. The volar part of the forearm is often large enough to fit the chambers if they are placed near the elbow fold. Do not place the chambers on the lower rotating part of the arm as movement may result in decreased pressure and leakage.
11. Blistering may be influenced by the temperature of the skin [28], and previous studies describe the use of external heating [22, 29, 30] during the creation of skin blisters. In our experience, however, a warm sweater is enough to yield good and reproducible blisters.
12. During creation of the skin blisters, a certain amount of pressure loss is unavoidable, and additional sporadic pumping is necessary to sustain the negative pressure around 300–400 mmHg.
13. The time to create blisters is correlated to the amount of negative pressure and could be adjusted. However, it is important to keep the negative pressure at a level that does not cause capillary bleedings, bruising, blister rupture, or pain.
14. For the purpose of kinetic studies of blister content, it is advisable to keep the time for blister drawing constant. In case blisters are to be denuded and covered with collection chambers, the time allowed for blister formation is not as critical.
15. As seen in Fig. 2, flow cytometric analyses of T0 blister fluid reveal a variety of events outside the leukocyte gates used. These events are CD45 negative (and thus non-leukocytes); microscopic analysis indicates that they are a mixture of anuclear debris, cell fragments, and occasional erythrocytes. Furthermore, the relative abundance of these events does not vary over time.
16. The skin blister method yields limited amounts of cells and experimental assays suited for small sample volumes, and

limited cell numbers are particularly helpful. We run our samples on a flow cytometer (Accuri C6, BD) that operates with minimal void volumes and a low-pressure pumping system (without vacuum) that allows for the use of any kind of tubes. In addition, all settings can be applied to samples after acquisition which is a great advantage for making the most out of a limited number of cells. As little as 2 μL blister fluid, diluted 1:10, can be used for flow cytometric analyses.

17. Multiplex analysis [31] is practical for evaluation of the content of inflammatory mediators in limited amounts of exudate fluids as it makes it possible to screen for multiple factors, e.g., cytokines, simultaneously. We have used a Bio-plex Pro Cytokine assay, 10-plex Group 1 (Bio-Rad Laboratories AB, Sundbyberg, Sweden), but other assays as Cytometric Bead Arrays, CBA (BD Bioscience, Stockholm, Sweden), are also available.
18. As stated in **Note 17**, we have successfully used a multiplex assay to evaluate the content of IL-1β, IL-6, IL-8, IL-10, IL-12, IL-17, TNF-α, IFN-γ, GM-CSF, and IP-10 in blister fluid [37]. All these cytokines, except for IL-12, IFN-γ, and IP-10, were increased in T0 blister fluid as compared to serum levels.
19. We have performed analysis of surface markers and viability [12], but also successfully analyzed intracellular markers and functional features of the transmigrated leukocytes [37].
20. Exclude blisters that display visible signs of bleeding.
21. To collect maximal volumes of blister fluid, light pressure can be applied to the blister roof (using, e.g., a pipette tip), pushing the fluid towards the pipette tip.
22. Since the cellular infiltrate typically consists of a mixture of different leukocytes, assays able to distinguish the cell type of interest are recommended, e.g., flow cytometry or microscopy. By flow cytometry, neutrophils can be easily distinguished from monocytes and lymphocytes on the basis of size and granularity (Fig. 2). Use of an anti-CD45 antibody can further facilitate the distinction of various leukocyte subsets [32], and for more detailed analyses of, e.g., different lymphocyte subsets, antibodies specific for additional surface markers can be added [12].
23. Our collection chambers hold 600 μL of serum per well, and after 24 h it is possible to collect exudate fluid containing approximately $5–30 \times 10^6$ cells, mainly neutrophils (more than 90 % of the total cell count, Fig. 2b). Most publications allow 20–24 h for transmigration which typically results in an abundant, and relatively pure, neutrophil population. Using 70 % autologous serum as a source of chemoattractants, Kuhns et al. [22] demonstrated that the accumulation of leukocytes

is finished after 18 h and that neutrophils dominate completely in the chamber fluid between 3 and 24 h. Only minimal amounts of monocytes and lymphocytes were detected in the chamber fluid, which is in contrast to findings at the dermal-epidermal interphase of the lesions where neutrophils are outnumbered by monocytes and lymphocytes during the early phase (up to 5 h) [22]. The massive neutrophil dominance seen in chamber fluid is also in contrast to the situation in blister fluid, where neutrophils are always accompanied by other leukocytes (Fig. 2).

24. Skin chamber neutrophils have been analyzed with respect to, e.g., granule mobilization [18], production of reactive oxygen species [15, 16], cytokine producing capacity [14, 7] gene expression [33], and regulation of cell death [14].
25. Aspirate blood (for preparation of serum) from the nondominant arm before the suction chambers are put in place and save the other arm until chambers are to be removed, as peripheral blood neutrophils are needed as control cells.
26. We put the serum tubes in 4 °C for the last 20 min before centrifugation (where cells and clotting factors are separated from the serum) as it in our experience results in a better serum yield.
27. Help from another person, or the person that will be wearing the skin chambers, facilitates the removal of the blister roofs. The choice of tweezers and scissors is also of importance; in our experience, this step is easier to perform with tweezers and scissors with curved blades.
28. It is important that the chambers are thoroughly cleaned and sterilized between experiments to avoid possible transfer of infectious microbes between the voluntary participants (*see* also **Note 7**).
29. The choice of cell-attracting medium regulates the transmigration process. Serum is a rich source of various protein structures, e.g., complement and coagulation factors that can be activated to attract leukocytes when it comes in contact with inflammatory factors in association with the lesions [13]. Small amounts of the complement factor C5 is cleaved and activated by serum preparation and results in presence of the chemotactic cleavage product C5a [21]. A kinetic analysis of chamber fluid, starting with 70 % autologous serum [22], has suggested that C5a is involved in the attraction of cells during the earlier time points of extravasation, but also other chemoattractants such as leukotriene B4 (LTB4) increase during the first hours. The neutrophil chemoattractant IL-8 is low during the first 8 h, but thereafter the concentration of this chemokine increased very steeply up to 24 h which is in correspondence with the increased migration of neutrophils at these time points [22]. Both LTB4 and IL-8 can be produced

by macrophages [34–37], and as this cell type is resident in most tissues, it is most likely that macrophages are in contact with the skin lesions and contribute to the release of attracting factors. However, serum has been shown to have an activating effect on resting blood neutrophils and to cause degranulation of secretory vesicles and gelatinase granules [18]. Even if the transmigration process per se also leads to mobilization of intracellular granule proteins, it could be worth remembering that serum may be inexpedient as skin chamber fluid for certain experimental settings. An alternative is to use plasma as chamber fluid, since it has less activating effect on cells. However, plasma is a poor chemoattractant and has also been shown to coagulate and clot after longer incubation times (>18 h) [13], so the use of plasma alone results in very poor cellular yields. Therefore, serum can be used for the first part (16–18 h), and when the inflammatory response is evoked and cells are migrating, it can be exchanged for plasma during the last 6 h of the experiment [18].

30. This part of the procedure is slightly challenging as it is important to fix the chambers firmly to avoid leakage of serum from the chambers without fixing them too tightly and affect circulation. The subject will be wearing the skin chambers for up to 24 h, and it is therefore important that discomfort due to chamber fixation is avoided.
31. It is also possible to use an elastic bandage, but we have found the self-adhering wrap to be superior in proper fixation of the chambers.
32. The lesions should be washed with lukewarm water and soap before covering them in a loose-fitting bandage for some hours. The lesions will heal completely within a matter of days and leave no scars. However, occasional hyperpigmentation can occur after healing of the lesions, but these changes are not permanent.
33. Ordinary Eppendorf tubes can be used to collect leukocytes from the skin chambers. The cellular yield from these chambers is high enough to make the loss of cells due to adherence to plastic, of minor importance.
34. We typically store cells at 5×10^6/mL to avoid aggregation.

Acknowledgments

This work was supported by the Swedish Research Council (521-2009-3443), the King Gustav V Memorial Foundation, Gothenburg Medical Society, Ingabritt and Arne Lundgren's Research Foundation, the Gothenburg Rheumatism Association, and the Swedish state under the LUA/ALF agreement.

References

1. Condliffe AM, Kitchen E, Chilvers ER (1998) Neutrophil priming: pathophysiological consequences and underlying mechanisms. Clin Sci (Lond) 94:461–471
2. Zarember KA, Kuhns DB (2011) Editorial: will the real neutrophil please stand up? J Leukocyte Biol 90:1039–1041
3. Kuhns DB, Long Priel DA, Gallin JI (1995) Loss of L-selectin (CD62L) on human neutrophils following exudation in vivo. Cell Immunol 164:306–310
4. Lukac J, Mravak-Stipetic M, Knezevic M et al (2003) Phagocytic functions of salivary neutrophils in oral mucous membrane diseases. J Oral Pathol Med 32:271–274
5. Briheim G, Stendahl O, Dahlgren C (1986) Factor-specific deactivation of leucocyte chemotaxis in vivo. Scand J Haematol 37: 253–258
6. Hustinx WN, Van Kessel CP, Heezius E et al (1998) Effects of granulocyte colony-stimulating factor (G-CSF) treatment on granulocyte function and receptor expression in patients with ventilator-dependent pneumonia. Clin Exp Immunol 112:334–340
7. Christenson K, Björkman L, Karlsson A et al (2013) Regulation of neutrophil apoptosis differs after in vivo transmigration to skin chambers and synovial fluid: a role for inflammasome dependent IL-1β release. J Innate Immun 5:377–388
8. Kiistala U, Mustakallio KK (1964) In-vivo separation of epidermis by production of suction blisters. Lancet 1:1444–1445
9. Bork K (1978) Physical forces in blister formation. The role of colloid osmotic pressure and of total osmolality in fluid migration into the rising blister. J Investig Dermatol 71:209–212
10. Hunter JA, McVittie E, Comaish JS (1974) Light and electron microscopic studies of physical injury to the skin. I. Suction. Brit J Dermatol 90:481–490
11. Kiistala U, Mustakallio KK (1967) Dermo-epidermal separation with suction. Electron microscopic and histochemical study of initial events of blistering on human skin. J Invest Dermatol 48:466–477
12. Thorén FB, Riise RE, Ousbäck J et al (2012) Human NK Cells induce neutrophil apoptosis via an NKp46- and Fas-dependent mechanism. J Immunol 188:1668–1674
13. Follin P (1999) Skin chamber technique for study of in vivo exudated human neutrophils. J Immunol Methods 232:55–65
14. Christenson K, Björkman L, Karlsson J et al (2011) In vivo-transmigrated human neutrophils are resistant to antiapoptotic stimulation. J Leukoc Biol 90:1055–1063
15. Follin P, Briheim G, Dahlgren C (1991) Mechanisms in neutrophil priming: characterization of the oxidative response induced by formylmethionyl-leucyl-phenylalanine in human exudated cells. Scand J Immunol 34:317–322
16. Karlsson A, Follin P, Leffler H et al (1998) Galectin-3 activates the NADPH-oxidase in exudated but not peripheral blood neutrophils. Blood 91:3430–3438
17. Paulsson JM, Moshfegh A, Dadfar E et al (2012) In-vivo extravasation induces the expression of interleukin 1 receptor type 1 in human neutrophils. Clin Exp Immunol 168:105–112
18. Sengelov H, Follin P, Kjeldsen L et al (1995) Mobilization of granules and secretory vesicles during in vivo exudation of human neutrophils. J Immunol 154:4157–4165
19. Boyum A (1968) Isolation of mononuclear cells and granulocytes from human blood. Isolation of monuclear cells by one centrifugation, and of granulocytes by combining centrifugation and sedimentation at 1 g. Scand J Clin Lab Invest Suppl 97:77–89
20. Boyum A, Lovhaug D, Tresland L et al (1991) Separation of leucocytes: improved cell purity by fine adjustments of gradient medium density and osmolality. Scand J Immunol 34:697–712
21. Follin P, Wymann MP, Dewald B et al (1991) Human neutrophil migration into skin chambers is associated with production of NAP-1/IL8 and C5a. Eur J Haematol 47:71–76
22. Kuhns DB, DeCarlo E, Hawk DM et al (1992) Dynamics of the cellular and humoral components of the inflammatory response elicited in skin blisters in humans. J Clin Invest 89: 1734–1740
23. Day RM, Harbord M, Forbes A et al (2001) Cantharidin blisters: a technique for investigating leukocyte trafficking and cytokine production at sites of inflammation in humans. J Immunol Methods 257:213–220
24. Gowland E (1964) Studies on the emigration of polymorphonuclear leucocytes from skin lesions in man. J Pathol Bacteriol 87:347–352
25. Perillie PE, Finch SC (1964) Quantitative studies of the local exudative cellular reaction in acute leukemia. J Clin Invest 43:425–430
26. Hellum KB, Solberg CO (1977) Human leucocyte migration: studies with an improved skin chamber technique. Acta Pathol Microbiol Scand C 85C:413–423
27. Wright DG, Gallin JI (1979) Secretory responses of human neutrophils: exocytosis of specific (secondary) granules by human neutrophils

during adherence in vitro and during exudation in vivo. J Immunol 123:285–294

28. Kiistala U (1972) Dermal-epidermal separation. II. External factors in suction blister formation with special reference to the effect of temperature. Ann Clin Res 4:236–246
29. Paulsson J, Dadfar E, Held C et al (2007) Activation of peripheral and in vivo transmigrated neutrophils in patients with stable coronary artery disease. Atherosclerosis 192: 328–334
30. Thylen P, Lundahl J, Fernvik E et al (2000) Impaired monocyte CD11b expression in interstitial inflammation in hemodialysis patients. Kidney Int 57:2099–2106
31. Vignali DA (2000) Multiplexed particle-based flow cytometric assays. J Immunol Methods 243:243–255
32. Preijers FW, Huys E, Leenders M et al (2011) The new violet laser dye, Krome Orange, allows an optimal polychromatic immunophenotyping based on CD45-KO gating. J Immunol Methods 372:42–51
33. Theilgaard-Monch K, Knudsen S, Follin P et al (2004) The transcriptional activation program of human neutrophils in skin lesions supports their important role in wound healing. J Immunol 172:7684–7693
34. Martin TR, Raugi G, Merritt TL et al (1987) Relative contribution of leukotriene B4 to the neutrophil chemotactic activity produced by the resident human alveolar macrophage. J Clin Invest 80:1114–1124
35. Nigon F, Rouis M, Foster SJ et al (1991) Native low-density lipoproteins stimulate leukotriene B4 production by human monocyte-derived macrophages. Biochim Biophys Acta 1083:230–234
36. Grimm MC, Elsbury SK, Pavli P et al (1996) Interleukin 8: cells of origin in inflammatory bowel disease. Gut 38:90–98
37. Winkler AR, Nocka KH, Sulahian TH et al (2008) In vitro modeling of human alveolar macrophage smoke exposure: enhanced inflammation and impaired function. Exp Lung Res 34:599–629. PMID:23570945

Chapter 5

Subcellular Fractionation of Human Neutrophils and Analysis of Subcellular Markers

Stine Novrup Clemmensen, Lene Udby, and Niels Borregaard

Abstract

The neutrophil has long been recognized for its impressive number of cytoplasmic granules that harbor proteins indispensable for innate immunity. Analysis of isolated granules has provided important information on how the neutrophil grades its response to match the challenges it meets on its passage from blood to tissues. Nitrogen cavitation was developed as a method for disruption of cells on the assumption that sudden reduction of the partial pressure of nitrogen would lead to aeration of nitrogen dissolved in the lipid bilayer of plasma membranes. We find that cells are broken by the shear stress that is associated with passage through the outlet valve under high pressure and that this results in disruption of the neutrophil cell membrane while granules remain intact. The unique properties of Percoll as a sedimentable density medium with no inherent tonicity or viscosity are used for creation of continuous density gradients with shoulders in the density profile created to optimize the physical separation of granule subsets and light membranes. Immunological methods (sandwich enzyme-linked immunosorbent assays) are used for quantitation of proteins that are characteristic constituents of the granule subsets of neutrophils.

Key words Nitrogen cavitation, Percoll density gradient centrifugation, Subcellular fractionation, Neutrophil granules, Secretory vesicles, Enzyme-linked immunosorbent assay, Myeloperoxidase, NGAL, Gelatinase, Latent alkaline phosphatase

1 Introduction

Human neutrophils undergo remarkable changes of activity in order to adjust to the different environments they encounter and to meet the demands required for fulfilling their role as the primary mobile innate immune defense system. Because most of the neutrophil's antimicrobial defense mechanisms can damage host tissues, inappropriate activation of neutrophils may cause severe tissue destruction and can be life threatening, as exemplified by Wegener's granulomatosis and adult respiratory distress syndrome (ARDS). To minimize the risk of inappropriate activation while circulating, and yet to secure a rapid and effective alertness for activation when needed, the circulating neutrophil has stored most

Mark T. Quinn and Frank R. DeLeo (eds.), *Neutrophil Methods and Protocols*, Methods in Molecular Biology, vol. 1124,
DOI 10.1007/978-1-62703-845-4_5,

of its antimicrobial armory in granules, and most of the receptors that are needed for activation of granule exocytosis and activation of the respiratory burst are inside vesicles. Thus, the circulating neutrophil is a dormant cell that does not readily respond to activation [1, 2]. The primary key to activation of the neutrophil is the endothelium of the postcapillary venules, which responds to microbial invasion or tissue damage by exposing selectins on the surface to capture bypassing dormant neutrophils and cause their awakening by signals that mobilize secretory vesicles as result of selectin and P-selectin glycoprotein ligand (PSGL)-1-mediated interaction. Secretory vesicles are the most readily mobilizable of the neutrophil's storage organelles, created by endocytosis during terminal neutrophil maturation in the bone marrow. Secretory vesicles contain plasma proteins and thus do not release toxic substances when they fuse with the plasma membrane and empty their contents. Their importance lies in their membrane, which is the main store of receptors that, when translocated to the cell surface, allow the neutrophil to interact with ligands presented by the epithelium and with soluble mediators released from microorganisms and other cells in response to a microbial threat. Thus, with the exception of a minor part of the membrane components of the NADPH oxidase, secretory vesicles are not the store of neutrophil antibacterial proteins but are better characterized as the key to neutrophil responsiveness.

Not all stored effector mechanisms are needed at the same time. Proteases that disrupt the collagenous network of the basement membrane are needed before the complement receptors that mediate phagocytosis of microorganisms opsonized by soluble innate bacterial recognition systems. In addition, pro-antibacterial proteins are stored away from their activating proteases as a means of preventing unleashing of the potential toxic effector mechanisms before creation of a phagocytic vacuole sets the stage for full orchestration of the antibacterial systems. Therefore, several different subsets of neutrophil granules exist, each with its characteristic profile of proteins and with its specific set point for degranulation. In fact, neutrophil granules are best described as a continuum, from the earliest appearing azurophil granules to the latest appearing gelatinase granules, each filled with proteins that are synthesized when the granules are formed. The differences and continuum are determined by the highly individual profiles for biosynthesis of granule proteins during neutrophil maturation in the bone marrow from promyelocyte to segmented neutrophil [3]. At the same time, the set point of the trigger that determines the propensity for degranulation is most likely determined by the density of fusion proteins on the surface of the granules, which increases during myelopoiesis such that azurophil granules contain the lowest amount and secretory vesicles the highest amount of fusion proteins. Thus, there is heterogeneity among both peroxidase-positive

(azurophil) and peroxidase-negative (specific and gelatinase) granules, but this is only associated with a heterogeneity of the set points for exocytosis with regard to the peroxidase-negative granules, while no difference in extent and direction of degranulation of the subsets of azurophil granules, defined by their presence or absence of defensins, has been documented [4].

The heterogeneity of neutrophil granules can be understood from the targeting by timing hypothesis (*see* Fig. 1). Although this hypothesis explains the fundamentals of neutrophil granule heterogeneity, it does not completely explain the presence or absence of proteins in all granules since another as yet not well-described mechanism(s) determines whether proteins are sorted to granules or to the constitutive secretory pathway. This is particularly clear for proteins, such as defensins and bactericidal permeability-increasing protein (BPI), which are only routed to granules during the promyelocyte stage and largely routed to the constitutive secretory pathway during the myelocyte stage where most of the proteins are synthesized.

Another fortuitous consequence of the heterogeneity of granules is that these differ by density. In general, the earliest formed granules are the densest, with the marked exception being granules that are high in defensins. Since defensins are present in such high concentrations in the defensin-positive azurophil granules, these are the granules of highest isopycnic density of the neutrophil but are produced at the myelocyte/metamyelocyte stage of maturation (*see* Fig. 1).

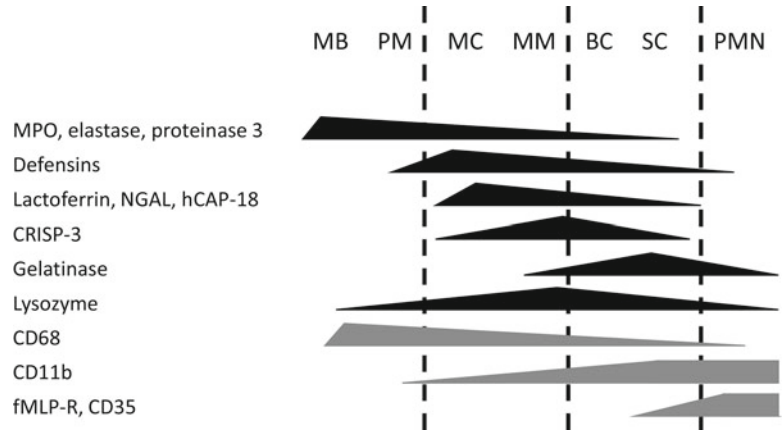

Fig. 1 Targeting by timing hypothesis. Hypothetical mRNA transcription profiles of neutrophil granule proteins during myelopoiesis (adapted from ref. 3). The distribution of transcripts for selected proteins is shown in *black* (matrix proteins) or *gray* (membrane proteins). *MB* myeloblasts, *PM* promyelocytes, *MC* myelocytes, *MM* metamyelocytes, *BC* band cells, *SC* segmented cells, *PMN* polymorphonuclear neutrophils. Reproduced by permission of Humana Press © 2007 [20]

1.1 Subcellular Fractionation on Percoll Density Gradients

The methods for subcellular fractionation that we have developed take advantage of the excellent properties of Percoll [5]. In contrast to the alternative, sucrose, density and tonicity are completely dissociated in Percoll, since Percoll owes its density to the concentration of silica macromolecules. The tonicity is thus determined by the medium in which Percoll is dissolved or diluted. Another fundamental advantage is that Percoll has close to no viscosity, again in contrast to sucrose solutions. This means that in a Percoll gradient, subcellular organelles reach their isopycnic density in a matter of minutes by high-speed centrifugation in contrast to the hours of ultra-speed centrifugation needed in a sucrose gradient. Finally, and perhaps most importantly, Percoll gradients are dynamic even during high-speed centrifugation. Since the large polyvinylpyrrolidone (PVP) covered silica molecules sediment by high-speed centrifugation, Percoll was introduced as a self-generating density profile medium where broken cells could be mixed with a uniform solution of Percoll. This would then form a self-generated density profile that decreases towards the top. Although this is certainly true, there is a shallow increase in density from the top of the gradient almost to the bottom where the density then rises almost exponentially, making Percoll less well suited for separation of organelles denser than plasma membranes and other light membranes, since these are separated by only a few milliliters of density medium even though they may differ significantly in isopycnic density (*see* Fig. 2).

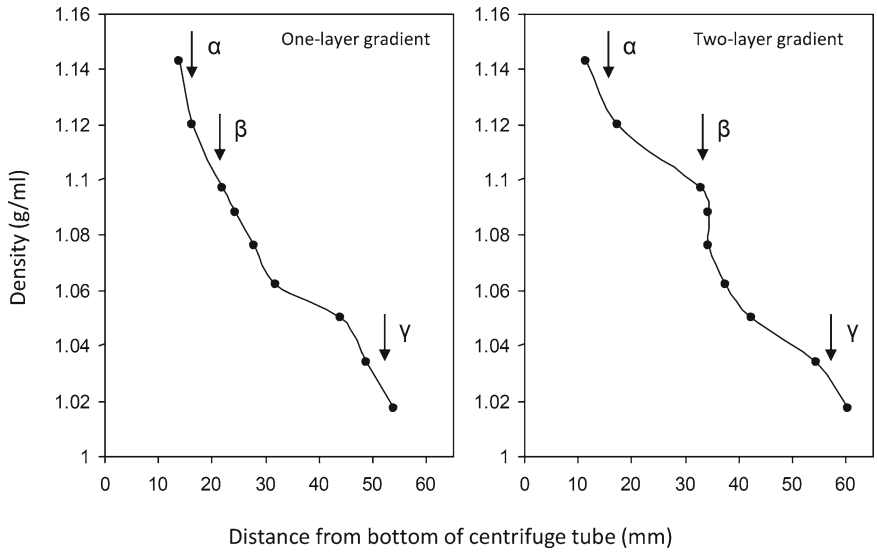

Fig. 2 Density profile of Percoll gradients after centrifugation. One-layer gradient: initial density 1.080 g/mL. Two-layer gradient: initial density 1.050/1.120 g/mL. *Arrows* indicate positions of the three visible bands (α, β, and γ bands) representing azurophil (peroxidase-positive) granules, peroxidase-negative (specific and gelatinase) granules, and light membranes, respectively. Reproduced by permission of Humana Press © 2007 [20]

We took advantage of the fact that Percoll does modulate its preset density profile even during short-term high-speed centrifugation and thus initially constructed a two-layer Percoll density gradient that would create a major physical separation between granules with the density of peroxidase-negative granules and the density of azurophil (peroxidase-positive) granules [6]. Thus, although constructed as a discontinuous density gradient, the two-layer Percoll density gradient works as a continuous density gradient with two main separating shoulders, one that separates light membranes from granules and one that separates peroxidase-negative from peroxidase-positive granules (*see* Fig. 2). When we subsequently discovered that gelatinase granules are distinctly lighter than specific granules (by analyzing the shoulder that separates azurophil from specific granules), we introduced yet another major shoulder that gives a large physical separation of gelatinase-rich granules from lactoferrin-rich granules [7, 8]. This three-layer gradient gives the same separation of light membranes as the two-layer gradient and thus allows the identification of secretory vesicles as distinct from plasma membranes but does not allow a major physical separation (*see* Fig. 3a). Such separation has been achieved by high-voltage free-flow electrophoresis [9] and also by flotation on density gradients [10]. In order to obtain both separation of the three granule subsets and separation of plasma membrane from secretory vesicles in one centrifugation step, we developed a four-layer gradient by combining the three-layer gradient with the flotation method [11] and hereby managed to separate these five subcellular compartments (s*ee* Fig. 3b).

1.2 Disruption of Neutrophils by Nitrogen Cavitation

Nitrogen cavitation is our method of choice for disruption of neutrophils. Neutrophils are pressurized in a Parr nitrogen bomb in cavitation buffer that mimics the intracellular environment to "welcome" organelles when these are released from the plasma membrane and relaxes the cytoskeleton to minimize trapping of granules to nuclei [6, 12]. We do not believe that the disruption of cells is a matter of aeration of nitrogen that has been dissolved in the lipid membranes when the pressure suddenly drops from the initial 375 psi to atmospheric pressure, but is a matter of breaking by shear stress when the neutrophils are forced through the valve at the outlet nozzle of the bomb. The arguments are that breaking is ineffective if the passage through the valve is too rapid. The cavitate should be let out dropwise, not as a continuous flow. Second, the same cavitation efficiently is achieved whether neutrophils have been pressurized for 2 or 20 min, which clearly has consequences for the amount of nitrogen that is dissolved in the lipid membranes. Finally, as the bomb wears (i.e., the valve wears) the nitrogen pressure needed to obtain efficient cavitation must be increased. We are currently operating at 550 psi. Thus, we believe that the breaking is achieved by shear force and not by

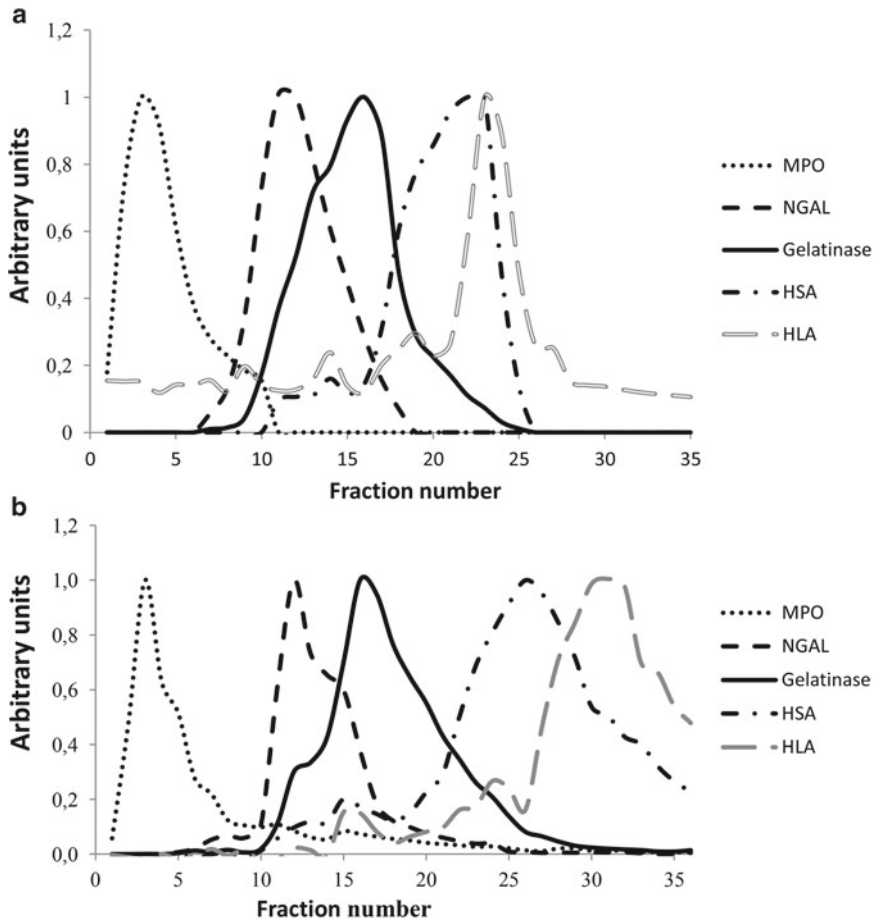

Fig. 3 (**a**) Subcellular fractionation of human neutrophils on a three-layer Percoll density gradient. (**b**) Subcellular fractionation of human neutrophils on a four-layer Percoll density gradient. The distribution profiles of marker proteins for the different granules and light membranes were determined by ELISA of individual fractions collected from the bottom of the tube. Markers are as follows: myeloperoxidase (MPO) for azurophil granules, NGAL for specific granules, gelatinase for gelatinase granules, albumin for secretory vesicles, and human leukocyte antigen (HLA) for plasma membrane. Concentrations for each protein are given as measured concentration in the fraction relative to the maximal concentration. Reprinted with permission from ref. 11 from Wiley Online Library

cavitation. This also explains the exquisite, gentle nature of this method for breaking of cells: only the surface membrane is broken, not the granule membrane.

After breaking of cells, the plasma membrane vesicles reseal, but this is not by random orientation. Based on the study of alkaline phosphatase, it has been documented that the plasma membrane vesicles are oriented right-side out [13]. Previous studies arguing to the contrary most likely were unaware of the presence of secretory vesicles in the plasma membrane preparations. Although the method is very gentle, it is recommended that the neutrophils are pretreated by an effective inhibitor of serine proteases before disruption. We recommend treatment with DFP.

1.3 Analysis of Subcellular Markers

Methods for detection and quantification of granule proteins with a known distribution in subcellular organelles and hence localization in the gradient are needed to evaluate the quality of the subcellular fractionation and to define the localization of a given protein. In general, immunological methods are preferred, because they may be less sensitive to proteases than activity-based assays. Additionally, the serine proteases in azurophil granules are irreversibly inhibited by treatment of cells with DFP, and the metalloproteases in peroxidase-negative granules are present in latent forms, which require activation before activity can be measured. We have developed an array of immunological assays (ELISAs) that are suitable for quantification of proteins from each of the subcellular compartments, which are separated in the four-layer Percoll gradient (Table 1). One advantage of the assays is that removal of Percoll is not necessary, as we have not observed interference of this substance with any of the ELISAs in the sample dilutions used. Furthermore, the same buffers and incubation times are used for all of the ELISAs, and the sample dilutions can be reused for more than one assay. This means that several marker proteins can be measured simultaneously in a few hours. Unfortunately, not all of the antibodies used in our assays are commercially available, and some require modification (affinity purification and/or biotinylation) before use. It should, however, be possible to develop similar assays using commercially available antibodies.

The granules and vesicles are characterized by their content of both matrix proteins and membrane proteins [1, 2], and both types of protein are useful as subcellular markers [14]. Azurophil (primary) granules are traditionally characterized by their content of myeloperoxidase (MPO), which also is our preferred marker for this granule subset. The other major azurophil granule protein, defensin, is absent from azurophil granules with the lowest density, and its precursor (prodefensin) is present in specific granules, which makes this protein less suitable as an azurophil granule marker [4, 15]. The two subsets of peroxidase-negative granules, specific (secondary) and gelatinase (tertiary) granules, are separated in the three-layer as well as the four-layer Percoll gradient. As marker for specific granules, we prefer neutrophil gelatinase-associated lipocalin (NGAL) and human cationic antimicrobial protein of 18 kDa (hCAP-18). Alternatively, lactoferrin can be used. Gelatinase granules are best identified by their high content of gelatinase (matrix metalloproteinase 9), which defines this granule subtype [7]. Secretory vesicles are characterized by their endocytic origin, which makes the plasma protein, albumin, a suitable marker [16]. Although we prefer matrix proteins for markers of subcellular organelles, a membrane protein is obviously necessary for detection of the plasma membrane. We use a mixed enzyme-linked immunosorbent assay for HLA class 1, which catches the histocompatibility complexes with an antibody against β_2-microglobulin and detects

Table 1
ELISA reagents

ELISA ***(marker for)***	**Capture Ab** ***(supplier, product)*** **(dilution)**	**Detecting Ab** ***(supplier, product)*** **(dilution)**	**HRP-conjugated reagent** ***(supplier, product)*** **(dilution)**	**Standard** ***(supplier, product)*** **(dilution)**
Myeloperoxidase (MPO) (20) *(azurophil gr.)*	Affinity-purified rabbit-anti-MPO *(Dako, A0398)*[a] (determined after purification)[a]	Biotinylated rabbit-anti-MPO *(Dako, A0398)*[b] (determined after biotinyl)[b]	HRP-Avidin *(eBioscience 18-4100)* (1:3,000)	MPO from neutrophils[c] (0–100 ng/mL)
NGAL (21, 22) *(specific gr.)*	Rabbit-anti-recombinant NGAL *(not commercially available)*	Biotinylated capture Ab *(not commercially available)*	HRP-Avidin *(eBioscience 18-4100)* (1:3,000)	NGAL monomer from neutrophils[c] (0–2 ng/mL)
Gelatinase (21, 23) *(gelatinase gr.)*	Rabbit-anti-gelatinase (-NGAL) *(not commercially available)*	Biotinylated, affinity-purified rabbit-anti gelatinase[a,b] *(not commercially available)*	HRP-Avidin *(eBioscience 18-4100)* (1:3,000)	Gelatinase from neutrophils[c] (0–5 ng/mL)
Albumin (HSA) (16) (secretory ves.)	Rabbit-anti-albumin *(Dako, A0001)* (1:2,500)	Biotinylated, affinity-purified rabbit-anti HSA *(A0001)*[a,b] (determined after biotinyl)[b]	HRP-Avidin *(eBioscience 18-4100)* (1:3,000)	Human serum albumin *(Sigma, A1887)* (0–250 ng/mL)
HLA class I (17) *(plasma membr.)*	Rabbit-anti-beta-2-microglobulin *(Dako, A0072)* (1:1,000)	Mouse-anti-HLA-ABC *(Dako, M0736)* (1:750)	HRP-rabbit anti-mouse-lg *(Dako, P0260)* (1:1,500)	Dilution buffer for subtraction of background (arb. units)

[a] *See* **Note 22**
[b] *See* **Note 23**
[c] *See* **Note 24**
The dilutions of antibodies are only intended as a guide and may need to be optimized in each laboratory (also batch dependable)

the complexes with an antibody against the HLA class 1 heavy chain [17]. Uncomplexed β_2-microglobulin, which is a constituent of peroxidase-negative granules matrix, is not detected in this assay.

Alkaline phosphatase is present in unperturbed cells both in the plasma membrane and in the membrane of secretory vesicles with a distribution of 30 and 70 %, respectively [13]. Because plasma membrane fragments reseal right-side out following disruption by nitrogen cavitation, the enzyme activity is present on the outside of plasma membrane vesicles. In contrast, the enzyme activity is present inside secretory vesicles, from where it is translocated to the outside of the plasma membrane after activation of the neutrophil. Using a substrate that does not penetrate membranes, it is possible to distinguish these two activities. Only activity in the plasma membrane is measured in the absence of detergent, whereas both plasma membrane- and secretory vesicle-associated activity are measured in the presence of a detergent that solubilizes membranes. The activity hidden inside secretory vesicles can thus be calculated as the difference between the two measures and is termed latent alkaline phosphatase activity.

One should bear in mind that co-localization of proteins in the gradient is not necessarily a result of localization in the same organelles. Proteins may be localized in different organelles of equal density. Serglycin, for example, is found in the light membrane fractions due to its localization in Golgi vesicles [18]. The argument for co-localization is strengthened if the proteins also follow the same pattern of mobilization in response to different stimuli. The degree of exocytosis can be evaluated using intact cells, but the mobilization is more elegantly visualized by comparing the distribution in subcellular fractionations of unperturbed and stimulated cells, respectively [8]. In this way, it is possible to demonstrate the disappearance of a protein from individual fractions in the gradient and the appearance of the same protein in the supernatant or in the plasma membrane fractions, depending on its matrix or membrane localization.

2 Materials

2.1 Subcellular Fractionation of Neutrophils

1. Isotonic saline solution.
2. Krebs-Ringer phosphate solution supplemented with glucose (KRG): 130 mM NaCl, 5 mM KCl, 1.27 mM $MgSO_4$, 0.95 mM $CaCl_2$, 10 mM NaH_2PO_4/Na_2HPO_4, pH 7.4, 5 mM glucose (*see* **Note 1**).
3. Freshly isolated neutrophils: suspend in isotonic saline or KRG (*see* **Note 1**). A total of 3×10^8 neutrophils is recommended for one Percoll gradient. This can usually be obtained from 400 to 500 mL of venous blood.

2.1.1 Inactivation of Neutrophil Serine Proteases

1. Diisopropyl fluorophosphate (DFP): store at 2–8 °C (*caution*: *DFP is very toxic*) (*see* **Note 2**).
2. Hamilton microliter syringe with blunt needle.
3. 2 % NaOH in water (*see* **Note 3**).

2.1.2 Disruption of Neutrophils by Nitrogen Cavitation

1. Disruption buffer (1×): 100 mM KCl, 3 mM NaCl, 3.5 mM $MgCl_2$, 10 mM 1,4-piperazinediethanesulfonic acid (PIPES) (*see* **Note 4**), pH 7.2. Stable for 1 month at 2–8 °C.
2. Adenosine 5′-triphosphate disodium salt [$ATP(Na)_2$] stock solution: 50 mM in water. Titrate to pH 7.0 with 1 N KOH. Store in aliquots at −20 °C.
3. Phenylmethylsulfonyl fluoride (PMSF) stock solution: 100 mM in anhydrous ethanol. Stable for months at 2–8 °C (*caution*: *PMSF is toxic*) (*see* **Note 5**).
4. EGTA stock solution: 100 mM in water. Titrate to pH 7.0. Store at 2–8 °C (*see* **Note 4**).
5. Parr cell disruption bomb model 4635 including an 1831 nitrogen filling connection (Parr Instrument Company).
6. Nitrogen gas cylinder.

2.1.3 Density Centrifugation on Percoll Gradient

1. Percoll solution. Density 1.130 ± 0.005 g/mL. Store at 2–8 °C.
2. Disruption buffer stock (10×): 1 M KCl, 30 mM NaCl, 35 mM $MgCl_2$, 15 mM EGTA, 100 mM PIPES (*see* **Note 4**). Titrate pH to 6.8 and adjust volume to 80 % of the final volume. Stable for 1 month at 2–8 °C. 10 mM $ATP(Na)_2$ is added from a 50 mM stock solution just before use and makes up the final volume.

2.1.4 Fractionation of Percoll Gradient

1. Automated fraction collector (e.g., FRAC-200, Amersham).
2. Peristaltic pump (e.g., Peristaltic pump P-1, Amersham).

2.2 Analysis of Subcellular Markers

2.2.1 ELISA

1. 96-well flat-bottom ELISA plates (e.g., Nunc-Immuno Plates MaxiSorp).
2. Capture antibodies, protein standards, detecting antibodies, and HRP-conjugated detection reagents (*see* Table 1).
3. Carbonate buffer: 50 mM Na_2CO_3/$NaHCO_3$, pH 9.6. Color buffer with 20 mg/L phenol red (optional). Stable for months at 2–8 °C.
4. Dilution buffer: 0.5 M NaCl, 3 mM KCl, 8 mM Na_2HPO_4/KH_2PO_4, 1 % (w/v) bovine serum albumin, 1 % (v/v) Triton X-100, pH 7.2. Color buffer with 20 mg/L phenol red (optional). Stable for 2 weeks at 2–8 °C.
5. Wash buffer: 0.5 M NaCl, 3 mM KCl, 8 mM Na_2HPO_4/KH_2PO_4, 1 % (v/v) Triton X-100, pH 7.2 (*see* **Note 6**).

6. Color buffer: 0.1 M Na_2HPO_4, 0.1 M citric acid monohydrate, pH 5.0. Store at 2–8 °C.
7. Color reagents: ortho-phenylenediamine (OPD) tablets 2 mg (Kem-En-Tec Diagnostics) and 30 % H_2O_2.
8. Stop solution: 2 N H_2SO_4. Store at room temperature.
9. Automated ELISA plate washer.
10. ELISA plate reader.

2.2.2 Assay for Latent Alkaline Phosphatase

1. 96-well flat-bottom plates (e.g., Nunc 96 MicroWell™ Plates).
2. Barbital buffer: 50 mM sodium diethylbarbiturate, 0.6 mM $MgCl_2$, pH 10.5.
3. Phosphatase substrate: 2 mg/mL p-Nitrophenyl phosphate disodium hexahydrate in water. Prepare fresh.
4. Triton X-100 stock: 10 % (v/v) in water.
5. ELISA plate reader.

3 Methods

3.1 Subcellular Fractionation of Neutrophils

All steps (*see* **Note 7**) are performed at 4 °C with precooled buffers and equipment. Cell suspensions are kept on ice (*see* **Note 8**).

3.1.1 Inactivation of Neutrophil Serine Proteases

1. Suspend the isolated neutrophils in isotonic saline or KRG at 3×10^7 cells/mL (*see* **Note 9**). Use a microliter syringe to aspirate the desired volume of DFP directly from the container (*see* **Notes 2** and **3**). Add 5 µl DFP per 10 mL of the cell suspension (for a final concentration of 5 mM DFP). Carefully mix the cell suspension and leave it on ice for 5 min.
2. Centrifuge for 6 min at 200 × *g* and decant the supernatant into an excess of 2 % NaOH (*see* **Note 3**).

3.1.2 Disruption of Neutrophils by Nitrogen Cavitation

1. Add 1 mM ATP$(Na)_2$ and 0.5 mM PMSF to the desired volume of (1×) disruption buffer just before use [for 10 mL of (1×) disruption buffer, add 0.2 mL from a 50 mM ATP$(Na)_2$ stock and 0.05 mL from a 100 mM PMSF stock].
2. Resuspend the DFP-treated cells in the initial volume of this buffer in a 50-mL conical polypropylene centrifuge tube. If the volume of the cell suspension exceeds 30–35 mL, it should be divided in two or more tubes.
3. Place the conical polypropylene tube(s) inside the precooled Parr bomb so that the bottom of the tube is as close as possible to the dip tube leading to the release valve (to ensure complete sample recovery). The tube should be placed in a plastic beaker cushioned with paper towel or similar (*see* Fig. 4).

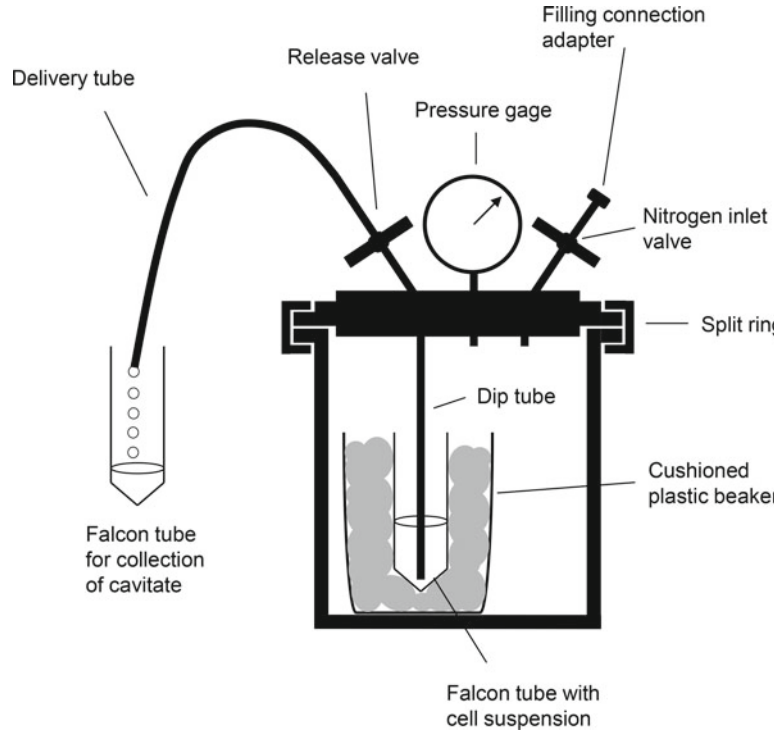

Fig. 4 Schematic illustration of the Parr bomb arrangement during nitrogen cavitation. Reproduced by permission of Humana Press © 2007 [20]

4. Set the head of the bomb (with the dip tube extending into the cell suspension) on the bottom part and attach the split ring cover clamp. Secure the parts by turning the thumbscrew finger tight. Close the two valves (nitrogen inlet valve and release valve) on the head of the bomb.
5. Attach the filling connection to a nitrogen cylinder and connect the filling hose to the Parr bomb inlet valve. Open the outlet valve on the nitrogen cylinder. Carefully open the nitrogen inlet valve on the Parr bomb and slowly raise the bomb pressure. Close the inlet valve, when the pressure inside the bomb reaches 375 psi (or more, *see* **Note 10**). Close the nitrogen cylinder outlet valve, depressurize the filling hose, and disconnect from the Parr bomb inlet valve. Leave the Parr bomb for approximately 5 min.
6. Prepare a 50-mL conical polypropylene tube for collection of the disrupted cells (i.e., the cavitate) by adding an amount of 100 mM EGTA that will result in 1.5 mM after collection of the cavitate (0.15 mL EGTA stock per 10 mL of cell suspension).
7. Place the EGTA-containing tube under the Parr bomb delivery tube and carefully open the release valve. Hold the tube in one hand and operate the release valve with the other hand.

By adjusting the valve opening, the cavitate should be released quickly dropwise and collected in the conical polypropylene tube. Close the release valve, when the majority of the cell suspension has been collected (*see* **Note 11**).

8. Centrifuge the cavitate at 400 × *g* for 15 min. Carefully decant the postnuclear supernatant (S_1) into a new tube. Resuspend the pellet of nuclei and unbroken cells (P_1) in 1 mL of disruption buffer and save it for determination of disruption efficiency, if desired (*see* **Note 10**).
9. Depressurize the bomb by opening the nitrogen inlet valve. Dismantle and clean the bomb later.

3.1.3 Density Centrifugation on a Three-Layer Percoll Gradient

1. Add 10 mM (final concentration) $ATP(Na)_2$ to the tenfold concentrated disruption buffer stock.
2. Prepare three Percoll solutions with different densities: 1.05, 1.09, and 1.12 g/mL as indicated in Table 2 (*see* **Note 12**). For one gradient, 10 mL of each is needed, but preparation of a larger volume is recommended. Add PMSF to a final concentration of 0.5 mM (0.15 mL PMSF stock for 30 mL of Percoll solution) and titrate the solutions to pH 7.0 by addition of a small volume of 1 N HCl.
3. Place 10 mL of the postnuclear supernatant (S1) in a 50-mL round botttom polycarbonate centrifuge tube using a syringe or a pipette for this procedure. Save a sample of the S1 for determination of disruption efficiency or recovery, if desired (*see* **Notes 10** and **20**).

Table 2
Preparations of Percoll solutions of different densities

Final density (g/mL)	Final volume (mL)	Percoll stock (1.130 g/mL)[a] (mL)	Disruption buffer (10×)[b] (mL)	H_2O (mL)
1.030	30	5.63	3.0	21.37
1.050	30	10.25	3.0	16.75
1.090	30	19.48	3.0	7.52
1.110	30	24.09	3.0	2.91
1.120	30	26.40	3.0	0.60

[a]If a Percoll stock solution with a different density is used (e.g., 1.129 g/mL) or if one desires to prepare a solution with a different final density, the volume of Percoll stock (V_P) can be calculated using the following formula: $V_P = V_0(D_0 - 1.056)/(D_P - 1)$, where V_0 is the final volume, D_0 the desired density of the Percoll solution, D_P the density of the Percoll stock, and 1.056 the density of the tenfold concentrated disruption buffer. The volume of H_2O (V_{H2O}) should be adjusted to make up the desired final volume [$V_{H2O} = (0.9 \times V_0) - V_P$]
[b]The volume of tenfold concentrated disruption buffer (including 10 mM $ATP(Na)_2$) is always one-tenth the final volume

4. Aspirate 10 mL of the solution with the lowest density (1.05 g/mL) using a 10-mL syringe and a pleuracenthesis needle (14-G × 3¼″). Carefully place 9 mL of the solution underneath the S1.
5. Aspirate 10 mL of the medium density solution (1.09 g/mL) with a new syringe and needle. Place 9 mL of this solution in the tube underneath the 1.05 g/mL solution. Make sure that a sharp demarcation between the two densities is obtained.
6. Likewise, aspirate 10 mL of the densest solution (1.12 g/mL) and place 9 mL of this underneath the medium dense Percoll solution without disturbing the gradient.
7. Centrifuge the gradient 37,000 × *g* for 30 min. After centrifugation, four distinct bands containing granules and light membranes should be clearly visible: from the bottom, the α-band containing azurophil granules, the β_1-band containing specific granules, the β_2-band containing gelatinase granules, and the γ-band containing secretory vesicles, plasma membranes, and other light membranes (ER and Golgi vesicles). The clear cytosol (S_2) is present on top of the γ-band (*see* Fig. 5a).

3.1.4 Density Centrifugation on a Four-Layer Percoll Gradient

1. Add 10 mM (final concentration) ATP$(Na)_2$ to the tenfold concentrated disruption buffer stock.
2. Prepare four Percoll solutions with different densities: 1.11, 1.03, 1.09, and 1.12 g/mL as indicated in Table 2 (*see* **Note 12**). For one gradient, 10 mL of each is needed, but preparation of a larger volume is recommended. Add PMSF to a final concentration of 0.5 mM (0.15 mL PMSF stock for 30 mL of Percoll solution) and titrate the solutions to pH 7.0 by addition of a small volume of 1 N HCl.

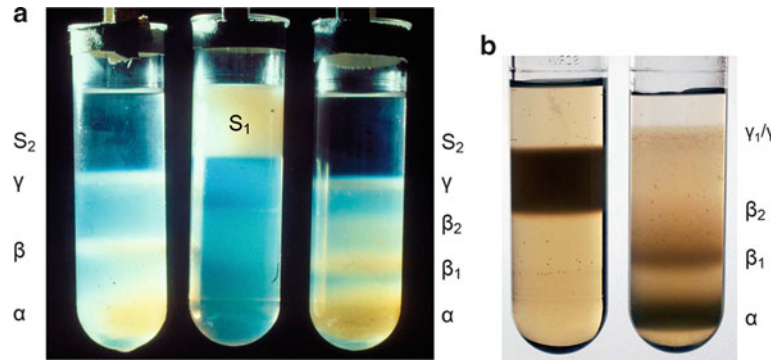

Fig. 5 (**a**) Photograph of the three-layer Percoll density gradient before (*middle*) and after centrifugation (*right*). A two-layer gradient after centrifugation (*left*) is shown for comparison. Reproduced by permission of Elsevier © 1999 [8]. (**b**) Photograph of a four-layer Percoll density gradient before (*left*) and after (*right*) centrifugation. The bands formed after centrifugation are indicated

3. Aspirate 10 mL of the solution with the density 1.03 g/mL using a 10-mL syringe and a pleuracenthesis needle (14-G × 3¼″). Place 9 mL of the solution in a 50-mL round bottom polycarbonate centrifuge tube.
4. The postnuclear supernatant is mixed in a ratio of 1:1 with the Percoll solution density of 1.11 g/mL resulting in a final density of 1.055 g/L. 9 mL of this is carefully placed underneath the 1.03 g/mL solution. Use a 10-mL syringe or a pipette for this procedure. Save a sample of the S_1 for determination of disruption efficiency or recovery, if desired (*see* **Notes 10** and **20**).
5. Aspirate 10 mL of the solution with density 1.09 g/mL with a new syringe and needle. Carefully place 9 mL of this solution in the tube underneath the 1.055 g/mL solution.
6. Finally aspirate 10 mL of the solution with density 1.12 g/mL with a new syringe and needle. Place 9 mL of this in the bottom of the tube underneath the 1.09 g/mL solution. Make sure that a sharp demarcation between the two densities is obtained.
7. Centrifuge the gradient 37,000 × *g* for 30 min in an SS-34 fixed angle rotor in a Sorvall RC-5B Superspeed centrifuge. Figure 5b displays the four-layer gradient before and after centrifugation. Three bands containing granules should be visible: from the bottom, the α-band containing azurophil granules, the β_1-band containing specific granules, and the β_2-band containing gelatinase granules. The γ-band containing secretory vesicles and light membranes is above these; however, the demarcation between the γ_1-band containing secretory vesicles and the γ_2-band containing plasma membranes and other light membranes (ER and Golgi vesicles) is not visually distinct, but will be revealed as the marker proteins are analyzed. The S_2 (which is placed above the γ-band in the three-layer gradient) is here merged in the flotation medium.

3.1.5 Percoll Gradient Fractionation

1. Cover the opening of the centrifuge tube with Parafilm and place the tube in a rack to secure the vertical position. Be careful not to disturb the gradient.
2. Stick a glass capillary tube through the center of the Parafilm to the bottom of the tube.
3. Attach a polyethylene tube to the glass capillary tube and connect it to a peristaltic pump and a fraction collector.
4. Collect 37 fractions of 1 mL each. Use transparent tubes, which expose the content (*see* **Note 13**).

3.2 Analysis of Subcellular Markers

All steps are performed at room temperature. The necessary volume of buffers, except carbonate buffer, should be brought to room temperature before use. It is recommended to use an 8-channel pipette for application of buffer and antibody dilutions.

3.2.1 ELISA

Day 1

1. Dilute capture antibodies in carbonate buffer according to Table 1 and immediately coat ELISA plates with 100 µL/well. Incubate plates overnight at room temperature (*see* **Note 14**).
2. Dilute samples (i.e., subcellular fractions and $S_1 + P_1$) in dilution buffer according to Table 3. Store samples at 2–8 °C (*see* **Note 15**).

Day 2

1. Wash ELISA plates in wash buffer (*see* **Note 16**). Quench the plates by applying dilution buffer 200 µL/well and incubate 1 h.
2. Bring samples to room temperature and prepare standard solutions according to Table 1 (*see* **Note 17**).
3. Wash ELISA plates in wash buffer. Apply standards and samples 100 µL/well. Standards are applied in duplicate in a two-fold dilution in lanes 1–2. Samples are applied in duplicate in lanes 3–12 (*see* Table 4). Incubate for 1 h.
4. Wash ELISA plates in wash buffer. Apply detecting antibody 100 µL/well and incubate 1 h.
5. Wash ELISA plates in wash buffer. Apply HRP-conjugated reagent 100 µL/well and incubate 1 h.
6. Prepare color solution: for one plate, dissolve three OPD tablets in 15 mL color buffer. Protect the solution from light (*see* **Note 18**, *caution*: OPD is toxic).
7. Wash ELISA plates in wash buffer. Equilibrate plates in color buffer by pouring 50–100 mL buffer over each plate. Remove buffer after 30 s–5 min.
8. Add H_2O_2 to the color solution just before use: add 1 µL 30 % H_2O_2/5 mL color solution. Apply 100 µL/well of this solution and incubate ELISA plates 10–30 min protected from light (*see* **Notes 18–19**).
9. Terminate color reaction by addition of 2 N H_2SO_4 100 µL/well and read the optical density at 492 nm in an ELISA plate reader.
10. Calculate the actual concentration of marker proteins in the undiluted samples (*see* **Note 20**).

3.2.2 Assay for Latent Alkaline Phosphatase

Alkaline phosphatase activity is simultaneously measured in the presence and absence of detergent.

1. Prepare two 96-well plates identically with material from each fraction (5 µL/well). Apply all fractions in duplicate on both plates.

Table 3
Dilutions of subcellular fractions for marker assays

ELISA[a]	Fractions[b]/dilutions	Peak fractions three-layer gradient	Peak fractions four-layer gradient	S_1	P_1
MPO	All fractions/1:2,000	Fraction 2–5 1:5,000	Fraction 2–5 1:5,000	1:2,000 and 1:5,000	1:5,000 and 1:10,000
NGAL	All fractions/1:2,000	Fraction 9–14 1:5,000	Fraction 9–14 1:5,000	1:2,000 and 1:5,000	1:5,000 and 1:10,000
Gelatinase	Fraction 1–11 and 18–36/1:2,000	Fraction 9–14/fraction 15–17 1:5,000/1:10,000	Fraction 9–14/fraction 15–17 1:5,000/1:10,000	1:5,000 and 1:10,000	1:10,000 and 1:20,000
Albumin	All fractions/1:15	Fraction 19–23 1:50	Fraction 19–31 1:50	1:15	1:15 and 1:50
HLA	All fractions/1:15	Fraction 19–23 1:50	Fraction 19–35 1:50	1:15 and 1:100	1:100 and 1:200

[a]Refers to the ELISA's described in Table 1 and Subheading 3.2.1

[b]In the subcellular fractions containing the cytosol, it is sufficient to measure granule markers in every second fraction (i.e., fractions 30, 32, 34, and 36). The sample dilutions are adjusted to subcellular fractionations obtained on a three-layer or four-layer Percoll gradient, respectively, with 3×10^8 cells (fractionated in 37 fractions of 1 mL each, as described in Subheading 3.1). The dilutions are only intended as a guide and may need to be optimized in each laboratory, especially if other antibodies or ELISA kits are used in marker assays

Table 4
Distribution of standards and samples on the ELISA plate for MPO ELISA

	1 (ng/mL)	2 (ng/mL)	3	4	5	6	7	8	9	10	11	12
A	0[a]	12.5	fr. 1 1/2,000	fr. 1 1/2,000	fr. 9 1/2,000	fr. 9 1/2,000	fr. 17 1/2,000	fr. 17 1/2,000	fr. 25 1/2,000	fr. 25 1/2,000	fr. 36 1/2,000	fr. 36 1/2,000
B	0[a]	12.5	fr. 2 1/2,000	fr. 2 1/2,000	fr. 10 1/2,000	fr. 10 1/2,000	fr. 18 1/2,000	fr. 18 1/2,000	fr. 26 1/2,000	fr. 26 1/2,000	fr. 2 1/5,000	fr. 2 1/5,000
C	1.56	25	fr. 3 1/2,000	fr. 3 1/2,000	fr. 11 1/2,000	fr. 11 1/2,000	fr. 19 1/2,000	fr. 19 1/2,000	fr. 27 1/2,000	fr. 27 1/2,000	fr. 3 1/5,000	fr. 3 1/5,000
D	1.56	25	fr. 4 1/2,000	fr. 4 1/2,000	fr. 12 1/2,000	fr. 12 1/2,000	fr. 20 1/2,000	fr. 20 1/2,000	fr. 28 1/2,000	fr. 28 1/2,000	fr. 4 1/5,000	fr. 4 1/5,000
E	3.13	50	fr. 5 1/2,000	fr. 5 1/2,000	fr. 13 1/2,000	fr. 13 1/2,000	fr. 21 1/2,000	fr. 21 1/2,000	fr. 29 1/2,000	fr. 29 1/2,000	fr. 5 1/5,000	fr. 5 1/5,000
F	3.13	50	fr. 6 1/2,000	fr. 6 1/2,000	fr. 14 1/2,000	fr. 14 1/2,000	fr. 22 1/2,000	fr. 22 1/2,000	fr. 30 1/2,000	fr.30 1/2,000	S_1 1/2,000	S_1 1/2,000
G	6.25	100	fr. 7 1/2,000	fr. 7 1/2,000	fr. 15 1/2,000	fr. 15 1/2,000	fr. 23 1/2,000	fr. 23 1/2,000	fr. 32 1/2,000	fr. 32 1/2,000	S_1 1/5,000	S_1 1/5,000
H	6.25	100	fr. 8 1/2,000	fr. 8 1/2,000	fr. 16 1/2,000	fr. 16 1/2,000	fr. 24 1/2,000	fr. 24 1/2,000	fr. 34 1/2,000	fr. 34 1/2,000	P_1 1/2,000	P_1 1/2,000

[a]Dilution buffer is applied for determination of background

2. Mix 15 mL of barbital buffer with 15 mL of phosphatase substrate. Divide the solution in two equal volumes. Add 300 μL of Triton X-100 stock to one and 300 μL of water to the other assay solution.
3. Apply assay solution 100 μL/well. Use assay solution with detergent (Triton X-100) on one plate and assay solution without detergent on the other.
4. Wrap plates in tin foil and incubate at 37 °C for 40 min.
5. Read the optical density at 405 nm in an ELISA plate reader.
6. Calculate the latent alkaline phosphatase activity: for each fraction, subtract the mean activity in the absence of detergent from the mean activity in the presence of detergent (*see* **Note 20**).

3.2.3 Removal of Percoll

1. We have not experienced any interference of Percoll with the assays described above; thus, Percoll is not removed from fractions prior to measurements. In other assays, e.g., Western blotting or functional assays, Percoll may pose a problem especially in the densest fractions with the highest content of Percoll.
2. It is possible to remove Percoll by ultracentrifugation at 100,000 × *g* for 45 min for light membranes or 90 min for granules (*see* **Note 21**).
3. After centrifugation, the Percoll will form a hard pellet and the membranous material will form a disc or lump above the Percoll.
4. The membranous material can easily be collected using a glass Pasteur pipette and subsequently resuspended in the desired buffer.

4 Notes

Unless stated otherwise, all solutions are prepared in water of MilliQ quality (i.e., deionized, depleted from organic content, and filtered). This is referred to as "water" in the text.

1. To avoid precipitation, KRG should be prepared fresh from stock solutions: (A) 154 mM NaCl, (B) 150 mM KCl, (C) 150 mM Mg_2SO_4, (D) 110 mM $CaCl_2$, and (E) 100 mM NaH_2PO_4/Na_2HPO_4, pH 7.4. Add 100 mL A, 4 mL B, 1 mL C, 1 mL D, and 12 mL E. Adjust to pH 7.4 if necessary. Supplement with 5 mM glucose.
2. DFP is an organophosphorus compound, which is a potent inhibitor of serine proteases including neutrophil elastase, proteinase 3, and cathepsin G. DFP is also an irreversible inhibitor of acetylcholinesterase, which makes it especially toxic by all

routes of administration (inhalation/skin contact/injection, etc.). All work with DFP should be carried out in a well-ventilated hood wearing suitable protective gloves and eye/face protection. Use of a blunt needle for aspiration of DFP from the container and delivery to the cell suspension is recommended to minimize the risk of skin penetration. DFP should be handled only by persons familiar with its properties, and a competent person (e.g., a physician) should be present and alerted of the plan to work with DFP. The antidote atropine sulfate including syringes and needles should be present if their use is required.

3. DFP is readily hydrolyzed by alkali. A beaker of 2 % aqueous NaOH should be ready in the hood. When aspirating DFP from the container, the needle should be wiped off using a soft tissue wetted in the NaOH solution. All contaminated equipment should be immersed into a large excess of the NaOH solution and left in the fume hood for at least 48 h to ensure complete hydrolysis. The solution can hereafter be neutralized and flushed with a huge amount of water into an appropriate disposal system.
4. PIPES is added to the disruption buffer (1×) from a 500 mM stock solution titrated to pH 7.0. For disruption buffer (10×), both PIPES and EGTA are added from stock solutions. The solubility of PIPES and EGTA in water is low but increases with the addition of NaOH (dissolve PIPES/EGTA directly in a small volume of 1 N NaOH or add 10 N NaOH or NaOH pellets to an aqueous solution).
5. PMSF is an inhibitor of serine proteases and cholinesterase but is less potent and toxic than DFP (*see* **Note 2**). For preparation of the stock solution, PMSF should be weighed in a fume hood while wearing protective gloves. PMSF is unstable in aqueous solution with a half-life <1 h at neutral pH, 25 °C, and should be added to buffers just before use.
6. A (5×) wash buffer stock can be prepared and stored for months at 2–8 °C: dissolve 584.4 g NaCl, 4.4 g KCl, 4.0 g KH_2PO_4, and 23.0 g Na_2HPO_4; $2H_2O$ in 4 L water. Do not adjust pH. Before use, the stock is diluted 5×, titrated to pH 7.2, and supplemented with 1 % Triton X-100. This working solution can be stored for at least 1 week at room temperature.
7. Isolation of neutrophils except for dextran sedimentation of erythrocytes is carried out at 4 °C to minimize unintended activation with exocytosis of especially the secretory vesicles. Nitrogen cavitation and collection of fractions are preferably carried out in a cold room.

8. The described method is also applicable to stimulated neutrophils: cells are preincubated 5 min at 37 °C in KRG before addition of stimulus (e.g., fMLP, PMA, or Ionomycin). After stimulation for 15 min at 37 °C, cells are pelleted by centrifugation ($200 \times g$ for 6 min) and the supernatant, termed S_0, aspirated. The cells are resuspended in the original volume of cold buffer before treatment with DFP. Exocytosis of a granule protein can be calculated as the amount in the supernatant divided by the total amount in the cells (i.e., in the supernatant after stimulation and in the postnuclear supernatant and unbroken cells and nuclei after cavitation and centrifugation, see later): $S_0/(S_0 + S_1 + P_1)$.
9. It is possible to use cell concentrations between 0.5×10^7 and 1.5×10^8 cells/mL throughout the fractionation procedure, but 3×10^7 cells/mL gives an excellent resolution of organelles, and the described marker assays are optimized for this cell concentration.
10. As the bomb (i.e., valves) wears, it may be necessary to increase the pressure. The disruption efficiency should be approximately 90 % and can be calculated if the amount of a granule marker protein is measured in the postnuclear supernatant (S_1) and the pellet (P_1) of nuclei and unbroken cells following centrifugation of the cavitate {disruption efficiency = $[S_1/(S_1 + P_1)] \times 100$ %}. Granules should be intact, i.e., less than 0.5 % of the granule proteins should be found in the cytosolic fractions after gradient centrifugation [8].
11. Prevent jet, bubbles, or foam when releasing the cell suspension. The last few drops of the disrupted cells will be ejected with high speed, if collection is not terminated. This may cause heavy splattering in the collection tube and loss of sample, because this is practically blown out of the tube. The opening of the conical polypropylene tube may be covered with Parafilm with a slit for the delivery tube and release of excess nitrogen. It is recommended to use a face shield and gloves for personal protection during the procedure.
12. If separation of gelatinase granules from specific granules is not desired, a two-layer Percoll gradient can be used instead. Percoll solutions of 1.05 and 1.12 g/mL are used, and 14 mL of each are placed in the centrifuge tube. The applied volume of S_1 and density centrifugation is unaltered. Following centrifugation it is sufficient to collect 25 fractions of 1.5 mL each.
13. It is possible to pool fractions corresponding to one or more types of granule/vesicle, preferably after marker assays have been performed. Usually, fractions 1–7 correspond to azurophil granules, fractions 8–13 to specific granules, fractions 14–20 to gelatinase granules, and fractions 21–27 to secretory

vesicles and plasma membranes. In the four-layer gradient, the fractions containing plasma membrane will be allocated to fractions 28–34.

14. Prepare 12 mL antibody solution for each ELISA plate. It is possible to analyze 40 samples on each plate, which is enough for one four-layer Percoll gradient.
15. Dilution of samples can be postponed to day 2, but it is often convenient to do this in advance. Diluted samples can be stored in a refrigerator for 1 week, before ELISA measurements.
16. Between each step, the ELISA plates are washed three times in wash buffer (3×300 µL) and left with 150 µL in each well, to prevent drying of the surface. Pour out the buffer over a sink and tap the plate against a towel to remove the last drops, just prior to application of the next layer.
17. Standard solutions, except for albumin and HLA ELISA, are made from concentrated stock solutions stored in aliquots at –20 °C. For preparation of standard stocks, pure standard protein is diluted in 50 mM Na-phosphate, pH 7.4 supplemented with 0.5 % (w/v) bovine serum albumin and 0.01 % (w/v) Na-azide. Aliquots should not be refrozen after use. Standard solution for the albumin ELISA should be prepared fresh from lyophilized albumin. No standard is used for HLA ELISA, but dilution buffer is used for subtraction of background.
18. Color solution should be prepared fresh, but dissolution of OPD tablets requires mixing (rotation end-over-end) for 10–15 min. If color solution is prepared for more than one plate, just make 10 mL/plate and 5 mL extra. Color solution will develop color if exposed to light; this will cause high background in the ELISA. OPD is toxic and possibly carcinogenic, and it is also harmful to the aquatic environment. Color solution should be used in a fume hood wearing protective gloves. Dispose excess color solution and developed ELISA plates according to local regulations.
19. Incubation time may differ between the ELISAs and from day to day partly depending on temperature. After termination of color reaction, the most concentrated standard should result in an optical density (at 492 nm) about 1.5 (1.2–1.8) and background should be below 0.1.
20. It is possible to calculate the recovery, as the total content of a marker protein in subcellular fractions expressed in percentage of the content in the postnuclear supernatant applied to subcellular fractionation. Recovery is usually 90–100 %.
21. For ultracentrifugation of small volumes, i.e., if Percoll should be removed from individual fractions, it is convenient to use a Beckman Airfuge CLS ultracentrifuge with an A-95 fixed angle

rotor and UltraClear (8 × 20 mm) centrifuge tubes. Centrifuge 300–450 μL of each fraction at 28 psi for 10–20 min (the densest fractions require the longest centrifugation time). To assure rotor balance, fill opposing tubes with fractions of similar density. After centrifugation, the membranous material can be collected above the Percoll pellet with a small pipette and resuspended in the desired volume of an appropriate buffer. A disadvantage of this method may be that cooling is not an option and samples are subjected to temperatures a little above room temperature.

22. Antibodies are affinity purified using columns containing the relevant marker protein (= ELISA standard) coupled to CNBr-activated Sepharose. The eluted antibodies are dialyzed against PBS and kept at 4 °C with the addition of 0.1 % (w/v) Na-azide. The proper dilution of antibody in the ELISA depends among other things on the IgG concentration and is determined by titration.
23. Biotinylation of antibodies is performed as described by Bayer and Wilchek [19]. In short, dialyze antibodies (2–5 mg/mL) against 0.1 M Na-carbonate, pH 8.0. For each mL, add 50–125 μL biotin-N-hydroxysuccinimide (Sigma) from a 2 mg/mL stock in dimethylformamide. Incubate 1 h at room temperature. Dialyze against PBS, with several changes of buffer to remove excess of free biotin. Keep at 4 °C with the addition of 0.1 % (w/v) Na-azide, protected from light. The proper dilution of antibody in the ELISA depends on the actual IgG concentration and efficiency of biotinylation and should be determined by titration.
24. Myeloperoxidase is purified from azurophil granules harvested manually from a two-layer Percoll gradient followed by removal of Percoll by ultracentrifugation (*see* **Notes 12** and **13**). NGAL and gelatinase are purified from exocytosed material from PMA-stimulated neutrophils.

References

1. Borregaard N, Cowland JB (1997) Granules of the human neutrophilic polymorphonuclear leukocyte. Blood 89:3503–3521
2. Faurschou M, Borregaard N (2003) Neutrophil granules and secretory vesicles in inflammation. Microbes Infect 5:1317–1327
3. Cowland JB, Borregaard N (1999) The individual regulation of granule protein mRNA levels during neutrophil maturation explains the heterogeneity of neutrophil granules. J Leukoc Biol 66:989–995
4. Faurschou M, Sorensen OE, Johnsen AH et al (2002) Defensin-rich granules of human neutrophils: characterization of secretory properties. Biochim Biophys Acta 1591: 29–35
5. Pertoft H, Laurent TC, Laas T et al (1978) Density gradients prepared from colloidal silica particles coated by polyvinylpyrrolidone (Percoll). Anal Biochem 88:271–282
6. Borregaard N, Heiple JM, Simons ER et al (1983) Subcellular localization of the b-cytochrome component of the human neutrophil microbicidal oxidase: translocation during activation. J Cell Biol 97: 52–61

7. Kjeldsen L, Sengelov H, Lollike K et al (1994) Isolation and characterization of gelatinase granules from human neutrophils. Blood 83:1640–1649
8. Kjeldsen L, Sengelov H, Borregaard N (1999) Subcellular fractionation of human neutrophils on Percoll density gradients. J Immunol Methods 232:131–143
9. Sengelov H, Borregaard N (1999) Free-flow electrophoresis in subcellular fractionation of human neutrophils. J Immunol Methods 232:145–152
10. Dahlgren C, Carlsson SR, Karlsson A et al (1995) The lysosomal membrane glycoproteins Lamp-1 and Lamp-2 are present in mobilizable organelles, but are absent from the azurophil granules of human neutrophils. Biochem J 311(Pt 2):667–674
11. Clemmensen SN, Jacobsen LC, Rorvig S et al (2011) Alpha-1-antitrypsin is produced by human neutrophil granulocytes and their precursors and liberated during granule exocytosis. Eur J Haematol 86:517–530
12. Klempner MS, Mikkelsen RB, Corfman DH et al (1980) Neutrophil plasma membranes. I. High-yield purification of human neutrophil plasma membrane vesicles by nitrogen cavitation and differential centrifugation. J Cell Biol 86:21–28
13. Borregaard N, Miller LJ, Springer TA (1987) Chemoattractant-regulated mobilization of a novel intracellular compartment in human neutrophils. Science 237:1204–1206
14. Sorensen O, Borregaard N (1999) Methods for quantitation of human neutrophil proteins, a survey. J Immunol Methods 232:179–190
15. Faurschou M, Kamp S, Cowland JB et al (2005) Prodefensins are matrix proteins of specific granules in human neutrophils. J Leukoc Biol 78:785–793
16. Borregaard N, Kjeldsen L, Rygaard K et al (1992) Stimulus-dependent secretion of plasma proteins from human neutrophils. J Clin Invest 90:86–96
17. Bjerrum OW, Borregaard N (1990) Mixed enzyme-linked immunosorbent assay (MELISA) for HLA class I antigen: a plasma membrane marker. Scand J Immunol 31:305–313
18. Niemann CU, Cowland JB, Klausen P et al (2004) Localization of serglycin in human neutrophil granulocytes and their precursors. J Leukoc Biol 76:406–415
19. Bayer EA, Wilchek M (1990) Protein biotinylation. Methods Enzymol 184:138–160
20. Udby L, Borregaard N (2007) Subcellular fractionation of human neutrophils and analysis of subcellular markers. Methods Mol Biol 412:35–56

Part III

Biochemistry, Biology and Signal Transduction of Neutrophils

Chapter 6

Rho Family and Rap GTPase Activation Assays

Richard T. Jennings and Ulla G. Knaus

Abstract

The detection of Ras superfamily GTPase activity in innate immune cells is important when studying signaling events elicited by various ligands and cellular processes. The development of high-affinity probes detecting the activated, GTP-bound form of small GTPases has significantly enhanced our understanding of initiation and termination of GTPase-regulated signaling pathways. These probes are created by fusing a high-affinity GTPase-binding domain derived from a specific downstream effector protein to glutathione *S*-transferase (GST). Such domains bind preferentially to the GTP-bound form of the upstream Rho or Ras GTPase. Coupling these probes to beads enables extraction of the complex and subsequent quantification of the active GTP-binding protein by immunoblotting. Although effector domains that discriminate efficiently between GDP- and GTP-bound states and highly specific antibodies are not yet available for every small GTPase, analysis of certain members of the Rho and Ras GTPase family is now routinely performed. Here, we describe affinity-based pulldown assays for detection of Rho GTPase (Rac1/2, Cdc42, RhoA/B) and Rap1/2 activity in stimulated neutrophils or macrophages.

Key words Rho GTPases, Rac, Cdc42, Rap, Affinity-based GTP activity probe, PBD assay, RBD assay, Pulldown assay

1 Introduction

Leukocytes are key cellular components of innate immunity. Almost all of their biological functions are under the control of small GTPases of the Ras superfamily. Specifically, the GTPases of the Rho family have been recognized for their crucial role in neutrophil phagocytic responses including chemotaxis, phagocytosis, and bacterial killing [1–3]. The ability to directly measure Rho GTPase activity in cell samples has become an important biochemical tool and has greatly aided our understanding of leukocyte responses to many different stimuli- or matrix-mediated changes. GTPases cycle from an inactive, GDP-bound form to an active GTP-bound form that interacts with effector proteins and regulates downstream intracellular signaling pathways. The identification of binding domains in

Mark T. Quinn and Frank R. DeLeo (eds.), *Neutrophil Methods and Protocols*, Methods in Molecular Biology, vol. 1124,
DOI 10.1007/978-1-62703-845-4_6,

particular target proteins that specifically recognize the active, GTP-bound form of a specific GTPase provides the basis for affinity-based GTPase activation assays.

Several different probes for monitoring small GTPase activity have been developed, all based on the use of high-affinity domains of various effector proteins. For analysis of leukocyte function, three examples of these probes are described here: two different Rho family member-specific probes (Rac/Cdc42 and Rho) and a Ras family member-specific probe (Rap). The Rac/Cdc42-specific probe is based on a domain within the N-terminal regulatory region of p21-activated kinase 1 (Pak1). This region, referred to as the CRIB domain (Cdc42/Rac interactive binding domain), contains a minimal sequence (amino acids 74–89) required for interaction with the active GTP forms of these GTPases [4, 5]. For enhanced affinity, a larger region of Pak1 is typically used as a Rac/Cdc42 activity probe, termed the p21-binding domain (PBD, amino acids 67–150). This PBD domain will bind to the active, GTP-bound form of several Rho GTPases expressed in leukocytes, namely, Rac1, Rac2, and Cdc42 [6–9]. For determination of active RhoA and RhoB proteins in neutrophils, a binding region in the effector protein Rhotekin (RhBD, amino acids 7–89) serves as affinity probe [10–12]. In migrating neutrophils RhoA is activated at the trailing edge, the uropod, and is essential for integrin-mediated adhesion signaling and the neutrophil "backness" program during polarization and chemotaxis [13–15]. For the Ras family member Rap, a specific binding site is contained within residues 1–97 of the RalGDS protein, and this domain provides the basis for a Rap-GTP-specific probe (RBD) [16–18]. The RBD domain provides a tool to study the activation of members of the Rap family in leukocytes, which primarily express Rap1A/B and Rap2B/C. Rap1 is activated by numerous stimuli in leukocytes and mediates responses connected to integrin inside-out signaling [19–21].

Addition of these probes to cell lysates, generated by ligand- or matrix-mediated immune cell stimulation, permits selectively binding the active form of GTPases (Fig. 1). The separated complexes containing the active GTPase bound to its specific binding domain are detected by immunoblotting using antibodies that recognize the particular GTPase being analyzed. By performing these "pull-down assays" at various time points, the activation kinetics can be assessed. We describe here in detail the methods for preparing these probes (PBD, RhBD, RBD) and for performing Rac/Cdc42/Rho/Rap activation assays based on the use of the Pak1-binding domain (PBD probe) [6], Rho activation assays based on the use of the Rhotekin-binding domain (RhBD probe) [11], and Rap activation assays based on the use of the RalGDS-binding domain (RBD probe) [16].

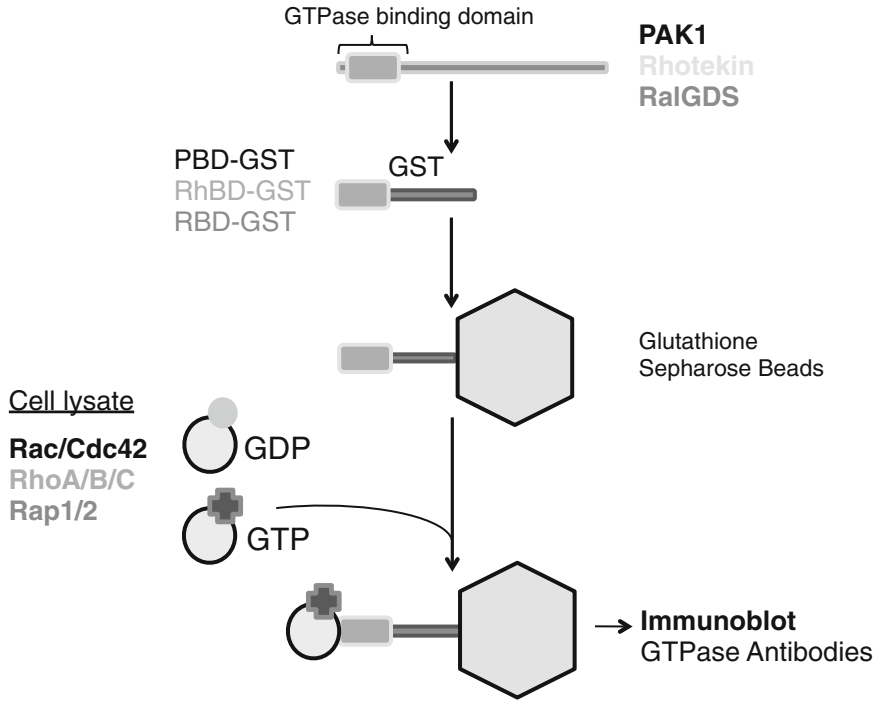

Fig. 1 Principle of the affinity precipitation assay for detection of active Rac, Cdc42, Rho, and Rap GTPases in cell lysates using the GST-PBD/RhBD/RBD

2 Materials

1. Rac-/Cdc42-binding domain of p21-activated kinase (Pak1) (GST-PBD, amino acids 67–150), RhoA-/B-/C-binding domain of Rhotekin (GST-RhBD, amino acids 7–89), and Rap1-/Rap2-binding domain of RalGDS (GST-RBD, amino acids 1–97) cloned into pGEX bacterial expression vectors (Amersham Biosciences) (*see* **Notes 1** and **2**).
2. Luria broth (LB).
3. Ampicillin: final concentration 100 μg/mL.
4. Isopropyl-β-D-thio-galactopyranoside (IPTG): 1 M in H_2O.
5. Bacterial lysis buffer: 50 mM Tris–HCl, pH 7.5, 150 mM NaCl, 5 mM $MgCl_2$, 1 mM EDTA, 1 mM dithiothreitol (DTT), 1 mM phenylmethylsulfonyl fluoride (PMSF), and 1 μg/mL aprotinin. Add the DTT, PMSF, and aprotinin to the freshly made, ice-cold buffer prior to use.
6. Bacterial wash buffer: 50 mM Tris–HCl, pH 8.0, 150 mM NaCl, 5 mM $MgCl_2$, 1 mM DTT, 1 mM PMSF, and 1 μg/mL aprotinin. Add the DTT, PMSF, and aprotinin to the freshly made, ice-cold buffer prior to use.

7. Glutathione Sepharose 4B beads (Amersham Biosciences).
8. Cell lysis buffer (Rac, Cdc42, Rap): 25 mM Tris, pH 7.5, 50 mM NaCl, 5 mM $MgCl_2$, 1 mM EDTA, 1 % NP-40, 10 % glycerol, 1 mM PMSF, 5 μg/mL aprotinin, 1 μg/mL leupeptin, and 2 mM sodium orthovanadate. Add protease and phosphatase inhibitors to the freshly made, ice-cold buffer prior to use.
9. Cell lysis buffer (Rho): 50 mM Tris, pH 7.5, 500 mM NaCl, 10 mM $MgCl_2$, 1 mM EDTA, 1 % NP-40, 10 % glycerol, 1 mM PMSF, 5 μg/mL aprotinin, 1 μg/mL leupeptin, and 2 mM sodium orthovanadate. Add protease and phosphatase inhibitors to the freshly made, ice-cold buffer prior to use.
10. Hanks' balanced salt solution with calcium and magnesium (HBSS).
11. GTPγS tetralithium salt: 1 mM in H_2O.
12. GDP tris salt: 1 mM in H_2O.
13. Laemmli sample buffer: 2 % sodium dodecylsulfate (SDS), 10 % glycerol, 2 % β-mercaptoethanol, 60 mM Tris–HCl, pH 6.8, and trace of bromophenol blue.
14. Ponceau S solution: 0.2 % Ponceau S in 3 % trichloroacetic acid.
15. Antibodies: Multiple commercial sources are available. Suggested are anti-Rac1 mouse mAb (R56220) (BD Transduction laboratories), anti-Rac2 rabbit pAb (Upstate), anti-Rap1 mouse mAb (BD Biosciences) or anti-Rap1 rabbit pAb (Santa Cruz Biotech), anti-Rap2 mouse mAb (BD Biosciences), anti-Cdc42 rabbit pAb (Santa Cruz Biotech), anti-RhoA mouse mAb (Santa Cruz Biotech), and anti-RhoB rabbit pAb (Santa Cruz Biotech).

3 Methods

3.1 Expression of GST-PBD, GST-RhBD, and GST-RBD Fusion Proteins in Bacteria

Competent *E. coli* strain BL21(DE3)LysE needs to be transformed with pGEX-PBD, pGEX-RhBD, or pGEX-RBD plasmids by standard procedures and grown on LB/agar plates with 100 μg/mL ampicillin.

1. Prepare bacterial stocks from a log phase LB/ampicillin culture after inoculating the culture with an individual bacterial colony.
2. Dilute the stock culture 1:1 with sterile 30 % v/v glycerol and snap-freeze in liquid nitrogen. Store at −80 °C (*see* **Note 3**).
3. From the frozen stock or a streaked plate, inoculate a 50 mL LB/ampicillin culture and grow overnight with shaking at 37 °C.

4. Transfer 25 mL of this culture to 1 L of LB/ampicillin broth and continue bacterial growth until the $OD_{600\ nm}$ reaches 0.6–0.8 (usually 2 h). Save 50 µL of bacteria culture for final SDS-PAGE analysis (this is the not induced sample).
5. Induce transcription with 0.8–1 mM IPTG and grow for 3–4 h at 30 °C. Save about 50 µL of this culture for final SDS-PAGE analysis (this is the induced sample).

3.2 Preparation of GST-PBD, GST-RhBD, and GST-RBD Probes

1. Prepare the *E. coli* lysate by spinning down the culture for 10 min at 2,300 × *g* at 4 °C.
2. Wash the pellet once with cold PBS followed by centrifugation.
3. Resuspend the pellet in 10 mL cold bacterial lysis buffer.
4. Incubate on ice for 10 min and then sonicate three times for 30 s on ice without foaming. If necessary, the *E. coli* pellet can be stored after the PBS wash at −80 °C. In this case, addition of 1 mg/mL lysozyme and 20 µg/mL DNAse I is recommended for efficient bacterial lysis and DNA shredding.
5. Clear the lysate by centrifugation (15 min, 9,300 × *g*, 4 °C).
6. Collect the supernatant and save 50 µL of supernatant sample for final SDS-PAGE analysis (this is the GST-PBD/RhBD/RBD total sample).
7. Prepare glutathione Sepharose 4B beads by aliquoting equivalent of 1 mL dry beads (for 1 L *E. coli* culture) and centrifuge for 5 min, 400 × *g*, 4 °C in a tabletop microcentrifuge.
8. Wash beads 2 times with 10 mL H_2O and two times with 5 mL bacterial lysis buffer.
9. Combine washed glutathione Sepharose 4B beads with *E. coli* supernatant from Subheading 3.2, **step 2** and incubate for 2 h (recommended) or overnight at 4 °C while inverting.
10. Centrifuge 5 min, 400 × *g*, at 4 °C and save 50 µL of supernatant as GST-PBD/GST-RhBD/GST-RBD unbound protein sample for final SDS-PAGE analysis.
11. Wash beads five times with 10 mL of ice-cold bacterial wash buffer.
12. Aliquot beads in wash buffer with 10 % v/v glycerol (1:1 slurry) and store at −80 °C.
13. Determine the protein concentration of GST-PBD, GST-RhBD, or GST-RBD bound to beads with commercially available protein assays.
14. To analyze the GST-PBD/GST-RhBD/GST-RBD purification process by SDS-PAGE, use ~5 µL of sample from not induced, induced, GST-PBD/RhBD/RBD total, GST-PBD/RhBD/RBD unbound, and final purified GST-PBD/RhBD/

RBD bound to beads aliquots (use 5 and 10 μL of 1:1 bead slurry) for SDS-PAGE and Coomassie blue staining. This provides a determination of protein induction, amounts of soluble and bound protein, and purity of the final GST-PBD/RhBD/RBD probe (*see* **Note 4**).

3.3 Identification of GTP-Bound Rac, Cdc42, Rho, and Rap with Activity-Specific Probes in Neutrophils

1. Neutrophils are suspended at 1×10^7 per ml in HBSS and preincubated for 15 min at room temperature in the presence of 1 mM diisopropyl fluorophosphate (DFP).
2. Aliquot neutrophils at 1 ml per timepoint and equilibrate to 37 °C in a heating block for 5 min.
3. Add 100 μL of stimulant at the appropriate concentration to each sample; stimulation is initiated for each time point separately.
4. Terminate stimulation by centrifugation at $4{,}500 \times g$ for 30 s at 4 °C.
5. Resuspend neutrophils in 100 μL ice-cold HBSS and lyse by the addition of 100 μL lysis buffer.
6. For adherent neutrophils, stimulation is terminated by removal of media and rapid washing with room temperature HBSS before ice-cold HBSS and cell lysis buffer is added, and neutrophils are scraped from the plates. For adherent neutrophils, lysis buffer includes 5 mM DFP (*see* **Notes 5–8**).
7. Keep the resulting neutrophil lysates on ice for 10 min for efficient extraction.
8. Vortex samples and clarify by centrifugation for 10 min at $10{,}000 \times g$ at 4 °C.
9. Aliquot the supernatants and snap-freeze in liquid nitrogen for analysis later, or placed the on ice for immediate use.
10. Retain 1/10th of the total supernatant volume for total GTPase detection. The remainder of the supernatant is subject to bead precipitation by adding ~10 μg of purified GST-PBD/RhBD/RBD beads to each sample and incubating for 1 h at 4 °C while inverting (*see* **Note 9**).
11. Centrifuge the samples at $250 \times g$ for 2 min at 4 °C.
12. Aspirate the supernatant, and wash five times with 1:1 cell lysis buffer/HBSS.
13. Add Laemmli sample buffer to the pellet, heat at 95 °C for 5 min, load the complete sample, and perform SDS-PAGE on a 15 % SDS-PAGE gel.
14. Transfer to nitrocellulose membrane, and stain the membrane with Ponceau S to ensure equal addition of GST-PBD/RhBD/RBD beads to every sample.

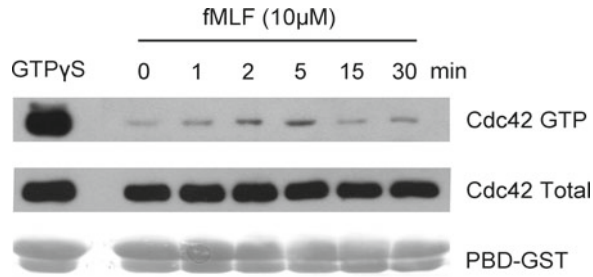

Fig. 2 Cdc42 activation in murine neutrophils. Bone marrow-derived neutrophils (BMDN) were stimulated in suspension with 10 μM fMLF for the indicated times (1×10^7 BMDN per time point). After lysis Cdc42-GTP was bound to the GST-PBD probe and detected by immunoblot analysis (*upper panel*). A GTPγS-loaded lysate of quiescent BMDN served as positive control. The *middle panel* shows a Cdc42 immunoblot using 1/10th of the BMDN lysate for each sample. The *lower panel* confirms equal GST-PBD loading as determined by Ponceau S staining prior to immunoblot

15. After blocking of the membrane, perform immunoblot analysis with appropriate Rac, Cdc42, Rho, or Rap antibodies (*see* **Notes 10**–**12**). A representative example of Cdc42 activation in fMLF-stimulated murine neutrophils including a GTPγS-loaded positive control is depicted in Fig. 2.

3.4 Control Reactions

Positive and negative controls for the assay should be performed with unstimulated neutrophil lysates, in which the endogenous GTPases are loaded with either GDP (negative control) or with GTPγS (positive control)—see below. In addition, lysates derived from cell lines (293 T, HeLa, etc.) overexpressing constitutively active Rho or Rap GTPase mutants can be used as positive binding controls, while dominant negative GTPase mutants serve as negative binding controls. Alternatively, a GTPase-regulatory protein such as a constitutively active exchange factor (GEF) can be expressed if a particular GTPase represents an in vivo target of a particular GEF (*see* **Note 13**).

1. For positive controls (GTP-bound form), add simultaneously 1 μL of 0.1 mM GTPγS and 2.1 μL of 0.1 M EDTA per 5 μL of lysate (*see* **Note 14**).
2. Incubate 8 min at 30 °C.
3. Place on ice and add 2 μL of 1 M $MgCl_2$ in order to stop nucleotide exchange.
4. As a negative control, 1 μL of 0.1 mM GDP is used instead of GTPγS and following **steps 1**–**3**.
5. The GTPγS- or GDP-loaded lysates should be kept on ice and used within the next 15–30 min by following the procedure

for the binding assays as described in Subheading 3.3, **steps 3** and **4**. It is crucial for nucleotide loading that the lysis buffer used contains the magnesium and EDTA concentrations listed when following this protocol.

4 Notes

1. The described GST-PBD probe will bind the active, GTP-bound form of all three Rac GTPases (Rac1, Rac2, Rac3) as well as the related GTPases Cdc42 and TC10. The GST-RBD probe described herein will bind to GTP-Rap1 isoforms and GTP-Rap2 isoforms. The GST-RhBD probe recognizes and binds the active conformation of Rho isoforms (RhoA, RhoB, and RhoC). Since other small GTPases may also have the ability to bind to GST-PBD/RhBD/RBD, identification of an activated GTPase is dependent on the specificity of the antibody used for immunoblotting.
2. Additional high-affinity probes for small GTPases have been developed, including the CRIB domain of WASP (Cdc42), the RBD domain of Raf-1 (Ras proteins), and the RBD domain of RalBP1/RLIP76 (Ral) to name a few. The experimental protocols for preparing and using these probes have to be adjusted to their specific requirements. Commercial kits are available for some of the GTPase affinity probes (Upstate, Cytoskeleton, Pierce, Millipore, etc.). Activation assays for some Rho GTPases are also available as G-LISA kits. The kit uses a 96-well plate coated with a binding domain (PBD, RhBD). After incubation of lysates in these wells, detection of bound active GTPases is performed in the plate by use of antibodies followed by luminometric or colorimetric detection. Multiple independent assays and stringent controls are essential for this assay format.
3. Various strains of *E. coli* can be tried to maximize protein expression and purity of the final product. Freshly inoculated and induced cultures give higher protein yields.
4. Breakdown products of the isolated GST-PBD/RhBD/RBD are often seen. These are usually not detrimental to the assay as long as the intact GST-PBD/RhBD/RBD is the major product (>75 % of total GST fusion protein).
5. Certain ligands may require priming or starvation of neutrophils before stimulation of the cells. These procedures can alter the GTPase activation state.
6. The short wash step is only recommended for adherent cells as it can be done very rapidly, while centrifugation of suspension cells would take too long for maintaining the accuracy of short time points.

7. The choice of the lysis buffer and the wash conditions for the beads after GTPase binding can be adjusted as long as GTP hydrolysis is minimized. Positive controls should give a strong clear signal, while negative controls and untreated control lysates should give little or no signal. Immediate use of cell lysates is recommended for better results, avoid freeze-thawing cycles.
8. Release of granule contents and high protease activation poses specific problems in neutrophil activation assays. Pretreatment with or inclusion of diisopropyl fluorophosphate in the lysis buffer greatly reduces protein degradation during the experiment. DFP is a neurotoxin, appropriate precautions must be taken. DFP treatment should take place in a chemical fume hood. DFP treatment prior to neutrophil stimulation may alter GTPase activation, thus a trail experiment has to be performed.
9. Binding of GTP-GTPase to the PBD reaches 75 % by 30 min and is maximal by 1 h at 4 °C. This time may need to be shortened if GTP hydrolysis in the cell lysate is high, although the binding of GTPase to the PBD, RhBD, or RBD inhibits hydrolysis. It is preferable to add the beads to the sample just after the lysis step to avoid any rapid hydrolysis of GTP to GDP.
10. This method only determines the relative increase of the GTP-bound form of a specific GTPase. One can assume that only about 5–10 % of the total GTPase pool will be activated by a given stimulus. This amount is further reduced by the intrinsic GTP hydrolysis rate of the GTPase and the activity of GAP proteins in the cell lysates. This loss can be minimized by shorter incubation and strict adherence to ice-cold conditions.
11. Unspecific binding of the GTPase to the affinity probe in unstimulated lysates may be due to stress-dependent activation of the GTPase during the isolation or handling of the cells. Careful handling of the cells as well as increasing the sodium chloride and/or detergent concentration in the wash buffer may reduce background effects.
12. Sensitivity of the assay will be determined to a large extent by the antibody used for detection. Certain antibodies are recommended here. However, before using the affinity probe, the sensitivity and specificity of the antibody need to be tested. The abundance of the GTPase in the cell together with the sensitivity of the antibody determines the amount of lysate necessary for efficient detection of the activated GTPase.
13. It is important to determine the maximal signal obtainable from GTPγS-bound GTPase in cell lysates. This allows adjusting the number of cells per sample in order to obtain a signal in the detectable range, assuming that the level of endogenously activated GTPase will usually be on the order of 5–10 % of the total GTPase pool. These controls also assure the quality of different preparations of the GST-PBD/RBD probe.

14. The concentration of EDTA has to be adjusted to the magnesium concentration in the lysis buffer (5–10 mM $MgCl_2$ in this protocol). Note that an excess of EDTA is critical for guanine nucleotide loading (a molar excess of two- to fivefold is recommended), while an excess of magnesium is required to stop guanine nucleotide exchange.

Acknowledgments

This work was supported by grants from Science Foundation Ireland and the Health Research Board.

References

1. Dinauer MC (2003) Regulation of neutrophil function by Rac GTPases. Curr Opin Hematol 10:8–15
2. Bokoch GM (2005) Regulation of innate immunity by Rho GTPases. Trends Cell Biol 15:163–171
3. Johnson DS, Chen YH (2012) Ras family of small GTPases in immunity and inflammation. Curr Opin Pharmacol 12:458–463
4. Burbelo PD, Drechsel D, Hall A (1995) A conserved binding motif defines numerous candidate target proteins for both Cdc42 and Rac GTPases. J Biol Chem 270:29071–29074
5. Thompson G, Owen D, Chalk PA, Lowe PN (1998) Delineation of the Cdc42/Rac-binding domain of p21-activated kinase. Biochemistry 37:7885–7891
6. Benard V, Bohl BP, Bokoch GM (1999) Characterization of Rac and Cdc42 activation in chemoattractant-stimulated human neutrophils using a novel assay for active GTPases. J Biol Chem 274:13198–13204
7. Geijsen N, van Delft S, Raaijmakers JA, Lammers JW, Collard JG, Koenderman L, Coffer PJ (1999) Regulation of p21rac activation in human neutrophils. Blood 94:1121–1130
8. Akasaki T, Koga H, Sumimoto H (1999) Phosphoinositide 3-kinase-dependent and -independent activation of the small GTPase Rac2 in human neutrophils. J Biol Chem 274:18055–18059
9. Arbibe L, Mira JP, Teusch N et al (2000) Toll-like receptor 2-mediated NF-kappa B activation requires a Rac1-dependent pathway. Nat Immunol 1:533–540
10. Ren XD, Kiosses WB, Schwartz MA (1999) Regulation of the small GTP-binding protein Rho by cell adhesion and the cytoskeleton. EMBO J 18:578–585
11. Ren XD, Schwartz MA (2000) Determination of GTP loading on Rho. Methods Enzymol 325:264–272
12. Teusch N, Lombardo E, Eddleston J, Knaus UG (2004) The low molecular weight GTPase RhoA and atypical protein kinase Czeta are required for TLR2-mediated gene transcription. J Immunol 173:507–514
13. Alblas J, Ulfman L, Hordijk P, Koenderman L (2001) Activation of RhoA and ROCK are essential for detachment of migrating leukocytes. Mol Biol Cell 12:2137–2145
14. Huveneers S, Danen EHJ (2009) Adhesion signaling: crosstalk between integrins, Src and Rho. J Cell Sci 122:1059–1069
15. Xu J, Wang FV, Keymeulen A et al (2003) Divergent signals and cytoskeletal assemblies regulate self-organizing polarity in neutrophils. Cell 114:201–214
16. Van Triest M, Bos JL (2004) Pulldown assays for guanoside 5′-triphosphate-bound Ras-like guanosine 5′-triphosphatases. Methods Mol Biol 250:97–102
17. Castro AF, Rebhun JF, Quilliam LA (2005) Measuring Ras-family GTP levels in vivo-running hot and cold. Methods 37:190–196
18. Herrmann C, Horn G, Spaargaren M, Wittinghofer A (1996) Differential interaction of the Ras family GTP-binding proteins H-Ras, Rap1A, and R-Ras with the putative effector molecules Raf kinase and Ral-guanine nucleotide exchange factor. J Biol Chem 271:6794–6800
19. M'Rabet L, Coffer P, Zwartkruis F, Franke B, Segal AW, Koenderman L, Bos JL (1998) Activation of the small GTPase Rap1 in human neutrophils. Blood 92:2133–2140
20. Abram CL, Lowell CA (2009) The ins and outs of leukocyte signaling. Annu Rev Immunol 27:339–362
21. Gloerich M, Bos JL (2011) Regulating Rap small G-proteins in time and space. Trends Cell Biol 21:615–623

Chapter 7

Measurement of Phospholipid Metabolism in Intact Neutrophils

Susan Sergeant and Linda C. McPhail

Abstract

Phospholipid-metabolizing enzymes are important participants in neutrophil signal transduction pathways. The methods discussed herein describe assays for assessing the activities of phospholipase A_2 (PLA_2), phospholipase C (PLC), phospholipase D (PLD), and phosphoinositide 3-OH-kinase in intact neutrophils. PLA_2 activity is measured as the release of radiolabeled arachidonic acid. PLC activity is measured as the accumulation of inositol 1,4,5-trisphosphate (IP_3), a water-soluble product, using a commercially available radioreceptor assay kit. PLD activity is measured as the appearance of its radiolabeled products, phosphatidic acid and phosphatidylethanol. PI3-K activity is measured as the appearance of its radiolabeled product, phosphatidylinositol-3,4,5-trisphosphate.

Key words Neutrophil, Phospholipase, Lipid kinase, Phospholipid, Signal transduction, Lipid second messengers

1 Introduction

Numerous phospholipid-metabolizing enzymes are expressed in neutrophils and many appear to play important roles in intracellular signaling pathways that regulate the functional responses of these cells. Thus, it is important to be able to accurately measure these enzymes in order to better define their role(s) in signaling pathways. Two approaches are generally used to assess the activity of phospholipid-metabolizing enzymes. The first measures the appearance of the radiolabeled product(s) and the second measures the increase in the mass of a product. Neither approach alone gives a complete picture of the activity of a particular enzyme because the products themselves are efficiently metabolized, interconverted, and recycled. Moreover, each approach has its limitations, which must be considered when evaluating the results. The ability to measure radiolabeled products requires a reasonably short (30 min to 2 h) incubation of neutrophils with radiolabeled precursors that will sufficiently label phospholipids without compromising cell

Mark T. Quinn and Frank R. DeLeo (eds.), *Neutrophil Methods and Protocols*, Methods in Molecular Biology, vol. 1124,
DOI 10.1007/978-1-62703-845-4_7,

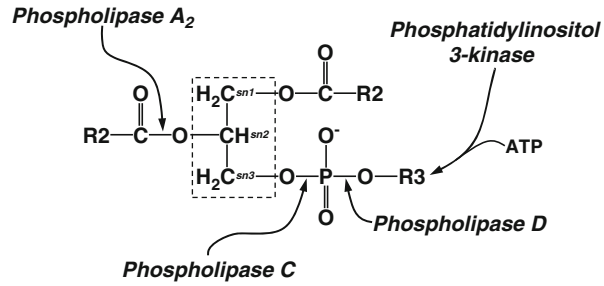

Fig. 1 Sites of phospholipid cleavage by the phospholipases A_2, C, and D and phosphorylation by PI3-K. The glycerol backbone (*dashed box*) is esterified to fatty acids (R1 and R2) through the *sn*-1 (*top*) and *sn*-2 (*middle*) carbons. The head group (R3; e.g., choline, inositol) is located on the *sn*-3 carbon (*bottom*) through a phosphodiester bond. Reproduced by permission of Humana Press©2007 [43]

viability and cell function. Although this scheme does not allow for equilibrium labeling [1], it can allow for the detection of product and its metabolites. The determination of product mass requires only detection methods with sufficient sensitivity to measure the small amounts of the transiently produced product(s). Here, we present the most widely used techniques for the activity measurements of phospholipase A_2 (PLA_2), phospholipase C (PLC), phospholipase D (PLD), and phosphoinositide 3-OH-kinase (PI3-K) in intact neutrophils. However, we have included references to detailed protocols for alternative activity measurements for each enzyme because of the limitations inherent in any single method. No attempt has been made to catalog or reference assays used to assess activity for these enzymes in cell-free systems using exogenous substrates.

PLA_2 cleaves the fatty acid chain from the *sn*-2 position of phospholipids (Fig. 1), generating a free fatty acid and a lysophospholipid. In neutrophils, the *sn*-2 position is enriched in arachidonic acid (AA), especially in phosphatidylcholine (PC), the most abundant (41 %) phospholipid [2]. Neutrophils contain several types of PLA_2, including secretory PLA_2 isoforms (in granules), cytosolic PLA_2, Ca^{2+}-independent PLA_2, and peroxiredoxin 6-PLA_2 [3–6]. A kit for measuring PLA_2 activity is currently available from Cayman Chemicals and is optimized for measurement of cytosolic PLA_2. We describe here a method for measuring PLA_2 activity that is commonly used to assess the release of [^{3}H]AA from labeled cellular phospholipids into the medium. This method compares favorably to [^{3}H]AA release assessed by total lipid analysis of cells using thin layer chromatography [7]. A more involved method designed to examine the release of [^{3}H]AA (extra- and intracellularly) and its metabolites can be found, described in detail, elsewhere [8].

Neutrophils contain multiple isoforms of PLC, in both the β and γ families [9, 10]. PLC primarily utilizes the low abundance

(~1 %, [2]) phosphatidylinositol (PI) family of phospholipids as substrates, generating diacylglycerol (DAG) and a water-soluble inositol phosphate as products (Fig. 1). The inositol head group of PI undergoes multiple phosphorylations by PI lipid kinases. A major substrate for PLC is phosphatidylinositol-(4,5)-bisphosphate (PIP_2). When metabolized by PLC, PIP_2 yields inositol 1,4,5-trisphosphate (IP_3) and its appearance is used as a measure of PLC activation. The method for evaluating PLC activation in neutrophils has been simplified in recent years by the appearance of commercially available kits for the measurement of IP_3 mass. This method eliminates a prolonged incubation to label neutrophils with tritiated *myo*inositol, needed for its incorporation into the phosphatidylinositide pool. However, this *myo*inositol labeling method [11–13] is still suitable when it is necessary to examine all inositol phosphate products, which are fractionated by liquid chromatography [14].

Neutrophils contain two isoforms of PLD, PLD1 and PLD2 [15, 16]. PLD primarily utilizes PC as a substrate, generating phosphatidic acid (PA) and choline as products (Fig. 1). PA production can be monitored as mass accumulation [16–18] or as generation of a radiolabeled product [19, 20]. The latter will be described here. A unique feature of PLD is its transphosphatidylation activity, which is often exploited to assay the activity of the enzyme. In the presence of a primary alcohol (e.g., ethanol, 1-butanol), a phosphatidylalcohol is generated at the expense of PA [21]. Metabolically more stable than PA, the phosphatidylalcohol is not subject to the normal degradative pathways of PA. This approach also provides unequivocal evidence of PLD-derived PA since PA can also be generated by the phosphorylation of DAG (derived from PLC activation) by DAG kinase. However, care must be taken with the use of alcohols since high concentrations can compromise cell viability and 1-butanol has been observed to inhibit one PLD isoform [22]. Although not discussed here, a detailed description of a chemiluminescence method for the detection of choline mass as an alternative means of assessing PLD activation has been published [23]. For those interested, a PLD assay kit for measuring the enzyme in cell extracts is available from Cayman Chemicals.

Phospholipids can also be metabolized by lipid kinases, which add phosphate groups to the head group (Fig. 1). PI, with its inositol ring, is the principal substrate of these enzymes. Of particular interest are the phosphoinositide 3-OH-kinases (PI3-K), since their activation is highly regulated and they are involved in intracellular signaling [24, 25]. Three methods are in use to assess PI3-K activation. One assesses the activity of PI3-K in immunoprecipitates by monitoring the generation of a radiolabeled lipid product from an exogenous substrate [26]. This method utilizes isoform-specific PI3-K or phosphotyrosine antibodies and it has been used to assess PI3-K activation in neutrophils [27, 28]. The other two methods detect total product formed in intact cells

either as product mass or as a radiolabeled product. Detection of mass can be via mass spectrometry [29] or a radioligand displacement assay [30]. The latter is comparable to the radioreceptor assay used to detect IP_3 for PLC activation, except that phosphatidylinositol-3,4,5-trisphosphate (PIP_3) in lipid extracts of cells must first be hydrolyzed to a water-soluble ligand (IP_4) before use in the binding assay [31]. Unfortunately, commercially available kits for this assay are not yet available, but a detailed description can be found in an earlier volume in this series [30], and this type of assay has been used to assess PI3-K activation in neutrophils [32]. The method described here detects total radiolabeled PIP_3, by thin layer chromatography, after cells are incubated with [^{32}P] inorganic phosphate to label the cellular ATP pool [33].

2 Materials

2.1 Common Materials (Used in Two or More Methods)

1. Buffer A (for labeling incubations): 138 mM NaCl, 5.3 mM KCl, 10 mM HEPES, 0.34 mM Na_2HPO_4, 0.44 mM KH_2PO_4, 4.2 mM $NaHCO_3$, 0.49 mM $MgCl_2$, 0.4 mM $MgSO_4$, and 5.5 mM glucose (pH 7.4) (*see* **Note 1**).
2. Buffer B (for stimulation incubations): buffer A plus 1.2 mM $CaCl_2$.
3. Fatty acid-free bovine serum albumin.
4. Chromatography grade solvents: chloroform, methanol, ethyl acetate, iso-octane, and acetone (*see* **Note 2**).
5. Acetic acid (glacial).
6. Silica Gel-GHL thin layer chromatography (TLC) plates (250 μm, 20 × 20 cm and 5 × 20 cm, inorganic binder; Analtech #11011 or comparable).
7. Silica Gel-G TLC plates (250 μm, 20 × 20 cm, no organic binder; Analtech #01011 or comparable).
8. Solvent system I (for phospholipid analysis): chloroform/methanol/acetic acid/water (100:50:16:6, v/v/v/v)
9. TLC plate guide.
10. TLC tank(s) with lid.
11. Oven (to 110 °C).
12. Screw-top glass tubes (13 × 100 mm) with Teflon-lined caps (*see* **Note 3**).
13. Nitrogen (N_2) tank and manifold (for drying lipid extracts).
14. Dry (glass bead) bath.
15. Pasteur pipets and bulbs.

16. Glass (capillary) micropipets (5, 10, 25, 50 µl; Drummond) and pipetor (Drummond) (*see* **Note 4**).
17. Iodine (solid) and a dedicated TLC tank with lid (*see* **Note 5**).
18. Weigh paper (10 × 10 cm).
19. Single-edge razor blades.
20. Scintillation vials.
21. Liquid scintillation counting fluid.

2.2 cPLA$_2$ Activity

1. [5,6,8,9,11,12,14,15-^{3}H] arachidonic acid (#NET298Z; 1 mCi/ml; 80–240 Ci/mmol; PerkinElmer). Store this radioactive material at –20 °C. Flush with N_2 after each opening.
2. 0.1 N NaOH.

2.3 PLC Activity

1. Ice-cold 20 % perchloric acid (v/v; PCA).
2. 5 M KOH.
3. Inositol 1,4,5-trisphosphate (IP_3) radioreceptor assay kit (PerkinElmer, NEK064). Kits contain [^{3}H]IP_3 (*see* **Note 6**).

2.4 PLD Activity

1. 1-O-[^{3}H] octadecyl lyso-platelet-activating factor (lysoPC; 1 mCi/ml; 30–60 Ci/mmol in toluene/ethanol; American Radiolabeled Chemicals). Store this radioactive material at –20 °C (*see* **Note 7**).
2. PLD label buffer: buffer A with 2.5 mg/ml BSA.
3. Unlabeled phospholipids [PC, PE (phosphatidylethanolamine), PS (phosphatidylserine), PI, PA, lyso-platelet-activating factor (PAF) from naturally occurring sources (brain, egg, or liver)], monoglyceride (18:1), diglyceride (18:1), triglyceride, and phosphatidylethanol (18:1) (Avanti Polar Lipids, Birmingham AL) for use as standards.
4. PLD quench mixture: chloroform/methanol/2% formic acid (1:2:0.2, v/v/v) (*see* **Note 8**).
5. Separatory funnel (1 l).
6. Solvent system II (for PA/phosphatidylethanol): ethyl acetate/iso-octane/acetic acid/water (110:50:20:100, v/v/v/v). Combine components in the separatory funnel. Mix thoroughly three times, venting between mixings. Let stand (1 h to overnight) in fume hood. Discard bottom (aqueous) phase. Pour the upper phase in TLC tank and let stand (covered, ~1 h) before use.

2.5 PI3-K Activity

1. [^{32}P]orthophosphate (HCl-free; PerkinElmer) (*see* **Note 9**).
2. Buffer C (for labeling incubation): 30 mM HEPES (pH 7.4), 110 mM NaCl, 10 mM KCl, 1 mM $MgCl_2$, and 5.5 mM glucose.

3. Buffer D (for stimulation incubation): buffer C plus 1.2 mM $CaCl_2$.
4. PI3-K quench mixture: chloroform/methanol (1:2, v/v).
5. Unlabeled PI, phosphatidylinositol-4-phosphate (PIP), PIP_2, and PIP_3 (Avanti Polar Lipids, Birmingham AL).
6. Solvent system III (for plate preparation): 1.2 % potassium oxalate in methanol/water (2:3, v/v).
7. Solvent system IV (for PIP_n separation): chloroform/acetone/methanol/acetic acid/water (80:30:26:24:14, v/v/v/v/v).
8. Lift-Away cleaner (Research Products International) or comparable cleaner for radioactive decontamination.
9. Plexiglass shields and boxes (to transport tubes), neoprene apron.

3 Methods

3.1 Common Thin Layer Chromatography (TLC) Methods and Assessment of Labeling

1. Preparation of plates:
   (a) Silica Gel-GHL plates (general use hard plates): Activate plates (100 °C, 30 min) and let cool before using (*see* **Note 10**). Mark the origin 1 cm above bottom of plate with a light pencil line using the TLC plate guide as a straight-edge. Mark lanes (maximum of 6 on a 20 × 20 cm plate) of equal width in a similar manner.
   (b) Silica Gel-G plates (soft plates with no binder): Activate plates (100 °C, 30 min) and let cool before using. Score lines for lanes with a pencil to remove silica gel between lanes using the TLC plate guide. Place the plate guide ~1 cm above bottom of plate to indicate the origin, but do not mark the origin with any pencil or scoring line (*see* **Note 11**). Lanes can be labeled in the silica gel-free top of the plate with a wax pencil (*not* a Sharpie-type marker).
2. *Test plates*: Use a 5 × 20-cm plate for test plates. Use microcapillary pipets to spot plates at the origin. Let spot dry between application of standard (or sample). Keeping spots as small as possible, apply each lipid standard individually and to a spot called "Mix," which contains all of the standards (*see* **Note 12**). No lane markings are needed on test plates. Develop the test plate in the appropriate solvent system to ensure that lipids will separate well before running radioactive samples. Let the plate air-dry in fume hood before visualization of lipids.
3. *Visualization of separated lipids*: Iodine vapor (*see* **Note 5**) is used to reversibly visualize separated lipids on TLC plates by virtue of the ability of iodine to interact with double bonds. Sprinkle a small amount of the solid in the TLC tank and

allow it to sublimate. Place an air-dried, developed plate in the iodine tank and observe until yellowish-brown spots appear. Remove plate from tank and lightly mark (with pencil) the lipid standard spots or the fractions to be scraped and counted. Allow iodine to evaporate in hood before scraping or analyzing plate.

4. *Scraping TLC plates and quantification* (for Subheadings 3.1, **step 6,** and 3.4, **step 15**): After TLC plates have been developed and lipids visualized, the separated lipid fractions are scraped and counted. Prepare the required number (based on number of samples and fractions for each) of scintillation vials. Using a clean razor blade, carefully scrape the silica gel fractions from the plate (lane by lane) onto a piece of weigh paper (*see* **Note 13**). Pour each fraction into a separate vial. To each vial, add 0.5 ml of methanol (to help elute lipids/counts from silica gel) and a suitable volume of liquid scintillation counting fluid. Cap tightly and shake well by hand. Place in liquid scintillation counter and count for 1 min with a program for [^{3}H] DPM.
5. *Estimation of tritiated-lipid incorporation into cells*: In initial experiments, it is necessary to determine the extent of tritiated-lipid incorporation into cells. Small (known) volumes of samples are collected after the labeling incubation and counted by liquid scintillation counting to calculate the percent of total radiolabel incorporated into cells. The samples are unincorporated (cell-free supernatant and washes; Subheading 3.2, **step 2** for PLA_2, Subheading 3.4, **step 4** for PLD) and incorporated (washed cells after labeling incubation; Subheading 3.2, **step 2** for PLA_2, Subheading 3.4, **step 5** for PLD). Count samples and calculate DPM in the final sample volume. Percent incorporation = [total DPM in cells/(total DPM in cells + total DPM in supernatant + washes)] × 100.
6. *Evaluation of tritiated-lipid incorporation into phospholipids* (for Subheadings 3.2 PLA_2 and 3.4 PLD): The radiolabeled precursors ([3H]AA and [3H] lysoPC) will predominantly label PC. Still, in initial experiments it is necessary to evaluate which phospholipid(s) the tritiated lipid has labeled. When labeled, washed cells are aliquoted for stimulation (Subheading 3.2, **step 3** for PLA_2, Subheading 3.4, **step 5** for PLD); reserve duplicate aliquots of cell suspension on ice for analysis of phospholipids. Extract lipids (Subheading 3.4, **steps 7–9**), add ~50 μg lysoPAF standard per tube [only for PLD (Subheading 3.4)], and dry the chloroform extract (Subheading 3.4, **step 11**). Prepare a TLC tank for solvent system I [Subheading 2.1, **item 8**; use a filter paper wick (*see* **Note 14**)] and run a test plate (Silica Gel-G, ~1.5-h development time) with the following lipid standards: PC, PS, lysoPAF [only for PLD (Subheading 3.4)], PE, and Mix (Subheading 3.1, **step 2**). Visualize separated lipids in iodine

vapor (Subheading 3.1, **step 3**, *see* **Note 5**) and carefully encircle separated lipids with etch lines. In this solvent system, lipids will separate from the origin as follows: lysoPAF, PC, PS, PE, and neutral lipids (near solvent front). Run samples on a prepared G plate (Subheading 3.1, **step 1**(**b**)), visualize lipids, and scrape fractions (Subheading 3.1, **step 4**; scrape the entire sample lane, even if no lipid is visualized, *see* **Note 15**) and count fractions by liquid scintillation counting. Average the DPM in lipid fractions of duplicates. Add the average DPM in all fractions for a sample to yield total DPM. Calculate the amount of radiolabel in each fraction as the percent of total DPM.

3.2 $cPLA_2$

Cells are labeled with [^{3}H]AA, washed to remove unincorporated label, and resuspended for stimulation. Cell stimulation is terminated by pelleting the cells. A volume of the cell-free supernatant is counted to determine the [^{3}H]AA release and the remaining cell-associated radioactivity is also counted in a sample of the solubilized cells. AA release is normalized to the total cell-associated radioactivity in unstimulated cells [34, 35].

1. *Labeling incubation*: Incubate isolated neutrophils (2×10^7/ml buffer A; Subheading 2.1, **item 1**) with [^{3}H]AA (1 μCi/ml) for 30 min at 37 °C in a shaking water bath.
2. *Pellet cells* and wash cells three times in cold buffer A with 1 mg/ml BSA. Take an aliquot of labeling supernatant and of washes to evaluate percent incorporation (Subheading 3.1, **step 5**; *see* **Note 16**). Resuspend cells to 1×10^7/ml with buffer B (Subheading 2.1, **item 2**) with BSA (1 mg/ml).
3. *Stimulation*: For each condition, aliquot cell suspension (2×10^6 cells/condition) to duplicate tubes on ice. Duplicate aliquots should also be added directly to liquid scintillation vials for total radioactivity per condition (total samples; *see* **Note 17**). Warm tubes at 37 °C, then add desired stimulus or solvent (final vol = 0.4 ml).
4. *Termination:* Stop the reaction (except total samples) with the addition of ice-cold buffer B (0.4 ml). Pellet cells ($600 \times g$, 10 min, 4 °C).
5. Remove an aliquot of the supernatant to a scintillation vial (AA released).
6. Discard any remaining supernatant (to radioactive waste), and solubilize cells in 0.4 ml 0.1 N NaOH. Transfer an aliquot of the resultant solution to a scintillation vial.
7. Add scintillation fluid, cap vials, and count vials for 1 min in a liquid scintillation counter with a program for an output of [^{3}H] DPM.

8. *Calculations:* For a sample, average the supernatant (AA released) DPM and the cell-associated DPM from duplicates. The sum of these two fractions should be constant for all conditions and should be similar to the counts in the total samples. Express the [^{3}H] AA release as the percent of the total DPM in the unstimulated cell suspension (total samples).

3.3 PLC

Cells are suspended for suitable stimulation. Cell stimulation is terminated by perchloric acid (PCA) extraction. The extract is neutralized. This aqueous extract is assayed for IP_3 mass using a commercially available radioreceptor assay kit. In this assay, the IP_3 in samples competes with radiolabeled IP_3 for binding to a specific IP_3-binding protein. The IP_3 concentration in samples is then calculated from a standard curve [36–38].

1. *Stimulation*: Warm isolated neutrophils (5×10^6 cell/ml buffer B; Subheading 2.1, **item 2**) and stimulate cells with desired agonist (final vol, 1–2 ml) (*see* **Note 18**).
2. *Extraction of product*: Stop the reaction with the addition of 0.4 vol of ice-cold 20 % PCA (*see* **Note 19**).
3. Vortex and let tube sit on ice 20 min.
4. Pellet precipitated proteins (1,000 × *g*, 10 min, 4 °C) and remove supernatant to a clean tube.
5. Neutralize the extract with 5 M KOH. Pellet (1,000 × *g*, 10 min, 4 °C) the resultant precipitate.
6. Remove neutralized extract to a clean tube and use as sample in the radioreceptor assay as described in the manufacturer's instructions (*see* **Note 20**).

3.4 PLD

Cells are labeled with alkyl-[^{3}H]-lysoPC, washed to remove unincorporated label, and resuspended for stimulation ± ethanol. Cell stimulation is terminated by extraction of cellular lipids. Unlabeled lipid standards are added to the extract, which is then concentrated by drying. The extracted lipids are separated by TLC, and radioactivity in lipid fractions is determined by liquid scintillation counting after scraping fractions from TLC plates. Radioactivity in the PA and/or phosphatidylethanol fractions is normalized to total lipid-associated radioactivity [19].

1. Suspend cells to 3.5×10^7 cells/ml in buffer A (Subheading 2.1, **item 1**) and keep on ice.
2. *Prepare label*: Dry an appropriate volume of stock [^{3}H]-lysoPC (3.2 μCi/ml of cell suspension) under N_2 in a microcentrifuge tube. Add 100 μl of PLD label buffer (Subheading 2.4, **item 2**) and vigorously vortex for 5 min to reconstitute the label. Count a small volume (0.5–1 μl) of the reconstituted label to estimate recovery (*see* **Note 21**).

3. *Labeling incubation*: Add reconstituted label to cell suspension and incubate (30 min, 37 °C) in a shaking water bath.
4. Pellet cells (225 × *g*, 10 min, 4 °C) and save the supernatant (to estimate incorporation of label; Subheading 3.1, **step 5**). Wash cells twice in 10 vol of cold buffer A. Save the supernatants from washes (to estimate incorporation of label; Subheading 3.1, **step 5**). Resuspend cells in cold buffer B (Subheading 2.1, **item 2**) to 1×10^7 cells/ml. Take a small volume (50–100 μl) of this cell suspension to estimate incorporation of label (Subheading 3.1, **step 5**).
5. *Stimulation*: For each condition, aliquot cell suspension (0.5 ml) to duplicate tubes (e.g., capped 15 ml polypropylene) on ice for stimulation and to tubes for analysis of phospholipids (Subheading 3.1, **step 6**). To stimulation tubes, add 0.5 ml buffer B ± ethanol (0.8 % final conc.). Warm tubes for 5 min at 37 °C. Add vehicle or stimulus for the desired time.
6. Stop the reaction with the addition of 3 ml of PLD quench mixture (Subheading 2.4, **item 4**). Vortex (*see* **Note 22**).
7. *Extraction of lipids*: Add 1 ml each chloroform and buffer A to tubes, vortex, and centrifuge (225 × *g*, 5 min, 25 °C) to split phases.
8. Remove bottom phase (chloroform) with a glass Pasteur pipet to screw-top glass tubes (13 × 100 mm; Subheading 2.1, **item 12**). Work in a fume hood.
9. Wash the aqueous (upper) phase twice with chloroform (1 ml). Centrifuge as in **step 7**. Pool bottom phases with the original extract in the glass tube (*see* **Note 23**).
10. Add 5–10 μg of unlabeled PA (egg), monoglyceride (18:1), and phosphatidylethanol (di-18:1) to each tube (*see* **Note 24**).
11. Dry samples under nitrogen. Wash sides of tube 2–3 times during the drying process with chloroform/methanol (9:1, v/v) to recover sample on the walls of tube. Dissolve dried samples in 50 μl chloroform/methanol (9:1, v/v) (*see* **Note 23**).
12. *TLC separation*: Prepare solvent system II (Subheading 2.4, **item 6**) and run a test plate (Silica Gel-GHL plate, 5 × 20 cm; Subheading 3.1, **step 2**) with lipid standards (PC, PE, PA, phosphatidylethanol, mono-, di-, triglycerides) individually and as a mixture to ensure good separation, as judged by visualization with iodine (Subheading 3.1, **step 3**). Develop plates for ~2 h (or ~1 cm from top of plate). In this system, the lipids separate from the origin as follows: PC/PE at the origin, PA, phosphatidylethanol, monoglyceride, diglyceride, triglyceride (near solvent front).
13. Prepare Silica Gel-GHL plate(s) for samples (Subheading 3.1, **step 1**). In a fume hood, spot samples at origin (*small* spots

along the origin line within a lane). Add ~30 μl chloroform/methanol (9:1, v/v) to tube as a rinse and spot the rinse in the appropriate lane. Allow lanes to dry before developing the plate in solvent system II (Subheading 2.4, **item 6**).

14. Let developed plate air-dry (in horizontal orientation) in fume hood. Visualize separated lipid in iodine vapors (Subheading 3.1, **step 3**). Lightly draw pencil lines to mark five fractions to scrape (#1, PC/PE at origin; #2, PA; #3, phosphatidylethanol; #4, monoglycerides; #5, di- and triglycerides).
15. *Scraping TLC plates and quantification: See* Subheading 3.1, **step 4**.
16. *Calculations*: For a sample, average the DPM in lipid fractions of duplicates. Add the average DPM in all fractions for a sample to yield total DPM. Calculate the data as the percent of total DPM in PA or phosphatidylethanol (if ethanol was included in the stimulation conditions; Subheading 3.4, **step 5**).

3.5 PI3K

Cells are incubated with [^{32}P]orthophosphate to label the ATP pool, washed to remove unincorporated label, and resuspended for stimulation. Cell stimulation is terminated by extraction of cellular lipids. Unlabeled lipid standards are added to the extract, which is then concentrated by drying. The extracted lipids are separated by thin layer chromatography (TLC), and radioactivity in lipid fractions is determined by analysis with imaging technology that detects the decay events of ^{32}P. Radioactivity in the PIP_3 fraction is normalized to total lipid-associated radioactivity [33].

1. *Label cells:* Suspend cells at 5×10^7 cells/ml in buffer C (Subheading 2.5, **item 2**). Add [^{32}P]orthophosphate (0.5 mCi/ml) and tightly cap the cell suspension tube (*see* **Note 25**). Incubate the suspension at 37 °C for 60 min (or 25 °C for 90 min) in a shaking water bath, suitably shielded.
2. Collect the labeled cells by centrifugation (225 × *g*, 10 min, 4 °C) and wash cells three times in cold buffer C. Collect the initial supernatant and washes in a well shielded radioactive liquid waste container. Since this is the bulk of the initial radioactivity, dispose of it as soon as possible (*see* **Note 9**).
3. *Stimulation:* Suspend the washed cells in cold buffer D (Subheading 2.5, **item 3**) at 2×10^7 cells/ml. For each condition, aliquot cell suspension (0.5 ml) to duplicate tubes (e.g., capped 15-ml polypropylene tubes) on ice. Warm tubes for 5 min at 37 °C. Add vehicle or stimulus for the desired time.
4. Stop the reaction with the addition of 3 ml of PI3-K quench mixture (Subheading 2.5, **item 4**). Vortex (*see* **Note 22**).
5. *Extraction of lipids*: To each tube add 2.1 ml chloroform, 2.1 ml 2.4 M HCl, and unlabeled phosphoinositides

(10 μg each; *see* **Note 24**). Vortex and centrifuge (225 × *g*, 5 min, 25 °C) to split phases.

6. Remove bottom phase (chloroform) with a glass Pasteur pipet to a screw-top glass tube (13 × 100 mm; Subheading 2.1, **item 12**). Work in fume hood.
7. Wash remaining aqueous phase four times with chloroform (1 ml). Centrifuge as in **Step 5**. Pool bottom phases with original extract in glass tube.
8. Wash each pooled bottom phase once with methanol/1 M HCl (1:1, v/v). Transfer the washed bottom phase to a clean glass tube (*see* **Note 23**).
9. Dry samples under nitrogen. Wash sides of tube 2–3 times during the drying process with chloroform/methanol (9:1, v/v) to recover sample on walls of tube. Dissolve dried samples in 50 μl chloroform/methanol (9:1, v/v) (*see* **Note 23**).
10. *Preparation of TLC plates*: Silica Gel-GHL plates are impregnated with potassium oxalate by developing in solvent system III (Subheading 2.5, **item 6**) overnight (*see* **Note 26**). Allow plate to air-dry. Activate plate by heating at 110 °C for 15 min. Let cool.
11. *TLC separation*: Run a prepared (Subheading 3.5, **step 10**) test plate with lipid standards (PIP, PIP_2, PIP_3, PA, individually and as a mixture) to ensure good separation in solvent system IV (Subheading 2.5, **item 7**), as judged by visualization with iodine (Subheading 3.1, **step 3**). Develop plates to the top of the silica gel, and then develop for an additional 15 min. In this system, the lipids separate from the origin as follows: PIP_3, then PIP_2 and PIP (as a doublet in mid-plate) and PA (near solvent front). When lipid separation is satisfactory, proceed with radiolabeled samples.
12. On prepared (Subheading 3.5, **step 10**) Silica Gel-GHL plates, spot samples at origin (*small* spots along the origin line within a lane). Add ~30 μl chloroform/methanol (9:1, v/v) to tube as a rinse and spot the rinse in the appropriate lane. Allow lanes to dry before developing plate in solvent system IV (Subheading 2.5, **item 7**; *see* **Note 27**).
13. Let developed plate air-dry (in horizontal orientation) in fume hood. Visualize and quantify separated, radiolabeled lipids with a phosphorimaging scanner (e.g., Molecular Dynamics) or comparable instrument. These instruments typically yield radioactivity in terms of density of user-selected areas of the image. This technology eliminates the need to scrape plates.
14. *Calculations*: For a sample, average the density output of the duplicates in each radiolabeled lipid fraction. Add the average density in all fractions for a sample to yield total density. Calculate the data as the percent of total density in PIP_3.

4 Notes

1. Comparable buffered solutions that maintain cell viability and function can be used. Ca^{2+} is excluded from the labeling incubations to minimize cell activation. Note that buffer A, which is phosphate buffered, is not suitable for labeling cells with inorganic phosphate for the measurement of PI3-K activity (Subheadings 2.5, **item 2,** and 3.5, **step 1**).
2. Use solvents in fume hood and collect solvent and radioactive wastes for disposal as prescribed by your institutional environmental safety department.
3. Only Teflon-lined caps should be used with chloroform-containing lipid extracts. Chloroform will dissolve other plastic-lined caps and Parafilm, resulting in contaminated samples. Do not use polystyrene plastics since they are unstable to chloroform. However, polypropylene tubes, which are commonly used for cell incubations, are resistant to chloroform for the short periods needed for the lipid extraction described here.
4. Use the pipetor designed for the glass capillary micropipets to dispense stock radiolabeled compounds and for spotting TLC plates. Do not mouth-pipet solvents or radioactive solutions. Minimize the use of plastic pipet tips for lipid-handling, especially when chloroform is the solvent.
5. Iodine vapor is poisonous. This tank must remain in a fume hood, and always wear gloves to handle any TLC plate.
6. In the previous version of this chapter, a second kit was available from Amersham/GE Healthcare. This kit has been discontinued, but the kit from PerkinElmer compares favorably and, as recently published in another volume of Methods in Molecular Biology [39], the PerkinElmer kit has several improved features. A complete instruction manual is supplied with the kit.
7. Neutrophils are efficiently labeled with this lysoPC, which is acylated in the *sn*-2 position to form PC [19]. The use of this lysoPC to label neutrophils is advantageous because labeling requires relatively short incubations (30–75 min) rather than overnight incubations with a tritiated fatty acid, which is a common practice for cultured cells [40]. A disadvantage of the lysoPC labeling method is that only the PC pool is labeled.
8. This is a modification (acidified) of the Bligh and Dyer [41] extraction mixture.
9. ^{32}P is a strong beta-emitting radionuclide with a short half-life and mCi amounts are required to adequately label cells. From a safety standpoint, it is recommended that fresh radionuclide

be obtained for each experiment and be disposed of quickly after use (through a Radiation Safety department) rather than storing the material in a laboratory setting. A thorough understanding of this radionuclide, its safe handling, and required shielding (plexiglass) is imperative before use.

10. Silica gel absorbs humidity. Heating the plates evaporates the water, which might otherwise compromise the separation of lipids. Let plates cool vertically or in a plate rack. Laying a hot plate on a cooler bench top will crack the plate.
11. Removal of the silica gel at the origin will prevent solvent migration up the plate. Avoid using side edges (~1 cm) of G plates. Lacking a binder, the silica gel on the edges of the plate can be easily scraped off if plates are not handled carefully.
12. Lipids can separate slightly differently when chromatographed in a mixture compared to when they are alone.
13. Scraping of plates should be performed on the bench (not a fume hood) on a clean piece of bench paper. Blades will become dull, use fresh blade as necessary. Weigh papers can be reused for several samples.
14. For solvent system I, add a wick (~50 × 20 cm piece of chromatography paper) to the inside perimeter of the tank when it is prepared. The wick aids in plate development.
15. Iodine interacts with unsaturated lipids, thus not all lipids can be visualized with it. Analysis of the entire plate will ensure that the extent of tritiated-label incorporation is not overestimated.
16. After counting, collect all supernatant and washes in a tritium waste container for disposal.
17. In initial experiments, reserve additional sets of duplicate aliquots for assessment of ^{3}H incorporation into cells (Subheading 3.1, **step 5**) and phospholipid analysis (Subheading 3.1, **step 6**).
18. The cell concentration and final volume can and should be adjusted for experimental dictates. However, an appropriate number of cells per sample should be between 10^6 and 10^7 cells.
19. Water-soluble inositol phosphates can also be extracted by adding an equal volume of ice-cold 15 % trichloroacetic acid. The extract is then washed three times with water-saturated diethyl ether and neutralized to pH 7.5 before assay. Diethyl ether is flammable; work in a fume hood and use suitable precautions.
20. The basal IP_3 content of neutrophils is reported to be 1–2 pmol/million cells [38, 42].

21. Alkyl-[^{3}H]-lysoPC is a sticky lipid and recovery of ≥80 % of the theoretical amount of radioactivity added is desirable using the conversion factor of 2.2×10^6 DPM/μCi. If recovery is low, vortex label again.
22. If two phases are apparent after vortexing, add a few drops of methanol.
23. Extracts can be stored overnight at –20 °C after the flushing tubes with N_2 and capping tightly. Tubes should be warmed to room temperature before proceeding.
24. A mixture of these lipids can be prepared for use as unlabeled carrier lipids. Unlabelled PC and di- and triglycerides need not be added since they are of suitable abundance in the neutrophil sample to be visualized with iodine.
25. Because of the safety issues involved in using these quantities of ^{32}P, it is important to carefully plan all aspects of the experiment, especially the cell labeling procedure, during which the risks of exposure and contamination are the greatest. An initial dry run experiment (without radioactivity) is recommended to help develop a procedure that will minimize exposure and maximize containment of all radioactive material and waste (solid and liquid). It is often necessary to dedicate certain equipment (pipetors, centrifuge buckets, vacuum flask) to ^{32}P-labeling protocols as a means of reducing contamination.
26. The potassium oxalate chelates cations that would otherwise interact with the polyphosphoinositides and thereby interfere with their ability to be separated by TLC.
27. Ensure that plates are run in the same direction in solvent system IV as for the pretreatment in solvent system III.

Acknowledgements

Development of the phospholipase D assay was partially supported by National Institutes of Health grant R01 AI-22564 to L.C.M.

References

1. Vadakekalam J, Metz S (1998) Isotopic efflux studies as indices of phospholipase activation. In: Bird IM (ed) Phospholipid Signaling Protocols. Humana Press, Totowa, NJ, pp 175–185
2. Mueller HW, O'Flaherty JT, Greene DG et al (1984) 1-O-alkyl-linked glycerophospholipids of human neutrophils: distribution of arachidonate and other acyl residues in the ether-linked and diacyl species. J Lipid Res 25:383–388
3. Solodkin-Szaingurten I, Levy R, Hadad N (2007) Differential behavior of sPLA$_2$-V and sPLA$_2$-X in human neutrophils. Biochim Biophys Acta Mol Cell Biol Lipids 1771:155–163
4. Bauldry SA, Wooten RE (1996) Leukotriene B_4 and platelet activating factor production in permeabilized human neutrophils: Role of

cytosolic PLA_2 in LTB_4 and PAF generation. Biochim Biophys Acta Lipids Lipid Metab 1303:63–73

5. Ayilavarapu S, Kantarci A, Fredman G et al (2010) Diabetes-induced oxidative stress is mediated by Ca^{2+}-independent phospholipase A_2 in neutrophils. J Immunol 184:1507–1515
6. Ambruso DR, Ellison MA, Thurman GW et al (2012) Peroxiredoxin 6 translocates to the plasma membrane during neutrophil activation and is required for optimal NADPH oxidase activity. Biochim Biophys Acta Mol Cell Res 1823:306–315
7. Cockcroft S, Stutchfield J (1989) The receptors for ATP and fMetLeuPhe are independently coupled to phospholipases C and A_2 via G-protein(s). Relationship between phospholipase C and A_2 activation and exocytosis in HL60 cells and human neutrophils. Biochem J 263:715–723
8. Bauldry SA, Wykle RL, Bass DA (1988) Phospholipase A_2 activation in human neutrophils. Differential actions of diacylglycerols and alkylacylglycerols in priming cells for stimulation by N-formyl-Met-Leu-Phe. J Biol Chem 263:16787–16795
9. Suire S, Lecureuil C, Anderson KE et al (2012) GPCR activation of Ras and PI3Kγ in neutrophils depends on PLCβ2/β3 and the RasGEF RasGRP4. EMBO J 31:3118–3129
10. Jakus Z, Simon E, Frommhold D et al (2009) Critical role of phospholipase Cβ2 in integrin and Fc receptor-mediated neutrophil functions and the effector phase of autoimmune arthritis. J Exp Med 206:577–593
11. Di VF, Vicentini LM, Treves S et al (1985) Inositol phosphate formation in fMet-Leu-Phe-stimulated human neutrophils does not require an increase in the cytosolic free Ca^{2+} concentration. Biochem J 229:361–367
12. Ferretti ME, Nalli M, Biondi C et al (2001) Modulation of neutrophil phospholipase C activity and cyclic AMP levels by fMLP-OMe analogues. Cell Signal 13:233–240
13. Skippen A, Swigart P, Cockcroft S (2012) Measurement of phospholipase C by monitoring inositol phosphates using [^{3}H]inositol labeling protocols in permeabilized cells. In: Lambert DG, Rainbow RD (eds) Calcium Signaling Protocols. Humana Press, Totowa, NJ, pp 163–174
14. Berridge MJ, Dawson RM, Downes CP et al (1983) Changes in the levels of inositol phosphates after agonist-dependent hydrolysis of membrane phosphoinositides. Biochem J 212:473–482
15. Ali WH, Chen Q, Delgiorno KE et al (2013) Deficiencies of the lipid-signaling enzymes phospholipase D1 and D2 alter cytoskeletal organization, macrophage phagocytosis, and cytokine-stimulated neutrophil recruitment. PLoS ONE 8:e55325
16. Norton LJ, Zhang Q, Saqib KM et al (2011) PLD1 rather than PLD2 regulates phorbol-ester-, adhesion-dependent and Fcγ-receptor-stimulated ROS production in neutrophils. J Cell Sci 124:1973–1983
17. Agwu DE, McPhail LC, Wykle RL et al (1989) Mass determination of receptor-mediated accumulation of phosphatidate and diglycerides in human neutrophils measured by Coomassie blue staining and densitometry. Biochem Biophys Res Commun 159:79–86
18. Wakelam MJO, Powner DJ, Pettitt TR (2008) Determination of phospholipase D, lysophospholipase D and DG kinase signaling pathways in disease states by mass spectrometry. Adv Enzyme Regul 48:254–260
19. Agwu DE, McPhail LC, Chabot MC et al (1989) Choline-linked phosphoglycerides. A source of phosphatidic acid and diglycerides in stimulated neutrophils. J Biol Chem 264:1405–1413
20. Bauldry SA, Elsey KL, Bass DA (1992) Activation of NADPH oxidase and phospholipase D in permeabilized human neutrophils. Correlation between oxidase activation and phosphatidic acid production. J Biol Chem 267:25141–25152
21. Pai JK, Liebl EC, Tettenborn CS et al (1987) 12-O-Tetradecanoylphorbol-13-acetate activates the synthesis of phosphatidylethanol in animal cells exposed to ethanol. Carcinogenesis 8:173–178
22. Hu T, Exton JH (2005) 1-Butanol interferes with phospholipase D1 and protein kinase Cα association and inhibits phospholipase D1 basal activity. Biochem Biophys Res Commun 327:1047–1051
23. Pedruzzi E, Hakim J, Giroud JP et al (1998) Analysis of choline and phosphorylcholine content in human neutrophils stimulated by f-Met-Leu-Phe and phorbol myristate acetate—contribution of phospholipase D and C. Cell Signal 10:481–489
24. Wymann MP, Sozzani S, Altruda F et al (2000) Lipids on the move: phosphoinositide 3-kinases in leukocyte function. Immunol Today 21:260–264
25. Hawkins P, Stephens L, Suire S et al (2011) PI3K signaling in neutrophils. Curr Top Microbiol Immunol 346:183–202

26. Endemann G, Yonezawa K, Roth RA (1990) Phosphatidylinositol kinase or an associated protein is a substrate for the insulin receptor tyrosine kinase. J Biol Chem 265:396–400
27. Ding J, Vlahos CJ, Liu R et al (1995) Antagonists of phosphatidylinositol 3-kinase block activation of several novel protein kinases in neutrophils. J Biol Chem 270:11684–11691
28. Naccache PH, Levasseur S, Lachance G et al (2000) Stimulation of human neutrophils by chemotactic factors is associated with the activation of phosphatidylinositol 3-kinase gamma. J Biol Chem 275:23636–23641
29. Wakelam MJO, Clark J (2011) Methods for analyzing phosphoinositides using mass spectrometry. Biochim Biophys Acta Mol Cell Biol Lipids 1811:758–762
30. van der Kaay J, Cullen PJ, Downes CP (1998) Phosphatidylinositol(3,4,5)trisphosphate (Ptdins(3,4,5)P3) mass measurement using a radioligand displacement assay. In: Bird IM (ed) Phospholipid Signaling Protocols. Humana Press, Totowa, NJ, pp 109–125
31. van der Kaay J, Batty IH, Cross DAE et al (1997) A novel, rapid, and highly sensitive mass assay for phosphatidylinositol 3,4,5-trisphosphate (PtdIns(3,4,5)P3) and its application to measure insulin-stimulated PtdIns(3,4,5)P3 production in rat skeletal muscle in vivo. J Biol Chem 272:5477–5481
32. Cadwallader KA, Condliffe AM, McGregor A et al (2002) Regulation of phosphatidylinositol 3-kinase activity and phosphatidylinositol 3,4,5-trisphosphate accumulation by neutrophil priming agents. J Immunol 169:3336–3344
33. Traynor-Kaplan AE, Thompson BL, Harris AL et al (1989) Transient increase in phosphatidylinositol 3,4-bisphosphate and phosphatidylinositol trisphosphate during activation of human neutrophils. J Biol Chem 264:15668–15673
34. Cockcroft S (1991) Relationship between arachidonate release and exocytosis in permeabilized human neutrophils stimulated with formylmethionyl-leucyl-phenylalanine (fMetLeuPhe), guanosine 5′-[gamma-thio]triphosphate (GTP[S]) and Ca^{2+}. Biochem J 275:127–131
35. Briand SI, Bernier SG, Guillemette G (1998) Monitoring of phospholipase A_2 activation in cultured cells using tritiated arachidonic acid. In: Bird IM (ed) Phospholipid signaling protocols. Humana Press, Totowa, NJ, pp 161–166
36. Anderson R, Steel HC, Tintinger GR (2005) Inositol 1,4,5-triphosphate-mediated shuttling between intracellular stores and the cytosol contributes to the sustained elevation in cytosolic calcium in FMLP-activated human neutrophils. Biochem Pharmacol 69:1567–1575
37. Zhang L (1998) Inositol 1,4,5-trisphosphate mass assay. In: Bird IM (ed) Phospholipid signaling protocols. Humana Press, Totowa, NJ, pp 77–87
38. Fruman DA, Gamache DA, Ernest MJ (1991) Changes in inositol 1,4,5-trisphosphate mass in agonist-stimulated human neutrophils. Agents Actions 34:16–19
39. Heilmann I, Perera IY (2013) Measurement of inositol (1,4,5) trisphosphate in plant tissues by a competitive receptor binding assay. In: Munnik T, Heilmann I (eds) Plant Lipid Signaling Protocols. Humana Press, Totowa, NJ, pp 33–41
40. Arun SN, Xie D, Howard AC et al (2013) Cell wounding activates phospholipase D in primary mouse keratinocytes. J Lipid Res 54:581–591
41. Bligh EG, Dyer WJ (1959) A rapid method of total lipid extraction and purification. Can J Biochem Physiol 37:911–917
42. Thompson NT, Bonser RW, Tateson JE et al (1991) A quantitative investigation into the dependence of Ca^{2+} mobilisation on changes in inositol 1,4,5-trisphosphate levels in the stimulated neutrophil. Br J Pharmacol 103:1592–1596
43. Sergeant S, McPhail LC (2007) Measurement of phospholipid metabolism in intact neutrophils. Methods Mol Biol 412:69–83

Chapter 8

Optical Methods for the Measurement and Manipulation of Cytosolic Calcium Signals in Neutrophils

Maurice B. Hallett, Maha Al-Jumaa, and Sharon Dewitt

Abstract

The measurement and manipulation of cytosolic free Ca^{2+} of neutrophils is crucial for investigating the mechanisms within living neutrophils which generate Ca^{2+} signals and the cellular responses triggered by them. Optical methods for this are the most applicable for neutrophils and are discussed here, especially the use of fluorescent indicators of Ca^{2+} and photoactivation of reagents involved in Ca^{2+} signaling. Both of these synthetic agents can be loaded into neutrophils as lipid-soluble esters or can be microinjected into the cell. In this chapter, we will outline some of the techniques that have been used to monitor, visualize, and manipulate Ca^{2+} in neutrophils.

Key words Calcium signaling, Cytosolic calcium flux, Fluorescent calcium indicator dye, Photoactivation, Calcium imaging

1 Introduction

The measurement and manipulation of cytosolic free Ca^{2+} permits the investigation of the mechanisms of generation of the Ca^{2+} signal and cellular responses to these Ca^{2+} signals within living neutrophils. The optical methods most applicable to neutrophils, which will be discussed here, are (1) the use of fluorescent indicators of Ca^{2+} and (2) photoactivation of reagents involved in Ca^{2+} signaling. Both of these synthetic agents can be loaded into neutrophils as lipid-soluble esters or can be microinjected into the cell. In this chapter, we will outline some of the techniques that have been used to monitor, visualize, and manipulate Ca^{2+} in neutrophils. Further details of some of these methods are given in ref. 1. A discussion of other methods not discussed here, such as the expression of luminescent and fluorescent indicators of Ca^{2+}, is given in ref. 2.

The fluorescent Ca^{2+} chelator probes developed by RY Tsien have opened up the study of cytosolic free Ca^{2+} in small cells, including neutrophils [3, 4]. The ester method of loading the

Mark T. Quinn and Frank R. DeLeo (eds.), *Neutrophil Methods and Protocols*, Methods in Molecular Biology, vol. 1124,
DOI 10.1007/978-1-62703-845-4_8,

probe into the cytosol of neutrophils works successfully. These indicators can be synthesized or purchased with the ester groups, which both "mask" the Ca^{2+} binding part of the molecule and make them lipid soluble. Thus the ester derivative readily crosses the plasma membrane and enters the neutrophil cytosol. Here, esterases cleave the ester bond to generate the acid form of the probe, which becomes entrapped within the cell as it is hydrophilic and thus unable to easily cross the plasma (or other) membrane. It is the acid form of the probe that is also the Ca^{2+} sensing form. There are two potential problems with this approach: (1) the accumulation of indicator into organelles and (2) partial (rather than full) hydrolysis of the probe to generate products with increased hydrophilicity, but that are insensitive to Ca^{2+} [5]. However, these problems are easily avoided in the protocols given and the measurement methodologies would detect such problems. It is, however, important to limit the amount of probe loaded in this way because (1) as the indicator is a Ca^{2+} chelator, it will buffer cytosolic free Ca^{2+} changes and "blunt" the very response that is being measured and (2) there is a toxicity associated with the products of de-esterification of the probe (namely, formaldehyde and H^+ ions), which can cause a reduction in ATP levels in neutrophils [6] and may have other toxic effects on the cell, including stimulation of cell aggregation. Some of these problems can be overcome by microinjection of nonesterified forms of the probes or high molecular weight forms that do not accumulate in organelles [1, 7], thereby circumventing the problems of location and toxicity associated with ester loading. SLAM (simple-lipid-assisted microinjection) and electroinjection (*see* Chapter 20) work well with neutrophils and are the methods of choice [8].

2 Materials

1. The properties of fluorescent Ca^{2+} probes suitable for use in neutrophils are given in Table 1. These reagents and those for manipulation of cytosolic free Ca^{2+} are available from many vendors.
2. SLAM micropipettes (Warner Instruments).

3 Methods

3.1 Selecting the Appropriate Fluorescent Ca^{2+} Probe

3.1.1 Ca^{2+} Affinity

There are now a myriad of commercially available Ca^{2+} probes, many of which are available as ester derivatives suitable for cytosolic loading into neutrophils (*see* Table 1). When selecting which probe to use, it is important to consider its Ca^{2+} affinity. As in other cell types, neutrophils have resting cytosolic free Ca^{2+} concentrations of near 100 nM. On stimulation this rises transiently to near 1 μM.

Table 1
Fluorescent Ca^{2+} probes useful in neutrophils

	K_d (Ca^{2+}, nM)	Excitation (nm)	Emission (nm)	Mode
Calcium crimson	205	588	611	S
Calcium green-1	189	506	534	S
Calcium green-2	574	506	531	S
Calcium green-5 N	3,300	506	531	S
Calcium orange	328	554	575	S
FFP-18	400	340 and 380	505	R
Fluo3	864	506	526	S
Fluo3FF	62,000	506	526	S
Fluo4	345	494	516	S
Fura red	133	420 and 480	640	R
Fura2	224	340 and 380	505	R
FuraFF	38,000	340 and 380	504	R
Indo-1	250	340	410 and 485	R
Mag-fura-2	25,000	340 and 380	504	R
Mag-fura-5	28,000	340 and 380	504	R
MOMO	nd	~495	~515	S
Quin2	114	340	490	S
Rhod-2	1,000	553	576	S

All these probes are available as cell-permeant esters. The mode of use is given as single wavelength (*S*) or the ratio of two wavelengths (*R*)

As the fluorescent signal depends upon the binding of Ca^{2+} to the probe, the Ca^{2+} dissociation constant, K_d, will define the range over which the probe can be usefully employed. A probe with a K_d of 300 nM will be only approx 25 % saturated in the resting cell, and thus, 75 % of its dynamic range will be available to monitor a rise in cytosolic free Ca^{2+}. It will, however, be difficult to measure cytosolic free Ca^{2+} concentrations above 1–3 μM, as the probe will be more than 90 % saturated with Ca^{2+}. In contrast, a probe with a k_d of 1 μM would be more useful for higher Ca^{2+} changes. The K_d for Ca^{2+} will also determine its Ca^{2+} buffering effect within the cytosol. Fortunately, neutrophils have high endogenous Ca^{2+} buffering, with estimates ranging from 1:1,000 to 1:3,000 [6, 9]. An intracellular fura2 concentration of 25–50 μM is thus estimated to increase the Ca^{2+} buffering by only about 10 %. With probes of higher k_d such as fluo3 or fluo4, the buffering effect would be even less.

3.1.2 Single or Dual Wavelength Ca^{2+} Probes

There are two types of fluorescent Ca^{2+} probe: (1) those that change their signal at two wavelengths, on either excitation or emission (ratiometric dyes), and (2) those that change their signal at only one wavelength (*see* Table 1). The single wavelength, non-ratiometric indicators, such as fluo3 or fluo4, can also be excited at visible wavelengths (such as 488 nm, a wavelength produced by laser light). Techniques involving confocal microscopy are powerful for locating the Ca^{2+} change within neutrophils and also can give information on fast time scales (1–10 ms). However, as the indicators produce only a single intensity change on binding Ca^{2+}, caution must be exercised in interpreting an increase in intensity as being solely due to an increase in cytosolic free Ca^{2+} concentration. For example, if a brightly loaded organelle moves into the confocal imaging plane, this would give an increased fluorescent signal unrelated to cytosolic free Ca^{2+} concentration. For this reason, it is recommended that Ca^{2+} measurements are initially performed using ratiometric indicators where there is certainty that the ratio change would be caused by a Ca^{2+} signal. The excitation spectrum of perhaps the most widely used indicator, fura2, shifts on binding Ca^{2+}, so that there is significant fluorescence from both the Ca^{2+}-bound and the Ca^{2+}-free forms of the probe. This permits monitoring of both the Ca^{2+}-free and the Ca^{2+}-bound forms of the indicator. By monitoring two wavelengths, one on either side of the isoemissive point (usually 340 and 380 nm), a reassuring fluorescent "Ca^{2+} signature" is observed, with the signal at one wavelength rising while the signal at the other wavelength declining.

3.2 "Ester Loading" Procedure for Neutrophils

It is crucial (*see* **Note 1**) that the loading medium contains Ca^{2+} (e.g., 1–2 mM) because as the Ca^{2+} chelator is generated within the cytosol, it will bind Ca^{2+} (the extent depending on its k_d). Without additional extracellular Ca^{2+} to replace this, Ca^{2+} will be displaced from Ca^{2+} stores within the cell (or worse, not replaced at all). Another important point in the method is the 1,000-fold dilution of the ester stock solution. This gives an acceptably low concentration of the solvent dimethyl sulfoxide (DMSO). DMSO can have toxic effect on neutrophils and it is therefore important that it is kept to a minimum. At 0.1 % (i.e., 1/1,000), the effects of DMSO are minimal. The steps given below marked by an asterisk can be omitted:

1. Dissolve ester in dry DMSO (*see* **Note 1**) to give a stock (1–5 mg/mL). Store at –20 °C.

2*. Mix 2.5 μL pluronic (25 %w/v in DMSO) with 5 μL of ester stock. This step may assist transfer into the neutrophils, pluronic being a "dispersing agent," which assists in keeping the ester in solution.

3. Add 1 μL of ester to 1 mL of neutrophil suspension (*see* **Note 2**) of $1–50 \times 10^6$ cell/mL in Ca^{2+} containing medium.

4. Incubate neutrophils for 20–60 min (room temperature or 37 °C). Note that for FFP18-AM, several hours are required to generate sufficient FFP on the inner surface of the plasma membrane to be useful.
5. Resuspend neutrophils in fresh medium.
6*. Store neutrophils on ice to reduce leakage of Ca^{2+} probe.
7. It is recommended that before accepting that loading has been successful, the following simple checks are made.
   (a) Check fluorescence at 360 nm excitation (505 nm emission) is significantly higher than in non-loaded cells. Record excitation or emission spectrum (quartz cuvette or optics) of loaded neutrophils to ensure that conversion of ester to its acid is complete. (For fura2, the ester and the acid have clearly different spectra, *see*, e.g., Molecular Probes Handbook.)
   (b) Treat neutrophils with either digitonin (150 mM) or Ca^{2+} ionophore (nonfluorescent ionomycin or Br A23187). Check the spectral change is consistent with Ca^{2+} saturation for the probe, e.g., for fura2 the excitation spectrum peaks at 340 nm. Add EGTA (20 mM) and check spectral change is consistent with zero saturation for the probe, e.g., for fura2 excitation peak is shifted towards 380 nm with the two spectra cross at ~360 nm.
   (c) Observe the fluorescence microscopically (e.g., Zeiss filters LP420/G365 or similar) to check loading has no obvious nonuniformity (i.e., in granules or phagosomes).

3.3 Measurement of Cytosolic Free Ca^{2+}

1. For a single wavelength indicator, the cytosolic free Ca^{2+} concentration can be calculated from:

$$Ca^{2+} = K_d \left(F - F_{min}\right) / \left(F_{max} - F\right) \quad (1)$$

where F is the fluorescent signal through the experiment, and F_{min} and F_{max} are the minimum and maximum obtainable signal from the indicator in the presence and absence of saturating amounts of Ca^{2+}. F_{max} and F_{min} are obtained at the end of the experiment by permeabilizing the cell (with ionophores) in the presence of Ca^{2+} and then chelating the Ca^{2+} with EGTA.

1. The single wavelength approach may be used confocally or flow cytometrically but is not advised for conventional fluorometry or imaging. For these latter procedures, ratio dyes are preferable.
2. The ratio of the two signals will be independent of the concentration (or amount) of probe, and the free Ca^{2+} required to give this signal ratio can be calculated:

$$Ca^{2+} = K_d \beta \left(R - R_{min}\right) / \left(R_{max} - R\right) \quad (2)$$

where $\beta = Sf2/Sb2$ and Sxy is the emission signal at wavelength y ($y = 1$ for 340 nm and 2 for 380 nm) from the fully Ca^{2+} saturated indicator ($x = b$), totally Ca^{2+}-free indicator ($x = f$) or variable Ca^{2+} saturation in the cell during the experiment ($x = v$), and $R = Sv1/Sv2$, $R_{max} = Sb1/Sb2$, and $R_{min} = Sf1/Sf2$.

3. The characteristic "Ca^{2+} signature" can be confirmed to originate solely from a change in Ca^{2+} by noting that the sum, $ASv1 + Sv2$ (where $A = (Sf2 - Sb2)/(Sb1 - Sf1)$, will be constant at all Ca^{2+} concentrations [6]. The R_{max} and R_{min} values are essential for the calculation and are usually taken at the end of the experiment by the addition of ionomycin or digitonin (to allow Ca^{2+} saturation) and then EGTA (to remove Ca^{2+} from the probe) (*see* **Note 3**).

3.4 Measurement Protocols

3.4.1 Fluorometry

1. Add cell suspension to quartz or UV transmissible cuvette. Keep stirred to ensure that cells remain in the illumination beam. Set temperature (37 °C).
2. Set fluorometer to illuminate and record emission at the appropriate wavelengths. Record single or dual wavelength data as appropriate (*see* Table 1).
3. Once data points are constant (i.e., after warm-up time), add stimulus while recording (*see* Fig. 1).
4. At the end of the experiment, add ionomycin (1–4 μM) or digitonin (150 mM) to saturate the probe.
5. Once saturation has occurred, add EGTA 20 mM (*see* Fig. 1).
6. Note the parameters listed below and calculate the cytosolic free Ca^{2+} concentration throughout the time-course using the appropriate equation given earlier and in Fig. 1.

3.4.2 Microfluorometry

1. By optically coupling a wavelength changer to the input port and a photomultiplier tube to the output port of a fluorescent microscope, the procedure given above can be used with individual cells.
2. In order to reduce background signal from areas of the field not occupied by the cells (or by other cells), a pinhole in the focal plane can be useful. This could be either fixed, so that the cell is moved to the pinhole by the microscope stage, or moveable. However, as neutrophils, by their nature, tend to move as part of their response, it is preferable to replace the photomultiplier tube with an intensified CCD camera.
3. A "virtual mask" can be set up by binning the data from the region of the image that includes the cell of interest (*see* **Note 4**). This approach has several advantages: (1) the cell is visualized

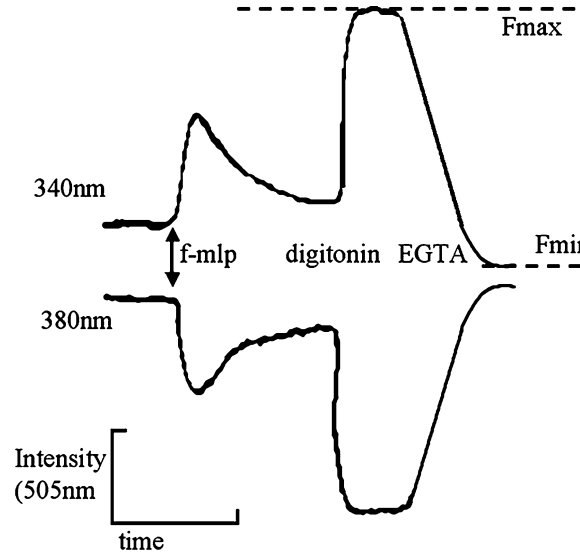

Fig. 1 A typical experiment in which cytosolic free Ca^{2+} concentration is monitored by fura2. The emission at 505 nm is recorded for excitation at 340 and 380 nm as indicated. A stimulus is added which produces the "Ca^{2+} signature." The addition of digitonin and then EGTA is for calibration. For a signal wavelength probe, the values of F_{max} and F_{min} are used. For a dual wavelength probes (as here), R_{max} and R_{min} are calculated from the two signals. Reproduced from [22] with permission from Humana Press

and so artifacts caused by cell movement are immediately apparent, and (2) as the masks are electronic, several "masks" can be defined that read out the ratio values of more than one individual cell in the field.

4. Digitonin should not be used in microfluorometry to determine F_{max}, as the Ca^{2+} indicator will be lost from the neutrophils (*see* **Note 3**). When this happens, the indicator will no longer be within the defined area and the information gathered will not be meaningful. It is therefore recommended that ionomycin is used to provide the maximum and minimum signals under these conditions.

3.4.3 *Flow Cytometry*

1. Measurement of cytosolic free Ca^{2+} concentration within individual cells as a cell population is possible using flow cytometry.
2. Time-course of Ca^{2+} changes can be achieved by addition of stimulus to the population as it passes through the cytometer. Caution must be exercised in the interpretation of these data as, although individual cells are being interrogated, no single cell is followed through the time-course and the same changes are merely population average changes. These often do not reflect changes at the single-cell level. For example, unless

stimulus-induced Ca^{2+} spikes are synchronized within the population, these will not be observed by flow cytometry).

3. With a UV laser cytometer, Indo-1, which can be used ratiometrically (*see* Table 1), is the probe of choice. However, single wavelengths indicators such as fluo3 and calcium green have been successfully used with conventional 488 nm lasers.

3.5 Imaging Ca^{2+} in Individual Neutrophils

3.5.1 Ratiometric Imaging

1. The fluorescent intensity at any point within the 2-D microscopic image of the cell will be proportional to the amount of probe in that "line of sight." Thus, it will be brighter at the center of the cell, where it is thicker, than at the edge, where the cell may become progressively thinner. Thus, it is helpful to use a ratiometric probe and take a ratio of two images to provide a "Ca^{2+} map" of the cytosolic free Ca^{2+} (*see* also **Note 5**). In order to achieve this, changing excitation wavelength must be synchronized with the acquisition of images, often by a spinning filter wheel, optical chopper, or rapid-changing monochromator. These are commercially available from many sources including PTI and Cairn Instruments.
2. Imaging is best achieved by coupling the wavelength changer to the "fluorescent input" of the microscope and either a digital camera or a video camera to the "output." Digitization of the signal to provide an array of pixels each with a value that corresponds to the intensity of the fluorescent image in that region of the field is then recorded.
3. After background subtraction, the ratio is calculated, and a lookup table (LUT) is used to provide color on the image corresponding to the cytosolic free Ca^{2+} concentration (Ca^{2+} map).
4. With an intensified video camera, the speed of acquisition is probably 25–30 frames/s, so that one ratio image would take about 80 ms. The time taken to change wavelengths can be minimized by using fast filter wheels, optical choppers, or rapid changing monochromators. However, the image quality is often poor at high speed and it is usually necessary to average a number of frames, thus increasing the signal but decreasing the time resolution or bin pixels to increase the signal (but decreased spatial resolution, **Note 4**). The need to do either is reduced by using image intensification, but in practice, useful ratio images can rarely be acquired faster than about 1 s^{-1}. The speed barrier is overcome by rapid confocal imaging (*see* Subheading 3.6).
5. Other problems associated with Ca^{2+} imaging include photobleaching of the probe (*see* **Note 4**) and light-induced activation of the neutrophil under view (*see* Subheading 3.8 and **Note 6**). Fuller details of Ca^{2+} imaging artifacts and their solution may be found in ref. 2.

3.5.2 Confocal Imaging

1. The single wavelength probes (e.g., fluo4 and calcium green) can only confidently be used with confocal imaging, because unlike conventional microscopy, confocal microscopy images only an optical section through the cell of a defined thickness. Therefore, the problems associated with cell thickness artifacts are eliminated. This optical sectioning enables Ca^{2+} to be monitored within the nucleus, through the cell perpendicular (*xz-plane*) to the normal viewing plane or at any predefined locus [10].
2. It is important to be aware that the cytoplasm of living cell is neither homogeneous nor static [11, 12]. This can give differences in the intensity of the fluorescence signal observed which are unrelated to Ca^{2+} concentration [11]. This problem is particularly apparent in granular cells, such as neutrophils, which undergo chemotaxis. The leading edge and pseudopodia (e.g., during phagocytosis) can often be devoid of granules and give significantly higher fluorescent signals [11–13].
3. One solution to this problem is to double label the neutrophils with both a Ca^{2+}-sensitive and Ca^{2+}-insensitive probe. A ratio of the two images will be independent of the spatial optical artifact and so give a spatial pure distribution of Ca^{2+} signaling despite changes in the cell morphology.

3.6 Rapid Ca^{2+} Imaging in Neutrophils

1. Many of the Ca^{2+} signals in neutrophils have time scales that can be measured over 10–100 s. However, it is becoming more evident that these Ca^{2+} events may be composed of faster events occurring on the millisecond time scale [14].
2. Confocal laser scanning of a single line repeatedly (*xt* scanning) through individual fluo3-loaded neutrophils can be used to accumulate data at a rate of at least 80 lines/s, giving a time resolution of greater than 12.5 ms with events in the cell distinguishable to about 0.1–0.2 μm lateral resolution [15].
3. Conventional confocal laser scanning in both *x* and *y* directions is necessarily slower, but resonant scanning in the *x* direction can generate useful images at 17.5 ms/frame and a rotating Nipkow disk (a series of pinpoints in the rotating disk) scans multiple laser beams across the field at up to 360 frames/s (3 ms/frame).

3.7 Near Membrane Ca^{2+} in Neutrophils

1. An analogue of fura2, FFP-18, with a long hydrophobic tail, accumulates in the membranes rather than the cytosol and has been used to monitor near plasma membrane Ca^{2+} in neutrophils [16, 17].
2. More recently, an equivalent "near membrane" probe excitable by visible light, MOMO (Table 1), has become available. However, this probe is more hydrophilic and partitions into the nuclear membrane of neutrophils (Fig. 2) and is excluded

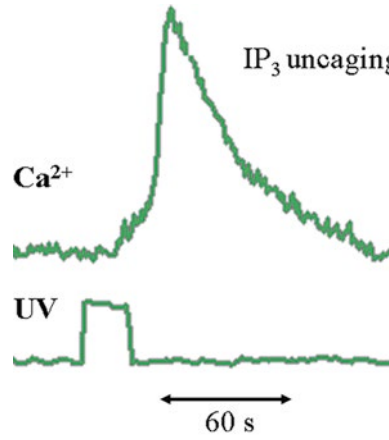

Fig. 2 Effect of uncaging IP_3 on neutrophil cytosolic free Ca^{2+}. The *upper trace* show the change in cytosolic free Ca^{2+}, monitored by fluo4 intensity, and the *lower trace* the pulse of UV illumination. It can be seen that there is a lag of several seconds before the Ca^{2+}begins to rise slowly. This is not observed when the cells are stimulated by fmlp or similar against. When the cytosolic Ca^{2+} reaches a critical point, a robust Ca^{2+} signal is fired. This latter signal is sufficient to trigger a cell spreading response

from within the nuclear lobes. It is useful for locating Ca^{2+} signals which originate near the nuclear boundary. In contrast, FFP-18-AM is hydrophobic and can be loaded into neutrophils from its AM ester [16, 17]. The esterified probe binds quickly to the neutrophil membrane and there follows a slow process (presumably limited by the rate of "flip-flop" diffusion of the probe across the cell membrane) where the AM ester is cleaved on the cytosolic facing leaflet of the plasma membrane [17]. Although the process is slow and requires hours to load, it may be useful approach to visualizing near membrane Ca^{2+} events. Furthermore, it can be used non-ratiometrically with an excitation from a UV diode lasers emitting at 410 nm.

3. With confocal imaging, the signal increase due to near membrane Ca^{2+} events can easily be seen. However, extreme caution must be exercised as the dye equilibrates across a number of membranes in the neutrophil, especially nuclear envelope.
4. Without ratiometric measurement, it is not possible to distinguish high fluorescence which results from high dye content from that which results from high Ca^{2+}.

3.8 Manipulating Cytosolic Ca^{2+} in Neutrophils by Photolysis

1. Cytosolic free Ca^{2+} within neutrophils can be manipulated on demand by photorelease of "caged Ca^{2+}" (e.g., nitr5), "caged Ca^{2+} chelator" (e.g., diazo-2), or caged IP_3 at defined times. These three "caged" compounds can be loaded into cells from

their available acetoxymethyl esters. Other (nonesterified) caged compounds can also be introduced into cells by microinjection techniques described in this volume.

2. The "caged" compound is inert until photolysis. In the case of "caged Ca^{2+}," the affinity of the chelator for Ca^{2+} changes dramatically on photolysis at 360 nm. In this way, the cytosolic free Ca^{2+} concentration can be elevated on photolysis [18].
3. Caged-IP_3 AM can be loaded into neutrophils in the same way as described above for fluorescent probes. The IP_3 concentration within the cytosol is then stepped up on photolysis (Fig. 2).
4. The efficiency of the uncaging system can be monitored using caged fluorescein as an easily quantifiable output. However, the optical situation within the neutrophil cytosol is more complex.
5. Another approach is to use nitr5 (caged Ca^{2+}) and to monitor the output (elevation of cytosolic Ca^{2+}). Our system causes of uncaging of Ca^{2+} (nitr5) to elevate cytosolic free Ca^{2+} in neutrophils at a rate of about 10 nM/s, equivalent to 1 μM/s total Ca^{2+} released (taking account of cytosolic Ca^{2+} buffering capacity of about 100:1).
6. Since the ratio of uncaging efficacy (uncaging index = $\varepsilon\phi$ of the photosensitive bonds in nitr5 to that in caged IP_3) is 0.24 [19], the rate of uncaged IP_3 can be estimated at 4 μM/s. We estimate that during the delay between the onset of uncaging and the Ca^{2+} signal, the IP_3 concentration in the neutrophils thus rises to about 20 μM.
7. Since the cytoplasm is optically nonuniform [11–13], the location of uncaging may be important. It is possible to compare the efficiencies of UV delivery to the cytosol using the photoconversion of dihydroethidium (Hydroethidine) to the ethidium, which fluoresces on binding to the neutrophil nucleus and acts as a surrogate monitor of cytosolic UV exposure [20].
8. Care must be taken to perform appropriate uncaging controls in neutrophils, e.g., performing sham photolysis (i.e., no caged compound) or photolysis of presumed biologically inert compounds (e.g., fluorescein).

4 Notes

1. De-esterification that is catalyzed enzymatically in the cell will also occur spontaneously (at a slow rate). If this occurs before presentation to the cells, the probe will either not be able to enter the cells or enter the cells in the partially de-esterified, but in the non-Ca^{2+}-sensitive form. Hydrolysis in the stored stock

solution is slowed by reduced temperature and the exclusion of water. As DMSO is hydroscopic and will readily absorb water from the air, standard laboratory-grade DMSO is not recommended. Dry DMSO can be purchased in sealed containers in smaller volumes (Sigma). Another precaution that can reduce the water content of the solution is to be sure when taking the container from the freezer (at –20 °C) to let it warm up to room temperature before opening it. If this is not done, water from the air may condense on the inner surface of the container, contaminate the stock solution, and increase ester hydrolysis.

2. Extracellular Ca^{2+} must be present during the time that the Ca^{2+} chelating probe is loaded into the cells, so that it can replace Ca^{2+}, which will be bound to the probe. Otherwise, Ca^{2+} will be removed from intracellular sites. However, provided these precautions are taken, Ca^{2+} chelating probes have little obvious (adverse) effect on Ca^{2+} signaling. However, omission of extracellular Ca^{2+} during loading has been used as a deliberate strategy for "depleting cell Ca^{2+}" in order to establish an intracellular role for this ion in a particular cell activity.
3. Digitonin is often preferred when measuring cytosolic free Ca^{2+} concentration in a cell population in suspension as it ensures that all fura2 gains access to high Ca^{2+} concentration in the extracellular medium. If ionomycin is used (e.g., during Ca^{2+} imaging), it is important that sufficient ionomycin is added to produce a truly maximal fluorescence signal, as it is possible to elevate cytosolic free Ca^{2+} with ionophores to concentrations that are less than μM. Under these latter conditions, the ionomycin signal will not correspond with R_{max} and cytosolic free Ca^{2+} concentration cannot be correctly calculated. The problem can be reduced by also increasing the extracellular Ca^{2+} concentration during the addition of ionomycin.
4. The information in a single pixel is limited by the noise associated with the detection system of the imager. A technique often used, called binning, is to collect the data from a pixel plus its neighbors and to treat the combined signal as though arising from a larger single pixel. Binning of information on neighboring pixels will increase the signal but decrease the spatial resolution. A statistical approach can be used to determine whether small areas within the cell truly have raised Ca^{2+}. Areas of interest in the image (with n pixels) can be chosen, for comparison of their cytosolic free Ca^{2+} concentration. The areas will have statistically significant cytosolic free Ca^{2+} concentrations when $n > 2[\sigma(Z_2\alpha + Z_{2\beta})/\delta]^2$ or $\delta > [\sqrt{(2/n)}][\sigma(Z_2\alpha + Z_{2\beta})]$, where n is the number of pixels in each of the two areas of the image, σ is the standard deviation of the distribution of Ca^{2+} values in the pixel arrays, Zx is the standard normal deviate exceeded with probability x, β is the significance level for the test, $(1 - \beta)$ is the

power of the test, and δ is the difference in cytosolic free Ca^{2+} concentrations [21]. It can be seen that the ability to detect small and localized changes in Ca^{2+} depends on both the magnitude of the Ca^{2+} change and the area it occupies. Detection of both very small and very localized Ca^{2+} changes is thus difficult and ultimately limited by the image noise, i.e., the variance (standard deviation) of individual pixel values.

5. The major problems associated with fluorescent imaging are photobleaching and image noise. Photobleaching arises where excessive excitation results in the destruction of the fluorescent molecules and hence a reduction in the emission intensity (bleaching). Each fluorescent molecule emits about 10^4–10^5 photons/molecule before photolysis. With ratiometric methods, photobleaching is less of a problem as the ratio will remain constant during the bleaching provided that the pairs of images are taken close together in time (when no significant bleaching has occurred). With non-ratiometric confocal Ca^{2+} imaging, bleaching during the time of the experiment can be avoided by attenuating the laser light and increasing the detector (photomultiplier) sensitivity so that the minimum usable emission intensity is employed.
6. Ratiometric dyes require excitation near the UV region, which stimulate fluorescence from endogenous molecules such as NADPH within neutrophils, and consequently the signal-to-noise ratio of the Ca^{2+} probe is reduced.

References

1. Hallett MB, Hodges R, Cadman M, Blanchfield H, Dewitt S, Pettit EJ et al (1999) Techniques for measuring and manipulating free Ca^{2+} in the cytosol and organelles of neutrophils. J Immunol Methods 232:77–88
2. Tepikin AV (2000) Calcium signalling: a practical approach, 2nd edn. Oxford University Press, Oxford, p 230
3. Pozzan T, Lew DP, Wollheim CB, Tsien RY, Rink TJ (1983) Is cytosolic ionized calcium regulating neutrophil activation? Science 221:1413
4. Hallett MB, Davies EV, Pettit EJ (1996) Fluorescent methods for measuring and imaging the cytosolic free Ca^{2+} in neutrophils. Methods 9:591–606
5. Scanlon M, Williams DA, Fay FS (1987) A Ca^{2+}-insensitive form of fura2 associated with polymorphonuclear leukocytes-assessment and accurate Ca^{2+} measurement. J Biol Chem 262:6308
6. Al-Mohanna FA, Hallett MB (1988) The use of fura 2 to determine the relationship between intracellular free Ca^{2+} and oxidase activation in rat neutrophils. Cell Calcium 8:17
7. Laffafian I, Hallett MB (1998) Lipid-assisted microinjection: introducing material into the cytosol and membranes of small cells. Biophys J 75:2558–2563
8. Laffafian I, Hallett MB (2000) Gentle microinjection for myeloid cells using SLAM. Blood 95:3270–3271
9. Von Tscharner V, Deranleau DA, Baggiolini M (1986) Calcium fluxes and calcium buffering in human neutrophils. J Biol Chem 261: 10,163
10. Pettit EJ, Hallett MB (1996) Localised and global cytosolic Ca^{2+} changes in neutrophils during engagement of CD11b/CD18 integrin visualised using confocal laser scanning reconstruction. J Cell Sci 109:1689–1694
11. Dewitt S, Darley R, Hallett MB (2009) Translocation or just location? Pseudopodia affect fluorescent signals. J Cell Biol 184: 197–203
12. Dewitt S, Hallett MB (2011) Optical complexities of living cytoplasm—implications for live cell imaging and photo-micromanipulation techniques. J Microsc 241:221–224

13. Hallett M, Dewitt S (2011) A trick of the light: the optical properties of living cytoplasm which can mislead. Integr Biol 3: 180–184
14. Hillson EJ, Hallett MB (2007) Localised and rapid Ca^{2+} micro-events in human neutrophils: conventional Ca^{2+} puffs and global waves without peripheral-restriction or wave cycling. Cell Calcium 41:525–536
15. Pettit EJ, Hallett MB (1995) Early Ca^{2+} signalling events in neutrophils detected by rapid confocal laser scanning. Biochem J 310:445
16. Davies EV, Hallett MB (1996) Near membrane Ca^{2+} changes resulting from store release in neutrophils: detection by FFP-18. Cell Calcium 19:355–362
17. Davies EV, Hallett MB (1998) High micromolar Ca^{2+} beneath the plasma membrane in stimulated neutrophils. Biochem Biophys Res Commun 248:679–683
18. Pettit EJ, Hallett MB (1998) Release of "caged" cytosolic Ca^{2+} triggers rapid spreading of human neutrophils adherent via integrin engagement. J Cell Sci 111:2209–2215
19. Ellis-Davies GCR (2007) Caged compounds: photorelease technology for control of cellular chemistry and physiology. Nat Methods 4:619–628
20. Brasen JC, Dewitt S, Hallett MB (2010) A reporter of UV intensity delivered to the cytosol during photolytic uncaging. Biophys J 98:L25–L27
21. Armitage P, Berry G (1987) Statistical methods in medical research, 2nd edn. Blackwell Scientific, Boston, MA, pp 181–182
22. Hillson EJ, Dewitt S, Hallett MB (2007) Optical methods for the measurement and manipulation of cytosolic free calcium in neutrophils. In: Quinn MT, DeLeo FR, Bokoch GM (eds) Methods in molecular biology, 412th edn. Humana Press, Totowa, NJ, pp 125–138

Chapter 9

Analysis of Electrophysiological Properties and Responses of Neutrophils

Deri Morgan and Thomas E. DeCoursey

Abstract

The past decade has seen increasing use of the patch-clamp technique on neutrophils and eosinophils. The main goal of these electrophysiological studies has been to elucidate the mechanisms underlying the phagocyte respiratory burst. NADPH oxidase activity, which defines the respiratory burst in granulocytes, is electrogenic because electrons from NADPH are transported across the cell membrane, where they reduce oxygen to form superoxide anion (O_2^-). This passage of electrons comprises an electrical current that would rapidly depolarize the membrane if the charge movement were not balanced by proton efflux. The patch-clamp technique enables simultaneous recording of NADPH oxidase-generated electron current and H^+ flux through the closely related H^+ channel. Increasing evidence suggests that other ion channels may play crucial roles in degranulation, phagocytosis, and chemotaxis, highlighting the importance of electrophysiological studies to advance knowledge of granulocyte function. Several configurations of the patch-clamp technique exist. Each has advantages and limitations that are discussed here. Meaningful measurements of ion channels cannot be achieved without an understanding of their fundamental properties. We describe the types of measurements that are necessary to characterize a particular ion channel.

Key words Proton current, Ion channels, pH, Zinc, Phagocyte, Respiratory burst, NADPH oxidase, Electrophysiology, Patch clamp

1 Introduction

Ion channels are a diverse group of proteins, representatives of which are found in all plasma membranes. Channels allow the regulated passage of ions across cell membranes, which otherwise have extremely low permeability to ions. Ion channels perform a wide variety of functions in a large number of cellular processes. The development of the voltage-clamp method revolutionized the study

AA arachidonic acid, *DPI* diphenylene iodonium, g_H proton conductance, $O_2^{\bullet-}$ superoxide anion, pH_i intracellular pH, pH_o extracellular pH, *PKC* protein kinase C, *PMA* phorbol myristate acetate, TEA^+ tetraethylammonium ion, TMA^+ tetramethylammonium, *ATP* adenosine triphosphate, *GTPγs* guanosine triphosphate γs, V_{rev} reversal potential, V_{hold} holding potential, $V_{thresbold}$ channel opening potential, g_H proton conductance, τ_{act} time constant of activation, P_{open} open probability, I_{hold} holding current, I_e electron current, E_H equilibrium potential for protons, γ single channel conductance

Mark T. Quinn and Frank R. DeLeo (eds.), *Neutrophil Methods and Protocols*, Methods in Molecular Biology, vol. 1124,
DOI 10.1007/978-1-62703-845-4_9,

of ion channels in excitable cells such as neurons and muscle [1]. The patch-clamp technique [2] dramatically extended the power of the voltage-clamp approach by making it possible to record current through individual ion channels and to faithfully record currents in the membranes of even the smallest cells. Knowledge of the presence and functions of ion channels in non-excitable cells, such as epithelial cells and immune cells, has mushroomed from virtually nothing a quarter of a century ago to thousands of papers. Researchers now have the luxury of engaging in heated arguments about the functions performed in these cells by ion channels that were not even known to exist a few decades ago. The first patch-clamp study on human granulocytes described nonselective cation channels activated by increased intracellular free calcium [3]. Subsequently, the patch-clamp technique has been used to explore proton, chloride, and potassium currents in neutrophils and eosinophils [4–8], as well as in many other non-excitable cells.

The phagocyte respiratory burst results in the production of large amounts of O_2^- via NADPH oxidase activation [9] (*see* **Note 1**). The patch-clamp technique has proven to be a powerful way to examine the phagocyte NADPH oxidase, and various configurations of this technique have been used to examine the respiratory burst measured as electron current in real time [5, 10, 11]. These techniques have been used to examine the dependence of NADPH oxidase activity on temperature, pH_o and pH_i, NADPH concentration, and membrane voltage [12–15]. The patch-clamp approach also enables recording current through voltage-gated proton channels (H^+ channels) during oxidase activation. Signaling pathways that regulate and coordinate the activity of NADPH oxidase and proton channels are an area of active investigation (*see* **Note 2**). A variety of evidence also implicates Cl^- channels in a host of neutrophil functions such as volume regulation, phagocytosis, chemotaxis, and host defense [16–21]. Thus, studies of granulocyte ion channels will undoubtedly continue to reveal the mechanisms of important physiological responses of these cells.

Although conceptually simple, the patch-clamp technique is a complicated experimental method. Collecting meaningful data requires appropriate experimental design that is based on a genuine understanding of the properties of ion channels. We hope to introduce the reader to the patch-clamp technique and provide an overview of the apparatus required, the general methods involved, and the application of this method to specific electrogenic transporters known to be present in human granulocytes. Figure 1 shows a schematic diagram of the patch-clamp setup and circuit. The essence of the patch-clamp technique is the formation of an electrically tight seal between the tip of a pipette and the plasma membrane of a cell. The glass pipette is filled with a solution that may (or may not, depending on the purpose of the experiment) mimic a physiological solution and makes contact with the electrode, shown as a wire. Electrical currents that pass through the

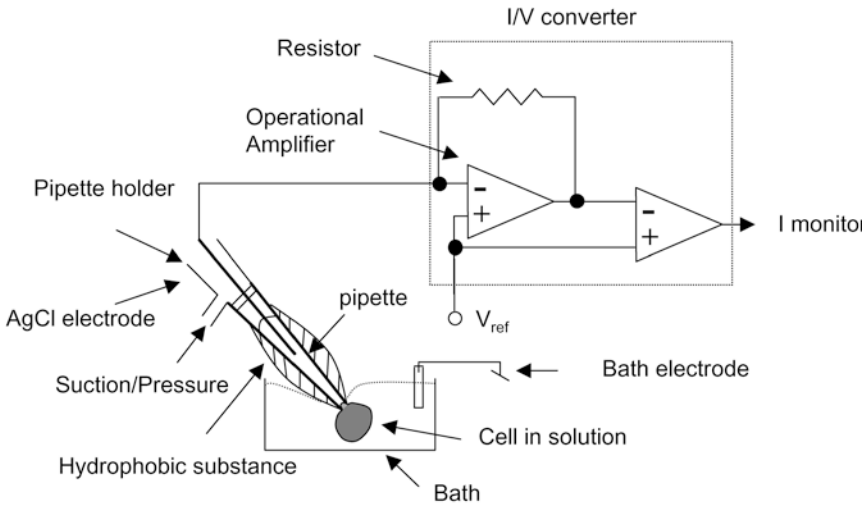

Fig. 1 A simplified diagram of a cell being studied by a patch clamp is shown [75, 80]. A cell in a physiological bath solution is sealed to a glass pipette that is filled with a solution that makes contact with the electrode (usually a chlorided silver wire). The small currents due to ion movements across the membrane are measured as a voltage drop across a resistor. The glass pipette is coated with a hydrophobic substance to reduce the pipette/bath solution capacitance. Reproduced by permission of Humana Press©2007 [91]

membrane are converted into voltage, which is amplified and sent to the data acquisition software (*see* **Note 3**).

The patch-clamp technique exists in several configurations that are distinguished by the size and orientation of the membrane through which current flow is measured. Whole-cell or perforated-patch configurations allow recording from the entire plasma membrane; in cell-attached or excised-patch configurations, only the channels in a small patch of membrane are studied. In the perforated-patch configuration the cytosol is intact; in whole-cell configuration the cytoplasm is replaced by the pipette solution (*see* **Note 4**). The choice of solutions depends on the experimental goals. We give examples of solutions that have been used to study granulocytes, but more importantly, we discuss strategies of solution design (*see* **Note 5**).

2 Materials

2.1 Patch-Clamp Equipment

The equipment comprising a patch-clamp setup is listed below. Nearly all of the apparatus can be purchased commercially. It is beyond the scope of this chapter to discuss the relative merits of products of different manufacturers.

1. Inverted microscope.
2. Perfusion bath and tubes.
3. Pipette electrode head-stage.
4. Micromanipulators.

5. Bath temperature control.
6. Pressure/vacuum unit.
7. Vibration isolation table.
8. Faraday cage.
9. Patch-clamp amplifier.
10. Computer with relevant data acquisition software.
11. Interface between computer and patch-clamp amplifier.
12. Bath electrode.
13. Patch pipette.

2.2 Bath (Reference) Electrode

1. Silver wire.
2. Epoxy resin.
3. Agar powder.
4. Glass or plastic tubing (3 mm bore).
5. Soldering iron and solder.
6. Bleach or NaOCl.
7. Hot plate.
8. Syringe with wide-bore needle.

2.3 Patch Pipette

1. Glass capillary tubes.
2. Pipette puller.
3. Sylgard 184® (Dow Corning Corp.)
4. Microscope.
5. Heating filament attached to a power supply.
6. Heat gun.
7. Pipette solution (*see* next section).

2.4 Solutions

Patch-clamp experiments involve exchanging solutions to vary the environment of the cell or membrane patch. The composition of the solutions is predicated on the specific channel of interest and the type of information that is to be extracted from the experiment. For example, the most fundamental measurement of a channel suspected of being K^+ selective would be to measure V_{rev} in solutions with quite different K^+ concentrations. Pipette solutions that are intended for whole-cell measurements are often made to approximate cytosolic constituents, with high $[K^+]$ and very low $[Ca^{2+}]_i$.

2.4.1 Proton Channel Solutions

1. To isolate proton currents from other conductances that might be present in the cell membrane, common cations and anions such as Na^+, K^+, and Cl^- may be replaced with larger, less permeant ions such as tetramethylammonium (TMA^+), tetraethylammonium (TEA^+), or *N*-methyl-D-glucamine$^+$ and

methanesulfonate ($MeSO_3^-$), aspartate$^-$, glutamate$^-$, isethionate ($HOCH_2CH_2SO_3^-$), cyanate (CN^-), or sulfate (SO_4^{2-}) [7, 22]. Occasionally Cs^+ is used as an impermeant cation [23], because Cs^+ blocks many K^+ channels.

2. Large H^+ currents tend to deplete intracellular protonated buffer, increasing pH_i. Because proton channels do not inactivate, any decay or "droop" of proton current during maintained depolarization indicates that depletion is occurring and that pH_i is increasing significantly [24–26]. To prevent or minimize such pH_i changes, a large concentration of buffer is required in the pipette solution [27]. Many studies have been done with ~100 mM buffer, and concentrations as high as 240 mM buffer have been used [14] (*see* **Note 6**). Table 1

Table 1
Examples of solutions used for proton channel characterization

Pipette solutions									
pH	**$MeSO_3$**	**CsCl**	**HCl**	**Base**	**EGTA**	**$CaCl_2$**	**$MgCl_2$**	**Buffer**	
5.5	96			80 TMA	1		2	100 MES	
5.5	70		10	TEA		2	1	100 MES	
6	80			130 TMA	1		2	100 MES	
6	70		10	TEA		2	1	100 MES	
6.5	128			75 TMA	1		2	100 BIS-TRIS	
6.5	70		10	TEA		2	1	100 PIPES	
7	128			115 TMA	1		2	100 HEPES	
7	70		10	TEA		2	1	100 HEPES	
7.5		75		50 CsOH				100 HEPES	
8		75		44 CsOH				100 TRIS	
Bath solutions									
pH	**$MeSO_3$**	**CsCl**	**HCl**	**Base**	**BAPTA**	**EGTA**	**$CaCl_2$**	**$MgCl_2$**	**Buffer**
5.5	96			80 TMA		1		2	100 MES
6	70		10	TEA			1		100 MES
6.5	70		10	TEA	5		2		100 PIPES
6.5		35		132 CsOH	10				100 PIPES
7	70		10	TEA	5		2		100 HEPES
7.2		75		30 CsOH	10		11.4		100 HEPES

The table lists examples of solutions used for pipette and bath solutions when recording proton currents in whole-cell configuration. Numbers indicate concentration in mM. Where no numbers are given, the base was used to titrate the solution to the correct pH

shows examples of solutions that have been used to study H^+ channels [6, 22, 28].

3. Buffers should be chosen that have a pK_a near the desired pH of the solution, in order to maximize the buffering power of the solution. One consideration is that many buffers bind divalent cations, which creates a problem because inhibition by Zn^{2+} or Cd^{2+} is a frequently studied characteristic of proton currents. Because tricine binds Zn^{2+} with high affinity [29], it removes Zn^{2+} from solution, so a different buffer would be preferred. Phosphate, a common constituent of solutions that mimic physiological ones, also binds zinc avidly [30]. The metal-binding constants for several buffers were measured by Cherny and DeCoursey [29].
4. Examples of buffers that have been used in solutions spanning a wide range of pH are as follows [numbers in brackets are pK_a at 20 °C]: homopiperazine-*N*,*N*′-bis-(2-ethanesulfonic acid (Homopipes) [4.61]; 2-(*N*-Morpholino) ethanesulfonic acid (MES) [6.15]; Bis-2-(hydroxyethyl)imino-tris(hydroxymethyl) methane (Bis Tris) [6.5]; piperazine-*N*-*N*-bis(2-ethanesulfonic acid (PIPES) [6.7]; *N*-*N*-bis(hydroxyethyl)-2-aminosulfonic acid (BES) [7.1]; *N*-(2-hydroxyethyl)-piperazine-*N*-(2-ethanesulfonic acid) (HEPES) [7.55]; Tris-(hydroxymethyl) aminomethanehydrochloride(Tris)[8.3];2-(*N*-cyclohexamino)-ethane sulfonic acid (CHES) [9.3]; and 3-(cyclohexamino)-1-propanesulfonic acid (CAPS) [10.37].

2.4.2 Potassium Channel Solutions

Solutions for studying K^+ channels usually include K^+. [K^+] can be varied, while maintaining constant ionic strength and osmolality, by replacing K^+ with Na^+. Table 2 shows solutions that were used to study K^+ channels in granulocytes [31].

2.4.3 Chloride Channel Solutions

It is possible to replace Cl^- with larger, less permeant ions. Table 3 shows examples of bath and pipette solutions that have been used to study Cl^- channels [7, 22].

2.4.4 Perforated-Patch Solutions

Perforated-patch recordings are achieved when a pore-forming antibiotic, such as amphotericin or nystatin, is included in the pipette solution. The antibiotic forms pores that allow only small monovalent ions (e.g., Na^+, K^+, Cl^-, or NH_4^+) to carry current between the pipette and the cell. In order to control pH_i, a proton donor/acceptor system such as an ammonium or methylamine gradient can be used [32] (*see* **Note 7**). Table 4 shows solutions that were used to change the pH symmetrically and asymmetrically [12]. The pH gradient can also be increased in increments by lowering $[NH_4^+]_o$ from 50 mM to 15, 9, 3, and 1 mM [32], although the lowest $[NH_4^+]_o$ controls pH_i less effectively [10, 32].

Table 2
Examples of solutions used for K^+ channel characterization

Pipette solutions											
pH	**NaCl**	**KCl**	**$CaCl_2$**	**$MgCl_2$**	**HEPES**	**Glucose**	**NaOH**				
7	137.6	5	2	1	10	6	2.4				
7	126.6	16	2	1	10	6	2.4				
7	117.6	25	2	1	10	6	2.4				
7	42.6	100	2	1	10	6	2.4				
7	2.6	140	2	1	10	6	2.4				
Bath solutions											
pH	**NaCl**	**KCl**	**$CaCl_2$**	**$MgCl_2$**	**Buffer**	**BAPTA**	**EDTA**	**MgATP**	**Na_2ATP**	**HCL**	**KOH**
7	5	97.6	0.7		10 HEPES	10		1			42.6
7	3	97.6	1.6		10 HEPES	10	10		1	2	41.5
5.5		102	0.06	0.69	10 MES	10			2.5	3.6	38
8	4	97.2	0.83	0.76	10 Taps	10			0.5		42.6

The table lists examples of solutions used for pipette and bath solutions when recording proton currents in whole-cell configuration. Numbers indicate concentration in mM

3 Methods

3.1 Patch-Clamp Setup

In a patch-clamp experiment, the pipette is positioned against the cell membrane, and suction is applied to the inside of the pipette until a seal of a very high resistance forms between the membrane and the glass. Hamill et al. [2] called the seal a "gigaohm seal" or "giga seal," because the resistance between the cell membrane and pipette is preferably in the gigaohm range. "Gigohm" is an accepted alternative spelling. The pipette usually contains a physiological salt solution to mimic the microenvironment of the cell membrane with a wire electrode immersed in the pipette solution.

The typical patch-clamp setup consists of an inverted microscope with a small bath placed on the stage. The inverted microscope allows room for the bath, pipette electrode, electrode manipulators, perfusion apparatus, and temperature controller/detector. The bath has a discontinuous solution inlet and outlet to enable exchange of bath solutions. It is impossible to perform normal patch-clamp measurements without exchanging bath solutions. A continuous perfusion system forms a conduction pathway that can act as an antenna that introduces a great deal of noise. A discontinuous perfusion system has a junction where the solution in the chamber does not make contact with fluid in the tubing to avoid this noise source.

Table 3
Examples of solutions used for K^+ channel characterization

Pipette solutions										
pH	**NaCl**	**Na_2SO_4**	**Na-Isethionate**	**TMA Cl**	**KCl**	**$CaCl_2$**	**$MgCl_2$**	**Mannitol**	**Base**	**Buffer**
7				145		2				20 BES
7.2	140				5	2	2			10 HEPES
7.2			140			2	2			10 HEPES
7.4	150				5	2	1		NaOH	10 HEPES
7.4		150			5	2	1	75	NaOH	10 HEPES
Bath solutions										
pH	**TMA $MeSO_3$**	**NaCl**	**K-Asp**	**KCl**	**EGTA**	**$MgCl_2$**	**Buffer**			
5.5	96				1	2	100 MES			
7.2		5		140	0.2	2	10 HEPES			
7.2		5	110	30	0.2	2	10 HEPES			

The tables list examples of pipette and bath solutions used for recording proton currents in whole-cell configuration. Numbers indicate concentration in mM. Where no numbers are given, the base was used to titrate the solution to the correct pH

Table 4
Examples of solutions used for perforated-patch recordings

Solution	TMA $MESO_3$	$(NH4)_2SO_4$	$MgCl_2$	$CaCl_2$	EGTA	Buffer	pH	pH_i
Pipette solution	100	25	2	1.5	1	BES 10	7	N/A
Bath 1	100	25	2	1.5	1	MES 10	5.5	5.5
Bath 2	100	25	2	1.5	1	MES 10	6.5	6.5
Bath 3	100	25	2	1.5	1	BES 10	7.5	7.5
Bath 4	100	25	2	1.5	1	Tricine 10	8.5	8.5
Bath 5	100	1.25	2	1.5	1	BES 10	7	6
Bath 6	100	1.25	2	1.5	1	Tricine 10	8.5	7.5
Bath 7	100	1.25	2	1.5	1	HEPES	7	6

The table lists examples of solutions used for pipette and bath solutions when recording proton currents in perforated-patch configuration. Numbers indicate concentration in mM. The pipette solution is the same for all bath solutions. pH_i is calculated from Eq. 8 (*see* **Note 7**)

Patch-clamp measurements are often performed at "room temperature" which may vary by a few degrees or more dramatically, depending on the building. Both proton and electron currents have unusually strong temperature dependence [13, 33, 34]; consequently, small temperature changes produce dramatic effects. For example, evaporative heat loss from a shallow chamber may lower the temperature in the bath, which will transiently increase when a new solution at room temperature is introduced. As a result, proton currents may transiently increase every time the bath solution is exchanged. Some designs for temperature control involve placing the chamber on a U-shaped piece of thermally conductive metallike copper, with Peltier devices sandwiched between the copper and a metal heat sink [35]. When this arrangement is used, care must be taken when decreasing the temperature, because contraction of the U-shaped metal lifts the chamber relative to the pipette, smashing it. Before lowering the temperature, it is advisable to lift the pipette and cell well above the bottom of the chamber.

A reference electrode is placed in the bath and the pipette is attached to micromanipulators that enable positioning the pipette in the bath. Fine movements are required to target the pipette accurately. Both hydraulic (manually controlled) and motorized micromanipulators may be used. The main requirement besides fine control is absence of drift. Cells are small, and drift of cellular dimensions can abruptly end an experiment by pulling the pipette away from the cell or by smashing the pipette against the chamber.

The microscope, electrodes, and manipulators are placed on a vibration isolation table to prevent electrode movement. Vibrations from the floor can cause movement artifacts that can introduce noise or break the pipette tip. A commonly used vibration isolation table is an air table in which the legs are supported on pressurized air cylinders. Other tables are made of large, heavy slabs of marble or granite and are placed in room corners to minimize floor vibration. Locating the table in a cellar can also reduce movement artifacts.

The signal from the pipette electrode is amplified by the head-stage amplifier, low-pass filtered, and sent to an analog-to-digital (A/D) converter and finally to the computer where it is recognized by data acquisition software. Extraneous electrical noise from power cords to the microscope light, head-stage, electrical thermometer, and micromanipulator motors can be shielded by surrounding them with braided wire. A Faraday cage (a wire screen cage) surrounding the entire microscope or just the microscope stage may be necessary to suppress electrical noise from overhead lights and other environmental electrical sources. Due to the sensitivity of the head-stage amplifier, it is important that all metal near the electrode be connected to the ground to prevent the detection of line frequencies. It is important to avoid ground loops. Proper grounding is both important and difficult to achieve.

3.2 Electrode Preparation

The electrodes require manual preparation. The bath (reference) electrode can be used for long periods of time, but the patch pipette should be made immediately before use.

3.2.1 Bath (Reference) Electrode)

The bath electrode provides the reference point from which voltage is measured. It is important that at each point in the recording apparatus where dissimilar materials meet, at least one current carrier can move freely in each direction. If this is not the case, electrode polarization may occur, in which large sustained currents decay because an opposing electromotive force develops at the offending interface. The most commonly used electrode in patch clamping is the silver–silver chloride electrode, made of a silver wire coated with AgCl. Current flowing into the solution or agar bridge is carried by Cl^-. A change in the bath chloride concentration will result in a voltage offset due to a liquid junction potential. Using an agar bridge between the AgCl and the bath solution keeps the concentration of chloride constant near the electrode and minimizes diffusion of the solution in the bridge into the chamber. Because patch-clamp chambers often have small volume (e.g., <1 mL), the use of saturated KCl in the bridge (typically used in of conventional microelectrodes) is avoided to prevent diffusion of these ions into the bath, which would change their concentrations. Bath electrodes are available for purchase but are often constructed on-site.

1. Cut the silver wire to a length of about 1½ in. and solder it to the end of the wire intended to connect the bath to the setup.
2. Immerse the silver wire in bleach for several hr or overnight (*see* **Note 8**).
3. Cut a piece of glass or plastic tubing ~1–2 in. in length, depending on its arrangement in the chamber, and epoxy the tube over the chlorided silver wire. Ensure that the epoxy completely encases the solder and any exposed, un-chlorided silver wire. The tube should extend past the wire by ½ in.
4. Heat 4 % agar/Ringer's solution (w/v) in a beaker until the solution begins to boil, and then remove from heat.
5. While the Ringer/agar solution is still hot, take up the solution with the syringe and inject the agar solution into the tube containing the silver wire.
6. Allow the electrode to cool and the agar to set.
7. When the electrode is not in use, it should be immersed in the solution used in the bridge and connected to the ground.

3.2.2 Patch Pipette

The glass patch pipette contains an electrode, commonly a chlorided silver wire that contacts the pipette solution. The pipette is manufactured using a pipette puller that produces a tip opening a few microns or less in diameter. Commercially available pipette-pulling instruments heat a filament that surrounds the pipette while pulling on either end. The filament may be alternately heated and cooled by an adjustable computer program until the capillary draws out and breaks at the center. The pipette is heat polished to optimize its shape and resistance [36]. Lower-tip resistance increases the fidelity of recording from whole cells (*see* **Note 9**). For small cells with currents of a few hundred picoamperes, a pipette resistance of 2–10 MΩ is typical and reasonable. Cells with larger currents require lower resistance pipettes. Conversely, for recording tiny currents or a small number of channels in excised patches, the tip resistance is not critical (*see* **Note 10**). Pipettes are best made immediately before use and should not be kept overnight.

1. Place the glass capillary tube (*see* **Note 11**) in the micropipette puller, and make two pipettes.
2. Coat the pipette tip with Sylgard, approaching very near the tip. Cure the Sylgard by heating with a heat gun.
3. Place the pipette on a microscope stage near a heating filament, and pass current through the filament to melt the pipette tip. The current can be adjusted empirically with a variable transformer. This process is observed through the microscope.

4. Switch off the current through the filament when the tip is rounded and the bore has narrowed to the desired diameter (*see* **Note 12**). If the microscope optics permits seeing the tip opening directly, direct observation is the easiest way to judge the progress of heat polishing (*see* **Note 13**).
5. Backfill the pipette with a pipette solution, taking care to ensure that no air bubbles are present in the tip of the pipette. Tiny bubbles near the tip can be seen with a dissecting microscope. Bubbles can be dislodged by flicking the pipette shank with a fingertip or by rubbing the serrated surface of a forceps against the shank of the pipette.
6. Mount the pipette in the pipette holder, place over the chlorided silver wire electrode, and tighten. When placed in the bath solution, the pipette resistance can be measured.

3.3 Seal Formation

The essence of the patch-clamp technique is the formation of a high-resistance seal (usually 10–100 GΩ or more) between the cell membrane and the pipette tip. Under optimal conditions, seals can reach the TΩ (10^{12} Ω) range [37]. This high-resistance seal allows recordings with very little background noise and small leak currents (i.e., current that flows from the pipette into the bath through the seal, rather than through the membrane). The process of positioning the pipette against the cell with the micromanipulators is similar for all adherent cells but differs when the cells are nonadherent. Filtering the pipette and bath solutions (e.g., at 0.2 μm) may improve seal formation.

3.3.1 Adherent Cells

1. Mount the pipette in the electrode holder taking care not to scratch the chlorided surface of the wire and tighten the pipette in place.
2. Apply positive pressure to the pipette interior and lower the pipette tip into the bath solution.
3. After the pipette tip enters the bath solution, adjust the offset current to zero.
4. Position the pipette directly above the cell and lower the pipette toward the cell.
5. Monitor the access resistance of the pipette by observing the current produced by a small voltage pulse.
6. When the pipette is near the cell, lower the pipette carefully (a) until the cell is slightly deformed by the pressure of the pipette or (b) until the pipette access resistance begins to increase, and then immediately apply gentle negative pressure (~2–5 in. of water).

3.3.2 Nonadherent Cells

1. Perform **steps 1–4** as in the method of adherent cells
2. When the pipette tip is near the cell, reduce the positive pressure to avoid pushing (or "blowing") the cell away and move the pipette tip near the cell.

3. Apply negative pressure and suck the cell onto the pipette.
4. It may not be possible to avoid pushing the cell away by reducing the positive pressure. If this is the case, the pipette can be aligned slightly to the side of the cell. Immediately after moving the pipette in line with the cell, apply negative pressure to pull the cell onto the pipette tip.

3.4 Patch-Clamp Configurations

There are several patch-clamp configurations: (1) cell-attached patch, (2) inside-out patch, (3) whole cell, (4) outside-out patch, and (5) perforated patch (Fig. 2). Each configuration has advantages and disadvantages that should be considered when deciding which is appropriate for the desired experiment.

3.4.1 Cell-Attached Patch

1. After the pipette has contacted the cell and a GΩ seal has been achieved, the configuration is cell-attached patch.

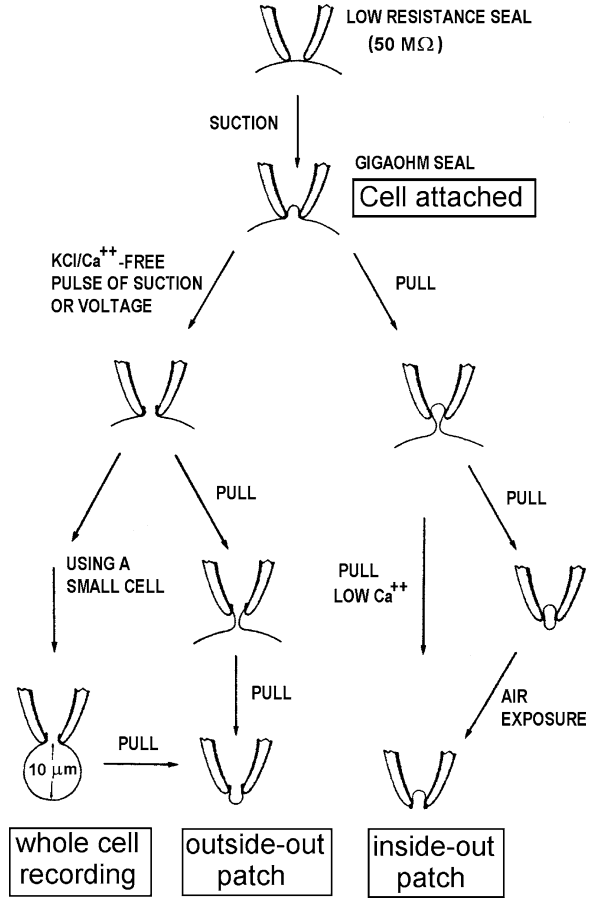

Fig. 2 The formation of the four main patch-clamp configurations is illustrated. See text for details. From ref. 2

2. The currents recorded will reflect only the ion channels in the patch of membrane that spans the tip of the pipette. Single-channel events may be detected, because the patch of membrane is very small.
3. Changing the bath solution will not directly affect channels in the patch, because the cell is still intact. Also because the cell is intact, there is very limited control over the conditions in the cytosol; thus, the pH, ionic composition, and membrane potential will be uncontrolled and unknown.
4. If the cell has a high membrane resistance, current flowing through a single open channel in the patch may change the membrane potential of the cell substantially, producing a decaying unitary current [38].
5. Because the pipette is extracellular, applied voltages (and recorded currents) need to be inverted to follow the convention of defining voltage as that inside the cell relative to that outside. The actual membrane potential will be the sum of the command potential and the membrane potential of the cell, which is not known.
6. Sometimes cells are bathed in an isotonic K^+ solution with the intent of clamping the membrane potential near 0 mV, on the assumption that most cells have K^+ channels that will perform this function. Most, but not all cells have K^+ channels. The patch potential is then simply the inverse of the voltage applied to the pipette.

3.4.2 Inside-Out Patch

1. This configuration is achieved by pulling the pipette away from the cell after forming a cell-attached patch in the case of adherent cells or by lifting the pipette briefly out of the bath solution for nonadherent cells.
2. It is best to excise the patch into solutions low in Ca^{2+}, because Ca^{2+} tends to "repair" membranes, producing a sealed vesicle on the end of the pipette, which is useless for recording.
3. As with the cell-attached patch, an inside-out patch permits recording single channels. The configuration allows complete control over the patch potential and the internal (bath) and external (pipette) solutions.
4. The bath solution (corresponding with the intracellular solution) can be exchanged easily during experiments.

3.4.3 Whole Cell

1. To form whole-cell configuration from the cell-attached patch configuration, the membrane across the tip of the pipette is ruptured by suction or a brief pulse of high voltage, allowing access to the entire membrane of the cell.
2. Sometimes it is difficult to rupture the patch. Attaching a large (e.g., 50 mL) syringe to the tubing connected to the

pipette interior and rapidly withdrawing the plunger is often effective. After membrane rupture, the pipette solution diffuses rapidly into the cell.

3. Whole-cell configuration enables recording macroscopic whole-cell currents that reflect all of the channels in the cell, with a defined internal solution. However, in this configuration the cytosol is removed, which may interrupt second messenger pathways that involve diffusible or unknown elements.

3.4.4 Outside-Out Patch

1. Outside-out patch configuration occurs when the pipette is pulled away from the cell after forming the whole-cell configuration.
2. Nonadherent cells tend to follow the pipette, but this may be remedied by pulling the cell away using a second pipette. The membrane ideally reforms across the tip of the pipette with the extracellular surface facing the bath solution.
3. This configuration is analogous to inside-out configuration, but with the opposite orientation, and has similar benefits and limitations, except that the external solution is readily varied.
4. The true orientation of the membrane in an excised patch can be verified readily if the membrane contains recognizable channels with known properties, such as voltage-gated channels. A depolarization-activated channel should open upon depolarization in an outside-out patch. This property may seem trivial, but in the real world, strange things do occasionally happen.

3.4.5 Perforated Patch

1. This configuration is topologically like the cell-attached patch, except the pipette solution contains a pore-forming molecule, such as ATP [39] or an antibiotic-like amphotericin (~1 mg/mL) [40] or nystatin [41], which perforates the membrane and allows small ions to permeate. Larger pores that allow entry of larger molecules into the cell are formed by β-escin [42].
2. Usually the tip of the pipette is dipped into solution lacking the pore-forming molecule to fill the tip before backfilling the pipette. This enables the seal to be formed before the membrane becomes perforated.
3. The perforated-patch configuration allows electrical access to the cell, but prevents the loss of proteins and large molecules from the cytosol. One can record from all channels in the cell membrane, with the advantage that many signaling pathways remain intact [39, 41].
4. The perforated-patch configuration permits activation of NADPH oxidase in phagocytes [10]; in many other cells it prevents the rundown of ionic currents that occurs in conventional whole-cell configuration [43, 44].

5. One problem with the perforated-patch configuration is that the patch may rupture spontaneously, producing a whole-cell configuration [13, 44, 45].

3.5 Electron Current Recordings

A useful application of the patch-clamp technique is to record plasma membrane electron current (I_e) produced by the NADPH oxidase [5]. The enzyme is electrogenic and is present at sufficiently large numbers in the plasma membranes of several human phagocytes that it passes currents large enough to be recorded (2–3 pA in neutrophils, 6–15 pA in eosinophils). Electron current can be measured in the perforated-patch configuration [10] or in excised, inside-out patches [11].

3.5.1 Recording I_e in Whole Cells

Schrenzel et al. [5] first reported I_e in phagocytes studied in the whole-cell configuration. Eosinophils were patched with a pipette solution consisting of 76 mM CsCl, 50 mM CsOH, 50 mM HEPES, pH 7.6, 10 mM TEACl, 1 mM $MgCl_2$, and 8 mM NADPH. The bath solution mimicked the pipette solution but lacked ATP or NADPH and was at pH 7.1. Under these conditions, the authors reported spontaneous appearance of I_e upon forming whole-cell configuration. The appearance of I_e without agonists suggests that these cells were activated spontaneously, perhaps by adhesion. In later experiments, I_e was observed with 25 μM GTPγs or 5 μM free Ca^{2+} in the pipette solution [46].

3.5.2 I_e in Perforated Patch

The perforated-patch configuration is highly suited to recording electron current. It is possible to record from the same cell before and after stimulation so that each cell is its own control. It appears to be beneficial to have glucose (1 mg/mL) in the bath solution to provide an energy source for the cells. Electron current can be recorded at −40 or −60 mV, voltages sufficiently negative to prevent activation of proton channels (at symmetrical pH) that would obscure the I_e.

1. After forming a giga seal, access to the cell increases over time as the amphotericin forms pores in the patch membrane. Depolarizing test pulses that activate H^+ current can be used to monitor the access resistance. As electrical access improves, the currents grow larger (*see* **Note 14**).
2. Begin recording when the H^+ current is stable.
3. The most reliable activator of NADPH oxidase is phorbol myristate acetate (PMA), which elicits I_e in almost all cells (*see* **Note 15**).
4. PMA produces a downward deflection of the holding current (I_{hold}) that usually stabilizes after a few minutes and persists for tens of minutes (Fig. 3).
5. If the increase in I_{hold} is due to NADPH oxidase activity, it should be sensitive to diphenylene iodonium (DPI), a well-

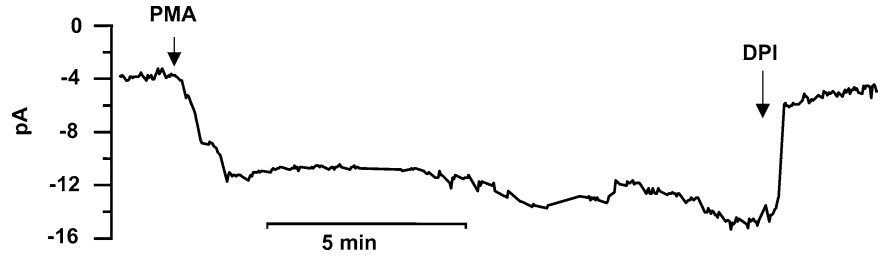

Fig. 3 A record from a human eosinophil in the perforated-patch configuration. The holding current is −60 mV. Pipette solution was 100 mM $KMeSO_3$, 1 mM $MgCl_2$, 1 mM EGTA, 25 mM $(NH_4)_2SO_4$, 10 BES, and 1 mg/mL amphotericin at pH 7. The bath solution was 100 mM $TMAMeSO_3$, 1 mM EGTA, 2 mM $MgCl_2$, 1.5 $CaCl_2$, 25 mM $(NH_4)_2SO_4$, and 10 mM BES pH 7. At the times indicated by the *arrows*, the cell was stimulated with 60 nM PMA, and I_e was inhibited by 12 μM DPI. Reproduced by permission of Humana Press©2007 [91]

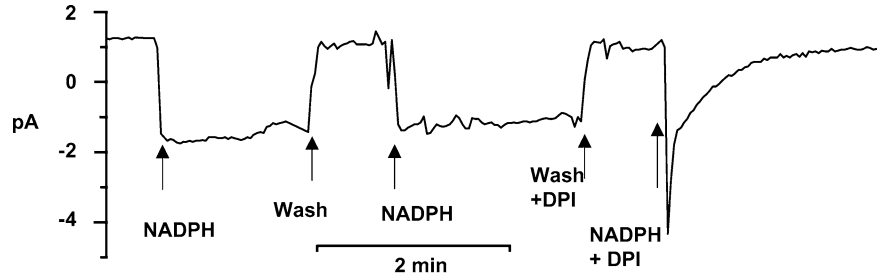

Fig. 4 I_e in an inside-out patch of membrane from a human eosinophil at −60 mV. The cell was stimulated with 60 nM PMA in cell-attached patch configuration 5 min before the patch was excised. Pipette solution was 200 mM HEPES, 2 mM MgCl, and 2 mM EGTA, titrated to pH 7.5 with $TMAMeSO_3$. The bath solution was the same as the pipette solution with 50 μM GTPγS and 3 mM MgATP added. The *arrows* indicate the addition of 2.5 mM NADPH or 12 μM DPI. Reproduced by permission of Humana Press©2007 [91]

known inhibitor of the NADPH oxidase [47]. If a high concentration of DPI inhibits the presumed I_e only partially, then the DPI-insensitive current is likely due to appearance of a leak conductance.

6. During perforated-patch recording, the patch sometimes ruptures spontaneously, producing whole-cell configuration. When this occurs, I_e vanishes rapidly [13], perhaps due to the diffusion of essential components from the cell into the pipette. I_e decreases several times faster when the patch is ruptured ($\tau = 5.6$ s) than when I_e is inhibited by DPI ($\tau = 25.5$ s) [13] (*see* **Note 16**).

3.5.3 I_e in Inside-Out Patch

Electron current can be recorded in the inside-out patch configuration [11]. A patch of membrane is excised from a stimulated granulocyte in which active oxidase complexes are already assembled. Exposing the internal surface of the patch membrane to NADPH enables electron flow across the membrane through the previously activated NADPH oxidase complexes (*see* Fig. 4 for a representative experiment) (*see* **Note 17**).

1. Patch a granulocyte in the cell-attached patch configuration in Ringer solution (pH 7.4) containing 50 μM GTPγS and 3 mM ATP.
2. Stimulate the cell by adding 60 nM PMA to the bath solution.
3. Lift the pipette briefly out of the bath solution to produce an inside-out patch, and then quickly replace the pipette in the bath.
4. Add NADPH to the bath to elicit I_e.

3.6 Ion Channel Recording

3.6.1 Optimizing Conditions to Record Specific Types of Currents

1. If more than one type of ion channel or electrogenic transporter is present in a cell, as is almost always the case, then the currents that are recorded will be an additive mixture of the various component currents.
2. To focus on one particular type of channel, the recording conditions may be adjusted to maximize the conductance of interest and to eliminate extraneous currents. To record ionic currents, the permeant ion must be present in appropriate concentrations. To record K^+ currents, K^+ must be present, although most K^+ channels are also permeable to Rb^+, NH_4^+, and, usually to a much smaller extent, other cations. To study currents carried by ions that are normally present at small concentrations, such as Ca^{2+} or H^+, it may be helpful to increase their concentration.
3. Eliminating extraneous currents can be achieved by several approaches:
   (a) Eliminate all ions permeant through a channel. This may be difficult for channels that are not very selective. For example, many anion channels are notoriously promiscuous, allowing large anions, such as aspartate or methanesulfonate, to permeate. Usually, replacing small physiological ions with larger ions of the same sign is sufficient to reduce the current (*see* **Note 18**).
   (b) If using impermeant ions is not possible, inhibitors can be used. These should be as specific as possible, so that they do not affect the currents of interest. Many channels have potent and specific inhibitors, often derived from venoms or toxins (*see* **Note 19**).
   (c) In some cases, the activation of a conductance can be prevented. To prevent activation of Ca^{2+}-activated channels, intracellular free Ca^{2+} $[Ca^{2+}]_i$ can be buffered to low levels. Voltage-gated channels can be prevented from opening simply by avoiding the voltage range that activates the channels. For example, electron current can be recorded without interference from proton channels at –60 mV, because at symmetrical pH, proton channels do not open

at that voltage. Most cells, including neutrophils [7], have volume-regulated anion channels that are activated when osmotic imbalance occurs. Typically, hypotonic solutions cause cell swelling, which activates stretch- or swelling-activated channels. When one first ruptures the membrane patch to begin whole-cell recording, there is often a transient osmotic imbalance thought to be caused by the higher mobility of small anions in the pipette solution than that of the large anionic proteins in the cytoplasm. This diffusional imbalance produces both a Donnan potential [38] and transient activation of stretch-activated anion currents in neutrophils [4, 7]. These stretch-gated currents usually go away after a few minutes [22].

3.6.2 Requirements for Complete Characterization of an Ion Channel

The selectivity of an ion channel is so important that channels are named for the ions they conduct. Potassium channels are selectively permeable to K^+, proton channels are selective for H^+, and so forth.

Selectivity: The Reversal Potential Must Be Measured!

1. Selectivity can be determined only by studying the channel in various ionic conditions to determine which ions permeate. Permeability can be evaluated in two ways.
   (a) Create conditions in which there is only a single ionic species (of one sign) on one side of the membrane, and determine whether that ion carries current in the correct direction. Although this approach seems straightforward, a prerequisite is a reliable method to determine whether the current is permeating the channel of interest. If the channel is voltage and time dependent, then the kinetics of the currents can be presumed to define the conductance; otherwise, using blockers may be necessary. Identification of a channel by pharmacology alone is unacceptable for several reasons. First, truly specific inhibitors are rare. Second, pharmacology can be messy. Some drugs have multiple effects, such as changing the pH or altering metabolism. If the inhibitors are irreversible, or if they act slowly, then positive identification becomes tricky. For example, one published study incorrectly identified volume-regulated anion currents as Na^+ currents. The putative Na^+ currents consistently ran down after addition of an inhibitor, and the rundown was mistaken for slow and irreversible block.
   (b) Selectivity is best determined by measuring the reversal potential, V_{rev}, and varying the species or concentration of ions in the bath. This approach can give precise information about relative permeability of a channel when many ions are measurably permeant. Addition or removal of

impermeant ions should not change V_{rev}, but changes in the concentration of a permeant ion should. The V_{rev} of voltage-gated proton currents does not change when the bath is changed among Cs^+, K^+, TMA^+, etc., although changes of a few millivolts are measured in some solutions which disappear when one corrects for liquid junction potentials. If one encounters a channel that indiscriminately conducts all cations or all anions (but does discriminate between ions of opposite charge), then the charge of the permeant ion can be identified by decreasing the ionic strength, replacing ions with uncharged molecules like glucose to maintain the osmolarity [48, 49]. Sometimes ions that are not permeant indirectly produce changes in V_{rev} that could be mistaken as an indication of permeability. For example, when the predominant cation in the bath solution is Na^+ or Li^+, compared with other cations, the measured V_{rev} of H^+ currents shifts in a positive direction [50]. Although such a shift would be expected if Na^+ were permeant, it is prevented by inhibiting Na^+/H^+-antiport and therefore is due to increased pH_i resulting from exchange of extracellular Na^+ for intracellular H^+ [50].

2. How does one measure V_{rev}? The answer depends on the situation. The idea is to determine the reversal potential of a conductance that presumably is due to a population of identical channels. However, all voltage-clamp data includes extraneous conductances that are observed as "leak" currents. If the conductance of interest is, for example, a non-voltage-gated (i.e., the conductance is "on" at all voltages) Ca^{2+}-activated K^+ conductance, then one might simply measure the voltage at which the current is zero to estimate V_{rev}. However, the measured V_{rev} will be incorrect unless the leak is corrected. Because leak conductances usually reverse near 0 mV, their effect is to decrease the absolute value of the measured V_{rev}. The larger the leak, the larger the error will be. If a specific inhibitor of the conductance of interest exists, one can subtract the current measured in the presence of blocker from that in its absence. The blocker-subtracted currents should reflect the properties of the conductance of interest. Two dangers exist. First, some drugs block channels in a voltage-dependent manner. In this case, the subtraction will give erroneous results unless block is essentially complete at all voltages. Second, the subtraction procedure introduces errors, because both the "leak" and conductance of interest may change with time, compromising the subtraction. One must recognize these limitations and accept that the results may have some error. One must be especially careful if two large numbers are subtracted to give a small result. If such a subtraction procedure results in V_{rev} values that follow the

Nernst prediction within 0.1 mV, then one must be extremely suspicious that wish fulfillment has entered into the data analysis process.

3. It is relatively easy to measure V_{rev} for channels that are voltage and time dependent. The two situations that may be encountered are illustrated in Fig. 5, when V_{rev} is outside (A) or within (B) the voltage range within which the conductance is activated. The classical method of estimating V_{rev} of voltage-gated channels, introduced by Hodgkin and Huxley [51] is the "tail-current" method (Fig. 5a). The membrane is held at a voltage at which the conductance is off, the "holding" potential, V_{hold}. A prepulse is applied to activate the conductance. Then the voltage is stepped to various voltages at which most channels close, in this example, –10 through +20 mV in 10-mV increments. The object is to determine the voltage at which the resulting "tail currents" vanish; this is V_{rev}. Often tail currents decay exponentially, and if the initial amplitude is difficult to resolve due to capacity current interference, the current can be fitted by an exponential decay function, which can be extrapolated to the time at the start of the pulse. One could then plot the "instantaneous" current against voltage and interpolate to determine where the currents cross the voltage axis. This would give the wrong answer, +8 mV in our example, because one must always consider the leak current. The conductance of interest in Fig. 5a is the voltage-gated proton conductance. At V_{hold} there is 2 pA of inward current that is unrelated to proton current and therefore considered "leak." We are not interested in the properties of leak current, except in so far as we want to eliminate their effects. The leak current will be different at each test voltage where tail currents were recorded. The simplest way to eliminate the leak is to look not at the absolute current value at the start of the pulse, but at the amplitude of time-dependent tail current. Generic leak currents are usually time independent, in contrast with proton currents. When we plot and interpolate the amplitudes of the tail current decay, we find that V_{rev} is actually +6 mV. The error due to leak was small here because the leak was small and reversed near V_{rev} for the proton conductance. Much larger errors have been published in reputable journals, including V_{rev} values that were described as being positive to voltages at which clearly outward tails currents decayed, because leak was not corrected. One presumption in the tail-current-decay-amplitude method is that the same number of channels is open at the end of each prepulse. In the example in Fig. 5a, one prepulse activated a smaller fraction of the total conductance, which we can see because the prepulse current was smaller. One can correct for this error retroactively by scaling the tail current according to

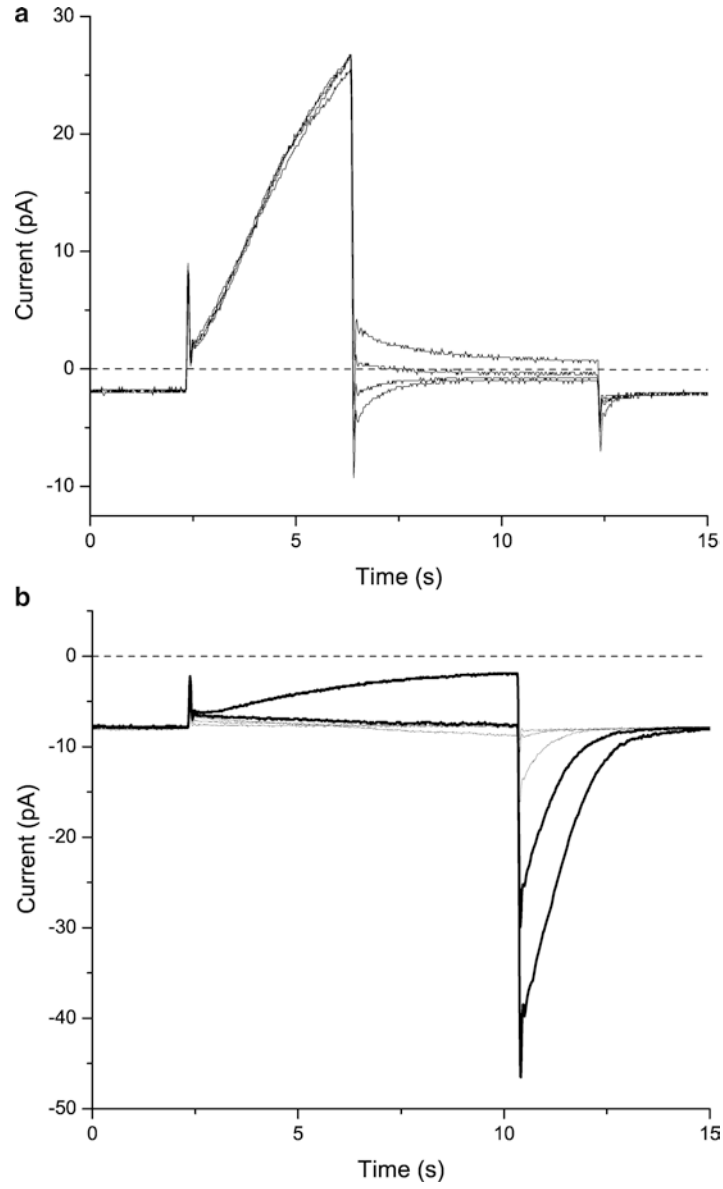

Fig. 5 Determining the reversal potential, V_{rev}, of a voltage-gated conductance, when V_{rev} is outside (**a**) or within (**b**) the voltage range at which the conductance is activated. (**a**) Tail-current method illustrated by voltage-gated proton currents in a human eosinophil at pH_o 7.0 and pH_i 7.0. From a holding potential of −60 mV, where H^+ channels are closed, a prepulse to +80 mV activates the conductance. The voltage is then stepped to various voltages at which most channels close, −10 to +20 mV in 10-mV increments in this example. Bath solution $TMAMeSO_3$ and pipette solution $KMeSO_3$, both with 50 mM NH_4^+ to control pH_i. (**b**) Determining V_{rev} from a family of depolarizing pulses. From $V_{hold} = -60$ mV, pulses were applied to −40 mV through 0 mV in 10-mV increments, with currents at −10 mV and 0 mV in *bold*. This human eosinophil was previously activated with PMA, and there is nearly −8 pA of electron current at V_{hold}. See text for details. Reproduced by permission of Humana Press©2007 [91]

the proportional decrease in prepulse current (in this example, the correction is negligible). Another presumption is that the tail current decays completely. In Fig. 5a, the tail current at +10 mV decayed only partially, resulting in maintained outward current. This can be confirmed by examining the secondary tail current when the voltage is finally returned to V_{hold}. There is a clear inward tail current after the pulse to +10 mV. One can determine whether complete decay can be expected at a given voltage by simply applying a pulse directly to that voltage to see if current is activated. If V_{rev} occurs at a voltage at which the conductance of interest is already activated, then a different approach must be used (see below).

4. Besides leak conductance, what other errors may occur? One systematic error arises from the necessity to activate the conductance in order to generate tail currents. The prepulse that activates the conductance also removes a large number of permeant ions from the cell. The result for proton currents is that the prepulse increases pH_i so that the measured V_{rev} tends to be more positive than the true value [26]. This error can be minimized by using high buffer concentrations in the pipette solution and by keeping the prepulse small and brief. However, if the prepulse is too small, the tail currents will be small and difficult to interpret. Although the error cannot be eliminated, it can be recognized. Because of this error, it is more reliable to consider the change in V_{rev} measured when pH_o is varied, rather than the absolute value of V_{rev}, which will also have errors due to liquid junction potentials. If similar depletion of protonated buffer occurs during each V_{rev} determination, then the shift in V_{rev} will be the best indicator of selectivity.

5. Sometimes, the conductance of interest is already activated at V_{rev}, and therefore, decaying tail currents do not occur. One solution is to cave in to error and simply measure the absolute current at various voltages, but this makes leak correction difficult. A simple and preferable alternative is to apply a family of depolarizing pulses and observe the time-dependent turn-on of current at various voltages, as illustrated in Fig. 5b. This human eosinophil was activated by PMA in perforated-patch configuration, and there is –8 pA of electron current at V_{hold}. That this large inward current is not leak can be deduced by noting the small spacing between the currents at the start of the four illustrated test pulses, before much proton current has turned on. During the pulse to –40 mV only leak current and I_e are evident, but the g_H is activated detectably at –30 mV, because a small tail current appears upon repolarization. During the pulses to –20 and –10 mV, inward H^+ current turns on slowly during the pulses, and large inward tail currents

are seen on repolarization. Finally, at 0 mV a large outward current turns on during the pulse. Despite the fact that this is clearly an outward current, its absolute value at the end of the pulse is still negative, because it is superimposed on the larger inward electron current. Only a computer program lacking the most rudimentary insight would declare that V_{rev} must be positive to 0 mV, simply because the total current at the end of the pulse is inward! It is obvious that V_{rev} for the voltage- and time-dependent proton conductance that we are interested in falls between –10 mV and 0 mV (the two darker records), because the time-dependent current is inward and outward, respectively, in the two records. To determine V_{rev} we can first measure the amplitude of inward current at –10 mV (–1.2 pA) and the outward current at 0 mV (+4.3 pA) that turned on during the pulses. However, simply interpolating between these values on a current–voltage graph, for example, would give the incorrect V_{rev} value of –8 mV, because the g_H activated at these two voltages was a very different fraction of the total g_H. We can determine precisely the relative g_H that was activated by each pulse from the amplitude of the tail current upon repolarization to –60 mV. We now scale the time-dependent current amplitudes according to the fraction of the g_H activated by the prepulse to arrive at the correct answer, –7 mV.

6. Under some conditions, one may use a "quick-and-dirty" method to determine V_{rev}. One such method is to use voltage ramps (Fig. 6). Here the voltage in a human eosinophil was ramped rapidly from +200 to –100 mV. Because H^+ current activation is faster at more positive voltages, nearly 200 pA of proton current was activated soon after the start of the ramp. The ramp was fast enough that the conductance was still active at 0 mV, and then in the negative voltage range, H^+ channels closed progressively. When the same ramp was applied after addition of high concentrations of Zn^{2+}, most, but not all of the proton, current was abolished. Because a major effect of divalent cations is to shift the voltage dependence of H^+ channel activation to more positive voltages [52, 53], the currents turned off at much more positive voltages. In the presence of Zn^{2+}, the current negative to +50 mV is almost entirely leak current. Estimating V_{rev} from voltage ramps suffers from at least three potential errors.

   (a) A capacitive artifact produces an offset of the current recorded during a voltage ramp, typically of a few picoamperes, because the capacity current is proportional to dV/dt, which is constant during a voltage ramp. Even if one uses analog capacity correction, the correction is rarely perfect and can change over time. This offset may be negligibly small, but can be problematic if the currents of interest are comparably small, as may occur in excised patches.

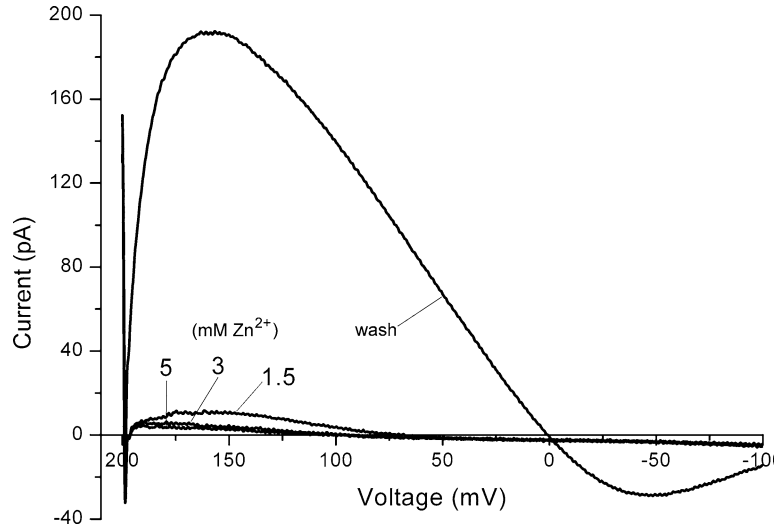

Fig. 6 Evaluation of V_{rev} using voltage ramps. Currents during voltage ramps (from +200 mV to −100 mV in 800 ms) in a human eosinophil studied in perforated-patch configuration with $KMeSO_4$ in the pipette solution and $TMAMeSO_4$ in the bath solution, both at pH 7.0 and both with 50 mM NH_4^+ to clamp pH_i near pH_o. The predominant conductance is due to voltage-gated proton channels, which are inhibited by Zn^{2+}. The sequence was 1.5 mM $ZnCl_2$, then 5 mM, and then 3 mM; then wash out with EGTA-containing bath solution. This cell was stimulated with PMA, and then DPI was added to inhibit NADPH oxidase. Reproduced by permission of Humana Press©2007 [91]

The offset increases with the speed of the ramp. A quick way to test whether the offset is a problem is to apply the same ramp (i.e., spanning the same voltage range) but in the opposite direction. If the currents do not superimpose, there is an offset problem. In the ramps in Fig. 6, the leak current intersects the *X*-axis near +70 mV. This may be the result of a small offset, because one expects leak currents to reverse near 0 mV, although this question was not studied systematically. However, the best estimate of V_{rev} in this experiment is not the point at which the control currents pass through the voltage axis (the zero-current potential), but rather the voltage at which the currents in the absence and presence of Zn^{2+} intersect, just negative to 0 mV.

(b) Significant numbers of the channel of interest must be open when the voltage passes V_{rev} to estimate V_{rev}. For example, voltage-gated proton channels generally open only positive to V_{rev}, and thus, V_{rev} can be estimated only by ramping from positive to negative voltages at a rate slow enough to allow H^+ channels time to open, but fast enough so that they do not all close by the time the voltage passes E_H.

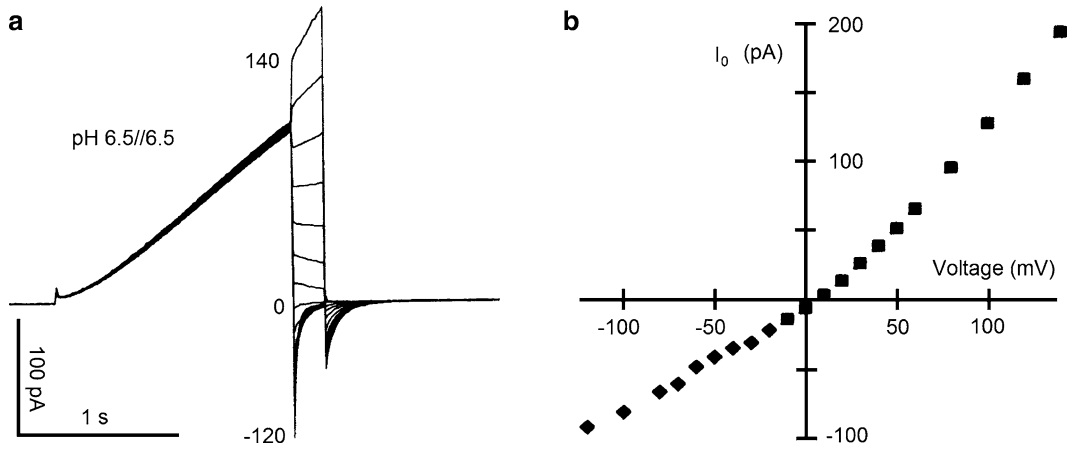

Fig. 7 Measurement of the instantaneous current–voltage relationship of proton channels. In (**a**) currents during repeated voltage pulses are superimposed. The first step, the "prepulse," is to a voltage at which the g_H is activated, and then the membrane is stepped to a range of voltages. Ideally, the same number of channels is open at the end of each prepulse, and therefore, the current at the start of the test pulse (**b**) reflects any rectification of the open-channel current. If one measured the current–voltage relationship of a single open channel, the result should have the same shape as that plotted in (**b**). If any gating that occurs during the test pulse, typically channels closing at negative voltages, is so rapid that the initial current cannot be resolved, one can fit the decaying current, usually to an exponential decay function, and extrapolate back to the start of the pulse. From ref. 90

Although it seems obvious that one can measure a meaningful V_{rev} only if the channels of interest are open at that voltage, papers on human neutrophil electrophysiology have been published in highly reputable journals in which this condition was not met. Naïve authors sometimes simply plot the total current and declare that V_{rev} is the voltage at which this current crosses the voltage axis, ignoring the fact that they have simply determined V_{rev} of the leak current!

(c) It is more difficult to separate the conductance of interest from leak or other conductances during ramps than during voltage pulses (see above).

7. A second "quick-and-dirty" way to estimate V_{rev} of a voltage-gated channel is to apply a single voltage pulse that activates the conductance and then repolarize to a voltage at which the channel closes. One can interpolate between the current at the end of the pulse and that at the beginning of the tail current to estimate V_{rev} [54]. This method assumes that the instantaneous current–voltage relationship is linear, i.e., that the open-channel conductance is ohmic. Figure 7 illustrates that the instantaneous current–voltage relationship for voltage-gated proton channels is not linear at symmetrical pH, but the rectification is weak enough that the error is not large if the two test voltages are close

together. Leak must also be corrected. In some situations, the complete tail-current method may be too time-consuming, and a rough estimate is better than none at all. An advantage of this "interpolation" method is that the two measurements are made at essentially the same time. Thus, although depletion would affect the result, the measurement is an accurate reflection of V_{rev} at that instant. Using the example in Fig. 5b, from the time-dependent outward current at 0 mV, +4.3 pA, and the inward tail current at –60 mV, –34 pA, we interpolate to arrive at –7 mV as an estimate of V_{rev} which is identical with the result calculated by the more laborious formal methods described above.

Rectification

Rectification means that the current flowing through a single open channel is not a linear function of the applied driving force (the applied voltage relative to V_{rev}).

1. Rectification can be determined from instantaneous current–voltage curves, like that in Fig. 7. Errors can arise if the current at the end of the prepulse is not the same each time, which this can be corrected by scaling, as already described. If the tail currents decay rapidly, their amplitude can be difficult to determine.
2. Another way to detect rectification is to measure single-channel currents directly at different voltages. The preferred method is to use repeated voltage ramps and then average segments of ramps containing either one or no open channels and subtract one from the other. Distinct advantages of this method include the following: (a) it is efficient; (b) by superimposing records, one can immediately see whether there has been a change in the leak current; (c) one can resolve tiny currents near V_{rev} more reliably than during sustained voltages pulses; and (d) it is much easier to confirm which channel is which when there are multiple types of channels in the patch. Obviously, this method requires that single-channel currents are large enough to detect. Single-proton channel currents are in the femtoampere range [37] and thus are not amenable to this method.

Activation by Ligands or Voltage, Gating Kinetics

1. Ion channels are classified according to the factors that cause them to open.
2. Some channels are ligand gated (i.e., they open when a particular substance binds). For example, end-plate channels at the neuromuscular junction open when acetylcholine binds. Ca^{2+}-activated channels open when $[Ca^{2+}]_i$ increases above resting levels.
3. Many channels are voltage gated. The voltage dependence of a channel can be described by applying a family of voltage pulses than span a voltage range in which the channel progresses from

being closed to having a high probability of being open (P_{open}). Ideally, the current is measured after it reaches a steady-state level. In practice, this ideal is often not achieved, especially for proton currents that activate slowly and may decay during prolonged large pulses due to H^+ current-induced pH_i increases. One can "correct" the current measured before steady state by fitting the current with a rising exponential, $I(t) = I_{max}\,(1 - e^{-t/\tau})$, and extrapolating to infinite time. This obviously assumes that an exponential describes the ideal activation behavior, which may not be the case, but may give a reasonable estimate. In this process, one also obtains the time constant (τ or τ_{act}) of activation of the current.

4. In most cells, proton currents activate with a sigmoidal time course, and thus a simple exponential does not accurately describe the kinetics. However, attempts to discover a simple model that fits the currents better have not been productive. Our philosophy is that if the main part of the current can be reasonably well described by a single exponential, then this provides a τ_{act} value that gives a rough indication of the rate at which most of the channels open, and it is a parameter that can be easily understood and communicated.
5. The resulting current–voltage relationship can be converted to a conductance–voltage relationship by dividing the current at each voltage (V) by the driving force (V–V_{rev}). The conductance ideally saturates at large voltages at which P_{open} is maximal. The single-channel correlate is the P_{open}–voltage relationship. Both of these relationships tend to be sigmoidal and are often fitted with a Boltzmann function (using proton channels as an example):

$$\frac{g_H}{g_{H,\max}} = \frac{1}{1 + e^{-\left(V - V_{1/2}\right)/k}} \tag{1}$$

$$\frac{P_{open}}{P_{max}} = \frac{1}{1 + e^{-\left(V - V_{1/2}\right)/k}} \tag{2}$$

The midpoint of the curve, at which the conductance is half maximal, is $V_{1/2}$ (in mV), and the slope factor k (in mV) indicates the steepness of the voltage dependence. A smaller value of k means steeper voltage dependence.

Single-Channel Conductance

Single-channel conductance (γ) is important because it determines how much current flows through the open channel. The total current across a cell membrane is described by:

$$I_{total} = \left(V - V_{rev}\right)\gamma N P_{open} \tag{3}$$

where (V–V_{rev}) is the driving force, N is the number of channels in the membrane, and P_{open} is the probability of any channel being open.

1. When ion channels open and close, the current increases and decreases in steps of identical amplitude, which sum together when many channels open to form a macroscopic current in which the unitary events cannot be clearly detected.
2. For many ion channels, γ is large enough that single-channel currents can be measured directly.
3. Detecting single-channel currents is usually done using excised patches of membrane, because it is desirable that either one channel or no more than a few channels are present.
4. There is additional noise when a channel is open, and the total noise increases with each open channel so that it is difficult to resolve unitary events when more than a few channels are open at one time. If multiple types of channels are present, identification becomes very difficult.
5. Single-channel currents can be recorded at constant voltage, during pulses or during voltage ramps. If there is only one channel in a patch, one can hold the membrane at each voltage for long times and determine mean open and closed times as well as P_{open} for that voltage. P_{open} can be efficiently determined by converting the data to an amplitude histogram and comparing the integrals when one or no channel is open.
6. Giving pulses is useful for voltage-gated channels to derive a sense of whether the channel behaves as expected from macroscopic currents.
7. Voltage ramps are an excellent way to determine the reversal potential and the voltage dependence of the conductance, i.e., its rectification. Under most circumstances, the open channel current is not ohmic, rather the conductance changes with voltage or rectifies. A voltage ramp is applied repeatedly, and the currents are analyzed afterwards. The average of current segments with no open channels can be subtracted from the average of segments with exactly one channel open to produce the open-channel current–voltage relationship.
8. If the unitary conductance is too small to measure directly, it can be deduced from current fluctuations or noise. Under stationary conditions (without time dependence of I_{total}, P_{open}, or driving force, etc.), the single channel current (i) can be calculated from the variance, σ^2, according to [55]:

$$i = \sigma^2 / \left[I_{total} \left(1 - P_{open} \right) \right] \tag{4}$$

The value used for σ^2 must have background noise subtracted, which can be determined from identical measurements in the presence of complete pharmacological blockade. If this is not feasible, one can determine background noise at subthreshold voltages, in the case of voltage-gated channels. The only parameter that is difficult to determine is P_{open}. The macroscopic conductance of a depolarization-activated channel may saturate at large positive voltages, but P_{open} at saturation may be much less than 1.0. However, by collecting data at different voltages, it is possible to deduce P_{open} (fig. 12 of [37]). One can also collect data near $V_{threshold}$ where P_{open} is close to 0, and the error in $(1 - P_{open})$ is negligible; this approach, however, produces estimates only within a narrow voltage range. For noise analysis, it is important that the data are collected using an appropriate sampling rate and appropriate filtering. These issues are beyond the scope of this chapter and have been discussed elsewhere at length [37, 56].

9. The transporters involved in the phagocyte respiratory burst have small conductance or transport rates. Proton channels have a conductance of ~15 fS at physiological pH [37], which corresponds with currents of a few femtoamperes, on the order of ~10,000 H^+/s, depending on the driving voltage. Store-operated Ca^{2+} (CRAC) channels may be present in neutrophils [57] and have similarly small conductance [58]. In comparison, the NADPH oxidase transports only ~300 e^-/s [59, 60]. It seems teleologically reasonable that in small cells, and especially in the much smaller phagosome, low transport rates would make the transporters more amenable to regulation and fine-tuning of their activity. A single large-conductance channel would produce a drastic and abrupt change in potential and ion concentrations and thus, from a teleological perspective, would be unwieldy [61].

4 Notes

1. The oxidase complex is assembled from two membrane-bound subunits (gp91^{phox} and p22^{phox}) and several cytosolic subunits (p67^{phox}, p47^{phox}, Rac, and p40^{phox}) [9]. The NADPH oxidase works by transporting electrons from cytoplasmic NADPH across the membrane, where they reduce O_2 to $O_2^{\bullet -}$. This electron movement can be recorded directly as an electrical current [5, 10]. Because the electron transport is not obligatorily coupled to a compensatory charge movement, it produces a separation of charge that leads to sustained depolarization of the membrane [62] well beyond 0 mV in intact granulocytes [63–66]. If this charge movement is not compensated, extreme

depolarization results [61, 67] that by itself directly opposes electron flux across the membrane [25]. In human neutrophils and eosinophils, almost all of this charge compensation is mediated by H^+ channels [25, 30, 61, 66–71].

2. H^+ channels are membrane proteins that are gated by both voltage and pH. They open with depolarization or an outward pH gradient (defined as $\Delta pH = pH_o - pH_i$). Increased pH_o and/or decreased pH_i causes the channels to open at lower voltages. Proton channels have two distinct gating modes, "resting" and "activated," which are observed before and after stimulation [10, 46, 70, 72]. Resting H^+ channels open almost exclusively positive to the Nernst potential for protons (E_H) and therefore extrude protons from cells. The activated mode occurs concurrently with NADPH oxidase activation and is manifested as an increased proton conductance, faster channel opening on depolarization, slower channel closing, and a negative shift in the threshold voltage at which the channels open. Enhanced gating of proton channels occurs when the protein is phosphorylated by PKC [73], at a single site, Thr^{29}, on the intracellular N-terminus of the protein [74].
3. The patch clamp allows the recording of small currents and the detection of single-channel currents in the cell membrane. Recording small currents with the patch-clamp technique requires a large signal-to-noise ratio. The smallest directly recorded single-channel currents were ~8 fA proton channel currents in human eosinophils [37]. Noise in the patch-clamp setup arises from the electronic circuitry, the pipette and holder assembly, the seal and cell membrane, and extraneous mechanical or electrical sources [36, 75]. Noise interferes with the recordings and should be minimized.
4. A patch-clamp experiment consists of a number of voltage pulses applied to a cell or membrane patch. Changes in pH, ion concentration, temperature, osmolality, and drug concentration can be exploited to reveal the properties of the channels present. Channels are characterized by the stimulus that causes them to open, their ion permeability, opening and closing kinetics, conductance, and pharmacological sensitivity.
5. The current that passes through a channel is described by Ohm's law:

$$V = IR \tag{5}$$

where V is the potential difference in volts (V), I is current in amperes (A), and R is resistance in ohms (Ω). The reciprocal of resistance is conductance (G, measured in Siemens, S) and indicates the facility of current flow.

The selectivity of an ion channel is determined by measuring the reversal potential (V_{rev}) and comparing it with the equilibrium potential or Nernst potential (E_X) of the ion (X) of interest. The Nernst equation shows that E_X depends on the ion concentrations inside and outside the cell:

$$E_X = (RT/zF)\ln\left([X]_i/[X]_o\right) \tag{6}$$

where R is the gas constant, T is the absolute temperature, z is the charge of ion X, F is Faraday's constant, and $[X]_i$ and $[X]_o$ are the concentrations (brackets indicate concentration) of the ion inside and outside the cell, respectively [55]. The term RT/zF is 25.26 mV for a monovalent cation at 20 °C. For a channel that is perfectly selective for a particular ion, the reversal potential is identical to the Nernst potential. When more than one ion is permeant, the relative permeability can be determined using the Goldman–Hodgkin–Katz voltage equation [49, 55, 76, 77]:

$$V_{rev} = \frac{RT}{F}\log\frac{P_{Cl^-}\left[Cl^-\right]_i + P_{K^+}\left[K^+\right]_o + P_{Na^+}\left[Na^+\right]_o + P_{H^+}\left[H^+\right]_o}{P_{Cl^-}\left[Cl^-\right]_o + P_{K^+}\left[K^+\right]_i + P_{Na^+}\left[Na^+\right]_i + P_{H^+}\left[H^+\right]_i} \tag{7}$$

where P_X is the permeability to ion X. This equation shows that the permeability of each ion, combined with its concentration, determines how large an effect it will have on V_{rev}.

6. For proton current recording, it is advisable to use a high intracellular buffer concentration to maximize control over pH. Reducing extracellular buffer from 100 to 1 mM had very little effect on voltage-gated proton currents [27], because the bath solution represents an effectively infinite sink for protons. Intracellular buffer concentration was more critical, with distinct limitation of H^+ current when buffer was reduced from 100 to 10 mM even in excised, inside-out patches [27]. Several whole-cell patch-clamp studies in which pH_i was determined have revealed that including 5–10 mM buffer in the pipette solution does not adequately control pH_i, compared with higher buffer concentrations, e.g., 100–120 mM [23, 53, 78, 79]. Even with high buffer, large proton currents can change pH substantially [26], which in a biological sense is fortunate, because extruding acid is a major function of proton channels in many cells.
7. The high membrane permeability of the uncharged form of these molecules and the impermeability of charged form provide a virtually unlimited reservoir of intracellular proton donor/acceptor. At equilibrium, the concentration of the uncharged form will be nearly equal on both sides of the membrane due to its freely diffusible nature. By changing pH_o and the concentration of the protonated donor, pH_i can be established

and maintained. In the case of ammonium, the relationship is give by [32]:

$$pH_i = pH_o - \log\left(\left[NH_4^+\right]_i / \left[NH_4^+\right]_o\right) \quad (8)$$

The internal NH_4^+ concentration is fixed by the pipette solution, and pH_i can be varied by changing the NH_4^+ concentration in the bath. It is possible to lower pH_i with respect to pH_o by decreasing the external NH_4^+ concentration. Decreasing $[NH_4^+]_o$ to one-tenth, $[NH_4^+]_i$ ideally will lower pH_i by one unit. In practice, the control of pH_i appears to be better at higher pH_o, perhaps because the neutral NH_3 is more abundant (the pK_a of ammonium is 9.4).

8. A more traditional method is to pass current repeatedly in both directions through a silver wire that is immersed in a Cl^--containing solution (e.g., 0.1 M HCl), to deposit a fine coat of AgCl. Sintered Ag/AgCl electrodes can also be purchased.
9. The pipette resistance (R_{pip}) is in series with the membrane resistance of the cell (R_m), and the applied voltage ($V_{command}$) will be divided according to these relative resistances. The result is that the actual voltage across the cell membrane (V_{true}) is less than the command voltage applied: $V_{true} = V_{command}\,[R_m/(R_m + R_{pip})]$. It should be noted that the resistance of the cell membrane decreases radically when a pulse that opens ion channels is applied, and therefore the series resistance error increases drastically when a large conductance is activated. Most patch-clamp amplifiers have a "series resistance compensation" circuit that can be adjusted to compensate some fraction of the series resistance. One easily detected manifestation of uncompensated series resistance is non-exponential decay of tail currents that normally decay exponentially.
10. A pipette filled with solution and placed into a bath solution acts as a capacitor. During a step change in voltage, there is a brief transient of current due to charging the pipette (fast) and cell membrane (slow) capacity. The pipette capacitance can be reduced by coating the part of the pipette that will be immersed with a hydrophobic substance, such as Sylgard® (Dow Corning Corp.), thus minimizing contact of the bath solution and the pipette and increasing the distance between the two conductors (the fluid in the bath and pipette) to reduce the capacitance [36]. When recording currents, it is necessary to null capacity transients using the analog capacity compensation controls of the patch-clamp amplifier.
11. Many types of glass have been evaluated for use as pipettes [36]. Glass with a lower softening temperature is easier to fire polish after pulling and forms blunt pipettes that have low

access resistance. Harder glass with a higher softening temperature tends to form long, gradually tapering pipettes with high resistance; hence, it is a poor choice for whole-cell recording. Hard glass may have other desirable properties, such as lower noise or better sealing proclivity [80]. Quartz pipettes have been used to minimize noise (especially in the high-frequency range) during single-channel recording [81]. Some types of glass, especially soft glasses used for whole-cell recording, contain heavy metals that can leach into the solution, affecting the recorded currents [82, 83]. Such effects can be controlled by including a divalent chelator-like EGTA in the pipette solution.

12. The wire filament is often coated with glass to prevent vaporization and deposition of metal on the pipette tip. Positioning a stream of air blowing toward the filament creates a steep temperature gradient that enables better control over the fire-polishing process.
13. If the tip opening cannot be seen, the tip resistance can be estimated by a "bubble test" in which a 10 mL syringe is attached to the base of the pipette via a tube. With the tip immersed in methanol and the syringe filled with 10 mL of air, apply pressure until bubbles first start to appear, and then note the amount of air left in the syringe. In one series of measurements, the resistance of the pipette filled with an isotonic KF solution and placed in a Ringer-containing bath was 3–5 MΩ for a bubble test number of 3, 5–8 MΩ for a bubble test number of 2, and 8–17 MΩ for a bubble test number of 1. Actual results may differ, depending on tip geometry and other factors. If the tip is too large, further polishing can be performed.
14. A more traditional way to monitor the access resistance is to apply a subthreshold test pulse and determine the time constant of decay of the capacity transient (τ_c). The decay becomes faster as the access resistance (R_a) decreases, because $\tau_c = R_a C_m$, where C_m is the capacity of the cell [40].
15. Unlike arachidonic acid (AA), PMA does not perturb the cell membrane. Unlike f-Met-Leu-Phe, PMA needs no priming.
16. The intactness of the patch membrane can be assessed by including a fluorescent dye (e.g., Lucifer yellow) in the pipette solution [13]. The cell will fluoresce if the patch has ruptured. The intactness of the patch can also be assessed by using a dye visible by light microscopy (e.g., eosin) in the pipette solution [45].
17. Petheö et al. [11] reported that the I_e in this method is susceptible to run down over time, which was reduced by addition of GTPγS and ATP to the bath (internal) solution. In our hands, I_e often persists in inside-out patches with minimal rundown, without addition of anything to the bath besides saline solution.

A speculative explanation for this difference is that our patches might include more cytoskeleton or other cytoplasmic structures that conceivably could influence oxidase stability.

18. Large, impermeant ions (methanesulfonate-, aspartate-, tetramethylammonium$^+$, *N*-methyl-D-glucamine$^+$) diffuse more slowly than the smaller physiological ions they replace, and thus significant liquid junction potentials may be present at the tip of the pipette [84, 85]. Contrary to popular opinion, liquid junction potentials are not corrected by nulling the current at the start of the experiment. If one wants to determine the absolute potential accurately, it is necessary to correct for liquid junction potentials. In many situations, such accuracy is not required, but if one wants to quantitate relative selectivity, for example, accuracy is desirable.
19. The apparent specificity of inhibitors historically often decreases with the passage of time. For example, charybdotoxin [86] and iberiotoxin [87] were originally thought to be specific for BK channels, but both were later found to also block other Ca^{2+}-activated K^+ channels [88], and charybdotoxin also blocks the purely voltage-gated Kv1.3 channel [89].

Acknowledgements

This work was supported in part by NIH grants HL61437 and GM087507 and NSF grant MCB-0943362.

References

1. Hodgkin AL, Huxley AF, Katz B (1952) Measurement of current–voltage relations in the membrane of the giant axon of *Loligo*. J Physiol 116:424–448
2. Hamill OP, Marty A, Neher E et al (1981) Improved patch-clamp techniques for high-resolution current recording from cells and cell-free membrane patches. Pflugers Arch 391:85–100
3. von Tscharner V, Prod'hom B, Baggiolini M et al (1986) Ion channels in human neutrophils activated by a rise in free cytosolic calcium concentration. Nature 324:369–372
4. DeCoursey TE, Cherny VV (1993) Potential, pH, and arachidonate gate hydrogen ion currents in human neutrophils. Biophys J 65:1590–1598
5. Schrenzel J, Serrander L, Bánfi B et al (1998) Electron currents generated by the human phagocyte NADPH oxidase. Nature 392:734–737
6. Gordienko DV, Tare M, Parveen S et al (1996) Voltage-activated proton current in eosinophils from human blood. J Physiol 496:299–316
7. Stoddard JS, Steinbach JH, Simchowitz L (1993) Whole cell Cl^- currents in human neutrophils induced by cell swelling. Am J Physiol 265:C156–C165
8. Krause KH, Demaurex N, Jaconi M et al (1993) Ion channels and receptor-mediated Ca^{2+} influx in neutrophil granulocytes. Blood Cells 19:165–173, discussion 173-165
9. Babior BM (1999) NADPH oxidase: an update. Blood 93:1464–1476
10. DeCoursey TE, Cherny VV, Zhou W et al (2000) Simultaneous activation of NADPH oxidase-related proton and electron currents in human neutrophils. Proc Natl Acad Sci U S A 97:6885–6889
11. Petheö GL, Maturana A, Spät A et al (2003) Interactions between electron and proton currents

in excised patches from human eosinophils. J Gen Physiol 122:713–726
12. Morgan D, Cherny VV, Murphy R et al (2005) The pH dependence of NADPH oxidase in human eosinophils. J Physiol 569:419–431
13. Morgan D, Cherny VV, Murphy R et al (2003) Temperature dependence of NADPH oxidase in human eosinophils. J Physiol 550:447–458
14. Petheő GL, Demaurex N (2005) Voltage- and NADPH-dependence of electron currents generated by the phagocytic NADPH oxidase. Biochem J 388:485–491
15. DeCoursey TE (2003) Interactions between NADPH oxidase and voltage-gated proton channels: why electron transport depends on proton transport. FEBS Lett 555:57–61
16. Moreland JG, Davis AP, Bailey G et al (2006) Anion channels, including ClC-3, are required for normal neutrophil oxidative function, phagocytosis, and transendothelial migration. J Biol Chem 281:12277–12288
17. Menegazzi R, Busetto S, Dri P et al (1996) Chloride ion efflux regulates adherence, spreading, and respiratory burst of neutrophils stimulated by tumor necrosis factor-α (TNF) on biologic surfaces. J Cell Biol 135:511–522
18. Matsuda JJ, Filali MS, Moreland JG et al (2010) Activation of swelling-activated chloride current by tumor necrosis factor-alpha requires ClC-3-dependent endosomal reactive oxygen production. J Biol Chem 285:22864–22873
19. Moreland JG, Davis AP, Matsuda JJ et al (2007) Endotoxin priming of neutrophils requires NADPH oxidase-generated oxidants and is regulated by the anion transporter ClC-3. J Biol Chem 282:33958–33967
20. Volk AP, Heise CK, Hougen JL et al (2008) ClC-3 and ICl_{swell} are required for normal neutrophil chemotaxis and shape change. J Biol Chem 283:34315–34326
21. Painter RG, Bonvillain RW, Valentine VG et al (2008) The role of chloride anion and CFTR in killing of Pseudomonas aeruginosa by normal and CF neutrophils. J Leukoc Biol 83:1345–1353
22. Cherny VV, Henderson LM, DeCoursey TE (1997) Proton and chloride currents in Chinese hamster ovary cells. Membr Cell Biol 11:337–347
23. Demaurex N, Grinstein S, Jaconi M et al (1993) Proton currents in human granulocytes: regulation by membrane potential and intracellular pH. J Physiol 466:329–344
24. DeCoursey TE, Cherny VV (1994) Voltage-activated hydrogen ion currents. J Membr Biol 141:203–223
25. DeCoursey TE, Morgan D, Cherny VV (2003) The voltage dependence of NADPH oxidase reveals why phagocytes need proton channels. Nature 422:531–534
26. Musset B, Cherny VV, Morgan D et al (2008) Detailed comparison of expressed and native voltage-gated proton channel currents. J Physiol 586:2477–2486
27. DeCoursey TE, Cherny VV (1996) Effects of buffer concentration on voltage-gated H^+ currents: does diffusion limit the conductance? Biophys J 71:182–193
28. Schrenzel J, Lew DP, Krause KH (1996) Proton currents in human eosinophils. Am J Physiol 271:C1861–C1871
29. Cherny VV, DeCoursey TE (1999) pH-dependent inhibition of voltage-gated H^+ currents in rat alveolar epithelial cells by Zn^{2+} and other divalent cations. J Gen Physiol 114:819–838
30. Femling JK, Cherny VV, Morgan D et al (2006) The antibacterial activity of human neutrophils and eosinophils requires proton channels but not BK channels. J Gen Physiol 127:659–672
31. Tare M, Prestwich SA, Gordienko DV et al (1998) Inwardly rectifying whole cell potassium current in human blood eosinophils. J Physiol 506:303–318
32. Grinstein S, Romanek R, Rotstein OD (1994) Method for manipulation of cytosolic pH in cells clamped in the whole cell or perforated-patch configurations. Am J Physiol 267:C1152–C1159
33. DeCoursey TE, Cherny VV (1998) Temperature dependence of voltage-gated H^+ currents in human neutrophils, rat alveolar epithelial cells, and mammalian phagocytes. J Gen Physiol 112:503–522
34. Kuno M, Ando H, Morihata H et al (2009) Temperature dependence of proton permeation through a voltage-gated proton channel. J Gen Physiol 134:191–205
35. Chabala LD, Sheridan RE, Hodge DC et al (1985) A microscope stage temperature controller for the study of whole-cell or single-channel currents. Pflugers Arch 404:374–377
36. Rae JL, Levis RA (1984) Patch voltage clamp of lens epithelial cells: theory and practice. Mol Physiol 6:115–162
37. Cherny VV, Murphy R, Sokolov V et al (2003) Properties of single voltage-gated proton channels in human eosinophils estimated by noise analysis and by direct measurement. J Gen Physiol 121:615–628
38. Fenwick EM, Marty A, Neher E (1982) A patch-clamp study of bovine chromaffin cells and of their sensitivity to acetylcholine. J Physiol 331:577–597
39. Lindau M, Fernandez JM (1986) IgE-mediated degranulation of mast cells does not require opening of ion channels. Nature 319:150–153
40. Rae J, Cooper K, Gates P et al (1991) Low access resistance perforated patch recordings

using amphotericin B. J Neurosci Methods 37:15–26
41. Horn R, Marty A (1988) Muscarinic activation of ionic currents measured by a new whole-cell recording method. J Gen Physiol 92:145–159
42. Fan JS, Palade P (1998) Perforated patch recording with β-escin. Pflugers Arch 436:1021–1023
43. Falke LC, Gillis KD, Pressel DM et al (1989) 'Perforated patch recording' allows long-term monitoring of metabolite-induced electrical activity and voltage-dependent Ca^{2+} currents in pancreatic islet B cells. FEBS Lett 251:167–172
44. Chung I, Schlichter LC (1993) Criteria for perforated-patch recordings: ion currents versus dye permeation in human T lymphocytes. Pflugers Arch 424:511–515
45. Strauss U, Herbrik M, Mix E et al (2001) Whole-cell patch-clamp: true perforated or spontaneous conventional recordings? Pflugers Arch 442:634–638
46. Bánfi B, Schrenzel J, Nüsse O et al (1999) A novel H^+ conductance in eosinophils: unique characteristics and absence in chronic granulomatous disease. J Exp Med 190:183–194
47. Robertson AK, Cross AR, Jones OTG et al (1990) The use of diphenylene iodonium, an inhibitor of NADPH oxidase, to investigate the antimicrobial action of human monocyte derived macrophages. J Immunol Methods 133:175–179
48. Barry PH (2006) The reliability of relative anion-cation permeabilities deduced from reversal (dilution) potential measurements in ion channel studies. Cell Biochem Biophys 46:143–154
49. Musset B, Smith SME, Rajan S et al (2011) Aspartate 112 is the selectivity filter of the human voltage-gated proton channel. Nature 480:273–277
50. DeCoursey TE, Cherny VV (1994) Na^+-H^+ antiport detected through hydrogen ion currents in rat alveolar epithelial cells and human neutrophils. J Gen Physiol 103:755–785
51. Hodgkin AL, Huxley AF (1952) The components of membrane conductance in the giant axon of *Loligo*. J Physiol 116:473–496
52. Byerly L, Meech R, Moody W Jr (1984) Rapidly activating hydrogen ion currents in perfused neurons of the snail, *Lymnaea stagnalis*. J Physiol 351:199–216
53. DeCoursey TE (1991) Hydrogen ion currents in rat alveolar epithelial cells. Biophys J 60:1243–1253
54. Humez S, Fournier F, Guilbault P (1995) A voltage-dependent and pH-sensitive proton current in *Rana esculenta* oocytes. J Membr Biol 147:207–215
55. Hille B (2001) Ion channels of excitable membranes, 3rd edn. Sinauer Associates, Inc., Sunderland, MA
56. Neher E, Stevens CF (1977) Conductance fluctuations and ionic pores in membranes. Annu Rev Biophys Bioeng 6:345–381
57. Demaurex N, Monod A, Lew DP et al (1994) Characterization of receptor-mediated and store-regulated Ca^{2+} influx in human neutrophils. Biochem J 297:595–601
58. Zweifach A, Lewis RS (1993) Mitogen-regulated Ca^{2+} current of T lymphocytes is activated by depletion of intracellular Ca^{2+} stores. Proc Natl Acad Sci U S A 90:6295–6299
59. Cross AR, Higson FK, Jones OT et al (1982) The enzymic reduction and kinetics of oxidation of cytochrome b_{-245} of neutrophils. Biochem J 204:479–485
60. Koshkin V, Lotan O, Pick E (1996) The cytosolic component $p47^{phox}$ is not a *sine qua non* participant in the activation of NADPH oxidase but is required for optimal superoxide production. J Biol Chem 271:30326–30329
61. Murphy R, DeCoursey TE (2006) Charge compensation during the phagocyte respiratory burst. Biochim Biophys Acta 1757:996–1011
62. Henderson LM, Chappell JB, Jones OTG (1987) The superoxide-generating NADPH oxidase of human neutrophils is electrogenic and associated with an H^+ channel. Biochem J 246:325–329
63. Bankers-Fulbright JL, Gleich GJ, Kephart GM et al (2003) Regulation of eosinophil membrane depolarization during NADPH oxidase activation. J Cell Sci 116:3221–3226
64. Geiszt M, Kapus A, Nemet K et al (1997) Regulation of capacitative Ca^{2+} influx in human neutrophil granulocytes. Alterations in chronic granulomatous disease. J Biol Chem 272:26471–26478
65. Jankowski A, Grinstein S (1999) A noninvasive fluorimetric procedure for measurement of membrane potential. Quantification of the NADPH oxidase-induced depolarization in activated neutrophils. J Biol Chem 274:26098–26104
66. Rada BK, Geiszt M, Káldi K et al (2004) Dual role of phagocytic NADPH oxidase in bacterial killing. Blood 104:2947–2953
67. Demaurex N, Petheõ GL (2005) Electron and proton transport by NADPH oxidases. Philos Trans R Soc Lond B Biol Sci 360:2315–2325
68. DeCoursey TE (2004) During the respiratory burst, do phagocytes need proton channels or potassium channels, or both? Sci STKE 2004:pe21
69. DeCoursey TE (2013) Voltage gated proton channels: molecular biology, physiology and

pathophysiology of the HV family. Physiol Rev 93(2):599–652
70. DeCoursey TE (2010) Voltage-gated proton channels find their dream job managing the respiratory burst in phagocytes. Physiology (Bethesda) 25:27–40
71. Henderson LM, Chappell JB, Jones OTG (1988) Superoxide generation by the electrogenic NADPH oxidase of human neutrophils is limited by the movement of a compensating charge. Biochem J 255:285–290
72. Musset B, Cherny VV, Morgan D et al (2009) The intimate and mysterious relationship between proton channels and NADPH oxidase. FEBS Lett 583:7–12
73. Morgan D, Cherny VV, Finnegan A et al (2007) Sustained activation of proton channels and NADPH oxidase in human eosinophils and murine granulocytes requires PKC but not $cPLA_2\alpha$ activity. J Physiol 579:327–344
74. Musset B, Capasso M, Cherny VV et al (2010) Identification of Thr^{29} as a critical phosphorylation site that activates the human proton channel *Hvcn1* in leukocytes. J Biol Chem 285:5117–5121
75. Sigworth FJ (1995) Electronic design of the patch clamp. In: Sakmann B, Neher E (eds) Single channel recording, 2nd edn. Plenum Press, New York, pp 95–127
76. Goldman DE (1943) Potential, impedance, and rectification in membranes. J Gen Physiol 27:37–60
77. Hodgkin AL, Katz B (1949) The effect of sodium ions on the electrical activity of giant axon of the squid. J Physiol 108:37–77
78. Byerly L, Moody WJ (1986) Membrane currents of internally perfused neurons of the snail, *Lymnaea stagnalis*, at low intracellular pH. J Physiol 376:477–491
79. Kapus A, Romanek R, Qu AY et al (1993) A pH-sensitive and voltage-dependent proton conductance in the plasma membrane of macrophages. J Gen Physiol 102:729–760
80. Levis RA, Rae JL (1992) Constructing a patch clamp setup. Methods Enzymol 207:14–66
81. Levis RA, Rae JL (1993) The use of quartz patch pipettes for low noise single channel recording. Biophys J 65:1666–1677
82. Cota G, Armstrong CM (1988) Potassium channel "inactivation" induced by soft-glass patch pipettes. Biophys J 53:107–109
83. Rojas L, Zuazaga C (1988) Influence of the patch pipette glass on single acetylcholine channels recorded from *Xenopus* myocytes. Neurosci Lett 88:39–44
84. Neher E (1992) Correction for liquid junction potentials in patch clamp experiments. Methods Enzymol 207:123–131
85. Ng B, Barry PH (1995) The measurement of ionic conductivities and mobilities of certain less common organic ions needed for junction potential corrections in electrophysiology. J Neurosci Methods 56:37–41
86. Miller C, Moczydlowski E, Latorre R et al (1985) Charybdotoxin, a protein inhibitor of single Ca^{2+}-activated K^+ channels from mammalian skeletal muscle. Nature 313:316–318
87. Galvez A, Gimenez-Gallego G, Reuben JP et al (1990) Purification and characterization of a unique, potent, peptidyl probe for the high conductance calcium-activated potassium channel from venom of the scorpion *Buthus tamulus*. J Biol Chem 265:11083–11090
88. Hermann A, Erxleben C (1987) Charybdotoxin selectively blocks small Ca-activated K channels in *Aplysia* neurons. J Gen Physiol 90:27–47
89. Sands SB, Lewis RS, Cahalan MD (1989) Charybdotoxin blocks voltage-gated K^+ channels in human and murine T lymphocytes. J Gen Physiol 93:1061–1074
90. Cherny VV, Markin VS, DeCoursey TE (1995) The voltage-activated hydrogen ion conductance in rat alveolar epithelial cells is determined by the pH gradient. J Gen Physiol 105:861–896
91. Morgan D, DeCoursey TE (2007) Analysis of electrophysiological properties and responses of neutrophils. Methods Mol Biol 412:139–175

Chapter 10

Assessment of Neutrophil Apoptosis

David A. Dorward, Adriano G. Rossi, Ian Dransfield, and Christopher D. Lucas

Abstract

Timely neutrophil apoptosis and cell clearance by surrounding phagocytes are essential components of the resolution phase of acute inflammation. Programmed cell death by apoptosis occurs with maintenance of an intact cell membrane in order to prevent the release of histotoxic intracellular products such as proteases and reactive oxidant species into the extracellular surroundings as occurs during necrosis. Macrophage phagocytosis results in attenuation of Toll-like receptor-driven proinflammatory mediator production further promoting inflammation resolution. Failures in this cascade of events can result in tissue damage, chronic inflammation and disease. By studying human neutrophil apoptosis and phagocytic clearance in vitro, it is possible to delineate key control mechanisms in the regulation of these processes and therefore also identify potential therapeutic targets. Apoptotic signalling pathways are well described in the literature using a variety of laboratory techniques. In this paper, we outline the key in vitro assays used to assess neutrophil apoptosis, activation of key components of the apoptotic machinery, and phagocytic clearance of these cells.

Key words Neutrophil, Apoptosis, Mitochondria, Caspase, Phagocytosis, DNA fragmentation

1 Introduction

Neutrophil migration into inflammatory sites in response to noxious stimuli is vital for the containment and clearance of inciting pathogens and control of acute inflammation [1]. Having performed a variety of functions including degranulation, production of reactive oxygen species (ROS), phagocytosis, and formation of antimicrobial neutrophil extracellular traps (NETs), the controlled and safe disposal of these cells is essential. Timely neutrophil apoptosis and subsequent clearance by surrounding phagocytes are therefore crucial components in the resolution of acute inflammation [2]. Dysregulation of either of these can result in perpetuation of the inflammatory process resulting in chronic inflammation and disease.

Neutrophils are terminally differentiated granulocytes that undergo spontaneous apoptosis within 8–24 h of culture in vitro [3].

Mark T. Quinn and Frank R. DeLeo (eds.), *Neutrophil Methods and Protocols*, Methods in Molecular Biology, vol. 1124,
DOI 10.1007/978-1-62703-845-4_10,

Induction of neutrophil apoptosis occurs due to "extrinsic" ligation of death receptors, including TRAIL (TNF-related apoptosis-inducing ligand) and FAS (CD95). Alternatively changes in the intracellular environment from cellular stress signals alter the balance between proapoptotic B cell lymphoma 2 (Bcl-2) family members Bax, and Bid and antiapoptotic proteins, predominantly Mcl-1 (myeloid leukemia cell differentiation protein) and Bcl-xl, leading to activation of the "intrinsic" apoptotic pathway. The resultant increase in mitochondrial membrane permeability allows cytochrome *c* translocation into the cytoplasm which, upon interaction with apoptotic protease activating factor 1 (APAF1), cleaves procaspase-9 to its active form, cysteine-aspartic protease (caspase) 9. Caspases are essential initiators (caspases 8, 9, and 10) and executioners (caspases 3, 6, 7, and 14) of the apoptotic pathway with caspase-8 cleavage occurring following death receptor ligation and formation of the death-inducing signalling complex (DISC) [4, 5]. Both intrinsic and extrinsic apoptotic signalling pathways converge upon caspase-3 which, once activated, induces cellular apoptosis. Conversely, neutrophil life span can be significantly prolonged through upregulation of antiapoptotic proteins including Mcl-1 and inhibitor of apoptosis (IAP) proteins in response to both intra- and extracellular factors including bacteria and bacterial-derived products, pH, hypoxia, temperature, and host-derived factors including G-CSF (granulocyte colony-stimulating factor) [6–8]. Phagocytosis of apoptotic cells is predominantly by surrounding macrophages whose phagocytic capacity is influenced by a variety of factors including cytokines, steroid hormones, prostaglandins, and lipoxins [9–11].

The study of neutrophil apoptosis in vitro is critically dependent on the isolation of a pure and unperturbed neutrophil population. A variety of methods are described for isolation of both human neutrophils from peripheral blood including hypotonic lysis, a Ficoll/Hypaque gradient or dextran sedimentation and discontinuous Percoll gradient. The merits of each technique are discussed elsewhere; we would guide readers to several useful articles on the topic for further information [12–15]. Given that neutrophil longevity is easily influenced by a wide variety of factors, minimizing experimental neutrophil activation and prolongation of life span is essential in in vitro culture. Most notably, careful choice of the method of cell isolation and control of pH, temperature, oxygen tension, and cell density and the presence of serum are key factors that will influence interpretation of experimental data.

Given the characteristic processes that occur during apoptosis, this cascade of events is amenable to in vitro study by a variety of different approaches and assays. These include observation of morphological changes such as cell shrinkage, apoptotic body formation, and chromatin condensation; mitochondrial permeability with loss of mitochondrial membrane potential; DNA cleavage into approximately 200 base pair fragments and multiples thereof; and

caspase activation and reorganization of the plasma membrane with externalization of phosphatidylserine and phosphatidylethanolamine. This chapter describes diverse methodologies to investigate each component of the apoptotic machinery as well as subsequent clearance by macrophage phagocytosis and is an updated version of our previous chapter in this journal [16].

2 Materials

2.1 In Vitro Culture of Human Neutrophils

1. Iscove's Modified Dulbecco's Medium (IMDM).
2. Penicillin/streptomycin 100×.
3. 10 % autologous serum (*see* **Note 1**).
4. 96-well flat-bottom plates.

2.2 Cytocentrifuge Preparations for Light Microscopy

1. Cytocentrifuge chambers; filter cards, glass slides, and coverslips.
2. Methanol, Diff-Quik™ stains, and DPX mounting medium (Sigma-Aldrich).

2.3 Preparation of Neutrophils for Electron Microscopy

1. 3 % glutaraldehyde: dilute 25 % stock solution in 0.1 M sodium cacodylate buffer, pH 7.2.
2. 1 % osmium tetroxide in 0.1 M sodium cacodylate.
3. 50, 70, 90, and 100 % normal grade acetones and analar acetone.
4. Araldite resin.
5. Reichert OMU4 ultramicrotome.

2.4 Plasma Membrane Alterations

1. 96-well flat-bottom plate.
2. Annexin V-conjugated fluorescein isothiocyanate (FITC; Roche).
3. Annexin-binding buffer: Hanks' balanced salt solution (HBSS) with 2.5 mM Ca^{2+}. Store at 4 °C.
4. Propidium iodide stock solution: 1 mg/mL propidium iodide in sterile H_2O.
5. Cytometry buffer: cation-free PBS, 0.1 % bovine serum albumin. Store at 4 °C.
6. APC-Cy7 antihuman CD16 (1:100 BioLegend).
7. Nonbinding murine isotype (IgG1) control (BioLegend).

2.5 Mitochondrial Permeability

1. MitoCapture™ Mitochondrial Apoptosis Detection Fluorometric Kit (BioVision, Milpitas, CA 95035, USA) contains MitoCapture™ reagent (store at –20 °C) and Incubation buffer (store at 4 °C).

2.6 Western Blotting for Regulators of Apoptosis

1. Tris-buffered saline (TBS 10×): 87.66 g of NaCl, 24.22 g Tris base, 800 mL of distilled water (ddH_2O). Adjust the pH to 7.4 with HCl and add ddH_2O to 1 L. Store at room temperature.
2. TBS 1×: dilute TBS 10× 1:10 with ddH_2O.
3. Protease inhibitor buffer (*see* **Note 2**): 0.78 mL of TBS, 20 μL of stock protease inhibitor cocktail for use with mammalian cell and tissue extracts (Sigma), 20 μL of 400 mM stock 4-(2-aminoethyl)benzenesulfonyl fluoride hydrochloride (AEBSF, stock in H_2O), 20 μL of 0.15 μM stock aprotinin (stock in H_2O), 20 μL of 20 mM stock leupeptin (stock in H_2O), 40 μL of 0.75 μM stock pepstatin A (stock in methanol), 20 μL of 1 M stock sodium vanadate (stock in H_2O, pH 10, boiled), 20 μL of 0.5 M stock benzamidine (stock in H_2O), 20 μL of 2 M stock levamisole (stock in H_2O), and 60 μL of 3.33 M stock β-glycerophosphate (stock in H_2O).
4. 10 % Nonidet P-40 (NP-40) in 1× TBS for cell lysis.
5. BCA protein assay.
6. Sample buffer (for 4×): 4 mL of 50 % glycerol, 4 mL of 20 % SDS, 2.5 mL of 1 M Tris–HCl (pH 6.8), and 20 μL of 1 % (w/v in ethanol) bromophenol blue. Add 400 μL of β-mercaptoethanol in a fume hood.
7. Benchmark™ prestained molecular weight standards (Invitrogen).
8. 12 % SDS-PAGE gel.
9. Running buffer (10×): 121 g Tris base, 10 g SDS, 238 g Hepes, and ddH_2O up to 1 L. Dilute in 1:10 ddH_2O prior to use.
10. Transfer buffer (10×): 30.3 g Tris base, 144.12 g glycine, and ddH_2O up to 1 L.
11. Transfer buffer (1×): 100 mL of 10× transfer buffer, 200 mL of methanol, and 700 mL of ddH_2O.
12. Polyvinylidene difluoride (PVDF) membrane (Millipore).
13. Blocking buffer: TBS, 0.1 % Tween 20 (polysorbate 20), and 5 % dried milk powder.
14. Primary antibodies: Mcl-1 (1:500; Santa Cruz Biotechnology), GAPDH (1:10,000; Sigma), cleaved caspase-3 (1:1,000; Cell Signalling), cleaved caspase-9 (1:1,000; Cell Signalling).
15. Secondary antibody: corresponding horseradish peroxidase-conjugated antibody (1:2,500; Dako).
16. ECL prime (GE Healthcare), light-sensitive film, and X-ray developer.

2.7 Fluorometric Caspase Kit

1. Homogeneous Caspase Assay Kit (Roche Diagnostics, Ltd) (*see* **Note 3**) contains 1× incubation buffer, stock caspase substrate solution (500 μM DEVD-R110 in DMSO), positive

control (lysate from apoptotic camptothecin-treated U937 cells), and R110 standard for calibration curve construction (1 mM in DMSO).

2.8 Caspase Profiling Plate

1. ApoAlert™ Caspase Profiling Plate (Clontech) contains 96-well microplate with immobilized substrates for caspase-2 (VDVAD-AMC), caspase-3 (DEVD-AMC), caspase-8 (IETD-AMC), and caspase-9 (LEHD-AMC) in 24 wells each, lysis buffer, 2× reaction buffer, 100× DTT solution, and inhibitors of caspases 2, 3, 8, and 9.

2.9 Gel Electrophoresis for DNA Fragmentation

1. Wizard® genomic DNA purification kit (Promega).
2. 0.5× TBE running buffer (5×): 54 g Tris base, 27.5 g boric acid, 20 mL of 0.5 M EDTA, up to 1 L of dH_2O, pH 8.0.
3. SeaKem LE agarose (Cambrex) for DNA electrophoresis.
4. Ethidium bromide solution: 10 mg/mL in dH_2O.
5. GelRed™ Nucleic Acid Gel Stain (Jencons, Lutterworth, England).
6. 6× blue/orange loading dye (Promega).

2.10 Propidium Iodide Staining for Hypodiploid Nuclei

1. 96-well flat-bottom plate.
2. PI solution: 250 μL of propidium iodide stock solution (10 mg/mL in ddH_2O), 2.2 mL of sodium citrate (2.2 g in 10 mL of ddH_2O), 50 μL Triton X-100; make up to 50 mL with ddH_2O. Store solution at 4 °C in the dark.

2.11 TUNEL Staining

1. 96-well flat-bottom flexible plate.
2. In Situ Cell Death Detection Kit, Fluorescein (Roche Diagnostics Ltd) contains 10× enzyme solution (TdT) in storage buffer and 1× labelled nucleotide mixture in reaction buffer. This protocol also requires PBS (wash buffer), 3 % H_2O_2 in methanol (blocking solution), 4 % paraformaldehyde in PBS at pH 7.4 (fixation buffer; freshly prepared), and 0.1 % Triton-X100 in 0.1 % sodium citrate (permeabilization buffer; freshly prepared).

2.12 Plate-Based Phagocytosis Assay

1. 2.5 % glutaraldehyde in PBS.
2. Dimethoxybenzidine (o-diansidine): 0.1 mg/mL of dimethoxybenzidine (o-diansidine) in PBS, made up fresh from 1 mg/mL frozen stock.
3. 30 % H_2O_2 solution.

2.13 Flow Cytometry-Based Phagocytosis Assay

1. 5-Chloromethylfluorescein diacetate (CMFDA; CellTracker™ Green, Invitrogen).
2. pHrodo™ Red succinimidyl ester (Invitrogen).
3. Trypsin/EDTA solution: 0.25 % trypsin, 1 mM EDTA.

3 Methods

3.1 Analysis of Neutrophil Morphology by Light Microscopy

Apoptotic neutrophils can be identified by their characteristic condensation of nuclear material, prominent nucleoli, and vacuolation of the cytoplasm (Fig. 1a, d). Morphological characterization of neutrophils by microscopy analysis allows rapid, cheap, and accurate assessment of neutrophil apoptosis (*see* **Note 4**).

1. Suspend freshly isolated peripheral blood neutrophils (at least 97 % purity—perform cytocentrifuge preparation, as described below) at 1×10^7 cells/mL in IMDM supplemented with 10 % autologous serum and penicillin/streptomycin (1×) (*see* **Note 1**).

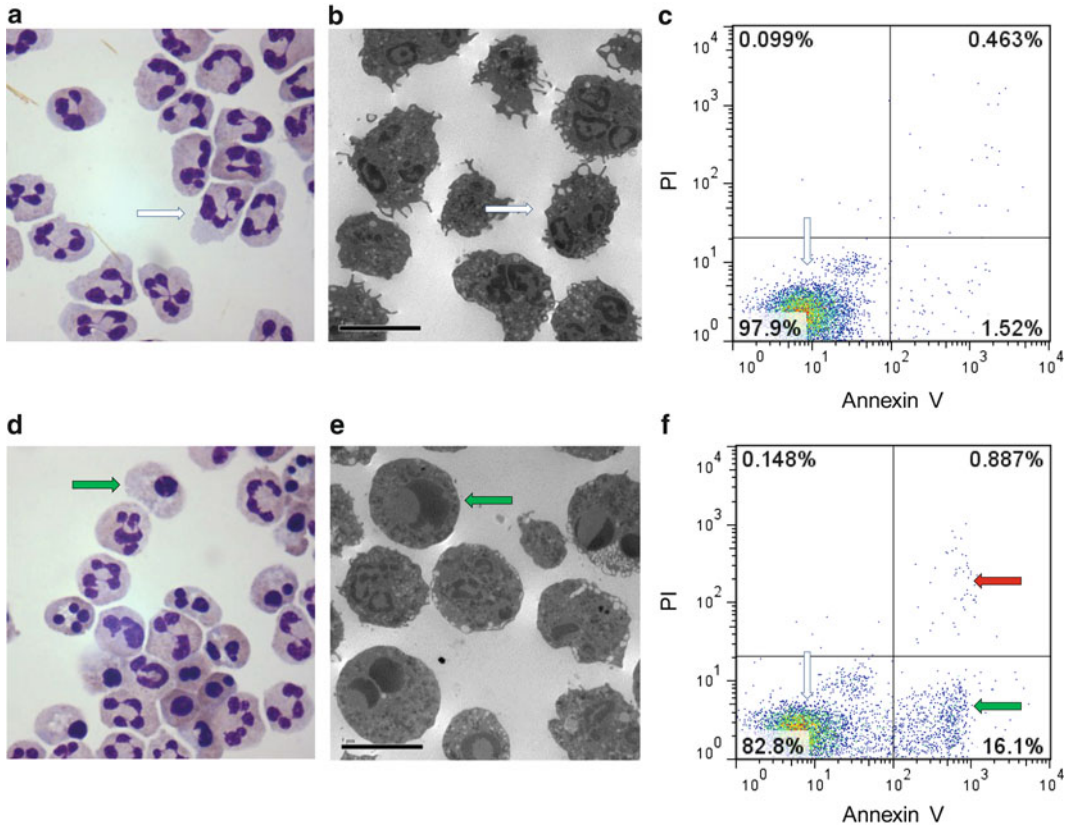

Fig. 1 Assessment of neutrophil apoptosis by microscopy and flow cytometry. Following 6 h in vitro culture, isolated neutrophils are predominantly viable with characteristic multilobed nucleus and irregular cell membrane (*white arrow*) as seen by light microscopy ((**a**); ×1000 magnification) and electron microscopy ((**b**); ×980 magnification). Cells are impermeable to propidium iodide (PI) and phosphatidylserine remains internalized; therefore no Annexin V (Ann V) binding occurs, and a viable cell population ($AnnV^{-ve}/PI^{-ve}$) is seen on flow cytometry (**c**). In contrast drug treatment with apoptosis-inducing agents induces neutrophil apoptosis with characteristic morphological changes of nuclear condensation and cell shrinkage (*green arrow*) visible by both light microscopy (**d**) and electron microscopy (**e**). Apoptotic cells are detected by flow cytometry as $AnnV^{+ve}/PI^{-ve}$ (*green arrow*). Necrotic cells with loss of cell membrane integrity are permeable to PI and are detected as $AnnV^{+ve}/PI^{+ve}$ (*red arrow*)

2. Add 75 μL of neutrophil suspension to wells of a 96-well flat-bottom plate.
3. To each well, add 15 μL of apoptosis-modifying agents (10× concentration) or buffer control and 60 μL of IMDM/10 % serum. If two agents are used in combination, only 45 μL of IMDM is required.
4. Cover with a lid. Incubate at 37 °C in a 5 % CO_2 incubator for the desired length of time.
5. Vigorously pipette the well to dislodge adherent cells, and load a cytospin chamber with 100 μL of aged neutrophil suspension.
6. Cytocentrifuge at 300 × *g* for 3 min.
7. Air-dry for 5 min.
8. Fix in methanol for 2 min. Drain.
9. Stain in Diff-Quik solution 1 or equivalent acid dye for 2 min. Drain.
10. Stain in Diff-Quik solution 2 or equivalent basic dye for 2 min.
11. Drain and rinse with distilled water.
12. Allow to dry, mount with a drop of DPX, and apply a coverslip.
13. View using a light microscope with a 40× or 100× (oil) objective, and count >300 cells per slide (*see* **Note 4**).

3.2 Analysis of Neutrophil Morphology by Electron Microscopy

Detailed structural analysis of the morphological changes that occur in apoptosis is observed best by electron microscopy and formed the basis of the initial observations of this cellular process [17] (Fig. 1b, d).

1. Suspend freshly isolated peripheral blood neutrophils (at least 97 % purity—perform cytocentrifuge preparation as described) at 1×10^7 cells/mL in IMDM/10 % autologous serum and penicillin/streptomycin.
2. Add 75 μL of neutrophil suspension to wells of a 96-well flat-bottom plate.
3. To each well add 15 μL of apoptosis-modifying agents (10× concentration) or buffer control and 60 μL IMDM with 10 % serum. If two agents are used in combination, only 45 μL of IMDM is required.
4. Cover with a lid, and incubate at 37 °C in a 5 % CO_2 incubator for the desired length of time.
5. Vigorously pipette the well to dislodge adherent cells, and pool multiple 5 wells together into 500 μL Eppendorf and centrifuge at 300 × *g* for 5 min.
6. Resuspend in 3 % glutaraldehyde in 0.1 M sodium cacodylate buffer, pH 7.3 for 2 h.

7. Centrifuge at 300×*g* for 5 min and resuspend in 0.1 M cacodylate. Incubate for 10 min and repeat three times.
8. Postfix in 1 % osmium tetroxide in 0.1 M sodium cacodylate for 45 min.
9. Centrifuge at 300×*g* for 5 min and resuspend in 0.1 M cacodylate. Incubate for 10 min and repeat three times.
10. Dehydrate in 50, 70, 90, and 100 % normal grade acetones for 10 min each and then for a further two 10-min changes in analar acetone.
11. Embed in araldite resin.
12. Cut 1 μm sections on an ultramicrotome, stain with toluidine blue, and view in a light microscope to select suitable areas for further study.
13. Cut 60 nm ultrathin sections from those areas identified and stain in uranyl acetate and lead citrate.
14. Viewed in a transmission electron microscope.

3.3 Annexin V/ Propidium Iodide Staining

Apoptosis is associated with the loss of phospholipid asymmetry and the externalization of phosphatidylserine on the outer surface of the plasma membrane. Annexin V (Ann V) binds specifically to phosphatidylserine in the presence of Ca^{2+}, and its fluorescent derivatives can be used to identify apoptotic cells. A range of conjugated fluorophores are available; however, Ann V-FITC is most commonly used. Propidium iodide (PI), a nucleophilic dye, is excluded from the cell in the presence of an intact cell membrane. In the absence of surrounding phagocytes in vitro, the apoptotic cell loses membrane integrity and becomes necrotic. In doing so PI is able to bind nuclear material and in combination with Ann V is able to discriminate viable, apoptotic, and necrotic cells by a simple and rapid flow cytometric method (Fig. 1c, f).

1. Suspend freshly isolated peripheral blood neutrophils (at least 97 % purity—perform cytocentrifuge preparation as described) at 1×10^7 cells/mL in IMDM supplemented with 10 % autologous serum and penicillin/streptomycin.
2. Add 75 μL of neutrophil suspension to wells of a 96-well flat-bottom plate. To each well add 15 μL of apoptosis-modifying agents (10× concentration) or buffer control and 60 μL of IMDM/10 % serum. If two agents are used in combination, only 45 μL of IMDM is required.
3. Cover with a lid, and incubate at 37 °C in a 5 % CO_2 incubator for the desired length of time.
4. Vigorously pipette the well to dislodge adherent cells, and transfer 75 μL of cells into a flow tube containing 250 μL of Annexin V buffer (*see* **Note 5**).

5. Incubate for 5 min on ice.
6. Immediately prior to running each sample on a flow cytometer, add PI (1 μL of 1 mg/mL stock solution).
7. Analyze by flow cytometry using FL-1/FL-2 channel analysis following appropriate compensation. Live cells are Annexin V negative and PI negative; apoptotic cells are Annexin V positive and PI negative; necrotic cells are both Annexin V and PI positive (Fig. 1c, f).

3.4 Loss of CD16 Expression

Neutrophil apoptosis is associated with a marked downregulation of FcγRIII (CD16) [18]. A simple flow cytometric method using an anti-CD16 monoclonal antibody will reliably discriminate apoptotic from non-apoptotic neutrophils in a mixed cell population. However, it should be noted that eosinophils express low levels of CD16 and that neutrophil expression of CD16 can be regulated during cellular activation, so it is important to verify that CD16 expression correlates with apoptosis using additional methods (*see* **Note 6**).

1. Suspend freshly isolated peripheral blood neutrophils (at least 97 % purity) at 2×10^6 cells/mL in IMDM/10 % autologous serum.
2. Add 90 μL of neutrophil suspension to wells of a 96-well flat bottom. To each well add 10 μL of apoptosis-modifying agents (10× concentration) or buffer control, cover with a lid, and incubate at 37 °C in a 5 % CO_2 incubator for the desired length of time.
3. Transfer 2×10^5 neutrophils (40 μL of a 5×10^6/mL suspension) to a 96-well U-bottom plate, and centrifuge at $200 \times g$ for 2 min at 4 °C. Discard the supernatants.
4. Briefly vortex the plate to disrupt the pelleted cells.
5. Incubate neutrophils with APC/Cy7 anti-CD16 (clone 3G8) or nonbinding control IgG1 in 50 μL of cytometry buffer on ice for 30 min.
6. Add 75 μL of cytometry buffer. Centrifuge at $200 \times g$ for 2 min at 4 °C. Discard the supernatants.
7. Resuspend cells in 125 μL of cytometry buffer. Centrifuge at $200 \times g$ for 2 min at 4 °C. Discard the supernatants and vortex the plate for 5 s to disrupt the pelleted cells.
8. Analyze cells using a flow cytometer. Apoptotic neutrophils have low CD16 expression fluorescence; non-apoptotic neutrophils have high CD16 fluorescence.

3.5 Measurement of Mitochondrial Membrane Potential Using MitoCapture™

Mitochondrial membrane potential (ΔΨM) is lost during apoptosis with the formation of pores which allow the passage of proteins from the mitochondria into the cytosol, leading to activation of caspase-9 and subsequently caspase-3. Changes in neutrophil

mitochondrial membrane potential may be measured using MitoCapture™ a cationic dye which exhibits membrane potential-dependent accumulation in mitochondria. In viable cells with intact mitochondrial membrane potential, MitoCapture™ is able to enter mitochondria and polymerize, where it fluoresces in the red (FL-2) channel indicated by a fluorescence emission shift from green (525 nm) to red (590 nm). However, when $\Delta\Psi M$ is lost during apoptosis, MitoCapture™ is unable to accumulate in the mitochondria and remains in monomeric form in the cytosol and fluoresces in the green (FL-1) channel. Apoptosis-associated mitochondrial depolarization is quantified flow cytometrically by an increase in FL-1 fluorescence (Fig. 2a) or alternatively as a plate-based fluorometric assay with a decrease in the red/green fluorescence intensity ratio (*see* **Note 7**).

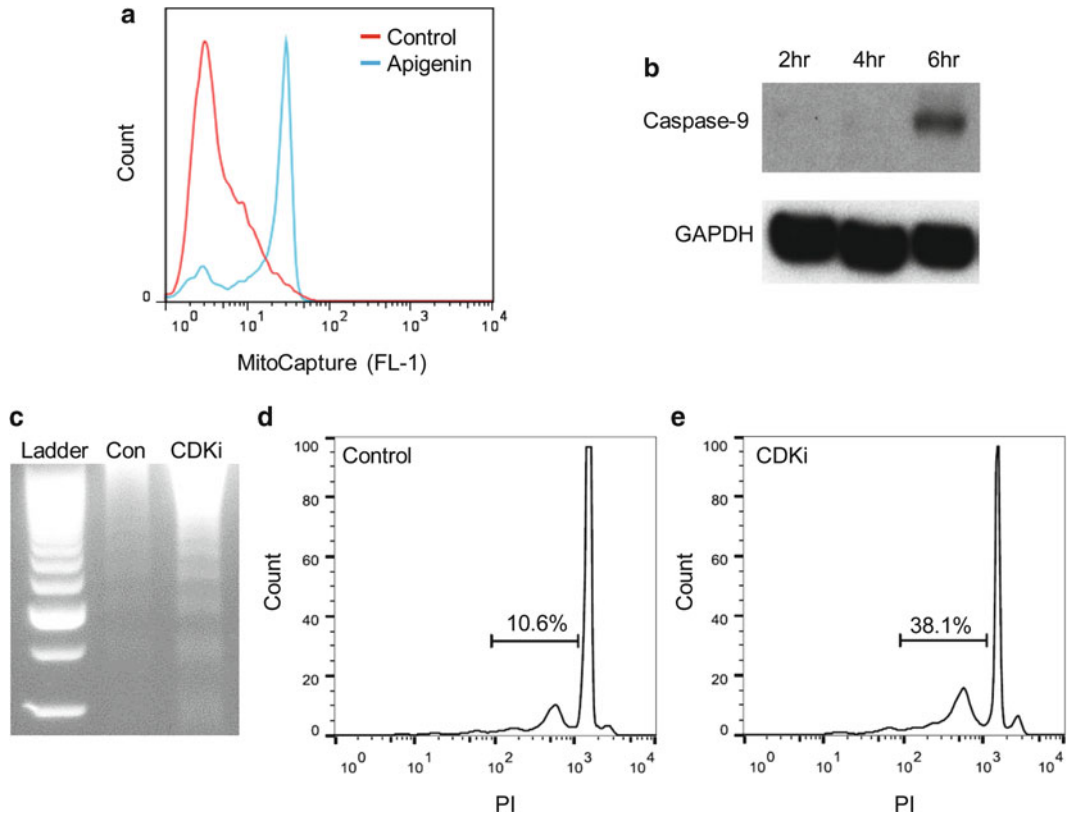

Fig. 2 Analysis of intracellular apoptotic events. Loss of mitochondrial membrane potential is demonstrated by increased fluorescence in MitoCapture™-labelled neutrophils after 2 h incubation with apigenin (50 mM), a known inducer of apoptosis, relative to vehicle control ((**a**) *red line*, control; *blue line*, apigenin). Constitutive apoptosis is associated with a time-dependent accumulation of intracellular-cleaved caspase-9 within neutrophils, GAPDH loading control (**b**). Increased apoptosis is also demonstrated by DNA fragmentation in cyclin-dependent kinase inhibitor (CDKi)-treated cells visible on gel electrophoresis with "laddering" ((**c**) 4 h). Hypodiploid DNA is also visible when analyzed by flow cytometry ((**d**), control; (**e**), CDKi 20 h)

1. This protocol assumes the use of a MitoCapture™ mitochondria permeability detection kit (BioVision).
2. For each experimental sample dilute 0.5 μL of MitoCapture™ reagent in 500 μL of pre-warmed (37 °C) MitoCapture™ Incubation buffer in a 1.5-mL Eppendorf tube.
3. Suspend freshly isolated peripheral blood neutrophils (at least 97 % purity) at 1×10^7 cells/mL in IMDM/10 % autologous serum.
4. Add 75 μL of neutrophil suspension to wells of a 96-well flat-bottom plate.
5. To each well add 15 μL of apoptosis-modifying agents (10× concentration) or buffer control and 60 μL of IMDM/10 % serum. If two agents are used in combination, only 45 μL of IMDM is required.
6. Cover with a lid, and incubate at 37 °C in a 5 % CO_2 incubator for the desired length of time.
7. Add 150 μL of cell suspension to 500 μL of diluted MitoCapture™ reagent.
8. Incubate on shaking heat block at 300 × *g*, 37 °C, 15 min.
9. Centrifuge at 300 × *g* for 5 min.
10. Resuspend in 300 μL of MitoCapture™ Incubation buffer.
11. Analyze on flow cytometer with an increase in fluorescence in FL-1 channel (Ex/Em = 48w8/530 + 30 nm) indicating loss of $\Delta\Psi M$.

3.6 Caspase Activation

Caspase signalling is central to both the initiation and execution of the apoptotic pathway with detection of the active forms of the protein, or disappearance of the inactive precursor, in response to apoptotic stimuli possible by Western blot. An example of Western blotting for active caspase-9 is shown in Fig. 2b (*see* **Note 8**).

3.6.1 Western Blotting for Caspases and Apoptotic Proteins

1. These instructions assume the use of an XCell SureLock™ Mini-Cell Electrophoresis System (Invitrogen).
2. Suspend freshly isolated peripheral blood neutrophils (at least 97 % purity) at 5×10^6 cells/mL in IMDM/10 % autologous serum. Dispense 1 mL of neutrophil suspension into 2-mL round-bottomed polypropylene tubes, and incubate ± apoptosis-modifying agents at 37 °C for the desired length of time.
3. Centrifuge the neutrophil suspensions at 13,000 × *g* for 1 min. Discard the supernatants.
4. Resuspend the cell pellets in protease inhibitor buffer (90 μL per 5×10^6 cells) and incubate on ice for 10 min.
5. Add 10 % NP-40 in TBS (10 μL per 5×10^6 cells), immediately vortex for 5 s, and incubate for a further 10 min on ice.

6. Centrifuge at 13,000×*g* for 20 min at 4 °C, and retain the detergent-soluble supernatant containing the cytosolic and membrane fractions. Samples can be stored at this point (−20 °C) prior to further analysis.
7. Calculate protein concentration of each sample using BCA protein assay per manufacturer's instructions.
8. Transfer volume equivalent to 30 μg of protein into fresh Eppendorf tubes, and make up to total volume of 30 μL with PBS (without cations) and 10 μL of 4× sample buffer.
9. Heat at 95 °C for 5 min.
10. Load samples (30 μL per lane) onto a 12 % polyacrylamide gel alongside molecular weight standards, and run at 110 V until the dye front reaches the bottom of the gel.
11. Transfer proteins from the gel to the PVDF membrane at 80 V for 1 h at 4 °C.
12. Wash the membrane in TBS/0.1 % Tween 20 for 5 min.
13. Block the membrane in 10 mL of 5 % dried milk powder in TBS/0.1 % Tween 20 at room temperature on a rocking platform for 1 h.
14. Wash the membrane three times in TBS/0.1 % Tween 20® for 5 min.
15. Incubate with the primary antibody at the indicated concentrations in TBS/0.1 % Tween 20 containing 5 % dried milk powder (5 mL volume). Incubate in a 50 mL conical polypropylene tube overnight at 4 °C on rollers.
16. Wash membrane three times in TBS/0.1 % Tween 20 each for 5 min at room temperature on a rocking platform.
17. Incubate with the secondary antibody (HRP-conjugated polyclonal goat anti-rabbit Ig (Dako)) diluted 1:2,500 in blocking buffer (5 mL). Incubate in a 50 mL conical polypropylene tube for 2 h at room temperature on a rocking platform.
18. Wash membrane three times in TBS/0.1 % Tween 20 each for 5 min at room temperature on a rocking platform.
19. Develop using enhanced chemiluminescence (ECL Prime; Amersham) according to the manufacturer's instructions.
20. Strip and reprobe blot with β-actin or GAPDH as a loading control.

3.6.2 Fluorometric Homogeneous Caspase Assay

Apoptosis usually occurs via caspase-dependent processes, and an increase in caspase activity gives a general indication of the occurrence of apoptosis. Commercial kits are available in which total caspase activity can be measured (homogeneous caspase assay). However, these kits do not dissect out precisely which caspases are active. They utilize cleavage of a fluorescence-conjugated, modified

nonspecific caspase substrate (e.g., VAD-fmk, DEVD) to generate a fluorescent product (e.g., FITC, rhodamine 110), and fluorescence correlates with the extent of total caspase activity.

1. These instructions assume the use of a Homogeneous Caspases Assay Kit (Roche Diagnostics Ltd) (*see* **Note 3**).
2. Suspend freshly isolated peripheral blood neutrophils (at least 97 % purity) at 1×10^6 cells/mL in IMDM/10 % autologous serum.
3. Plate neutrophils (1×10^5 per well; *see* **Note 9**), and incubate at 37 °C ± apoptosis-modifying agents for the required time in a black 96-well microplate (total volume 100 μL).
4. Dilute stock caspase substrate 1:10 in incubation buffer. Add 100 μL of freshly prepared caspase substrate to each well, plus duplicate wells containing medium alone (negative control), and duplicate wells containing positive control lysate.
5. Cover the plate and incubate at 37 °C for at least 1 h.
6. Measure fluorescence with a plate reader (excitation, 470–500 nm; emission, 500–560 nm).

3.6.3 Caspase Profiling Assay

Fluorometric assays for specific caspases work in a similar way to the homogeneous caspase assays, but exploit a certain degree of specificity between the substrates of individual caspases or groups of caspases. Fluorescence-conjugated substrates specific for certain caspases (e.g., 2, 3, 8, and 9) are immobilized in a 96-well plate. When cell lysates are added to the wells and incubated with the substrates, the amount of fluorescence generated correlates with the activation of that particular caspase. They can therefore be used to study particular pathways of apoptosis by looking for activity of a caspase protease that is specific for a particular pathway or cell type (e.g., caspase-8 in death receptor-mediated death).

1. These instructions assume the use of the ApoAlert™ Caspase Profiling Plate (Clontech) (*see* **Notes 10** and **11**).
2. Suspend freshly isolated peripheral blood neutrophils (at least 97 % purity) at 2×10^6 cells/mL in IMDM/10 % autologous serum. Dispense 1 mL of neutrophil suspension (2×10^6 cells) into 2-mL round-bottomed polypropylene tubes, and incubate ± apoptosis-modifying agents at 37 °C for the desired length of time.
3. Centrifuge at $220 \times g$ for 5 min at 4 °C. Discard the supernatants.
4. Resuspend the cells in 400 μL of ice-cold lysis buffer and incubate for 10 min on ice.
5. Meanwhile, add 10 μL DTT per 1 mL of 2× reaction buffer, and then add 50 μL of this mixture to each well of the

96-well Caspase Profiling Plate. Cover the plate with film and incubated for 5 min at 37 °C.

6. Vortex the neutrophil lysates, and then add 50 μL from each lysate to duplicate wells of each caspase substrate.
7. Cover the plate with film and incubate for 2 h at 37 °C.
8. Measure fluorescence using a plate reader (excitation, 380 nm; emission, 460 nm).

3.7 Gel Electrophoresis of DNA

A characteristic event of apoptosis is the endonuclease-mediated cleavage of DNA at regular intervals along its length, thus generating single-nucleosome fragments of around 180 bp, or oligonucleosomal fragments at multiples thereof, following earlier large-scale (50–200 kbp) degradation. Such ordered fragmentation produces discrete sized lengths of DNA, which produce a distinct "laddering" pattern on electrophoresis, in contrast to necrotic cell death in which DNA is cleaved randomly, thus producing a smear on a DNA gel (Fig. 2c).

1. Suspend freshly isolated peripheral blood neutrophils (at least 97 % purity) at 5×10^6 cells/mL in IMDM/10 % autologous serum. Dispense 1 mL of neutrophil suspension into 2-mL round-bottomed polypropylene tubes, and incubate ± apoptosis-modifying agents at 37 °C for the desired length of time.
2. Extract the genomic DNA using a Wizard® Genomic DNA Purification Kit (Promega).
3. Run the DNA (23 μL DNA plus 7 μL of loading dye) on a 2 % agarose gel containing either ethidium bromide (2.5 μg/mL) or GelRed (5 μL in 50 mL) in TBE buffer at 10 V/cm. Visualize under ultraviolet illumination. DNA from apoptotic cells exhibits a characteristic ladder pattern.

3.8 Hypodiploid DNA Content

DNA fragmentation also leads to an apparent reduction in nuclear DNA content of triton-permeabilized cells, so that staining with a DNA-intercalating dye such as propidium iodide allows detection of a "hypodiploid" cell population. This technique works particularly well with neutrophils, because they are terminally differentiated cells which do not undergo proliferation and consequently generate only two peaks when DNA content is measured: diploid (viable) cells and hypodiploid (apoptotic) cells (Fig. 2d, e).

1. Suspend freshly isolated peripheral blood neutrophils (at least 97 % purity) at 1×10^7 cells/mL in IMDM/10 % autologous serum and penicillin/streptomycin.
2. Add 75 μL of neutrophil suspension to wells of a 96-well flat-bottom plate. To each well add 15 μL of apoptosis-modifying agents (10× concentration) or buffer control and 60 μL of

IMDM/10 % serum. If two agents are used in combination, only 45 μL of IMDM is required.

3. Cover with a lid, and incubate at 37 °C in a 5 % CO_2 incubator for the desired length of time.
4. Vigorously pipette the well to dislodge adherent cells, and transfer 50 μL into flow tubes containing 250 μL of PI solution.
5. Incubate at 4 °C for 15 min in the dark.
6. Analyze by flow cytometry (FL-2 channel) to determine the percentage of cells with hypodiploid DNA content.

3.9 TUNEL Staining for DNA Breaks

The presence of DNA strand breaks can be assessed by enzymatic methods, since DNA breaks create acceptor sites for enzymes such as terminal deoxyribonucleotidyltransferase (TdT). Addition of TdT together with fluorescein-12-2′deoxyuridine-5′-triphosphate is used to reveal DNA fragmentation in the TUNEL technique.

1. These instructions assume the use of the In Situ Cell Death Detection Kit, Fluorescein (Roche Diagnostics Ltd).
2. Suspend freshly isolated peripheral blood neutrophils (at least 97 % purity) at 2×10^7 cells/mL in IMDM/10 % autologous serum and penicillin/streptomycin.
3. Add 90 μL of neutrophil suspension to wells of a 96-well flat-bottom plate. To each well add 10 μL of apoptosis-modifying agents (10× concentration) or buffer control.
4. Cover with a lid, and incubate at 37 °C in a 5 % CO_2 incubator for the desired length of time.
5. Transfer 100 μL of neutrophil suspension to a 96-well U-bottom flexible plate, and centrifuge at 200 × *g* for 2 min at 4 °C. Discard the supernatants.
6. Wash the cells three times by adding 100 μL of PBS per well, centrifuging the plate at 200 × *g* for 3 min at 4 °C, discarding the supernatants, and vortexing the plate for 5 s.
7. Add 100 μL of fixation solution to each well.
8. Incubate on a shaker for 60 min at room temperature.
9. Add 200 μL of PBS to each well, then centrifuge the plate at 200 × *g* for 10 min at 4 °C, and discard the supernatants.
10. Resuspend the cells in permeabilization solution for 2 min on ice.
11. Add 50 μL of nucleotide mixture to the two negative control wells. The TUNEL reaction mixture is then made up by mixing the enzyme solution (50 μL) with the remaining 450 μL of nucleotide mixture.
12. The two positive control wells are treated for 10 min at room temperature with DNase I to introduce DNA strand breaks.

13. Wash twice in PBS (200 μL per well) then resuspend in TUNEL reaction mixture (50 μL per well).
14. Cover the plate and incubate at 37 °C for 60 min in the dark.
15. Wash twice in PBS (200 μL per well) and then transfer to flow cytometry tubes for analysis of fluorescence levels (FL-1).

3.10 Plate-Based Assay for Phagocytosis of Apoptotic Neutrophils

Macrophage phagocytosis of apoptotic neutrophils may be assessed using minor modifications of a serum-free phagocytosis assay first described by Newman et al. in 1982. This method uses adherent human monocyte-derived macrophages which are most efficient at ingesting apoptotic cells, but it has also been used successfully with murine peritoneal and bone marrow-derived monocytes. Depending on the phagocytosis pathway being examined, one could add specific opsonins such as C1q, MFG-E8, or other ligands as required. NB it is important to wash neutrophils in HBSS prior to assay to ensure they are free of serum opsonins (e.g., Protein S).

1. This method assumes the use of adherent macrophages in 48-well TC-treated microplates.
2. Suspend 10^8 freshly isolated peripheral blood neutrophils (at least 97 % purity) in 20 mL of IMDM/10 % autologous serum. Dispense the neutrophil suspension into a 75 cm^2 cell culture flask, and stand the flask on its end in an incubator for 20 h at 37 °C in a 5 % CO_2 atm.
3. Harvest the neutrophil suspension into a 50-mL conical polypropylene tube, and wash twice in warm IMDM (50 mL volume per wash) by centrifuging at $220\times g$ for 5 min and discarding the supernatant. After each wash, gently resuspend the neutrophil pellet in 1 mL of warm (37 °C) IMDM using a plastic pipette to avoid clumping of the cells. Count the cells using a hemocytometer, and finally resuspend the aged neutrophils at 4×10^6 cells/mL in warm (37 °C) IMDM (no serum).
4. Rinse the macrophage monolayer with warm (37 °C) IMDM to remove nonadherent cells.
5. Overlay the macrophage monolayer with 0.5 mL (2×10^6 cells) of the suspension of aged neutrophils in IMDM (serum-free), and incubate for 60 min at 37 °C in a 5 % CO_2 atm.
6. Wash each well with ice-cold PBS (without cations). Use an inverted microscope to check that non-ingested neutrophils have been largely removed.
7. Repeat the wash as necessary, continually checking by microscopy to ensure that the macrophage monolayer is not disrupted.
8. Fix in 2.5 % glutaraldehyde for 30 min and rinse with PBS.
9. Stain for myeloperoxidase (MPO) with 0.1 mg/mL dimethoxybenzidine and 0.03 % (v/v) H_2O_2 in PBS for 60 min at room temperature.

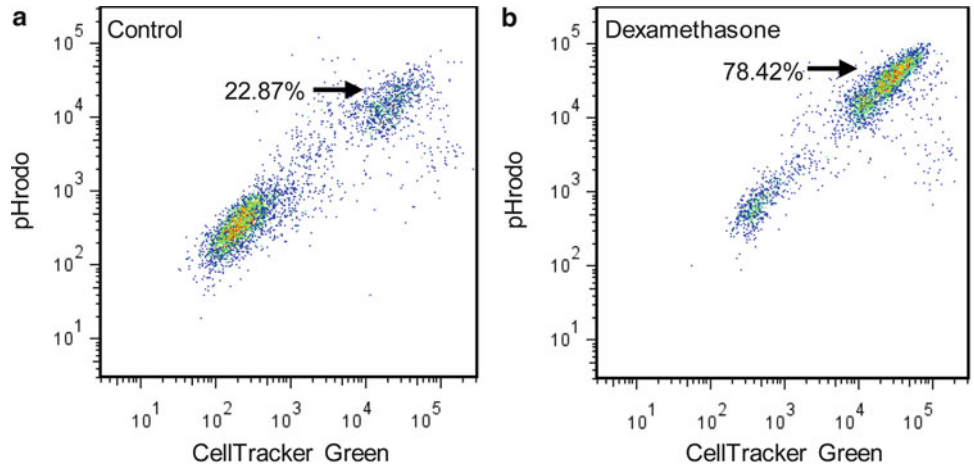

Fig. 3 Analysis of macrophage phagocytosis of apoptotic cells by flow cytometry reveals increased uptake following steroid treatment. (**a**) Control and (**b**) dexamethasone-treated monocyte-derived macrophages (100 μM for 5 days) were incubated with apoptotic neutrophils for 1 h prior to flow cytometry. Neutrophils were pre-labelled with CellTracker™ Green and pHrodo™. Phagocytosis was quantified as percentage of CellTracker^{+ve}/pHrodo^{+ve} cells

10. Count the percentage of macrophages (MPO negative) that have phagocytosed one or more apoptotic neutrophils (MPO positive) by examination with an inverted microscope of at least five fields (minimum 400 cells), and record as the mean percent phagocytosis of duplicate or triplicate wells.

3.11 Flow Cytometry-Based Phagocytosis Assay

This modification of the plate-based phagocytosis assay utilizes a fluorescent chloromethyl dye that diffuses freely through plasma membranes to label the cytoplasm of live neutrophils without altering their functional activity. This method avoids the need for vigorous washing of the macrophage monolayer following interaction with aged neutrophils and eliminates potential observer bias when counting macrophages. It is less laborious than the plate-based counting method and is therefore particularly suitable for repeated measurements and screening assays. Used in conjunction with a pH-sensitive succinimidyl ester (pHrodo™), this method allows definite discrimination of phagocytosis of apoptotic cells. pHrodo™ dyes are nonfluorescent at a neutral pH but fluoresce brightly in acidic conditions (i.e., within the phagolysosome); therefore macrophages display dual fluorescence upon phagocytosis of apoptotic CM-green-labelled neutrophils (Fig. 3). We do recommend however that new investigators validate this method against the "gold standard" plate-based counting assay in their own laboratories.

1. This method assumes the use of adherent macrophages in 48-well TC-treated microplates.
2. Suspend freshly isolated peripheral blood neutrophils (at least 97 % purity) at 2×10^7 cells/mL in IMDM/10 %

autologous serum and penicillin/streptomycin in a 15-mL conical polypropylene tube. Add 2 μg/mL of 10 mM 5-chloromethylfluorescein diacetate (CellTracker™ Green), mix gently, and incubate at 37 °C for 30 min.

3. Centrifuge at 220×*g* for 5 min and discard supernatant. Resuspend in PBS and centrifuge again at 220×*g* for 5 min.
4. Resuspend cells at 4×10^6 cells/mL in IMDM/10 % autologous serum and penicillin/streptomycin. Dispense the neutrophil suspension into a 75 cm^2 cell culture flask, and stand the flask on its end in an incubator for 20 h at 37 °C in a 5 % CO_2 atm.
5. Harvest the neutrophil suspension into a 50-mL conical polypropylene tube, and wash twice in warm IMDM (50 mL volume per wash) by centrifuging at 220×*g* for 5 min and discarding the supernatant. After each wash, gently resuspend the neutrophil pellet in 1 mL of warm IMDM using a plastic pipette to avoid clumping of the cells. Count the cells using a hemocytometer, and resuspend the aged neutrophils at 1×10^6 cells/mL in warm (37 °C) HBSS.
6. Incubate cells with 20 ng/mL pHrodo™ for 30 min at room temperature.
7. Centrifuge at 220×*g* for 5 min and discard supernatant. Resuspend in PBS and centrifuge again at 220×*g* for 5 min.
8. Resuspend cells at 4×10^6/mL in warm (37 °C) IMDM (serum-free).
9. Rinse the macrophage monolayer with warm (37 °C) IMDM to remove nonadherent cells.
10. Overlay the macrophage monolayer with 500 μL (2×10^6 cells) of the suspension of labelled aged neutrophils in IMDM (serum-free), and incubate for 60 min at 37 °C in a 5 % CO_2 atm. Note that this is an excess number of apoptotic neutrophils in order to determine macrophage phagocytic capacity and not a surrogate marker of neutrophil apoptosis.
11. Aspirate the neutrophil suspension from the wells and wash macrophages three times with PBS.
12. Detach the macrophages by incubation with 500 μL 0.25 % trypsin/EDTA solution for 10 min at 37 °C followed by 10 min at 4 °C (*see* **Note 12**).
13. Harvest the detached macrophages by vigorous pipetting and place on ice.
14. Analyze the entire samples (unfixed) immediately using a flow cytometer, aiming to collect at least 5,000 events in the macrophage gate.
15. Apoptotic cells and macrophage populations are identified by their distinct laser scatter properties. The number of the

CellTracker^{+ve}/pHrodo^{+ve} events in the macrophage gate is divided by the total number of macrophages to obtain the proportion of macrophages that have internalized apoptotic cells.

4 Notes

1. We culture neutrophils in IMDM containing 10 % serum. We routinely use autologous platelet-rich plasma-derived serum, prepared from platelet-rich plasma (harvested after centrifugation of citrate-anticoagulated blood) by recalcification with 20 mM $CaCl_2$ for 1 h at 37 °C in glass tubes. However, bovine serum may also be used. Alternatively, neutrophils may be cultured in the absence of serum with a small amount of added protein (e.g., 0.5 % (w/v) serum albumin), but apoptosis will proceed more rapidly. Cell saver pipette tips should be used when pipetting neutrophils to minimize cell damage.
2. Neutrophil granules contain high concentrations of proteases. Extreme care must be taken to keep all samples on ice during the preparation of neutrophil lysates in order to prevent the protein of interest being degraded before blotting. Higher protease inhibitor concentrations are required for neutrophils than for other cell types. The protocol describes high protease inhibitor concentrations that we have used successfully in our laboratory; however, some experimentation with regard to manipulation of concentrations may be required. Preincubation of neutrophils with 1 mM phenylmethanesulfonyl fluoride (PMSF) for up to 1 h prior to lysis may be required to prevent neutrophil protease-mediated cleavage of intracellular proteins following addition of lysis buffer [17].
3. The protocol described is based on the homogeneous caspase kit available from Roche Diagnostics and represents the simplest method for fluorometric detection of total caspase activity. However, other commercial kits are available, which may be based on either the same or slightly different protocol.
4. Some investigators add extra serum to the cells in the cytospin chamber to avoid artifacts caused by cell breakage during centrifugation. We have observed that adding serum reduces the effectiveness of deposition of neutrophils that have progressed to a late stage of apoptosis (late apoptotic or post-apoptotic cells), so potentially underestimating the true rate of neutrophil apoptosis. Late apoptotic neutrophils appear as cell ghosts with little or no evidence of nuclear staining, having undergone “nuclear evanescence.” Furthermore, late apoptotic cell ghosts in a cell population may be overlooked because the lack of nuclear material means that they stain very faintly with Romanowsky stains such as Diff-Quik, and in the past late

apoptotic cells may have been gated out as "debris" when analyzed by flow cytometry.

5. Dilutions prior to flow cytometry should be performed using Annexin-binding buffer, because in the absence of Ca^{2+}, Annexin V will rapidly dissociate from PS on the apoptotic cell surface.
6. Eosinophils present in the granulocyte population also have low levels of CD16 expression, so eosinophil counts (by analysis of cell morphology in cytocentrifuge preparations or CD16 expression) should be performed at baseline.
7. Another way of analyzing mitochondrial changes associated with apoptosis is Western blotting of the Bcl-2 family proteins that are important in the control of the intrinsic (mitochondrial) apoptotic pathway. The expression profile of Bcl-2 family proteins in peripheral blood neutrophils has been analyzed and shows expression of Bak, Bad, Bcl-w, and Bfl-1 in these cells, but relatively little Bcl-2, Bcl-xL, Bik, and Bax [19]. Therefore, the more abundant proteins should be considered first for analysis for roles in neutrophil apoptosis, although some proteins, such as Bax, may be transcriptionally upregulated in response to certain apoptotic stimuli under the control of p53 and may therefore still be important in neutrophil apoptosis. For a detailed Western blotting protocol, please refer to **step 1** of Subheading 3.4 as the method is identical to that for caspases.
8. The 12 % gel recommended in this protocol is based on blotting for cleaved caspase-3 (14–21 kDa). However, gel percentages may be altered according to the size of the protein of interest. In general, low-percentage gels are used to blot for high-MW proteins and high-percentage gels for low-MW proteins. Therefore, the composition of the gel may have to be altered depending on the size of the protein of interest. Some proteins that are important in apoptosis are of similarly low size to cleaved caspase-3, e.g., Bax (21 kDa) and truncated Bid (15 kDa), and therefore a similar percentage gel will probably be appropriate, whereas other proteins such as procaspase-8 (55 kDa) and procaspase-3 (32 kDa) are larger and may require a lower-percentage gel for optimal resolution.
9. The protocol for this kit recommends a cell number of 4×10^4 cells per well in a volume of 100 μL. However, in assays involving neutrophils, cell numbers are often boosted in order to amplify the signals obtained from the assay, particularly as neutrophils are so abundant. On the other hand, cell density may affect the rate of spontaneous apoptosis of these cells during culture, with a high cell density promoting survival, especially at densities of 8×10^6 cells/mL and above (25). Therefore, some experimentation may be require, to manipulate the cell

density, volume, and time of culture in order to gain the best results with this assay.

10. Colorimetric assays for single-caspase activity are also available. These are similar to the fluorometric assays and follow a similar protocol, but instead utilize cleavage of a chromophore (e.g., *p*-nitroanilide) from caspase substrates as a measure of caspase activation. Development of color can be monitored using a spectrophotometer or microplate reader (405 nm) and activity quantified by comparison with a calibration curve constructed using known standards.
11. This protocol applies to any cell type, as caspase activation is a general event of apoptosis and is not unique to neutrophils. However, differences may exist between the expression profiles of the various caspases in different cell types, and this must be borne in mind when selecting an assay to use in neutrophils. Caspases 1, 3, 4, and 7–10 are expressed in neutrophils [19]. In contrast, it has been reported that caspase-2 is absent from peripheral blood neutrophils, although it is expressed in HL-60 cells.
12. Treatment with trypsin–EDTA may lead to clumping of cells leading to blockage of the flow cytometer's sample intake nozzle. Clumping may be minimized by adding 50 μL of bovine serum to each well following incubation with trypsin–EDTA.

Acknowledgements

The authors would like to acknowledge funding from the Wellcome Trust WT096497 (D.A.D.) and WT094415 (C.D.L.) and the MRC G0601481 (A.G.R.) and Dr John A. Marwick for provision of macrophage phagocytosis flow cytometry data (Fig. 3).

References

1. Dorward DA, Lucas CD, Rossi AG, Haslett C, Dhaliwal K (2012) Imaging inflammation: molecular strategies to visualize key components of the inflammatory cascade, from initiation to resolution. Pharmacol Ther 135: 182–199
2. Fox S, Leitch AE, Duffin R, Haslett C, Rossi AG (2010) Neutrophil apoptosis: relevance to the innate immune response and inflammatory disease. J Innate Immun 2:216–227
3. Lucas CD, Allen KC, Dorward DA, Hoodless LJ, Melrose LA, Marwick JA, Tucker CS, Haslett C, Duffin R, Rossi AG (2013) Flavones induce neutrophil apoptosis by down-regulation of Mcl-1 via a proteasomal-dependent pathway. FASEB J 27:1084–1094
4. Rossi AG, Hallett JM, Sawatzky DA, Teixeira MM, Haslett C (2007) Modulation of granulocyte apoptosis can influence the resolution of inflammation. Biochem Soc Trans 35:288–291
5. Duffin R, Leitch AE, Fox S, Haslett C, Rossi AG (2010) Targeting granulocyte apoptosis: mechanisms, models, and therapies. Immunol Rev 236:28–40
6. Hasegawa T, Suzuki K, Sakamoto C, Ohta K, Nishiki S, Hino M, Tatsumi N, Kitagawa S (2003) Expression of the inhibitor of apoptosis (IAP) family members in human neutrophils: up-regulation of cIAP2 by granulocyte colony-stimulating factor and overexpression of cIAP2 in chronic neutrophilic leukemia. Blood 101: 1164–1171

7. Murray J, Walmsley SR, Mecklenburgh KI, Cowburn AS, White JF, Rossi AG, Chilvers ER (2003) Hypoxic regulation of neutrophil apoptosis role: of reactive oxygen intermediates in constitutive and tumor necrosis factor alpha-induced cell death. Ann N Y Acad Sci 1010: 417–425
8. Pryde JG, Walker A, Rossi AG, Hannah S, Haslett C (2000) Temperature-dependent arrest of neutrophil apoptosis. Failure of Bax insertion into mitochondria at 15 degrees C prevents the release of cytochrome c. J Biol Chem 275:33574–33584
9. Elliott MR, Ravichandran KS (2010) Clearance of apoptotic cells: implications in health and disease. J Cell Biol 189:1059–1070
10. Ravichandran KS, Lorenz U (2007) Engulfment of apoptotic cells: signals for a good meal. Nat Rev Immunol 7:964–974
11. Liu Y, Cousin JM, Hughes J, Van Damme J, Seckl JR, Haslett C, Dransfield I, Savill J, Rossi AG (1999) Glucocorticoids promote nonphlogistic phagocytosis of apoptotic leukocytes. J Immunol 162:3639–3646
12. Hu Y (2012) Isolation of human and mouse neutrophils ex vivo and in vitro. Methods Mol Biol 844:101–113
13. Youssef PP, Mantzioris BX, Roberts-Thomson PJ, Ahern MJ, Smith MD (1995) Effects of ex vivo manipulation on the expression of cell adhesion molecules on neutrophils. J Immunol Methods 186:217–224
14. Macey MG, McCarthy DA, Vordermeier S, Newland AC, Brown KA (1995) Effects of cell purification methods on CD11b and L-selectin expression as well as the adherence and activation of leucocytes. J Immunol Methods 181: 211–219
15. Haslett C, Guthrie LA, Kopaniak MM, Johnston RB Jr, Henson PM (1985) Modulation of multiple neutrophil functions by preparative methods or trace concentrations of bacterial lipopolysaccharide. Am J Pathol 119:101–110
16. Taylor EL, Rossi AG, Dransfield I, Hart SP (2007) Analysis of neutrophil apoptosis. Methods Mol Biol 412:177–200
17. Kerr JF, Wyllie AH, Currie AR (1972) Apoptosis: a basic biological phenomenon with wide-ranging implications in tissue kinetics. Br J Cancer 26:239–257
18. Dransfield I, Buckle AM, Savill JS, McDowall A, Haslett C, Hogg N (1994) Neutrophil apoptosis is associated with a reduction in CD16 (FcγRIII) expression. J Immunol 153:1254–1263
19. Santos-Beneit AM, Mollinedo F (2000) Expression of genes involved in initiation, regulation, and execution of apoptosis in human neutrophils and during neutrophil differentiation of HL-60 cells. J Leukoc Biol 67:712–724

Chapter 11

Microinjection Methods for Neutrophils

Iraj Laffafian, Kimberly J. Lewis, K. Benjamin Masterman, and Maurice B. Hallett

Abstract

The ability to microinject substances into the cytosol of living neutrophils opens the possibility of manipulating the chemistry within the cell and also of monitoring changes using indicators which otherwise cannot be introduced into the cell. However, neutrophils cannot be microinjected by the conventional glass pipette insertion method. Here, we outline two techniques which work well with neutrophils, namely, SLAM (simple lipid-assisted microinjection) and electroinjection.

Key words Microinjection, SLAM, Electroinjection, Cell signaling

1 Introduction

Microinjection of molecules into the cytosol of living cells is a powerful technique in cell biology. However, microinjection of neutrophils has always been difficult to achieve without damaging the cell. In conventional microinjection, the penetration of the plasma membrane is achieved by a rapid entry and exit "stab." The period of time for ejection of material, when the pipette tip is within the cell, is thus short (on the order of 100 ms) and so requires high pressure (100–200 mbar) to introduce sufficient material from the micropipette into the cell during that time. This must be carefully controlled, as insufficient pressure results in too little material being injected and excessive pressure causes cell damage or even cell rupture. Additionally, in the absence of full 3D control of the micropipette tip, the tip's location within the cell is uncontrolled and is liable to cause damage to intracellular organelles. Whereas this may not be a problem for larger cells, the percentage of the cell cytoplasm occupied by organelles, such as the nucleus and granules in neutrophils, is high. Since the velocity at which the micropipette tip enters the cell may be on the order of

Mark T. Quinn and Frank R. DeLeo (eds.), *Neutrophil Methods and Protocols*, Methods in Molecular Biology, vol. 1124,
DOI 10.1007/978-1-62703-845-4_11,

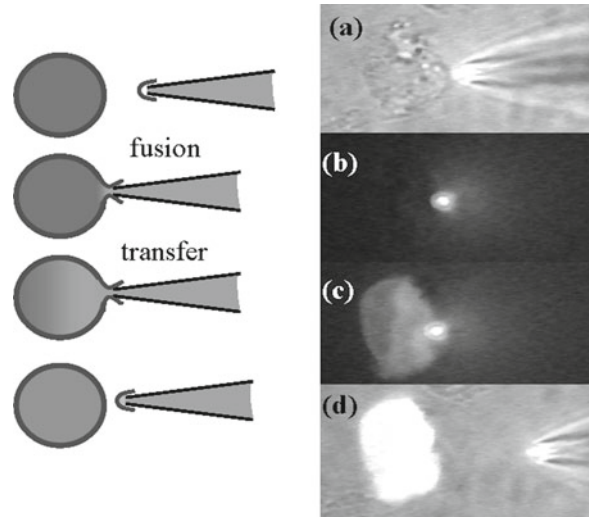

Fig. 1 SLAM transfer of Lucifer yellow into a human neutrophil. The process is illustrated by the diagrams on the *left* and an example of the experimental transfer: (**a**) the approach of the lipid-coated micropipette, (**b**) the fusion of the lipid on the micropipette with the cell membrane, (**c**) the transfer of fluorescent material, and (**d**) withdrawal of the micropipette

700 μm/s [1], it is likely to displace, damage, or enter the nucleus rather than directly enter the cytosol.

We have found only two approaches useful for microinjection, namely, simple lipid-assisted microinjection (SLAM) and electroinjection. The principles underlying each of these are discussed first before the methodology protocols are provided. An older approach that does not involve glass micropipettes employs lipid fusion, either liposomes (e.g., [2, 3]) or erythrocyte ghost fusion [4, 5], as a means of introducing materials into small cells. However, this approach has two limitations. First, the amount of material injected per cell is limited by the space within the liposome or erythrocyte ghost and can thus be very small. The technique is thus useful for introducing nucleic acid into cells, as with lipofection, where amplification of the effect of the injected molecule can occur but may be insufficient for experiments with no amplifying effect. The SLAM technique is a "hybrid" technique involving both the glass micropipette and lipid fusion approaches [6]. The micropipette tip is coated with a lipid bilayer so that contact with the neutrophil plasma membrane results in fusion between the lipid at the micropipette tip and the cell membrane (Fig. 1). This results in a channel into the cell cytosol and the transfer of molecules into the neutrophil cytosol at low pressure [6, 7]. In a similar manner to internal perfusion, the pipette tip does not enter the cytosol, thus avoiding the possibility of organelle damage. However, unlike internal perfusion, the micropipette can be withdrawn, and cell survival is good.

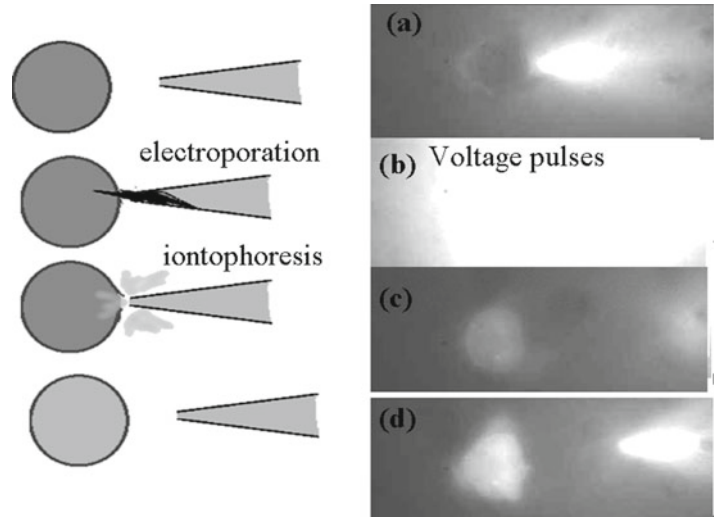

Fig. 2 Electroinjection of Lucifer yellow into a human neutrophil. The process is illustrated by the diagrams on the *left* and an example of the experimental transfer: (**a**) the approach of the micropipette, (**b**) the voltage pluses causing electroporation and ejection of fluorescent material, (**c**) the transfer of fluorescent material, and (**d**) the ability of the cell to undergo chemotaxis after electroinjection

Furthermore, the low pressure in the micropipette ensures that the amount of material injected is controlled and does not unduly damage the cell [6, 8]. This technique has been used successfully to introduce large molecular weight inhibitors of the IP3 receptor [9] and high molecular weight Ca^{2+} indicators (e.g., dextran fura2) [10]. The cells retain low cytosolic Ca^{2+} and the ability to undergo chemotaxis and phagocytosis [10].

Although many problems are overcome by SLAM, the fusion requires a close contact between the two bilayers for several, often tens of seconds, making it difficult to use on cells which are moving or undergoing other dynamic shape changes. Electroinjection is a "no-touch" approach which we found was surprisingly benign and can be used on neutrophils engaged in chemotaxis without affecting their motile behavior. The technique involves passing controllable electrical voltage pulses from the open tip of a small bore micropipette (containing the molecules to be injected) through the cell to be injected. Provided that the pipette is close to the cell, the voltage pulses will cause a localized and transient electroporation of the cell membrane, during which time molecules diffusing out of the micropipette will enter the cell (Fig. 2). Since many molecules also carry a charge, provided the electrical polarity is in the appropriate direction, the voltage pulses will also have an ionotophoretic effect forcing molecules out of the pipette synchronously with the opening of the electroporation pore. Since the electroporation effect is dependent on the membrane curvature

[11], it is selective for the larger radius of curvature of the cell membrane over the smaller curvatures of intracellular organelles. Haas and Cline have used this approach for transfecting neurons in vivo with GFP-expressing plasmids [12, 13] and for other molecules [14]. We have also shown that it is useful for neutrophils and that the approach is surprisingly gentle and simple, resulting in a no-touch (point and shoot) method for introducing material into the cell cytosol with minimal impact of cell shape change dynamics.

2 Materials

1. Micropipettes: either be pulled using a micropipette puller to give the required tip diameter of 0.5–1 μm or pre-made (Eppendorf).
2. Micromanipulator: a good micromanipulator is required to achieve the fine control required for neutrophils (e.g., Eppendorf manipulator).
3. Phosphatidylcholine-oleoyl-palmitoyl (POPC): 20 mg/mL in $CHCl_3$. Store below 0 °C. Dilute aliquots of this solution with $CHCl_3$ before use to a final POPC concentration of 1 mM.
4. DiIC18(3) (1,1′-dioctadecyl-3,3,3′,3′-tetramethylin docarbocyanine perchlorate) (Molecular Probes).
5. Lucifer yellow CH (Sigma).

3 Methods

3.1 SLAM

3.1.1 Lipid Coating of Micropipette

1. Dip the tip of the micropipette into the lipid solution (1 mM POPC in anhydrous $CHCl_3$), or a 10 μl drop of the lipid solution may be applied to the tip of the micropipette. The POPC solution should be stored under desiccation at 4 ºC.
2. Evaporation of the chloroform after the micropipette is withdrawn from the lipid solution results in a coating of lipid on the glass.
3. Back-load the micropipette with sufficient volume of the injection medium containing the material to be injected (*see* **Notes 1** and **2**) to exert a pressure to offset capillary pressure.
4. Connect the micropipette to a control pressure device (microinjector) with the pressure set to zero.
5. Carefully lower the micropipette into the aqueous medium bathing the neutrophils on the microscope stage. This results in swelling of the dried lipid on the tip of the micropipette and the formation of a bilayer across the open tip (*see* **Note 3**).

3.1.2 SLAM Procedure

1. Move the loaded lipid-coated micropipette into the field of view of the neutrophils, which have been allowed to sediment onto a glass coverslip (*see* **Note 4**).
2. Neutrophils are microscopically "small," so a high magnification objective, e.g., 100× or 63× oil immersion objective, and a motorized, microprocessor-controlled micromanipulator are required.
3. Allow the tip of the SLAM pipette to gently contact the surface of the chosen neutrophil.
4. A short delay of 1–5 s is often required before the transfer of lipid, and the aqueous contents of the micropipette to the cell are observed.
5. Do not increase the pressure within the micropipette during the microinjection but hold it constant at 5–10 mbar (*see* **Note 5**).
6. When the required amount of material has been transferred (as monitored by the fluorescent signal), remove the tip of the pipette from the neutrophil.
7. The effect of the injected molecule on neutrophil behavior/responsiveness can now be observed (*see* **Note 6**).

3.2 Electroinjection

1. Backfill the micropipette with appropriate loading solution (~1–2 μl) (*see* **Notes 1** and 7).
2. Pass a silver wire (0.25 mm diameter) through the micropipette holder, into the micropipette, and then into the loading solution.
3. Fix a second silver wire in place in the cell-containing medium on a microscope slide.
4. Connect the two wires to a voltage stimulator terminal. We use a Grass SD9 stimulator, but any stimulator capable of delivering low voltage pulses could be used.
5. Position the micropipette next to the target neutrophil (preferably within 1 μm) using a micromanipulator (Eppendorf InjectMan).
6. Initiate electroporation using a 1 s train of voltage pulses. We use 1 ms square pulses, 10–50 V, and 200 Hz (*see* **Note** 7).
7. This should result in the expulsion of fluorescent material from the pipette tip and its incorporation into the neutrophil (Fig. 2).

4 Notes

1. It is advisable to include a fluorescent marker along with the material to be injected. We routinely use Lucifer yellow (10–50 mg/mL). Often however, the injectate is itself fluorescent (e.g., GFP-tagged protein or FITC-labeled sample).

2. It is important to remember that there will be a large dilution of the material within the micropipette when it enters the cell. This can be quantified by monitoring fluorescence transfer and quantified from the intensity of the injected cell. However, the dilution may be of the order of 1:100 (i.e., 0.1 %) to 1:100 (1 % transfer). This may limit the use of some proteins which cannot be solubilized at these high concentrations. In this case, prolonged transfer time can be tried (similar to internal perfusion, where a far smaller dilution occurs). However, it must be remembered that diffusion of molecules out of the cytosol will also occur, and therefore it is important to include in the micropipette molecules which might be important for the survival of the microinjected cells and for its responsiveness (e.g., ATP).
3. The formation of a lipid bilayer at the micropipette tip can be checked by increasing the pressure in the micropipette to 5–10 mbar. Lack of ejection or leakage of the dye from the micropipette provides evidence that an effective lipid seal had formed at the micropipette tip.
4. For good cell response, it is important to maintain the neutrophils at 37 °C using a microscope stage heater or similar device.
5. This low pressure was important to prevent rupture of the lipid seal at the micropipette tip and to prevent subsequent damage to the cell undergoing microinjection.
6. The lipid-coated micropipette can be used more than once, but the number of possible successful injections depended on the amount of lipid in the coating and the amount of cell "debris" picked up as the micropipette is raised and lowered into the cell-bathing medium. This results in blockage of the pipette tip by particulate material. Blockage can often be dislodged by applying a high pressure to the micropipette (cleaning pressure), and the lipid seal may reform.
7. We have found a range of parameters work, but the stated parameters may not be optimal for the molecules of your particular interest. The duration and voltage should be experimentally varied to establish the optimum delivery of your material into the neutrophil. It is important to remember that using Lucifer yellow as a surrogate marker may be misleading with this technique (which relies on molecular charge) and that ideally the material being injected should itself be fluorescent.

References

1. Guse AH, Berg I, da Silva CP et al (1997) Ca^{2+} entry by cyclic ADP-ribose in intact T-lymphocytes. J Biol Chem 272:8546–8550
2. Hallett MB, Campbell AK (1980) Uptake of liposomes containing the photoprotein obelin by rat isolated adipocytes; adhesion, endocytosis or fusion? Biochem J 192:587–596
3. Gao X, Huang L (1995) Cationic liposome-mediated gene transfer. Gene Ther 2:710–722
4. Hallett MB, Campbell AK (1982) Measurement of changes in cytoplasmic free calcium in fused cell hybrids. Nature 294:155–158
5. Campbell AK, Hallett MB (1983) Measurement of intracellular calcium ions and oxygen radicals in polymorphonuclear leukocyte–erythrocyte "ghost" hybrids. J Physiol 338:537–550
6. Laffafian I, Hallett MB (1998) Lipid-assisted microinjection: introducing material into the cytosol and membranes of small cells. Biophys J 75:2558–2563
7. Peters R, Sikorski R (1998) Gentle slam. Science 282:2213–2214
8. Laffafian I, Hallett MB (2000) Gentle microinjection for myeloid cells using SLAM. Blood 95:3270–3271
9. Davies-Cox EV, Laffafian I, Hallett MB (2001) Control of Ca^{2+} influx in human neutrophils by IP3 binding: differential effects of microinjected IP3 receptor antagonists. Biochem J 355:139–143
10. Dewitt S, Laffafian I, Hallett MB (2003) Phagosomal oxidative activity during β2 integrin (CR3)-mediated phagocytosis by neutrophils is triggered by a non-restricted Ca^{2+} signal: Ca^{2+} controls time not space. J Cell Sci 116:2857–2865
11. Zimmermann U (1986) Electrical breakdown, electropermeabilization and electrofusion. Rev Physiol Biochem Pharmacol 105:175–256
12. Haas K, Sin WC, Javaherian A et al (2001) Single-cell electroporation for gene transfer *in vivo*. Neuron 29:583–591
13. Haas K, Jensen K, Sin WC et al (2002) Targeted electroporation in Xenopus tadpoles in vivo – from single cells to the entire brain. Differentiation 70:148–154
14. Bestman JE, Ewald RC, Chiu SL, Cline HT (2006) *In vivo* single-cell electroporation for transfer of DNA and macromolecules. Nat Protoc 1:1267–1272

Chapter 12

Generation of Functionally Mature Neutrophils from Induced Pluripotent Stem Cells

Colin L. Sweeney, Randall K. Merling, Uimook Choi, Debra Long Priel, Douglas B. Kuhns, Hongmei Wang, and Harry L. Malech

Abstract

Induced pluripotent stem cells (iPSCs) are pluripotent stem cells established from somatic cells. The capability of iPSCs to differentiate into any mature cell lineage under the appropriate conditions allows for modeling of cell processes as well as disease states. Here, we describe an in vitro method for generating functional mature neutrophils from human iPSCs. We also describe assays for testing these differentiated cells for neutrophil characteristics and functions by morphology, cell surface markers, production of reactive oxygen species, microbial killing, and mobilization of neutrophils to an inflammatory site in an in vivo immunodeficient mouse infusion model.

Key words iPSCs, Neutrophils, Giemsa stain, Dihydrorhodamine 123, Staphylocidal assay, Thioglycollate mobilization

1 Introduction

Polymorphonuclear neutrophils are important for phagocytosis and destruction of bacterial and fungal microorganisms via nonoxidative and oxidative killing mechanisms. Our laboratory has had a particular interest in the oxidative killing respiratory burst that generates reactive oxygen species (ROS) through the phagocytic NADPH oxidase complex. Deficiencies of any of the NADPH oxidase components, as in chronic granulomatous disease (CGD), result in a failure to produce ROS and subsequent susceptibility to a distinct subset of microbial infections [1, 2].

Induced pluripotent stem cells (iPSC) are embryonic-like stem cells that can be established from adult somatic cells [3, 4]. Many types of somatic cells have been reprogrammed, including from different human disease types [5–7]. The pluripotent ability of iPSCs to differentiate into cells of all three germ layers allows for unprecedented modeling of diseases and therapeutic treatments in

Mark T. Quinn and Frank R. DeLeo (eds.), *Neutrophil Methods and Protocols*, Methods in Molecular Biology, vol. 1124,
DOI 10.1007/978-1-62703-845-4_12,

relevant mature cell lineages following directed differentiation of patient iPSCs. Additionally, the capacity of iPSCs for unlimited proliferative self-renewal potentially allows for the generation of therapeutic quantities of cells for regenerative medicine.

A number of neutrophil differentiation methods from pluripotent cells have been established [8–11], involving methodologies for the intermediate generation of hematopoietic stem/progenitor cells (albeit stem/progenitor cells seemingly lacking long-term hematopoietic engraftment capabilities), followed by further differentiation to produce mature neutrophils. The majority of these methods use coculture with mouse OP9 stromal cells [12] for neutrophil maturation, although a feeder-free neutrophil differentiation method has also been described [8]. Although the production of hematopoietic stem cells capable of engraftment and long-term repopulation from human iPSCs is still a challenge, the production of short-lived mature neutrophils from pluripotent stem cells could potentially provide a replacement or supplement for current clinical neutrophil infusions for treatment of severe neutropenia.

In this chapter, we describe an in vitro method [11] for directed differentiation of human iPSCs into functional mature neutrophils. Further, we outline techniques for characterization of these differentiated cells for neutrophil morphology, cell surface markers, ROS production, microbial killing, and migration to a site of inflammation, at which they compare favorably to healthy human peripheral blood neutrophils. This multistage differentiation method involves embryoid body (EB) formation to generate hematopoietic stem/progenitor cells, which are then cocultured with OP9 stromal cells for cell expansion and induction of neutrophil maturation. We have previously used the mature neutrophils generated by this differentiation technique both for disease modeling of the neutrophil ROS defect of X-linked CGD in patient iPSCs and to test gene therapy approaches in those iPSCs [6].

2 Materials

2.1 General Cell Culture

Specified cell culture reagents may be readily replaced with comparable materials from other suppliers. We recommend that all prepared cell culture media be filter-sterilized (0.22 μm filter).

1. Complete iPSC media: Knockout DMEM/F12 (Life Technologies), 20% Knockout Serum Replacement (Life Technologies), 1 % nonessential amino acids, 2 mM L-glutamine, 100 U/mL penicillin, 100 μg/mL streptomycin, 10 ng/mL basic fibroblast growth factor, 0.1 mM β-mercaptoethanol.
2. Collagenase or dispase: 1 mg/mL in DMEM/F12.
3. Y-27632 ROCK inhibitor (CalBioChem): 5 mM stock in ultrapure deionized water. Inhibits anoikis-induced apoptosis in iPSCs.

4. Mouse embryonic fibroblasts (MEFs): mitotically inactivated primary CF-1 MEFs (GlobalStem).
5. Phosphate-buffered saline, pH 7.4, without $CaCl_2$ or $MgCl_2$ (PBS).
6. Gelatin suitable for cell culture: 0.1 % solution in PBS or ultrapure deionized water; filter-sterilized.
7. 0.25 % trypsin-EDTA.
8. 0.05 % trypsin-EDTA.
9. 100-mm and 6-well tissue culture-treated plates and dishes.
10. Cesium-137 irradiator or mitomycin C.

2.2 Neutrophil Differentiation Culture

1. First stage differentiation media (for day 0 of differentiation): StemSPAN SFEM (Stem Cell Technologies), 10 μM Y-27632 (*see* **Note 1**).
2. Iscove's modified Dulbecco's media (IMDM).
3. Second stage differentiation media (for days 1 through 17 of differentiation): IMDM, 15 % fetal bovine serum, 1 % nonessential amino acid, 2 mM L-glutamine, 100 U/mL penicillin, 100 μg/mL streptomycin, 0.1 mM β-mercaptoethanol, plus the following human cytokines—25 ng/mL bone morphogenic protein-4, 50 ng/mL stem cell factor (SCF), 50 ng/mL Flt-3 ligand (Flt-3 L), 50 ng/mL interleukin-6 (IL-6), and 20 ng/mL thrombopoietin (TPO).
4. Third stage differentiation media (for days 18 through 24 of differentiation): IMDM, 10 % FBS, 10 % horse serum, 5 % protein-free hybridoma medium (Life Technologies), 100 U/mL penicillin, 100 μg/mL streptomycin, 0.1 mM β-mercaptoethanol, plus the following human cytokines: 100 ng/mL SCF, 100 ng/mL Flt-3 ligand, 100 ng/mL IL-6, 10 ng/mL TPO, and 10 ng/mL interleukin-3.
5. Fourth stage differentiation media (for days 25 through 31–32 of differentiation): IMDM, 10 % FBS, 100 U/mL penicillin, 100 μg/mL streptomycin, 0.1 mM β-mercaptoethanol, and 50 ng/mL human granulocyte colony-stimulating factor.
6. Ultralow attachment 100-mm dishes or 6-well plates.
7. Cell strainers: 40, 70, or 100 μm cell strainers.
8. OP9 mouse marrow stroma cell line: obtain from the American Type Culture Collection (ATCC # CRL-2749).

2.3 Cytospin and Giemsa Staining

1. Cytocentrifuge with compatible cytology funnels and microscope slides.
2. Modified Giemsa stain.
3. Optional: Mounting medium (e.g., Permount) and coverslips.

2.4 Surface Marker Antibodies and ROS Production Assays

1. FACS buffer: 0.5 % bovine serum albumin in PBS.
2. Fluorochrome-conjugated antibodies to human CD45, CD13, CD16, or CD16b.
3. Hank's balanced salt solution without Ca^{2+} or Mg^{2+} ($HBSS^{-}$).
4. Hank's balanced salt solution with Ca^{2+} and Mg^{2+} ($HBSS^{+}$).
5. Dimethyl sulfoxide (DMSO).
6. Dihydrorhodamine 123 (DHR): 10 mg in 1 mL of DMSO for 29 mM stock. Store in 25 μL aliquots at −20 °C or colder. Protect from light.
7. Catalase: 560,000 U in 400 μL of $HBSS^{-}$. Store in 10 μL aliquots at −20 °C or colder.
8. Phorbol 12-myristate 13-acetate (PMA): 1 mg in 500 μL of DMSO. Store in 10 μL aliquots at −20 °C or colder.
9. 37 °C heat block or water bath.
10. Optional: ACK lysis buffer (Quality Biological) for red blood cell lysis of peripheral blood samples prior to use as a positive control for DHR assay.
11. Nitro blue tetrazolium (NBT): 10 mg NBT in 5 mL of PBS. Use within 1 month.

2.5 Staphylocidal Assay

1. Human AB sera for opsonization: Arrange for a same-day collection of 50 mL of blood using serum separator tubes from each of 6 to 10 donors with AB blood type. Immediately after the blood has clotted, spin the tubes in a centrifuge at 500 × *g* for 10 min. Harvest the serum from each donor and pool all sera into one flask, keeping the flask at 4 ° C. Transfer 1 mL aliquots of the pooled AB sera to cryotubes and store as single-use aliquots at −80 °C.
2. Sterile distilled water adjusted to pH 11 with 10 N NaOH for neutrophil lysis.
3. Trypticase soy agar (TSA).
4. Trypticase soy broth (TSB).
5. Centrifuge with carriers equipped with biosafety domes.
6. 2-mL screw-cap conical tubes.
7. 37 °C incubator containing a rotator for end-over-end mixing of 2-mL tubes.
8. Disposable sterile glass tubes: 18 × 150 mm with metal caps.
9. Petri dishes: round, polystyrene, 60 × 15 mm.
10. Spectrophotometer.
11. Optional: Image analysis system including CCD camera, software, and light box for enumeration of colonies.

12. *Staphylococcus aureus* 502A (ATCC # 27217) frozen stocks. *See Safety considerations* in Subheading 3.7 prior to use. Prepare stocks as follows:
    (a) Resuspend vial of lyophilized *Staphylococcus aureus* 502A into 1.0 mL of TSB and transfer to a flask containing 50 mL of TSB.
    (b) Determine $O.D._{650\,nm}$ at time = 0, use TSB as the blank.
    (c) Incubate bacterial suspension at 37 °C in a shaking water bath.
    (d) Determine $O.D._{650\,nm}$ at 30-min intervals, plot log $O.D._{650\,nm}$ versus time.
    (e) Continue the incubation until the bacteria enter early stationary phase.
    (f) Add an equal volume of 20 % glycerol (sterilized, reagent grade) to the bacterial suspension and transfer 1-mL aliquots to cryotubes.
    (g) Store bacterial aliquots for single-use in the vapor phase of a liquid N_2 freezer.

2.6 Neutrophil Mobilization to Thioglycollate-Induced Inflammation

1. Carboxyfluorescein diacetate, succinimidyl ester (CFSE/CFDA SE): 10 mM stock in high-quality DMSO, per manufacturer's guidelines. Freeze aliquots. Prior to use, thaw aliquot and prepare 10 μM working solution in HBSS. Protect from light.
2. Cell injection buffer: PBS containing 0.2 % BSA. Filter-sterilize.
3. Thioglycollate: sterile 4 % (w/v) thioglycollate solution. Prepare from powdered thioglycollate brewer-modified medium in water (BD BBL) (*see* **Note 2**).
4. Immunodeficient NODCg-*Prkdc*^{scid} *Il2rg*^{tm1Wjl}/SzJ (NSG) mice (The Jackson Laboratory).

2.7 Human Subjects Protocol and Animal Studies Protocols

1. Human subjects are required as a source of peripheral blood for generating iPSC and to obtain peripheral blood neutrophils. Obtain blood following approved IRB protocol and informed consent. [Studies described were approved under NIH-approved protocol 05-I-0213 (HLM Principle Investigator).]
2. Animal studies using NSG mice are needed to observe migration of intravenously injected human neutrophils to thioglycollate inflamed peritoneum. [Studies described were approved under NIAID-approved ACUC animal protocol LHD 3E (HLM Principle Investigator).]

3 Methods

3.1 iPSC Culture

1. Culture iPSC in the presence of MEFs using complete iPSC media [6, 7].
2. Alternately, feeder-free culture media and techniques may be used. Detailed explanations of these culture techniques are beyond the scope of this protocol.

3.2 Neutrophil Differentiation

This protocol for differentiation of iPSCs into neutrophils [6] was adapted from a previously published protocol [11] for differentiation of human embryonic stem cells involving EB (Fig. 1a) formation (first stage) and culture for 18 days (second stage), followed by cell dissociation and 2 weeks of coculture (third and fourth stages) with OP9 stroma cells (*see* **Note 3**). Hematopoietic cells first begin to develop near the end of the EB stage (second stage), and hematopoietic stem/progenitor cells may expand during the first week of OP9 coculture (third stage). Mature, functional neutrophils develop during the second week of OP9 coculture (fourth stage). Since only nonadherent cells are carried forward in the third and fourth stages, typically >99 % of the final harvested cell population is hematopoietic (based on antibody staining, as described below). The efficiency of this differentiation can vary

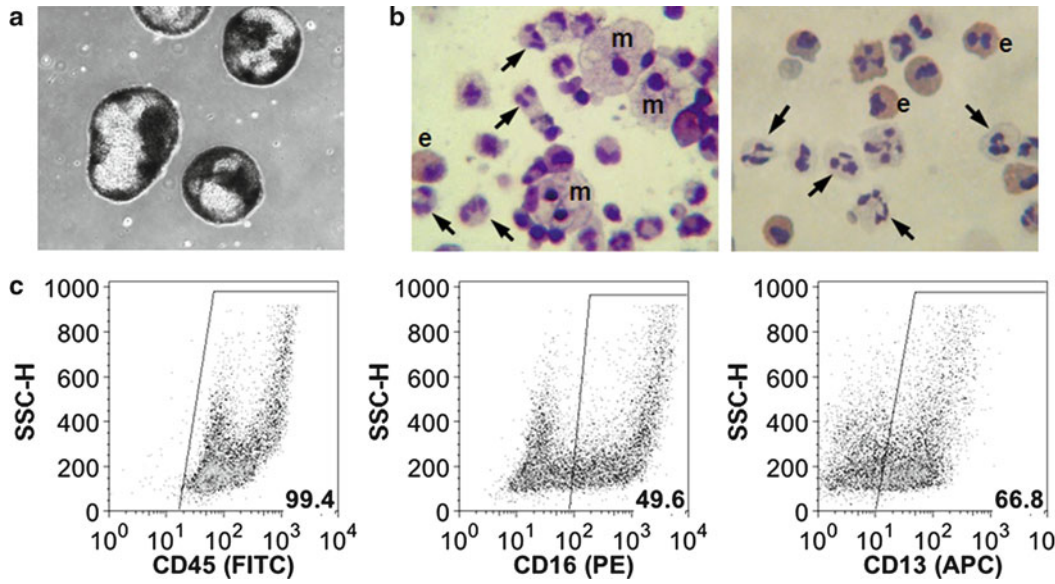

Fig. 1 Morphology and surface marker expression of neutrophils differentiated from iPSCs. (**a**) Characteristic appearance of hollow, clear EBs at day 17 of neutrophil differentiation, photographed at 10× magnification. (**b**) Morphology of Giemsa-stained cells following directed neutrophil differentiation. *Arrows* indicate representative neutrophils; macrophages ("m") and eosinophils ("e") are also indicated. (**c**) Flow cytometry of cells stained with antibodies to hematopoietic- and neutrophil-associated surface markers after directed neutrophil differentiation of iPSCs. Typically >99 % of the endpoint differentiated cells express the pan-leukocyte hematopoietic marker CD45

greatly between different iPSC lines and even to a lesser degree within the same cell line, depending on the status of the iPSCs and the initial size of the EBs (*see* **Note 4**). The final yield of differentiated neutrophils can be as low as 1–2 % of the initial number of undifferentiated iPSCs (although we have achieved neutrophil cell numbers as high as 50 % of the initial iPSC numbers on rare occasions), and so the number of starting iPSCs should be adjusted based on the desired neutrophil number and the possibility of low yields. Morphological and functional neutrophil assays for characterizing the differentiated cells are described below.

1. *Day 0*: For EB formation (*see* **Note 4**), completely detach colonies of pluripotent iPSCs from MEFs by incubating with dispase for 20–30 min at 37 ° C. Alternately, treat iPSCs on MEFs with collagenase for 5 min at 37 °C, then scrape iPSCs and MEFs from plates using a cell scraper.
2. Gently collect detached iPSCs and transfer to a conical tube (*see* **Note 5**).
3. Wash cells with iPSC media to dilute dispase or collagenase, centrifuging at $220 \times g$ for 2 min.
4. Aspirate and repeat the wash twice with fresh iPSC media (or DMEM/F12 or HBSS).
5. Gently resuspend iPSCs in first stage differentiation media (*see* **Note 5**).
6. Plate iPSCs onto ultralow attachment surface 100-mm dishes; for every two confluent plates of undifferentiated iPSCs cultured on MEFs (approximately $12–18 \times 10^6$ total iPSCs), use one 100-mm ultralow attachment dish containing 10–15 mL of 1st stage differentiation media. Culture at 37 °C, 5 % CO_2 for 24 h for EB formation.
7. *Day 1*: Gently collect EBs and centrifuge at $220 \times g$ for 2 min (*see* **Notes 5** and **6**).
8. For each 100-mm dish of EBs, gently resuspend in 10–15 mL of second stage differentiation media and replate into the same ultralow attachment plate. Culture at 37 °C, 5 % CO_2.
9. *Days 2 through 18*: Gently change second stage differentiation media every 2–3 days, as in **steps 5** and **6** (*see* **Notes 5**–7).
10. *Day 17*: Coat 100-mm tissue culture dishes (*not* ultralow attachment plates) with 0.1 % gelatin at 37 °C for at least 30 min. Irradiate OP9 cells at 1,500–2,000 rad (or mitotically inactivate using mitomycin C).
11. Plate 9×10^5 irradiated OP9 cells into each 100-mm tissue culture plate. Culture at 37 °C, 5 % CO_2.
12. *Day 18*: Collect EBs in a conical tube by centrifugation or using a cell strainer (*see* **Notes 5** and **6**).
13. Wash cells with PBS or HBSS to remove serum.

14. Add 0.5 % trypsin to EBs. Incubate at 37 °C for 10–15 min, vortexing or pipetting occasionally to break apart EBs.
15. Inactivate trypsin with media containing FBS and centrifuge at 880 × *g* for 5 min.
16. Aspirate and resuspend cells in third stage differentiation media. Count cells.
17. Plate up to 3×10^6 EB-derived cells in 10–12 mL of third stage media into each 100-mm plate of irradiated OP9 cells from day 17 (*see* **Note 8**). Culture at 37 °C, 5 % CO_2.
18. *Day 22*: Change to fresh third stage media by collecting nonadherent cells from OP9 coculture, centrifuging cells at 880 × *g* for 5 min, resuspending in fresh third stage media (10–15 mL per 100-mm plate), and replating back into same plate of irradiated OP9 cells (*see* **Note 9**).
19. *Day 24*: Coat 100-mm tissue culture dishes (*not* ultralow attachment plates) with 0.1 % gelatin at 37 °C for at least 30 min. Irradiate OP9 cells and plate as in **step 10**.
20. *Day 25*: Collect nonadherent cells from OP9 coculture (*see* **Note 10**).
21. Centrifuge cells at 880 × *g* for 5 min.
22. Plate up to 3×10^6 differentiated cells in 10–15 mL of fourth stage media into each 100-mm dish of new irradiated OP9 cells (from **step 19**). Culture at 37 °C, 5 % CO_2.
23. *Day 28 or 29*: Change to fresh fourth stage media by collecting nonadherent cells from OP9 coculture, centrifuging cells at 880 × *g* for 5 min, resuspending in fresh fourth stage media (10–15 mL per 100-mm plate), and replating back into same plate of irradiated OP9 cells.
24. *Day 31 or 32*: Harvest nonadherent differentiated cells as in **step 20** (*see* **Note 11**), and count cells for subsequent neutrophil analyses, as described below.
25. For smaller scale differentiations, 6-well plates may be used instead of 100-mm dishes in **steps 6**, **10**, **19**, and **22**, with adjusted volumes and cell numbers to scale.

3.3 Cytospin and Giemsa Stain

Differentiated mature neutrophils should contain granules and a characteristic segmented, multilobed (typically 2–4 lobes) nucleus (Fig. 1b). Neutrophils typically comprise 30–80 % of the total differentiated cell population. Macrophages and monocytes often comprise the majority of the remaining cells, although eosinophils and basophils are occasionally present as well.

1. The recommended number of differentiated cells is 1,000–10,000 cells (*see* **Note 12**).
2. Resuspend cells in 20–200 μL of PBS. Apply cells to assembled cytofunnel.

3. Cytospin cells onto a microscope slide at 70 × *g* for 5 min using a cytocentrifuge.
4. Fix cells on slide with methanol for 5–7 min. Air dry.
5. Add Giemsa stain to cover cells on slide. Stain for 15–30 min.
6. Rinse in deionized water. Air dry.
7. Optional: For permanent storage, mount coverslip on slide with Permount.
8. Visualize by light microscopy.

3.4 Neutrophil Surface Marker Analyses

For flow cytometry analysis of neutrophil surface markers (Fig. 1c), we typically stain for expression of CD45 (a pan-leukocyte marker) and one or more of: CD13 (granulocyte/monocyte marker), CD16 (granulocyte/macrophage marker), or CD16b (neutrophil marker; *see* **Note 13**).

1. The recommended number of differentiated cells is 200,000–1,000,000 cells.
2. Wash cells with PBS, centrifuging at 880 × *g* for 5 min.
3. Resuspend cells in 100 μL of FACS buffer.
4. Stain cells with fluorochrome-conjugated antibodies according to manufacturer's recommendations (e.g., 20 μL of antibody at room temperature for 20–30 min), keeping them protected from light.
5. Wash with a 20× volume of PBS, centrifuging at 880 × *g* for 5 min.
6. Resuspend cells in FACS buffer, analyze by flow cytometry.

3.5 DHR Assay of ROS Production

The DHR assay [13] measures cellular production of ROS as detected by oxidation of nonfluorescent DHR to fluorescent rhodamine-123, which can be detected by flow cytometry (Fig. 2a). DHR can be performed with as few as 5×10^4 cells, although for optimal analysis we recommend at least 10^5 cells. If iPSC differentiation results in too few neutrophils for DHR assay, the NBT assay (*see* below) may be used instead. ROS production is stimulated by addition of PMA; if sufficient neutrophils are available for analysis, an unstimulated negative control for DHR should be prepared by excluding PMA in a replicate sample. For a positive control, 400 μL peripheral blood can be used after red blood cell lysis (*see* **Note 14**). Flow cytometry analysis should be performed within 25 min of initial addition of DHR reagent to cells (*see* **Note 15**).

1. The recommended number of differentiated cells for analysis is 100,000–500,000 cells.
2. Thaw catalase, PMA, and DHR aliquots to room temperature. Protect DHR from light.
3. Prepare a 100 U/μL working solution of catalase by adding 10 μL of stock catalase to 130 μL of $HBSS^-$.

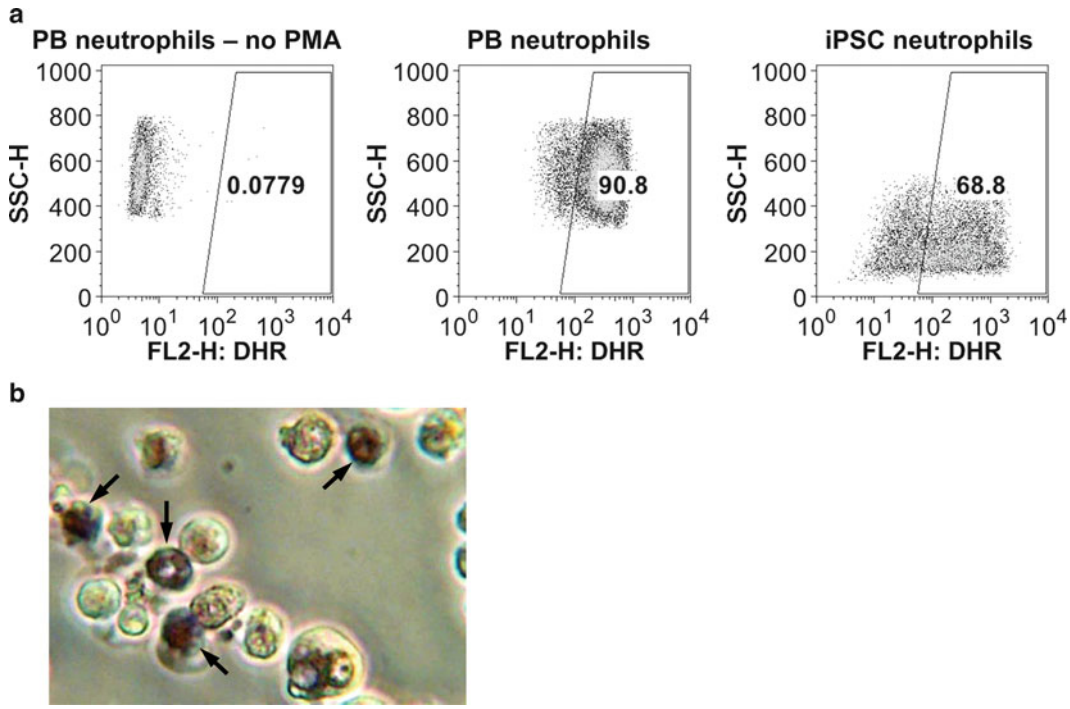

Fig. 2 Functional assays of ROS production in differentiated neutrophils. (**a**) DHR flow cytometry analysis of peripheral blood neutrophils ("PB neutrophils") compared to cells after directed neutrophil differentiation of iPSCs reprogrammed from a normal, healthy volunteer ("iPSC neutrophils"). Upon PMA stimulation, iPSC-derived neutrophils are capable of producing ROS. An unstimulated negative control of peripheral blood neutrophils without PMA treatment ("PB neutrophils—no PMA") is also included. (**b**) NBT assay of cells following directed neutrophil differentiation from iPSCs. *Arrows* indicate ROS-producing cells, identified by colorimetric change

4. Prepare a 5 μg/mL working solution of PMA by adding 5 μL of 2 μg/μL stock to 2 mL of $HBSS^+$.
5. Resuspend cells in 400 μL of $HBSS^-$ in a flow cytometry tube.
6. Add 1.8 μL of 29 mM DHR to all cell samples.
7. Quickly add 5 μL of 100 U/μL catalase to all cell samples.
8. Vortex cells and incubate at 37 °C for 5 min in heat block or water bath.
9. Add 100 μL of 5 μg/mL PMA to cells to stimulate ROS production (or add 100 μL of $HBSS^-$ for unstimulated negative controls).
10. Incubate at 37 °C for 14 min in heat block or water bath.
11. Analyze cells by flow cytometry for DHR fluorescence in the FL2 channel (*see* **Notes 15** and **16**).

3.6 NBT Assay of ROS Production

The NBT assay [14, 15] is an alternative to the DHR assay for ROS production and requires fewer cells (as few as 1,000 viable cells).

Upon stimulation with PMA, ROS reaction with NBT dye results in formation of blue-black formazan precipitates inside cell vacuoles that can be visualized by light microscopy (Fig. 2b). An unstimulated negative control can be prepared by excluding PMA in a replicate sample.

1. The recommended number of differentiated cells for analysis is 1,000–10,000 cells.
2. Thaw PMA aliquot to room temperature. Prepare 1 μg/mL working solution of PMA by adding 1 μL of 2 μg/μL stock to 2 mL of PBS.
3. Cytospin cells onto microscope slides at 70 × *g* for 5 min.
4. Add 250 μL of 1 μg/mL PMA to cells on slide (or 250 μL of PBS for unstimulated negative control).
5. Add 250 μL of 2 mg/mL NBT to cells on slide.
6. Incubate slide at 37 °C for 20–30 min on top of heat block or in incubator (*see* **Note 17**).
7. Fix cells on slide with 1.5 % paraformaldehyde to stop NBT reaction.
8. Wash three times with deionized water.
9. Visualize by light microscopy.

3.7 Staphylocidal Assay

The determination of staphylocidal activity of neutrophils [16] provides an overall assessment of multiple neutrophil functions, including recognition of microorganisms by surface receptors, cytoskeleton rearrangement during phagocytosis, assembly of NADPH oxidase, production of ROS, and migration and fusion of cytoplasmic granules with the phagosome. For this assay, a negative control without neutrophils and a positive control of normal peripheral blood neutrophils can be included for comparison with iPSC-derived neutrophils (Fig. 3a). Prepare these samples in triplicate for statistical analysis, if desired.

Safety considerations: *Staphylococcus aureus* is a human pathogen, which can cause endocarditis, meningitis, and toxic shock syndrome in humans. *S. aureus* cultures are a biological hazard, and all labware which come in contact with these cultures should be decontaminated with a 10 % solution of household bleach for at least 30 min and subsequently autoclaved. For safety, personal protective equipment (safety eyewear, gloves, and lab coat) and a biosafety cabinet should be used. Vacuum aspiration of supernatant should be performed with the employment of proper engineering design (i.e., house vacuum system outfitted with engineered safety controls, in-line waste receptacles, and aerosol filters). Also, take steps to minimize the generation of aerosols, including using sealable tubes, a centrifuge with carriers equipped with sealable biosafety domes, and cotton-plugged pipettes. Use “to deliver” pipettes rather than “blowout” pipettes.

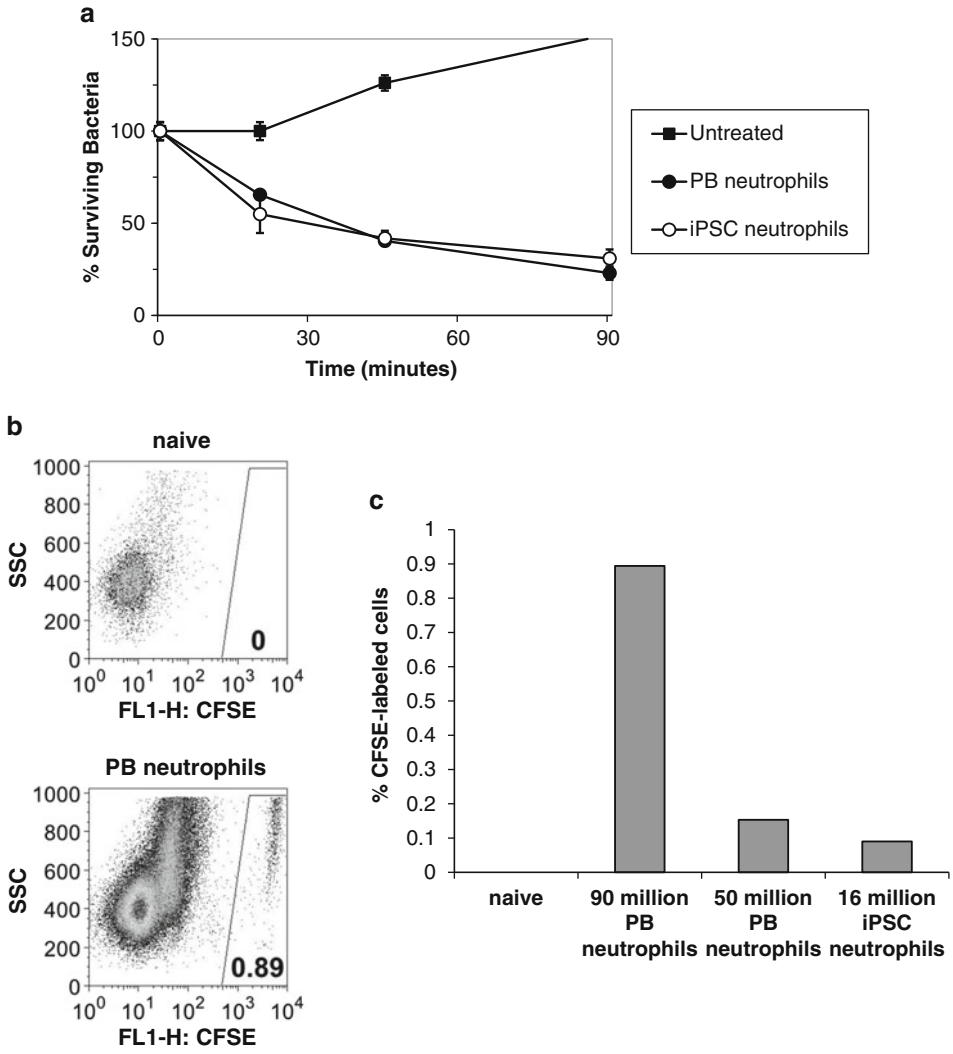

Fig. 3 Functional assays of iPSC-derived neutrophils for bacterial killing and mobilization to an inflammatory site. (**a**) Staphylocidal assay demonstrating that neutrophils differentiated from iPSCs exhibit bacterial killing activity comparable to normal peripheral blood neutrophils. Shown are bacterial colony counts from plating into agarose culture after various times of incubation with peripheral blood or iPSC-derived neutrophils, expressed as a percentage of the number of bacterial colonies plated any prior incubation (at time = 0). "Untreated" samples were plated after incubation in the absence of neutrophils as a negative control for bacterial killing. (**b**) Flow cytometry analysis of the peritoneal exudate cell population after thioglycollate-induced mobilization of 90 million CFSE-labeled peripheral blood neutrophils ("PB neutrophils") injected into an NSG mouse. The intensity of CFSE fluorescence allows for unambiguous detection of the labeled human cells. Also included is the exudate of an untreated control mouse ("naive"). (**c**) Summary of flow cytometry data for thioglycollate-induced mobilization of CFSE-labeled neutrophils, in mice injected with either 90 million or 50 million peripheral blood ("PB") neutrophils, or 16 million iPSC-derived neutrophils; an untreated ("naive") mouse control is included

1. The recommended number of differentiated cells for analysis is $2–5 \times 10^6$ million cells without replicates (or $6–15 \times 10^6$ cells for analyzing in triplicate).
2. On the day of the assay, prepare *S. aureus* inoculum from stock *S. aureus* as follows:

(a) Thaw one aliquot of stock *S. aureus* at 37 °C, and transfer the contents to 50 mL of TSB in a 100-mL bottle.

(b) Incubate the bacterial suspension in a 37 °C shaker water bath (*see* **Note 18**) for approximately 4 h, monitoring the $O.D._{650\ nm}$ until the bacteria enters early log phase of growth.

(c) Transfer *S. aureus* culture to a 50-mL centrifuge tube.

(d) Centrifuge at $1{,}800 \times g$ for 5 min at 4 °C.

(e) Remove the supernatant fluid from the bacteria pellet using vacuum with appropriate safety controls.

(f) Wash the bacterial pellet twice with $HBSS^-$, each time spinning at $1{,}800 \times g$ for 5 min at 4 °C to pellet the bacteria.

(g) Resuspend the bacterial pellet in 10 mL of $HBSS^+$ (*see* **Note 19**).

(h) Adjust the $O.D._{650\ nm} = 0.235–0.260$, corresponding to 1×10^8 bacteria/mL.

3. In a 500-mL bottle, add 15 g of TSA to 375 mL of distilled water (normal pH). Autoclave for 30 min. Place in 56 °C water bath to prevent solidifying (*see* **Note 20**).
4. Resuspend iPSC-derived neutrophils in 500 μL of $HBSS^+$ in a 2-mL screw-cap conical tube (experimental tube). For a positive control, use peripheral blood neutrophils in 500 μL of $HBSS^+$ in a separate tube. For a negative control, use 500 μL of $HBSS^+$ without cells in a separate tube. Set up all samples in triplicate for statistical analyses, if desired.
5. Add 100 μL of AB sera (or other opsonizing agent) to each sample.
6. Add 300 μL of HBSS + to each sample.
7. Add *S. aureus* in 100 μL of $HBSS^+$ to each sample at a neutrophil/bacteria (i.e., effector/target) ratio of 1:2 (*see* **Note 21**).
8. Immediately place the experimental and positive control conical tubes on a rotator in a 37 °C incubator and begin timing.
9. Transfer 10 μL from the negative control conical tube to a disposable 18×150 mm glass tube containing 10 mL of sterile water, pH 11 (*see* **Note 22**) for determination of the initial inoculum at time = 0 (this will also serve as the time = 0 sample for the positive control and experimental samples). Cap glass tube and vortex vigorously. Set aside this "0-min" sample until **step 11**.
10. Place the negative control conical tube on the rotator in the 37 °C incubator.
11. At 20, 45, and 90 minutes, remove 10 μL from each conical tube (experimental, positive, and negative) and transfer it to an

appropriately labeled 18 × 150 mm glass tube containing 10 mL of sterile water, pH 11 (*see* **Note 22**). Cap glass tubes and vortex vigorously.

12. For each of the 0-, 20-, 45-, and 90-min time point samples of the negative control, transfer 25 μL from the appropriate glass tube to the center of a separate correspondingly labeled Petri dish. Do the same for the 20-, 45-, and 90-min samples of the positive control and experimental glass tubes, except use 25 μL for each 20-min time point and 75 μL for each of the 45- and 90-min time points.
13. Remove agar from 56 °C water bath. Wait 3–5 min to cool agar slightly.
14. Add agar to each dish. Swirl clockwise eight times and then counterclockwise eight times to ensure homogeneous distribution of the bacteria within the agar before it solidifies.
15. After the agar on the Petri dishes has solidified, invert the dishes and incubate them in a dry incubator at 37 °C for 48 h.
16. Count surviving bacterial colonies for each plate, either manually or with the use of image analysis software. If imaging software is used, a light box with uniform light source is needed for backlighting of the colonies on the Petri dishes.
17. Calculate the total surviving bacteria for each tube = the number of colonies counted/volume of aliquot $\times 10^6$. Divide the total surviving bacteria at each time point by the total surviving bacteria in the initial inoculum of the negative control at "time = 0" to determine the percent survival at that time point (Fig. 3a).

3.8 In Vivo Assay of Neutrophil Mobilization

Thioglycollate injection into mouse peritoneum induces inflammation resulting in mouse neutrophil recruitment to the site [17]. Human neutrophils injected via tail vein into nonablated NSG mice can also mobilize to the site of thioglycollate-induced inflammation, although the human cells present within the peritoneal exudate are greatly outnumbered by mouse neutrophils, even when up to 9×10^7 human peripheral blood neutrophils are injected. Fluorescent labeling of human neutrophils with CFSE prior to injection allows for unambiguous detection of the relatively rare human cells (Fig. 3b). Using this in vivo model, we have observed that human neutrophils differentiated from iPSCs exhibit a similar capacity for mobilization in response to thioglycollate as a comparable number of human peripheral blood neutrophils (Fig. 3c).

1. The recommended number of differentiated cells for analysis is $\geq 10^6$ cells.
2. Resuspend neutrophils in 1 mL of HBSS.

3. Add 1 mL of HBSS containing 10 μM CFSE. Mix immediately (*see* **Note 23**).
4. Incubate in 37 °C water bath for 10 min.
5. Centrifuge cells at 880 × *g* for 5 min.
6. Resuspend cells in 150 μL of cell injection buffer per mouse. Inject cells via tail vein into NSG mice without prior preconditioning.
7. Inject 1 mL of 4 % thioglycollate intraperitoneally into mouse.
8. At 3–5 h after thioglycollate injection (*see* **Note 24**), euthanize mice and carefully dissect to expose the peritoneal cavity without puncturing the cavity.
9. Using a 12-mL syringe with a 19-G needle, lavage peritoneum with 10 mL of PBS, injecting posterior to the xyphoid process at the bottom center of the ribcage to avoid organs. Avoid moving the needle so as not to puncture organs. Leaving the needle in place, draw liquid back into syringe (typically recovering 8–9 mL containing 1–2 × 10^6 cells maximum).
10. Centrifuge exudate at 880 × *g* for 5 min.
11. Resuspend cell pellet in FACS buffer and analyze by flow cytometry for CFSE fluorescence (FL1 channel).

4 Notes

1. Inclusion of Y-27632 ROCK inhibitor [18] in the 1st stage differentiation media may enhance iPSC survival during the initial EB formation. However, it may also make EBs stickier, resulting in individual EBs fusing together.
2. Older solutions (≥1 month old) of thioglycollate work better for inducing inflammation. For long-term storage, store at 4 °C.
3. OP9 cells are sensitive to both over- and under-confluence during cell culture. Over-confluence (>80 %) during routine OP9 cell culture can result in OP9 cell adipogenesis, which may hinder their ability to support hematopoiesis. To reduce problems of OP9 cell over-confluence, pre-coat culture flasks or plates with 0.1 % gelatin at 37 °C for at least 30 min prior to OP9 culture.
4. The initial EB size can affect the efficiency of hematopoietic differentiation. It has been reported [19] that myeloid differentiation from human embryonic stem cells (using a different differentiation methodology than the one we describe) was optimal with EBs of at least 1,000 cells in size, while smaller EBs resulted in reduced hematopoietic differentiation. In our experience, small EBs are more likely to disintegrate during the first 18 days of culture. To overcome this, either grow the

undifferentiated iPSC colonies to a larger size and detach these large, intact iPSC colonies (using dispase or collagenase) for EB formation without breaking the colonies into smaller pieces, or use a "spin EB" methodology [19] to generate EBs of a standard, defined size.

5. Vigorous pipetting can break iPSC colonies into small pieces and should be avoided. Using larger bore 25-mL pipets instead of 5- or 10-mL pipets will help prevent this.
6. Larger hollow EBs are buoyant and may not pellet properly during centrifugation. In this case, media can be changed by collecting EBs using a 40–100 μm cell strainer to capture the EBs while passing the old media through, then inverting the cell strainer and gently washing EBs from the strainer into a tube or plate using fresh media.
7. While often initially dark in color, healthy EBs should take on a clear, hollow, spherical appearance within the first 3–7 days of the culture (Fig. 1a). If media color turns to orange or yellow between media changes, increase media volume (and increase the number of ultralow attachment plates, if necessary) or decrease duration between media changes. A change in EB appearance from clear to dark may be a sign of insufficient nutrients.
8. A greater density of differentiated hematopoietic stem/progenitor cells during this first week of OP9 coculture can result in better hematopoietic expansion.
9. Following plating of the EB-derived cells, the majority of cells will be adherent; nonadherent cells are greatly enriched for hematopoietic cells. This corresponds with a low level of $CD45^+$ hematopoietic cells present at day 18 (typically <5 %).
10. If numerous round, loosely adherent cells remain attached to OP9 cells, these cells can be recovered by washing the plate with PBS or HBSS, then briefly treating plate with 0.05 % trypsin-EDTA for 1–2 min.
11. Again, loosely adherent cells can be collected by washing and brief trypsin treatment (*see* **Note 9**), but more care must be taken to avoid detaching OP9 cells at day 31/32 in order to exclude OP9 cells from subsequent analyses of neutrophil function.
12. If there are too few differentiated cells for all desired analyses, the cytospin/Giemsa protocol can be performed on the residual fluorescently stained cells after antibody (Subheading 3.4) or DHR (Subheading 3.5) flow cytometry analysis.
13. Since there are two major antigen variants of CD16b (neutrophil antigen 1/human neutrophil antigen 1a and neutrophil antigen 2/human neutrophil antigen 1b) [20], care should be

taken that the CD16b antibody either recognizes both forms (such as CD16b antibody clone 1D3) or recognizes the particular variant present in your iPSCs.

14. To prepare a peripheral blood sample for DHR, add 4 mL of pre-warmed (37 °C) ACK lysis buffer to 400 μL of peripheral blood. Incubate at 37 °C for 5 min, then centrifuge at 220 × *g* for 5 min. Aspirate and add 4 mL of $HBSS^-$ to wash, centrifuging as above. Care should be taken not to overtreat with ACK lysis buffer, since neutrophils are sensitive to prolonged lysis.
15. Prolonged incubation with DHR reagent in the absence of ROS stimulation can result in a gradual false-positive fluorescent signal (notably in neutrophils from chronic granulomatous disease patients lacking ROS activity). Consequently, flow cytometry analysis should ideally be performed within 25 min of the initial addition of DHR reagent.
16. Although rhodamine-123 can also be detected in the FL1 channel, we observe a greater increase in fluorescence intensity of ROS-positive cells compared to ROS-negative cells when using the FL2 channel.
17. Prolonged incubation with NBT reagent in the absence of ROS stimulation can result in a gradual false-positive color change (notably in neutrophils from chronic granulomatous disease patients lacking ROS activity). The incubation time can be adjusted between 20 and 30 min, depending on cell numbers (less incubation time for fewer cells).
18. Lid should be fitted loosely to allow for aeration.
19. When resuspending the bacterial pellet, pipette the HBSS along the interior wall of the tube. If additional manipulation is required to resuspend the pellet, cap the tube and use a swirling rotary motion rather than a shaking motion. Permit the aerosol to settle for a few minutes before uncapping the tube.
20. Swirl the agar before placing into the water bath to ensure that the solution is homogeneous and before pouring plates to verify that solidification has not occurred.
21. If a higher effector/target ratio is required, the volume of bacteria can be increased up to 400 μl with corresponding decreases in the volume of $HBSS^+$ added in **step 5**.
22. Use of water at pH 11 allows complete lysis of neutrophils and dispersal of live, cell-associated *S. aureus* [21].
23. Cells will quickly uptake CFSE, so failure to mix immediately after adding can result in unequal staining and/or a lack of staining in some cells.
24. This 3–5 h time frame allows for migration of mouse and human neutrophils to the site of thioglycollate-induced inflammation [17]. Longer periods (i.e., overnight or longer) can result in increased migration of macrophages.

Acknowledgements

All of the authors were supported by the intramural research program of the National Institute of Allergy and Infectious Diseases. This work was supported in part by an intramural award to HLM from the NIH Center for Regenerative Medicine.

References

1. Winkelstein JA, Marino MC, Johnston RB Jr et al (2000) Chronic granulomatous disease. Report on a national registry of 368 patients. Medicine 79:155–169
2. van den Berg JM, van Koppen E, Åhlin A et al (2009) Chronic granulomatous disease: the European experience. PLoS ONE 4:e5234
3. Takahashi K, Tanabe K, Ohnuki M et al (2007) Induction of pluripotent stem cells from adult human fibroblasts by defined factors. Cell 131:861–872
4. Yu J, Vodyanik MA, Smuga-Otto K et al (2007) Induced pluripotent stem cell lines derived from human somatic cells. Science 318: 1917–1920
5. Park I-H, Arora N, Huo H et al (2008) Disease-specific induced pluripotent stem cells. Cell 134:877–886
6. Zou J, Sweeney CL, Chou BK et al (2011) Oxidase-deficient neutrophils from X-linked chronic granulomatous disease iPS cells: functional correction by zinc finger nuclease-mediated safe harbor targeting. Blood 117: 5561–5572
7. Merling RK, Sweeney CL, Choi U et al (2013) Transgene-free iPSCs generated from small volume peripheral blood non-mobilized $CD34^+$ cells. Blood. doi:10.1182/blood-2012-03-420273
8. Saeki K, Saeki K, Nakahara M et al (2009) A feeder-free and efficient production of functional neutrophils from human embryonic stem cells. Stem Cells 27:59–67
9. Choi K-D, Vodyanik M, Slukvin II (2011) Hematopoietic differentiation and production of mature myeloid cells from human pluripotent stem cells. Nat Protoc 6:296–313
10. Morishima T, K-i W, Niwa A et al (2011) Neutrophil differentiation from human-induced pluripotent stem cells. J Cell Physiol 226:1283–1291
11. Yokoyama Y, Suzuki T, Sakata-Yanagimoto M et al (2009) Derivation of functional mature neutrophils from human embryonic stem cells. Blood 113:6584–6592
12. Kodama H, Nose M, Niida S et al (1994) Involvement of the c-kit receptor in the adhesion of hematopoietic stem cells to stromal cells. Exp Hematol 22:979–984
13. Henderson LM, Chappell JB (1993) Dihydrorhodamine 123: a fluorescent probe for superoxide generation? Eur J Biochem 217: 973–980
14. Buescher ES, Alling DW, Gallin JI (1985) Use of an X-linked human neutrophil marker to estimate timing of lyonization and size of the dividing stem cell pool. J Clin Invest 76: 1581–1584. doi:10.1172/jci112140
15. Malech HL, Maples PB, Whiting-Theobald N et al (1997) Prolonged production of NADPH oxidase-corrected granulocytes after gene therapy of chronic granulomatous disease. Proc Natl Acad Sci U S A 94:12133–12138
16. Metcalf JA, Gallin JI, Nauseef WM et al (1986) Microbicidal assay. In: Laboratory manual of neutrophil function. Raven Press, New York, pp 134–143
17. Baron EJ, Proctor RA (1982) Elicitation of peritoneal polymorphonuclear neutrophils from mice. J Immunol Methods 49:305–313
18. Watanabe K, Ueno M, Kamiya D et al (2007) A ROCK inhibitor permits survival of dissociated human embryonic stem cells. Nat Biotechnol 25:681–686
19. Ng ES, Davis RP, Azzola L et al (2005) Forced aggregation of defined numbers of human embryonic stem cells into embryoid bodies fosters robust, reproducible hematopoietic differentiation. Blood 106:1601–1603
20. Ortolani C (2011) CD16 antigen. In: Flow cytometry of hematological malignancies, 1st edition. Wiley-Blackwell, Oxford, UK, pp 45–48
21. Decleva E, Menegazzi R, Busetto S et al (2006) Common methodology is inadequate for studies on the microbicidal activity of neutrophils. J Leukoc Biol 79:87–94

Part IV

Neutrophil Adhesion and Chemotaxis

Chapter 13

Neutrophil Migration Through Extracellular Matrix

Richard T. Jennings and Ulla G. Knaus

Abstract

Neutrophil migration from the bloodstream to sites of infection or injury is a multistep process that requires, dependent on the tissue structures being encountered, different modes of movement. Neutrophil locomotion can range from mesenchymal to amoeboid movement and may include multiple shape changes, contractile squeezing through gaps, and adhesion/de-adhesion cycles. In vitro migration assays reflect only some aspects of the complex in vivo neutrophil recruitment. For two-dimensional in vitro migration chemotaxis chambers, microscopic analysis of movement towards a pipette gradient or Boyden chambers is used. To analyze three-dimensional in vitro migration neutrophils can be embedded into matrices of diverse biophysical properties or can be placed onto matrices that are layered on a wide-pore filter, enabling migration through the matrix and the filter of a transwell plate towards a gradient of chemoattractant. We utilize here a commercially available setup for migration of murine neutrophils from the top of a loose collagen type I matrix, which determines the ability of neutrophils to attach to the matrix, sense the chemoattractant, polarize, digest the matrix, and move through the matrix into the lower transwell chamber. While the mode of migration inside the matrix cannot be studied in detail, this assay permits quantitative assessment of migrated neutrophils during a defined period of time.

Key words Murine neutrophils, Three-dimensional (3D) migration, Extracellular matrix (ECM), Chemotaxis

1 Introduction

As first responders in infection or tissue injury, neutrophils play a central role in clearance of microorganisms and initiation of immune and inflammatory responses. Recruitment of neutrophils circulating in the bloodstream to a site of insult follows a defined sequence of sensing the pathogen, slower rolling, stopping, attaching to the endothelial wall, diapedesis, and following a chemotactic gradient towards the pathogen [1]. Neutrophils are highly motile cells with speeds up to 17–21 μm/min on linear microfluidic devices that can rapidly adjust direction [2]. As very diverse tissues need to be infiltrated, neutrophils have evolved a wide repertoire of migratory modes enabling penetration of varied matrix types.

Mark T. Quinn and Frank R. DeLeo (eds.), *Neutrophil Methods and Protocols*, Methods in Molecular Biology, vol. 1124,
DOI 10.1007/978-1-62703-845-4_13,

Neutrophils encounter soft, malleable matrices such as interstitial tissue but also stiffer substrates such as basement membrane or fibrin matrices. Migration on two-dimensional (2D) surfaces follows a well-defined cycle of lamellipodium (protrusion) formation, adhesion, polarization at the leading edge, nucleus translocation, and subsequent uropod retraction [3]. This mesenchymal mode of 2D motility depends on adhesion and detachment, both dependent on integrins. Neutrophils will often engage in three-dimensional migration (3D) when they chemotax in vivo. Several modes of 3D migration have been documented such as mesenchymal, amoeboid, or microtubule-directed blebbing. The primary mode of leukocyte migration in 3D environments is the amoeboid type characterized by gliding without or minimal integrin involvement [4]. While integrin-mediated adhesion is an integral part of diapedesis, interstitial migration may only require protrusive F-actin flowing [5]. When neutrophils encounter very small openings, contraction of the actomyosin network facilitates squeezing of the nucleus through gaps. In some cases, such as recruitment into the airways, neutrophils will get trapped in small pulmonary capillaries and the alveolar wall and migrate directly into the lung parenchyma without integrin-dependent attachment [6]. Current 3D model systems have limitations, often not reflecting in vivo environment, but they permit mechanistic studies and analysis of matrix-based 3D motility. The type of ECM used is chosen to reflect the composition, elasticity, and density of barriers and tissues that migrating neutrophils encounter. Common ECMs include type I collagen of varying density, laminin-rich hydrogels derived from tumor cell extracts resembling basement membrane (Matrigel), fibrin gels, or RGD peptide functionalized hydrogels [7]. For instance, the porous matrix formed from fibrillar collagen is often used when modelling neutrophil/interstitium interactions while gelled collagen I polymerizes into a more rigid structure and is often used to model basement membranes or tumor stroma. Neutrophils adjust their mode of migration according to ECM composition. The encountered ECM environment determines the input of β1 or β2 integrins, actin polymerization, and myosin II-driven forces to the motile behavior. For example, neutrophils encountering stiff 2D matrices will engage β2 integrins for adhesion-based, polarized migration, while 3D loose matrix such as fibrillar collagen will result in amoeboid crawling [8]. During diapedesis, proteolytic remodelling of the basement membrane is integral for efficient migration while interstitial migration of neutrophils usually does not require matrix degradation, although matrix metalloproteinase activity may enhance directed migration by generating chemotactic collagen fragments [7]. We describe here a transwell assay that uses fibrillar ECM for directed migration of murine neutrophils towards a chemotactic fMLF gradient. The assay system is flexible and easily adapted to changes in the composition and biophysical properties of the ECM or to various chemoattractant stimuli.

2 Materials

1. 10× phosphate buffered saline without calcium and magnesium (10× $PBS^{-/-}$).
2. Phosphate buffered saline without calcium and magnesium ($PBS^{-/-}$).
3. Percoll.
4. 100 % Percoll: Percoll buffered by the addition of 10× $PBS^{-/-}$ (nine parts to one part) (*see* **Note 1**).
5. 81 % Percoll: 5.7 ml 100 % Percoll, 1.3 ml $PBS^{-/-}$ (*see* **Note 1**).
6. 62 % Percoll: 3.1 ml 100 % Percoll, 1.9 ml $PBS^{-/-}$ (*see* **Note 1**).
7. 55 % Percoll: 2.75 ml 100 % Percoll, 2.25 ml $PBS^{-/-}$ (*see* **Note 1**).
8. 50 % Percoll: 2.5 ml 100 % Percoll, 2.5 ml $PBS^{-/-}$ (*see* **Note 1**).
9. 45 % Percoll: 3.15 ml 100 % Percoll, 3.85 ml $PBS^{-/-}$ (*see* **Note 1**).
10. Hanks balanced-salt solution without calcium and magnesium ($HBSS^{-/-}$).
11. 1 M HEPES-NaOH pH 7.0–7.6.
12. 2.5-ml syringes.
13. 28-G and 18-G needles.
14. Filter (70 μm).
15. ACK lysis buffer: 155 mM NH_3Cl, 1 mM $KHCO_3$, 10 mM EDTA (pH 8.0).
16. Collagen type I: 6 mg/ml bovine collagen (e.g., Nutragen).
17. 10× $HBSS^{+/+}$ PR^{+}: 10× $PBS^{-/-}$ with phenol red.
18. Buffer A: $HBSS^{+/+}$, 2 % FCS, 10 mM HEPES.
19. Fetal calf serum (FCS; low endotoxin).
20. Fluorescein isothiocyanate isomer I (FITC, ≥90 % HPLC).
21. 24-well transwell plate (8 μm pore).
22. *N*-Formyl-Met-Leu-Phe (fMLF, ≥97 % HPLC).
23. LPS from *Salmonella enterica*.
24. Hoechst 33342.
25. Superfrost glass slides.
26. Mowiol 4-88.
27. Borosilicate glass coverslips (19 mm, thickness No. 0).
28. Transmission light microscope with camera.
29. Confocal microscope with image and data processing software.

3 Methods

3.1 Murine Neutrophil Isolation

1. Sequentially layer 2 ml of 62 %, 2 ml of 55 %, and 2 ml of 50 % Percoll above 3 ml of 81 % Percoll in a 15-ml polypropylene tube. (*see* **Notes 1** and **2**).
2. Prior to euthanasia, 10 ml of $HBSS^{-/-}$ containing 10 mM HEPES-NaOH (pH 7.0–7.6) in a 50 ml tube and 2 ml $PBS^{-/-}$ per well in a 6-well plate are placed on ice.
3. Mice are euthanized by an IACUC-approved method, and femurs and tibias are harvested into the 2 ml of cold $PBS^{-/-}$.
4. Crush epiphyses, and flush bone marrow out using a 28-G needle with 2 ml of cold HEPES-buffered $HBSS^{-/-}$ per bone.
5. Filter bone marrow through a 70 μm filter and pellet by centrifugation at 400 × *g* for 4 min at 4 °C with low acceleration and low brake.
6. Resuspend pelleted bone marrow in 3 ml of 45 % Percoll and layer upon the premade gradient.
7. Centrifuge gradients at 1,600 × *g* for 30 min at 10 °C with low acceleration and no brake. Neutrophils and contaminating erythrocytes sediment at the 62–81 % interface.
8. Remove Percoll above the 62–81 % interface by aspiration.
9. Remove Percoll layers below the interface using an 18-G needle attached to a 2.5 ml syringe.
10. Wash harvested neutrophils and erythrocytes with 10 ml of $PBS^{-/-}$, and pellet twice by centrifugation at 400 × *g* for 4 min at 4 °C with low acceleration and low brake.
11. Remove contaminating erythrocytes through hypotonic lysis by adding 3 ml of ice-cold ACK lysis buffer per gradient pellet.
12. After 3 min at room temperature, terminate lysis by adding 10 ml of $PBS^{-/-}$.
13. Pellet neutrophils by centrifugation at 400 × *g* for 4 min at 4 °C with low acceleration and low brake.
14. Resuspend cells in 10 ml $PBS^{-/-}$.
15. Use a hemocytometer to count cells and calculate neutrophil yield (*see* **Notes 3**–**7**).

3.2 ECM and Chemoattractant Gradient Setup

1. Mix 800 μl of bovine collagen with 100 μl of 10× $HBSS^{+/+}$ PR^{+} (8:1).
2. Add 0.1 N NaOH in 2.5–5 μl aliquots. After each addition, mix the collagen and assess pH by phenol red color change.
3. When the solution remains neutral (orange), add H_2O to reach a final 1× $HBSS^{+/+}$ solution.

4. Dilute the 4.8 mg/ml solution (4.8 mg/ml) with 1× $HBSS^{+/+}$ to achieve a 1 mg/ml collagen concentration.
5. Add 2 % FCS (v/v), 10 mM HEPES, and 1 μg/ml FITC to the solution (*see* **Notes 8–11**).
6. Place 40 μl of neutralized and diluted collagen solution in each insert of a 24-well transwell plate and incubate for 45–60 min at 37 °C.
7. To rehydrate the collagen and establish the chemoattractant gradient, add 300 μl of buffer A containing a chemoattractant (e.g., fMLF, KC, MIP2, fMIFL) in the lower chamber of each transwell.
8. Return the plate to 37 °C at least 2 h prior to running experiments (*see* **Notes 12** and **13**).

3.3 Neutrophil Migration and Analysis

3.3.1 Neutrophil Labeling

1. Dilute neutrophils to 1×10^7 neutrophils per ml in $PBS^{-/-}$ supplemented with 2 % FCS.
2. Label neutrophils by incubation with 100 ng/ml Hoechst 33342 for 30 min on ice.
3. Wash cells twice with $PBS^{-/-}$ and pellet by centrifugation at $400 \times g$ for 4 min at 4 °C with low acceleration and low brake.

3.3.2 Neutrophil Migration and Experiment Termination

1. Gently add 100 μl of buffer A to the transwell upper chamber and pre-warm to 37 °C.
2. Resuspend isolated neutrophils at a concentration of 1×10^7 cells/ml in buffer A.
3. Add 25 μl of the cell suspension (2.5×10^5 neutrophils) to the transwell upper chamber above the set collagen and chemoattractant gradient.
4. Return the transwell plate to 37 °C.
5. At different time intervals (for example after 3 h), terminate migration by fixation with formaldehyde at 4 °C.
6. For fixation, remove transwell inserts and placed them in a fresh 24-well transwell plate. Add 1 ml of $PBS^{-/-}$-buffered 4 % formaldehyde (w/v) to the lower chamber and 200 μl of the same solution to the upper chamber.
7. Incubate plates for 24 h at 4 °C for complete fixation.

3.3.3 Microscopy Analysis

1. Neutrophils capable of migrating through ECM and the transwell membrane can be visualized at the bottom of the transwell using transmission light microscopy. Acquire triplicate images per transwell.
2. To analyze neutrophils which have migrated through the matrix but have not migrated through the transwell membrane, rehydrate transwell membranes and associated ECM with $PBS^{+/+}$ for at least 2 h at 4 °C.

3. Carefully cut from each transwell using a sharp ethanol-cleaned scalpel.
4. Mount membrane and attached ECM on the superfrost glass slides using acid-washed borosilicate glass coverslips and Mowiol.
5. Visualize membranes using transmission light through a 60×/1.35 (oil) objective; visualization of FITC-labeled ECM requires a 488-nm laser line, and Hoechst requires a UV (405 nm) laser line (*see* **Note 14**).
6. Focus the microscope to the interface between the ECM and membrane using the 488 nm laser line.
7. Take confocal pictures within this plane using the 405-nm laser line to visualize nuclei (cells) in plane with the membrane.
8. Quantify images using imaging software, such as ImageJ cell counter software. Data analysis can then be performed using software (e.g., Graphpad Prism). Migrated neutrophil numbers can be represented as cells per field, cells per membrane area, or percentage of total neutrophils loaded into the transwell. Acquire triplicate images per transwell and calculate mean and SEM (standard error of the mean) in order to apply statistics.
9. When examining migration through the 1 mg/ml collagen matrix and insert membrane using a 20× objective, 700–800 cells per field should be expected when wild-type neutrophils are allowed to migrate for 3 h towards 10 μM fMLF.
10. After 3 h, 150–200 neutrophils per field should be expected when examining transwell membranes using a 60× objective with no digital magnification(*see* **Note 15**).
11. Application of a two-tailed equal variance student's *t*-test between treatments indicates whether results are statistically relevant. A representative experiment of neutrophil chemotaxis towards fMLF or LPS through fibrillar collagen is shown (Fig. 1) (*see* **Notes 16** and **17**).

4 Notes

1. Prior to Percoll gradient setup, all buffers and reagents should be at room temperature.
2. Quality of neutrophil preparation is dependent upon the quality of the gradient. All interfaces should be clearly visible. For optimal purity gradients should be loaded with bone marrow within 10–15 min of being prepared.
3. Neutrophil activation during purification is avoided by limiting vibration during centrifugation steps. Therefore, all acceleration and deceleration steps are low, and all tubes including gradients should be perfectly balanced.

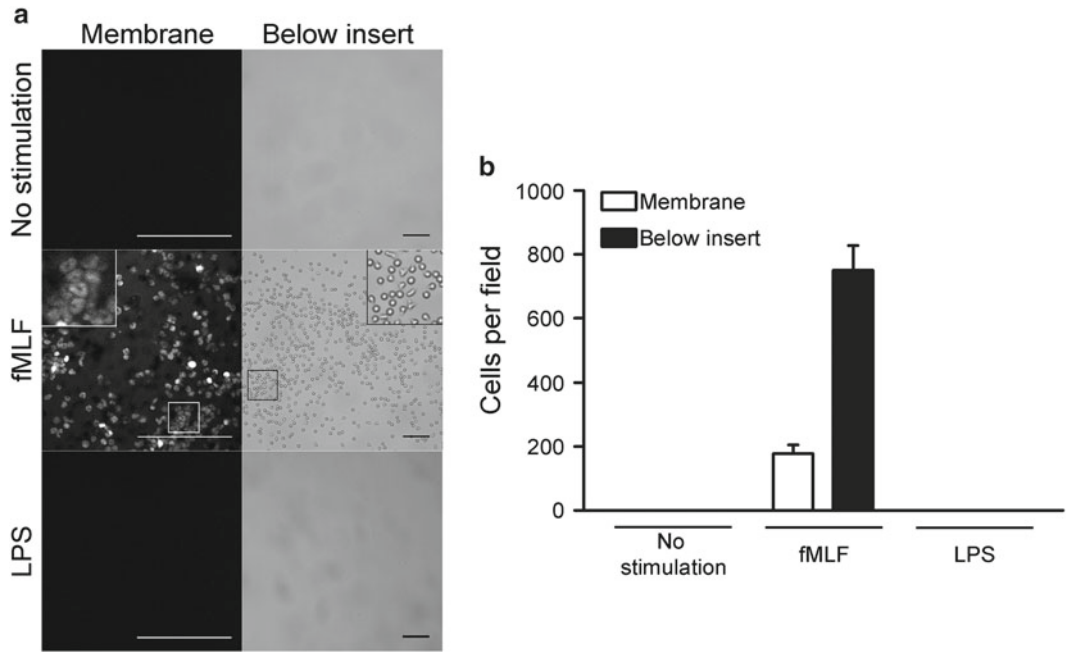

Fig. 1 Migration of murine neutrophils through collagen type I. Hoechst 33342-stained bone marrow-derived neutrophils (BMDN) were placed on top of the ECM followed by migration for 3 h through 1 mg/ml collagen towards either buffer A alone, or 10 μM fMLF, or 10 ng/ml LPS in buffer A. (**a**) After 3 h transmission light images were acquired at the bottom of the transwell (*right*); inserts were fixed, membranes and ECM removed, mounted and confocal images were taken in plane with the membrane (*left*), and *scale bars* represent 100 μm. *Boxed areas* are digitally magnified and displayed *top/left* (confocal) or *top/right* (transmission). (**b**) Quantification of neutrophil numbers per field presented as mean ± standard error of the mean of three independent fields

4. Neutrophils can be directly harvested from the gradient through drawing neutrophils off the gradient using an 18-G needle attached to a 2.5-ml syringe. Directly harvesting neutrophils may result in activation during preparation. Removing the Percoll from above and below the neutrophil/erythrocyte interface eliminates cell activation.
5. Approximately 1×10^7 neutrophils are commonly obtained per mouse. Purity is above 90% and can be measured through techniques including flow cytometry (SSC/FSC or Gr-1 staining) and cytospin.
6. Neutrophil isolation will take approximately 1 h after euthanasia. Prolonged handling may result in neutrophil activation and/or a reduction in purity.
7. Greater neutrophil purity and quality is obtained when one gradient is used per mouse, bone marrow from up to two mice can be loaded onto one gradient. Overloading Percoll gradients will lower purity and activate neutrophils.
8. All Nutragen® handling is performed in an ice water bath; the temperature must remain 4–8 °C. pH-regulated, buffered

Nutragen®, which has a concentration of 4.8 mg/ml, is often used at concentrations between 1 and 3 mg/ml; at a concentration lower than 1 mg/ml incomplete gellation may occur.

9. A variety of ECMs can be used for neutrophil 3D migration. For example, MatriGel™ and Geltrex®, which are mixtures of membrane proteins secreted by Engelbreth-Holm-Swarm (EHS) mouse sarcoma cells; fibrinogen gelled with thrombin; functionalized hydrogels incorporating RGD peptides; and collagen type I, either fibrillar or gelled, can be used. Collagen is usually supplied as a high-concentration solution dissolved in acetic acid with a pH ~ 2. Commercially available MatriGel™ in solution exhibits basic pH. Matrix pH should be neutralized prior to gellation, with NaOH and/or HCl being commonly used. pH meters can be used to determine pH, but due to the small volume of matrix used per experiment (<1 ml), the use of pH paper or phenol red indicator permits more accuracy in pH estimation without substantial loss of matrix. Of note, due to the preparation procedure of MatriGel™ and its origin, a high degree of inter-batch variation should be expected [8–10]. References 8–10 indicate the broad range of ECMs that have been used during migration experiments.
10. Fibrinogen can be gelled at concentrations ranging from 2 to 50 mg/ml, but most concentrations have not been tested with neutrophils [8, 11]. References 8 and 11 indicate the range of fibrinogen concentrations are often used.
11. MatriGel™ at concentrations lower than 0.3 mg/ml may not polymerize. Concentrations that have been tested in neutrophil migration assays range from 0.3 to 5 mg/ml, migration through MatriGel™ has been shown to occur within 6 h [12, 13].
12. FITC is incorporated into the matrix to allow ECM visualization during analysis by confocal microscopy. FITC enables low-cost ECM labeling but rapidly bleaches during image acquisition. FluoSpheres® are photostable, fluorescent beads that enable ECM visualization at specified excitation and emission wavelengths. Available excitation/emission wavelengths (nm) include 365/415, 505/515, and 580/605.
13. Antibodies including fluorophore-conjugated anti-Gr1 can also be used as neutrophil stains. Nonspecific cell membrane stains such as the CellMask™ plasma membrane stains and CellVue® dyes permit neutrophil membrane visualization during migration. Dyes which are cell membrane permeable and selectively label live cells such as Calcein AM can also be used. It is important that any staining protocol does not impede neutrophil migration. Preliminary experiments comparing stained and non-stained neutrophils should be performed before using any dyes or labels.

14. The majority of standard confocal microscopes are equipped with 405- and 488-nm laser lines. For other ECMs and cell stains optimization may be required to ensure visualization during microscopy.
15. Neutrophils can be visualized at 10–100× magnification, 60× magnification is preferred for obtaining quantification of migrated neutrophils and qualitative data regarding cell morphology. Pictures should be taken by focussing at the middle of the membrane to avoid bias due to the ECM meniscus.
16. A variety of chambers are available including transwell plates or various 2D and 3D migration chambers from Ibidi GmBH, Martinsried, Germany. Custom-built chambers are often used, but these individualized chambers prevent standardization between laboratories. For higher throughput, modified 24-well transwell plates or microfluidic devices are preferable [14].
17. Additional chemoattractants, which have been tested to elicit murine neutrophil migration through 3D collagen type I ECM within 3 h, include 10 nM fMILF (*N*-formyl-Met-Ile-Leu-Phe), 10 ng/ml KC/CXCL1, and 10 ng/ml MIP2/CXCL2.

Acknowledgments

This work was supported by grants from Science Foundation Ireland and the Health Research Board.

References

1. Borregaard N (2010) Neutrophils, from marrow to microbes. Immunity 33:657–670
2. Butler KL, Ambravaneswaran V, Agrawal N et al (2010) Burn injury reduces neutrophil directional migration speed in microfluidic devices. PLoS ONE 5:e11921
3. Nourshargh S, Hordijk PL, Sixt M (2010) Breaching multiple barriers: leukocyte motility through vascular walls and the interstitium. Nat Rev Mol Cell Biol 11:366–378
4. Huttenlocher A, Horwitz AR (2011) Integrins in cell migration. Cold Spring Harb Perspect Biol 3:a005074
5. Lammermann T, Sixt M (2009) Mechanical modes of 'amoeboid' cell migration. Curr Opin Cell Biol 21:636–644
6. Yoshida K, Kondo R, Wang Q et al (2006) Neutrophil cytoskeletal rearrangements during capillary sequestration in bacterial pneumonia in rats. Am J Respir Crit Care Med 174: 689–698
7. Wolf K, Friedl P (2011) Extracellular matrix determinants of proteolytic and non-proteolytic cell migration. Trends Cell Biol 21:736–744
8. Van Goethem E, Poincloux R, Gauffre F et al (2010) Matrix architecture dictates three-dimensional migration modes of human macrophages: differential involvement of proteases and podosome-like structures. J Immunol 184: 1049–1061
9. Koenderman L, Van der Linden JAM, Honing H et al (2010) Integrins on neutrophils are dispensable for migration into three-dimensional fibrin gels. Thromb Haemost 104:599–608
10. Zaman MH, Trapani LM, Sieminski AL et al (2006) Migration of tumor cells in 3D matrices is governed by matrix stiffness along with cell-matrix adhesion and proteolysis. Proc Natl Acad Sci U S A 103:10889–10894
11. Duong H, Wu B, Tawil B (2009) Modulation of 3D fibrin matrix stiffness by intrinsic fibrinogen–thrombin compositions and by extrinsic cellular activity. Tissue Eng A 15:1865–1876

12. Wang Q, Teder P, Judd NP et al (2002) CD44 deficiency leads to enhanced neutrophil migration and lung injury in *Escherichia coli* pneumonia in mice. Am J Pathol 161: 2219–2228
13. Steadman R, St John PL, Evans RA et al (1997) Human neutrophils do not degrade major basement membrane components during chemotactic migration. Int J Biochem Cell Biol 29:993–1004
14. Sixt M, Lammermann T (2011) *In vitro* analysis of chemotactic leukocyte migration in 3D environments. Methods Mol Biol 769: 149–165

Chapter 14

Spinning Disk Confocal Imaging of Neutrophil Migration in Zebrafish

Pui-ying Lam, Robert S. Fischer, William D. Shin, Clare M. Waterman, and Anna Huttenlocher

Abstract

Live-cell imaging techniques have been substantially improved due to advances in confocal microscopy instrumentation coupled with ultrasensitive detectors. The spinning disk confocal system is capable of generating images of fluorescent live samples with broad dynamic range and high temporal and spatial resolution. The ability to acquire fluorescent images of living cells in vivo on a millisecond timescale allows the dissection of biological processes that have not previously been visualized in a physiologically relevant context. In vivo imaging of rapidly moving cells such as neutrophils can be technically challenging. In this chapter, we describe the practical aspects of imaging neutrophils in zebrafish embryos using spinning disk confocal microscopy. Similar setups can also be applied to image other motile cell types and signaling processes in translucent animals or tissues.

Key words Spinning disk, Confocal microscopy, Neutrophils, Migration, In vivo imaging, Zebrafish

1 Introduction

The zebrafish (*Danio rerio*) immune system is remarkably similar to its mammalian counterpart and it has therefore gained tremendous popularity as a vertebrate disease model of both innate and adaptive immunity (reviewed in [1, 2]). Zebrafish embryos are largely translucent for the first few days of development, allowing for noninvasive in vivo imaging and studies of cell behavior in a physiologically relevant context.

Here, we describe methods for in vivo live imaging of neutrophils in zebrafish embryos. Neutrophil imaging is usually performed at 2–3 days post fertilization (dpf). At this stage of development, adaptive immunity has not sufficiently matured, allowing the direct study of innate immunity in isolation. Neutrophils at this stage are considered to be fully functional, as they can directionally migrate (chemotaxis) to wounds or infections and perform immune functions

Mark T. Quinn and Frank R. DeLeo (eds.), *Neutrophil Methods and Protocols*, Methods in Molecular Biology, vol. 1124,
DOI 10.1007/978-1-62703-845-4_14,

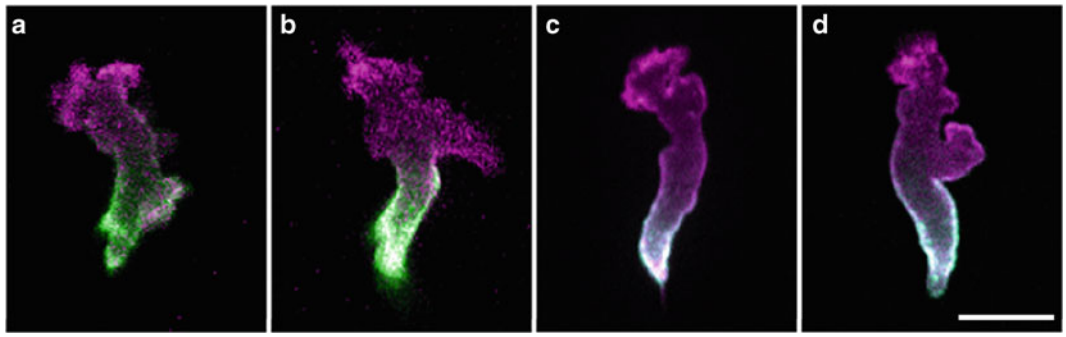

Fig. 1 Comparison of laser scanning confocal (LSM) and spinning disk confocal (SDCM) on in vivo neutrophil imaging. Maximum intensity projection image of a neutrophil expressing GFP-UtrCH (*green*) and Lifeact-Ruby (*magenta*), which labels stable F-actin and all F-actin, respectively. (**a**, **b**) Image acquired using an LSM (Olympus). Olympus LUMFL 60×/1.1NA Water objective (**a**) or Olympus PlanApo N 60×/1.45NA Oil objective (**b**) was used with S.U. 200, optimal step size and 3.8× zoom in. (**c**, **d**) Image acquired using SDCM (Zeiss). LCI Plan-Neofluar 63×/1.3NA Water objective (**c**) or Plan Apo 63×/1.4NA Oil objective (**d**) was used with 300 EM gain, 55 ms exposure for both channels and 0.4 μm step size. SDCM images showed superior image quality compared to that of the LSM images. The difference between using an oil objective with a higher NA than the water objective is less significant. Scale bar: 10 μm

to fight off pathogens. In addition, neutrophils migrate spontaneously (random migration) in the interstitial tissue within the head region (reviewed in [2]). The ability to image both neutrophil chemotaxis and random motility in the same organism allows for the dissection of the molecular regulators required for basic motility and directional sensing. One thing to note is that neutrophils at this developmental stage are not terminally differentiated, since they retain the ability to undergo cell division under some conditions and possess an elongated nucleus instead of the multi-lobulated nucleus observed in human neutrophils.

This protocol describes the use of spinning disk confocal microscopy (SDCM) for live imaging of genetically encoded fluorescent reporters expressed in zebrafish embryos. The benefits of imaging using SDCM over conventional single-point laser scanning confocal microscopy (LSM) including acquisition speed, detection efficiency, resolution, reduced photobleaching, and improved signal-to-noise ratio (SNR), both in vitro and in vivo, has been discussed elsewhere [3–5]. One common concern regarding high-speed imaging is the trade-off between speed and resolution. In our experience, acquiring a Z-stack time series using an SDCM system with optimal camera setup offers improved temporal and spatial resolution as compared to laser scanning confocal microscopy (Fig. 1). One of the major differences between the acquisition speed of the LSM and SDCM is that the former collects signals from the specimen one pixel at a time through a single pinhole. The speed of the LSM thus depends on the line frequency of the scanner, which is limited by the galvanometer mirrors that

move the laser beams, along with the number of lines needed for the field of view imaged. However, because the galvanometer speed is fixed, the limitation on image acquisition speed in practice is the dwell time for each XY position (pixel) to produce sufficient signal over background. The detector for LSM is typically a photomultiplier tube (PMT). Although PMTs have a huge capacity for amplification of signal, they also have relatively low quantum efficiency (~10–15 % is typical depending on wavelength). Thus, in order to increase speed for a given signal, one must increase excitation laser power, which can result in faster photobleaching and/or increased phototoxicity with LSM [5]. In addition, PMT amplification applies to both signal and noise, thus reducing the overall SNR in LSM images.

In contrast to point scanning with an LSM, a spinning disk confocal utilizes a rotating Nipkow disk with thousands of pinholes arranged in a series of nested spirals to simultaneously illuminate and collect signals from the entire specimen field, thus leading to significantly faster frame rates than LSM systems. Perhaps more significantly, SDCM systems use a charge-coupled device (CCD) camera or camera as a detector, which have both higher quantum efficiencies (~60 %) and lower noise than PMTs, resulting in significantly higher SNR and increased sensitivity [6, 7]. Due to the improved SNR and sensitivity, SDCM imaging has the added advantage of requiring lower levels of excitation laser light, leading to less photobleaching and/or phototoxicity of the imaged samples. In recent years, electron multiplying CCDs (EMCCDs) have been introduced that have even greater quantum efficiency (~90 %) and low-noise signal amplification resulting in exceptionally high SNR and sensitivity.

When imaging any live specimen by fluorescence microscopy, high expression of fluorescent fusion proteins can produce cytotoxicity or unintended phenotypic effects, including developmental defects in zebrafish. However, live cells expressing fluorescent fusion proteins expressed at approximately endogenous levels of the target protein are often very dim. With samples in which a fluorescent signal is relatively weak, the enhanced sensitivity of SDCM is clearly advantageous. In addition, low fluorescence emission intensity can be compensated for by using longer exposure times; however, this too will decrease the speed advantages of using a SDCM. Further improvements in sensitivity and SNR can be gained through pixel binning, at the cost of lateral resolution. For example, 2×2 binning will increase the SNR by a factor of four, but reduce the lateral resolution by 50 %. An EMCCD camera can sometimes abrogate the need for pixel binning, but it should be noted that native pixel sizes vary with camera type (*see* **Notes 1** and **18**).

A major advantage of using SDCM for live, fast motile cell imaging lays in the image quality, which arises from the aforementioned

high SNR due to the use of CCD and EMCCD camera technologies. One notable downside of SDCM for intravital imaging is pinhole cross talk, which can degrade image quality. This effect is particularly problematic with specimens that have high light scattering properties [5]. Newer model spinning disk heads with greater pinhole spacing can mitigate this problem to some degree. Another potential downside of standard SDCM systems relative to LSM is that they do not have the inherent ability to select a region of interest (ROI) for high power illumination as is required in photobleaching or photoactivation experiments. However, ROI illumination can be achieved via separate illumination paths. Despite these potential drawbacks, SDCM is a powerful system for high-speed three-dimensional imaging of fast-moving cells like neutrophils.

In the following sections, we provide protocols for performing live spinning disk confocal microscopy of transgenic zebrafish expressing fluorescent-tagged proteins in neutrophils. This includes protocols for optimizing neutrophil-specific protein expression, preparation of transgenic fish for imaging, microscope setup, and image acquisition.

2 Materials

2.1 Zebrafish Embryos

1. Zebrafish husbandry according to The Zebrafish Book [8]. Available online http://zfin.org/zf_info/zfbook/zfbk.html. Accessed 14 Feb 2013.

2.2 Microscope Supplies and Components

This is just a reference of the setup we use to acquire the images presented in the figures (Figs. 2 and 3). Other vendors also provide similar systems.

1. Inverted microscope (Zeiss Observer Z1) (*see* **Note 2**).
2. Spinning disk (Yokogawa CSU X1) (*see* **Note 3**).
3. EMCCD camera (Photometrics Evolve 512 EMCCD) (*see* **Notes 1** and **18**).
4. Objective (LCI Plan-Neofluar 63×/1.3 Imm Corr DIC M27; water or glycerine immersion) (*see* **Note 4**).
5. Immersion medium (Carl Zeiss Immersol W 2010; distilled water is also suitable for short-term imaging; *see* **Note 5**).
6. Heating stage/heating chamber (PECON Incubator P, compact S1 and Heating Insert P S1; heating is optional depending on room setup and stage of embryo).
7. Scanning stage with Z-piezo (*see* **Note 6**).
8. Multi laser module (laser unit 488/20 mW (OPSL laser) and 561 nm/20 mW (DPSS laser)) (*see* **Note 7**).

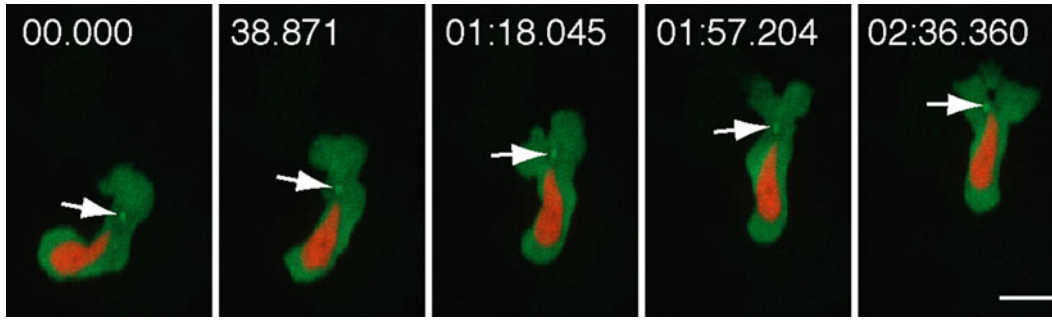

Fig. 2 Spinning disk confocal imaging of F-actin cytoskeleton dynamics. Time-lapse maximum intensity projection image of a neutrophil undergoing random motility in a zebrafish embryo in vivo. The neutrophil expresses GFP-UtrCH (*green*) and Lifeact-Ruby (*red*), which labels stable F-actin and all F-actin, respectively. A SDCM equipped with an EMCCD camera was used for the acquisition. LCI Plan-Neofluar 63×/1.3 Water objective; 300 EM gain; 55 ms exposure (GFP-UtrCH), 36 ms exposure (Lifeact-Ruby); emission filter BP 525/50 and FF02-617/73-25; 0.4 μm step size. Acquisition was made as fast as possible and consecutive images are shown in the panel. Scale bar: 10 μm

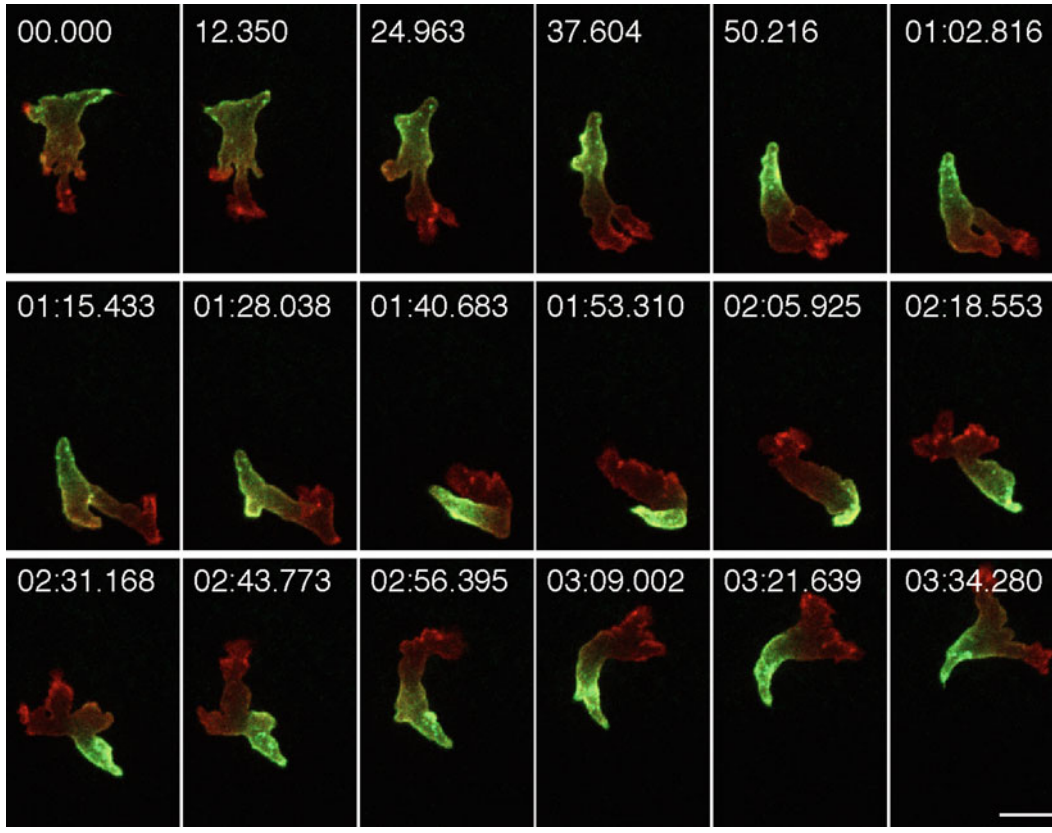

Fig. 3 Spinning disk confocal imaging of organelle subcellular localization. Time-lapse maximum intensity projection image of a neutrophil expressing γtubulin-GFP (*green*) and a nuclear probe, mCherry-histone H2B (*red*). The Microtubule Organizing Center (MTOC-*arrow*) is localized in front of the nucleus during neutrophil random motility in vivo. Scale bar: 10 μm

9. Emission filter (BP 525/50 DMR 25; FF02-617/73-25) (*see* **Note 8**).
10. Vibration isolation table (Newport Vision IsoStation).
11. Glass bottom Petri dish (*see* **Note 9**).
12. Zen 2011 (Carl Zeiss) image acquisition software.

2.3 Buffers and Other Reagents (Image Acquisition Components)

1. 60× E3: 17.2 g NaCl, 0.17.2 g NaCl, 2.9 g $CaCl_2$, 4.9 g $MgSO_4$. Fill to 1 L with reverse osmosis (RO) water. Adjust pH to 7.2 with NaOH.
2. 1× E3: Dilute 60× E3 with RO water to 1×. Add 0.1 % methylene blue.
3. E3/PTU: 0.003 % 1-phenyl-2-thiourea in 1× E3.
4. 20× Tricaine: 400 mg tricaine (MS-222) powder, 97.9 mL RO water, ~2.1 mL 1 M Tris (pH 9). Adjust pH to ~7. Store at 4 °C.
5. 1× Tricaine: Dilute 20× Tricaine to 1× in E3/PTU.
6. Water bath at 42 °C.
7. 1 % low melting point agarose (L.M.A.) in E3 solution for embryo mounting: microwave to melt the L.M.A. The solution remains fluid at 37 °C but quickly hardens when cooled. Maintain the melted L.M.A. in a 42 °C water bath.

2.4 Image Processing Components

Image acquisition software usually contains some image viewing and/or imaging analysis functions. Additional commonly used software includes but is not limited to the following:

1. ImageJ (free software; http://rsbweb.nih.gov/ij. Accessed 14 Feb 2013).
2. FIJI (free software; http://fiji.sc. Accessed 14 Feb 2013).
3. FluoRender (free software; http://www.sci.utah.edu/software/127-fluorender.html. Accessed 14 Feb 2013).
4. Bitplane Imaris (http://www.bitplane.com/go/products/imaris. Accessed 14 Feb 2013).
5. MetaMorph (http://www.moleculardevices.com/products/software/meta-imaging-series/metamorph.html. Accessed 14 Feb 2013).
6. Volocity (http://www.perkinelmer.com/pages/020/cellular-imaging/products/volocity.xhtml. Accessed 14 Feb 2013).

3 Methods

3.1 Neutrophil-Specific Protein Expression

For imaging purposes, transient mosaic expression is usually sufficient. However, in the case where high levels of expression of the transgene affect neutrophil function, generation of a transgenic line may be desired, as gene expression can be lower and specific

transgenic lines with low copy number of the transgene can be identified (*see* **Note 10**). Preparation of transient expression or transgenic zebrafish embryos that express the gene of interest in a neutrophil-specific manner requires the use of a neutrophil-specific promoter such as the myeloperoxidase (*mpx*) [9, 10] or the lysozyme C (*lyz*) promoter [11, 12] (*see* **Note 11**):

1. For plasmid construction, use DNA expression vectors containing minimal Tol2 elements for efficient integration [13] flanking either *mpx* or *lyz* promoter, the gene of interest and an SV40 polyadenylation sequence (Clonetech).
2. Prepare plasmid DNA. Transformation of plasmid into regular cloning competent cells, e.g., *E. coli* DH5α is sufficient with the exception of plasmids containing the *mpx* promoter (*see* **Note 12**).
3. Extract and purify DNA using a commercially available miniprep kit (Promega Wizard *Plus* SV Minipreps DNA purification system) (*see* **Note 13**).
4. Prepare Tol2 transposase mRNA by in vitro transcription (Ambion mMESSAGE mMACHINE), followed by column purification (Qiagen-RNeasy Mini Kit).
5. Microinject zebrafish embryos using standard routine procedures. Different laboratories will have slightly different setups. For basic setup information and injection procedures, please refer to The Zebrafish Book [8] and a video demonstration published elsewhere [14].
6. Expression of construct is obtained by injection of 3 nL of 12.5 ng/μL DNA plasmid with 17.5 ng/μL Tol2 transposase mRNA into the cytoplasm of one-cell stage embryos.

3.2 Preparation of 35-mm Glass Bottom Petri Dish

Embryos will stick to polystyrene and glass surfaces without coating, and this will create unwanted wounds on the embryos.

1. Submerge the 35-mm glass bottom Petri dish (*see* **Note 9**) in 1 % BSA or 1 % skim milk for 10 min.
2. Rinse several times with RO water and air dry before use.

3.3 Preparation of Samples

Imaging is usually performed at 2–3 days post fertilization (dpf). To prevent pigmentation, exchange regular media with E3 containing 0.003 % 1-phenyl-2-thiourea (PTU) as early as 15 h post fertilization and no later than 1 dpf before pigment starts appearing. Keep the embryos in the E3/PTU medium throughout. Before imaging, remove chorion using ultrafine forceps if embryos are still unhatched. Mounting of an embryo in L.M.A., which will stabilize the embryo and prevent movement, is required for high-magnification imaging, since even the slightest movement by

an embryo will affect image quality. Proceed to the mounting procedures as follows:

1. Place embryos in 0.2 mg/mL tricaine in E3/PTU for 1 min.
2. Transfer 1–2 embryos onto a glass bottom Petri dish using a plastic or glass transfer pipette. Remove as much E3 as possible without drying out the embryo using a P100 pipette or transfer pipette. Any exposure of the embryo to air is enough to create injury on the epithelium and may affect neutrophil behavior.
3. Add ~80 μL of the melted L.M.A. directly onto the drop of liquid containing the embryo. In order to achieve an even consistency of L.M.A. around the embryo, remove the L.M.A. and add in new L.M.A.
4. Repeat the removal and addition of L.M.A. steps again and let it settle. Embryos usually lay down on the bottom of the plate laterally at this stage and are ideal for imaging. Otherwise, adjust the angle of the embryo before the L.M.A. hardens.
5. Wait for approximately 5 min at room temperature to ensure that the L.M.A. has hardened (*see* **Note 14**).
6. Slowly add in 2–4 mL E3/PTU with tricaine. Check if embryos are still attached to the bottom and have not floated. If floating occurs, perform the mounting steps again.

3.4 Microscopy, Image Acquisition, and Analysis

Perform imaging at the desired developmental stage, typically at 2–3 dpf. Imaging of spontaneous neutrophil motility is performed in the head region. The typical average speed of neutrophils undergoing random motility that we have observed is between 80 and 130 nm/s. Directional migration can be performed with different stimulants, i.e., tail fin or ventral fin wounding using a needle or surgical scalpel [12, 15], $CuSO_4$ induced neuromast damage [16], and LTB4 injection [17], incubation [18], etc.

Common applications include imaging the dynamics of the cytoskeleton, such as F-actin (Fig. 2); subcellular localization of organelles, such as the microtubule organizing center and the nucleus (Fig. 3); subcellular localization of proteins; subcellular localization of signaling molecules and protein activity using various bioprobes and ratio analysis; and morphological and tracking analysis during cell trafficking.

Different SDCM setups and image acquisition programs can be used. Here, we describe a general inverted microscope setup and the acquisition parameters to be considered before image acquisition. There is no fixed parameter for each acquisition, as every sample is different, and adjustments are often required to determine the optimal settings. The key is the balance between the

speed of acquisition, phototoxicity, and image SNR. The following is a general procedure of setting up a Z-stack time series for single or multiple channel image acquisition:

1. Turn on heating stage and set at 28.5 °C.
2. Apply a small drop of immersion medium to the objective (*see* **Note 5**).
3. Secure the glass bottom Petri dish with samples on the microscope stage. Make sure that the dish is seated flat and firmly in the stage, as this will minimize focus drift during imaging. If stage clips are present, clip the sample in tightly.
4. Locate target cell using eyepiece (*see* **Note 15**).
5. Choose a suitable emission filter for acquisition (*see* **Note 16**).
6. Adjust laser power to as low as possible while still obtaining a good SNR image, especially for long time imaging (*see* **Note 17**).
7. Adjust optimal exposure time (usually around 50–100 ms) and EM gain (around 300–500 for Evolve EMCCD) (*see* **Note 18**). Note that exposure time and laser power will be interdependent. In general, lower laser power at the cost of longer exposure times will result in less phototoxocity and photobleaching, assuming that the time resolution for Z-stack collection is not limiting for the experiment.
8. Set spinning disk revolution speed to maximum (*see* **Note 19**).
9. Set the Z-range with a little buffer distance above and below the cell's initial position, as the cell is actively migrating in a three-dimensional tissue.
10. Set the step size for Z-acquisition (*see* **Note 20**).
11. Set time interval and total duration of the acquisition (*see* **Note 21**).
12. Set the mode of acquisition as all channels per Z-slice (*see* **Note 22**).
13. Start acquiring image.
14. Common post-acquisition image analysis programs include but not limited to freeware like ImageJ/Fiji and FluoRender or commercially available Bitplane Imaris, Volocity, and MetaMorph. Each program has a different capacity and details of such are out of the scope of this chapter.

4 Notes

1. Photometrics Evolve 512 EMCCD and CoolSNAP HQ2 CCD are the common high-performance cameras of choice for SDCM. Sensitivity and resolution are the main criteria for choosing a suitable camera. Evolve EMCCD offers a higher

sensitivity but a relatively big 16 × 16 μm pixel size. CoolSNAP HQ2 has a 6.45 × 6.45 μm pixel size; however, binning may be needed for image acquisition to reduce illumination intensity and exposure time needed. It is highly recommended that you evaluate different cameras by demonstration to find out which one is better suited for your specific application. For our applications, we selected the Evolve EMCCD taking into consideration the speed of neutrophil migration and fluorescent levels of live cells (also *see* **Note 18**). One thing to note is that because the Evolve EMCCD is very sensitive, it can pick up cosmic ray signals stochastically that appear sporadically as very bright transient dots/comets within the image [19]. These transient dots/comets are very bright and are easily distinguishable from the real signal generated by fluorescent protein expression.

2. The inverted microscope stand provides a stable base for minimizing vibration as well as providing long-term stability for time-lapse imaging. As most microscope models will have manual parts, automation of the stand is not necessary for spinning disk confocal image acquisition. Motorized components of the stand conveniently allow for fast and seamless switching between preconfigured settings for sample viewing and image acquisition. The stand should include a filter-cube turret to allow switching between different dichromatic mirrors for specimen viewing and image acquisition, a multi-position objective lens nose piece for switching between magnifications, transilluminator for phase/DIC imaging/viewing, and an epi-illuminator for wide-field excitation of the sample for viewing. Having multiple imaging ports provides flexibility for introducing illumination, mounting digital cameras, and sample observation. Incorporating electronic shutters in the transillumination and epifluorescence illumination path will help to minimize photobleaching and phototoxicity when imaging/viewing the sample.
3. The Yokogawa CSU X1 spinning disk confocal unit is a dual-disk scan head design that consists of a disk with microlenses that are in conjugate with the pinholes of the Nipkow disk. This has several advantages for high temporal and spatial resolution live cell imaging over other spinning disk confocal systems. Single Nipkow disk systems only transmit 5 % of the incident illumination, whereas the microlenses in the second disk of the Yokogawa CSU X1 increase the illumination efficiency theoretically up to 40 %. Slit-scanning systems do not reject out-of-focus fluorescence along the axis of the slit and thus suffer from higher backgrounds. Compared to previous models (CSU 10, CSU 22), the CSU X1 has increased

illumination throughput and improved beam expanding optics providing flatter field of illumination. The CSU X1 is available as a manual or motorized version and has a wide range of configurations such as two camera port and bright field bypass module. For our application, we chose the basic manual version with six position electronic emission filter wheel.

4. Imaging deep in the sample and far away from the coverslip with an oil immersion objective can suffer from optical artifacts such as spherical aberration. Utilizing a high NA water immersion objective with a correction collar can minimize these induced spherical aberrations caused by mismatched refractive indices of the sample and immersion medium. In addition, the correction collar not only allows one to compensate for coverslip thickness variations but also changes in refractive medium due to temperature.
5. For extended time-lapse imaging experiments, Carl Zeiss Immersol W 2010 instead of distilled water is used as a water objective immersion medium. This reduces evaporation of the immersion medium and allows uninterrupted long-term imaging.
6. A piezoelectric Z-stage allows higher Z-focusing speeds than a stepper- or servomotor-driven Z-stage. In our experience, it can cut down on the time for a Z-stack acquisition by nearly half. As an alternative, a piezoelectric-driven objective lens mount can be used. Note that piezo devices have much smaller focus range limits (typically 100 μm, some as high as 300 μm) compared to motor-driven devices (tens of millimeters).
7. Developments in diode lasers and diode-pumped solid state (DPSS) lasers have made them a cost-effective alternative to gas lasers. They are small and quiet, have low heat loads and large range of wavelength selection, and don't require bulky water coolers. Most microscope manufacturers provide fiber-coupled laser combiners to deliver the laser beam, which use an acousto-optic tunable filter (AOTF) or TTL modulation to quickly select, shutter, and modulate the wavelength power. When choosing from the wide selection of available laser lines, the wavelength should optimally excite the fluorescent protein. Common laser wavelengths used for exciting fluorophores are 405 nm for DAPI, 442 nm for CFP, 488 nm for GFP, 514 nm for YFP, 561 nm for RFP, and 647 nm for Cy5. In addition, when considering power selection of individual lines, it should be noted that for fiber-coupled laser combiners, 40–60 % of the illumination power (wavelength dependent) is loss due to fiber coupling efficiency. For our application, 20 mW has proven to be sufficient for live zebrafish imaging (also *see* **Note 17**).

8. Individual band-pass emission filters, denoted by the center wavelength and bandwidth, should be chosen based on the spectral properties of the fluorophore. When selecting band-pass filters, it is important that the bandwidth be wide enough for efficient emission collection of the fluorophore, as well as provides sufficient blocking to eliminate the excitation source and signal from other fluorescent channels. For our filters, we chose a center wavelength of 525 nm with a 50 nm bandwidth (BP 525/50 DMR 25) and a 617 nm center wavelength with a 73 nm bandwidth (FF02-617/73-25). Manufacturers, such as Chroma Technology Corp and Semrock, Inc., can provide suggestions for filter selection based on the fluorophore spectral properties.
9. Glass bottom dishes are commercially available, but an inexpensive and relatively easy alternative is to make them in house. Drill a 16–18 mm hole in the center of a 35-mm tissue culture dish bottom. Apply a thin layer of Norland Optical Adhesive 68 on the outside surface around the hole. Place a 22-mm round #1 coverslip on top of the adhesive and press down slightly. The adhesive is cured by UV light. Overnight exposure of UV light in a tissue culture hood or approximately 1 h on a UV transilluminator is sufficient to cure the adhesive.
10. To make a transgenic line, injected embryos displaying mosaic transgene expression are raised to sexual maturity (as early as 2.5 months). F_0 founders are screened by outcrossing with wild-type zebrafish and checked for transgene expression in the neutrophils in the F_1 embryos at 2–3 dpf. The positive F_1 transgenic progeny can then be used for imaging or propagation of the transgenic line.
11. Since the *mpx* promoter is much larger than that of the *lyz* promoter (8 Kb vs. 4.1 Kb, respectively), it is easier to express larger transgenes (i.e., >3 Kb) driven under the *lyz* promoter in our experience. The *mpx* promoter drives gene expression mainly in neutrophils, although there may be very low levels of expression in macrophages as well [9]. The *lyz* promoter drives gene expression in neutrophils at later stages (≥ 2 dpf) [12]. However, in earlier stage embryos (i.e., 1 dpf), expression can be seen in primitive macrophages [20].
12. Cloning with the *mpx* promoter is better achieved using bacterial strains specific for unstable DNA inserts, e.g., Stbl3 (Invitrogen).
13. Not all DNA extraction and purification procedures/kits produce high enough DNA quality for microinjection. Injecting poor quality DNA will result in embryo death. For small amounts of DNA preparation, the Promega Wizard *Plus* SV Minipreps DNA purification system yields good DNA quality in our experience.

14. A small amount of L.M.A. just covering the embryo is enough for securing the position of the embryo on the glass bottom dish. The water tension of a small drop of L.M.A. helps hold the embryo close to the bottom of the dish. A larger volume of L.M.A. may result in an agarose gap between the embryo and the glass bottom, which is not obvious under low-power magnification. As higher magnification and higher NA objectives usually have a shorter working distance, this may make a substantial difference in image quality.
15. Ideally, find neutrophils that are close to the objective lens (i.e., not deep into the embryo) and have a normal morphology, i.e., elongated cell shape and display pseudopod formation. Rounding of neutrophils is a common sign of abnormality due to transgene overexpression. If neutrophils have multiple fluorescent proteins expressed, find neutrophils that have similar fluorescent intensity of both fluorophores.
16. When performing ratio image analysis or imaging more than one fluorescence channel, caution should be taken to check for bleed-through between fluorescence channels. If this happens, separate single band-pass emission filters in an electronic filter wheel should be used instead of a multiband emission. Although the time needed for the filter wheels to switch between filters limits the acquisition speed of multicolor images on a single camera, sequential acquisition of different channels is necessary to produce an accurate co-localization and/or ratio quantitative analysis. It is recommended to acquire the longest wavelength emission probe first to avoid possible bleed-through (also *see* **Note 22**). Careful control of total signal for each channel is also important in limiting the contribution of cross talk. In addition, the intensity of fluorescence emission varies from one channel to another, in order to acquire two channels with comparable exposure time and signal intensity, it is best to adjust laser power without introducing excessive phototoxicity.
17. We usually use ≤30 % laser power with our laser unit for imaging experiments. Too high of a laser intensity will result in unhealthy neutrophils or even cell death (also *see* **Note 7**). Ideally, set the initial maximum signal to 50 % of the dynamic range of the camera bit depth. Fiber optic coupling efficiency and final output power at the objective will vary depending on the microscope setup, so empirical testing or direct power measurements should be done to optimize imaging quality and embryo health.
18. EM gain technology multiplies the charge signal from each pixel on a CCD array to a level above the read noise. Therefore, EMCCD cameras can further improve image acquisition speed by reducing the exposure time needed compared to a CCD camera.

It can also reduce the amount of excitation illumination needed that may cause photobleaching and phototoxicity of the cell and therefore can extend the possible imaging time of the sample. This is important when performing long-term time-lapse acquisition, especially with Z-stack acquisition of each time point. However, the cost of EMCCD cameras is much higher than traditional CCD cameras. If an EMCCD camera is used, adjust EM gain settings, preferably to the camera optimal setting. Increasing EM gain will increase signal intensity but may introduce noise at the same time. In the case where a bright field image is needed, EM gain for bright field acquisition can be reduced to zero to decrease graininess. Alternatively, 2×2 binning on a CCD camera with small pixel sizes (e.g., 6.45 μm in the case of the Photometrics HQ2) will improve its sensitivity but will still lack the signal amplification afforded by an EMCCD.

19. In practice, it is best to synchronize the spinning disk speed and camera exposure time so that the pinholes traverse an integral number of frame crossings during exposure. When the disk speed is not optimal, striped patterns can be observed especially for shorter exposure times (smaller than 50 ms). As it takes time for the spinning disk to change its speed, the disk speed should be set constant throughout the acquisition. For this reason, it is best to set similar exposure times for different channels during multiple channel acquisition.
20. Ideally, as a minimum requirement, a Nyquist theorem satisfying step size is preferred, which is equal to half the Z resolution (depth of field/optical depth). This is determined by the objective used and any additional magnification in the light path, as well as the wavelength of excitation used. As an example, for the microscope setup and objective that we use (LCI Plan-Neofluar 63×/1.3 Imm Corr DIC M27), we usually set the step size as 0.4 μm.
21. In general, 0.5–1 min intervals for a duration of 30 min using a 20× objective is sufficient for imaging neutrophil long distance migration. Allowing the specimen to experience maximal "dark periods" (no laser exposure) during the collection will generally result in less phototoxic effects over longer imaging times. For imaging neutrophil pseudopod dynamics, acquire images for ≥10 min continuously at maximal speed or at minimum with a time interval of 10–30 s using a 60× objective.
22. Caution should be taken in choosing to acquire all channels per Z-slice or whole Z-stack per channel. It is recommended to use all channels per Z-slice, as it will acquire an image of each channel for each Z-plane sequentially, resulting in a more accurate temporal comparison between channels. However, switching between filters for each Z-plane will increase the overhead time.

Acknowledgements

Dr. Benjamin Ng (Carl Zeiss) has provided valuable advice on the SDCM setup. This work was supported by the National Institutes of Health (grant number GM074827) to A. H. and the Hong Kong Croucher Foundation, Joint Universities Summer Teaching Laboratory (JUSTL) program to P-Y.L.

References

1. Meeker ND, Trede NS (2008) Immunology and zebrafish: spawning new models of human disease. Dev Comp Immunol 32:745–757
2. Deng Q, Huttenlocher A (2012) Leukocyte migration from a fish eye's view. J Cell Sci 125:3949–3956
3. Graf R, Rietdorf J, Zimmermann T (2005) Live cell spinning disk microscopy. Adv Biochem Eng Biotechnol 95:57–75
4. Wang E, Babbey CM, Dunn KW (2005) Performance comparison between the high-speed Yokogawa spinning disc confocal system and single-point scanning confocal systems. J Microsc 218:148–159
5. Fischer RS, Wu Y, Kanchanawong P, Shroff H, Waterman CM (2011) Microscopy in 3D: a biologist's toolbox. Trends Cell Biol 21: 682–691
6. Salmon WC, Waters JC (2011) CCD cameras for fluorescence imaging of living cells. Cold Spring Harb Protoc 2011:790–802
7. Murray JM, Appleton PL, Swedlow JR, Waters JC (2007) Evaluating performance in three-dimensional fluorescence microscopy. J Microsc 228:390–405
8. Westerfield M (2000) The zebrafish book: a guide for the laboratory use of zebrafish (*Danio rerio*), 4th edn. University of Oregon Press, Eugene
9. Mathias JR, Perrin BJ, Liu TX, Kanki J, Look AT, Huttenlocher A (2006) Resolution of inflammation by retrograde chemotaxis of neutrophils in transgenic zebrafish. J Leukoc Biol 80:1281–1288
10. Renshaw SA, Loynes CA, Trushell DM, Elworthy S, Ingham PW, Whyte MK (2006) A transgenic zebrafish model of neutrophilic inflammation. Blood 108: 3976–3978
11. Hall C, Flores MV, Storm T, Crosier K, Crosier P (2007) The zebrafish lysozyme C promoter drives myeloid-specific expression in transgenic fish. BMC Dev Biol 7:42
12. Lam PY, Yoo SK, Green JM, Huttenlocher A (2012) The SH2-domain-containing inositol 5-phosphatase (SHIP) limits the motility of neutrophils and their recruitment to wounds in zebrafish. J Cell Sci 125:4973–4978
13. Urasaki A, Morvan G, Kawakami K (2006) Functional dissection of the Tol2 transposable element identified the minimal cis-sequence and a highly repetitive sequence in the subterminal region essential for transposition. Genetics 174: 639–649
14. Rosen JN, Sweeney MF, Mably JD (2009) Microinjection of zebrafish embryos to analyze gene function. J Vis Exp 25:1115
15. Yoo SK, Huttenlocher A (2011) Spatiotemporal photolabeling of neutrophil trafficking during inflammation in live zebrafish. J Leukoc Biol 89:661–667
16. d'Alencon CA, Pena OA, Wittmann C, Gallardo VE, Jones RA, Loosli F, Liebel U, Grabher C, Allende ML (2010) A high-throughput chemically induced inflammation assay in zebrafish. BMC Biol 8:151
17. Tobin DM, Vary JC Jr, Ray JP, Walsh GS, Dunstan SJ, Bang ND, Hagge DA, Khadge S, King MC, Hawn TR, Moens CB, Ramakrishnan L (2010) The lta4h locus modulates susceptibility to mycobacterial infection in zebrafish and humans. Cell 140:717–730
18. Yoo SK, Starnes TW, Deng Q, Huttenlocher A (2011) Lyn is a redox sensor that mediates leukocyte wound attraction in vivo. Nature 480: 109–112
19. Groom D (2002) Cosmic rays and other nonsense in astronomical CCD imagers. Exp Astron 14:45–55
20. Zhang Y, Bai XT, Zhu KY, Jin Y, Deng M, Le HY, Fu YF, Chen Y, Zhu J, Look AT, Kanki J, Chen Z, Chen SJ, Liu TX (2008) In vivo interstitial migration of primitive macrophages mediated by JNK-matrix metalloproteinase 13 signaling in response to acute injury. J Immunol 181:2155–2164

Chapter 15

Detection of Bidirectional Signaling During Integrin Activation and Neutrophil Adhesion

Stuart M. Altman, Neha Dixit, and Scott I. Simon

Abstract

Neutrophil arrest and migration on inflamed endothelium is dependent upon a conformational shift in CD11a/CD18 (LFA-1) from a low to high affinity and clustered state which determines the strength and lifetime of bond formation with intracellular adhesion molecule 1 (ICAM-1). Cytoskeletal adaptor proteins kindlin-3 and talin-1 anchor clustered LFA-1 to the cytoskeleton and support the transition from neutrophil rolling to arrest. We employ microfluidic flow channels and total internal reflection fluorescence microscopy to evaluate the spatiotemporal regulation of LFA-1 affinity and bond formation that facilitate the transition from neutrophil rolling to arrest. Methodology is presented to correlate the relationship between integrin conformation, bond formation with ICAM-1, and cytoskeletal engagement and adhesion strengthening necessary to achieve a migratory phenotype.

Key words Integrin, Selectin, ICAM-1, Intercellular adhesion molecule-1, Leukocyte function associated protein-1 (LFA-1), Macrophage protein-1 (Mac-1), Adhesion strengthening, G-protein coupled receptors, Cytoskeleton

1 Introduction

Leukocyte recruitment to sites of inflammatory insult is a multistep process governed by chemokines, selectins, and integrins that engage in a stepwise manner to initiate intracellular signals and adhesive bond formation [1–3]. Key stages in the neutrophil recruitment cascade include: rolling, capture, arrest, adhesion strengthening, polarization, and transmigration (Fig. 1). Integrins are transmembrane heterodimeric cell adhesion proteins with distinct combinations of α and β subunits. There are 18 α and 8 β subunits and thus together generate 24 heterodimeric forms. In neutrophils, β_2 integrins are most abundant and $\alpha_L\beta_2$ (LFA-1) and $\alpha_M\beta_2$ (Mac-1) are of specific significance in transitioning neutrophils from rolling to arrest to a polarized and transmigrating phenotype. β_2 integrins are key adhesion receptors in this process as they perform both adhesion and signaling functions. In the circulation,

Mark T. Quinn and Frank R. DeLeo (eds.), *Neutrophil Methods and Protocols*, Methods in Molecular Biology, vol. 1124,
DOI 10.1007/978-1-62703-845-4_15,

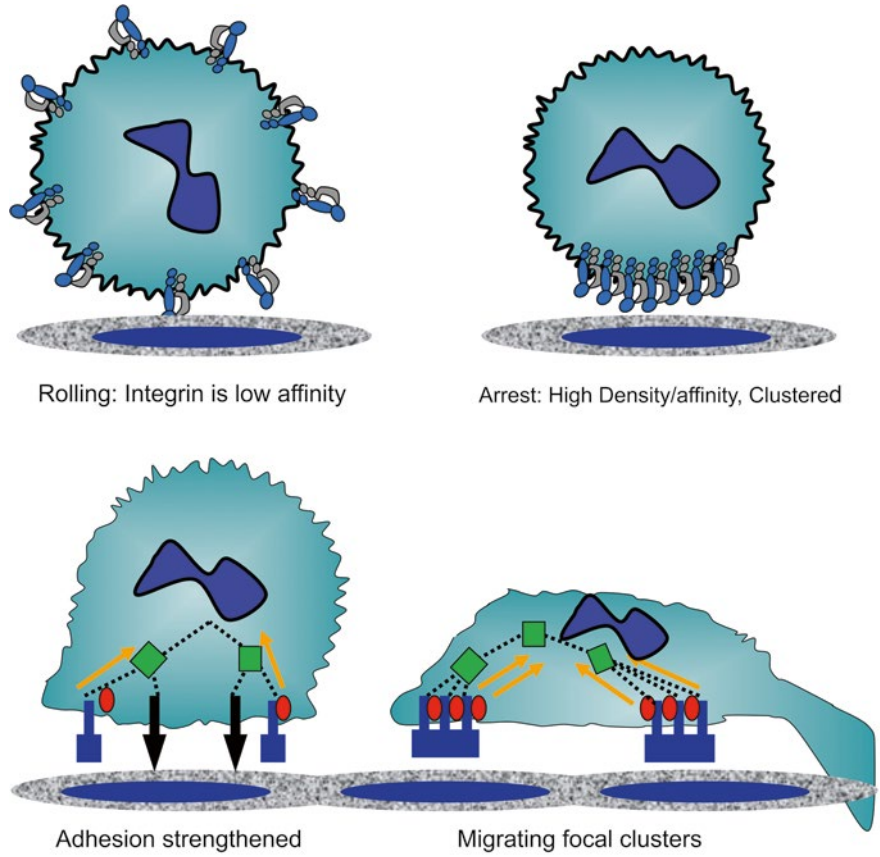

Fig. 1 Illustration of multistep process of neutrophil recruitment. Adhesion strengthening and migrating neutrophil shown with focal adhesions transmitting outside-in signals to adaptor and cytoskeletal proteins

β_2-integrins are expressed on the membrane at low numbers (~100,000 copies) and in a low affinity state that rapidly shift to high affinity and increase in number, and surface density as they make contact with endothelium at sites of inflammation. This chapter will provide tools that facilitate quantitative measurement of the activation state of neutrophils for clinical evaluation to delve the mechanism of recruitment in basic science studies of neutrophil acute response to inflammation.

1.1 Inside-Out and Outside-In Signaling of Integrin Activation

Affinity is regulated via allosteric changes in integrin structure that in turn modulate their potential to adhere to each other and inflamed endothelium. Activation of integrins can be achieved by engagement and rolling on selectins, which facilitates the initial capture of leukocytes on the endothelial surface [2, 3]. Specifically, E-selectin, P-selectin, and L-selectin are critical to leukocyte and lymphocyte capture and rolling through PSGL-1 and other glycosylated ligands. While E- and P-selectin are expressed on the endothelium, L-selectin is expressed only on leukocytes and is involved

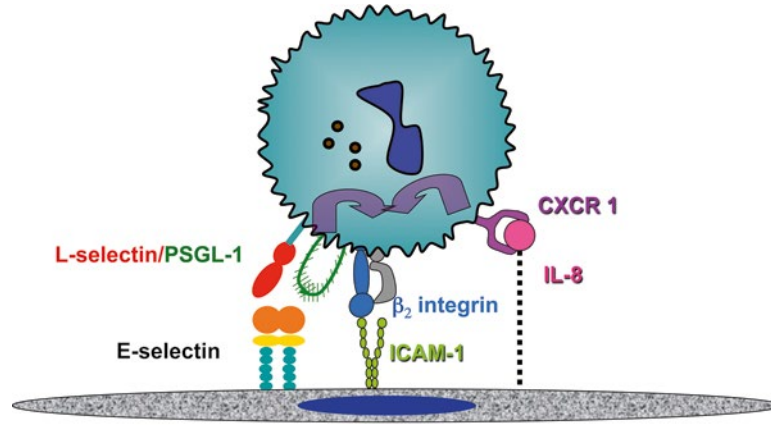

Fig. 2 Neutrophil engaging adhesion receptors and CXC chemokine. E-selectin and ICAM-1 engagement with respective neutrophil adhesion receptors are cooperative with chemokine signaling during rolling to arrest

in secondary capture of neutrophils during recruitment [4, 5]. Selectins form adhesive bonds with their sialylated and fucosylated ligands with high on and off rates and require a threshold level of hydrodynamic shear stress to support rolling and subsequent signaling [6–8]. E-selectin binding to PSGL-1 activates tyrosine kinase Syk and MAPK, which together signal a shift in LFA-1 conformation to an extended and intermediate affinity state [9, 10]. This inside-out signaling of an intermediate affinity state in LFA-1 facilitates deceleration of neutrophil rolling on the endothelium and can trigger firm arrest in the presence of a sufficient density of ICAM-1 [8, 11]. Rolling on E-selectin is synergistic with the so-called inside-out signaling via GPCRs in activation of integrin-dependent arrest (Fig. 2). The mechanism is not completely elucidated but may involve calcium acting as a secondary messenger to amplify conversion of additional integrins to a high affinity state and facilitate their formation into focal clusters [1, 11–13].

Following selectin-dependent capture and rolling, an upshift occurs from a low affinity bent conformation to an extended conformation associated with intermediate affinity that can bind to endothelial ligands and effect deceleration of rolling leukocytes. Chemokines play a key role in inside-out signaling of an upshift in integrin conformation from intermediate to high affinity that is associated with adhesive stabilization, such that the leukocyte becomes resistant to tensile and shear repulsive forces of blood flow. In fact, it is control of the number and density of high affinity integrins and endothelial presentation of their cognate ligands that determines when and where leukocytes are recruited to emigrate during inflammation [11, 14–18]. Neutrophil receptors for chemokine binding such as CXCR1 and CXCR2 are linked to G-protein coupled receptor (GPCR) pathways that activate an upshift in

affinity and focal clustering of Mac-1 and LFA-1 β_2-integrins to initiate firm arrest and subsequent migration [19]. These integrins once activated to a high affinity state can bind ligand and themselves initiate outside-in signals to remodel the cytoskeleton facilitating the next step in the process of pseudopod extension and transendothelial migration [20].

1.2 Detection of Activation State of Integrins on Neutrophils

LFA-1 is the first integrin to be activated during a PMN's transition from rolling to arrest but is rapidly followed by upregulation of Mac-1 surface expression achieved by exocytosis of receptor from cytosolic granules. Both integrin subunits dynamically shift from low to intermediate to high affinity states, the latter of which is required to stabilize adhesion and activate intracellular signaling. These integrins link with the actin cytoskeleton on the inside of the cell and can signal from the outside-in a change in cell shape and motility. Perhaps the most common means of gauging the activation state of a neutrophil is via detection of the number and conformational state of β_2-integrins. Within seconds of stimulation with chemotactic factors at sub-nanomolar concentrations, corresponding to ligation of 10–100 GPCRs, upregulation of Mac-1 can be detected [21]. Thus, use of fluorescence imaging techniques can serve to elucidate the link between the numerical increase in activated integrins and adhesion and migratory function [11].

Shear stress is an omnipresent and necessary component of leukocyte recruitment and this chapter endeavors to describe techniques to image bidirectional signaling of integrins dynamically becoming activated upon ligand binding. The process by which they signal from the outside-in involves mechanotransduction of signals in a process that involves buildup of tensile force at focal sites of integrin adhesion in an arrested neutrophil [22, 23]. Shear forces exerted by flowing blood are known to play a significant role in neutrophil activation as it integrates signals derived from GPCR and selectin-ligand ligation and engagement of intermediate and high-affinity LFA-1/ICAM-1 bonds. Absence of shear causes impairment in neutrophil recruitment and the upshift in affinity of β_2 integrins that are catalyzed by the tensile forces transmitted from shear stresses under flow [3, 24]. Downstream effects of shear-induced adhesion has been demonstrated in leukocytes as evidenced by the absence of effective transendothelial migration of T cells under shear-free conditions even in the presence of appropriate chemokines [25]. However, shear forces have been shown to cooperate with chemokine-induced signals to enhance calcium signaling through bound selectins and integrins during neutrophil rolling and arrest [13]. Hence, there have been reports of shear force in mediating activation of integrins and promoting leukocyte TEM. Current data support the contention that bond force promotes the formation of a strong clustered adhesive complex between LFA-1, Mac-1, and their cognate ligands on inflamed

endothelium. Transduction of directional shear forces is associated with normal mechanotaxis, a process that appears to assist in guidance of neutrophils as they migrate in a directionally biased manner perpendicular to the direction of shear or circumferentially along the blood vessel to nearest sites of transendothelial immigration. The methods that follow can be used to detect integrin number, topography, activation state, association with adaptor molecules that assist in linkage of cytoskeletal molecules, and correlation with neutrophil shape change and migratory behavior.

2 Materials

2.1 Substrate: Derivitization

1. Piranha solution: 95.0–98.0 % H_2SO_4.
2. 30 % H_2O_2 solution.
3. Acetone.
4. 3-aminopropltriethoxysilane.
5. Deionized water (diH_2O).
6. 35-mm diameter glass coverslips.
7. Plastic coverslip rack.
8. 60-mm diameter polystyrene disposable Petri dishes.
9. 70 % ethanol solution.
10. 35-mm aminosilanated coverslips.
11. Recombinant human ICAM-1 (rhICAM-1) (R&D Systems).
12. Recombinant mouse ICAM-1 (rmICAM-1) (R&D Systems).
13. E-selectin-IgG.
14. 240Q antibody.
15. TS1/18 antibody.
16. CD45 antibody.
17. Goat antihuman IgG F(ab′)^2 fragments.
18. Phosphate-buffered saline without cations (PBS$^{-/-}$).
19. 1 % casein solution in PBS.

2.2 Flow Channel Assembly

1. 35-mm diameter glass coverslips with absorbed proteins.
2. Poly(dimethylsiloxane) (PDMS) microfluidic flow chambers and reservoirs.
3. Syringe pump with 1-mL syringe.
4. 20 cm of PE 20 tubing.

2.3 PMN Isolation

1. Whole blood obtained by venipuncture based upon an institutional review board approved human materials protocol.
2. Hemocytometer.

3. 12-mL syringe.
4. 16-G syringe needle.
5. PMN isolation media (Thermo Fisher Scientific).
6. Human serum albumin (HSA).
7. Hanks balanced salt solution (HBSS).
8. 1 M calcium chloride ($CaCl_2$) solution.

2.4 Analysis of the Integrin State

1. Primary antibody conjugated directly to fluorophore: free of sodium azide.
2. Fluorescent microscope with excitation and emission filter wheels, a high-sensitivity camera, and excitation/brightfield shutters.
3. Fluo-5F.
4. 4 % paraformaldehyde (PFA).
5. 0.1 % Triton X-100.
6. Secondary antibodies.
7. Human serum albumin (HSA).
8. L-Ascorbic acid.

2.5 Analysis of Cell Arrest and Adhesion Strengthening

1. HEPES-buffered saline: 10 mM KCl, 110 mM NaCl, 10 mM glucose, 1 mM $MgCl_2$, and 30 mM HEPES, pH 7.4, 290 mOsm.
2. Fura-2 AM.

2.6 Analysis of Cytoskeletal Assembly

1. Talin-1 antibody (Abcam).
2. Kindlin-3 (Abcam).
3. Phalloidin (cell signaling).

3 Methods

3.1 Substrate: Derivatization

Clean coverslips with piranha solution and coat with aminosilane. Then derivatize either ICAM-1-IgG in presence or absence of E-selectin-IgG or antibodies that recognize a common or allosterically defined integrin conformation onto aminosilanated coverslips.

1. Fill two 600-mL glass beakers with approximately 450 mL of diH_2O each, and fill a 2-L glass beaker with approximately 1,500 mL of diH_2O.
2. Using tweezers, completely load plastic coverslip racks with clean 35-mm glass coverslips. Transfer assembled supplies to a fume hood.
3. Under a fume hood, add 300 mL of 95.0–98.0 % H_2SO_4 solution to a 600-mL beaker.

4. Add 150 mL of 30 % H_2O_2 solution to achieve a 2:1 ratio of H_2SO_4 to H_2O_2, and let the solution stand for 5 min.
5. Carefully place coverslip racks into the piranha solution and let sit in solution for 15 min.
6. In two glass 100-mL beakers, add ~90 mL of acetone. Also add 100 mL of acetone to a 100-mL Nalgene beaker.
7. Aliquot 2 mL of 3-aminopropyltriethoxysilane into the Nalgene beaker containing acetone to achieve an aminosilane solution at a ratio of 1:50 aminosilane to acetone.
8. After the 15 min, transfer the coverslip racks from the piranha solution into one of the 600-mL beakers of water. Let them sit for at least 1 min.
9. Arrange your workspace: from left to right, place one of the 100-mL beakers with ~90 mL (sufficient volume to submerge) acetone, then the 250-mL Nalgene beaker with the aminosilane solution, and lastly the other 100-mL glass beaker containing acetone.
10. Carefully remove one coverslip rack from the water, submerge in acetone for 10 s, submerge in aminosilane solution for 5 min, submerge in the last acetone beaker for 10 s, and place into an unused 600-mL beaker of diH_2O.
11. Repeat **step 10** for the second rack.
12. Take the beaker of water with the racks in it over to the workstation. Remove racks. Blow-dry with air. Make sure to remove all water.
13. Once the coverslips are completely dry, place individual slips into 60 mm Petri dishes.
14. Absorb either recombinant ICAM-1, E-selectin, or antibodies 240Q (stabilizes CD18 at high affinity), TS1/18 (stabilizes LFA-1 at low affinity), or CD45 (control non-integrin), at 5 μg/mL to coverslips cleaned with piranha solution [26] and coated with aminosilane.
15. In a 1.5-mL Eppendorf tube, make a 250 μL solution of $PBS^{-/-}$, goat antihuman IgG $F(ab')^2$ fragments, and ICAM-1 or antibody. Adjust the volumes of goat antihuman IgG $F(ab')^2$ fragments and ICAM-1 or antibody added to achieve concentrations of 5 μg/mL, respectively.
16. Dispense 200 μL of the prepared solution onto an aminosilanated coverslip in a 60-mm Petri dish, and place coverslip at 4 °C for 1 h.
17. Use a pipette to wash the coverslip with 2 mL of $PBS^{-/-}$, aspirate, and repeat once.
18. Block nonspecific binding with casein by carefully suctioning proteins from the top of the coverslip (*see* **Note 1**) and then

adding 200 μL of casein to the coverslip. Incubate at room temperature for 30 min.

19. Suction off casein, wash with 2 mL of $PBS^{-/-}$, suction off PBS, and repeat once. Add 2 mL of PBS to the coverslip and use for experiment.

3.2 Flow Channel Assembly

1. For a removable vacuum-sealed channel, soak all PDMS devices in separate Petri dishes containing sufficient deionized water to completely submerge chambers.
2. Position a chamber with the channel-engraved surface facing down, and use needle nose tweezers to position the chamber against the wall of the dish. Keep the chamber under the level of the deionized water, but such that it is not in contact with the bottom of the dish.
3. Use a 200-μL pipette to remove any air bubbles trapped within the channels. Position the pipette tip at the entrance to one of the channels on the top surface of the chamber and draw in with the pipette. Withdraw the pipette, expend the contents into the dish, and repeat for each channel.
4. Connect the PDMS device to its vacuum leads, and invert it such that several drops of deionized water can be dispensed onto the channel-engraved surface (*see* **Note 2**).
5. Use needle nose tweezers to place a protein-absorbed coverslip on top of the wetted PDMS and initialize the vacuum using a stopcock.
6. Use a stage heater to maintain experimental conditions at 37 °C. A heated and humidified enclosure provides optimal experimental conditions. For oil objectives, begin heating at least 1 h in advance of the experiment in order to allow optics to equilibrate at the experimental temperature.
7. To prevent desiccation of channels, place drops of deionized water on top of all channel access holes. Use blunt tweezers to hold down the PDMS and press fit fluid-filled reservoir and pump fluidic tubes into prepunched holes in the PDMS device.
8. Draw fluid through the microchannels into the pump tubing using the syringe pump. Set the volumetric flow rate of the syringe pump based on the desired fluid shear stress and Eq. 1.

$$\tau_w = 6\mu Q / wh^2. \quad (1)$$

where τ_w is shear stress, μ is fluid viscosity, Q is volumetric flow rate, w is channel width, and h is channel height (Fig. 3).

3.3 PMN Isolation

1. Dispense 4 mL of isolation media into a 15-mL conical polypropylene tube using a serological pipette, taking care to minimize the amount of media that gets on the side of the tube.

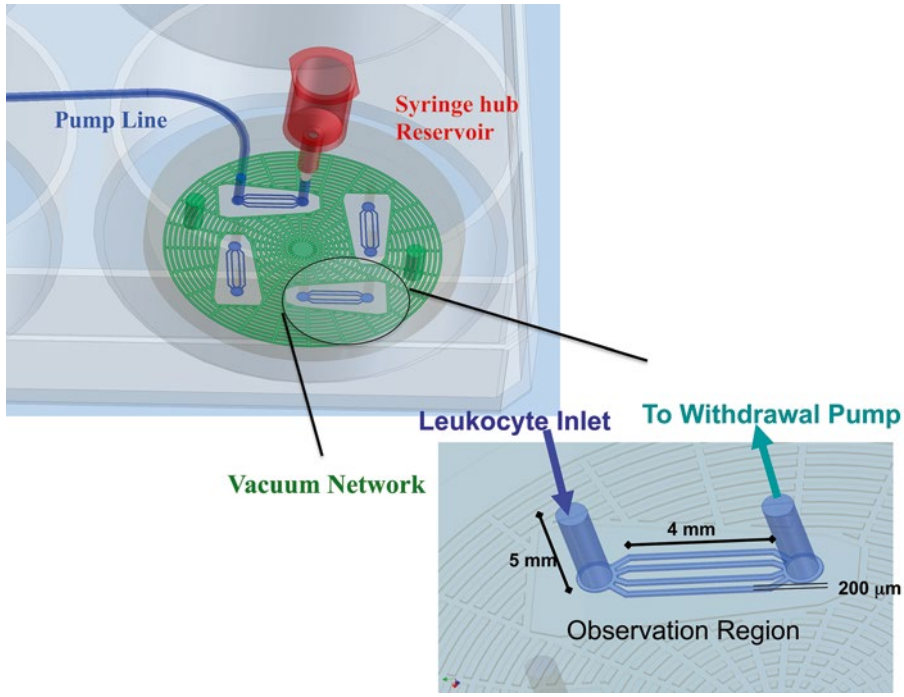

Fig. 3 Vascular mimetic microfluidic flow channels. A schematic of a 25 mm PDMS microfluidic disc assembled on a well of a 6-well plate. The pump line is connected to a syringe pump for variable control of the negative pressure flow rate at the exit of one of four flow channels used for each of four experiments. Two holes conduct a vacuum line to the spider webbed set of channels to anneal the flow channel to the substrate with negative static pressure. The hub of a syringe pump is affixed to a port connecting the inlet to the channel that serves as the reservoir for the neutrophil suspension. Dimension of an individual four-channel flow chamber provides a 100 μm height × 200 μm width rectangular flow area

2. Layer 4 mL of whole blood over separation media to achieve a 1:1 ratio of blood to isolation media.
3. Repeat **steps 1** and **2** to prepare a second tube for a 10 mL whole blood sample.
4. Centrifuge the tubes for 30 min at 760 × *g*.
5. In a 50 mL conical polypropylene tube, add 120 μL of HSA to 30 mL of HBSS. In a 15 mL conical polypropylene tube, add 40 μL of HSA to 10 mL of HBSS that will serve as the buffer to resuspend the PMN and use in the experiment later.
6. Use a 12-mL syringe with 16-G needle that has approximately 2 mL of HBSS/0.1%HSA drawn in from the 50-mL tube to extract the appropriate density layer from the centrifuged samples. Try to minimize collection of other blood constituents such as lymphocytes and platelets.
7. Wash the extracted cells by dispensing the syringe into the 50-mL HBSS/0.1 % HSA tube and centrifuging for 8 min at 190 × *g* (*see* **Note 3**).

Table 1
Summary of antibodies that can be used for the analysis of integrin activation state

Clone/subunit	Activation state	Activating/ blocking/detection	Commercial source or reference
IB4/CD18	Common epitope	Detection	Santa Cruz Biotechnology
327C/CD18	Detects extended conformation epitope	Detection	Eli Lilly Corp
240Q/CD18	Induces extended conformation epitope	Activating	Eli Lilly Corp
TS2/4/CD11a	Common epitope	Detection	BioLegend
Mab24/CD18	Extended conformation epitope	Detection	Hycult Biotech
Kim127/CD18	Common epitope	Detection	ATCC
TS1/18/CD11a	Stabilizes bent or low affinity conformation	Blocking	BioLegend

Antibodies for detecting and inducing defined activation states of β_2 integrins

8. Dispense the supernatant and resuspend isolated PMN in 500 μL of HBSS/0.1 % HSA from the 15-mL tube.
9. Use a hemocytometer to count cells, and suspend to a concentration of 2×10^6 cells/mL.
10. Add 1.5 mM $CaCl_2$ to the cell suspension just prior to the experiment. The cells remain viable and unactivated up to 4–6 h after isolation.

3.4 Analysis of the Integrin State

1. For real-time total internal reflection fluorescence (TIRF) calcium measurements, label cells with 1 μM fluo-5 F for 30 min at 37 °C.
2. Fix PMN that were perfused over protein-absorbed glass coverslips in a microfluidic flow chamber with 4 % PFA.
3. Permeabilize the cells with 0.1 % Triton X-100 and label with primary (*see* Table 1) and secondary antibodies to specific proteins.
4. Excite arrested PMNs with a 488-nm laser using TIRF microscopy at 1 frame/s to observe changes in intracellular calcium in a focal section of the PMNs approximately 100 nm from the surface of the coverslip [27].
5. The topography of LFA-1, Mac-1, and high affinity CD18 can be imaged in real time during neutrophil rolling and arrest in shear flow with epifluorescence (within plane of focus) or total internal reflection fluorescence microscopy (within 100 nm of substrate).

6. Dilute neutrophils to a concentration of 1×10^6 cells/mL in HSA and 20 μg/mL of the appropriate labeling control antibody. Preincubate neutrophils with nonblocking fluorescent monoclonal antibodies and allosteric inhibitors at 37 °C for 10 min.
7. Centrifuge the labeled neutrophils, and resuspend the pellet to a concentration of 1×10^6 cells/mL in HEPES-buffered saline containing 0.5 mM ascorbic acid, 1.5 mM Ca^{2+}, and 1 mg/mL of HSA.
8. Use these washed, labeled neutrophils as the sample for a microfluidic flow chamber by adding them to the inlet reservoir. Draw the sample into the flow chamber at the desired shear rate.
9. Optimize camera settings for the labeling conditions by taking single images of the fist neutrophils that adhere to the substrate. When imaging moving cells, it is important to use the minimum exposure time necessary to obtain a clear image.
10. Once a number of neutrophils adhere to the underlying substrate, acquire images of immunofluorescence microscopy coupled with phase-contrast microscopy at one frame/s using a 60× objective. Use an automated brightfield source shutter and an optical excitation filter wheel with filters appropriate for fluorescent labels (i.e., Alexa-488, Alexa-546, and PE labels) [11] (*see* **Note 4**).
11. The distribution of the labeled neutrophil surface epitopes may be processed and analyzed using Image-Pro (Media Cybernetics), MetaMorph (Molecular Devices), or National Institutes of Health (NIH) image analysis software. Defining clusters of epitopes as regions with signal intensity three standard deviations above the background intensity, one may quantify the number, size, and location of high-density adhesion molecules (i.e., β_2 integrins) on the neutrophil surface.

3.5 Analysis of Cell Arrest and Adhesion Strengthening

1. Suspend PMN at a concentration of 2×10^6/mL in HEPES-buffered salt solution.
2. Label PMN with Fura-2 AM for 30 min at 37 °C.
3. Wash and resuspend cells in HEPES-buffered salt solution.
4. Perfuse labeled cells into microfluidic flow chamber at desired shear stress (4 dyn/cm^2 is the venular magnitude of shear stress).
5. Sequentially image cells over time with alternating excitation by 340 and 380 nm light generated by a mercury lamp attached to a filter wheel with 0.1 s switch time.
6. Images can be acquired with an Orca-ER camera (Hamamatsu Corp) coupled to a Nikon 1200 microscope running Simple PCI 5.3 software.

7. Analyze image sequences for the ratio between emission at 340 and 380 nm using custom macros written for Image-Pro Plus 5.1.
8. Identify the average intensity of each cell in a confined area of interest around each cell for both the 340 and 380 nm exposures. This method of cell identification and local overlap accounts for any motion of rolling PMN during image acquisition.

3.5.1 Adhesion Strengthening Experiments

1. Differentiate control, talin, and kindlin-3 shRNA transfected HL-60 cells to a neutrophil phenotype over 3 days with 1.3 % DMSO and human isolated PMN.
2. Treat cells with Mac-1 blocking antibody present in excess in the media (ICRF44 for human and M1/70 for mouse) to ensure LFA-1 dependent adhesion.
3. To study the role of Ca^{2+} flux in adhesion strengthening, treat PMN with Fura-2 to detect intracellular Ca^{2+}.
4. Block Ca^{2+} signal by chelation with 50 μM BAPTA or block CRAC channels with 100 μM 2-APB.
5. Perfuse cells and allow to settle over an ICAM-1 + 240Q substrate derivatized on the substrate at 1:1 ratio (5 μg/mL each) to activate and stabilize high affinity LFA-1 at adhesive contact sites.
6. Ramp shear up at 30 s intervals from 0, 4, 10, 20, and 40 dyn/cm^2.
7. Measure the number of cells that remain adhered over separate fields of view at each shear level.

4 Notes

1. For vacuuming excess solution from coverslips, an aspiration setup with primary containment will be sufficient. A sterile filter can be placed on the end of the plastic tubing that attaches to the laboratory vacuum spigot to prevent particulates from being aspirated. When vacuuming proteins off of the coverslips, be careful not to contact the surface of the coverslip with the tip of the aspirating pipette. It helps to tilt the Petri dish and displace the protein solution to one side of the slip and aspirate from there. Be careful not to fully dry the coverslip during aspiration.
2. It is not necessary to completely cover the bottom of the PDMS chamber with water. Simply dispense a few drops such that the channel entrances are covered and place the coverslip on top in the correct orientation. Dispensing too much water on the bottom of the chamber can result in improper coverslip alignment and difficulty attaining proper suction.

3. Throughout the entire neutrophil isolation process and especially during this part of the procedure when transferring the isolated PMN to the 50 mL Falcon tube, be careful to minimize the chances of physically activating the cells. For example, dispense the PMN from the syringe at a slow but steady pace to prevent inadvertent activation as a result of imparted high shear stress.
4. When a microscopic field becomes unsuitable for further imaging as a result of photobleaching, move the stage to another region of the flow chamber and resume imaging.

Acknowledgements

This work was supported by National Institutes of Health (NIH) grant AI472294 to S.I.S.

References

1. Campbell JJ, Hedrick J, Zlotnik A et al (1998) Chemokines and the arrest of lymphocytes rolling under flow conditions. Science 279: 381–384
2. Ley K (2002) Integration of inflammatory signals by rolling neutrophils. Immunol Rev 186: 8–18
3. Simon SI, Green CE (2005) Molecular mechanics and dynamics of leukocyte recruitment during inflammation. Annu Rev Biomed Eng 7:151–185
4. Dwir O, Kansas GS, Alon R (2001) Cytoplasmic anchorage of L-selectin controls leukocyte capture and rolling by increasing the mechanical stability of the selectin tether. J Cell Biol 155: 145–156
5. Taylor AD, Neelamegham S, Hellums JD et al (1996) Molecular dynamics of the transition from L-selectin- to beta 2-integrin-dependent neutrophil adhesion under defined hydrodynamic shear. Biophys J 71:3488–3500
6. Thomas WE, Trintchina E, Forero M et al (2002) Bacterial adhesion to target cells enhanced by shear force. Cell 109:913–923
7. Zhu C, McEver RP (2005) Catch bonds: physical models and biological functions. Mol Cell Biomech 2:91–104
8. McDonough DB, McIntosh FA, Spanos C et al (2004) Cooperativity between selectins and beta2-integrins define neutrophil capture and stable adhesion in shear flow. Ann Biomed Eng 32:1179–1192
9. Zarbock A, Lowell CA, Ley K (2007) Spleen tyrosine kinase Syk is necessary for E-selectin-induced alpha(L)beta(2) integrin-mediated rolling on intercellular adhesion molecule-1. Immunity 26:773–783
10. Simon SI, Hu Y, Vestweber D et al (2000) Neutrophil tethering on E-selectin activates beta 2 integrin binding to ICAM-1 through a mitogen-activated protein kinase signal transduction pathway. J Immunol 164:4348–4358
11. Green CE, Schaff UY, Sarantos MR et al (2006) Dynamic shifts in LFA-1 affinity regulate neutrophil rolling, arrest, and transmigration on inflamed endothelium. Blood 107: 2101–2111
12. Alon R, Feigelson S (2002) From rolling to arrest on blood vessels: leukocyte tap dancing on endothelial integrin ligands and chemokines at sub-second contacts. Semin Immunol 14: 93–104
13. Schaff UY, Yamayoshi I, Tse T et al (2008) Calcium flux in neutrophils synchronizes beta2 integrin adhesive and signaling events that guide inflammatory recruitment. Ann Biomed Eng 36:632–646
14. Beals CR, Edwards AC, Gottschalk RJ et al (2001) CD18 activation epitopes induced by leukocyte activation. J Immunol 167: 6113–6122
15. Constantin G, Majeed M, Giagulli C et al (2000) Chemokines trigger immediate beta2 integrin affinity and mobility changes: differential regulation and roles in lymphocyte arrest under flow. Immunity 13:759–769
16. Kim M, Carman CV, Yang W et al (2004) The primacy of affinity over clustering in regulation of adhesiveness of the integrin $\alpha_L\beta_2$. J Cell Biol 167:1241–1253

17. Sarantos MR, Raychaudhuri S, Lum AF et al (2005) Leukocyte function-associated antigen 1-mediated adhesion stability is dynamically regulated through affinity and valency during bond formation with intercellular adhesion molecule-1. J Biol Chem 280:28290–28298
18. Bachmann MF, Kopf M, Marsland BJ (2006) Chemokines: more than just road signs. Nat Rev Immunol 6:159–164
19. Zarbock A, Deem TL, Burcin TL et al (2007) Galphai2 is required for chemokine-induced neutrophil arrest. Blood 110:3773–3779
20. Alon R, Ley K (2008) Cells on the run: shear-regulated integrin activation in leukocyte rolling and arrest on endothelial cells. Curr Opin Cell Biol 20:525–532
21. Lum AF, Green CE, Lee GR et al (2002) Dynamic regulation of LFA-1 activation and neutrophil arrest on intercellular adhesion molecule 1 (ICAM-1) in shear flow. J Biol Chem 277:20660–20670
22. Dixit N, Simon SI (2012) Chemokines, selectins and intracellular calcium flux: temporal and spatial cues for leukocyte arrest. Front Immunol 3:188
23. Dixit N, Yamayoshi I, Nazarian A et al (2011) Migrational guidance of neutrophils is mechanotransduced via high-affinity LFA-1 and calcium flux. J Immunol 187:472–481
24. Alon R, Dustin ML (2007) Force as a facilitator of integrin conformational changes during leukocyte arrest on blood vessels and antigen-presenting cells. Immunity 26:17–27
25. Schreiber TH, Shinder V, Cain DW et al (2007) Shear flow-dependent integration of apical and subendothelial chemokines in T-cell transmigration: implications for locomotion and the multistep paradigm. Blood 109: 1381–1386
26. Mitchon LN, White JM (2006) Growth and analysis of octadecylsiloxane monolayers on Al2O3 (0001). Langmuir 22:6549–6554
27. Schaff UY, Dixit N, Procyk E et al (2009) Orai1 regulates intracellular calcium, arrest, and shape polarization during neutrophil recruitment in shear flow. Blood 115:657–666

Part V

Neutrophil Phagocytosis and Bactericidal Activity

Chapter 16

Immunofluorescence and Confocal Microscopy of Neutrophils

Lee-Ann H. Allen

Abstract

Rapid recruitment of neutrophils to sites of infection and their ability to phagocytose and kill microbes is an important aspect of the innate immune response. Challenges associated with imaging of these cells include their short lifespan and small size and the fact that unstimulated cells are nonadherent. In addition, although cytoplasmic granules are plentiful, the abundance of many other organelles is diminished. Here we reprise methods for analysis of resting and activated cells using immunofluorescence and confocal microscopy, including kinetic analysis of phagosome maturation and degranulation, and detection of intraphagosomal superoxide accumulation. We describe approaches for rapid cell fixation and permeabilization that maximize antigen detection and discuss other variables that also affect data interpretation and image quality (such as cell spreading, degranulation, and phagocytosis). Finally, we show that these methods are also applicable to studies of neutrophil interactions with the extracellular matrix.

Key words Neutrophil, Immunofluorescence, Confocal microscopy, Phagosome, Granule, Talin, Myeloperoxidase, Fibrinogen, Bacteria, Zymosan

1 Introduction

Distinctive characteristics of neutrophils (polymorphonuclear leukocytes, PMNs) are their small size, lobed nucleus, and abundant cytoplasmic granules. Fundamental initial insight into the composition of gelatinase and specific and azurophilic granules and the subcellular localization of NADPH oxidase subunits in resting, primed, and activated cells was obtained using subcellular fractionation [1, 2]. However, the application of fluorescence microscopy approaches to studies of neutrophils has lagged behind other cell types. In part for this reason, much less is known about fundamental processes such as phagosome maturation in PMNs as compared with macrophages [3].

Summarized here are methods we developed originally for analysis of macrophages [4, 5] and then optimized for immunofluorescence

Mark T. Quinn and Frank R. DeLeo (eds.), *Neutrophil Methods and Protocols*, Methods in Molecular Biology, vol. 1124,
DOI 10.1007/978-1-62703-845-4_16,

and confocal analysis of human neutrophils [6–12]. Our approaches address general issues such as methods of cell fixation and permeabilization that are also relevant to studies of other cell types. In addition, we address factors particular to neutrophils such as cell size, adhesion, spreading, degranulation, and phagocytosis in the context of image analysis using immunofluorescence and confocal microscopy.

2 Materials

2.1 Cell Culture

1. Neutrophils: isolate from the peripheral blood of healthy donors using dextran sedimentation and density gradient separation on Ficoll-Hypaque [13]. Cell purity should be >95 % PMNs.
2. Fresh human serum: to coat coverslips and also as a source of active complement factors that can be used for particle opsonization. Transfer a sample of non-heparinized venous blood (10 ml) to a sterile glass tube and incubate for 1 h at room temperature followed by 1 h on ice. Detach the clot from the tube wall using a sterile pipette tip and centrifuge at 1,500 × *g* for 15 min at 4 °C. Transfer the serum layer to a sterile polypropylene tube and keep on ice to preserve bioactivity. Fresh serum should be used within 2 h or stored in single-use aliquots at −80 °C for future use. Either autologous serum or serum pooled from several donors is suitable for this purpose.
3. Heat-inactivated fetal bovine serum (HI-FBS): incubate serum at 56 °C for 30 min with occasional swirling. Filter (0.45 μm) to remove any particulates and store at −20 °C.
4. Endotoxin-free, HEPES-buffered RPMI-1640 medium containing L-glutamine. Store at 4 °C. Supplement with HI-FBS or human serum to 10 % final concentration.
5. 10 mM HEPES solution, pH 7.2.
6. 10 mM glucose solution.
7. Endotoxin-free Hank's buffered salt solution containing calcium and magnesium (HBSS), supplemented with 10 mM HEPES and 10 mM glucose. Sterile filter (0.2 μm) and store at room temperature.
8. 35 mm tissue culture dishes.
9. Sterile 15 and 50 ml conical polypropylene tubes.
10. Rectangular, flat-bottom aluminum pans (approximately 7 × 11 in.).
11. Refrigerated tissue culture centrifuge with swinging bucket rotor and microplate carriers such as the Allegra 6KR (Beckman Coulter).

2.2 Particulate and Soluble Stimuli

1. Zymosan (yeast cell wall particles, Sigma-Aldrich, St. Louis, MO): rehydrate 200 mg zymosan in 20 ml sterile PBS in a 50 ml sterile conical polypropylene tube. Vortex briefly and then place in a water bath sonicator for 5 min. Transfer zymosan to a boiling water bath for 10 min, collect particles by centrifugation (400 × *g* for 10 min), decant PBS, and repeat the sonication and boiling steps twice using fresh changes of PBS. Resuspend the final zymosan pellet in 10 ml tissue culture medium (without serum) or sterile HBSS, and store in 250 µl (5 mg) aliquots at –20 °C. Prepare a working stock solution by diluting one aliquot of zymosan with three volumes of buffer or tissue culture medium (5 mg/ml final concentration). Before each use, briefly sonicate the thawed working stock to disperse any aggregates (*see* **Note 1**).
2. Complement-opsonized zymosan (COZ) particles are obtained by incubating an aliquot of the zymosan working stock with fresh human serum (50 % final concentration) at 37 °C for 30 min. Pellet COZ using a microfuge (2 min, 16,000 × *g*) and then wash twice with PBS or serum-free tissue culture medium. Keep COZ on ice and use within 2 h. IgG-opsonized zymosan (IgG-Z) particles are prepared using Molecular Probes/Invitrogen/Life Technologies (Grand Island, NY) zymosan opsonizing reagent. Store IgG-Z in small aliquots at –20 °C. Dynabeads precoated with IgG are available from life technologies. Bacteria can also be opsonized with complement factors, antibodies, or immune serum (*see* **Note 1**).
3. Phorbol myristate acetate (PMA) is dissolved in endotoxin-free, tissue culture grade DMSO (Sigma-Aldrich) at a final concentration of 5 mM. Store at –80 °C in small aliquots. Because PMA is rapidly inactivated in aqueous solution, thaw stocks at room temperature and use immediately after dilution into buffer or medium.
4. f-Met-Leu-Phe (fMLF) and TNFα are dissolved in tissue culture grade, endotoxin-free DMSO at a final concentration of 4 mM and 10 µM, respectively, and stored in aliquots at –80 °C.

2.3 Microscopy Supplies

1. Round glass coverslips (12 mm diameter).
2. Unlabeled fibrinogen (Sigma-Aldrich): 0.1 mg/ml stock solution in sterile HBSS, store at –20 °C.
3. Oregon Green-labeled fibrinogen (Molecular Probes/Invitrogen/Life Technologies): 0.1 mg/ml stock solution in sterile HBSS, store at –20 °C.
4. Straight needle-point stainless steel forceps.
5. Glass Petri dishes (60 mm), store at –20 °C.
6. Disposable microbeakers (10 ml capacity).

7. Pre-cleaned microscopy slides with frosted marking area.
8. Lids from 24-well tissue culture cluster plates. These do not need to be sterile and can be lids saved after use in other experiments.
9. Plastic flat-bottom plastic boxes with lids (Tupperware type), large enough to accommodate one–three lids from 24-well tissue culture dishes.
10. Cardboard slide folders.

2.4 Buffers and Other Reagents

1. Nitric acid.
2. 95 % ethanol.
3. 70 % ethanol: dilute 95 % ethanol using tissue culture grade sterile deionized water.
4. 10 % neutral buffered formalin solution (*see* **Note 2**).
5. Acetone: store at room temperature and chilled rapidly to −20 °C prior to use (*see* **Note 3**).
6. Phosphate-buffered saline (PBS): 137 mM NaCl, 2.68 mM KCl, 8.1 mM Na_2HPO4, and 1.47 mM KH_2PO4 (pH 7.4).
7. Blocking buffer: PBS supplemented with 5 mg/ml bovine serum albumin (BSA), 0.5 mg/ml NaN_3, and 10 % horse serum (*see* **Note 4**). Sterile (0.2 μm) filter and store at 4 °C.
8. Washing buffer (PBS-azide-BSA, "PAB"): blocking buffer without horse serum, store at 4 °C.
9. Antibodies directed against specific marker proteins of neutrophils obtained from commercial sources or prepared in your own laboratory (*see* **Note 5**).
10. DyLight 488 and rhodamine-conjugated $F(ab')_2$ secondary antibodies (Jackson ImmunoResearch Laboratories, West Grove, PA): rehydrate with sterile deionized water according to the manufacturer's directions and store at 4 °C. Secondary antibodies conjugated to other fluors can also be used (*see* **Note 6**).
11. Gelvatol mounting medium (*see* **Note 7**): mix 2.4 g polyvinyl alcohol with 6 g glycerol, 6 ml deionized water, and 12 ml 200 mM Tris–HCl (pH 8.0) in a beaker on a stir plate for several hours until dissolved. Heat the solution to 50 °C for 10 min and then clarify by centrifugation at $5{,}000 \times g$ for 15 min. Decant the supernatant into a new 50 ml polypropylene tube and add 625 mg 1,4-diazobicyclo-[2.2.2]-octane (DABCO). Invert the tube to dissolve DABCO. Store in 1 ml aliquots in Eppendorf tubes in a frost-free freezer at −20 or −80 °C. DABCO reduces photobleaching of fluorescence.

3 Methods

3.1 Preparation of Acid-Washed Coverslips

Acid washing is essential since it removes manufacturing residue, oils, and other contaminants such as LPS that may inadvertently activate PMNs, impair cell adhesion, and/or cause high nonspecific background fluorescence after antibody staining.

1. Transfer one package of 12 mm round glass coverslips into a small glass bottle.
2. Inside a fume hood, pour nitric acid over the coverslips making sure they are all submerged.
3. Cap the bottle and swirl gently to ensure all coverslips are in contact with the acid.
4. Incubate in the fume hood for at least 48 h.
5. Carefully decant the acid and then rinse the coverslips with 15–20 changes of sterile deionized tissue culture grade water (pour water over the coverslips, cap bottle, rotate gently to rinse coverslips, decant water, and repeat).
6. Rinse the coverslips with two changes of 95 % ethanol to remove residual water.
7. Store coverslips in 70 % ethanol at room temperature. Use after ≥16 h in ethanol.

3.2 Preparation of Coated Coverslips

Bloodstream neutrophils are nonadherent, whereas PMNs at a site of infection have attached to, and migrated along, the extracellular matrix. Freshly isolated peripheral blood PMNs will associate with glass coverslips precoated with serum proteins or purified fibrinogen (*see* **Note 8**). Adherent PMN are preferred since these cells are more similar to neutrophils at sites of infection and because it is easier to synchronize phagocytosis of adherent cells than cells in suspension.

3.2.1 Flaming of Coverslips and Dispersal in 35 mm Dishes

1. Set up 35 mm tissue culture dishes in a rectangular metal pan. Each dish will hold three coverslips which provide triplicate samples for each experimental condition or time point.
2. Use forceps to remove a few coverslips from their ethanol storage bottle and place on a pile of Kimwipes.
3. Fill one small microbeaker with 70 % ethanol and light a Bunsen burner.
4. Working with one coverslip at a time, grasp with forceps, dunk into ethanol, and drain off excess ethanol by touching edge of the coverslip to the pile of Kimwipes.
5. Pass the coverslip through the flame and then place it into a 35 mm dish. Because the 35 mm dishes are opened only briefly, this procedure can be performed on the bench top. Failure to remove excess ethanol will cause coverslips to shatter when passed through the flame.

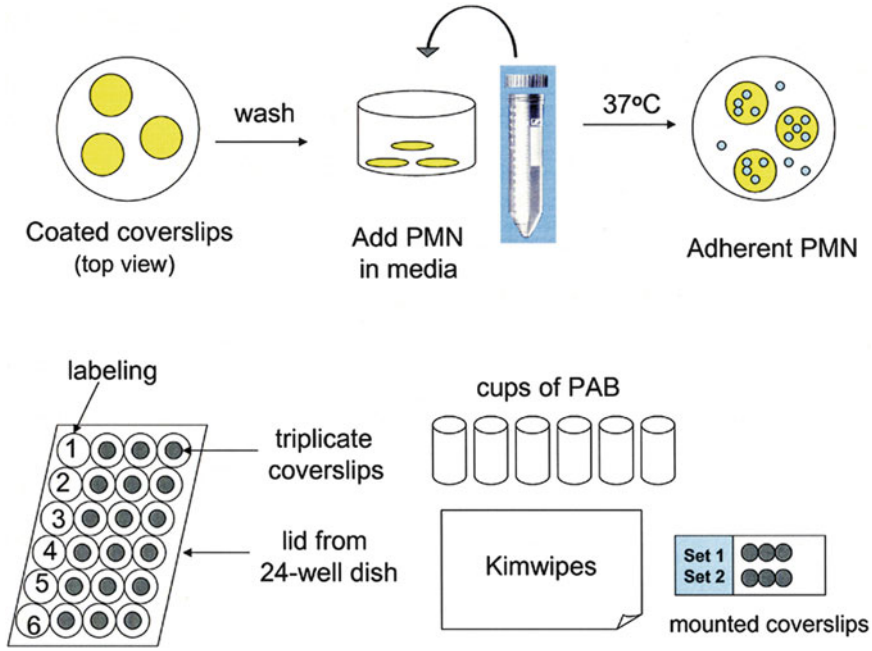

Fig. 1 Cell plating and staining schematic. The process of coverslip coating and neutrophil plating is shown (*top row*) as well as the process of cell staining and washing and coverslip mounting (*bottom row*). Reprinted from [12] with permission from Humana press

3.2.2 Coating Coverslips with Serum or Fibrinogen

6. Transfer 35 mm dishes containing coverslips into a tissue culture hood.
7. Open all dishes and, using a sterile probe (such as a P200 Pipetman tip), position the coverslips in each dish such that they are not touching the side of the dish or touching one another (Fig. 1).
8. Pipette 50 µl of 0.1 mg/ml fibrinogen or 50 µl fresh serum directly onto each coverslip. The coating agent will spread evenly over the acid-washed glass, and surface tension holds the domes of liquid in place.
9. Close all dishes, transfer back into the metal pan, and place inside a 37 °C tissue culture incubator for 30–60 min.
10. Rinse coverslips by flooding each dish with about 3 ml of sterile HBSS or PBS. Note that failure to remove excess fibrinogen may cause coverslips to become glued to the tissue culture dish if they air dry.

3.3 Plating Neutrophils on Coated Coverslips

1. Dilute PMNs to 1×10^6 cells per ml in tissue culture medium in a conical tube.
2. Invert the tube gently to mix cells, do not vortex.

3. Place 1 ml of this suspension in each 35 mm dish containing coated coverslips. Be sure that the coverslips are not overlapping one another.
4. Push any floating coverslips to the bottom of the dish using a sterile pipette tip.
5. Place dishes in a 37 °C incubator for 1 h. Neutrophils will adhere to the coated coverslips in preference to the uncoated tissue culture dish (Fig. 1). For microscopy, a moderate cell density is optimal.

3.4 Stimulation of Adherent PMNs

Because PMNs are only loosely adherent, it is important to add stimuli to dishes carefully so as not to detach the cells. For this same reason, cells are not fluid changed before addition of stimuli. Rather, particles or soluble stimuli are added to adherent neutrophils in a volume of 1 ml to achieve a total volume of 2 ml per 35 mm dish. Most stimuli will enhance PMN adhesion and spreading via their ability to trigger upregulation of surface β2 integrins (*see* **Notes 8** and **9**).

3.4.1 Soluble Stimuli

1. Human PMNs are optimally activated by exposure to 200 nM PMA or 1–10 μM fMLF and can be primed or activated by TNFα depending on the concentration used.
2. Dilute each agonist in tissue culture medium to achieve to twice the desired final concentration.
3. Vortex to mix.
4. Add 1 ml of the desired stimulus to each dish.
5. Transfer to 37 °C incubator for the desired amount of time (generally 0.5–5 min for fMLF and 5–30 min for PMA).

3.4.2 Synchronized Phagocytosis of Opsonized Zymosan

Centrifugation of opsonized zymosan particles or bacteria onto adherent neutrophils at low temperature allows particle binding but not phagocytosis, and rapid transfer of samples to 37 °C supports synchronized ingestion.

1. Dilute COZ in cold (4 °C) tissue culture medium (use 1–2 μl of 5 mg/ml COZ per dish to achieve ~2–3 phagosomes per cell).
2. Add 1 ml of cold, diluted COZ to each dish of PMN (already containing 1 ml warm medium). Mixing warm and cold medium will reduce the overall temperature below the threshold for phagocytosis (16 °C).
3. Rapidly and carefully transfer the dishes onto plate carriers in a refrigerated tissue culture centrifuge cooled to 12–15 °C.
4. Centrifuge for 2 min at 2,000 rpm (~$600 \times g$) with maximum braking. For smaller particles such as bacteria, increase the centrifugation time to 3.5–4 min.

5. Carefully transfer dishes to a 37 °C incubator to allow phagocytosis or fix cells immediately ($t = 0$ min). If samples remained cold during centrifugation, the particles or bacteria in the 0 min samples should be cell associated but not internalized, and forming phagosomes are typically apparent within 1 min of transfer to 37 °C [5, 6], though this is subject to manipulation by pathogenic microbes [14, 15]. For Fcγ receptor-mediated phagocytosis, samples can be cooled to 4 °C instead of 15 °C, but in our hands the lower temperature does not support tight binding to CD11b/CD18.

3.5 Fixation

1. Gently aspirate medium from each dish and then cover cells with 10 % formalin.
2. Incubate at room temperature for 10–15 min (*see* **Note 10**). For certain applications, fixing cells with 4 % paraformaldehyde may be preferred (*see* **Note 2**).

3.6 Permeabilization

1. Fill chilled glass Petri dishes with −20 °C acetone.
2. Using forceps, transfer coverslips (one at a time) into chilled acetone.
3. After 5 min, rehydrate coverslips by transferring into new tissue culture dishes filled with room temperature PBS. Longer incubations in acetone (at least up to 30 min) will not harm cells.
4. Alternatively, cells can be permeabilized using a 1:1 mixture of −20 °C acetone–methanol which is compatible with tissue culture plastic (*see* **Notes 2** and **3**).

3.7 Blocking

1. Aspirate PBS from each dish and cover the fixed and permeabilized cells with 2–4 ml blocking buffer.
2. Incubate at room temperature for 1 h or overnight at 4 °C.

3.8 Antibody Staining for Fluorescence Microscopy

For each antibody the optimal concentration for fluorescence microscopy must be determined empirically. As a general rule, higher concentrations of antibodies are needed for microscopy than for immunoblotting. It is also essential to determine whether the antibodies of choice exhibit nonspecific binding to opsonized zymosan, bacteria, or other particulate stimuli you may be using. In most cases, nonspecific staining can be eliminated by antibody affinity purification.

3.8.1 Primary Antibodies

1. Dilute primary antibodies in blocking buffer to the desired final concentration (*see* **Note 11**). Each coverslip requires 30 μl of antibody. For double or triple staining, primary antibodies can be mixed together. Prepare only what is needed for each experiment since diluted antibodies are unstable and cannot be reused on subsequent days.

2. Centrifuge diluted antibodies (10 min, 4 °C, 10,000 × *g*) to pellet any aggregates.
3. Label a 24-well dish lid and set up a pile of Kimwipes and six microbeakers of PAB (Fig. 1).
4. Using forceps, remove one coverslip from blocking buffer.
5. Touch the edge of coverslip to the pile of Kimwipes to drain off liquid, rinse (swish) in one microbeaker of PAB, and drain again.
6. Dry the back (non-cell side) of the coverslip using a fresh Kimwipes and place it on the 24-well dish lid. Immediately cover with 30 μl antibody (do not let coverslips dry out).
7. Repeat this process for other coverslips.
8. Place coverslips into a plastic box lined with moist paper towels and incubate for 1 h.

3.8.2 Washing and Secondary Antibody Staining

1. Prepare diluted secondary antibodies in blocking buffer. Appropriate dilutions will not stain cells in the absence of primary antibody. For example, we use the DyLight 488- or rhodamine-conjugated Jackson ImmunoResearch $F(ab')_2$ antibodies at 1:600 and 1:200 dilution, respectively. Once again, 30 μl of antibody is used per coverslip. Prepare the amount needed for each experiment. Secondary antibodies generally do not need to be centrifuged prior to use.
2. Lift the first coverslip off of the 24-well dish lid using forceps (grasp as close to the edge as possible) and drain primary antibody into Kimwipes.
3. Wash the coverslip sequentially in six microbeakers of PAB with thorough draining between washes.
4. After the final rinse, carefully blot dry the back of the coverslip and return it to the 24-well dish lid.
5. Cover cells with 30 μl secondary antibody. Repeat for other coverslips.
6. Incubate for 1 h in a covered box lined with moist paper towels.

3.8.3 Non-antibody Stains

Actin filaments can be detected by staining cells with fluorophore-conjugated phalloidins. Several nucleic acid stains can be used to label cell nuclei as well as microbes. Phalloidin conjugates can be added along with primary or secondary antibodies. For most DNA stains, a 5–10-min incubation is sufficient. Wash samples thoroughly before proceeding (*see* **Note 6**).

3.8.4 Mounting Coverslips Onto Slides

1. Label microscopy slides in the frosted marking area. Up to six coverslips will fit onto one slide (Fig. 1). It is important to place the coverslips as close as possible to the frosted marking

area of the slide, as the other edge supports the slide by resting on the microscope stage and as a result any coverslips in this area cannot viewed.

2. Thaw one tube of mounting medium.
3. Working with coverslips for one slide at a time, place six small drops (~15 μl) of gelvatol mounting medium onto the glass slide (*see* **Note 7**).
4. Wash each coverslip in six beakers of PAB, as described above, followed by a final rinse in deionized water. The water rinse prevents a dried salt crust from forming on mounted coverslips.
5. Blot excess water off the back of the coverslip and then invert it (cell side down) onto a bead of mounting medium (start from one edge of the coverslip and lower it slowly to avoid trapping air bubbles). Repeat for the other coverslips on this slide.
6. Gently press down on the top of each coverslip to ensure that their edges are not overlapping (this will also push out small air bubbles). If necessary, excess mounting medium can be removed using an aspirator.
7. Place slides in a cardboard slide folder; this keeps the slides flat and protected from light.
8. Let the mounting medium set overnight at 4 °C. Leftover mounting medium can be refrozen for future use. Very high humidity will prevent the mounting medium from hardening, so do not store samples in a cold room or refrigerator near dripping or condensed water.

3.9 Microscopy, Image Acquisition, and Analysis

1. Neutrophil shape, phagocytosis, and recruitment of granule markers and other proteins to large phagosomes, such as those containing opsonized zymosan particles, can be evaluated using conventional fluorescence microscopy [6]. The phase contrast objectives that are present on most fluorescence microscopes are our preferred method for analysis of cell morphology, as greater detail is revealed relative to the Nomarski (differential interference contrast, DIC) objectives that are typically found on confocal microscopes.
2. We prefer phase contrast objectives for analysis of intraphagosomal superoxide accumulation revealed by nitroblue tetrazolium staining, as we find that color images obtained in this manner can reveal details and subtleties that are more difficult to discern in similar grey-scale NBT-DIC merged images that we obtain by confocal microscopy [7, 9–11].
3. Analysis of granule distribution [12] and the composition of small bacterial phagosomes [7–10] is more readily analyzed by, and may require, the enhanced imaging capacity that is available

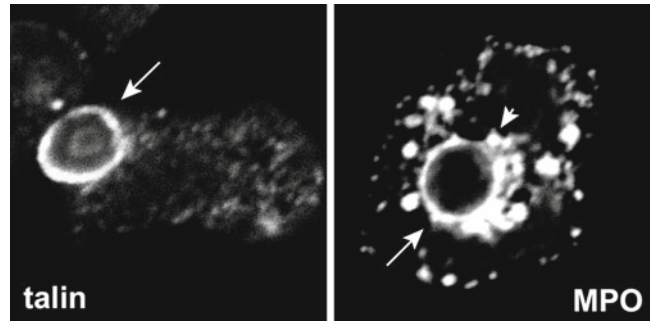

Fig. 2 Images of nascent and mature phagosomes. Confocal images of PMNs on serum-coated coverslips show the accumulation of the cytoskeletal protein talin on 1 min COZ phagosomes and the azurophilic granule protein MPO on 15 min COZ phagosomes. *Arrows* indicate phagosomes; *arrowhead* indicates periphagosomal azurophilic granules

with confocal microscopy. Advantages of confocal microscopy include the ability to zoom in on single cells and the ability to examine cells as sequential (or merged stacks) of thin optical sections. Using this approach, specific and azurophilic granules can be detected in the vicinity of COZ phagosomes prior to phagosome-granule fusion (Fig. 2) [12].

4. The ability to capture several images using identical confocal and laser settings allows distinct fixation and permeabilization conditions [12], or effects of different stimuli (Fig. 3) to be compared directly, and the software packages associated with confocal microscopes allow extensive image analyses such as measurement of pixel intensity at different points within a single image or on a single phagosome [7, 16].
5. When testing new antibodies or particulate stimuli, all samples should be carefully evaluated for specificity of intracellular staining (if the antigen distribution is known) and absence of nonspecific staining of zymosan or bacteria. We have used the methods described here to study neutrophils from persons with chronic granulomatous disease and to analyze PMNs that have ingested opsonized zymosan, *Neisseria meningitidis*, *Helicobacter pylori*, *Staphylococcus aureus*, and *Francisella tularensis* [6–10, 12]. As reported previously [12], we find that that acetone or methanol–acetone permeabilization significantly enhances the sensitivity of detection of many granule proteins and NADPH oxidase subunits in PMNs (*see* **Note 3**) and, in general, cytoplasmic granules are dispersed more evenly under these conditions as compared with detergent-permeabilized neutrophils. This approach also enhances the sensitivity of detection of lamp-1, a prominent marker of late endosomes and multivesicular bodies, in macrophages as well as neutrophils (data not shown). Neutrophil spreading and degranulation can also affect antigen detection [12] (*see* **Note 11**).

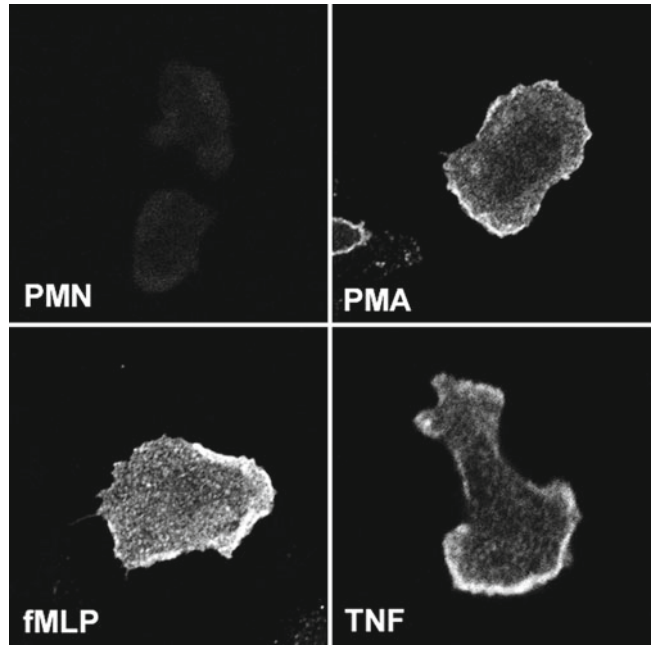

Fig. 3 Detecting upregulation of proteins at the cell surface. Neutrophils plated on fibrinogen-coated coverslips were left untreated or stimulated with 200 nM PMA, 1 μM fMLF, or 0.02 μM TNFα as indicated. Fixed, intact cells were stained with mAb 7D5 to show upregulation of flavocytochrome b_{558} at the cell surface. All four images were acquired using identical confocal settings

4 Notes

1. Other particulate stimuli can be substituted for zymosan including live or killed microorganisms, latex beads, or opsonized sheep red blood cells. Zymosan, latex beads, and red blood cells are visible using phase contrast, bright field, or DIC optics [6]. On the other hand, the small size of many bacteria makes them more difficult to detect in the absence of a direct probe (such as green-fluorescent protein or a specific antibody) [7, 9, 10, 17]. Opsonization of encapsulated bacteria can be inefficient, and particle to serum ratios may need to be adjusted to ensure that complement deposition or antibody biding is sufficient to confer phagocytosis [17]. When using IgG or immune serum, it is also important to ensure that particles are not aggregated [10]. Prelabeled fluorescent beads, *Escherichia coli,* or other BioParticles should be used with caution as we find that the intense fluorescence of these particles overwhelms all other signals and appears as nonspecific fluorescence (bleed through) across a wide spectrum of wavelengths or channels using either conventional or confocal immunofluorescence microscopy.

2. Neutral buffered solutions of 10 % formalin are equipotent to 4 % paraformaldehyde. We prefer formalin because it does not need to be prepared fresh each day. However, the small amount of methanol used to stabilize formalin makes it unsuitable as a fixative when intact cell membranes are required, for example, when fixing cells that have pinocytosed fluorescent dextrans or Lucifer yellow [18] or when strict detection of a surface-exposed (but not intracellular) antigen or epitopes is desired [7] (Fig. 3). In these instances, cells should be fixed using fresh 4 % paraformaldehyde. Direct exposure of live cells to cold methanol (which can fix and permeabilize neutrophils in one step) is compatible with some (but not all) antigens.
3. Detergents such as Triton X-100 are commonly used to permeabilize fixed cells for fluorescence microscopy. However, this approach is prone to artifacts, particularly when used to detect soluble proteins [19]. We find that permeabilization of formalin-fixed cells with −20 °C acetone (or acetone–methanol mixtures) provides superior preservation of cell morphology and enhances the sensitivity of detection of many antigens including $p22^{phox}$ and CD66b [12]. These data are noteworthy since the epitope on $p22^{phox}$ that is recognized by monoclonal antibody 44.1 is cytosolic [20, 21]. As such, the limited detection conferred by 0.1 % Triton X-100 cannot be explained by differential permeabilization of granule and plasma membranes by this detergent. Similarly, we have shown previously that acetone permeabilization enhances detection of lamp-1 on *Helicobacter pylori* phagosomes in macrophages [16]. On the other hand, detergent permeabilization is preferred if cells contain pinocytosed dextrans or Lucifer yellow (*see* **Note 2**).
4. In our hands, the type of serum used in blocking buffer is not critical. We find that Sigma-Aldrich horse serum works well and is cost effective (as compared with FBS, goat serum, or donkey serum (*see also* **Note 6**)).
5. We routinely use the following antibodies for immunofluorescence microscopy of human neutrophils [6–10]. To detect NADPH oxidase components, antibodies specific for $p22^{phox}$ (mAb 44.1) and $gp91^{phox}$ (mAb 54.1) [20, 21] are now available from Santa Cruz Biotechnology (Santa Cruz, CA); mAb 7D5 detects an epitope of $gp91^{phox}$ present in mature flavocytochrome b_{558} [22] and can be used on intact PMNs to detect protein upregulation at the cell surface [7]; a rabbit mAb specific for human $p40^{phox}$ (Epitomics, Burlingame, CA); an antibody that specifically detects active Rac (NewEast Biosciences, Malvern, PA); and rabbit antisera from William Nauseef (University of Iowa) specific for $p47^{phox}$ and $p67^{phox}$ [6]. Mouse mAbs specific for human CD63, lamp-1, and CD11b are obtained from the University of Iowa Developmental

Studies Hybridoma Bank. Mouse mAb to human lactoferrin and myeloperoxidase are purchased from Meridian Life Sciences (Saco, ME) or other vendors.

6. For dual and triple staining, optimal results are obtained using secondary antibodies that are cross-absorbed against other species (such as those available from Jackson ImmunoResearch Labs), and $F(ab')_2$ antibodies are preferred to whole immunoglobulins. If whole IgG are used, it may be necessary to use blocking buffer containing serum matched to the species of secondary antibody in order to prevent nonspecific binding to Fcγ receptors. On the other hand, the choice of fluorescent conjugate is largely a matter of personal preference. For double staining "green–red" combinations are standard. In this regard, DyLight 488 (Jackson ImmunoResearch) or Alexa 488 (Molecular Probes/Invitrogen/Life Technologies) is brighter, more photostable, and less pH sensitive than FITC. Rhodamine and similar DyLight or Alexa conjugates emit strong red–orange fluorescence that often appears brighter than the darker red of Alexa 594 and Alexa 610 conjugates. For triple labeling it is typical to include a far red dye such as Cy5, Cy7, or Alexa 635, which is then false-colored blue in merged images.

   The ultraviolet-excitable dye DAPI is often used to stain cell nuclei [17], and fluor-conjugated phalloidins are used to detect actin filaments [6]. However, antibodies to cytoskeletal proteins such as talin (Fig. 2) or coronin [6] may give superior results in neutrophils for detection of forming phagosomes, as actin filaments in this cell type are less robust than in macrophages.

7. We prefer the polyvinyl alcohol base of gelvatol mounting medium because it hardens rapidly and completely. A common alternative to gelvatol is buffered glycerol (supplemented with an anti-fading agent). Because glycerol mounting solutions do not harden, coverslips must be attached to microscope slides using nail polish (which is more time consuming to apply and more apt to leak).

8. We described previously the phenotype of PMNs attached loosely to serum- or fibrinogen-coated coverslips [6–10, 12]. Here, we extended these results to show that the ability of PMNs to digest or bleach and migrate along surfaces coated with extracellular matrix proteins can also be analyzed (Figs. 4 and 5). Because these interactions are physiological, they are also preferred to the nonspecific adhesion obtained using polylysine-coated surfaces. Moreover, the general "stickiness" of polylysine can impair phagocytosis of particulate stimuli and increase background due to trapping of debris. If polylysine is used, 0.1 mg/ml poly-D-lysine is less toxic to most cell types than poly-L-lysine.

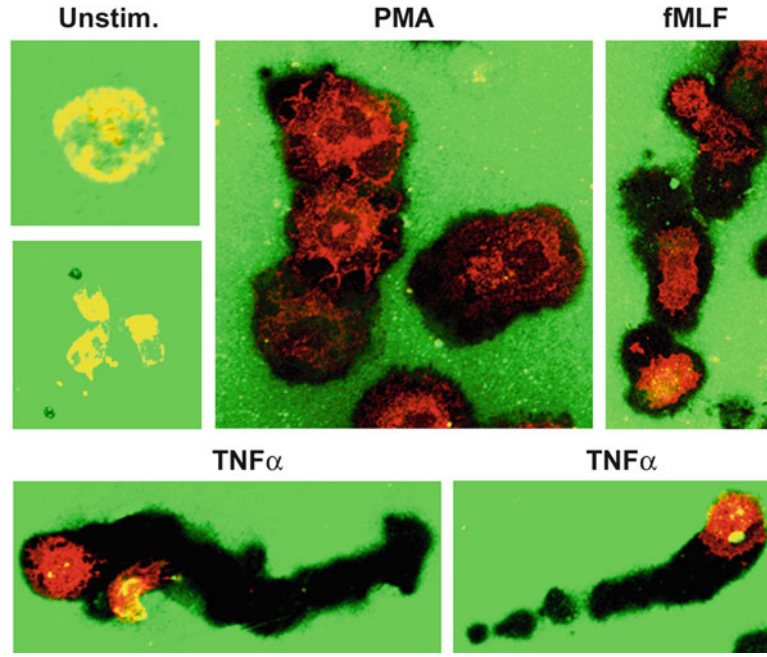

Fig. 4 Neutrophil modulation of the extracellular matrix. PMNs were plated on coverslips coated with Oregon Green-labeled fibrinogen and then left untreated or stimulated with PMA, TNFα, or fMLF as indicated. PMNs were counterstained with mAb to gp91^{phox} after fixation and permeabilization. Fluorescence microscopy images show the ability of activated cells to bleach and/or degrade fibrinogen. Differential effects of these stimuli on cell migration are also apparent

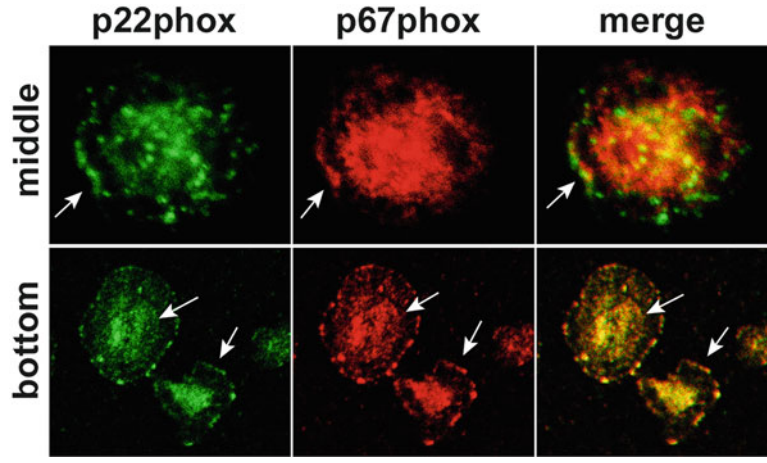

Fig. 5 Localization of NADPH oxidase subunits. Neutrophils were plated on fibrinogen-coated coverslips and then stimulated with TNFα for 30 min. Fixed and permeabilized cells were double stained to detect p22^{phox} (*green*) and p67^{phox} (*red*). Confocal sections taken through the center of cells or at the substrate-adherent surface indicate colocalization of NADPH oxidase subunits at the leading edge and throughout the plasma membrane (*arrows*). In contrast, p67^{phox} was not detected on p22^{phox}-positive specific granules (*arrowheads*)

For several reasons we also prefer coated coverslips to chamber slides (Nunc). First, coverslips are more cost effective, in part because only six of the eight wells on each chamber slide can be used (because the wells on the far right side of the slide rest on the microscope stage). Second, neutrophils distribute evenly over coated coverslips yet bind preferentially near the edges of each chamber due to the meniscus of liquid in each well. Third, the binding interactions that mediate cell attachment to the proprietary slide coating are unclear and can trigger cell activation. Therefore, chamber slides should be coated with serum proteins or fibrinogen before use. Finally, 70 µl of antibody is needed for each well as compared with 30 µl for each 12 mm coverslip (despite similar surface area).

9. To stimulate neutrophils in suspension, dilute cells to 1×10^6 PMN/ml in desired medium or buffer and disperse into sterile polypropylene tubes. Add particulate or soluble stimuli and incubate at 37 °C (with tumbling). Terminate incubations by rapidly diluting each sample into 20 volumes of ice cold PBS and keep on ice. Attach cells to acid-washed coverslips using a cytocentrifuge (such as a Shandon CytoSpin). Assemble slides and filter papers as directed by the manufacturer and place a dry (uncoated) coverslip between the microscope slide and the absorbent paper with the coverslip positioned to receive the sample. Centrifuge 50,000–100,000 PMN onto each coverslip. Transfer coverslips to a tissue culture dish, cover with fixative, and continue as described for adherent cells. Do not fix and stain cells prior to cytocentrifugation. It is also important not to submerge the coverslips in dishes prefilled with fixative as they can cause cells to detach. Precise synchronization of phagocytosis is not achieved using this method.
10. Both the time and temperature of cell fixation are important. Room temperature fixation preserves cell morphology, whereas chilled fixatives can cause cells to contract or detach. Cells incubated in fixative for prolonged periods of time will appear dark using phase contrast optics. Inadequately fixed cells will have poor organelle morphology and, because antigens are not appropriately fixed in place, antibody staining may appear less distinct or poorly localized as compared with properly fixed cells. It is also important to note that aldehyde fixation is reversible. For this reason paraformaldehyde or formalin-fixed cells that have been permeabilized with detergents must be analyzed within a day or so. In contrast, aldehyde fixed samples that have been permeabilized using methanol and/or acetone are more stable and can be stored at 4 °C for 2–3 weeks.
11. Appropriate antibody concentrations vary with changes in cell morphology and the extent of degranulation. Concentrations of antibody appropriate for activated, spread PMN that have

undergone some degranulation can be too high when applied to round, unstimulated cells. Similarly, the amount of antibody needed to detect high concentrations of granule-associated proteins may not be sufficient to detect the same marker once it is distributed over a large phagosome or throughout the plasma membrane [12]. In this regard it is important to evaluate each antibody separately and also to realize that the appropriate dilution of primary antibody may vary depending on the fluor conjugated to the secondary antibody.

Acknowledgements

This work was supported by funds from the National Institutes of Health (R01AI073835, P01AI044642) and a VA Merit Review Grant.

References

1. Faurschou M, Borregaard N (2003) Neutrophil granules and secretory vesicles in inflammation. Microbes Infect 5:1317–1327
2. Nauseef WM (2004) Assembly of the phagocyte NADPH oxidase. Histochem Cell Biol 122:277–291
3. Nordenfelt P, Tapper H (2011) Phagosome dynamics during phagocytosis by neutrophils. J Leukoc Biol 90:271–284
4. Allen L-AH, Aderem A (1995) A role for MARCKS, the α isozyme of protein kinase C and myosin I in zymosan phagocytosis by macrophages. J Exp Med 182:829–840
5. Allen L-AH, Aderem A (1996) Molecular definition of distinct cytoskeletal structures involved in complement- and Fc receptor-mediated phagocytosis in macrophages. J Exp Med 184: 627–637
6. Allen L-AH, DeLeo FR, Gallois A, Toyoshima S, Suzuki K, Nauseef WM (1999) Transient association of the nicotinamide adenine dinucleotide phosphate oxidase subunits p47phox and p67phox with phagosomes in neutrophils from patients with X-linked chronic granulomatous disease. Blood 93:3521–3530
7. Allen L-AH, Beecher BR, Lynch JT, Rohner OV, Wittine LM (2005) *Helicobacter pylori* disrupts NADPH oxidase targeting in human neutrophils to induce extracellular superoxide release. J Immunol 174:3658–3667
8. DeLeo FR, Allen L-AH, Apicella M, Nauseef WM (1999) NADPH oxidase activation and assembly during phagocytosis. J Immunol 163: 6732–6740
9. McCaffrey RL, Allen L-AH (2006) Pivotal advance: *Francisella tularensis* evades killing by human neutrophils via inhibition of the respiratory burst and phagosome escape. J Leukoc Biol 80:1224–1230
10. McCaffrey RL, Schwartz JT, Lindemann SR, Moreland JG, Buchan BW, Jones BD, Allen L-AH (2010) Multiple mechanisms of NADPH oxidase inhibition by type A and type B *Francisella tularensis*. J Leukoc Biol 88:791–805
11. Schulert GS, McCaffrey RL, Buchan BW, Lindemann SR, Hollenback C, Jones BD, Allen L-AH (2009) *Francisella tularensis* genes required for inhibition of the neutrophil respiratory burst and intramacrophage growth identified by random transposon mutagenesis of strain LVS. Infect Immun 77: 1324–1336
12. Allen L-AH (2007) Immunofluorescence and confocal microscopy of neutrophils. Methods Mol Biol 412:273–287
13. Nauseef WW (2007) Isolation of human neutrophils from venous blood. Methods Mol Biol 412:15–20
14. Allen L-AH, Schlesinger LS, Kang B (2000) Virulent strains of *Helicobacter pylori* demonstrate delayed phagocytosis and stimulate homotypic phagosome fusion in macrophages. J Exp Med 191:115–127
15. Allen L-AH (2008) Rate and extent of *Helicobacter pylori* phagocytosis. Methods Mol Biol 431:147–157
16. Schwartz JT, Allen L-AH (2006) Role of urease in megasome formation and *Helicobacter pylori* survival in macrophages. J Leukoc Biol 79:1214–1225
17. Schwartz JT, Barker JH, Long ME, Kaufman J, McCracken J, Allen L-AH (2012) Natural IgM

mediates complement-dependent uptake of *Francisella tularensis* by human neutrophils via complement receptors 1 and 3 in nonimmune serum. J Immunol 189:3064–3077
18. Botelho RJ, Tapper H, Furuya W, Mojdami D, Grinstein S (2002) FcγR-mediated phagocytosis stimulates localized pinocytosis in human neutrophils. J Immunol 169:4423–4429
19. Melan MA, Sluder G (1992) Redistribution and differential extraction of soluble proteins in permeabilized cultured cells: implications for immunofluorescence microscopy. J Cell Sci 101:731–743
20. Burritt JB, Quinn MT, Jutila MA, Bond CW, Jesaitis AJ (1995) Topological mapping of neutrophil cytochrome b epitopes with phage-display libraries. J Biol Chem 270:16974–16980
21. Burritt JB, Busse SC, Gizachew D, Siemsen DW, Quinn MT, Bond CW, Dratz EA, Jesaitis AJ (1998) Antibody imprint of a membrane protein surface. Phagocyte flavocytochrome b. J Biol Chem 273:24847–24852
22. Yamauchi A, Yu LX, Potgens AJG, Kuribayashi F, Nunoi H, Kanegasaki S, Roos D, Malech HL, Dinauer MC, Nakamura M (2001) Location of the epitope for 7D5, a monoclonal antibody raised against human flavocytochrome b_{558}, to the extracellular peptide portion of primate gp91(phox). Microbiol Immunol 45:249–257

Chapter 17

Expression of Genetically Encoded Fluorescent Probes to Monitor Phospholipid Dynamics in Live Neutrophils

Benjamin E. Steinberg, Marco A.O. Magalhaes, and Sergio Grinstein

Abstract

Essential functions of neutrophils, including chemotaxis and phagocytosis, are directed in part by phospholipid signaling. Detailed elucidation of these pathways was hampered by the paucity of methods to study phospholipid localization and dynamics. The development of genetically encoded lipid-specific probes circumvented this limitation. The probes are chimeric constructs consisting of a specific lipid-binding domain fused to a fluorescent protein. This chapter describes a protocol to transiently transfect primary murine neutrophils with such probes in order to localize phospholipids in live cells, and provides a compendium of the types of lipid-binding domains currently used to visualize phospholipids.

Key words Phospholipids, Phosphoinositides, Lipid-binding domains, Phagocytosis, Chemotaxis

1 Introduction

Protein–protein interactions have long been the focus of biochemical analyses of signal transduction; however, other cellular components are now thought to be equally important contributors of signaling networks. In particular, there has been increased appreciation for the role of phospholipids, such as the phosphoinositides and phosphatidylserine, as directors of a multiplicity of cell physiologic processes. The phosphoinositides consist of a phosphatidylinositol moiety that can be either mono-, *bis-* or *tris-*phosphorylated at the 3, 4, and/or 5 positions of the inositol head-group.

The unique physiology of these lipids is largely attributable to the distinctive phosphorylation of their head-groups. Individual phosphoinositides can be recognized stereospecifically by defined domains of ligand proteins For example, the pleckstrin-homology (PH) domain of phospholipase C-delta binds selectively to phosphatidylinositol 4,5-*bis*phosphate ($PI(4,5)P_2$), while the phox (PX) domain of the p40 subunit of the NADPH oxidase recognizes phosphatidylinositol 3-phosphate. As a result of these interactions,

Mark T. Quinn and Frank R. DeLeo (eds.), *Neutrophil Methods and Protocols*, Methods in Molecular Biology, vol. 1124,
DOI 10.1007/978-1-62703-845-4_17,

signaling proteins can be recruited to the membrane; these include enzymes that can convert phosphoinositides into second messengers such as diacylglycerol and inositol 3,4,5-*tris*phosphate.

At physiological pH, phosphatidylserine (PS) and the phosphoinositides are anionic, the magnitude of their charge varying with the extent of phosphorylation of the inositol ring. This negative charge confers onto the membrane a surface charge and an associated surface potential, which dictate the accumulation and attachment of cationic molecules (notably polycationic proteins) near and on the membrane surface, respectively. Note that the surface potential is distinct from the trans-membrane potential, which refers to an electro-diffusional voltage generated primarily by the differential permeability of inorganic ions through the membrane. While the inner surface charge affects the association of peripheral proteins with the cytosolic aspect of the membrane, the orientation and structure of transmembrane proteins is affected by the net effects of the transmembrane and surface potentials. Thus, the lipidic composition of the membrane can affect the biochemistry and physiology of the cells in multiple ways: through stereospecific and electrostatic recruitment of peripheral components, by providing substrates for the generation of second messengers, and by altering the orientation and physiology of transmembrane proteins.

The involvement of phosphoinositides in neutrophil function is slowly being elucidated. For example, the polarization of migrating neutrophils is now known to involve the asymmetric accumulation of phosphatidylinositol(3,4,5)-*tris*phosphate or PI(3,4,5)P_3 at their leading edge, where the phosphoinositide regulates the recruitment of effector proteins to the plasma membrane (*see* ref. 1 for example). Modulation of this phosphoinositide is also critical for neutrophil phagocytosis and bactericidal activity [2]. Similarly, the membrane surface charge generated by phospholipids is now appreciated to modulate the differential recruitment of Rac1 and Rac2 during neutrophil chemotaxis and phagocytosis [3].

While we now understand that phospholipids participate in many key processes of neutrophil physiology, the field is nevertheless at an embryonic stage. Progress has been limited by the difficulties inherent to the measurement of phospholipid distribution and dynamics in live neutrophils with suitable spatial and temporal resolution. Indeed, until recently, this problem was technically intractable. Lipids and their signaling metabolites are chemically unstable, scarce in quantity, and spatially localized to specific signaling foci within cell membranes. Traditional biochemical methods useful in defining protein–protein interactions are not transferable to lipid analysis. For instance, cell lysis and fractionation are accompanied by lipid redistribution, hydrolysis, and/or oxidation. Immunochemical analysis is similarly limited by a paucity of lipid-specific antibodies and aggravated by the requirement for

permeabilization, which generally involve the use of detergents or solvents that interfere with lipid distribution.

Recently, the study of lipid signaling pathways has benefited from our ability to visualize phospholipids using genetically encoded chimeric proteins consisting of a specific lipid-binding protein domain fused with a fluorescent protein, such as green fluorescent protein (GFP). When combined with fluorescence microscopy, this strategy—first introduced by Tamas Balla, Tobias Meyer, and others [4–6]—allows for noninvasive, highly sensitive analysis of spatially localized and temporally fleeting lipid signaling platforms. Employing these protein lipid sensors to investigate neutrophils is accompanied by the additional difficulty of introducing the cDNA constructs and expressing the chimeric protein probes in short-lived primary cells. This chapter describes a protocol to transiently transfect primary murine neutrophils in order to monitor phospholipid localization in live cells, and provides a compendium of the variety of lipid-binding domains used to visualize phospholipids and measure surface charge.

2 Materials

1. Minimum Essential Minimum α (αMEM).
2. Iscove's Modified Dulbecco's Medium (IMDM).
3. Phosphate-buffered saline (PBS): 140 mM NaCl, 5 mM KCl, 8 mM NaH_2PO_4, and 2 mM KH_2PO_4, adjusted to pH 7.4 with 1 M NaOH.
4. Hank's Buffered Salt Solution (HBSS): 137 mM NaCl, 5.4 mM KCl, 0.25 mM Na_2HPO_4, 0.44 mM KH_2PO_4, 1.3 mM $CaCl_2$, 1.0 mM $MgSO_4$, and 4.2 mM $NaHCO_3$.
5. Fetal bovine serum (FBS).
6. Polystyrene beads (Bangs Laboratories, Inc.): Various sized particles are available from the manufacturer. The protocol described herein uses 3.87 μm diameter beads.
7. Percoll.
8. Human IgG.
9. Formyl-Met-Leu-Phe-OH (fMLF).
10. Lipid-binding chimeric protein cDNA constructs: multiple constructs have been developed by various laboratories. Some constructs are available from nonprofit repositories such as Addgene (http://www.addgene.org/). Table 1 provides a representative list of lipid-binding domains and their target lipids.
11. Electroporation systems for transient transfection of mammalian cells: the protocol described was optimized for the Amaxa Nucleofector (Lonza Biosciences).

Table 1

Lipid	Binding domains
PI3P	FYVE, PH, PX
PI4P	GOLPH3, PH, PTB, PX
PI5P	ING2 PHD
$PI(3,4)P_2$	PH, PX
$PI(3,5)P_2$	PH, PROPPINs
$PI(4,5)P_2$	ANTE, ENTH, C2, FERM, PDZ, PH, PTB, PX, Tubby
$PI(3,4,5)P_3$	C2, PH, PX
PS	Lact-C2
ANTH	AP180 N-terminal homology
C2	Conserved region-2 of protein kinase C
ENTH	Epsin N-terminal homology
FERM	4.1, ezrin, radixin, moesin
FYVE	Fab1, YOTB, Vac1, and EEA1
GOLPH3	Golgi phosphoprotein 3
ING2 PHD	Inhibitor of growth 2 Plant homeo-domain
PDZ	Postsynaptic density 95, disk large, zonula occludens
PH	Pleckstrin homology
PROPPINs	β-Propellers that bind PIs
PTB	Phosphotyrosine-binding
PX	Phox homology

12. Hardware necessary for fluorescence imaging of live neutrophils: our laboratory has employed a Quorum spinning-disk confocal system mounted on a Leica DMIRE2 microscope (Leica Microsystems Inc., Bannockburn, IL, USA) equipped with a Hamamatsu back-thinned electron-multiplying charged-coupled device camera and the Volocity 4.2 software platform). Multiple imaging hardware and software systems are available. Live-cell imaging chambers, including the Attofluor live-cell chamber from Invitrogen or glass-bottom dishes, are available from a variety of manufacturers (e.g., MatTek, Ashland, MA).

13. Chemokine gradients for chemotaxis studies can be generated using micropipette and micromanipulator systems. For example, we employ the Eppendorf InjectMan setup. Other systems are commercially available.

3 Methods

3.1 Neutrophil Harvest and Purification

Neutrophils are harvested from the tibias and femurs of both hindlegs after implementation of an appropriate protocol for the humane killing of the mice.

1. Remove the tibias and femurs of freshly euthanized animals and free them of attached connective tissue.
2. Remove the proximal and distal extremities of both bones.
3. Using a 30 G needle, force cold αMEM through the marrow space, and collect the medium in a petri dish. Repeat this step if necessary until you completely remove the bone marrow.
4. By repeated passage through a 20 G needle, mix the collected medium aliquots to disperse any cell clumps.
5. Transfer the solution into a 15 mL tube and centrifuge at 500 × *g* for 5 min at room temperature.
6. Resuspend the cell pellet into 1 mL HBSS at room temperature.
7. Isolated bone marrow cells are purified using a three-layer Percoll gradient. Prepare 85, 65, and 55 % Percoll solutions in PBS according to the manufacturer's specification.
8. Create a three-layer column and place the 1 mL cell solution on top of the Percoll gradient.
9. Centrifuge at 1,000 × *g* for 30 min at room temperature.
10. Collect mature neutrophils at the interface between the 85 and 65 % layers.
11. Wash the collected cells three times using ice-cold HBSS. For each wash, a volume of HBSS equivalent to five times the volume of the Percoll collected is used.
12. The harvested layer will include contaminating red blood cells. Lyse red blood cells by hypotonic lysis. This is carried out by suspending the cells in distilled water at room temperature for 30 s and immediately restoring osmolarity by adding a volume of HBSS equivalent to five times the volume of distilled water.
13. Wash the neutrophils three times in HBSS.

It is important to perform the neutrophil isolation in an efficient manner (preferably completing the process within 2 h of sacrificing the animals) and immediately follow with the transfection protocol.

3.2 Transient Transfection of Primary Neutrophils

The transient transfection protocol is based on electroporation, whereby DNA is introduced into the neutrophils through the application of an external electric field (*see* **Note 1**). The protocol listed below is adapted from the manufacturer's instructions.

1. Mix 2–4 × 10^6 freshly isolated primary neutrophils in 100 μL of Nucleofector solution V at 4 °C.
2. Add 2–5 μg of the purified DNA construct of choice. The precise amount of DNA needs to be adjusted based on the type of construct used.
3. Gently mix the solution and immediately transfer to the electroporation cuvette. Make sure that all of the solution is located within the electroporation well.
4. Transfect using the program Y-001 of the Nucleofector.
5. Immediately and gently add 500 μL of IMDM supplemented with 10 % fetal bovine serum (FBS) at 37 °C.
6. Gently mix the solution inside the electroporation well. Ensure that the cells are suspended from the bottom of the well. This is a critical time and all efforts have to be made to avoid cell lysis. A proportion of the cells will be lysed during the electroporation, forming a white gelatinous material.
7. Transfer the transfected cells into an appropriate uncoated culturing vial filled with IMDM at 37 °C supplemented with 10 % FBS (minimum 2 mL of medium in total). Avoid unnecessary agitation to the cells.
8. Allow the cells to recover for 2 h at 37 °C in a humidified CO_2 incubator.
9. Evaluate transfection efficiency using appropriate methods, such as fluorescence microscopy. Examples of transfected primary neutrophils, visualized by fluorescence microscopy, are shown in Fig. 1.

3.3 Phosphoinositide Imaging in Live Cells by Fluorescence Microscopy

Once transfected, the primary neutrophils can be employed in a variety of functional assays. Protocols to assay neutrophil phagocytosis and chemotaxis are provided below.

3.3.1 Phagocytosis

The phagocytosis protocol employs IgG-opsonized polystyrene beads as the phagocytic prey. Other phagocytic targets—such as zymosan, red blood cells, and bacteria—can be substituted with only minimal modification to the protocol provided here. For example, the opsonization of sheep red blood cells with either IgG or the complement component C3bi have been described [7].

1. Opsonize polystyrene beads by mixing 200 μL of PBS with 10 μL of 3.87 μm polystyrene beads (3.1 × 10^9 beads/mL) and 20 μL of human IgG (50 mg/mL stock).

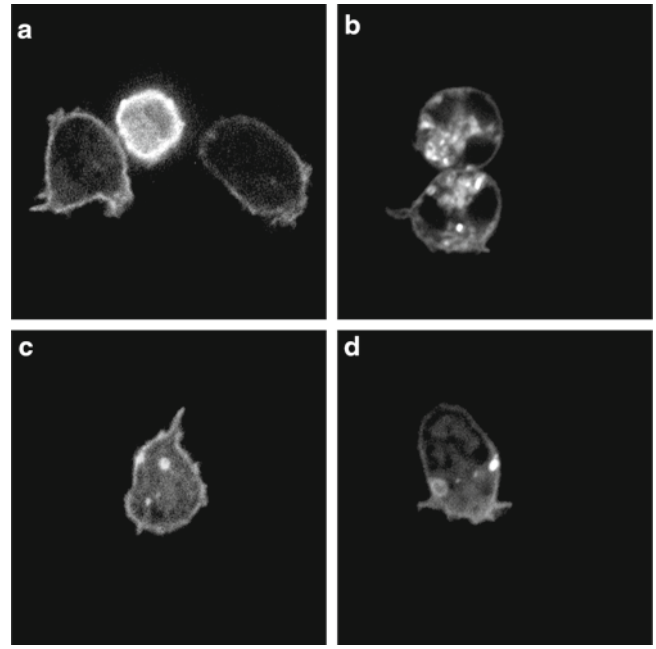

Fig. 1 Primary murine neutrophils transiently transfected with (**a**) PH-PLCδ-GFP, and (**b**) Lactadherin-C2-GFP or PH-AKT-GFP (**c**, **d**). The distribution of PH-AKT-GFP is shown in resting (**c**) and chemotaxing (**d**) cells. Note the polarization of the PH-AKT to the cell's leading edge in panel (**d**). Refer to the text for protocol details and the table for a list of the phospholipids recognized by the respective lipid-binding domains

2. Incubate the suspension for 1 h on a rotating shaker at room temperature.
3. Wash the beads with 1 mL of PBS three times before being resuspending in 250 μL of PBS (*see* **Note 2**).
4. Phagocytic targets can be presented to neutrophils in several ways depending on whether the cells are maintained in suspension or allowed to adhere to a substrate. Here, we consider suspended neutrophils; however, the interested reader is referred to ref. 7 for methods using cells adherent to fibronectin. For suspended, transiently transfected neutrophils, centrifuge the cells along with the IgG-coated beads at 4 °C for 30 s (3,000 × *g*). A ratio of approximately 3–5:1 (beads–cells) should be achieved for optimal phagocytosis.
5. Resuspend the pellet containing the cells and beads and transfer to a live-cell imaging chamber.
6. Image the cells using an appropriate live imaging/fast acquisition system with appropriate temperature control and imaging filters to capture the fluorescent protein construct of choice.

3.3.2 Chemotaxis

1. Transfer cells to glass coverslips pre-coated with 50 μL/mL fibronectin and mounted in a live-cell imaging chamber.
2. Allow the cells to attach to the matrix (approximately 1–3 min).
3. Gently rinse twice with the incubation buffer to remove non-adherent neutrophils.
4. Deliver 1 μM fMLF using a micropipette under continuous flow. The neutrophils will polarize towards the fMLF gradient (Fig. 1).
5. Image the cells using an appropriate live-imaging/fast acquisition system with appropriate temperature control.

4 Notes

1. The transient transfection of primary murine neutrophils represents one of the limiting steps to the above protocol. The protocol described here is very sensitive to changes in cell isolation, timing and manipulation. Our experience shows that cell viability after transfection is variable but is often low compared to other cell lines. Transfection efficiencies are also variable and tend to be low compared to other cell lines, varying from 2 to 30 %. Protocol optimization of cell number and DNA construct amount is highly recommended.
2. Polystyrene beads opsonized with IgG can be stored rotating at 4 °C for several hours, even up to several days. In contrast, when the above protocol is modified to employ other phagocytic targets such as sheep red blood cells coated with complement-derived opsonins, the particles should be used shortly after preparation.

Acknowledgments

The authors wish to acknowledge the support of Dr. Michael Glogauer in the establishment of the above-described transfection protocol. B.E.S. is supported by the Department of Anesthesia at the University of Toronto. M.A.O.M. is supported by the Dental Research Institute (DRI) grant, Javenthey Soobiah Scholarship and the Heidi Sternbach Scholarship. S. G. is the current holder of the Pitblado Chair in Cell Biology; research in the authors' laboratory is supported by Cystic Fibrosis Canada and by the Canadian Institutes of Health Research.

References

1. Kuiper JW, Sun C, Magalhaes MAO et al (2011) Rac regulates $PtInsP_3$ signaling and the chemotactic compass through a redox-mediated feedback loop. Blood 118:6164–6171
2. Prasad A, Jia Y, Chakraborty A et al (2011) Inositol hexakisphosphate kinase 1 regulates neutrophil function in innate immunity by inhibiting phosphatidylinositol-(3,4,5)-trisphosphate signaling. Nat Immunol 12:752–760
3. Magalhaes MAO, Glogauer MJ (2010) Pivotal advance: phospholipids determine net membrane surface charge resulting in differential localization of active Rac1 and Rac2. J Leukoc Biol 87:545–555
4. Várnai P, Balla T (1998) Visualization of phosphoinositides that bind pleckstrin homology domains: calcium- and agonist-induced dynamic changes and relationship to myo-[3H]inositol-labeled phosphoinositide pools. J Cell Biol 143:501–510
5. Stauffer TP, Ahn S, Meyer T (1998) Receptor-induced transient reduction in plasma membrane PtdIns(4,5)P2 concentration monitored in living cells. Curr Biol 8:343–346
6. Burd CG, Emr SD (1998) Phosphatidylinositol(3)-phosphate signaling mediated by specific binding to RING FYVE domains. Mol Cell 2:157–162
7. Steinberg BE, Grinstein S (2007) Assessment of phagosome formation and maturation by fluorescence microscopy. Methods Mol Biol 412:289–300

Chapter 18

Quantitative Assessment of Neutrophil Phagocytosis Using Flow Cytometry

Pontus Nordenfelt

Abstract

Neutrophils have an incredible ability to find and eradicate intruders such as bacteria and fungi. They do this largely through the process of phagocytosis, where the target is internalized into a phagosome, and eventually destroyed by the hostile phagosomal environment. It is important to study phagocytosis in order to understand how neutrophils interact with various pathogens and how they respond to different stimuli. Here, I describe a method to study neutrophil phagocytosis of bacteria using flow cytometry. The bacteria are fluorescently labeled before being introduced to neutrophils. After phagocytosis, both any remaining extracellular bacteria and neutrophils are labeled using one-step staining before three-color analysis. To assess phagocytosis, first the average time it takes for the neutrophils to internalize all bound bacteria is determined. Experiments are then performed using that time point while varying the bacteria-to-neutrophil ratio for full control of the analysis. Due to the ease with which multiple samples can be analyzed, and the quantitative nature of flow cytometry, this approach is both reproducible and sensitive.

Key words Neutrophil, Phagocytosis, Flow cytometry, Bacteria, Opsonization, *Streptococcus pyogenes*

1 Introduction

The process of phagocytosis, where a cell identifies a target and internalizes it into a membrane-bound phagosome, is a critical part of the immune response. Through phagocytosis, many pathogens are cleared effectively from the body before causing harm (reviewed in refs. 1, 2). The neutrophil, our most abundant leukocyte, is a professional phagocyte and is very efficient at attacking bacteria and fungi, often internalizing them in very short amounts of time and possesses a large arsenal of antimicrobial measures (reviewed in ref. 3). To fully understand the neutrophil's role vis-à-vis a specific pathogen, careful analysis of phagocytosis is necessary. Traditionally, this is done with microscopy, and advanced fluorescence microscopy is the de facto method of choice for highly detailed studies [4]. However, microscopy is not as suitable for high-throughput

Mark T. Quinn and Frank R. DeLeo (eds.), *Neutrophil Methods and Protocols*, Methods in Molecular Biology, vol. 1124,
DOI 10.1007/978-1-62703-845-4_18,

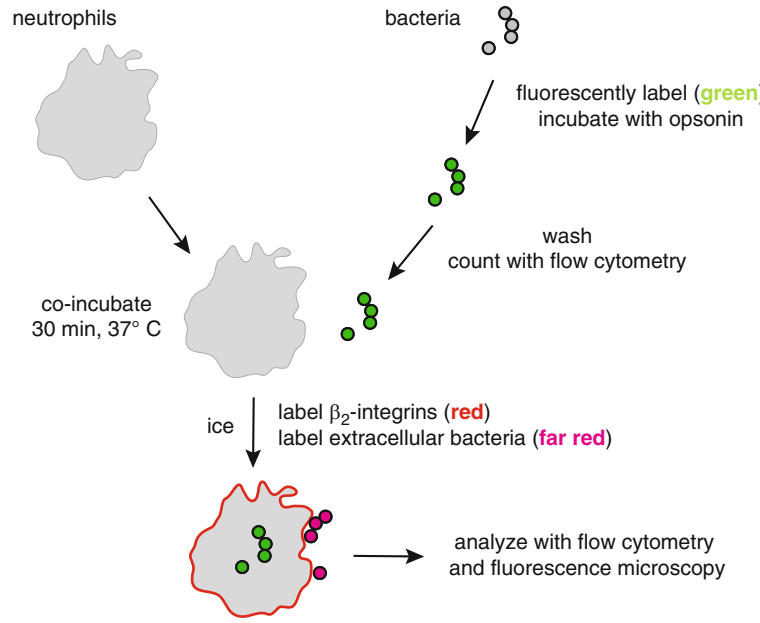

Fig. 1 Schematic workflow of the phagocytosis assay. Briefly, bacteria are fluorescently labeled, incubated with opsonin, washed, and counted using flow cytometry. After co-incubating bacteria with freshly isolated neutrophils, the samples are put on ice. PE-conjugated anti-CD18 (β_2-integrins) and DyLight649-conjugated anti-bacterial Fab fragments are added before analysis

experiments or for quantitative measurements of neutrophil–pathogen interactions. The use of flow cytometry is a potent approach to address the shortcomings of microscopy and the combination of the two is ideal. With flow cytometry, it is easy to acquire quantitative data on multiple and parallel samples in a reproducible manner. This makes it possible to discern and quantify even small differences between conditions.

Here, I present one way to study neutrophil phagocytosis. The method has been successfully employed in the analysis of interactions between *Streptococcus pyogenes* and human neutrophils [5]. The sequence of sample preparation, labeling and phagocytosis is summarized in Fig. 1. First, bacteria are labeled with an organic fluorophore, Oregon Green, but they could also be expressing a fluorescent protein, such as GFP. They are optionally opsonized and then washed before being carefully counted using flow cytometry; accurate counting is essential for reproducibility. At the same time as the bacteria are being prepared, neutrophils are purified and activated. They are then brought together and incubated under end-over-end rotation. At the last step both neutrophils and extracellular bacteria are fluorescently labeled before analysis with flow cytometry.

Phagocytosis can be studied in many different ways, and the analysis strategy used here is to first determine the time it takes for the neutrophils to completely internalize all the bacteria that are bound to their surface. The internalization process itself is preferably studied using fluorescence microscopy [6]. The kinetics of complete internalization are then used as a guide for the time point used when varying the ratio of bacteria to neutrophils (often defined as the multiplicity of infection, MOI). In this way, the experiments are carried out in a step-way fashion and only varying one factor at a time, allowing for complete control of the analysis.

In this chapter, the workflow from determining the kinetics of internalization to quantitative assessment of neutrophil phagocytosis using flow cytometry is described.

2 Materials

2.1 Phagocytosis and Bacterial Preparation

1. Na-medium: 5.6 mM glucose, 127 mM NaCl, 10.8 mM KCl, 2.4 mM KH_2PO_4, 1.6 mM $MgSO_4$, 10 mM Hepes, and 1.8 mM $CaCl_2$; pH adjusted to 7.4 with NaOH.
2. Human plasma or other opsonin: for preparation of human plasma *see* protocol by Rai et al. [7].
3. f-Met-Leu-Phe (f-MLF).
4. Microcentrifuge tube centrifuge with swing-out rotor (such as Eppendorf 5417).
5. VialTweeter (Hielscher).
6. CountBright counting beads (Invitrogen).
7. Low-binding microcentrifuge tubes (Costar).

2.2 Antibodies and Fluorescent Dyes for Flow Cytometry

1. Phycoerythrin (PE)-conjugated Mouse Anti-Human CD18 (BD Pharmingen).
2. Oregon Green (OG) 488X succinimidyl ester (Invitrogen).
3. DyLight 649 anti-human IgG Fab (Jackson) to detect bacteria-bound antibodies.
4. Far red (such Alexa 647 or DyLight 649) species-matched anti-bacterial IgG.

3 Methods

The analysis described here is as performed on BD Biosciences flow cytometers, but should be applicable to any type of flow cytometer.

3.1 Flow Cytometry Settings and Gates

1. Set forward (FSC) and side scatter (SSC) gain and voltage to find cell population.
2. Adjust FSC threshold to limit cell debris.
3. Activated neutrophils will cover a fairly wide range and thus a large gate is used to analyze them (Fig. 2).
4. To make sure that we are looking at leukocytes and not clusters of bacteria, the samples are stained with PE-conjugated anti-CD18 antibodies. This is detected in the FL-2 channel and is the second gating parameter (Fig. 2) (*see* **Note 1**).

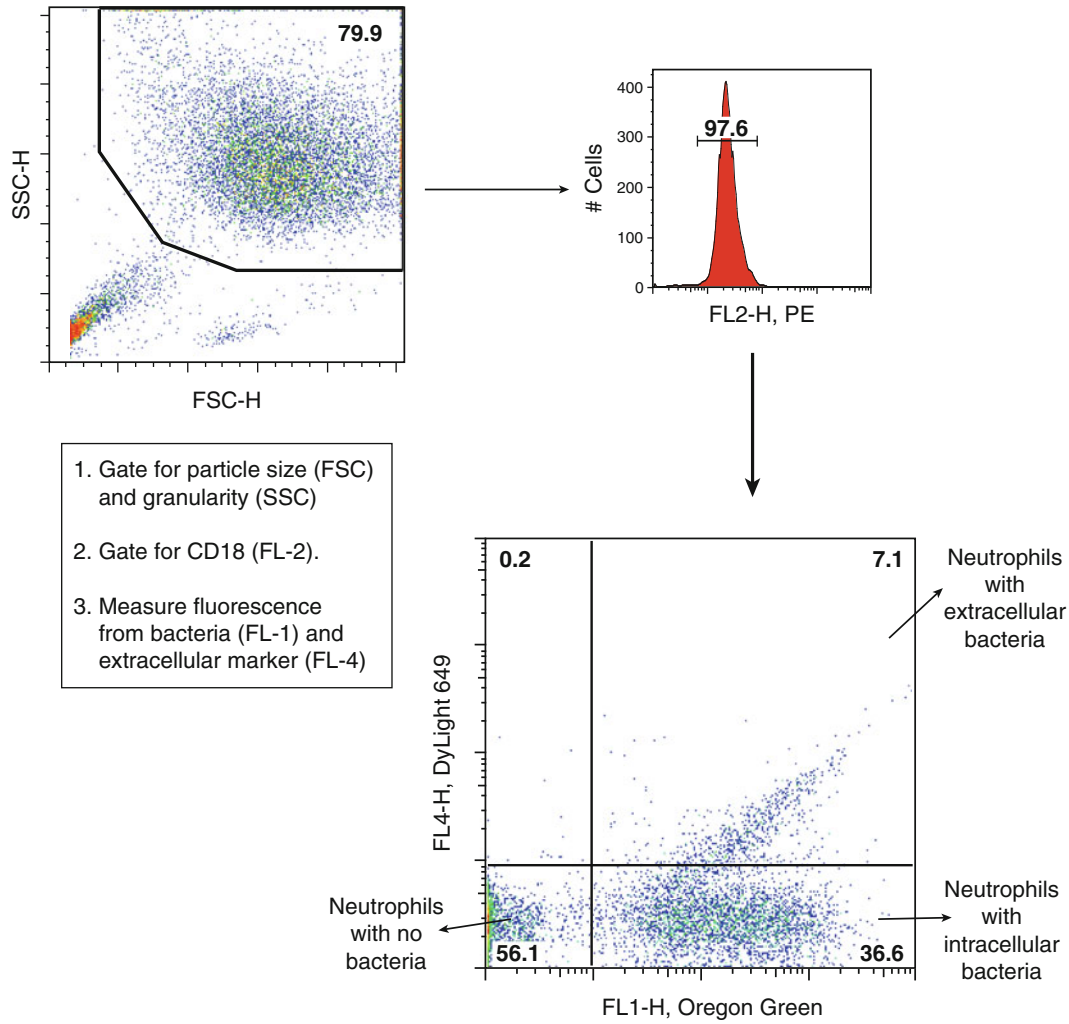

Fig. 2 Gating strategy for the measure of phagocytosis. Human neutrophils are gated based on light scatter properties (1) and then gated for CD18 (2) before analysis of OG/DyLight649-labeled bacteria (3). The upper right quadrant represent neutrophils associated with extracellular bacteria; the lower right quadrant represent neutrophils associated with only intracellular bacteria, and the lower left are cells that are not associated with bacteria

5. Fluorescence from the OG-labeled bacteria is collected in FL-1. As there is a spectral overlap between OG and PE this needs to be compensated. Single-labeled controls with OG and PE are used to set compensation settings (*see* **Note 2**).
6. DyLight 649 anti-bacterial Fab fragments are used to detect non-internalized bacteria. This fluorescence is collected in FL-4 (*see* **Note 3**).
7. The final gate is a quadrant with FL-4 versus FL-1 (Fig. 2). Double positive will indicate cells that have non-internalized bacteria and those with only FL-1 will indicate cells that have completed phagocytosis (*see* **Note 4**).
8. To control for correctly stained samples it is recommended to analyze them with fluorescence microscopy as well (*see* **Note 5**).

3.2 Phagocytosis and Efficient Sample Handling for Flow Cytometry

1. Purify neutrophils from peripheral donor blood according to standard protocols [8].
2. Count the cells and resuspend them in Na-medium at a density of 10–30 million/ml.

3.2.1 Purification of Neutrophils

3. Put tube on a microcentrifuge tube rotator for end-over-end rotation (8 rpm) at RT until start of experiment (*see* **Note 6**).

3.2.2 Preparation of Opsonized and Non-opsonized Oregon Green-Labeled Bacteria

1. Centrifuge live or heat-killed bacteria (500–2,000 million) and resuspend in 500 µl Na-medium with 5 µM Oregon Green (*see* **Notes 7** and **8**).
2. Briefly sonicate the samples to disperse aggregates (*see* **Note 9**).
3. Centrifuge gently (200×*g*, 2 min, swing-out) and continue with the supernatant to remove any remaining bacterial aggregates.
4. Incubate for 30 min at 37 °C.
5. Centrifuge for 5 min at 5,000×*g* using a swing-out rotor (*see* **Note 10**).
6. Resuspend in 250 µl Na-medium.
7. Split bacteria into different opsonizing (e.g., plasma) or control solutions by taking 50 µl OG-labeled bacteria and adding to 500 µl.
8. Incubate for 30 min at 37 °C.
9. Wash twice with 500 µl Na-medium (swing-out, 5,000×*g*, 10 min).
10. Resuspend in 200 µl Na-medium.

3.2.3 Count Prepared Bacteria with Flow Cytometry

1. Vortex counting beads and bacteria.
2. In triplicate, add 5 µl opsonized and OG-labeled bacteria, and 25 µl counting beads to 970 µl Na-medium.

3. Count 1,000 beads and record the number of bacteria.
4. Since the number of beads is known (25,000), multiplying the bead concentration (25/μl) with the bacteria–bead ratio will give the bacterial concentration after accounting for possible dilutions.

3.2.4 Phagocytosis

1. Add neutrophils and bacteria to Na-medium for a total reaction volume of 1,000 μl. Per sample, add 2.5 million neutrophils to a suitable volume of Na-medium (based on how much bacterial volume will be added, *see* **Note 11**).
2. Activate neutrophils by adding 1 μM f-MLF and incubate at 37 °C for 15 min (*see* **Note 12**).
3. Add bacteria to activated neutrophils and incubate for chosen time period at 37 °C with end-over-end rotation (8 rpm). Up to four samples can be started at the same time. Stagger remaining groups of samples with 1 min delay.
4. At each desired time point, withdraw 100 μl from each group of samples and add to 300 μl of ice-cold Na-medium.
5. Keep on ice until all samples are ready for analysis.

3.2.5 Staining of Cells and Bacteria

1. The staining solution consists of PE-conjugated anti-CD18 and DyLight 649- or Alexa 647-conjugated anti-bacterial Fab fragments (*see* **Note 13**).
2. When all phagocytosis samples are on ice, add staining solution and incubate for 15 min on ice (*see* **Note 14**).
3. Analyze samples on flow cytometer, keeping all samples on ice throughout the analysis.

3.3 Determining Internalization Kinetics

3.3.1 Preparations, Phagocytosis, and Staining

1. Follow Subheadings 3.2.1–3.2.3.
2. Choose a single MOI for which to determine the kinetics for complete internalization of neutrophil-associated bacteria (*see* **Note 15**).
3. Add 2.5 million neutrophils to yield 1,000 μl Na-medium as final volume (based on how much bacterial volume will be added, *see* **Note 11**).
4. Activate neutrophils by adding 1 μM f-MLF and incubate at 37 °C for 15 min (*see* **Note 12**).
5. Add bacteria to activated neutrophils and incubate up to 2 h at 37 °C with end-over-end rotation (8 rpm).
6. Withdraw 100 μl aliquot at 5, 15, 30, 60, and 120 min and add to 300 μl of ice-cold Na-medium.
7. Add 100 μl staining solution as described in Subheading 3.2.5.
8. After 15 min incubation on ice, samples can be analyzed continuously.

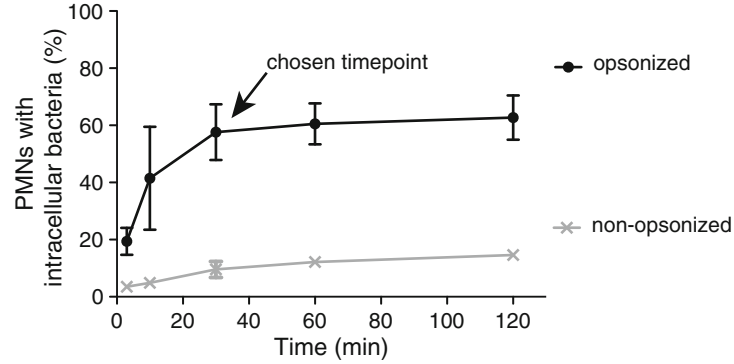

Fig. 3 Kinetics for complete internalization of bacteria by neutrophils. The diagram shows neutrophil phagocytosis of *S. pyogenes* bacteria with or without opsonization with human plasma at MOI 10. The *arrow* indicates the chosen time point (30 min) for the experiments described in Fig. 4. The data are representative of three independent experiments

3.3.2 Analysis of Internalization Kinetics

1. Gate according to Subheading 3.1.
2. Choose cells that are found in the lower right quadrant (Fig. 2), corresponding to neutrophils with only intracellular bacteria.
3. Plot the percentage of the neutrophils that have completed phagocytosis versus time (Fig. 3). Typically, there will be a clear plateau occurring after a certain time that represents when most neutrophils have internalized all bacteria associated with them (*see* **Note 16**).

3.4 Analyzing Phagocytosis at Multiple MOIs

3.4.1 Preparations, Phagocytosis, and Staining

1. Follow Subheadings 3.2.1–3.2.3.
2. Choose a single time point where uptake appears saturated (based on a kinetics curve as Fig. 3) to determine the impact of changing the ratio of bacteria versus neutrophils (MOI).
3. Add 0.5 million neutrophils to yield 500 µl Na-medium as final volume (based on how much bacterial volume will be added) in a 0.65 ml low-bind microcentrifuge tube.
4. Activate neutrophils by adding 1 µM f-MLF and incubate at 37 °C for 15 min (*see* **Notes 12** and **17**).
5. Add bacteria to activated neutrophils and incubate for 30 min (based on kinetics, Fig. 3) at 37 °C with end-over-end rotation (8 rpm).
6. Put samples on ice.
7. Optional: withdraw 150 µl for microscopy analysis (*see* **Note 5**).
8. Add 100 µl staining solution as described in Subheading 3.2.5.
9. Keep on ice until analysis (*see* **Note 14**).

3.4.2 Analysis of Multiple MOIs

1. Gate according to Subheading 3.1.
2. Choose cells that are found in the lower right quadrant (Fig. 2), corresponding to neutrophils with only intracellular bacteria.
3. Plot the percentage of the neutrophils that have completed phagocytosis versus MOI (Fig. 4a). This will reflect how efficient both the bacteria–neutrophil interaction and phagocytosis are.
4. Plot the mean fluorescence intensity versus MOI (Fig. 4b). This will reflect the number of internalized bacteria per cell (*see* **Note 18**).

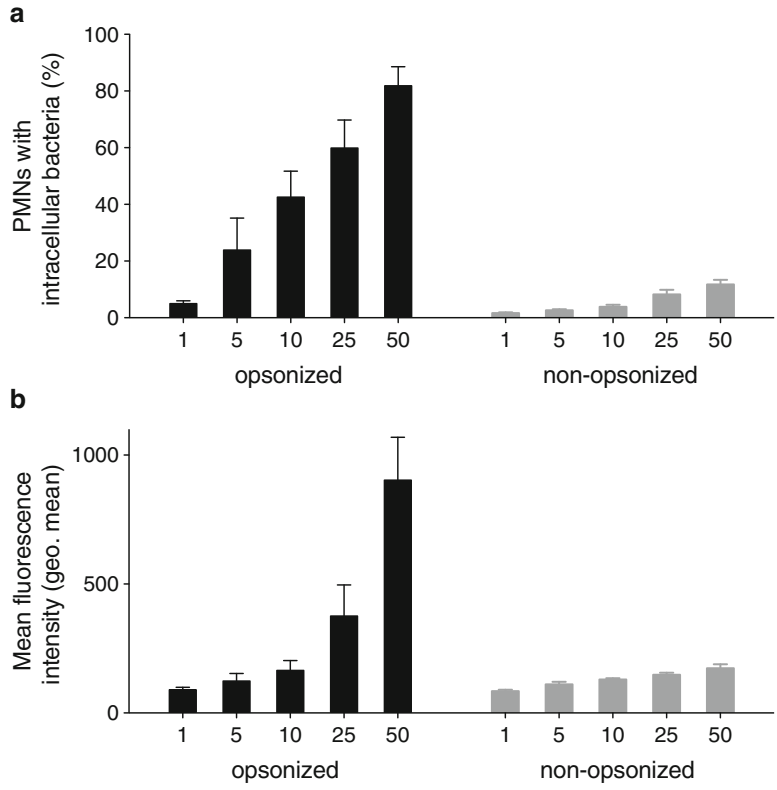

Fig. 4 Phagocytosis of bacteria at multiple MOIs. The diagrams show neutrophil phagocytosis of *S. pyogenes* bacteria with or without opsonization with human plasma. The bars in groups of five represent MOI 1, 5, 10, 25, and 50 (30 min phagocytosis). (**a**) Percentage of neutrophils that has fully internalized at least one bacterium. (**b**) Mean fluorescence intensity of intracellular bacteria as a relative measure of the number of internalized bacteria per neutrophil. Data are representative of three independent experiments

4 Notes

1. Many other cell markers could be used, as long as they do not bind to the bacteria.
2. Spectral overlap can vary with staining efficiency and compensation should be checked routinely; ideally include compensation samples for every experiment. See the manual for your respective flow cytometer on how to set up compensation for spectral overlap.
3. Ideally anti-bacterial Fab fragments are used as they will have minimal interaction with neutrophil Fc receptors, but antibodies that show low binding to neutrophil will work as well.
4. Typically there will be a slope in the upper right quadrant (as in Fig. 2). This represents neutrophils with large numbers of bacteria bound to the surface and over time, as bacteria are phagocytosed, this population will move into the lower right quadrant. This is not to be confused with incorrect compensation, which can have a similar appearance.
5. Microscopy is not described in detail in this chapter but is recommended as a control for the flow cytometry staining. Briefly, fix samples with 2–4 % PFA for 30–60 min on ice. Add the same staining solution as used for flow cytometry and incubate for 15 min at RT. Wash samples three times with PBS and add to poly-L-lysine coated coverslips. After settling for 30 min at RT, aspirate and mount on an object slide with mounting medium (ProLong Gold, Invitrogen).
6. If multiple lab members are involved, the purification of neutrophils and preparation of bacteria/particles should preferably be done in parallel.
7. Use standard protocols to grow bacteria (not referenced here since it will be species- and strain-dependent). In my experience, this labeling works well for both live and heat-killed *E. coli*, *S. aureus*, and *S. pyogenes*.
8. Fluorescein isothiocyanate (FITC) or other dyes and proteins (such as GFP) with similar spectral properties could also be used.
9. Ultrasonic water baths work but the VialTweeter used here is recommended because of its reproducibility. For the first few experiments, monitor the sonication with a standard light microscope to determine time and pulse required for the VialTweeter.
10. The use of swing-out rotors is recommended to minimize loss of bacteria in washing steps; the use of low binding tubes is also helpful in this respect.

11. Example: if there are 30 million neutrophils per ml and 550 million opsonized bacteria per ml the volumes will be as follows for MOI 10: add 871 μl Na-medium, 83 μl neutrophils, and 46 μl bacteria.
12. fMLF can be omitted but will typically result in lower phagocytosis.
13. Directly conjugated fluorophores are essential as it is a one-step staining. Kits are available to conjugate fluorescent molecules to antibodies (Invitrogen). Fab fragments might not be necessary, and antibodies can be used instead if it can be shown that the neutrophils do not bind the Fc of the bacteria-detecting antibodies. Fab fragments are otherwise prepared using standard biochemical protocols [9].
14. To save time, it is good to transfer the samples to FACS tubes (on ice) during the incubation time.
15. Typically this will be in the middle of the planned MOI range; it should not be in the lower range as this could cause an underestimation of the time it takes for complete internalization of cell-associated bacteria.
16. This time will be system-dependent and has to be determined again if any significant changes are introduced, such as changing opsonin, bacterial species, reaction volume, rotation times, etc. It also important to keep in mind that choosing a late time point might lead to an increase of false negatives as the fluorophores can be broken down in the phagosome.
17. Do this in a staggered fashion or with multipipette to allow time for handling multiple samples.
18. As can be seen from the example presented in Fig. 4b, if different MOIs had not been analyzed (and after appropriate time (Fig. 3), important differences between the conditions could easily be missed, especially at low MOIs. For instance, at MOI 5 there is no apparent difference in the number of internalized bacteria, but there is a large difference in the number of neutrophils that are involved.

Acknowledgements

This work was supported by the Swedish Research Council (524-2011-891), Swedish Society of Medicine (SLS-173751), and the Blanceflor Foundation.

References

1. Flannagan RS, Jaumouillé V, Grinstein S (2012) The cell biology of phagocytosis. Ann Rev Path 7:61–98
2. Swanson JA (2008) Shaping cups into phagosomes and macropinosomes. Nat Rev Mol Cell Biol 9:639–649
3. Nordenfelt P, Tapper H (2011) Phagosome dynamics during phagocytosis by neutrophils. J Leukoc Biol 90:271–284
4. Sarantis H, Grinstein S (2012) Monitoring phospholipid dynamics during phagocytosis: application of genetically-encoded fluorescent probes. Methods Cell Biol 108:429–444
5. Nordenfelt P, Waldemarson S, Linder A et al (2012) Antibody orientation at bacterial surfaces is related to invasive infection. J Exp Med 209:2367–2381
6. Nordenfelt P, Bauer S, Lönnbro P et al (2009) Phagocytosis of *Streptococcus pyogenes* by all-trans retinoic acid-differentiated HL-60 cells: roles of azurophilic granules and NADPH oxidase. PLoS ONE 4:e7363
7. Rai AJ, Gelfand CA, Haywood BC et al (2005) HUPO Plasma Proteome Project specimen collection and handling: towards the standardization of parameters for plasma proteome samples. Proteomics 5:3262–3277
8. Nauseef WM (2007) Isolation of human neutrophils from venous blood. Methods Mol Biol 412:15–20
9. Andrew SM, Titus JA (2001) Fragmentation of immunoglobulin G. Curr Prot Cell Biol 16(4): 16.4.1–16.4.10

Chapter 19

Analysis of Neutrophil Bactericidal Activity

Heather A. Parker, Nicholas J. Magon, Jessie N. Green, Mark B. Hampton, and Christine C. Winterbourn

Abstract

This chapter describes two methods for measuring the bactericidal activity of neutrophils. These are a new simple fluorescence-based assay, which quantifies bactericidal activity by measuring changes in bacterial fluorescence associated with a loss of membrane potential over time, and a more traditional colony counting protocol. Two variations of these techniques are presented: a "one-step" protocol providing a composite measure of phagocytosis and killing, and a "two-step" protocol that allows calculation of separate rate constants for both of these processes.

Key words Neutrophil, Bacteria, Killing, Bactericidal activity, *Staphylococcus aureus*, Method

1 Introduction

Neutrophils are the immune system's key defenders against bacterial infection, their primary function being to destroy invading pathogens. One of the ways they achieve this is by engulfing the pathogen into an intracellular compartment, the phagosome, then subjecting it to an array of both oxygen-dependent and oxygen-independent killing mechanisms. These involve the release of antimicrobial and proteolytic peptides into the phagosomal space, along with the production of reactive oxygen species by an NADPH oxidase complex that assembles in the membrane [1–3]. If the bactericidal capacity of neutrophils is defective, an individual may suffer from enhanced susceptibility to potentially fatal microbial infection. To identify such defects, or to investigate the mechanisms used to kill bacteria, the bactericidal activity of neutrophils must be accurately quantified.

Bactericidal activity is measured as the loss in viability of bacteria cocultured with neutrophils. Methods include measuring the ability of bacteria to form colonies on nutrient agar, or to incorporate [^{3}H]-thymidine into newly synthesized DNA. Alternatively, fluorescent dyes such as acridine orange can distinguish viable from

Mark T. Quinn and Frank R. DeLeo (eds.), *Neutrophil Methods and Protocols*, Methods in Molecular Biology, vol. 1124,
DOI 10.1007/978-1-62703-845-4_19,

dead bacteria by intercalating into the less structurally organized DNA of the dead bacteria, resulting in a shift in emission peak. The advantages and disadvantages of these various methods have been reviewed elsewhere [4].

This chapter provides details of a new assay we recently developed that is based on the ability of live bacteria to take up a fluorescent membrane potential dye 3, 3′-diethyloxacarbocyanine iodide ($DiOC_2(3)$). This assay is less time consuming than methods that involve colony counting. It does, however, require the use of a fluorescent plate reader capable of scanning excitation (*see* **Note 1**). Therefore, we also describe the protocol for the colony forming unit (CFU) assay, which uses standard laboratory equipment.

$DiOC_2(3)$ is a positively charged lipophilic, green fluorescent dye which accumulates in cells or organelles that maintain a negative membrane potential (live bacteria and mitochondria). At high intracellular concentrations $DiOC_2(3)$ forms aggregates that exhibit a red shift in fluorescence [5]. Thus live bacteria emit red fluorescence and this is lost in dead cells due to dissipation of the bacterial membrane potential. $DiOC_2(3)$ has been used in drug development for screening of compounds with potential antibacterial activity [6, 7]. We have adapted this assay to assess the bactericidal activity of neutrophils.

Two variations of the fluorescence and colony counting procedures are described. In the "one-step" protocol, extracellular bacteria remain with the neutrophils that contain phagocytosed and dead bacteria. Therefore, a composite measure of both phagocytosis and killing is obtained. The "two-step" protocol (illustrated in Fig. 1) incorporates a differential centrifugation step [8] that separates extracellular bacteria from those ingested by the neutrophils. The proportions of viable extracellular and intracellular bacteria are measured at various times and a kinetic analysis is then undertaken, allowing separate rate constants to be calculated for phagocytosis and killing. The one-step protocol requires less manual sample processing and can be used when it is not critical to distinguish which function (phagocytosis or killing) is affected. It is also useful for screening numerous samples or conditions. If differences are detected, samples can then be investigated in more depth using the two-step protocol. The two-step protocol is preferable for elucidating which aspect of the bactericidal process is defective.

2 Materials

1. Tryptic soy broth: autoclave before use.
2. Phosphate buffered saline (PBS) (10× stock): KH_2PO_4 (15 mM), Na_2HPO_4 (80 mM), KCl (27 mM) in 900 mL of

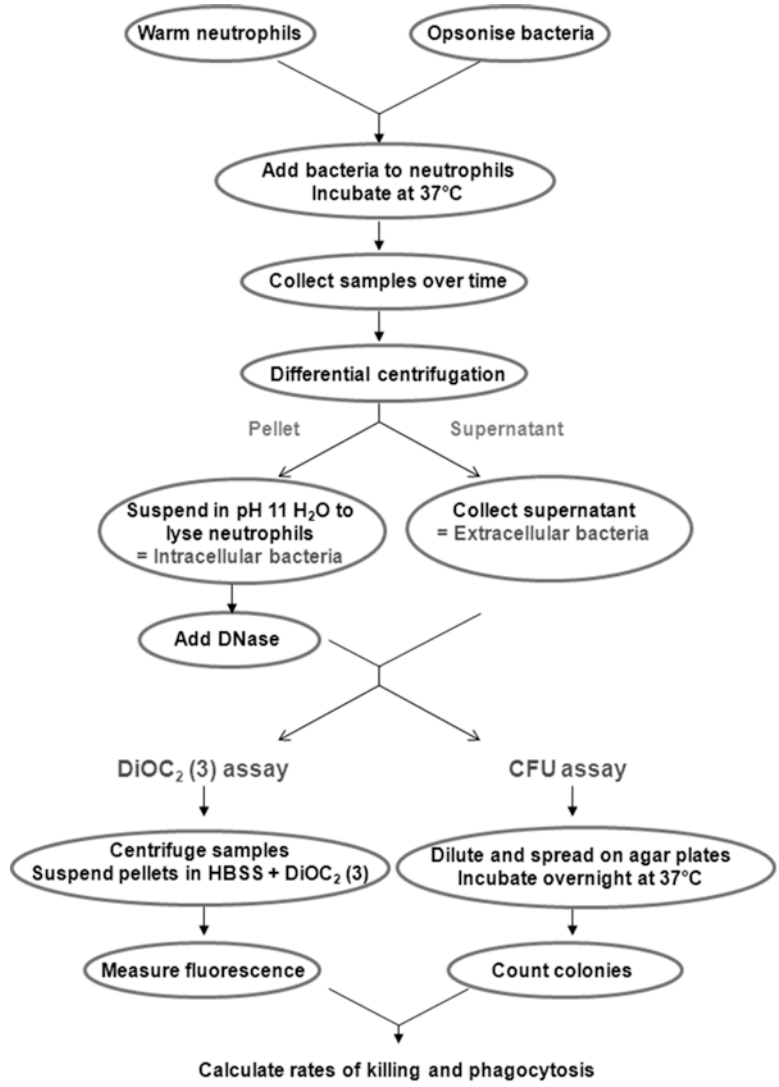

Fig. 1 Outline of the two-step method for measuring bactericidal activity of neutrophils

water. Adjust to pH 7.4 with HCl if necessary, then add NaCl (1.37 M) and bring the final volume to 1 L. Store at room temperature.

3. PBS (1×): 1 part 10× PBS, 9 parts water. Autoclave before use (*see* **Note 2**).
4. Hank's balanced saline solution (HBSS): 1 mM $CaCl_2$, 0.5 mM $MgCl_2$, 1 mg/mL glucose in PBS. Filter-sterilize before storage for up to 1 month at 4 °C.
5. Autologous human serum: For ~1 mL of serum, reserve 2–3 mL of blood (without anticoagulant) from the donor

whose neutrophils are being examined. Allow to clot in a glass tube at 37 °C for ~1.5 h. "Ring" the clot by running a sterile Pasteur pipette tip around the side of the tube. Separate the serum from the clot by centrifugation at 1,200 × *g* for 2 min, transferring the serum to a clean tube. Centrifuge at 12,000 × *g* for 30 s to remove contaminating erythrocytes.

6. pH 11 water: Bring water to pH 11.0 by adding NaOH. For the CFU assay, sterile water should be used.
7. DNase mix: Tris–HCl pH 7.4 (250 mM), $CaCl_2$ (25 mM), $MgCl_2$ (12.5 mM), and DNase (Roche) (2,500 U/mL).
8. $DiOC_2(3)$ (Molecular Probes): 3 mM in DMSO. Store in the dark at 4 °C.
9. Columbia sheep blood agar plates: suitable for the fastidious growth requirements of *Staphylococcus aureus*.

3 Methods

These protocols have been optimized for use with the target bacteria *Staphylococcus aureus*. Other target microorganisms can be used with the colony counting assay. However, sampling times and dilution factors may need adapting. The fluorescence assay has not as yet been tested with other organisms.

3.1 Neutrophil Preparation

1. Isolate neutrophils from whole blood as described in detail elsewhere in this volume (*see* **Note 3**).
2. Suspend neutrophils at a final concentration of 1×10^7 cells/mL in HBSS. Keep at room temperature and use within 1 h.

3.2 Preparation of Bacteria

1. Inoculate 10 mL of sterile tryptic soy broth with a single colony of *S. aureus* grown on sheep blood agar. Culture overnight at 37 °C in a shaking incubator at 200 rpm.
2. Take a 1 mL sample of the overnight culture and centrifuge at 12,000 × *g* for 4 min to pellet the bacteria.
3. Wash the pellet twice in PBS and suspend in 1 mL of HBSS.
4. Centrifuge at 100 × *g* for 5 min to remove any clumped bacteria (*see* **Note 4**).
5. Calculate the concentration of bacteria in the sample by measuring the optical density at 550 nm and relating to a previously established standard curve of optical density vs. CFU.
6. Opsonize the bacteria by suspending (for example, 2×10^8 CFU/mL for a 20:1 ratio of bacteria to neutrophils) in HBSS containing 10 % autologous serum in a glass tube. Rotate end-over-end (6 rpm) for 20 min at 37 °C, then use immediately.

3.3 One-Step Assay for Neutrophil Bactericidal Activity

3.3.1 Fluorescence Assay

1. Prepare 1.5-mL Eppendorf tubes (in triplicate for each time point or treatment) containing 300 μL of freshly isolated neutrophils (at 1×10^7/mL) with 30 μL of autologous serum.
2. Incubate at 37 °C for 10 min to pre-warm. Any experimental drugs or inhibitors are added at this stage and pre-incubated for the appropriate time required.
3. Prepare 4–6 identical "control" tubes of bacteria alone for time zero and the last time point and for each treatment by replacing the neutrophils with 300 μL of HBSS (*see* **Note 5**). This control allows fluorescence measurement of the starting number of bacteria, their growth over the time-course of the experiment, and the effects of opsonisation and any experimental drugs on bacterial growth.
4. Prepare a control of neutrophils alone by replacing the bacteria with HBSS (*see* **Note 6**).
5. Add 300 μL of freshly opsonized bacteria to start the reaction. The final ratio of bacteria to neutrophils in our example is 20:1, and the serum concentration is approximately 10 % (*see* **Note 7**).
6. To follow a time course (e.g., 5, 10, and 20 min; *see* **Note 8**), add bacteria immediately after opsonisation to all experimental tubes then incubate for the chosen times.
7. Incubate the tubes at 37 °C with end-over-end rotation (6–10 rpm) (*see* **Note 9**).
8. After incubation, immediately place tubes on melting ice (*see* **Note 10**).
9. Pellet the cells and bacteria ($30{,}000 \times g$, 2 min, 4 °C) and suspend in 1 mL of freshly made pH 11 H_2O.
10. Allow the neutrophils to lyse by standing at room temperature for 5–10 min, then vortex briefly (*see* **Note 11**).
11. To degrade the released neutrophil DNA, add 40 μL of DNase mix (*see* **Note 12**). Mix by inverting the tubes and incubate at 37 °C for 10 min (*see* **Note 13**). Incubate the control bacteria under the same conditions.
12. Add 20 μL of a 25 mg/mL solution of saponin (final concentration 0.05 %) and gently rotate tubes for 2 min to prevent the bacteria from sticking to the tubes. Pellet all samples ($30{,}000 \times g$, 2 min, 4 °C) and suspend in 98 μL HBSS.
13. Add 1.7 μL $DiOC_2(3)$ (final concentration 50 μM) and pipette briefly to mix.
14. Prepare three "blank" tubes with HBSS and dye alone.
15. Incubate samples and blanks at room temperature for 5 min in the dark then transfer the entire contents of each tube to the wells of a clear 96-well flat-bottomed microtiter plate (*see* **Note 14**).

16. Measure fluorescence signal (Excitation 350–550 nm; Emission 700 nm; bandwidth 5 nm) and calculate the area under the curve between 380 and 430 nm (*see* **Note 15**).
17. Subtract the fluorescence of neutrophils alone (*see* **Note 6**).
18. Adjust the fluorescence to account for growth of the bacteria over the time course of the assay by plotting the fluorescence of "control" bacteria at the start and end of the experiment. Fit a linear curve to this data. The fluorescence of experimental samples at a particular time is then divided by the ratio of the extrapolated fluorescence of "control" bacteria at this time to that of time zero. These calculations are based on the assumption that bacteria grow at the same rate in the presence of neutrophils.

3.3.2 Colony Forming Unit Assay

1. Prepare 1.5-mL Eppendorf tubes containing 300 μL of freshly isolated neutrophils (at 1×10^7/mL) with 30 μL of autologous serum. Prepare a single experimental tube for each condition and one control for bacterial growth (*see* **Note 16**). There is no need to include a control of neutrophils alone.
2. Incubate at 37 °C for 10 min to pre-warm. Any experimental drugs or inhibitors are added at this stage and pre-incubated for the appropriate time required.
3. Add 300 μL of freshly opsonized bacteria to start the reaction.
4. Incubate the tubes at 37 °C with end-over-end rotation (6–10 rpm) (*see* **Note 9**).
5. For a time course, take 50 μL samples from the experimental tubes at each time point (e.g., 5, 10, and 20 min; *see* **Note 8**) and from the controls at time zero and last time point and place on melting ice.
6. Dilute into 910 μL of pH 11 water (*see* **Note 17**). Allow the neutrophils to lyse by standing at room temperature for 5–10 min, then vortex vigorously for ~5 s to disperse the bacteria.
7. Treat with DNase as described above in Subheading 3.3.1, **step 11** (*see* **Note 18**).
8. Dilute in ice-cold pH 11 H_2O to give a concentration of approximately 5,000 CFU/mL (refer to Table 1, *see* **Note 19**).
9. Spread 20 μL on half of an agar plate, giving approximately 100 CFU per half plate. Plate at least four half plates per sample.
10. Incubate the plates overnight at 37 °C and count the number of colonies formed.
11. Convert colony counts to bacterial concentrations by multiplying with the appropriate dilution factor (refer to Table 1).
12. Adjust bacterial numbers to account for growth over the time course of the assay as described in Subheading 3.3.1, **step 18**.

Table 1
Dilution guidelines for the one-step colony counting protocol

Dilutions for one-step protocol				
	Sample time			
	0 min	5 min	10 min	20 min
Approx. undiluted concentration/mL[a]	1×10^8	1×10^8	7×10^7	4×10^7
Dilution due to sample processing[b]	20×	20×	20×	20×
Dilution incurred by plating 20 µL[b]	50×	50×	50×	50×
Additional dilution required to get approx. 100 colonies per 20 µL[c]	1,000×	1,000×	700×	400×
Total dilution factor	1×10^6	1×10^6	7×10^5	4×10^5

[a]From experience, these are the approximate bacterial concentrations expected at time of sampling. These values are likely to vary under different conditions. If the numbers of bacteria detected are too high or low to make accurate colony counts, the additional dilutions should be adjusted accordingly
[b]These are dilutions that will be automatically incurred through following the protocol as written
[c]These are the further dilutions required in the second to last step of either the one-step or two-step protocol

3.3.3 Data Analysis for the One-Step Assay

1. Plot raw values of fluorescence or viable bacteria against time, or convert to percentage killing or percentage survival relative to the number of bacteria at the corresponding time point. Expression of data as a percentage normalizes any variation in the initial concentration of bacteria and enables experiments on different days to be compared.
2. Different experiments can also be compared by obtaining the slope of a semi-natural log plot or fitting an exponential curve ($y = y_0 e^{-kx}$) to the data to provide a single rate, k, which is a composite measure of phagocytosis and killing. The ½ life for killing can be calculated from $t_{1/2} = \ln(2)/k$ min. Figure 2a, b show examples of time course data fitted to an exponential curve. In Fig. 2c, d, the percentage of viable bacteria is shown after 20 min incubation. Killing is inhibited by treatment with diphenyleneiodonium (DPI), an inhibitor of the NADPH oxidase, or the MPO inhibitor thioxanthine-1 (TX1) [9].

3.4 Two-Step Assay for Neutrophil Bactericidal Activity

3.4.1 Fluorescence Assay

1. Prepare 1.5-mL Eppendorf tubes (in triplicate for each time point or treatment) containing 300 µL of freshly isolated neutrophils (at 1×10^7/mL) with 30 µL of autologous serum.
2. Incubate at 37 °C for 10 min to pre-warm. Any experimental drugs or inhibitors are added at this stage and pre-incubated for the appropriate time required.

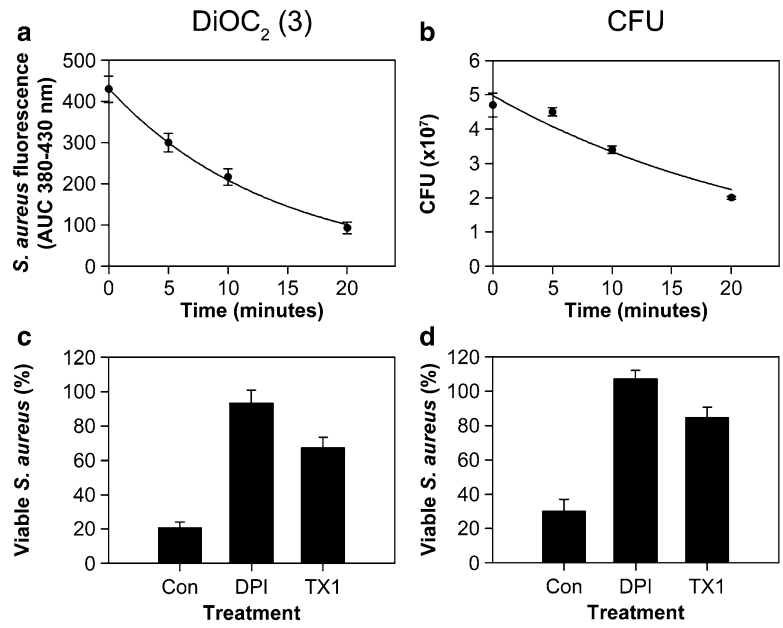

Fig. 2 Measurement of the bactericidal activity of neutrophils by $DiOC_2(3)$ fluorescence and colony forming unit assays. (**a** and **c**) show data for $DiOC_2(3)$ fluorescence assays and (**b** and **d**) for colony forming unit (CFU) assays. (**a** and **b**) Bacteria were incubated with neutrophils (20:1 ratio) for 0–20 min. (**c** and **d**) *S. aureus* were incubated for 20 min with control neutrophils (Con) or neutrophils pre-treated with 10 μM of either the NADPH oxidase inhibitor DPI or the myeloperoxidase inhibitor TX1. All samples were processed as described in the text using the one-step protocol. Data are means ± SE of 3–5 separate experiments using neutrophils from different donors. For **a** and **b**, data are fitted to an exponential decay curve (two parameter) using the curve fitting program in SigmaPlot

3. Prepare four tubes of "control" bacteria alone for the start and end of the experiment. Prepare a control of neutrophils alone by replacing the bacteria with HBSS (*see* **Note 6**).
4. Incubate the tubes at 37 °C with end-over-end rotation (6–10 rpm) (*see* **Note 9**).
5. To follow a time course, add bacteria immediately after opsonisation to all experimental tubes then incubate for the chosen times (e.g., 5, 10, and 20 min; *see* **Note 8**).
6. After incubation, place on melting ice (*see* **Note 10**).
7. Centrifuge experimental samples at 100 × *g* for 5 min at 4 °C using a swing-out rotor (*see* **Note 20**).
8. Collect the supernatant, being careful not to disturb the neutrophil pellet (*see* **Note 21**).
9. Wash the pellet twice more with 400 μL ice-cold PBS (100 × *g*, 5 min, 4 °C), pooling the supernatants. The pooled supernatant contains the bacteria that have not been phagocytosed (*extracellular* bacteria), while the phagocytosed bacteria are in the neutrophil pellet (*intracellular* bacteria).

10. Centrifuge the supernatants, control bacteria and control neutrophils (30,000 × *g*, 2 min, 4 °C).
11. Suspend all pellets in 1 mL of pH 11 water. Let stand at room temperature for 5–10 min then vortex briefly (*see* **Note 11**).
12. Treat with DNase as described above in Subheading 3.3.1, **step 11** (*see* **Notes 12** and **13**).
13. Add 20 μL of a 25 mg/mL solution of saponin (final concentration 0.05 %) and gently rotate tubes for 2 min to prevent the bacteria from sticking to the tubes and to lyse any contaminating neutrophils (*see* **Note 22**).
14. Pellet all samples (30,000 × *g*, 2 min, 4 °C) and suspend in 98 μL HBSS.
15. Add 1.7 μL $DiOC_2(3)$ (final concentration 50 μM) and pipette briefly to mix.
16. Prepare three "blank" tubes with HBSS and dye alone.
17. Incubate samples and blanks at room temperature for 5 min in the dark then transfer the entire contents of each tube to the wells of a clear 96-well flat-bottomed microtiter plate (*see* **Note 14**).
18. Measure fluorescence signal (Excitation 350–550 nm; Emission 700 nm; bandwidth 5 nm) and calculate the area under the curve between 380 and 430 nm (*see* **Note 15**).
19. Subtract the fluorescence of neutrophils alone (*see* **Note 6**).
20. We have developed an Excel file that calculates the rate constants for phagocytosis and killing. This can be found in the online *Supplementary material* and at http://www.otago.ac.nz/christchurch/research/freeradical/assays. This file contains instructions for its use. Add the raw data (with the fluorescence of neutrophils alone subtracted where appropriate) to the required cells in the Excel spreadsheet.

3.4.2 Colony Forming Unit Assay

1. Prepare 1.5-mL Eppendorf tubes containing 300 μL of freshly isolated neutrophils (at 1×10^7/mL) with 30 μL of autologous serum. Prepare a single experimental tube for each condition and one control for bacterial growth (*see* **Note 16**). There is no need to include a control of neutrophils alone.
2. Incubate at 37 °C for 10 min to pre-warm. Any experimental drugs or inhibitors are added at this stage and pre-incubated for the appropriate time required.
3. Add 300 μL of freshly opsonized bacteria to start the reaction.
4. Incubate the tubes at 37 °C with end-over-end rotation (6–10 rpm) (*see* **Note 9**).
5. For a time course, take 50 μL samples from the experimental tubes at each time point (e.g., 5, 10, and 20 min; *see* **Note 8**) and from the controls at time zero and last time point. Dilute the samples into 950 μL of ice-cold PBS to halt neutrophil activity.

6. After incubation, place on melting ice (*see* **Note 10**).
7. Centrifuge experimental samples at 100 × *g* for 5 min at 4 °C using a swing-out rotor (*see* **Note 20**).
8. Collect the supernatant, being careful not to disturb the neutrophil pellet (*see* **Note 21**).
9. Wash the pellet twice more with 400 µL ice-cold PBS (100 × *g*, 5 min, 4 °C), pooling the supernatants. The pooled supernatant contains the bacteria that have not been phagocytosed (*extracellular* bacteria), while the phagocytosed bacteria are in the neutrophil pellet (*intracellular* bacteria).
10. Suspend all pellets to a volume of 950 µL in pH 11 water. Let stand at room temperature for 5–10 min then vortex briefly (*see* **Note 23**).
11. Treat with DNase as described above in Subheading 3.3.1, **step 11** (*see* **Notes 12** and **13**).
12. Dilute each sample, including supernatants and controls, in ice-cold pH 11 water to give a bacterial concentration of ~5,000 CFU/mL (refer to Table 2, *see* **Note 19**).
13. Spread 20 µL on half of an agar plate, giving ~100 CFU per half plate. Plate at least four half plates per sample.

Table 2
Dilution guidelines for the two-step colony counting protocol

Dilutions for two-step protocol								
	Sample							
	Control		Extracellular			Intracellular		
	0 min	20 min	5 min	10 min	20 min	5 min	10 min	20 min
Approx. undiluted concentration/mL[a]	1×10^8	1×10^8	4×10^7	3×10^7	1×10^7	2×10^7	2×10^7	1×10^7
Dilution due to sample processing[b]	20×	20×	30×	30×	30×	20×	20×	20×
Dilution incurred by plating 20 µL[b]	50×	50×	50×	50×	50×	50×	50×	50×
Additional dilution required to get approx 100 bacteria per 20 µL[c]	1,000×	1,000×	267×	200×	67×	200×	200×	100×
Total dilution factor	1×10^6	1×10^6	4×10^5	3×10^5	1×10^5	2×10^5	2×10^5	1×10^5

[a]From experience, these are the approximate bacterial concentrations expected at time of sampling. These values are likely to vary under different conditions. If the numbers of bacteria detected are too high or low to make accurate colony counts, the additional dilutions should be adjusted accordingly
[b]These are dilutions that will be automatically incurred through following the protocol as written
[c]These are the further dilutions required in the second to last step of either the one-step or two-step protocol

14. Incubate the plates overnight at 37 °C and count the number of colonies formed.
15. Add the raw data and the dilution factors to the appropriate cells in the Excel spreadsheet provided in the *Supplementary material*. This file contains instructions for its use.

3.4.3 Kinetic Basis for Data Analysis of the Two-Step Assay

1. Using data obtained with the two-step protocol, killing can be quantified using a kinetic analysis. As both phagocytosis and killing approximate first order processes [10], rate constants for these processes can be calculated.
2. The number of extracellular bacteria (A) decreases with time, while the number of viable intracellular bacteria (B) initially increases but then decreases as the bacteria are killed (C). These two events can be represented as occurring in series.

$$A \xrightarrow{k_p} B \xrightarrow{k_k} C$$

By obtaining values for A and B at different time points, rate constants for phagocytosis (k_p) and killing (k_k) can be calculated.

3. Phagocytosis and killing are represented by Eqs. 1 and 2, which can be integrated to give Eqs. 3 and 4, where A_0 = the initial number of bacteria added to the system and t = time.

$$\frac{\partial[A]}{\partial t} = k_p[A] \tag{1}$$

$$\frac{\partial[B]}{\partial t} = k_p[A] - k_k[B] \tag{2}$$

$$A = A_0 e^{-k_p t} \tag{3}$$

$$B = \frac{A_0 k_p}{k_k - k_p}\left(e^{-k_p t} - e^{-k_k t}\right) \tag{4}$$

4. The calculation of rate constants requires that both processes follow first-order kinetics (*see* **Note 24**). Solving for k_p from Eq. 3 involves obtaining the slope of a semi-log plot of A with time. A linear fit confirms that phagocytosis follows first-order kinetics.
5. To calculate k_k, Eq. 4 can be rearranged and solved using the Lambert W function ($W(X)$). The solution to the Lambert W function can be determined using a mathematical software package or can be calculated as described in the *Supplementary material*. The k_k values for each time point are then averaged, giving an overall k_k value. k_p and k_k can also be converted to half-lives of phagocytosis and killing using the equation $t_{1/2} = \ln(2)/k$ min.
6. Figure 3 shows the graphical outputs obtained after several steps of the calculation are completed. Data for these analyses

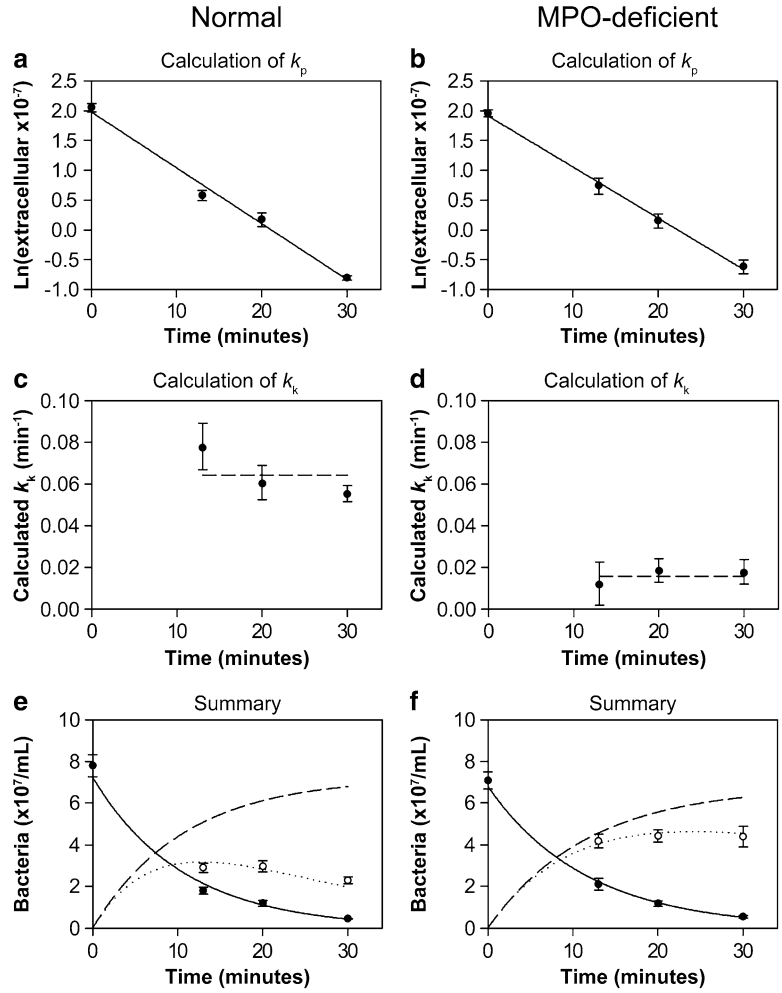

Fig. 3 Calculation of rate constants for phagocytosis (k_p) and killing (k_k) of *S. aureus* using two-step protocol results. Colony counts of control, extracellular and intracellular bacteria were obtained using the two-step protocol with neutrophils from a healthy and an MPO-deficient donor. These have been converted back to bacterial concentrations using the appropriate dilution factors and adjusted at each time according to the growth of control bacteria. (**a** and **b**) k_p was determined from a semi-log plot of extracellular bacteria with time, where the slope of the regression line is equal to k_p. In this example $k_p = 0.094$ min^{-1}, $t_{1/2} = 7.4$ min and $k_p = 0.085$ min^{-1}, $t_{1/2} = 8.1$ min for normal and MPO-deficient, respectively. (**c** and **d**) Rate constants of killing (k_k) calculated for each sampling time. The *dashed line* is the mean k_k. In this example $k_k = 0.064$ min^{-1}, $t_{1/2} = 11$ min and $k_k = 0.016$ min^{-1}, $t_{1/2} = 44$ min for normal and MPO-deficient, respectively. The error bars in this graph reflect the error in the intracellular colony counts and the degree of phagocytosis. When limited phagocytosis has occurred, a small variation in the intracellular colony counts will have a much larger effect on the calculated k_k value than if a lot of bacteria have been phagocytosed. (**e** and **f**) Theoretical curves of extracellular (*solid*) and intracellular bacteria (*dotted*) were generated using the calculated rate constants and the experimentally obtained values for both extracellular (*filled circle*) and intracellular (*open circle*) bacteria. The *dashed line* represents the expected number of viable intracellular bacteria if none were killed

were obtained in a two-step assay using neutrophils from a healthy and an MPO-deficient donor. While the rate of phagocytosis is similar between donors, the rate of killing is reduced in MPO-deficient neutrophils.

4 Notes

1. We have found that exciting $DiOC_2(3)$ by scanning from 350 to 550 nm and detecting the emission at 700 nm, rather than measuring at the excitation maximum of 482 nm, minimizes the interference of neutrophil fluorescence which can be a problem in this assay.
2. In the $DiOC_2(3)$ assay, sterility is not important once the neutrophils have been lysed as the effects of any contamination at this stage will be negligible. However, in the CFU assay all reagents and equipment should be sterilized before use. Handling can be undertaken on the bench since contamination will be very minor in comparison to the numbers of experimental bacteria present. Aseptic technique should be used when plating samples to avoid plate contamination with airborne microorganisms.
3. We use dextran sedimentation and Ficoll-Hypaque density-gradient separation, followed by hypotonic lysis of erythrocytes. This is gentler than ammonium chloride lysis and helps to preserve neutrophil function.
4. It is important to remove clumped bacteria that otherwise can pellet with the neutrophils during the differential centrifugation step in the two-step protocol.
5. This value is critical for accuracy. Therefore, four to six replicates are prepared and their fluorescence averaged.
6. As the fluorescence of lysed neutrophils is above background, this value must be subtracted from the fluorescence of neutrophils plus bacteria.
7. Alternative bacteria to neutrophil ratios can be used but at ratios <10:1 the $DiOC_2(3)$ assay loses sensitivity.
8. The time points at which viable bacteria are measured should be selected to coincide with the period when most of the phagocytosis and killing occurs. For *S. aureus*, sampling up to 30 min is appropriate [10]. Samples taken at longer times generally show little further reduction in bacterial numbers as the rate of killing begins to decrease. The killing mechanisms at these later times may differ from those functioning during the initial period when the bulk of the bacteria are killed. If using other bacterial species or ratios it may be necessary to adjust the sampling times. Under conditions where phagocytosis is

slow, rates of killing at early time points are variable (*see* "k_k variability at different time points" in *Supplementary material*). Therefore, under these conditions it is better to start measurements later (e.g., 10–15 min).

9. Continuous, slow, end-over-end rotation of the tubes is very important to prevent the neutrophils from sedimenting and clumping, and to ensure continual contact between neutrophils and uningested bacteria. The rotation speed must not be too vigorous or neutrophil function is disrupted.
10. Melting ice rather than fresh ice cools the samples rapidly to halt further phagocytosis and killing.
11. Dilution into pH 11 water results in osmotic lysis of the neutrophils without affecting viability of *S. aureus*. The sensitivity of other bacteria to pH 11 water should be checked.
12. The presence of released DNA after pH 11 water lysis interferes with a subsequent centrifugation step. Therefore, the lysate solution is brought to an appropriate pH, and magnesium and calcium are added for optimized DNase activity. The final concentration of DNase is approximately 100 U/mL.
13. We find that the DNA degrades better over this time if the samples are mixed by pipetting half-way through the incubation.
14. It is critical to transfer the total contents of each tube to the 96-well plate. Leaving a small volume behind, such as 10 μL, will significantly affect the fluorescence measured.
15. We use a Thermo Scientific VARIOSKAN® Flash plate reader, scanning the excitation between 350 and 550 nm and measuring the emission at 700 nm. The area under the curve between 380 and 430 nm is then calculated, using the macro function in SigmaPlot, to minimize the interference of the neutrophil fluorescence. Within this wavelength range neutrophil background fluorescence is lower and a good bacterial signal is observed.
16. The greatest variation in the CFU assay is incurred during plating. Therefore, it is better to plate more aliquots from a single replicate than to plate less aliquots of two or more replicates. This contrasts with the $DiOC_2(3)$ assay where the greatest variation is observed between replicates.
17. When water at neutral pH is used, there is incomplete lysis of the neutrophils and ineffective dispersal of bacteria associated with the cell debris [11]. This results in an overestimation of bactericidal activity due to multiple bacteria being counted as only a single colony. In this situation, partial defects may be overlooked and complete defects may appear as only partial. To overcome this problem, pH 11 water is used [11, 12]. Decleva et al. [11] found this to be more effective than other

lysis methods, including dilution into neutral pH water or into detergent-containing buffer. Experiments in our laboratory have confirmed that pH 11 water is more effective than 0.1 % saponin. In addition, use of pH 11 water for all subsequent dilution steps seems to avoid the clumping of *S. aureus* that is sometimes seen with PBS.

18. DNA, often released after vortexing lysed neutrophils, presents a problem in the CFU assay. Bacteria become trapped in the DNA, hindering their dispersal and causing bactericidal activity to be overestimated.
19. If different bacteria-neutrophil ratios are used, dilutions for the colony counting assay must be adjusted accordingly.
20. This is a low speed centrifugation to sediment the neutrophils and their ingested bacteria, but not extracellular bacteria. A small, diffuse, white pellet of neutrophils should be seen in the experimental tubes and no bacterial pellet in the control tubes. If this is not the case, the differential centrifugation speed should be adjusted.
21. As the centrifugation speed is low, the pellet does not adhere strongly to the tube wall and care must be taken to avoid disturbing it as the supernatant is removed.
22. Ideally there should not be any neutrophils in the pooled supernatants. However, slight contamination may occur. The fluorescence of even a small percentage of live neutrophils will lead to an overestimation of extracellular bacteria. Therefore, saponin is added to lyse the neutrophils. The fluorescence of a small percentage of lysed neutrophils will be minimal and should not affect results.
23. If the residual volume over the pellets is greater than 100 μL, the amount of pH11 water added may need to be increased to maintain the pH at or near to 11. The volume of DNase mix will also need to be increased. This needs to be accounted for when calculating the final dilutions.
24. There may be some conditions when this first-order relationship does not hold. Results can then be presented as percentages of bacteria phagocytosed, and percentages of phagocytosed bacteria that have been killed at any time point. Impaired killing will be evident, but the degree of quantification is much less than with kinetic analysis, as it will be different at each time point.

Acknowledgements

This work was supported by the Health Research Council of New Zealand.

References

1. Winterbourn CC, Kettle AJ (2013) Redox reactions and microbial killing in the neutrophil phagosome. Antioxid Redox Signal 18:642–660
2. Nauseef WM (2007) How human neutrophils kill and degrade microbes: an integrated view. Immunol Rev 219:88–102
3. Segal AW (2008) The function of the NADPH oxidase of phagocytes and its relationship to other NOXs in plants, invertebrates, and mammals. Int J Biochem Cell Biol 40:604–618
4. Hampton MB, Winterbourn CC (1999) Methods for quantifying phagocytosis and bacterial killing by human neutrophils. J Immunol Methods 232:15–22
5. Shapiro HM (2008) Flow cytometry of bacterial membrane potential and permeability. Methods Mol Med 142:175–186
6. Gentry DR, Wilding I, Johnson JM et al (2010) A rapid microtiter plate assay for measuring the effect of compounds on Staphylococcus aureus membrane potential. J Microbiol Methods 83:254–256
7. Silverman JA, Perlmutter NG, Shapiro HM (2003) Correlation of daptomycin bactericidal activity and membrane depolarization in *Staphylococcus aureus*. Antimicrob Agents Chemother 47:2538–2544
8. Leijh PCJ, van Furth R, van Zwet TL (1986) In vitro determination of phagocytosis and intracellular killing by polymorphonuclear and mononuclear phagocytes, Handbook of experimental immunology. Blackwell Scientific Publishers, Oxford, pp 41–46.21
9. Tiden AK, Sjogren T, Svensson M et al (2011) 2-thioxanthines are mechanism-based inactivators of myeloperoxidase that block oxidative stress during inflammation. J Biol Chem 286:37578–37589
10. Hampton MB, Vissers MC, Winterbourn CC (1994) A single assay for measuring the rates of phagocytosis and bacterial killing by neutrophils. J Leukoc Biol 55:147–152
11. Decleva E, Menegazzi R, Busetto S et al (2006) Common methodology is inadequate for studies on the microbicidal activity of neutrophils. J Leukoc Biol 79:87–94
12. Gargan RA, Brumfitt W, Hamilton-Miller JM (1989) Failure of water to lyse polymorphonuclear neutrophils completely. Role of pH and implications for assessment of bacterial killing. J Immunol Methods 124:289–291

Chapter 20

Induction and Quantification of Neutrophil Extracellular Traps

Alejandro Sanchez Gonzalez, Bart W. Bardoel, Christopher J. Harbort, and Arturo Zychlinsky

Abstract

Neutrophil extracellular trap (NET) formation is a recently discovered process in the field of innate immunity. It is important to have consistent standards in inducing and quantifying NET formation to compare data from different labs in this new area of investigation. Here we describe the conditions of neutrophil isolation from peripheral blood and stimulation that we find allow the study of NETosis in vitro. The criteria for conclusively identifying the process of NETosis, and the pros and cons of various quantification methods are discussed.

Key words Neutrophil extracellular traps, NET quantification, Neutrophil isolation, Immunofluorescence

1 Introduction

Stimulated neutrophils can undergo a novel form of cell death resulting in the extracellular release of NETs—structures composed of DNA complexed with antimicrobial proteins [1]. During NETosis, the nucleus expands within the cell and mixes with the cytoplasm before being released into the extracellular space. This mechanism has been shown to be dependent upon reactive oxygen species (ROS), myeloperoxidase (MPO), and neutrophil elastase (NE) [2, 3]. NETs contribute to immunity by trapping microbes and aiding in their elimination, and have been shown to be involved in infections with many diverse pathogens. Additionally, they are implicated in the development and pathogenesis of autoimmune diseases, such as systemic lupus erythematosus (SLE) [4, 5].

For in vitro assays of NETosis, neutrophils are isolated from fresh peripheral blood by density gradient separation. Purified neutrophils are seeded in tissue culture plates or on glass coverslips and activated with phorbol myristate acetate (PMA), microbes, or

Mark T. Quinn and Frank R. DeLeo (eds.), *Neutrophil Methods and Protocols*, Methods in Molecular Biology, vol. 1124,
DOI 10.1007/978-1-62703-845-4_20,

other compounds of interest. Conclusive demonstration of NET formation requires multiple assays. Fluorescence assays to measure extracellular DNA in supernatants after DNase digestion should be interpreted cautiously, as they provide no information about how the cells died, and overlook cells undergoing NETosis that have not yet released their trap. By immunofluorescence, NETs appear as clouds of DNA that stain for granular proteins such as MPO and NE, and are larger than the cells they derive from. Care must be taken during fixing and staining to preserve the cloud-like NET structure, or else NETs will appear as elongated, string-like structures which affect nuclear area quantification. Cells undergoing NETosis, but that have not yet released their trap, display delobulated and expanded nuclei. By quantifying the nuclear area, NET formation prior to DNA release can be quantified robustly. However, as this assay cannot differentiate unactivated from dead neutrophils, live microscopy and staining with nonpermeable DNA dyes, such as Sytox green, without fixing can be performed to determine if cytotoxic effects kill cells before NETosis is initiated. Additionally, to support an argument that extracellular DNA is released as the result of NETosis, as opposed to cell lysis or other mechanisms, it should be examined whether or not the DNA release is dependent upon ROS, MPO, and/or NE activity.

2 Materials

1. Percoll.
2. Phosphate buffered saline (PBS).
3. 10× PBS.
4. 100 % Isotonic Percoll solution: 36 mL of Percoll, 4 mL of 10× PBS.
5. 85 % Isotonic Percoll solution: 34 mL of 100 % Isotonic Percoll, 6 mL of 10× PBS.
6. 80 % Isotonic Percoll solution: 32 mL of 100 % Isotonic Percoll, 8 mL of 10× PBS.
7. 75 % Isotonic Percoll solution: 30 mL of 100 % Isotonic Percoll, 10 mL of 10× PBS.
8. 70 % Isotonic Percoll solution: 28 mL of 100 % Isotonic Percoll, 12 mL of 10× PBS.
9. 65 % Isotonic Percoll solution: 26 mL of 100 % Isotonic Percoll, 14 mL of 10× PBS.
10. EDTA tubes.
11. Fresh blood.
12. Histopaque 1119.

13. RPMI-1640 medium (RPMI).
14. Human serum albumin.
15. HEPES.
16. Phorbol 12-myristate 13-acetate (PMA).
17. Antibody incubation buffer: 3 % BSA in PBS.
18. Washing buffer: 3 % BSA in PBS.
19. Blocking buffer: 3 % normal goat serum, 3 % cold water fish gelatin, 1 % BSA, 0.05 % Tween 20 in PBS.
20. Permeabilization buffer: 0.5 % Triton X-100 in blocking buffer (*see* **Note 1**).
21. Sytox Green.
22. Albumin Fraction V (BSA).
23. 13 mm Coverslips 13 mm.
24. Triton X-100.
25. Aqua Poly/Mount (Polysciences).
26. Tween 20.
27. Goat serum.
28. Cold water fish gelatin.
29. Hoechst 33342.
30. Donkey anti-mouse Cy3.
31. Subnucleosomal complex antibody [6].
32. Fluorescent microscope with appropriate filters and camera.

3 Methods

3.1 Isolation of Peripheral Blood Neutrophils Using a Percoll Density Gradient

Isolation of neutrophils can be performed in several different ways. The method described below results in highly purified unactivated neutrophils that have minimal background in NET formation. Perform all steps at room temperature.

1. Collect whole blood in tubes with EDTA as anticoagulant. The expected yield from 50 mL of blood is 10^8 cells (*see* **Note 2**).
2. Carefully layer 7 mL of blood on top of equal amount of Histopaque 1119 in a 15-mL conical polypropylene centrifugation tube.
3. Spin tubes at 800 × *g* for 20 min. Use centrifuge program with slow braking to prevent mixture of layers.
4. Discard the lymphocytes and monocytes (upper cell layer) and collect the lower peripheral blood neutrophils (PMN) layer, which is the diffuse, red phase directly above the red blood cell pellet with a plastic Pasteur pipette (Fig. 1a).

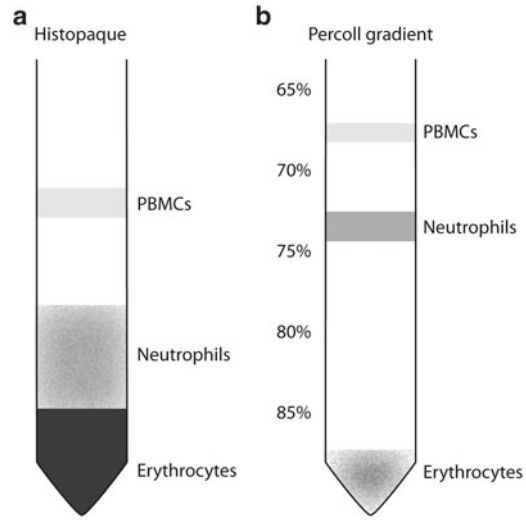

Fig. 1 Layering of cells after Histopaque separation (**a**) and Percoll density gradient (**b**)

5. Transfer the collected PMNs from each tube to a fresh 15-mL tube and fill with PBS to wash the cells.
6. Centrifuge cells at 300 × *g* for 10 min.
7. Prepare Percoll gradients by carefully layering 2 mL each of 85, 80, 75, 70, and 65 % isotonic Percoll solutions on top of each other in a 15 mL centrifugation tube, starting with 85 % solution at the bottom.
8. Resuspend and pool cell pellets originating from 50 mL of whole blood in 4 mL of PBS and transfer 2 mL onto the top of each Percoll gradient.
9. Centrifuge gradients for 20 min at 800 × *g*. Use a centrifuge program with slow acceleration and brake to prevent disturbance of the gradient.
10. Collect the interphase between 70 and 75 % Percoll layers in a 15-mL tube (Fig. 1b).
11. Fill tube with PBS and centrifuge at 300 × *g* for 10 min.
12. Resuspend cells in RPMI + 10 mM HEPES + 0.5 % HSA.
13. Determine the concentration of neutrophils.

3.2 NET Induction

1. Seed freshly isolated neutrophils at a density of 10^6 cells/mL in RPMI + 10 mM HEPES + 0.5 % HSA (e.g., 300 µl cell suspension in wells of a 24-well plate).
2. Incubate neutrophils for 20 min at 37 °C to allow them to adhere.

3. Add 25 nM PMA, or other compound of interest, to the neutrophils to induce NET formation. Include unstimulated controls to check for background NET formation (*see* **Note 3**).
4. Incubate for 3–4 h and analyze the morphology of the cells under the microscope. Neutrophil morphology changes after about 2 h into NET formation.
5. Add 160 nM Sytox to each well, incubate in dark for 10 min at room temperature. Prevent agitation of the plate (*see* **Note 4**).

3.3 Quantification of Nuclear Expansion

The present protocol to quantify the NET formation by nuclear area expansion was described and used in Papayannopoulos et al. [2, 3].

1. Take images of each sample by using an inverted fluorescence microscope. Capture images of the fluorescence and of its corresponding phase contrast of at least five random fields with the FITC filter (ex = 480/495; em = 535/50) using the 20× objective (*see* **Note 5**).
2. The image processing is made with ImageJ (version 1.47 h or newer) (*see* **Note 6**).
3. Open the phase contrast image of the sample and count the total number of cells. This can be done by using the cell counter plug-in of the program and entering the number in an Excel document as the total number of cells (Plug-in → Analyze → Cell counter → Initialize → Select type 1 → count; *see* **Note 7**).
4. Open and transform the fluorescence Sytox image into a black and white 8-bit image (Image → Type → 8-bit).
5. Adjust the image brightness and contrast in order to make clearly discernible the whole cells against a noiseless background, click Apply (Image → Adjust → Brightness/Contrast → Apply) (*see* **Note 8**).
6. Adjust the image threshold: in the image tab select adjust and then threshold, in the settings select Default, Red and Dark background. Move the upper sliding tab until the red color cover completely the cells avoiding the appearance of noise in the image, click Apply (Image → Adjust → Threshold (select Default, Red and Dark background) → Apply) (*see* **Note 9**).
7. Using the drawing tools (located under the alternated macro tool set) eliminate the cells on the border and noise that could appear (*see* **Note 10**). Additionally, sometimes the program cannot divide the cells properly and it is absolutely necessary to do it manually; for this, select the paintbrush tool and proceed to separate the cells manually (*see* **Note 11**).
8. Analyze the image to obtain the pixel area corresponding to each cell. Under Analyze tab select "Analyze particles," set the

Size values to "100-Infinity," "Show Outlines" and check "Display results" and click OK [Analyze → Analyze Particles (set Size: 100-Infinity, Show: Outlines and check Display results) → OK] (*see* **Note 12**).

9. New windows appear, and in the one named "Drawing of (file name)" are shown the outlines of each cell. If the cells were divided properly (**step 9**), the program should be able to count individual cells (denoted by a red number inside each cell); if not, close the new windows, proceed to correct the mistakes and repeat **step 10**. Once satisfied, copy the data for the event number and area shown in the Results window and paste it into the Excel document under a new column named "ImageJ results."
10. In Excel, create a BINS array, this is a range of increasing numbers that covers the lower and maximum values obtained for the Area of all the treatments.
11. In the next cell calculate the frequency of each data in the treatment, to do this, insert the function "FREQUENCY" and enter the range of data for the area of the treatment in the Data_array and the range of data for the BINS on the Bins_array and click OK. The function will only return the first value; from this extend the selection for the whole array of BINS values (*see* **Note 13**), now click on the formula and enter the command <Ctrl> + <Shift> + <Enter>. Now the correct frequencies for the data appear.
12. Convert the data to a percentage of Sytox-positive cells by dividing the frequency values by the total amount of cells determined from the phase contrast images.
13. Plot the percentage of Sytox-positive cells within the DNA area range in μm^2 (Fig. 2) (*see* **Note 14**).
14. A cell that presents decondensed nuclei and exceeds the normal average area of an unstimulated neutrophil (80 μm^2) can be considered NETotic (*see* **Note 15**).

It is now recognized that NET formation consists of many stages, and this method quantifies neutrophils that are undergoing NETosis by directly measuring nuclear decondensation. This method is particularly useful with inducers that promote a high quantity of NETs (i.e., PMA). The main drawback of this method is that it cannot quantify NETs once they are released, and hence is restricted to measure cells in the process of NETosis. NETs that are already expanded cannot be quantified because the thresholds of the images cannot be set due of their stringy character.

3.4 Immunofluorescence

The present protocol has been optimized to stain NETs using low concentrations of antibodies (Fig. 3).

1. Prepare all antibodies by dilution in antibody incubation buffer.

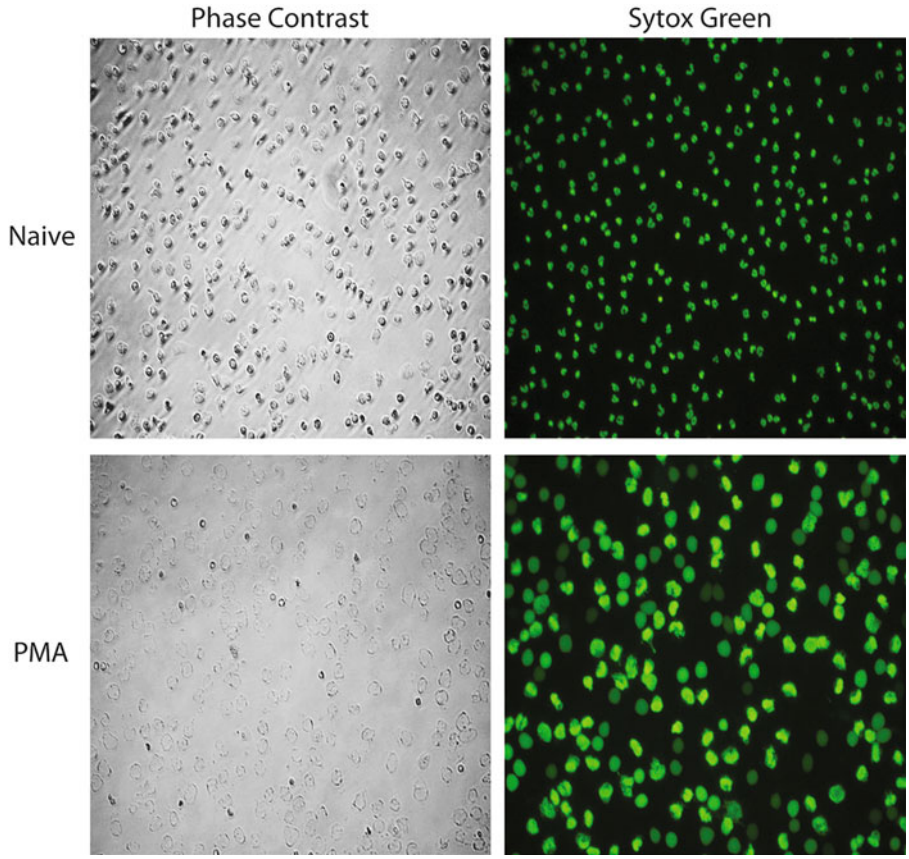

Fig. 2 NET detection with Sytox Green staining. The *left* column shows the phase contrast image of naive and PMA-stimulated neutrophils, whereas the *right* column shows the nuclear pattern of neutrophils after staining with Sytox

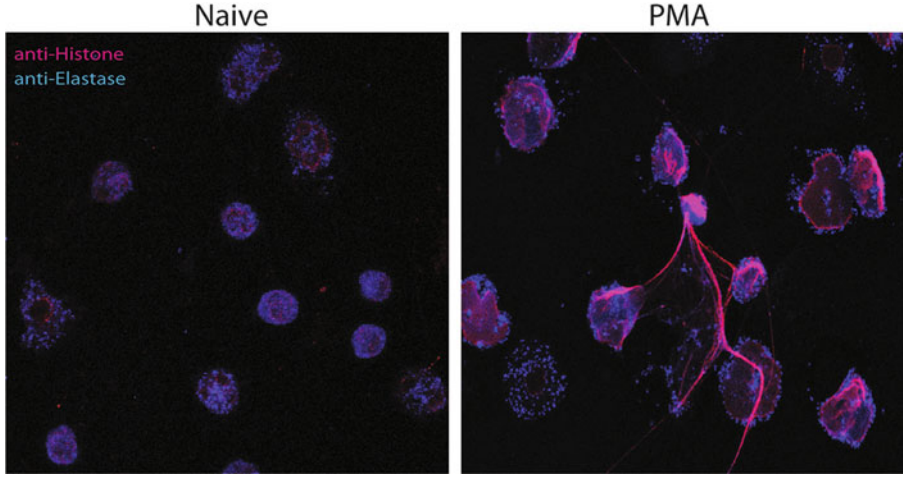

Fig. 3 Immunofluorescence of NETs. Neutrophils were stained with anti-elastase (*blue*) and anti-histone (*red*). The staining pattern for naive neutrophils and after 4 h stimulation with 25 nM PMA is shown (Color figure online)

2. Seed 10^5 cells/well in RPMI supplemented with glutamine/pyruvate/0.5 % HSA) over 13 mm coverslips in 24-well plates.
3. Add 25 nM PMA and incubate for 3–4 h at 37 °C to induce NET formation.
4. Fix the cells with 4 % paraformaldehyde (final concentration).
5. Incubate for 10 min at room temperature.
6. Wash carefully twice with 300 μL of washing buffer.
7. Permeabilize the cells by adding enough permeabilization buffer to cover each coverslip. Incubate for 5 min at room temperature (*see* **Note 16**).
8. Wash three times with 300 μL of washing buffer.
9. Block nonspecific binding with blocking buffer. Incubate for 30 min at room temperature.
10. Wash twice with 300 μL of washing buffer.
11. Prepare a humid chamber by covering the bottom of a tray with wet paper towels, discard the excess water and stretch to eliminate wrinkles. Cut Parafilm of the proper size and put over the wet paper towels adding water again and eliminating the excess.
12. Using tweezers and a needle, take out the coverslips from the wells and place in the humid chamber (*see* **Note 17**).
13. Add 100 μL of washing buffer to each slide (*see* **Note 18**).
14. Add the primary antibody diluted in antibody incubation buffer (100 μL) and incubate for 1 h at 37 °C.
15. Wash three times with 100 μL of washing buffer (*see* **Note 19**).
16. If directly labeled antibodies are used, proceed to **step 18**.
17. Add the fluorescent secondary antibody and incubate for 45 min at 37 °C in the dark (*see* **Note 20**).
18. Wash three times with 100 μL of washing buffer.
19. Remove coverslips from well and mount on Aqua Poly/Mount (*see* **Note 21**).
20. Seal the coverslips with nail polish and store at 4 °C until analysis.
21. Acquire the images (*see* **Note 22**).

3.5 Automated Quantification of NETs

This method is suited to calculate the percentage of neutrophils that undergo NETosis in an automatic and operator independent way [7]. Analysis of larger image sets can be performed with this method, however NET strings cannot be divided automatically by the program, resulting in an underestimation of NETosis.

1. Include neutrophils with PMA for 10 min as a control to determine background staining.

2. Stain neutrophils with antibody directed against the subnucleosomal complex, consisting of histones H2A and H2B together with DNA. Use the same method described in the immunofluorescence section.
3. Stain using a secondary antibody with a compatible fluorophore.
4. Wash samples with distilled water.
5. Incubate with 100 ng/mL Hoechst 33342 in distilled water for 10 min.
6. Wash samples with distilled water before mounting.
7. Take five images (resolution 1,360 × 1,024) from different regions from each coverslip with a fluorescence microscope using a 10× lens (*see* **Note 23**).
8. Calibrate on a bright representative sample and keep exposure time for all channels constant for all images of the experiment.
9. Import images in ImageJ as an image stack. File → Import → Image sequence and select a file in the folder of the experiment and use the field "file name contains" to select images with the same staining to generate a stack.
10. Transform all images to 8-bit and save the image stacks.
11. Determine total number of cells per image by binarizing the Hoechst 33342 stack using the Bernsen automatic local threshold function set to radius 15 and parameter 1–35 (Image → Adjust → Auto local threshold).
12. Set (Analyze →) Automatic particle analysis to "20 pixels-infinity" (*see* **Note 23**) and check "stack", "pixel unit", and choose "bare outlines". Save the output values representing the number of cells per image in an Excel file.
13. Switch to the stacks stained for chromatin to determine number of NET events per image.
14. Set the threshold (Image → Adjust → Threshold) in such a way that an image of neutrophils stimulated with PMA for 10 min is negative, except for a few cells (Setting upper value usually around 50 and lower value to 255).
15. Analyze particles with setting size from 75 pixels to infinity (check "Pixel units", *see* **Note 23**), show "Bare outlines", and check "Summarize".
16. Save the output values in the same Excel file as for the Hoechst staining.
17. Save the image showing the outlines of the counted events and create an overlay of this image with the saved image stacks of point 7 to check if the program recognized neutrophils undergoing NETosis appropriately.

18. Calculate percentage of NET forming neutrophils by dividing the events counted in the chromatin channel (multiplied by 100) by the events counted in the Hoechst channel.

4 Notes

1. Vortex the solution until no detergent remnants can be seen.
2. Use fresh blood for neutrophil isolation. Heparin can be used as alternative anticoagulant.
3. Several other NET inducers other than PMA have been described; however PMA is the most robust reproducible stimulus to induce NET formation and serves as a good positive control.
4. Do not add the solution directly over the medium since we have observed that letting the drop fall directly on the cells and excessive agitation can induce false positives. This can be solved by adding the Sytox very slowly by the side of the well just above the interphase of the medium and allowing the drop to fall by gravity.
5. The magnification used to take the pictures determines the value range needed to calculate the DNA Area, thus, at less magnification a smaller range of DNA area values are needed and vice versa. In this protocol pictures taken at 20× were used. Additionally, in order to make the nuclear area quantification simpler it is really important to avoid taking images of air bubbles in the sample, and more importantly to avoid the edges of the well, since in these areas high numbers of preactivated cells and thus false positives can be observed.
6. Rasband, W.S., ImageJ, US National Institutes of Health, Bethesda, Maryland, USA, http://imagej.nih.gov/ij/, 1997–2012.
7. In this step it is important to only count the complete cells and not the ones appearing just partially in the border of the image to best avoid artifacts in the quantification.
8. At this point it is important to avoid excessive noise in the image but be able to observe clearly the periphery of the cells against the background since this can make the threshold step difficult.
9. The noise can be easily observed as small red dots in the periphery of the cells initially and in the whole image later.
10. In this step the noise can be observed as small black dots not corresponding to the size of any cell.

11. It is useful to compare the corresponding original fluorescence image side by side with the working one to divide the cells manually easily. Select the same color as that in the background to draw the line by first clicking over the color picker icon and then over any space of the background of the working image. To divide the cells more precisely set the paintbrush tool width to 3; this can be done by right clicking over the paintbrush tool.
12. The pixel size value is important to diminish the probability of counting noise by the program. We find that establishing the pixel size value to 100-Infinity for the majority of our images is useful; however, this value should be modified for particular cases.
13. This first set of values is incorrect (denoted by the program with a mark in the upper left corner of each cell) because this is an array function and therefore requires the input of a CSE Excel command to work properly. For this, with the area of selection still over the cells, click on the formula and enter the command <Ctrl> + <Shift> + <Enter>.
14. To convert the data for the BINS array into DNA range divide this value by the estimated diameter in an unstimulated stage of the human neutrophils (10 μm).
15. It is calculated that the average area of a resting neutrophil to be approximately 80 μm^2 (assuming a circular shape and using $\pi \times r^2$).
16. Be sure that the permeabilization solution covers the cells completely.
17. Do this step very carefully to avoid breaking the coverslip and always be sure to keep the cells facing up in all the next steps.
18. Add the washing buffer very carefully on top of the coverslip trying to avoid spills.
19. Add the solution as in **Note 5** and aspirate the liquid with a pipette slowly by the side of the coverslip. Do the same for the next washing steps.
20. When using Alexa conjugated antibodies, spin down the diluted antibody for 30 s at $300 \times g$ and add 100 μL of this supernatant to each coverslip to get rid of fluorescent crystals in the preparation.
21. First place a drop of the mounting solution on the slide and then place the coverslip on top with the cells facing the drop. Once the coverslip touches the drop release it very carefully avoiding further manipulation. At this point you will see the mounting solution slowly cover the whole coverslip.

22. Be very careful at this step to prevent the microscope objective from touching the coverslip.
23. This method is optimized for images with a resolution of 0.973 pixels/μm. Adjust the parameters of **steps 9** and **12** when analyzing images with a different resolution.

References

1. Brinkmann V, Reichard U, Goosmann C, Fauler B, Uhlemann Y, Weiss DS, Weinrauch Y, Zychlinsky A (2004) Neutrophil extracellular traps kill bacteria. Science 303(5663):1532–1535. doi:10.1126/science.1092385
2. Metzler KD, Fuchs TA, Nauseef WM, Reumaux D, Roesler J, Schulze I, Wahn V, Papayannopoulos V, Zychlinsky A (2011) Myeloperoxidase is required for neutrophil extracellular trap formation: implications for innate immunity. Blood 117(3):953–959. doi:10.1182/blood-2010-06-290171
3. Papayannopoulos V, Metzler KD, Hakkim A, Zychlinsky A (2010) Neutrophil elastase and myeloperoxidase regulate the formation of neutrophil extracellular traps. J Cell Biol 191(3):677–691. doi:10.1083/jcb.201006052
4. Hakkim A, Furnrohr BG, Amann K, Laube B, Abed UA, Brinkmann V, Herrmann M, Voll RE, Zychlinsky A (2010) Impairment of neutrophil extracellular trap degradation is associated with lupus nephritis. Proc Natl Acad Sci USA 107(21):9813–9818. doi:10.1073/pnas.0909927107
5. Lande R, Ganguly D, Facchinetti V, Frasca L, Conrad C, Gregorio J, Meller S, Chamilos G, Sebasigari R, Riccieri V, Bassett R, Amuro H, Fukuhara S, Ito T, Liu YJ, Gilliet M (2011) Neutrophils activate plasmacytoid dendritic cells by releasing self-DNA–peptide complexes in systemic lupus erythematosus. Sci Transl Med 3(73):73–19. doi:10.1126/scitranslmed.3001180
6. Losman MJ, Fasy TM, Novick KE, Monestier M (1992) Monoclonal autoantibodies to subnucleosomes from a MRL/Mp(−)+/+ mouse. Oligoclonality of the antibody response and recognition of a determinant composed of histones H2A, H2B, and DNA. J Immunol 148(5):1561–1569
7. Brinkmann V, Goosmann C, Kuhn LI, Zychlinsky A (2012) Automatic quantification of in vitro NET formation. Front Immunol 3:413. doi:10.3389/fimmu.2012.00413

Part VI

NADPH Oxidase and Production of Reactive Oxygen Species

Chapter 21

Measurement of Respiratory Burst Products, Released or Retained, During Activation of Professional Phagocytes

Johan Bylund, Halla Björnsdottir, Martina Sundqvist, Anna Karlsson, and Claes Dahlgren

Abstract

Activation of professional phagocytes, potent microbial killers of our innate immune system, is associated with an increase in cellular consumption of molecular oxygen (O_2). The consumed O_2 is utilized by an NADPH-oxidase to generate highly reactive oxygen species (ROS) by a one electron reduction, initially generating superoxide anion (O_2^-) that then dismutates to hydrogen peroxide (H_2O_2). The ROS are strongly bactericidal molecules but may also cause tissue destruction, and are capable of driving immune competent cells of both the innate and the adaptive immune systems into apoptosis. The development of basic techniques to measure/quantify ROS generation by phagocytes during activation of the respiratory burst is of great importance, and a large number of methods have been used for this purpose. A selection of methods, including chemiluminescence amplified by luminol or isoluminol, the absorbance change following reduction of cytochrome c, and the fluorescence increase upon oxidation of PHPA, are described in detail in this chapter with special emphasis on how to distinguish between ROS that are released extracellularly, and those that are retained within intracellular organelles. These techniques can be valuable tools in research spanning from basic phagocyte biology to more clinically oriented research on innate immune mechanisms and inflammation.

Key words Reactive oxygen species, Superoxide, Hydrogen peroxide, Myeloperoxidase, Intracellular NADPH-oxidase activity, Plasma membrane NADPH-oxidase activity, Subcellular granules, Chemiluminescence, Cytochrome c reduction, PHPA oxidation

1 Introduction

Professional phagocytes of the innate immune system increase their consumption of molecular oxygen (O_2), during phagocytosis of microbial intruders or upon interaction with inflammatory mediators. The electron transport system responsible for O_2 consumption, the NADPH-oxidase, is essential for protection against invading pathogens, as demonstrated by the susceptibility of persons with a nonfunctional oxidase, e.g., suffering from chronic granulomatous disease (CGD), to bacterial and fungal infections [1, 2] (*see* **Note 1**).

Mark T. Quinn and Frank R. DeLeo (eds.), *Neutrophil Methods and Protocols*, Methods in Molecular Biology, vol. 1124,
DOI 10.1007/978-1-62703-845-4_21, © Springer Science+Business Media, LLC 2014

In resting phagocytes, the cytosolic components of the NADPH-oxidase are separated from the two membrane-bound components that constitute the so-called flavocytochrome b. During phagocyte activation, the cytosolic and membrane components assemble to form a functional electron-transfer system, which ferries electrons over the membrane from cytosolic NADPH to O_2, forming superoxide anion (O_2^-) [3]. This primary product of the NADPH-oxidase, together with its initial metabolite, hydrogen peroxide (H_2O_2), is not sufficiently reactive to account for the bactericidal effects seen in phagocytes, but can be metabolized also into other reactive oxygen species (ROS) that are strongly antimicrobial (*see* **Note 2**).

Assembly of the NADPH-oxidase at the plasmalemma results in release of ROS to the extracellular milieu or intracellularly into a phagosome. It is however becoming increasingly evident that neutrophils are able to produce substantial amounts of intracellular ROS also in the total absence of phagosome formation (reviewed in ref. 4). In neutrophils, 80–85 % of the flavocytochrome b is localized in the membranes of the peroxidase-negative granules [5, 6], suggesting that NADPH-oxidase activation in granule membranes could explain these intracellular (non-phagosomal) ROS [7, 8]. The biological relevance of granule-localized, non-phagosomal ROS is still not clear, but they likely participate in cell signaling. Specific defects in intracellular ROS production have been described for neutrophils derived from distinct patients with hyper-inflammation as a common denominator. In neutrophils from a novel type of CGD, carrying a non-functional $p40^{phox}$ NADPH-oxidase component, extracellular ROS production was normal, whereas intracellular ROS was potently decreased [9]. Also, neutrophils from patients with the inflammatory syndrome SAPHO (synovitis, acne, pustulosis, hyperostosis, osteitis) displayed severely decreased intracellular ROS production while extracellular production was intact [10, 11].

Different agonists activate the two pools of NADPH-oxidase (in the plasma membrane or in the granules) differently, suggesting that the signaling as well as the molecular mechanisms for regulation differ depending on the localization of the oxidase [12–16]. Not much is known about the signals leading to the differential activation of the two pools of oxidase, but clearly $p40^{phox}$ is needed only for intracellular activation [9]. In addition, the dependency of PI-3-kinase activity in the two responses differs, as does the PKC isotype specificity [14, 17–19].

The importance of ROS for the antimicrobial and pathophysiological activity of phagocytes makes it essential to have access to adequate techniques for their analysis. Although there is an urgent need for better methods to measure the different types of ROS generated and to determine the precise subcellular site for their generation [20], we have for now, to rely on the techniques that

are at hand, with their pros and cons. Here we describe some basic, easy-to-perform methods that are frequently used to follow cellular production of ROS, not only in the extracellular milieu but also in intracellular compartments.

2 Materials

1. 5 M NaOH stock solution.
2. A balanced-salt solution, such as Krebs–Ringer phosphate buffer (KRG): 120 mM NaCl, 5 mM KCl, 1.7 mM KH_2PO_4, 8.3 mM Na_2HPO_4, 10 mM glucose, 1 mM $CaCl_2$, 1.5 mM $MgCl_2$, pH 7.3.
3. 5-Amino-2,3-dihydro-1,4-phtalazinedione (Luminol) solution: 50 mM luminol in freshly prepared 0.1 M NaOH (from 5 M stock). Luminol stock solution can be stored at room temperature, protected from light, for several months. Prepare 500 μM luminol working solution fresh on the day of the experiment.
4. 6-Amino-2,3-dihydro-1,4-phtalazinedione (Isoluminol) solution: 50 mM isoluminol in freshly prepared 0.1 M NaOH (from 5 M stock). Isoluminol stock solution can be stored at room temperature, protected from light, for several months. Prepare 500 μM isoluminol working solution fresh on the day of the experiment.
5. Horseradish peroxidase (HRP) solution: 80 U/mL HRP in physiological saline. Store in small aliquots at –20 °C.
6. *p*-Hydroxyphenylacetate (PHPA) solution: 10 mg/mL PHPA powder in physiological saline. The solution is acidic and should be pH adjusted to 7.3. Store in small aliquots at –70 °C.
7. Superoxide dismutase (SOD) solution: 5,000 U/mL SOD in physiological saline. Store in small aliquots at –70 °C.
8. Catalase solution: wash particulate catalase (Worthington) twice by suspending in H_2O and centrifugation at 15,000 × *g* for 10 min. Dissolve the final pellet in physiological saline at 200,000 U/mL. Store in small aliquots at –70 °C. It should be noticed that many catalase batches contain endotoxin in rather large amounts.
9. Sodium azide (NaN_3) solution: 10 mM NaN_3 in KRG. NaN_3 solution can be stored at 4 °C for several months.
10. Cytochrome C (cytC) solution: 15 mg/mL (~1.2 mM) cytC in KRG. Prepare solution fresh on the day of the experiment.
11. WST-1 (2-(4-iodophenyl)-3-(4-nitrophenyl)-5-(2,4-disulfophenyl)-2-tetrazolium, monosodium salt (Dojindo Laboratories, Kumamoto, Japan): 33 mg/mL (~5 mM) WST-1 in KRG. Prepare solution fresh on the day of the experiment.

12. Dihydrorhodamine 123 (DHR123) solution: 5 mg/mL DHR123 in dimethyl sulfoxide (DMSO). Store in small aliquots at −20 °C. Prepare 10 μg/mL working solution fresh on the day of the experiment.
13. Diphenyleneiodonium chloride (DPI) solution: 10 mM DPI, a widely used inhibitor of NADPH-oxidase activity, in DMSO. This stock solution can be kept at room temperature protected from light for very long time. Prepare the working solution fresh on the day of the experiment by diluting the stock 1/100 in phosphate buffered saline (37 °C) during heavy mixing. Adding DPI to any of the measuring systems described here, at concentrations between 1 and 10 μM [21], inhibits the NADPH-oxidase activity by 50–95 % (*see* **Note 3**).
14. Neutrophils purified from peripheral human blood by standard techniques (or any cell that can generate ROS). Store the cells on melting ice until use.
15. Chemiluminometer: preferentially equipped with a temperature-controlled sample holder.
16. Photometer: preferentially equipped with a temperature-controlled cuvette holder.
17. Fluorometer: preferentially with a temperature-controlled cuvette holder.
18. Flow cytometer.

3 Methods

A large number of techniques have been developed over the years to measure the cellular production of different ROS (Table 1). Ideally, techniques for measuring cellular production of ROS should (1) be specific for a particular oxygen metabolite, (2) be sensitive, (3) not interfere with cellular function, (4) distinguish the localization of the ROS production, (5) not require specialized laboratory equipment that is expensive or complicated to handle, and (6) be easy to standardize. Nevertheless, no single technique has hitherto been found that satisfies all of these criteria [20]. The drawbacks of the various techniques differ, and more than one technique usually has to be included in the methodological repertoire of oxygen radical scientists. Described in detail below are three techniques (luminol or isoluminol-amplified chemiluminescence, cytochrome C reduction, and PHPA-oxidation) that we routinely use to study respiratory burst activity in human phagocytes. These methods serve as valuable tools in both basic and clinically oriented research involving phagocyte function. We also describe DHR123 fluorescence since it is a widely used method, despite the fact that it suffers from a variety of drawbacks making it unsuitable for quantitative and kinetic studies.

Table 1
Techniques used for measuring cellular production of different reactive oxygen species

Technique	Measuring principle	Cellular localization	Comment
Superoxide anion			
Photometry	SOD-inhibitable reduction of cytochrome c (or WST-1)	Extracellular	Easy to follow kinetics of the response, provided that the stimulus is non-particulate; H_2O_2 may interfere with the assay; low sensitivity
Luminometry	Peroxidase-dependent isoluminol-amplified chemiluminescence	Extracellular	High sensitivity; easy to follow kinetics of the response; detects O_2^- despite the requirement for a peroxidase
	Lucigenin-amplified chemiluminescence	Extracellular	High sensitivity, but less than the isoluminol system; easy to follow kinetics of the response
Precipitation reaction	NBT reduction	Intracellular	Simple to count the number of positive cells microscopically, but laborious to make quantitative; should include SOD and catalase to remove released metabolites
Hydrogen peroxide			
Fluorometry	Peroxidase-dependent oxidation of PHPA ± azide	Extracellular	Fluorescence increases, making kinetics easy to follow; SOD is required for conversion of O_2^- to H_2O_2; low sensitivity
		Intracellular	NaN_3 inactivates MPO and catalase, thus allowing H_2O_2 generated intracellularly to leak out and be detected extracellularly
	Peroxidase-dependent oxidation of scopoletin ± azide	Extracellular	Fluorescence decreases, making kinetics more difficult to follow; SOD is required for conversion of O_2^- to H_2O_2; higher sensitivity than the PHPA system. See above regarding NaN_3
		Intracellular	
Non-identified oxygen radical			
Precipitation reaction	DAB oxidation	Intracellular	Simple to count the number of positive cells microscopically, laborious to make quantitative; should include SOD and catalase to remove released metabolites
Flow cytometry or fluorometry	Oxidation of DHR123, or 2,7-dichlorofluorescein	Intracellular	Many different oxidants can change the fluorescence of these substrates, making it difficult to use the technique quantitatively; difficult to follow kinetics
Luminometry	Peroxidase-dependent luminol-amplified chemiluminescence	Intracellular	Possibly detects O_2^-; high sensitivity; easy to follow kinetics; dependent on endogenous peroxidase activity; should include SOD and catalase to remove extracellularly produced metabolites

3.1 Detection of Extracellular ROS

It is generally assumed that the NADPH-oxidase is assembled and activated either in the plasma membrane or in the membranes of phagosomes [22, 23]. The ROS generated will then either be released from the cells (activation in the plasma membrane) or be retained inside the phagocyte (activation in the phagosomal membrane). In addition, neutrophils are clearly able to produce significant amounts of intracellular ROS in the absence of phagosome formation (reviewed in ref. 4). Thus, it is important to measure both intra- and extracellular ROS production by phagocytes treated with various activating stimuli.

3.1.1 Extracellular O_2^- Detection by Chemiluminescence

There are several dyes that after being excited by ROS release energy in the form of light (i.e., chemiluminescence). Among these dyes, the membrane-permeable luminol (Fig. 1) is the most intensively characterized and most frequently used in the free radical research field (*see* **Note 4**). Luminol is an activity amplifier that decreases the detection limit substantially, thus making the technique very sensitive (*see* **Note 5**). The system described here is a robust, highly sensitive technique that enables kinetic monitoring of phagocyte O_2^- production both in basic research and for more clinically oriented investigations of phagocyte function. There are some

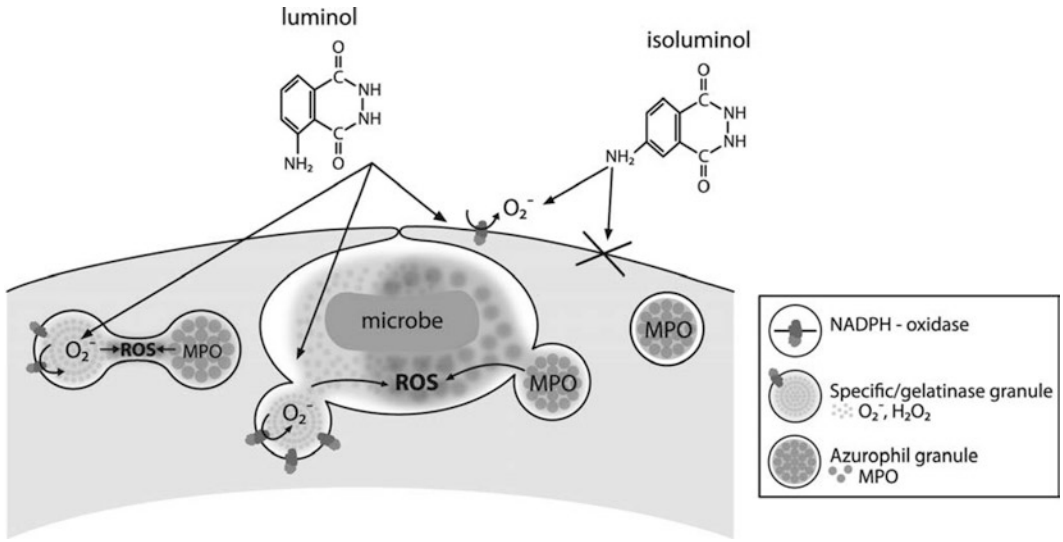

Fig. 1 Molecular structures and membrane permeability of luminol and isoluminol. Whereas isoluminol is unable to cross the plasma membrane and exclusively reacts with extracellular ROS, luminol is cell permeable and may also react with ROS generated within intracellular compartments. In order for the intracellular chemiluminescence reaction to take place, MPO needs to be present at the site of ROS production. This typically occurs within phagosomes after fusion with MPO-containing azurophil granules, but can also take place in the total absence of phagosome formation and is likely the result of heterotypic granule fusion involving granules equipped with the flavocytochrome b (gelatinase- and/or specific granules) and azurophil granules as a source of MPO [4, 36]

alternative substrates for the chemiluminescence reaction, but there are no strong arguments for using these in neutrophil respiratory burst measurements (*see* **Note 6**).

Luminol has an amino group in position 5 of the phthalate ring, and changing the position of the amino group in that ring does not change the ability of the molecule to detect ROS. However, moving the amino group away from the first carbon atom in the aromatic ring makes the molecule more hydrophilic and less able to pass over biological membranes. Thus, isoluminol (Fig. 1) can be used to exclusively measure ROS *released* from activated cells [24, 25]. While this method provides a relative measure of ROS, it does not quantify the specific amount of O_2^- present in the sample.

1. Add 600 µL of KRG to Eppendorf tubes or luminometer tubes for each sample (*see* **Note 7**).
2. Add 100 µL of fresh 500 µM isoluminol solution.
3. Add 100 µL of HRP solution (*see* **Note 8**).
4. Add 100 µL of cells in KRG (10^2–10^6 cells, depending on the activity of the cells and the sensitivity of the luminometer; *see* **Note 9**).
5. Equilibrate samples to the desired temperature.
6. Add 100 µL of a stimulus dissolved in KRG to activate the cells (*see* **Note 10**).
7. Measure chemiluminescence with an ordinary β-counter or one of the many luminometers present on the market (preferentially equipped with a temperature-controlled sample holder), including those adapted to microtiter plates (*see* **Notes 10** and **11**).

3.1.2 Spectrophotometric Determination of Extracellular O_2^-

Reactive oxygen species can reduce a number of different substrates, and techniques that exploit the absorbance change of chromogenic substrates are commonly used to measure ROS production. Here we describe a simple and highly reproducible technique that relies on the O_2^--dependent reduction of the membrane-impermeable substrate cytochrome C (cytC). The same method can be used with other substrates, e.g., the tetrazolium salt WST-1, without making any other changes. The reduction of cytC can be detected by a photometric change in absorbance at 550 nm, while WST-1 reduction is followed at 540 nm. As there is a one-to-one molar stoichiometry between the amount of O_2^- produced and the number of cytC molecules reduced, the actual amount of O_2^- produced can be quantified with this technique.

1. Prepare two cuvettes for each sample (i.e., a sample and a reference cuvette).
2. Add 700 µL of KRG to the sample cuvette and 690 µL of KRG to the reference cuvette (*see* **Note 7**).

3. Add 100 μL of cytC solution to both cuvettes.
4. Add 10 μL of SOD solution to the reference cuvette only (*see* **Note 12**).
5. Add 100 μL of cells ($\geq 5 \times 10^5$ cells) in KRG to both cuvettes.
6. Equilibrate both samples to the desired temperature in a temperature-controlled cuvette holder or water bath.
7. Add 100 μL of a stimulus dissolved in KRG to activate the cells (*see* **Note 10**).
8. Continuously monitor the change is absorbance at 550 nm (for cytC) in a spectrophotometer.
9. Determine the change in absorbance (ΔOD_{550} for cytC) for each sample by subtracting the absorbance of the reference cuvette containing SOD from that of the sample cuvette for each sample for each time point.
10. Calculate the molar amount of O_2^- generated per unit time and volume using the Beer-Lambert law with an extinction coefficient (ε) of 21.1 mM^{-1} cm^{-1} for reduced cytC at 550 nm. For a standard 1 mL assay containing 10^6 cells in a cuvette with a 1 cm light path, the amount of O_2^- generated can easily be calculated using Eq. 1 (*see* **Notes 13** and **14**):

$$\Delta OD \times 47.4 = \text{nmol } O_2^- \,/\, 10^6 \text{ cells} \,/\, \text{time unit} \qquad (1)$$

11. When a particulate prey (e.g., bacteria) is used to activate the cells, a discontinuous assay system has to be used in which the samples are centrifuged (to remove the bacteria that could otherwise scatter the light) and O_2^- production is determined from the sample and reference supernatants.
12. When comparing the two substrates, WST-1 generates a somewhat greater increase in absorbance, but this cannot be directly transferred to an increased sensitivity. With a diluted cell suspension, the sensitivity of the cytC reduction assay is actually somewhat greater than the WST-1 assay system (*see* **Note 15**).

3.1.3 Extracellular H_2O_2 Detection by PHPA Fluorescence

Membrane-impermeable PHPA is oxidized by H_2O_2 in the presence of HRP (which does not penetrate intact phagocytes), resulting in an increase in fluorescence. Production of H_2O_2 can subsequently be followed continuously using a fluorometer, including microtiter plate fluorometers.

1. Add 550 μL of KRG to Eppendorf tubes for each sample (*see* **Note 7**).
2. Add 100 μL of PHPA solution.
3. Add 50 μL of HRP solution.
4. Add 100 μL of SOD solution (*see* **Note 16**).

5. Add 100 μL of cells ($\geq 5 \times 10^5$ cells) in KRG.
6. Equilibrate samples to the desired temperature.
7. Add 100 μL of a stimulus dissolved in KRG to activate the cells (*see* **Note 10**).
8. Measure change in fluorescence emission at 400 nm with an excitation wavelength of 317 nm.
9. Calculate the amount of H_2O_2 produced from a standard curve of the PHPA system, calibrated with different concentrations of H_2O_2 added to non-activated cell samples (*see* **Note 17**).

3.2 Detection of Intracellular ROS

As mentioned above, intracellular production of ROS in neutrophils is not restricted to phagosomes, indicating that a complete NADPH-oxidase can be assembled and activated also in flavocytochrome b-containing granule membranes (*see* **Note 18**). Here we describe methods for measuring intracellular ROS production by phagocytes treated with various activating stimuli.

3.2.1 Intracellular ROS Detection by Chemiluminescence

The membrane-permeable dye, luminol (Fig. 1), is excited by phagocyte-generated ROS, resulting in chemiluminescence. By adding membrane-impermeable enzymes, SOD and catalase, to reaction mixtures, extracellularly released O_2^- and H_2O_2 are removed, leaving ROS generated specifically in intracellular compartments to be measured (*see* **Note 5**).

1. Add 680 μL of KRG to Eppendorf tubes or luminometer tubes for each sample (*see* **Note 7**).
2. Add 100 μL of fresh 500 μM luminol solution.
3. Add 10 μL of SOD solution.
4. Add 10 μL of catalase solution.
5. Add 100 μL of cells in KRG (10^2–10^6 cells, depending on the activity of the cells and the sensitivity of the luminometer; *see* **Note 9**).
6. Equilibrate samples to the desired temperature.
7. Add 100 μL of a stimulus dissolved in KRG to activate the cells (*see* **Note 10**).
8. Measure chemiluminescence with a β-counter or luminometer, including those adapted to microtiter plates (*see* **Note 19**).

3.2.2 Intracellular H_2O_2 Detection by PHPA Fluorescence

The O_2^- generated inside an intracellular compartment cannot normally be determined extracellularly, simply because neutrophils lack the anion channels needed for O_2^- to pass biological membranes [26]. Similarly, H_2O_2 generated in an intracellular compartment cannot be measured extracellularly, but for other reasons. The H_2O_2 can pass biological membranes but is rapidly consumed by endogenous peroxidases and catalase on its way from intracellular

compartments to the plasma membrane. However, if endogenous MPO and catalase are inhibited (e.g., with NaN_3), the intracellularly produced H_2O_2 can leak out of the cell and be detected extracellularly by the PHPA technique described above (Subheading 3.1.3) [27, 28].

1. Prepare two Eppendorf tubes for each sample (i.e., a sample and a reference tube).
2. Add 550 μL of KRG to the sample tube and 600 μL of KRG to the reference tube (*see* **Note 7**).
3. Add 100 μL of PHPA solution.
4. Add 50 μL of HRP solution
5. Add 100 μL of NaN_3 (1 mM final) to the reference sample only (*see* **Note 20**).
6. Add 100 μL of cells ($\geq 5 \times 10^5$ cells) in KRG.
7. Equilibrate samples to the desired temperature.
8. Add 100 μL of a stimulus dissolved in KRG to activate the cells (*see* **Note 10**).
9. Measure change in fluorescence emission at 400 nm with an excitation wavelength of 317 nm.
10. Calculate intracellular H_2O_2 generation by subtracting the fluorescence of samples lacking NaN_3 (extracellular H_2O_2) from that of samples containing NaN_3 (total H_2O_2).
11. Calculate the amount of H_2O_2 produced from a standard curve of the PHPA system, calibrated with different concentrations of H_2O_2 added to non-activated cell samples (*see* **Note 17**).

3.2.3 Intracellular ROS Detection by DHR123

Several probes exist for the detection of cellular ROS by flow cytometry. One of the most widely used is dihydrorhodamine 123 (DHR123; *see* **Note 21**), which is a nonfluorescent molecule that readily diffuses across cell membranes. Once inside the cell, DHR123 can be oxidized by ROS to the highly fluorescent, cationic rhodamine 123, which can be measured by flow cytometry or fluorometrically. Using flow cytometry, the dye should theoretically measure mainly intracellular ROS, but extracellular H_2O_2 may also pass over the plasma membrane and react with the probe intracellularly [29], which complicates the interpretation of data. Further, the technique is neither directly quantitative nor reliable for kinetic studies, and it is not clear which particular oxygen species directly reacts with DHR123 to generate fluorescence [30]. Thus, DHR123 (and similar probes) is likely more useful as a generic redox sensitive probe (*see* **Note 22**) than for detailed studies of phagocyte respiratory burst products.

In the protocol described below, extracellular ROS are neutralized by the addition of SOD and catalase to the measuring system,

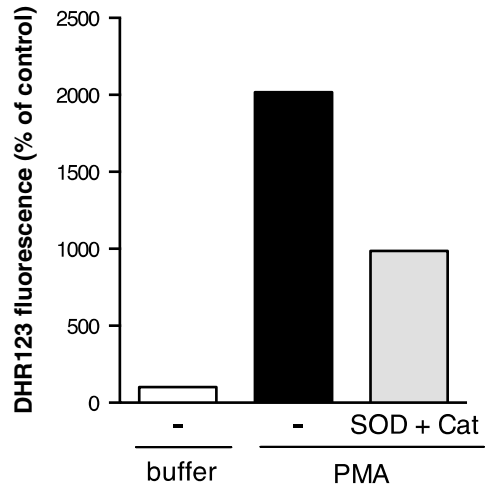

Fig. 2 Detection of neutrophil-derived ROS by DHR123. Human neutrophils stimulated with PMA for 15 min (*black*) display substantially increased DHR123 fluorescence compared to unstimulated control cells (*white*), when analyzed by flow cytometry. The presence of SOD (catalyzes the reduction of O_2^- to H_2O_2) and catalase (catalyzes the reduction of H_2O_2 to H_2O) during activation potently decreases the fluorescent signal, indicating that DHR123 is sensitive to extracellular, as well as intracellular ROS

and a comparison between the fluorescent signals obtained in the presence or absence of these antioxidants reveals that the relative contribution of extracellular ROS is quite significant (Fig. 2).

1. Add 100 µL of isolated neutrophils (5×10^5–10^6 cells/mL) in KRG to Eppendorf tubes or FACS tubes.
2. Add 1 µL of SOD solution to a final concentration of 50 U/mL.
3. Add 1 µL of catalase solution to a final concentration of 2,000 U/mL.
4. Add 10 µL of fresh 10 µM DHR123 solution (*see* **Note 23**).
5. Incubate samples for 15 min at 37 °C.
6. Add 10 µL of stimulus dissolved in KRG to activate the cells (e.g., PMA; 50 nM).
7. Incubate samples for an additional 15 min at 37 °C.
8. Add 200 µL ice cold KRG.
9. Keep tubes in darkness on ice and analyze directly by flow cytometry using an excitation/emission spectrum of 488/525 nm. Set up samples in duplicates, with one sample containing SOD and catalase. After gating away cellular debris, record the geometric mean fluorescence values of stimulated samples and compare to an unstimulated sample.

4 Notes

1. The phagocyte NADPH-oxidase is sometimes incorrectly called NOX2, even though this name refers only to the larger of the two membrane-bound subunits (also called $gp91^{phox}$).
2. Subsequent to receptor activation in neutrophils (or sometimes through receptor-independent activation of the cells), O_2 undergoes a one electron reduction to form O_2^- that dismutates to H_2O_2. The electron donor, NADPH, is formed by the oxidation of glucose in the hexose monophosphate shunt. Superoxide anion and H_2O_2 may be further reduced by a number of different cellular protection systems, including superoxide dismutase (catalyzes the reduction of O_2^- to H_2O_2), catalase (catalyzes the reduction of H_2O_2 to H_2O), and glutathione peroxidase (catalyzes the oxidation of glutathione by H_2O_2). The O_2^- and H_2O_2 can act as substrates for reactions with other cellular ROS (e.g., O_2^- reacts with nitric oxide to form the very reactive peroxynitrite molecule [31]) or cellular enzymes, such as MPO, that uses H_2O_2 in combination with chloride ions to generate the highly microbicidal HOCl [32].
3. The most widely used pharmacological inhibitor of NADPH-oxidase activity, DPI, effectively blocks NADPH-oxidase-derived ROS formation. However, DPI also affects a number of other cellular systems, and it was in fact originally described as an inhibitor of mitochondria by blocking the flavin components of the electron transport chain [33]. Thus, the use of DPI for the purpose of claiming that the ROS detected in a cellular system originate from the activated NADPH-oxidase is not convincing. Despite extensive research in the matter, we have not found a single reagent that specifically blocks the NADPH-oxidase dependent generation of ROS.
4. In order for luminol to react with oxidants in an intracellular compartment, it has to cross one or more biological membranes. Currently, very little is known about the diffusion properties of luminol or the diffusion limitations in different phagocyte membranes (plasma membrane, granule membranes, and/or phagolysosomal membranes).
5. The requirement for ROS in the luminol-dependent chemiluminescence reaction is shown by the absence or very low levels of chemiluminescence obtained when stimulating cells isolated from patients with CGD [34]. In addition, neutrophils isolated from donors with a deficiency of the azurophil granule protein MPO produce very low levels of chemiluminescence, despite a pronounced (in fact higher than normal) production of O_2^- and H_2O_2 (as measured with other techniques described here) [35], demonstrating that MPO participates in

the chemiluminescence-producing reaction. The fact that addition of MPO to the extracellular fluid is not sufficient to fully regenerate the chemiluminescence activity of MPO-deficient cells to that of control cells suggests that intracellular MPO (stored in the azurophil granules) also participates in the excitation of luminol by reacting with ROS generated in an intracellular compartment. This suggestion is further supported by the fact that part of the chemiluminescence response is insensitive to cell-impermeable extracellular scavengers of O_2^- and H_2O_2 [16]. Furthermore, we have recently shown that inhibition of phospholipase A2 (PLA2) can abrogate intracellular chemiluminescence specifically, without affecting intracellular ROS production or MPO activity [36]. This indicates that PLA2 activity is not needed for activation of the NADPH-oxidase per se, but rather contributes to the intracellular processing of ROS and facilitates fusion between MPO-containing (azurophil) granules and flavocytochrome b-containing (specific and/or gelatinase) granules. This study also highlights the value of combining more than one method for the measurements of ROS.

6. The luminol derivative, L-012, which is an even more sensitive CL amplifier than luminol [37, 38], has been used in model systems of whole animals to measure ROS produced by inflammatory cells in vivo [39]. The basic measuring characteristics of L-012 are the same as for isoluminol (*see* Subheading 3.1.1), but the high light output makes it difficult to work with; it is e.g., necessary to decrease the exposure time in the photomultiplier. The background activity of L-012 is also very high, while the signal to noise ratio is basically the same as for luminol or isoluminol. Hence, there are no strong arguments for using L-012 instead of luminol or isoluminol as a probe to measure phagocyte NADPH-oxidase activity.

   The chemiluminescence kit from National Diagnostics (Atlanta, GA, USA), called Diogenes Cellular Luminescence Enhancement System is a chemiluminescence enhancer of unknown origin that is non-denaturing to living cells. Oxygen radicals generated in neutrophils by the chemoattractant fMLF can be followed using this kit and most of the activity is inhibited by superoxide dismutase. The kit (used as suggested by the manufacturer) is however less sensitive than the HRP–isoluminol technique (Subheading 3.1.1). Neutrophils activated by fMLF produce O_2^- mainly at the plasma membrane (extracellular release) but the enhancer manufactured by National Diagnostics can be used to measure also intracellular ROS formation in a way similar to the luminol–SOD–catalase system (Subheading 3.2.1). Given that this kit is less sensitive, much more expensive, and that it has a very limited shelf life as compared to the luminol or isoluminol systems described in

this chapter, there are no strong arguments for using this kit to measure phagocyte NADPH-oxidase activity.

7. The methods described are for 1 mL assay volumes; however, they can easily be adapted to a microtiter plate format by adjusting the volumes accordingly. Based on a 200 μL assay volume for microtiter plate wells, the volumes for each step would then be reduced to a fifth of those used in the 1 mL assay. Microtiter plate assays are quite convenient and reduce sample and reagent requirements, as well as time required to measure signal readouts. *See* also **Note 10** below.
8. Although the light-generating reaction is peroxidase-dependent, the amount of H_2O_2 released from the cells does not affect the activity detected [25]. Peroxidases (MPO and HRP) catalyze the reaction using mainly O_2^- and not H_2O_2, and samples can be analyzed in the presence and absence of SOD, in parallel, to directly determine the portion of the activity that reflects O_2^- production.
9. Future developments of new luminescent dyes that are more sensitive than isoluminol should allow measurements of respiratory burst activity in individual cells, or even measurements at the subcellular level.
10. The neutrophil respiratory burst can be activated by a number of different soluble and particulate stimuli, including chemoattractants, certain cytokines, phorbol esters, calcium ionophores, certain lectins, and various microorganisms (opsonized as well as unopsonized). All of these stimuli elicit a neutrophil chemiluminescence response in the presence of luminol [14, 15, 34, 40–44]. Different stimuli trigger ROS production with markedly different kinetics, which is especially important to keep in mind when analyses are to be performed on microtiter plate based assays; for slow ROS responses (induced by for example PMA stimulation) it is often possible to add stimuli manually (with a multipipette) to wells of a microtiter plate. In contrast, to properly follow rapid responses (induced for example by chemoattractants) a plate reader equipped with injectors is required.
11. The relation between the amount of O_2^- produced and the amount of detected light or change in absorbance is dependent on the luminometer, but can easily be determined by a direct comparison with the SOD-inhibitable reduction of cytC [45].
12. In order to specifically determine the amount of O_2^- produced, SOD is added to reference samples so that any part of the signal that is not SOD-inhibitable (i.e., not due to O_2^-) can be subtracted.
13. The O_2^- production is often calculated and reported as the amount produced by 10^6 cells. If the number of cells in the

sample differs from 10^6, then the equation will need to be adjusted by dividing by the actual number of cells in units of 10^6. For example, if 5×10^5 (0.5×10^6) or 1×10^5 (0.1×10^6) cells are in the sample, then the value obtained from Eq. 1 must be divided by 0.5 and 0.1, respectively, and so on.

14. If a microtiter plate format is used for the cytC assay, two parameters will need to be changed in the formula: (1) the light path length will no longer be 1 cm and should be determined by measuring the distance from the bottom of the plate to the top of the sample liquid meniscus (usually about 0.75 cm) and (2) the assay volume is now 200 µL instead of 1 mL. As an example: O_2^- can be calculated for a 200 µL assay in a microtiter plate well with a 0.75 cm light path using Eq. 2:

$$\Delta OD_{550} \times 12.64 = \text{nmol } O_2^- / \text{ time unit} \qquad (2)$$

This number can then be divided by the number of cells in the well to obtain O_2^- production per unit of cells (*see* **Note 13**).

15. Accumulation of H_2O_2 in the measuring system (which can occur when a large proportion of the available cytC is reduced and the H_2O_2 consuming enzymes are inhibited) can result in a reoxidation of the ferrous form of cytC, thus giving an underestimated result. For stoichiometrical reasons, the problematic level of substrate consumption is reached more rapidly in the cytC reduction assay than when WST-1 is used as substrate.

16. In order to reflect the release of ROS using PHPA (which specifically detects H_2O_2), SOD has to be added to the system to convert all O_2^- to H_2O_2.

17. The PHPA can be replaced by other fluorogenic substrates, that when oxidized by the peroxidase-H_2O_2 complex, changes its fluorescence properties. Scopoletin (7-hydroxycoumarin) is such a substrate that in reduced form emits light at 460 nm when activated at 350 nm, and in oxidized form loses its fluorescence [46]. The scopoletin-assay system is more sensitive than the PHPA system but has the disadvantage that the fluorescence is lost in relation to H_2O_2 production, making the "measuring window" rather narrow.

18. Human neutrophils contain at least four types of granules that are mobilized (induced to fuse with the plasma membrane) hierarchically during in vivo extravasation of the cells from the blood stream to the tissue ([47, 48]; see also the Chapter 4 by Christenson et al. in this volume). Apparently, the membranes of the mobilizable granules store most of the cellular content of flavocytochrome b, the membrane component of the NADPH-oxidase complex, and translocation of flavocytochrome b from the granules to the plasma membrane is associated with a reduction of the NADPH-oxidase activity in the

granule fraction (as measured in a cell-free system using subcellular fractions from activated neutrophils) [7].

19. The light-generating reaction is dependent on the endogenous peroxidase, MPO. It is possible for MPO to use O_2^- as well as H_2O_2 in the light-generating reaction, but the actual oxygen metabolite(s) measured, has not been identified. It is not possible to directly quantify the amounts of O_2^- produced with this technique, and a change in luminescence could be due to either a change in O_2^-/H_2O_2 production, a change in the availability of MPO [36], or a change in the basic conditions (protein content; pH; ionic composition) in the intracellular compartment in which the reaction takes place. It should also be noted that luminol can in some situations inhibit the release of O_2^- [49], suggesting that this dye should only be used to measure ROS generated in an intracellular compartment, and the molecular basis for any detected responses should be verified with another technique.
20. Even though NaN_3 inhibits the major H_2O_2-consuming enzymes (i.e., catalase and MPO) in neutrophils, intracellularly generated H_2O_2 may be consumed or scavenged by other routes. Thus, the calculated amount of intracellularly generated H_2O_2 will most likely be an underestimation of what is really produced.
21. An alternative probe that we have used, with very similar results, is H_2DCFDA. In the protocol described, DHR123 can be exchanged for H_2DCFDA (Molecular Probes/Invitrogen) at a final concentration of 1–10 μM. The excitation/emission spectrum of H_2DCFDA is 492–495/517–527 nm.
22. The DHR123 is by no means specific for NADPH-oxidase derived ROS, as evidenced by the fact that non-phagocytes [50] give rise to DHR123 signals. The same is true also for CGD neutrophils, although in contrast to control neutrophils, these cells do not increase DHR123 signal after stimulation [51].
23. For the protocol described, a final concentration of DHR123 between 1 and 10 μg/mL has been used with similar results.

Acknowledgements

This work was supported by the Swedish Medical Research Council, the Swedish Society for Medical Research, the IngaBritt and Arne Lundberg Research Foundation, the Swedish state under the LUA-ALF agreement, and the King Gustaf V Memorial Foundation. We thank Maria Hjulström and Hülya Çevik-Aras for performing chemiluminescence determinations with the National diagnostic kit and L-012, respectively.

References

1. Quie PG, White JG, Holmes B et al (1967) In vitro bactericidal capacity of human polymorphonuclear leukocytes: diminished activity in chronic granulomatous disease of childhood. J Clin Invest 46:668–679
2. Segal AW (2005) How neutrophils kill microbes. Ann Rev Immunol 23:197–223
3. Quinn MT, Gauss KA (2004) Structure and regulation of the neutrophil respiratory burst oxidase: comparison with nonphagocyte oxidases. J Leukoc Biol 76:760–781
4. Bylund J, Brown KL, Movitz C et al (2010) Intracellular generation of superoxide by the phagocyte NADPH oxidase: how, where, and what for? Free Radic Biol Med 49:1834–1845
5. Borregaard N, Heiple JM, Simons ER et al (1983) Subcellular localization of the b-cytochrome component of the human neutrophil microbicidal oxidase: translocation during activation. J Cell Biol 97:52–61
6. Hager M, Cowland JB, Borregaard N (2010) Neutrophil granules in health and disease. J Internal Med 268:25–34
7. Dahlgren C, Johansson A, Lundqvist H et al (1992) Activation of the oxygen-radical-generating system in granules of intact human neutrophils by a calcium ionophore (ionomycin). Biochim Biophys Acta 1137:182–188
8. Karlsson A, Dahlgren C (2002) Assembly and activation of the neutrophil NADPH oxidase in granule membranes. Antioxid Redox Signal 4:49–60
9. Matute JD, Arias AA, Wright NA et al (2009) A new genetic subgroup of chronic granulomatous disease with autosomal recessive mutations in p40 phox and selective defects in neutrophil NADPH oxidase activity. Blood 114:3309–3315
10. Björkman L, Dahlgren C, Karlsson A et al (2008) Phagocyte-derived reactive oxygen species as suppressors of inflammatory disease. Arthritis Rheum 58:2931–2935
11. Ferguson PJ, Lokuta MA, El-Shanti HI et al (2008) Neutrophil dysfunction in a family with a SAPHO syndrome-like phenotype. Arthritis Rheum 58:3264–3269
12. Dahlgren C, Karlsson A (2002) Ionomycin-induced neutrophil NADPH oxidase activity is selectively inhibited by the serine protease inhibitor diisopropyl fluorophosphate. Antioxid Redox Signal 4:17–25
13. Karlsson A, Follin P, Leffler H et al (1998) Galectin-3 activates the NADPH-oxidase in exudated but not peripheral blood neutrophils. Blood 91:3430–3438
14. Karlsson A, Nixon JB, McPhail LC (2000) Phorbol myristate acetate induces neutrophil NADPH-oxidase activity by two separate signal transduction pathways: dependent or independent of phosphatidylinositol 3-kinase. J Leukoc Biol 67:396–404
15. Lock R, Dahlgren C, Linden M et al (1990) Neutrophil killing of two type 1 fimbria-bearing *Escherichia coli* strains: dependence on respiratory burst activation. Infect Immun 58:37–42
16. Serrander L, Larsson J, Lundqvist H et al (1999) Particles binding beta(2)-integrins mediate intracellular production of oxidative metabolites in human neutrophils independently of phagocytosis. Biochim Biophys Acta 1452:133–144
17. Brown GE, Stewart MQ, Liu H et al (2003) A novel assay system implicates PtdIns(3,4)P(2), PtdIns(3)P, and PKC delta in intracellular production of reactive oxygen species by the NADPH oxidase. Mol Cell 11:35–47
18. Kent JD, Sergeant S, Burns DJ et al (1996) Identification and regulation of protein kinase C-delta in human neutrophils. J Immunol 157:4641–4647
19. Sergeant S, McPhail LC (1997) Opsonized zymosan stimulates the redistribution of protein kinase C isoforms in human neutrophils. J Immunol 159:2877–2885
20. Murphy MP, Holmgren A, Larsson NG et al (2011) Unraveling the biological roles of reactive oxygen species. Cell Metab 13:361–366
21. Hancock JT, Jones OT (1987) The inhibition by diphenyleneiodonium and its analogues of superoxide generation by macrophages. Biochem J 242:103–107
22. Hampton MB, Kettle AJ, Winterbourn CC (1998) Inside the neutrophil phagosome: oxidants, myeloperoxidase, and bacterial killing. Blood 92:3007–3017
23. Kobayashi T, Robinson JM, Seguchi H (1998) Identification of intracellular sites of superoxide production in stimulated neutrophils. J Cell Sci 111:81–91
24. Dahlgren C, Karlsson A (1999) Respiratory burst in human neutrophils. J Immunol Methods 232:3–14
25. Lundqvist H, Dahlgren C (1996) Isoluminol-enhanced chemiluminescence: a sensitive method to study the release of superoxide anion from human neutrophils. Free Radic Biol Med 20:785–792
26. Halliwell B, Gutteridge JM (1985) The importance of free radicals and catalytic metal ions in human diseases. Mol Aspects Med 8:89–193
27. Root RK, Metcalf J, Oshino N et al (1975) H_2O_2 release from human granulocytes during phagocytosis. I. Documentation, quantitation, and some regulating factors. J Clin Invest 55:945–955

28. Root RK, Metcalf JA (1977) H_2O_2 release from human granulocytes during phagocytosis. Relationship to superoxide anion formation and cellular catabolism of H_2O_2: studies with normal and cytochalasin B-treated cells. J Clin Invest 60:1266–1279
29. van Pelt LJ, van Zwieten R, Weening RS et al (1996) Limitations on the use of dihydrorhodamine 123 for flow cytometric analysis of the neutrophil respiratory burst. J Immunol Methods 191:187–196
30. Wardman P (2007) Fluorescent and luminescent probes for measurement of oxidative and nitrosative species in cells and tissues: progress, pitfalls, and prospects. Free Radic Biol Med 43:995–1022
31. Beckman JS, Koppenol WH (1996) Nitric oxide, superoxide, and peroxynitrite: the good, the bad, and ugly. Am J Physiol 271:C1424–C1437
32. Klebanoff SJ (2005) Myeloperoxidase: friend and foe. J Leukoc Biol 77:598–625
33. Holland PC, Sherratt HS (1972) Biochemical effects of the hypoglycaemic compound diphenyleneiodonnium. Catalysis of anion-hydroxyl ion exchange across the inner membrane of rat liver mitochondria and effects on oxygen uptake. Biochem J 129:39–54
34. Lundqvist H, Follin P, Khalfan L et al (1996) Phorbol myristate acetate-induced NADPH oxidase activity in human neutrophils: only half the story has been told. J Leukoc Biol 59:270–279
35. Dahlgren C, Stendahl O (1983) Role of myeloperoxidase in luminol-dependent chemiluminescence of polymorphonuclear leukocytes. Infect Immun 39:736–741
36. Björnsdottir H, Granfeldt D, Welin A et al (2013) Inhibition of phospholipase A(2) abrogates intracellular processing of NADPH-oxidase derived reactive oxygen species in human neutrophils. Exp Cell Res 319:761–774
37. Imada I, Sato EF, Miyamoto M et al (1999) Analysis of reactive oxygen species generated by neutrophils using a chemiluminescence probe L-012. Anal Biochem 271:53–58
38. Nishinaka Y, Aramaki Y, Yoshida H et al (1993) A new sensitive chemiluminescence probe, L-012, for measuring the production of superoxide anion by cells. Biochem Biophys Res Commun 193:554–559
39. Kielland A, Blom T, Nandakumar KS et al (2009) In vivo imaging of reactive oxygen and nitrogen species in inflammation using the luminescent probe L-012. Free Radic Biol Med 47:760–766
40. Almkvist J, Dahlgren C, Leffler H et al (2002) Activation of the neutrophil nicotinamide adenine dinucleotide phosphate oxidase by galectin-1. J Immunol 168:4034–4041
41. Fu H, Belaaouaj AA, Dahlgren C et al (2003) Outer membrane protein A deficient *Escherichia coli* activates neutrophils to produce superoxide and shows increased susceptibility to antibacterial peptides. Microbes Infect 5:781–788
42. Fu H, Karlsson J, Bylund J et al (2006) Ligand recognition and activation of formyl peptide receptors in neutrophils. J Leukoc Biol 79:247–256
43. Karlsson J, Fu H, Boulay F et al (2005) Neutrophil NADPH-oxidase activation by an annexin AI peptide is transduced by the formyl peptide receptor (FPR), whereas an inhibitory signal is generated independently of the FPR family receptors. J Leukoc Biol 78:762–771
44. Thoren F, Romero A, Lindh M et al (2004) A hepatitis C virus-encoded, nonstructural protein (NS3) triggers dysfunction and apoptosis in lymphocytes: role of NADPH oxidase-derived oxygen radicals. J Leukoc Biol 76:1180–1186
45. Foyouzi-Youssefi R, Petersson F, Lew DP et al (1997) Chemoattractant-induced respiratory burst: increases in cytosolic Ca2+ concentrations are essential and synergize with a kinetically distinct second signal. Biochem J 322:709–718
46. Boveris A, Martino E, Stoppani AO (1977) Evaluation of the horseradish peroxidase-scopoletin method for the measurement of hydrogen peroxide formation in biological systems. Anal Biochem 80:145–158
47. Faurschou M, Borregaard N (2003) Neutrophil granules and secretory vesicles in inflammation. Microbes Infect 5:1317–1327
48. Zarember KA, Kuhns DB (2011) Editorial: will the real neutrophil please stand up? J Leukoc Biol 90:1039–1041
49. Fäldt J, Ridell M, Karlsson A et al (1999) The phagocyte chemiluminescence paradox: luminol can act as an inhibitor of neutrophil NADPH-oxidase activity. Luminescence 14:153–160
50. Leutner S, Schindowski K, Frolich L et al (2005) Enhanced ROS-generation in lymphocytes from Alzheimer's patients. Pharmacopsychiatry 38:312–315
51. Mauch L, Lun A, O'Gorman MR et al (2007) Chronic granulomatous disease (CGD) and complete myeloperoxidase deficiency both yield strongly reduced dihydrorhodamine 123 test signals but can be easily discerned in routine testing for CGD. Clin Chem 53:890–896

Chapter 22

Cell-Free NADPH Oxidase Activation Assays: "In Vitro Veritas"

Edgar Pick

Abstract

The superoxide ($O_2^{\bullet-}$)-generating NADPH oxidase complex of phagocytes comprises a membrane-imbedded heterodimeric flavocytochrome, known as cytochrome b_{558} (consisting of Nox2 and $p22^{phox}$) and four cytosolic regulatory proteins, $p47^{phox}$, $p67^{phox}$, $p40^{phox}$, and the small GTPase Rac. Under physiological conditions, in the resting phagocyte, $O_2^{\bullet-}$ generation is initiated by engagement of membrane receptors by a variety of stimuli, followed by specific signal transduction sequences leading to the translocation of the cytosolic components to the membrane and their association with the cytochrome. A consequent conformational change in Nox2 initiates the electron "flow" along a redox gradient, from NADPH to oxygen, leading to the one-electron reduction of molecular oxygen to $O_2^{\bullet-}$. Methodological difficulties in the dissection of this complex mechanism led to the design "cell-free" systems (also known as "broken cells" or in vitro systems). In these, membrane receptor stimulation and all or part of the signal transduction sequence are missing, the accent being placed on the actual process of "NADPH oxidase assembly," thus on the formation of the complex between cytochrome b_{558} and the cytosolic components and the resulting $O_2^{\bullet-}$ generation. Cell-free assays consist of a mixture of the individual components of the NADPH oxidase complex, derived from resting phagocytes or in the form of purified recombinant proteins, exposed in vitro to an activating agent (distinct from and unrelated to whole cell stimulants), in the presence of NADPH and oxygen. Activation is commonly quantified by measuring the primary product of the reaction, $O_2^{\bullet-}$, trapped immediately after its generation by an appropriate acceptor in a kinetic assay, permitting the calculation of the linear rate of $O_2^{\bullet-}$ production, but numerous variations exist, based on the assessment of reaction products or the consumption of substrates. Cell-free assays played a paramount role in the identification and characterization of the components of the NADPH oxidase complex, the deciphering of the mechanisms of assembly, the search for inhibitory drugs, and the diagnosis of various forms of chronic granulomatous disease (CGD).

Key words NADPH oxidase, Superoxide, Cell-free assays, Cytochrome b_{558}, Nox2, Noxes, Cytosolic components, $p47^{phox}$, $p67^{phox}$, Rac, Anionic amphiphile, Arachidonic acid, Superoxide dismutase, Isoprenylation, Peptide walking

1 Introduction

> Less is More
>
> Ludwig Mies van der Rohe (German-American architect)

Mark T. Quinn and Frank R. DeLeo (eds.), *Neutrophil Methods and Protocols*, Methods in Molecular Biology, vol. 1124,
DOI 10.1007/978-1-62703-845-4_22, © Springer Science+Business Media, LLC 2014

1.1 Background

Phagocytic cells (principally, neutrophils, monocytes, and macrophages) destroy engulfed bacterial, fungal, and protozoal pathogens by a number of effector mechanisms. Among these, reactive oxygen species (ROS) occupy a prominent position. ROS are derived from the primordial oxygen radical, superoxide ($O_2^{\cdot-}$), which is produced in response to appropriate engagement of membrane receptors by a tightly regulated enzyme complex, known as the $O_2^{\cdot-}$-generating phagocyte NADPH oxidase (briefly, "oxidase") (reviewed in ref. 1). The oxidase catalyzes the formation of $O_2^{\cdot-}$ by the NADPH-driven one-electron reduction of molecular oxygen (O_2). The functionally competent oxidase complex is composed of a membrane-associated flavocytochrome b_{558}, which is a heterodimer of two subunits (Nox2, also known as gp91^{phox}, and p22^{phox}), and four cytosolic components, p47^{phox}, p67^{phox}, p40^{phox}, and the small GTPase Rac1/2 (reviewed in ref. 2). The catalytic component is Nox2, which consists of six transmembrane α-helices linked by three external and two cytosol-facing loops and a cytosolic segment, also known as the dehydrogenase region (DHR). Nox2 is harboring all redox stations carrying the flow of electrons from NADPH to O_2, namely, an NADPH-binding site and non-covalently bound FAD, both present in the DHR, and two hemes, bound to histidine pairs present in the second and fifth membrane helices. In resting phagocytes, the components of the complex exist as distinct entities, oxidase activation being the consequence of the interaction of flavocytochrome b_{559} with cytosolic components, a process requiring translocation of the cytosolic components to the membrane environment of flavocytochrome b_{558}. This process involves a complex set of protein–protein and protein–lipid interactions and is defined as oxidase assembly (reviewed in refs. 3–5) (*see* Fig. 1).

For oxidase assembly, the decisive interaction is that of the DHR of Nox2 with one or more cytosolic components, resulting in a conformational change that initiates electron flow. In one model of oxidase assembly, p67^{phox} is seen as the only cytosolic component responsible for an "activating" interaction with Nox2 [6, 7]. Because p67^{phox} does not possess a membrane attachment signal of its own, it requires the assistance of p47^{phox} and Rac, to be brought in contact with Nox2 [6, 8, 9]. This fact was the reason for naming p47^{phox} and p67^{phox} homologues, associated with some of the non-phagocytic oxidases (Noxes), as Nox organizer 1 (NOXO1), and Nox activator 1 (NOXA1), respectively (reviewed in refs. 3, 5, 10). The roles of p47^{phox} and Rac in helping the association of p67^{phox} with Nox2 are not interchangeable; under certain in vitro conditions, oxidase activation can take place in the absence of p47^{phox} but not that of Rac [11, 12]. These differences in the "assistance" provided to p67^{phox} are of significance in the design and interpretation of cell-free assays and will be discussed in this chapter.

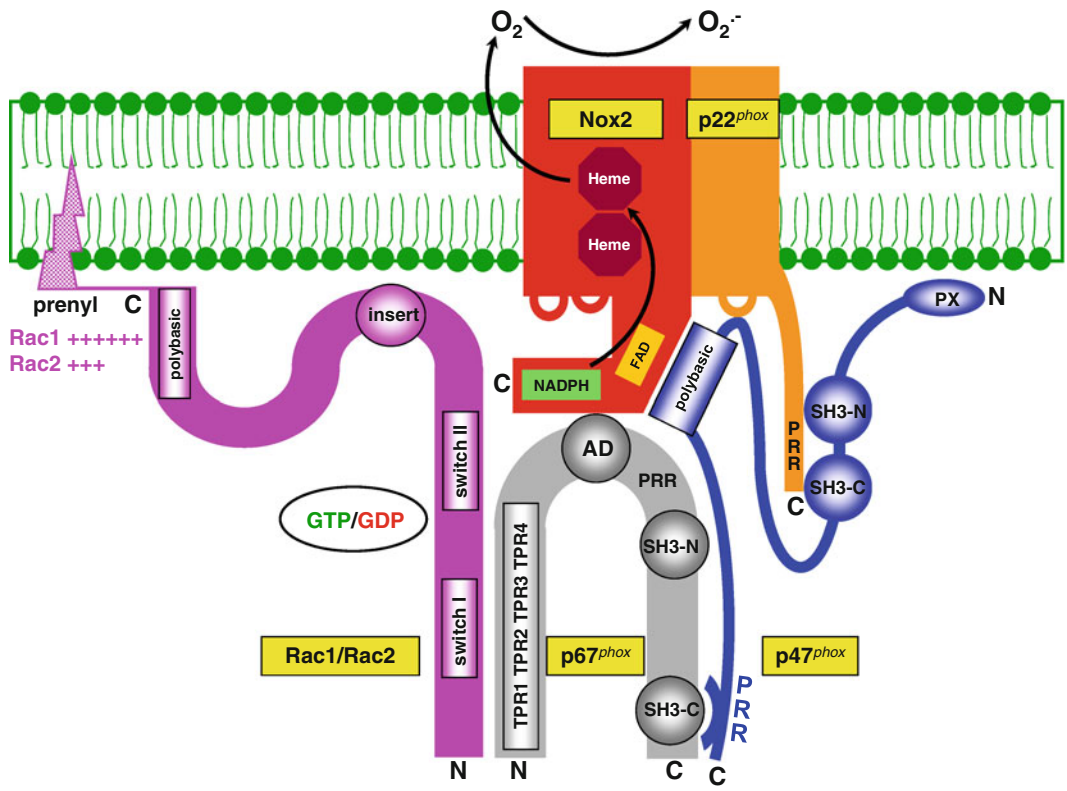

Fig. 1 Schematic representation of the assembled phagocyte NADPH oxidase. TPR = tetratricopeptide repeat; AD = activation domain; SH3 = Src homology 3; PRR = proline rich region; PX = *phox* homology. Reproduced by permission from [124]

The early literature on the assay of NADPH oxidase was rooted in the awareness of the multiplicity of stimulants causing ROS production by phagocytes [13, 14] and on the finding that, independent of the nature of the stimulant, NADPH oxidase activity could be demonstrated in the particulate (membrane) fraction of stimulated but not resting cells [15]. Thus, subjection of phagocytes to a stimulant, followed by cell disruption, separation of the cell homogenate into a particulate (membrane) and a cytosolic fraction, and measurement of NADPH-dependent $O_2^{\bullet-}$ production by the membrane fraction, became the standard procedure for assessing NADPH oxidase activity [16]. In the course of work with the membrane fraction of stimulated phagocytes, two facts became firmly established: first, the physiological substrate of the enzyme was NADPH and not NADH [15], and, second, the enzyme required supplementation with FAD for optimal activity [17]. Working with membranes from stimulated cells was technically difficult because the activity, as expressed in reaction rates, declined rapidly over time, was inactivated at 37 °C, and was sensitive to high salt concentrations and to harsh sonic disruption of the cells [16].

These difficulties prompted a search for an alternative procedure for the assay of NADPH oxidase. An additional stimulus for such a search was the unexplained mechanism responsible for the majority of the autosomal recessive form cases of chronic granulomatous disease (CGD). In the early 1980s, cytochrome b_{558} was the only known component of the oxidase and it was not known that the oxidase was a complex consisting of more than one component (a useful historical perspective of oxidase research "prehistory" appears in ref. 18). Thus, the finding that most patients with autosomal recessive CGD possessed a normal cytochrome b_{558} (found to be missing in the X-linked form of the disease) was puzzling.

This introduction would be incomplete without mentioning the marked increase of interest in non-phagocytic Noxes (reviewed in refs. 3, 5, 10). Nox family members are membrane-associated proteins with an electron carrier function involving the conserved functional modules also present in Nox2: NADPH- and FAD-binding sites, six transmembrane α-helices, and two histidine-bound hemes. The family includes five members, known as Nox1, Nox2, Nox3, Nox4, and Nox5; Nox2 representing the catalytic subunit of the phagocyte oxidase. Noxes 1, 2, and 3 are dependent on or regulated by cytosolic components; Nox4 is constitutively active and cytosol-independent, and Nox5 is Ca^{2+}-activated. Non-phagocytic Noxes generate much smaller amounts of ROS than Nox2, the identity of the activators is much less known, and the availability of purified and recombinant components lags behind that of the phagocyte oxidase. As will become apparent in the following subsections, the design of cell-free assays for non-phagocytic oxidases is a yet only partially fulfilled challenge.

1.2 The Canonical Cell-Free System

As with many discoveries, the design of a system to allow activation of the oxidase in subcellular fractions derived from resting (non-stimulated) phagocytes has a complex parenthood. In the laboratory of the author, the development of a cell-free oxidase activation system was not the result of a focused search for a better methodology, but the consequence of the finding that inhibition of phospholipase A_2 in intact macrophages prevented $O_2^{\cdot-}$ production by many stimulants [19]. These stimulants also caused liberation of arachidonic acid (C20:4) and we proposed that C20:4, generated by phospholipase A_2 action on membrane phospholipids, serves as a second messenger of oxidase activation, leading to the idea that C20:4 might be capable of activating the oxidase in disrupted resting phagocytes. Further encouragement was derived from work on the activation of adenylate cyclase in broken cell preparations by cholera toxin, which exhibited a requirement for both membranes and a cytosolic component [20].

In a paper published in 1984, the NADPH-dependent production of $O_2^{\cdot-}$ by guinea pig macrophage homogenates exposed to a critical concentration of C20:4 and several other long-chain

unsaturated (but not saturated) fatty acids in the ionized (but not in the esterified) forms, was described [21] (*see* **Note 1**). None of the numerous stimulants, eliciting $O_2^{\cdot-}$ production in intact phagocytes were capable of acting as activators in the cell-free system. A finding of paramount importance for future developments in oxidase research was that neither membrane nor cytosolic fractions of the phagocyte homogenate were, by themselves, capable of supporting fatty acid-elicited $O_2^{\cdot-}$ production, but recombining the two fractions resulted in full reconstitution of oxidase activity [21]. The "cell-free concept" was clearly ripe for discovery, as shown by the fact that similar cell-free oxidase activating systems were described within 1 year by three other groups. These were derived from resting horse [22] or human [23, 24] neutrophils, and in all cases, a requirement for cooperation between membrane and cytosol was found. An important finding made by two of these groups was that patients with the X-linked form of CGD possess a defective membrane component but a normal cytosolic component(s) [22, 24]. This observation was followed by the reciprocal finding that most CGD patients with the autosomal recessive mode of inheritance have a normal membrane component but a defective cytosolic component(s) [25]. These clinical correlates were essential for "legitimizing" the cell-free system as reflecting the activity of the $O_2^{\cdot-}$-forming oxidase, known from work in intact phagocytes. It is, perhaps, of interest to mention that the cell-free system was received with skepticism by some experts in the field (see lack of acceptance of the system in ref. 26, in which it was stated that it represents "nonphysiologic changes in the lipophilic environment of the enzyme").

Soon after the introduction of the cell-free system, the mechanism by which fatty acids cause oxidase activation became a subject of intense investigation. One of the first breakthroughs was the discovery that fatty acids act as anionic amphiphiles, as shown by the ability of sodium or lithium dodecyl sulfates (SDS; LiDS) to replace fatty acids as activators in the cell-free system, with very similar dose–response curves [27]. Other anionic detergents, such as sodium cholate, sodium deoxycholate, digitonin, and saponin, containing fused aromatic rings, are inactive. Sodium dodecyl sulfonate, like SDS, consists of an aliphatic hydrophobic moiety and an anionic polar head and thus serves as an activator [27]. Cell-free oxidase activation by fatty acids and some detergents was clearly one and the same and the term anionic amphiphiles became the accepted term for activators belonging to this category. This generalizing thesis was not well received by some reviewers of the manuscript on oxidase activation by SDS, when first submitted for publication (*see* **Note 2**).

The predominant explanation for the oxidase-activating ability of some anionic amphiphiles is that they disrupt an intramolecular bond in $p47^{phox}$ between a C-terminal polybasic region and the Src

homology 3 (SH3) tandem. In the intact phagocyte, this bond is severed by the phosphorylation of critical serines within the polybasic stretch, freeing the SH3 domains of $p47^{phox}$ for intermolecular interaction with a proline-rich region at the C-terminus of $p22^{phox}$, a critical step in the assembly of the oxidase complex [28]. Direct experimental evidence was provided for the induction of a conformational change in $p47^{phox}$ by C20:4 and SDS, a change which is also achieved by phosphorylation of $p47^{phox}$ by protein kinase C in vitro [29].

Some caution is, however, required concerning this "single target" interpretation because of the existence of a massive body of evidence for a direct effect of anionic amphiphiles on cytochrome b_{558}, leading to conformational changes which might also participate in oxidase activation [30–32]. Cell-free oxidase activation can also be induced by the synergistic action of phosphatidic acid (product of phospholipase D) and diacylglycerol (product of phospholipase C), again requiring participation of both the membrane and cytosolic fractions of the phagocytes and involving phosphorylation of $p47^{phox}$ and $p22^{phox}$ [33, 34]. A cell-free oxidase activating system, involving phosphorylation of $p47^{phox}$ (and of an unidentified membrane component) by protein kinase C in vitro was designed with the idea of being as close as possible to the in vivo reality [35, 36]. The latter system led to an activation level inferior to that induced by anionic amphiphiles and did not achieve widespread use.

A methodological but also conceptual revolution was the introduction of the semi-recombinant cell-free system. In this, the membrane is either used in the native form or represented by a purified and relipidated cytochrome b_{558} preparation, but the cytosol is replaced by a mixture of purified recombinant components [37]. This system permits introduction of strict quantification of the components participating in cell-free oxidase activation, the performance of dose–response assays, and control over the ratios among cytosolic components, among these and cytochrome b_{558}, and among the activating amphiphile and the membrane and cytosolic components. The amphiphile-activated cell-free system is the most frequently used and deserves to be coined the "canonical" cell-free assay. A modification of the cell-free system is the "two-step" assay, the purpose of which is to separate the assembly and catalytic phases in oxidase function (*see* **Note 3**).

1.3 Variations on the "Cell-Free" Theme

Recently, variations of the semi-recombinant amphiphile-dependent cell-free system have been introduced in which individual cytosolic components were replaced by chimeric constructs of either [$p47^{phox}$-$p67^{phox}$] [38] or [$p67^{phox}$-Rac1] [7, 39–41], supplemented by the missing third component (Rac1 and $p47^{phox}$, respectively), or by a tripartite chimera [$p47^{phox}$-$p67^{phox}$-Rac1] [42].

These chimeras consist of fusions of either full-length or truncated individual components and will be discussed in more detail further down. A further variation is represented by a cell-free system in which Rac is replaced by a complex of Rac1-GDP and GDP dissociation inhibitor for Rho (RhoGDI) [43].

1.4 A Cell-Free System Based on Cell Cores and Cytosol

The canonical cell-free system is not capable of detecting the participation of $p40^{phox}$ in oxidase activation [44]. To enable this, a system was designed based on permeabilization of neutrophils by streptolysin-O, resulting in the formation of cytosol-free "cores" [45]. These are used as a source of membranes, with the maintenance of membrane morphology and preservation of intracellular granules. Upon supplementation with cytosol, ATP, GTP, and NADPH, a cell-free-like system is generated which responds to stimulants normally acting on intact cells, such as phorbol myristate acetate (PMA), by $O_2^{\bullet-}$ production. Using this system, a role for $p40^{phox}$ in oxidase activation in human neutrophils could be demonstrated [46].

1.5 A Cell-Free System Without Cytosolic Components

A later methodological development was the design of a cell-free system in which macrophage membrane-derived cytochrome b_{558} was relipidated with a mixture of crude (14–23 %) soybean phosphatidylcholine (PC) and pure phosphatidic acid. The relipidated cytochrome b_{558} was found to generate $O_2^{\bullet-}$ in vitro in the presence of FAD, NADPH, and a low amount of anionic amphiphile, in the absence of cytosolic components [47, 48]. The level of $O_2^{\bullet-}$ production was about four times lower than that found in the canonical cytosol-dependent cell-free system, but the discovery of a cytosol-independent oxidase activation process provided definitive functional proof for the presence of all redox stations on cytochrome b_{558}. The cytosol-independent cell-free assay was used successfully for the elucidation of the defect in some cases of the $X91^+$ form of CGD [49].

1.6 Cell-Free Activation in the Absence of an Activator

1.6.1 Relieving Autoinhibition

The elucidation of the mechanism by which anionic amphiphiles induce oxidase activation in the cell-free system (severing the intramolecular bond in $p47^{phox}$ between the $(SH3)_2$ tandem and the polybasic C-terminus) led to the design of a new type of amphiphile-independent cell-free system. In this, truncation of $p47^{phox}$ at residue 286, which removes the polybasic C-terminus [50], or engineered mutations in $p47^{phox}$, which cause unmasking of $(SH3)_2$ [51], make the system amphiphile-independent. The need for amphiphile is circumvented because, in both cases, spontaneous interaction between the $(SH3)_2$ of $p47^{phox}$ and the proline-rich region at the C-terminus of $p22^{phox}$ is made possible. Surprisingly, amphiphile-independent activation involving $p47^{phox}$ truncated at residue 286, required $p67^{phox}$ to be truncated, too, at a residue N-terminal to the N-terminal SH3 domain, suggesting that the amphiphile might also have an effect on $p67^{phox}$ [50].

1.6.2 A Lipid Anchor

We developed a conceptually different amphiphile-independent cell-free system based on the use of prenylated Rac1 [9, 52], which binds to phagocyte membranes with high affinity and serves as a chaperone for $p67^{phox}$, leading to oxidase activation in the absence of amphiphile and without the need for $p47^{phox}$. Later variations of this system are represented by a prenylated [$p67^{phox}$-Rac1-GTP] chimera, which activates the oxidase in the absence of amphiphile and of any other component [7, 41, 53], a tripartite chimera, consisting of the functional domains of $p47^{phox}$, $p67^{phox}$, and full-length prenylated Rac1-GTP [54], and prenylated Rac-GDP, in conjunction with a guanine nucleotide exchange factor (GEF) for Rac and GTP or ATP [55]. The essential difference between amphiphile-dependent and amphiphile-independent, Rac prenylation-dependent cell-free systems is poignantly illustrated by the specific inhibitory effects of a peptide corresponding to the C-terminus of Rac1 (prevents only amphiphile-dependent activation) and of RhoGDI (prevents only amphiphile-independent activation) [7].

1.6.3 "Reversed" Activation: Making the Membrane Anionic

The plasma membrane of mammalian cells contains 15–20 % anionic phospholipids, a fact of considerable importance in leukocyte function (reviewed in ref. 56). Yet another group of cell-free systems was developed, based on the rationale of artificially enriching phagocyte membranes with anionic phospholipids. This is expected to result in an increase in the negative charge at the cytosolic aspect of the membrane and should promote the binding of cationic cytosolic components (or positively charged regions in chimeras resulting from their fusion) to the membrane and, possibly, decrease the electrostatic repulsion of the positively charged cytochrome b_{558}. There are several examples of such cell-free systems. Thus, a combination of a [$p67^{phox}$(1-210)-$p47^{phox}$(1-286)] chimera and Rac1-GTP activates phagocyte membranes enriched in anionic phospholipids, in the absence of amphiphile [38]. The tripartite chimera, [$p47^{phox}$(1-286)-$p67^{phox}$(1-212)-Rac1(192)], is a potent oxidase activator in the absence of anionic amphiphile, provided that the membrane is enriched with one of the anionic phospholipids, phosphatidic acid (PA), phosphatidylglycerol (PG), phosphatidylserine (PS), or phosphatidylinositol (PI) [42]. Also, enrichment of phagocyte membrane with the anionic phospholipids PG and PA enables oxidase activation in vitro by $p67^{phox}$ combined with [Rac1(GTP)-RhoGDI] complexes [57], and supplementation of membranes with phosphatidylinositol 3,4,5-triphosphate promotes oxidase activation by $p67^{phox}$ and [Rac1(GDP)-RhoGDI] complexes in conjunction with GTP and a GEF [58], both in the absence of an anionic amphiphile and $p47^{phox}$. The fine mechanism behind this form of "spontaneous" activation is not explained by simple electrostatic attraction between the membrane and the cytosolic components and their chimeric variations because the overall charges of [$p67^{phox}$(1-210)-$p47^{phox}$(1-286)] and [$p47^{phox}$(1-286)-$p67^{phox}$(1-212)-Rac1(192)]

chimeras are close to neutral, and thus, it is likely that positively charged domains in the cytosolic proteins and their chimeric constructs are participating in the interaction. An example of the major effect of electrostatics on cell-free activation is illustrated in Table 1.

1.7 Beginning and End

All cell-free systems are reductionist constructions. The systems, in most of their variations, are missing all or part of the initiating transduction mechanism from membrane receptors to the enzyme and also lack the "termination" process occurring in the intact phagocyte. In vivo, NADPH oxidase activity is transient and $O_2^{\bullet-}$ production is regulated by the balance between assembly and disassembly of the complex (reviewed in ref. 59). An in vivo study concluded that the turnover of cytochrome b_{558}-bound p67^{phox} and Rac is very high, indicating a continuous exchange of bound for free cytosolic components [60]. Cell-free systems are not the methodology of choice for the assessment of oxidase complex stability and the apparent decrease or termination of activity, when occurring in short-term assays, is due either to the exhaustion of NADPH or to the consumption of the reagents serving as $O_2^{\bullet-}$ traps. The brief duration of most contemporary cell-free assays also assures that the reaction components are unlikely to be inactivated in the course of the assay. In the past, it was thought that part of the $O_2^{\bullet-}$ generated in the system, which has escaped the intrinsic trap meant to bind the radical, might be dismutated to H_2O_2 and inactivate one or more of the oxidase components. To prevent this, catalase was added to the reaction in order to degrade any H_2O_2 that might have been produced [61], but such supplementation is unnecessary in brief kinetic assays and in the presence of sufficient $O_2^{\bullet-}$-trapping reagent.

In spite of the existing limitations, the stability of the assembled oxidase complex was also studied in cell-free systems, and was found to be significantly increased by chemical cross-linking of membrane and unidentified cytosolic components [62], by chimerization of p47^{phox} with p67^{phox} [38] or with Rac1 [39], and, most pronouncedly, by using a tripartite chimera consisting of functional domains of p47^{phox}, p67^{phox}, and Rac1, as the activator [42]. It, thus, appears that procedures replacing the natural association–dissociation cycles between cytosolic components and between cytosolic and membrane components by covalent bonds, enhances the half-life of the oxidase complex.

1.8 The "Subcellular" in the "Cell-Free"

The "primordial" cell-free assays consisted of mixtures of various membrane preparations and cytosol. Neither of these two components was properly characterized. In parallel with the isolation and characterization of the cytosolic components, the dominant form of cell-free assay became the one coined "semi-recombinant" [37]. This consists of recombinant p47^{phox}, p67^{phox}, and Rac and relipidated cytochrome b_{558}, purified from native or cell-line-derived

Table 1
Amphiphile-independent cell-free oxidase activation by enrichment of membrane with anionic phospholipids

Cytosolic activator(s)	NADPH oxidase activity (mol $O_2^{\cdot -}$/s/mol cytochrome b_{558} heme)			
	Membrane + phosphatidic acid (PA)	Membrane + phosphatidyl-glycerol (PG)	Membrane + phosphatidyl-serine (PS)	Membrane + phosphatidyl-inositol (PI)
No activator (membrane only)	11.70 ± 1.11	2.47 ± 0.13	1.75 ± 0.08	1.87 ± 0.04
$p47^{phox}$ + $p67^{phox}$	32.60 ± 2.60	12.37 ± 1.28	6.81 ± 0.58	2.91 ± 0.19
$p67^{phox}$ + Rac1	95.41 ± 3.64	34.29 ± 5.07	12.80 ± 1.20	5.63 ± 0.40
$p47^{phox}$ + $p67^{phox}$ + Rac1	112.83 ± 12.85	69.95 ± 8.46	48.57 ± 7.73	22.50 ± 3.22
[$p67^{phox}$(1-212)-Rac1(1-192)] chimera[a]	62.46 ± 4.81	12.92 ± 0.55	5.62 ± 0.57	3.11 ± 0.06
[$p67^{phox}$(1-212)-Rac1(1-192)] chimera + $p47^{phox}$	80.03 ± 4.99	44.87 ± 2.43	22.23 ± 0.42	6.12 ± 0.13
[$p47^{phox}$(1-286)-$p67^{phox}$(1-210)] chimera[b]	19.76 ± 0.86	3.21 ± 0.29	1.90 ± 0.35	2.27 ± 0.15
[$p47^{phox}$(1-286)-$p67^{phox}$(1-210)] chimera + Rac1	93.68 ± 2.97	68.94 ± 3.06	48.65 ± 1.46	30.25 ± 3.39
[$p47^{phox}$(1-286)-$p67^{phox}$(1-212)-Rac1(1-192)] chimera[c]	92.05 ± 2.38	50.76 ± 1.01	41.58 ± 1.72	37.80 ± 3.19

Assay mixtures contained solubilized macrophage membrane relipidated with PA, PG, PS, or PI, corresponding to 5 nM heme, and cytosolic activator(s), at 300 nM. $p47^{phox}$, $p67^{phox}$, and Rac1 were full-length proteins. Rac1 and the chimeras were nonprenylated. Rac1 and the chimeras were exchanged to the GTPase-resistant GTP analog, guanylyl imidodiphosphate (GMPPNP). The final concentrations of membrane phospholipid in the assays were 12 μM endogenous membrane phospholipid and 80 μM PA, PG, PS, or PI. Activation was in the absence of an anionic amphiphile. Methodology was as described in ref. 42. The results represent means ± SE derived from three experiments

[a]Reference 40
[b]Reference 38
[c]Reference 42

phagocyte membranes, following the demonstration that the only membrane component participating in cell-free activation is cytochrome b_{558} [63]. Due to the methodological difficulties associated with the preparation and purification of cytochrome b_{558}, membranes or solubilized membrane are routinely used. In the case of human neutrophils, a "whole" membrane fraction contains the plasma membranes, as well as the specific and azurophilic granules. Most of cytochrome b_{558} is found in the specific granules, with a lesser amount present in the plasma membranes [64]. $O_2^{\bullet-}$ production in intact neutrophils occurs both at the level of the plasma membrane and in an intracellular compartment corresponding to granules [65]. An analysis of the subcellular compartmentalization of membranes in the neutrophil, which respond with NADPH-dependent $O_2^{\bullet-}$ generation when exposed to cytosol and an amphiphilic activator, reveals that both plasma membranes and specific granules are involved [66]. To the best of our knowledge, the subcellular nature of macrophage/monocyte membranes participating in cell-free activation has not been ascertained.

One of the great advantages of the cell-free system is that the catalytic component of the enzyme (Nox2) is accessible to all reaction substrates (NADPH, FAD, oxygen) and the reaction product ($O_2^{\bullet-}$) has direct contact with the trapping reagent, maximizing the likelihood that we are measuring the full extent of the oxidase activity. When native membranes are replaced by solubilized membrane liposomes [67] or by purified and relipidated cytochrome b_{558} [63], the accessibility of Nox2 to the substrates and the $O_2^{\bullet-}$ trapping reagent is unknown, but our personal experience is that oxidase activity values are significantly superior to those obtained with native membranes.

1.9 What Are We Measuring in Cell-Free Assays

All cell-free systems are designed to mimic oxidase activation in vivo under in vitro conditions, starting from the equivalent of the state of the enzyme in resting cells. Enzyme activity is expressed as the reaction rate, based on the quantification of a reaction product or on the consumption of a reaction substrate. The most commonly used techniques are as follows:

1. *Reduction of cytochrome c by* $O_2^{\bullet-}$. This method is by far the most reliable, easy to perform, and convertible to a high-throughput assay. It was first described in the landmark paper by Babior et al. [68] on the production of $O_2^{\bullet-}$ by phagocytosing leukocytes. The specificity of cytochrome *c* reduction is checked by its elimination in the presence of superoxide dismutase (SOD). This assay is also used in less common situations, such as in Nox1-based cell-free systems [69], and for assessing the cytosol-independent diaphorase activity of the DHR of Nox4 [70].

2. *Reduction of iodonitrotetrazolium violet (INT)*. This method was introduced with the claim that INT is reduced by electrons originating in $FADH_2$ bound to the DHR of Nox2, by two-electron reduction and, thus, is measuring a step before the reduction of the two hemes and the generation of $O_2^{\bullet-}$ [71]. Most of the INT reduction was described as being SOD-resistant and not being dependent on $p47^{phox}$ (*see* **Note 4**).
3. *Reduction of nitrotetrazolium blue (NBT)*. This method is used almost exclusively for measuring NADPH-dependent diaphorase activities of the DHR of Nox2 and other Noxes, in the presence or absence of cytosolic activators [72–74].
4. *Other artificial electron acceptors*. These include dichloroindophenol, potassium ferricyanide, and cytochrome b_5. Together with INT and NBT, they are used for measuring the constitutive diaphorase activities of the DHR of Nox4 [70, 75].
5. *Measuring the production of* H_2O_2. Quantification of the primordial ROS generated in the cell-free system, $O_2^{\bullet-}$, should, in most cases, be the default choice. On rare occasions, H_2O_2, derived by non-enzymatic dismutation of $O_2^{\bullet-}$, is measured in Nox2 cell-free systems. Unlike Nox2, Nox4 produces mainly H_2O_2 [76] and cell-free systems centered on Nox4 are based on the quantification of H_2O_2 [70], utilizing a fluorescence method, involving the H_2O_2- and horseradish peroxidase-dependent oxidation of Amplex Red [77]. Assay buffers containing horseradish peroxidase should not contain NaN_3, an inhibitor of peroxidases. Oxidase assay buffers intended for quantifying $O_2^{\bullet-}$ production, routinely contain 2 mM NaN_3 (*see* Subheading 2.1.5).
6. *Chemiluminescence assay for measuring* $O_2^{\bullet-}$. On some occasions, an enhanced sensitivity is required for the detection of $O_2^{\bullet-}$ in cell-free assay. For this purpose, lucigenin is used as the chemiluminescent detector and its validity as a specific probe was rigorously demonstrated [78]. Its use in a canonical amphiphile-dependent cell-free system is illustrated in ref. 79.
7. *NADPH consumption*. This is a simple technique, easily applicable to cell-free assays [80]. Its principal use is in situations in which a compound added to the reaction interferes with the detection reagent (*see* ref. 81). As is the case for all substrate consumption assays, it has the disadvantage that the product of the reaction is presumed but not ascertained. However, when applied to the semi-recombinant type of cell-free assay [37], there is an almost absolute certainty that NADPH is used exclusively for $O_2^{\bullet-}$ production.
8. *Oxygen consumption*. This assay is rarely used at present in cell-free systems because of the cumbersome equipment required. It was popular in the early history of the cell-free system in order to establish the stoichiometry between oxygen consumption and $O_2^{\bullet-}$ production [82, 83].

1.10 Uses of Cell-Free Systems

Cell-free assays are extensively used in both basic research and clinical medicine. The tremendous expansion of the field of non-phagocytic NOXes has provided further impetus to their use and to the development of variations of the assay adapted to specific NOXes. At the time of the writing of this review, the original descriptions of the C20:4 and SDS-activated cell-free systems [21, 27] have accumulated a total of 635 citations and many authors cite later applications of the original method. The principal uses of cell-free assays are as follows:

1. The identification, quantification and functional assessment of oxidase components. At present this refers almost exclusively to components produced by recombinant technology and less commonly to those purified from cells. Although cell-free assays, if properly performed, are among the most sensitive techniques for the detection of oxidase components, obtaining quantitative data requires basing these on careful dose–response experiments with highly purified components. Thus, cell-free assays are mainly used to assess the functional competence of recombinant oxidase components.
2. Structure–function studies on recombinant oxidase components, subjected to mutagenesis, truncations, deletions, chimerization, and posttranslational modifications, such as prenylation. This is, at present, one of the most popular applications, due to the very high sensitivity of the system, enabling detection of the effect of minor structural modifications on function.
3. The availability of numerous variations of the cell-free system has opened the way to novel applications that were not possible when only the canonical assay was available. Some examples are: the cell-free system in the absence of cytosolic activator [47, 48], used in the diagnosis of some forms on CGD [49]; the amphiphile- and $p47^{phox}$-independent variations [9, 12, 52], allowing focusing on the interaction of cytochrome b_{558} with $p67^{phox}$, or a system centered on the detection of GEFs [55].
4. Investigating the mechanism of action of oxidase inhibitors. With the increasing interest in the development of Nox inhibitors [84, 85], cell-free assays are key components in the search for such compounds (predominantly in the form of high-throughput screening).
5. Diagnosis of the various forms of CGD and follow up on the success of therapeutic approaches applied to CGD patients. One of the first indicators of the importance of the cell-free system was its application to distinguishing between CGD caused by mutations in cytochrome b_{558} [22, 24] and in the cytosolic components [25].

6. A more recent development is the design of cell-free systems applicable to non-phagocytic Noxes, in either cytosolic components-dependent or -independent variations [69, 70, 75].

Cell-free assays are characterized by simplicity, speed, and repeatability and are ideal for being converted to high-throughput applications.

1.11 Methodological Reductionism Triumphant

Methodological reductionism is the concept that complex biological events should, if possible, be studied at the most elementary level, preferably down to that of interacting molecules [86]. Complex processes, such as activation of an oxidative burst in the intact phagocyte, are deconstructed to its component parts.

The cell-free system is one of the best examples for the successful application of methodological reductionism. Soon after its discovery it was described in the following terms: "What was really needed to achieve an understanding of oxidase activation at the molecular level was a cell-free oxidase activating system that can be taken apart and analyzed component by component using biochemical techniques. In a major advance that has capped years of work on this problem, activation of the oxidase in a cell-free system has at last be realized" [87], and "Through diligent research… whose pace has accelerated greatly since the ground-breaking discovery of a method to activate the respiratory burst oxidase in a cell-free system, the operation of this complex enzyme is now beginning to be understood" [88]. A useful brief review of the role of cell-free methodology in opening the "black box" of oxidase function is provided by ref. 89.

The overwhelming majority of the results obtained employing cell-free methodology fully overlapped those obtained by working with whole cells (transfection) or whole organisms (knock-out or natural disease). Occasionally, results obtained in the cell-free system differ from those obtained in whole cells, providing proof for the statement that "the whole is more than the sum of its parts." Examples for such discrepancies are the findings that truncation of $p67^{phox}$ at residue 246 (which removes both SH3 domains) [90] or deletion of the N-terminal SH3 domain [90, 91] led to the elimination of $O_2^{\bullet-}$ production by stimulated cells transfected with the $p67^{phox}$ mutants whereas both mutants were found to be fully capable of supporting both amphiphile-dependent and -independent $O_2^{\bullet-}$ production in a cell-free system [90, 92].

In this chapter, we describe the basic methodology for performing the different versions of the cell-free assay, commonly used for studying the NADPH oxidase, and shall deal with theoretical considerations to be taken into account, interpretation of results, possible problems and their solutions, available alternatives, and the multiple applications of this approach.

2 Materials (*See* Note 5)

2.1 Chemicals and Reagents

2.1.1 Preparation of Phagocyte Membranes

1. Paraffin oil, weight/mL = 0.85 (highly liquid) or 0.83–0.86 (BDH). This was used for eliciting a sterile peritoneal exudate as a source of macrophages for the preparation of membranes.
2. Earle's balanced-salt solution: 6.8 g NaCl, 0.4 g KCl, 0.125 g $NaH_2PO_4 \cdot H_2O$, 0.2 g $MgSO_4 \cdot 7\ H_2O$, 1 g glucose, 0.2 g $CaCl_2$ (anhydrous), 1.25 g $NaHCO_3$, H_2O up to 1 L.
3. Sonication buffer: 8 mM potassium, sodium phosphate buffer, pH 7.0 (made from 61 parts K_2HPO_4 and 39 parts NaH_2PO_4 stock solutions), 131 mM NaCl, 340 mM sucrose, 2 mM NaN_3, 5 mM $MgCl_2$, 1 mM ethylene glycol-bis(β-aminoethyl ether)-*N,N,N′,N′*-tetraacetic acid (EGTA), 1 mM dithiothreitol (DTT), 1 mM 4-(2-aminoethyl)-benzene-sulfonyl fluoride hydrochloride (AEBSF) (*see* **Note 6**), and 0.021 mM leupeptin hemisulfate. It is best to add DTT (200 mM), AEBSF (100 mM), and leupeptin (2.1 mM) from concentrated stock solutions (concentrations are listed in parentheses) just before using the buffer.
4. 3.5 M KCl solution: made in 20 mM Tris–HCl buffer, pH 7.5, for mixing with sonication buffer to reach a final concentration of 1 M KCl. It is used to wash macrophage membranes for removal of non-integral membrane-attached proteins.
5. Octyl-β-D-glucopyranoside (octyl glucoside).
6. Solubilization buffer: 120 mM sodium phosphate buffer, pH 7.4, 1 mM $MgCl_2$, 1 mM EGTA, 2 mM NaN_3, 10 μM flavin adenine dinucleotide, disodium salt (FAD), and 20 % v/v glycerol. Add 40 mM octyl glucoside (from powder), 1 mM DTT, 1 mM AEBSF, and 0.021 mM leupeptin from concentrated stock solutions just before using the buffer. Unused buffer can be divided in aliquots of 25–50 mL and stored frozen at –20 °C. The same basic buffer, not supplemented with octyl glucoside, FAD, and AEBSF, serves for dialysis of solubilized membranes leading to the formation of membrane liposomes.
7. Sodium dithionite.
8. Phospholipids: 3-sn-phosphatidic acid (sodium salt, from egg yolk, 98 %) and L-α-phosphatidyl-DL-glycerol (ammonium salt, synthetic, 99 %). Dissolve at 5 mM in solubilization buffer containing 40 mM octyl glucoside (but lacking protease inhibitors, DTT, and FAD). Dispense into aliquots of 0.5 mL and store at –75 °C.

2.1.2 Expression of Recombinant Cytosolic Components

For the last 5 years we have switched from glutathione *S*-transferase (GST) fusion proteins to proteins with an N-terminal 6His tag. This applies to $p47^{phox}$, $p67^{phox}$, and Rac1. The basic procedure for

the expression and purification of the recombinant proteins is described elsewhere [54].

1. *E. coli* competent cells (Rosetta 2(DE3)pLysS; Novagen).
2. pET-30a expression vector (Novagen).
3. LB Broth.
4. Isopropyl β-D-1-thiogalactopyranoside (IPTG).
5. Triton X-100 solution: 10 % (v/v) solution in H_2O.
6. Protease inhibitor mixture Complete EDTA-free (Roche).
7. 50 % (w/v) Poly(ethyleneimine) solution (PEI).

2.1.3 Purification of Recombinant Cytosolic Components

1. Imidazole solution: 2 M in H_2O, adjust to pH 7.4 with 3 M HCl.
2. Ni Sepharose 6 Fast Flow (GE Healthcare).
3. *E. coli* lysis buffer and Binding Buffer for metal affinity chromatography on Ni Sepharose: 20 mM sodium phosphate buffer, pH 7.4, 0.5 M NaCl, 20 mM imidazole.
4. Wash buffer: 20 mM sodium phosphate buffer, pH 7.4, 0.5 M NaCl, 40 mM imidazole.
5. Elution buffer: 20 mM sodium phosphate buffer, pH 7.4, 0.5 M NaCl, 300 mM imidazole.
6. FPLC gel filtration columns: HiLoad 10/60 Superdex 75 prep grade (fractionation range: 3–70 kDa) for purification of $p47^{phox}$, $p67^{phox}$ (1-212) and Rac; HiLoad 10/60 Superdex 200 prep grade (fractionation range: 10–600 kDa) for purification of $p67^{phox}$ (1-526).
7. Phosphate buffered saline (PBS): 137 mM NaCl, 2.7 mM KCl, 4.3 Na_2PO_4, 1.4 mM KH_2PO_4, 2 mM NaN_3, pH 7.3.
8. Protein assay concentrate for measuring protein concentration by the Bradford assay [93].
9. Bovine gamma globulin standard: 2 mg/mL for Bradford assay.
10. NuPage 12 % Bis-Tris electrophoresis gels: 1 mm gel thickness (Invitrogen, Life Technologies).
11. NuPage MOPS SDS running buffer (Invitrogen, Life Technologies).
12. NuPage LDS sample buffer (4×), and NuPage reducing agent (10×) (Invitrogen, Life Technologies).
13. Precision Plus SDS-PAGE protein standards, unstained (10–250 kDa) (Bio-Rad).
14. Coomassie Blue protein gel stain.

2.1.4 Reagents Required for Nucleotide Exchange on Rac (See **Note 7***)*

1. Buffer for diluting recombinant Rac1 for nucleotide exchange: 50 mM Tris–HCl, pH 7.5, 150 mM NaCl, 4 mM $MgCl_2$, 2 mM DTT. PBS is not compatible with high concentrations of $MgCl_2$.
2. Guanylylimidodiphosphate, trisodium salt (GMPPNP): 10 mM stock in H_2O, aliquot, and store –75 °C.
3. Guanosine-5′-*O*-(3-(thio)triphosphate, tetralithium salt (GTPγS): 10 mM stock in H_2O, aliquot, and store –75 °C.
4. (Ethylene-dinitrilo)-tetraacetic acid, disodium salt (EDTA): 0.5 M stock in H_2O. In order to dissolve EDTA, the solution has to be brought to pH 8.0 with 10 M NaOH.
5. $MgCl_2$ solution: 1 M stock in H_2O.
6. Recombinant rat geranylgeranyl transferase I made in *E. coli* (Calbiochem, EMD Millipore, Merck KGaA). One unit transfers 1 nmol geranylgeranyl pyrophosphate to Rho proteins per hour at 37 °C, at pH 8.0.
7. Geranylgeranyl pyrophosphate: 1 mg/mL solution in methanol/10 mM aqueous NH_4OH (7/3).
8. Prenylation buffer: 50 mM Tris–HCl buffer, pH 7.7, 0.1 mM $ZnCl_2$, 5 mM $MgCl_2$, 2 mM DTT.
9. Triton X-114: 10 % (v/v) solution in H_2O.

2.1.5 Cell-Free Assays

1. Cytochrome *c*, from equine heart, 95 %.
2. *p*-iodonitrotetrazolium violet (INT): 10 mM solution in ethanol, keep frozen at –20 °C, in the dark.
3. β-nicotinamide adenine dinucleotide 2′-phosphate reduced, tetrasodium salt, min. 95 % (NADPH): 5 mM stock in H_2O, divide in 1 mL aliquots, and store at –20 °C. Avoid frequent thawing and freezing, and do not store over 2 months.
4. Lithium dodecyl sulfate, >99 % (LiDS): 10 mM stock in H_2O, store at 4 °C for unlimited periods, provided that evaporation is prevented. Unlike SDS, LiDS does not precipitate out of aqueous solutions at low temperature.
5. Superoxide dismutase (SOD), from bovine erythrocytes: 10,000 U/mL stock in H_2O, aliquot in amounts of 100 µL, store at –20 °C.
6. Oxidase assay buffer: 65 mM sodium phosphate buffer, pH 7.0 (made from 61 parts K_2HPO_4 and 39 parts NaH_2PO_4 stock solutions), 1 mM EGTA, 10 µM FAD, 1 mM $MgCl_2$, 2 mM NaN_3, 0.2 mM cytochrome *c* (*see* **Note 8**). The conductivity of this buffer is 7.7 mS/cm. When reduction of INT is measured, cytochrome *c* is replaced by 100 µM INT. When the assay is based on NADPH consumption, the buffer does not contain cytochrome *c* or INT. When the concentration of LiDS to be

used in a large number of assays is known, this can be dissolved in the buffer. Assay buffer with and without LiDS can be divided into batches of 100 mL and stored at –20 °C for unlimited periods of time, in the dark, to prevent damage to FAD. The rationale for the components of the buffer is discussed below.

2.2 Disposable Plasticware

1. 96-well microplates, polystyrene, flat bottom, clear, with a well volume of 382 μL and a maximal height of 10.9 mm. When the wells in these plates are filled with a 0.21 mL reaction volume, the vertical light path is 0.575 cm. Plates intended for use in ELISA assays of medium or high hydrophilic protein-binding capacity are not recommended for use in cell-free assays. For the performance of the NADPH consumption assay, 96-well microplates permitting passage of UV light are recommended (e.g., UV-Star plate, flat bottom).
2. For the preparation of dilutions and the storage of recombinant proteins and membrane liposomes, tubes made of polypropylene are recommended, to reduce binding of the proteins to the tube wall. Glass and polystyrene tubes should not be used.
3. For batch metal affinity purification of 6His-tagged recombinant proteins, we found the disposable centrifuge columns (polypropylene (22 mL capacity) with polyethylene bottom filter (30 μm pore size) very useful.
4. Centrifugal concentrators, 10,000 molecular weight cutoff, 4- and 15-mL, for the concentration of all recombinant cytosolic components and buffer exchange.

2.3 Large and Small Equipment

1. Electronic single channel pipettors (range from 0.5 to 1,000 μL). These have a "dispensing" mode, very useful for adding small equal amounts of reagents to 96-well plates.
2. Multipette Plus (manual) or Multipette Stream (electronic) pipettors and various Combitips (Eppendorf).
3. Finnpipette digital 12-channel pipette (50–300 μL range) (Thermo Scientific).
4. Innova 4230 refrigerated incubator shaker (New Brunswick Scientific).
5. Refrigerated low-speed centrifuge (up to 7,000 × *g*), with a swing-out rotor (e.g., Sorvall RC-3B or RC-3C, and H-6000A rotor).
6. Refrigerated high-speed centrifuge (up to 48,000 × *g*), with fixed angle rotor (e.g., Sorvall RC-5 or RC-5 Plus, and SS-34 rotor).
7. Ultracentrifuge and fixed angle rotor (e.g., Beckman L5-50 ultracentrifuge and 60-Ti rotor).

8. High intensity ultrasonic processor (400- or 500-W) fitted with exchangeable regular and microprobe and cup horn.
9. Akta Basic 10 chromatography system, to be used for FPLC (GE Healthcare).
10. Rotating tube mixer (e.g., Rotamix RM1, ELMI).
11. XCell SureLock Mini-Cell for SDS-PAGE of mini-gels (Invitrogen, Life Technologies).
12. Electrophoresis power supply (e.g., Power Pac 300, Bio-Rad).
13. Microplate spectrophotometer (SPECTRAmax 340 or 190), preferably with PathCheck, fitted with SOFTmax PRO software (Molecular Devices, *see* **Note 9**).
14. Spectrophotometer (double-beam) UV/visible.
15. Thermomixer Comfort, rotary mixer and heater/cooler (Eppendorf).
16. Mini orbital shaker for 96-well plates.
17. Optical microscope (with 10× and 40× magnification objective lenses).

3 Methods

Cell-free assays are used in an almost limitless variety of forms and applications. In the original form of the assay, cytochrome b_{558} was represented by a total macrophage membrane preparation and the cytosolic components, by total cytosol [21]. In the variants developed later, a more sophisticated membrane preparation is utilized or the membrane is altogether replaced by purified relipidated cytochrome b_{558}. In all the assays to be described, we use a modified membrane preparation, originating from guinea pig peritoneal exudate macrophages, and the cytosol is replaced by purified and well-characterized recombinant proteins ($p47^{phox}$, $p67^{phox}$, and Rac). Although a number of anionic amphiphiles can act as activators in cell-free systems (*see* **Note 1** and refs. 21, 27), we shall limit our description to LiDS as the prototype activator. We describe two methods for the detection of ROS, based on the trapping of $O_2^{\cdot-}$ produced in the cell-free system by oxidized cytochrome *c* [68] or INT [71] and one method, based on the consumption of NADPH [80].

3.1 Cytochrome b_{558} (The Membrane Component)

3.1.1 Membrane Preparation

We here describe the preparation of membranes from elicited guinea pig peritoneal macrophages [27, 82]. Considering the paucity of granules in macrophages, differential centrifugation is not required to obtain granule-free pure plasma membrane preparations from these cells. Instead, we prepare a "total" membrane

fraction, defined by its sedimentation at 160,000 × *g*. The use of an uncharacterized membrane preparation is made possible by the fact that, in the cell-free assays to be described, the amounts of membrane added to the assay are based strictly on the cytochrome b_{558} content.

1. Inject guinea pigs (male or female, weighing 300–500 g) intraperitoneally with sterile light paraffin oil (15 mL per animal).
2. After 4 days, sacrifice the animals by CO_2 inhalation, and collect the peritoneal content via a 3-cm-long incision in the abdominal wall and repeated introduction and aspiration of 50-mL volumes of ice-cold Earle's balanced-salt solution.
3. Pass the collected peritoneal lavage through a 180 μm pore size nylon mesh sheet and collect in ice-cooled Erlenmeyer flasks (*see* **Note 10**).
4. Centrifuge fluid for 20 min at 940 × *g* and 4 °C to sediment the cells.
5. Repeat the procedure once more, and suspend the cell sediment in ice-cold distilled H_2O (20 mL to a cellular pellet derived from 400 mL lavage fluid) to lyse red cells.
6. After 3 min, add an equal volume of ice-cold 0.29 M NaCl solution in water (20 mL), resulting in an isotonic NaCl concentration (0.145 M), mix well, and recentrifuge at 940 × *g*, as above. If necessary, the lysis procedure can be repeated once more.
7. Resuspend the cell pellet in Earle's solution (10 mL per animal), and count cells after diluting the suspension 1:10 in 1 % v/v acetic acid in H_2O. The expected cell harvest varies from 1 to 2×10^8 cells per animal.
8. Pellet the cells at 940 × *g* and resuspend in sonication buffer at a concentration of 10^8 cells/mL in 16 × 100 mm polypropylene tubes (4 mL/tube).
9. Sonicate samples (400-W ultrasonic processor), keeping tubes immersed in ice-water, with the microprobe lowered into the cell suspension 2/3 of its entire depth. Submit cells to three cycles of sonic disruption at an amplitude of 10 %, each cycle consisting of sonication for 9 s, followed by a 1-s rest, repeated three times. Check for quality of cell disruption by phase-contrast microscopy at 40× magnification (~90 % cell disruption is expected).
10. Centrifuge the cell homogenate for 10 min at 3,000 × *g* and 4 °C in a swinging-bucket rotor to remove unbroken cells, aggregates, and nuclei. Collect the supernatant (postnuclear supernatant).

11. Centrifuge the supernatant for 2 h at 160,000 × *g* and 4 °C. The supernatant from this step is collected and represents the cytosol. If an ultracentrifuge is not available, centrifuge for 4 h at 48,000 × *g* in a high-speed centrifuge.
12. Resuspend the membrane pellet in sonication buffer supplemented with 1 M KCl (*see* **Note 11**) at a volume identical to the original volume of the homogenate. Resuspend directly in the ultracentrifuge tubes (kept in ice-water) by adding buffer with 1 M KCl in small aliquots (1–2 mL) and very briefly and gently sonicate after each addition, using a microprobe, until all the membrane is suspended (*see* **Note 12**).
13. Centrifuge the mixture for 2 h at 160,000 × *g* and 4 °C.
14. Discard the supernatant and freeze the membrane pellet at –75 °C. The membranes can be kept frozen indefinitely for future use. We found no reason for flash freezing or keeping membranes at a lower temperature.

3.1.2 Preparation of Membrane Liposomes

Although membrane preparations obtained as described above are quite adequate for use, we routinely use solubilized membrane preparations consisting of liposomes of uniform size as our source of cytochrome b_{558} in cell-free assays. Liposomes are obtained by solubilizing membranes with octyl glucoside and then removing the detergent by dialysis [67, 82].

1. Suspend frozen membranes in ice-cold solubilization buffer at a concentration of 5×10^8 cell equivalents/mL using the original ultracentrifuge tubes as containers.
2. Stir suspension with a small magnetic bar by placing the tube in a beaker containing ice-water. Continue solubilization until no intact membrane fragments remain. This might take 3–6 h, and it is important to keep the tubes ice-cooled throughout this period.
3. Centrifuge the solution for 1 h at 48,000 × *g* and 4 °C in a fixed angle rotor.
4. Transfer supernatant containing the solubilized membrane into a fresh tube (appears as a pale-yellow opalescent solution). Discard pellet.
5. Place solution in dialysis tubing with a 25,000 molecular weight cutoff (*see* **Note 13**), and dialyze against a 100-fold excess of detergent-free solubilization buffer for 18–24 h at 4 °C (*see* **Note 14**). The dialyzed detergent-free solubilized membrane consists of liposomes, 250–300 nm in diameter.
6. Measure the concentration of cytochrome b_{558} as described below.
7. Supplement the preparation with 10 μM FAD, divide into aliquots of 1–1.5 mL, and store at –75 °C (*see* **Note 15**). The

preparation is now ready to be used in all forms of cell-free assays (*see* **Note 16**).

3.1.3 Quantification of Cytochrome b_{558} Content

The results of cell-free assays are commonly expressed in turnover values (mol $O_2^{\bullet-}$ produced per time unit [s] per mol cytochrome b_{559} heme). Thus, it is essential that the cytochrome b_{558} content of membranes is known. Cytochrome b_{558} content is expressed by heme concentration.

1. Dilute membrane liposome preparation in solubilization buffer without octyl glucoside and FAD (1:5 or 1:10 dilution). Place diluted samples in spectrophotometer cuvette (*see* **Note 17**).
2. Place cuvette in the sample compartment of a double-beam spectrophotometer, and place a cuvette containing the buffer used for diluting the membrane preparation in the reference compartment.
3. Run an absorption spectrum scan, from 400 to 600 nm, using a band-width of 1 nm, a scanning interval of 1 nm, and a scanning speed of 100 nm/min (*see* **Note 18**). Save this as "oxidized spectrum" in the computer linked to the spectrophotometer.
4. Add a few grains of sodium dithionite, rapidly mix, and run a spectral scan again. Save this as "reduced spectrum."
5. Subtract the "oxidized spectrum" from the "reduced spectrum," and save the resulting "reduced *minus* oxidized spectrum."
6. Detect and record absorbance values of major cytochrome b_{558} peaks, located at 558/559, 529, and 426/427 nm. Detect and record absorbance at the "valley," at 410/411 nm.
7. Calculate heme content, based on the Δ extinction coefficient of the 427 nm peak/411 nm valley pair, using $\Delta\varepsilon_{427-411\ nm} = 200\ mM^{-1}\ cm^{-1}$ [94] (*see* **Note 19**).
8. Normally, we obtain a concentration of cytochrome b_{558} heme of 400 pmol/10^8 cell membrane equivalents. Thus, the membrane liposome suspension of 5×10^8 cell membrane equivalents/mL has a heme concentration of 2 μM (*see* **Note 20**).

3.2 Cytosolic Components

All recombinant cytosolic components are expressed in *E. coli* as N-terminal 6His-tagged proteins. The methodology is described elsewhere [54]. The key steps are briefly summarized below:

3.2.1 Preparation of Recombinant $p47^{phox}$, $p67^{phox}$, and Rac1

1. Transform *E. coli* competent cells (Rosetta 2(DE3)pLysS) with the expression vector pET-30a-6His Kan^R, carrying cDNAs encoding each of the three cytosolic components, following a standard protocol (pET System Manual, 11th edition, Novagen, Merck KGaA).

2. Induce bacteria with 0.4 mM IPTG and grow at 18 °C for 14–16 h in a refrigerated incubator shaker. Induction at 18 °C is important for maximizing the recovery of the recombinant proteins in the soluble fraction after disruption of the bacteria.
3. Sediment bacteria by centrifugation at 3,500 × *g*, resuspend in lysis buffer, supplement with Complete EDTA-free and 1 % v/v Triton X-100 (40 mL for 1 L bacterial culture),
4. Sonicate sample for 5 min in an ice-water-cooled glass beaker, using a 500-W ultrasonic processor with a 12-mm diameter probe, at an amplitude of 20 %, and alternating cycles consisting of sonication for 2 s, followed by a 2-s rest.
5. Centrifuge at 48,000 × *g* for 30 min and decant supernatant containing the soluble protein.
6. Precipitate DNA with PEI at a final concentration of 0.3–0.4 % (w/v) for cationic proteins [$p47^{phox}$, Rac1, and $p67^{phox}$(1-212)] or 0.05 % for anionic proteins ($p67^{phox}$) [95].
7. Sediment DNA–PEI precipitate by centrifugation at 48,000 × *g* at 4 °C for 30 min. Use supernatant for purification on Ni Sepharose.
8. Measure protein concentration by the Bradford assay [93] modified for use with 96-well microplates (*see* Bio-Rad Technical Bulletin 1177 EG and **Note 21**).

3.2.2 Purification of Recombinant Cytosolic Components

Recombinant cytosolic components are purified in two stages. First, by batch affinity metal chromatography on Ni Sepharose, and second, by preparative FPLC gel filtration.

1. Mix 3 mL of washed packed Ni Sepharose beads with soluble fraction derived from sonic disruption of bacteria from 1 L culture. Incubate for 1 h at room temperature with top/bottom rotation using a rotating tube mixer at 10 RPM.
2. Transfer contents into a centrifuge column and allow the fluid to flow by gravity.
3. Wash beads twice with 15 mL volumes of binding buffer and twice with 15 mL volumes of washing buffer.
4. Add 10 mL of column elution buffer, seal bottom and top apertures, and incubate for 30 min at room temperature with top/bottom rotation using a rotating tube mixer at 10 RPM.
5. Allow the eluate to run by gravity into a collecting tube and repeat procedure once or twice.
6. Measure protein concentrations in all eluates and analyze by SDS-PAGE for purity. The purity requirements for the performance of cell-free assays are easily achieved by purification on Ni Sepharose. Purity ≥90 % is adequate, and the only problem

encountered with lower purity preparations is that the actual concentrations of the components present in the assay cannot be accurately determined.

7. When high purity preparations are desired, proceed to purification by gel filtration on HiLoad 16/60 Superdex 200 prep grade for $p67^{phox}$ and tripartite [$p47^{phox}$-$p67^{phox}$-Rac1] chimeras, and HiLoad 16/60 Superdex 75 prep grade for $p47^{phox}$, $p67^{phox}$(1-212), Rac1, and [$p67^{phox}$-Rac1] and [$p47^{phox}$-$p67^{phox}$] bipartite chimeras. The reason for using Superdex 200 for gel filtration of full-length $p67^{phox}$ is the non-globular nature of the protein, which causes its elution at an apparent molecular weight much higher than 67,000 [96].
8. Concentrate eluates from Ni Sepharose to a volume of 2.5–5 mL by centrifugal filters and inject onto the column using PBS buffer and a flow rate of 1 mL/min. Keep the column refrigerated. Record absorbance at 280, and collect 1 mL fractions. Analyze fractions by SDS-PAGE and pool those of highest purity.
9. Supplement purified recombinant proteins with 20 % v/v glycerol, divide in small aliquots in polypropylene tubes with low protein binding quality (Eppendorf, Protein LoBind) and store at –75 °C. Avoid repeated thawing–refreezing. In this state, they are active for an unlimited time period (*see* **Note 22**).

3.2.3 The Preference for Rac1

Rac2 is the predominant form of Rac in neutrophils [97], whereas monocytes and macrophages use Rac1 in oxidase activation [43, 98, 99]. The oxidase can be activated in the cell-free system by both Rac1 and Rac2 in their nonprenylated forms. However, one should be aware that this is an artifact, since nonprenylated Rac does not exist, as such, in phagocytes. Translocation to the membrane of nonprenylated Rac is dependent exclusively on the net positive charge of the polybasic domain at the C-terminus. Because Rac1 contains six contiguous basic residues in this domain whereas Rac2 contains only three that are only partially contiguous, nonprenylated Rac1 is much more active in the cell-free system than Rac2 [8, 54, 100]. Native, recombinant Rac1 contains exclusively GDP [101, 102]. Thus, before use in cell-free assays, subject Rac1 to nucleotide exchange with a non-hydrolyzable GTP analog (GMPPNP or GTPγS; for choosing between the two analogs *see* **Note 23**). Recently, we have started to use predominantly the Rac1 mutant Q61L, which is constitutively in the GTP-bound form [103].

3.2.4 Nucleotide Exchange on Rac

The procedure described here is for exchange to GMPPNP, but the same procedure is used for exchange to GTPγS. It is based on the removal of bound endogenous GDP by chelation of Mg^{2+} and replacement of the bulk of GDP by the GTP analog.

1. Decide on the size of the batch of recombinant Rac that is to be to subject to guanine nucleotide exchange. For use in cell-free assays, we normally perform exchange on aliquots of 10–20 nmol of Rac in Tris–HCl buffer. Place in 1.5- or 2-mL Eppendorf polypropylene tube.
2. Add GMPPNP stock solution in a quantity representing a ten-fold molar excess over the amount of Rac. For example, if you intend to perform exchange on 10 nmol of Rac, add 100 nmol of GMPPNP (10 µL from the 10 mM stock solution).
3. Add EDTA solution to a final concentration of 12.5 mM. Incubate for 30 min at 30 °C in a rotary mixer set at 600 rotations/min.
4. Stabilize the exchanged state of Rac by adding $MgCl_2$ solution to a final concentration of 25 mM.
5. Store exchanged protein frozen at –75 °C (*see* **Notes 24** and **25**).

3.2.5 Prenylation of Rac In Vitro

In the past, 6His-tagged Rac1 was cloned into the baculovirus genome, and this recombinant virus was used to infect cultures of Sf9 cells [9]. In this procedure, prenylated Rac was expressed in the cell membrane and thus had to be purified following membrane solubilization. This procedure was replaced by a much simpler method using in vitro enzymatic prenylation of nonprenylated recombinant Rac1 [53].

1. Add 10 nmol of nonprenylated Rac (*see* **Note 26**) to a 1.5 or 2 mL polypropylene Eppendorf tube.
2. Add 10 µL (20 nmol) of geranylgeranyl pyrophosphate stock solution, 10 µL (10 U) of geranylgeranyl transferase I stock solution, and prenylation buffer containing $ZnCl_2$ (*see* **Note 27**) to a final volume of 0.9 mL.
3. Incubate for 45 min at 37 °C in a rotary mixer set at 600 rotations/min (*see* **Note 28**).
4. Add 60 µL of 70 mM octyl glucoside in H_2O (final octyl glucoside concentration is 4.375 mM), and reincubate for 45 min under the same conditions as above.
5. Sonicate the protein in a 400-W ultrasonic processor fitted with a cup horn filled with ice-water for five cycles of 10 s each at 50 % amplitude.
6. Add 0.24 mL of glycerol to bring the final volume to 1.2 mL. The final concentrations of components are 8.33 µM Rac, 3.5 mM octyl glucoside, and 20 % v/v glycerol (this does not take into account the glycerol carried into the reaction by nonprenylated Rac itself).
7. Prenylated Rac can be stored at –75 °C. After thawing it should be centrifuged for 15 min at 10,000 × *g* to check for the presence of aggregates. If sediment is found, use the supernatant only after measuring its protein content.

3.2.6 Checking the Degree of Rac Prenylation

Prenylation in vitro is a very reliable methodology provided that a trusted source of geranylgeranyl transferase I is available. Nevertheless, it is recommended that until enough experience is acquired, the degree of prenylation should be checked [104].

1. Remove an aliquot from the completed prenylation mixture before adding glycerol. Since the final detection method is based on SDS-PAGE, one has to remove sufficient protein to make detection easy. Normally, one third of a 10 nmol Rac prenylation mixture is used for confirming prenylation (about 3 nmol Rac). The procedure is best performed in 1.5 mL conical microcentrifuge tubes.
2. Add prenylation buffer up to a total volume of 0.9 mL.
3. Add 0.1 mL of 10 % Triton X-114 (1 % final concentration).
4. Place the tube in ice-water for 30 min, vortexing the tube every 5 min.
5. Heat the mixture at 37 °C for 10 min in a heating block or a water bath. Keep the tubes stationary—do not mix. This will cause the solution to become cloudy due to aggregation of Triton X-114 above its cloud point. Amphiphilic proteins, such as prenylated Rac, will associate with the detergent aggregates, whereas nonprenylated Rac will remain in the aqueous phase.
6. Centrifuge the mixture at 10,000–12,000 × *g* in a microfuge at room temperature. This will result in phase separation with the upper (aqueous) phase containing nonprenylated Rac and the lower (detergent-enriched) phase containing prenylated Rac. Transfer upper phase into a fresh tube.
7. Add prenylation buffer to the lower phase to make the total volume equal to that of the upper phase, and mix well.
8. Take equal sample volumes from the two phases and subject to SDS-PAGE.
9. Compare intensity of the Rac bands (21 kDa) in the two phases visually or by densitometry (*see* **Note 29**).

3.3 An Overview of Cell-Free Assay Design

For the proper application of cell-free assays, it is essential to recall a number of theoretical considerations, as outlined below.

1. The $O_2^{\bullet-}$-producing component is cytochrome b_{558} found in the membrane and results are to be related to the amount of cytochrome b_{558} present in the reaction.
2. All cytosolic components must be present at saturating quantities in relation to cytochrome b_{558}. These quantities are determined with dose–response experiments in which the concentration of one or all cytosolic components is varied in the presence of a constant amount of cytochrome b_{558} (membrane).
3. The amphiphile-independent cell-free system is a very useful variant of the canonical system, with specific applications in

situations in which the emphasis is on interaction between Nox2 and $p67^{phox}$. In spite of the fact that it was described more than a decade ago [9], and is technically simple, it has not gained wide acceptance.

4. Normally, amphiphile-dependent cell-free assays are performed with nonprenylated Rac1. However, identical results are obtained with prenylated Rac1, provided that $p47^{phox}$ and $p67^{phox}$ are present in the reaction. In the absence of $p47^{phox}$, amphiphile exerts a paradoxical inhibitory effect in cell-free assays containing prenylated Rac and $p67^{phox}$ [52].
5. All cell-free assays comprise two stages: (a) the stage of oxidase complex assembly, in the course of which cytosolic components translocate to the membrane, leading to the induction of conformational change in Nox2, and (b) the catalytic stage, initiated by the addition of NADPH, resulting in the production of $O_2^{\bullet-}$. In some forms of cell-free assay, the two stages are separated by the interruption of assembly just before the initiation of catalysis. In most assays, the assembly merges with the catalytic stage, although an effort is usually made to bring assembly to completion before the addition of NADPH.
6. Amphiphile-dependent oxidase assembly is time- and temperature-dependent (*see* **Note 30**).
7. Kinetic models of anionic amphiphile-induced oxidase assembly have been proposed both before [105, 106] and after [107] the identification of the components of the oxidase. These contain useful information, which, paradoxically, had relatively little influence on the design and methodological aspects of cell-free assays.
8. Oxidase activation in cell-free systems is reduced by an increase in the ionic strength of the assay buffer (*see* **Note 31**).

3.4 The Canonical Amphiphile-Dependent Cell-Free Assay: "Don't Leave Home Without It"

We describe here the basic methodology for performing cell-free oxidase activation in what is called the "semi-recombinant" system. This is a modification of the original amphiphile-activated (membrane + cytosol) system [21–24, 27]. Since measuring ROS production by phagocytes by microplate spectrophotometers became the standard procedure [108, 109], spectrophotometric kinetic methodology in microtiter plates also became the routine procedure for the performance of cell-free assays. This required adjustment of the assay from the 1–3 mL volumes, used in standard spectrophotometers, to 100–300 μL volumes used with 96-well microtiter plates (96-well plates). We describe a kinetic cell-free oxidase activation assay performed in 96-well plates in which the reaction components comprise solubilized macrophage membrane liposomes, recombinant $p47^{phox}$, $p67^{phox}$, and nonprenylated Rac1.

3.4.1 Cytochrome c Reduction

1. Add 20 μL of solubilized membrane liposomes (50 nM cytochrome b_{558} heme) to the wells of a 96-well plate. This is intended to result in a final concentration of 5 nM cytochrome b_{558} heme in 200 μL (the total volume of the reaction before addition of NADPH) and equals 1 pmol cytochrome b_{558} heme/well.
2. Add 20 μL of a mixture of $p47^{phox}$, $p67^{phox}$, and nonprenylated Rac1-GMPPNP (or Rac1 Q61L mutant), each at a concentration tenfold higher than that desired as the final concentration in 200 μL. As an example, if a final concentration of 100 nM is to be achieved for all three components, add 20 μL of a solution containing 1 μM of each component (*see* **Note 32**). Make all dilutions of membrane and cytosolic components in oxidase assay buffer without LiDS. Dispensing 10 or 20 μL aliquots of membrane or cytosolic components to the wells is best performed with electronic pipettors, in the dispensing mode, or with multichannel pipettors.
3. Add 160 μL/well of assay buffer containing an optimized concentration of LiDS. We typically use a digital 12-channel pipette. For this protocol, the final concentration of LiDS causing maximal activation is 120–130 μM (Fig. 2) (*see* **Note 33**). Because the amphiphile is diluted 1.25-fold by the volumes of

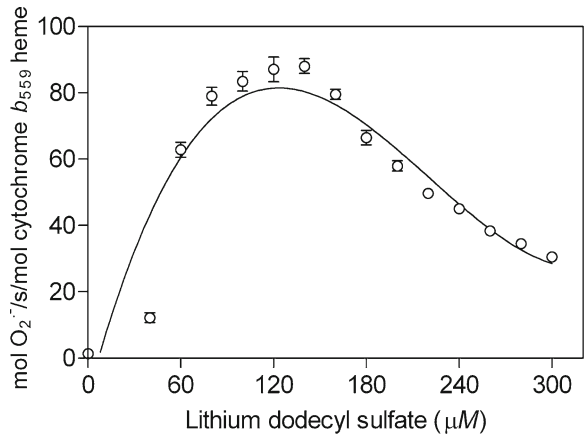

Fig. 2 Dose–response curve of lithium dodecyl sulfate (LiDS) in the amphiphile-dependent cell-free system. Assay mixtures consisting of solubilized macrophage membrane liposomes (5 nM cytochrome b_{558} heme) and recombinant $p47^{phox}$ (100 nM), $p67^{phox}$ (100 nM), and non-prenylated Rac1-GMPPNP (100 nM) were incubated with varied concentrations of LiDS as indicated. $O_2^{\cdot-}$ production was initiated by the addition of NADPH and measured by the kinetic cytochrome *c* reduction assay for 5 min. Results represent means ± SE of three experiments. Reproduced from [142] by permission of Humana Press©2007

membrane and cytosolic components previously added to the wells, the concentration of the amphiphile in the assay buffer has to be adjusted accordingly (as an example, to achieve a final concentration of 130 μM, add 160 μL of a 162.5 μM solution).

4. Place the plate on an orbital shaker and mix contents for 90 s at 500–600 movements/min and room temperature (*see* **Note 34**).
5. Dispense 10 μL of NADPH/well using a multichannel pipettor, as fast as possible. This results in a final concentration of 238 μM NADPH in a total volume of 210 μL per well, which is well above the K_m for NADPH of the oxidase in the cell-free system [21].
6. Transfer the plate quickly to the microplate spectrophotometer and mix contents for 5 s using the mixing option of the reader. The instrument should be set to record increase in absorbance at 550 nm over a time period of 5 min with 28 readings being executed at 0.11 min intervals at room temperature (temperature regulation by the microplate spectrophotometer is set "off"). Include blank wells containing 200 μL assay buffer to which 10 μL of 5 mM NADPH were added simultaneously with its addition to the sample wells.
7. For most instruments, results in the kinetic mode are expressed in $Abs_{550\ nm}$/min units. The software of the instrument calculates these values by dividing the ΔAbs_{550nm} or, preferably, $\Delta mAbs_{550nm}$ over time, by the number of minutes elapsed. Thus, it is essential for the increase in absorbance curve to be linear. The curves turn nonlinear whenever one or more components of the reaction is/are exhausted. Although every effort is made to prevent this from occurring, by choosing the right amounts of enzyme (cytochrome b_{558} in the membrane), cytochrome *c*, and NADPH per well (*see* **Note 35**), it occasionally happens (*see* Fig. 3). In this case, the linear portion of the curve is chosen, and values are recalculated as $\Delta mAbs_{550nm}$/min for the revised time interval (shorter than 5 min). Contemporary microplate readers are fitted with the appropriate software, allowing fast and simple recalculation of the slopes after selecting the linear segment. $\Delta mAbs_{550nm}$/min values are transformed to nnmol cytochrome *c* reduced per min per well content of 210 μL, based on the extinction coefficient $\Delta E_{550} = 21\ mM^{-1}\ cm^{-1}$ for reduced minus oxidized cytochrome *c* (nmol $O_2^{\bullet-}$/min/well) (*see* **Note 36**).
8. Express the final results as "turnover": the amount of $O_2^{\bullet-}$ produced per time unit per mol membrane cytochrome b_{558} heme (mol $O_2^{\bullet-}$/s/mol cytochrome b_{558} heme; *see y*-axis of graphs in most figures in this chapter). This is easily calculated by knowing the nmol $O_2^{\bullet-}$/min/well values and the amount of cytochrome

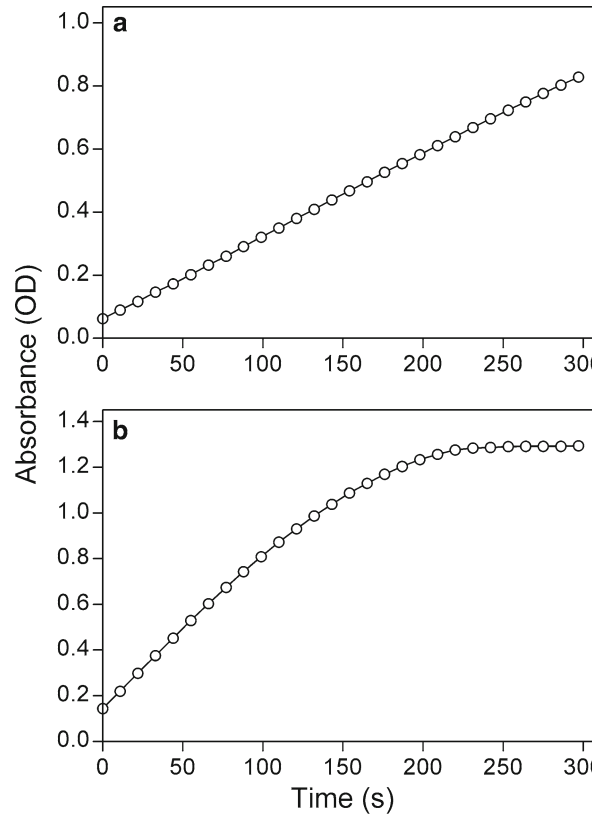

Fig. 3 Actual data displays of the results of two kinetic cell-free assays, showing the increase in absorbance at 550 nm over a 300-s interval. (**a**) Increase is linear throughout the 300 s period. (**b**) Increase is linear up to 120 s, after which time it starts leveling off. In this situation, the ΔAbs_{550nm}/min should be recalculated for the first 120 s. Turnover values were found to be 41 mol $O_2{\cdot}^-$/s/mol cytochrome b_{558}, for panel **a**, and 106 mol $O_2{\cdot}^-$/s/mol cytochrome b_{558}, for panel **b** (recalculated value). Reproduced from [142] by permission of Humana Press©2007

b_{559} heme per well (1 pmol, when 20 μL of membrane, containing 50 nM of cytochrome b_{558} heme, are added per well). For each experimental condition, perform the assay in triplicate wells and make the software calculate mean values and standard deviations (*see* **Note 37**).

9. It is essential to include SOD control wells in cell-free assays to assure that the reduction of cytochrome *c* is indeed due to $O_2{\cdot}^-$. This requires that parallel SOD-containing wells are included for every group of wells in which $O_2{\cdot}^-$ production is detected. Use a large excess of 100 U SOD/mL by adding 10 μL/well of a 2,000 U/mL of SOD solution before the addition of NADPH. Addition of SOD is expected to prevent cytochrome *c* reduction by 95 % or more (*see* **Note 38**).

10. A number of additional control reactions are requirements for the proper execution of cell-free assays, and no assay is complete without the inclusion of reactions wells in which one of the following components is omitted (i.e., anionic amphiphile, NADPH, membrane, and all or each of the individual cytosolic components).

3.4.2 INT Reduction

Cytochrome *c* reduction can be replaced by INT reduction. The method is identical to that described under Subheading 3.4.1, with the exception that the assay buffer contains 100 μM INT instead of cytochrome *c* (*see* **Note 39** for converting increase in absorbance at 490 nm data to $O_2^{\bullet-}$ values).

Three problems are related to the use of the INT technique:

1. The first is the possibility that INT is reduced by electrons originating from reduced Nox2-bound FAD ($FADH_2$) [71]. In our hands, however, when using the canonical semi-recombinant amphiphile-activated cell-free system, at least 80 % of INT reduction is SOD-sensitive and, thus, mediated by $O_2^{\bullet-}$.
2. Second, SDS and LiDS react with INT, forming an unidentified material that absorbs at 490 nm. We have no experience with using C20:4 to replace the anionic detergents.
3. Third, in our hands, INT is about 50 % less effective than cytochrome *c* in detecting $O_2^{\bullet-}$ production in the canonical cell-free assay, under strictly identical conditions. The reason for this is unclear.

INT reduction should, therefore, be used predominantly for measuring the diaphorase activity of the DHR of Nox2 [72–74] and, possibly, other Noxes [70, 75].

3.4.3 NADPH Consumption

The method is similar to that described under Subheading 3.4.1, with the exception that the assay buffer contains no electron acceptor and a negative slope, corresponding to the conversion of NADPH to $NADP^+$, is recorded [80] (*see* **Note 40** for converting *decrease* in absorbance at 340 nm data to $O_2^{\bullet-}$ values). As in the cytochrome *c* and INT assays, the catalytic phase of the reaction is initiated by the addition of NADPH to the wells. A number of issues are to be taken into consideration:

1. The technique is useful when there is evidence for interference by a component of the cell-free reaction with electron acceptors, as illustrated previously for INT [71] and cytochrome *c* [81], or in the presence of a reducing agent.
2. It is ideal for use with amphiphile-dependent semi-recombinant cell-free systems, in which the presence of contaminating NADPH reductases is unlikely. Even in their presence, the absolute dependence on an amphiphile activator makes the assay applicable.

3. The sensitivity of the assay is comparable to that based on cytochrome *c* reduction.
4. A possible limitation is the requirement for microplates allowing passage of UV light.

3.5 Amphiphile-Independent Cell-Free Assays

The ability to activate the oxidase in vitro in the absence of an anionic amphiphile was first reported by Sumimoto et al. [50], based on C-terminal truncation of both $p47^{phox}$ and $p67^{phox}$. Amphiphile-independent systems were also described by Tamura et al. [38], using a chimeric construct consisting of truncated $p67^{phox}$ and $p47^{phox}$, and by Kleinberg et al. [51], who prevented the establishment of intramolecular bonds in $p47^{phox}$, by mutagenesis. The two latter groups and we [42] also observed that acidification of the membrane phospholipid environment made the presence of an anionic amphiphile unnecessary.

A conceptually distinct situation, in which oxidase activation can be achieved in the absence of amphiphile and of $p47^{phox}$, is represented by a cell-free system consisting of membrane liposomes, $p67^{phox}$, and prenylated Rac [9]. We proposed that proper targeting of $p67^{phox}$ to the membrane in conjunction with the induction of a conformational change in $p67^{phox}$ by Rac is sufficient for the initiation of electron flow in Nox2 [7, 9, 53]. Variations of this system include activation by combinations of $p67^{phox}$, prenylated Rac, GTP, and a Rac GEF [55], and the recently described amphiphile-independent oxidase activation by $p67^{phox}$ and prenylated [Rac-RhoGDI] complexes [57, 58].

We describe two methods for amphiphile-independent cell-free oxidase activation. One assay is based on the use of prenylated Rac and does not require the participation of $p47^{phox}$; the other makes use of our ability to modify the charge of phospholipids in phagocyte membranes and works with nonprenylated Rac.

3.5.1 Amphiphile-Independent Cell-Free Oxidase Activation in Mixtures of Membrane, $p67^{phox}$, and Prenylated Rac1

The amphiphile-independent cell-free system is useful for investigating the role of Rac and Rac-$p67^{phox}$ interaction in oxidase assembly. This particular aspect of assembly is more difficult to explore in the presence of $p47^{phox}$, which has not only an assembly-initiating function but also a role in the stabilization of the assembled complex [41]. Other situations in which the amphiphile-independent cell-free system is the assay of choice are when the effects of regulators of Rac are to be explored in vitro. One example is provided by Rac GEF-dependent oxidase activation in a cell-free system consisting of membrane, $p67^{phox}$, prenylated Rac1-GDP, GTP, and a Rac GEF, such as Trio or Tiam1 [55]. Another example is the ability of [prenylated Rac1-RhoGDI] complexes in conjunction with $p67^{phox}$, to activate the oxidase when added to phagocyte membrane liposomes enriched in anionic phospholipids [57] or specific phosphoinositides, in the presence of GTP and a GEF [58], in the absence of amphiphile.

Applications of amphiphile-independent cell-free assays also comprise the study of inhibitors (proteins, peptides, phospholipids, nucleotides, detergents, drugs) on the various stages of oxidase assembly. An example is the study of the effect of the amphiphilic activator LiDS on oxidase activation by $p67^{phox}$ and prenylated Rac1-GMPPNP, in the absence of $p47^{phox}$. We found LiDS to exert a marked dose-dependent inhibitory effect, in the 25–200 μM concentration range, which was relieved by the presence of $p47^{phox}$ [52]. Further examples are the distinct effects of a number of compounds (GTP and GDP, a C-terminal Rac1 peptide, RhoGDI, the p21-binding domain of p21-activated kinase (PBD of PAK), and neomycin sulfate) on amphiphile-dependent and -independent cell-free oxidase assembly, reflecting the existence of different pathways of assembly [52].

1. Subject Rac1 to nucleotide exchange with GMPPNP or use Rac1 Q61L mutant. It is preferable to perform nucleotide exchange before prenylation. This will reduce possible loss of prenylated protein during exchange by binding to surfaces due to hydrophobicity.
2. Prenylate Rac1-GMPPNP, as described above.
3. Add 20 μL/well of solubilized membrane liposomes (50 nM cytochrome b_{558} heme) to the wells of a 96-well plate. This is intended to result in a final concentration of cytochrome b_{558} heme of 5 nM in 200 μL (the total volume of the reaction, before the addition of NADPH) and equals 1 pmol cytochrome b_{558} heme/well.
4. Add 20 μL of a mixture of $p67^{phox}$ and prenylated Rac1-GMPPNP, each at a concentration tenfold higher that that desired as the final concentration in 200 μL. If the requirements of the experiment are to add each component separately, add 10 μL of each component from a 20-fold concentrated stock solution. All dilutions of membrane and cytosolic components are made in assay buffer without LiDS (*see* **Note 41**).
5. Add 160 μL/well of assay buffer without LiDS using a digital 12-channel pipette. Place the plate on an orbital shaker and mix for 90 s at 500–600 movements/min and room temperature (*see* **Note 42**).
6. Dispense 10 μL of NADPH solution/well using an electronic pipettor, in the dispensing mode, or a multichannel pipette. This results in a final concentration of 238 μM NADPH in a total volume of 210 μL per well.
7. Record activity and convert to turnover values as described for the amphiphile-dependent system (*see* Subheading 3.4). An example of such an assay, with the required control mixtures, is illustrated in Fig. 4.

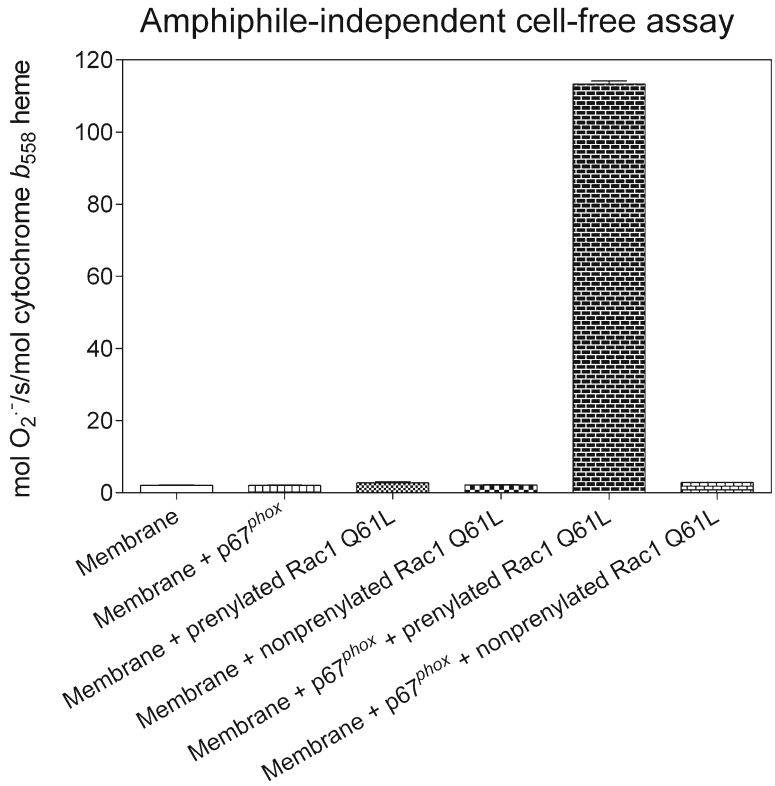

Fig. 4 Typical amphiphile-independent cell-free assay. The complete reaction mixture contained solubilized macrophage membrane liposomes (5 nM cytochrome b_{558} heme), recombinant p67^{phox} (300 nM), and recombinant Rac1 Q61L prenylated in vitro (300 nM). The contents were incubated without amphiphile for 5 min at room temperature. $O_2^{\cdot-}$ production was initiated by the addition of NADPH (238 μM) and measured by the kinetic cytochrome *c* reduction assay for 5 min. The compositions of the control (incomplete) assay mixtures are indicated on the *x*-axis. Results represent means ± SE of three experiments

3.5.2 Amphiphile-Independent Cell-Free Oxidase Activation in Mixtures of Negatively Charged Membrane, p47^{phox}, p67^{phox}, and Nonprenylated Rac1

Preparing Membrane Liposomes Enriched In Anionic Phospholipids

1. Dilute solubilized macrophage membrane in solubilization buffer containing 40 mM octyl glucoside to a concentration of cytochrome b_{558} heme of 1.2 nmol/mL.
2. Add PA or PG, both at a concentration of 5 mM, at a ratio of one part membrane and four parts phospholipids. This results in a final concentration of 240 pmol/ml cytochrome b_{558} heme and 4 mM anionic phospholipids.
3. Dialyze the membrane-phospholipid mixture (*see* **Note 13**) against a 100-fold excess of detergent-free solubilization buffer (also lacking AEBSF and FAD) for 18–24 h at 4 °C (*see* **Note 14**).
4. Measure the concentration of cytochrome b_{558}, and supplement the preparation with 10 μM FAD.
5. Divide into aliquots of 1–1.5 mL and store at –75 °C.

Amphiphile-Independent Cell-Free Oxidase Activation with Anionic Membrane Liposomes

This cell-free assay is a hybrid between the canonical amphiphile-dependent system (from which it borrowed the anionic charge requirement and the fact that Rac is nonprenylated) and the amphiphile-independent assay (based on the use of prenylated Rac).

1. Add 20 μL/well of membrane liposomes enriched in PA or PG (50 nM cytochrome b_{558} heme and about 0.8 mM anionic phospholipid) to the wells of a 96-well plate. This is intended to result in a final concentration of cytochrome b_{558} heme of 5 nM and close to 80 μM anionic phospholipid in 200 μL (the total volume of the reaction, before the addition of NADPH) and equals 1 pmol cytochrome b_{558} heme/well.
2. Add 20 μL of a mixture of $p47^{phox}$, $p67^{phox}$, and nonprenylated Rac1-GMPPNP or Rac1 Q61L mutant, each at a concentration tenfold higher that that desired as the final concentration in 200 μL (*see* **Note 43**). All dilutions of membrane and cytosolic components are made in assay buffer without LiDS. In most situations, concentrations of $p47^{phox}$, $p67^{phox}$, and nonprenylated Rac required for reaching maximal activation in this system are higher than those customary in the canonical amphiphile-dependent assay.
3. Add 160 μL/well of assay buffer without LiDS. Place the plate on an orbital shaker and mix for 90 s at 500–600 rotations/min and room temperature.
4. Dispense 10 μL of NADPH solution/well. This results in a final concentration of 238 μM NADPH in a total volume of 210 μL per well.
5. Record activity and convert to turnover values as described for the amphiphile-dependent system.

3.6 Sense and Sensitivity in Cell-Free Assays

Here, we discuss a number of methodological issues related to the proper way of performing cell-free assays. Emphasis will be placed on untested or unproven assumptions and some "sacred cows" will be questioned.

3.6.1 LiDS, SDS, or Arachidonate?

1. Unless the purpose of performing the cell-free assay is to explore the oxidase activating capabilities of C20:4 itself or of C20:4 isomers or C20:4 oxidation products, there are few occasions justifying the use of C20:4 as an activator.
2. C20:4 acid activates the oxidase only in its ionized salt form, and stock solutions are tedious to prepare and are unstable. We recommend using LiDS or SDS as standard amphiphilic activators.
3. SDS is as good an activator as LiDS, but concentrated solutions of SDS must be kept at room temperature. LiDS and SDS yield more reproducible results than C20:4. We find no basis for the claim that C20:4 is to be preferred because it represents a more "physiologic" form of activation.

3.6.2 To Supplement or Not to Supplement?

1. Calcium: in early experiments, we found that activation was reduced by Ca^{2+} and moderately enhanced by the Ca^{2+} chelator EGTA [21] (*see* **Note 44**). We reinvestigated the necessity of Ca^{2+} chelation in the LiDS-activated and amphiphile-independent systems by examining the effect of EGTA, alone or in association with other supplements. As seen in Fig. 5a, b, EGTA had no enhancing effect on oxidase activation in both the amphiphile-dependent and -independent systems.
2. FAD: a flavin requirement was observed in the oxidase isolated from stimulated phagocytes [17], and, early in the development of the C:20-activated cell-free system, it was found that exogenous FAD enhanced activation [21]. The most likely explanation is that Nox2 lost the noncovalently bound FAD during preparation of membranes, leading to a need to reflavinate cytochrome b_{558}. Here, we compared cell-free oxidase activation in the presence and absence of 10 μM FAD in the assay buffer by using solubilized membrane liposomes, which are routinely supplemented with FAD. As apparent in Fig. 5, FAD enhanced both amphiphile-dependent (Fig. 5a) and amphiphile-independent (Fig. 5b) oxidase activation, the effect being more pronounced on the amphiphile-dependent activation (*see* **Note 45**).
3. Magnesium: a requirement for Mg^{2+} was described early in cell-free studies, and it was suggested that the metal interacted with a saturable oxidase component at a K_m of about 1 mM [105]. The identity of this component was not established at the time, but after the discovery of the involvement of Rac in oxidase assembly, it became common belief that the requirement for millimolar concentrations of Mg^{2+} was related to its role in preventing the dissociation of GTP from Rac [97]. As shown in Fig. 5, supplementation of the assay buffer with 1 mM Mg^{2+} enhanced oxidase activation in both the amphiphile-dependent (Fig. 5a) and -independent (Fig. 5b) systems. Higher concentrations of Mg^{2+} (up to 5 mM) were not more effective than 1 mM (results not shown). Combining supplementation with FAD with that with Mg^{2+} did not result in an additive or synergistic effect; activities were identical to those found with FAD alone. Also, combining supplementation with FAD or Mg^{2+} with EGTA, or adding all three supplements, had no additive or synergistic effect. The almost identical ability of FAD and Mg^{2+} to improve assembly and the lack of an additive or cooperative effect suggest that they act by the same mechanism, most likely related to the stability of the Nox2-FAD bond and not to that of the Rac-GTP bond (*see* **Note 46**).

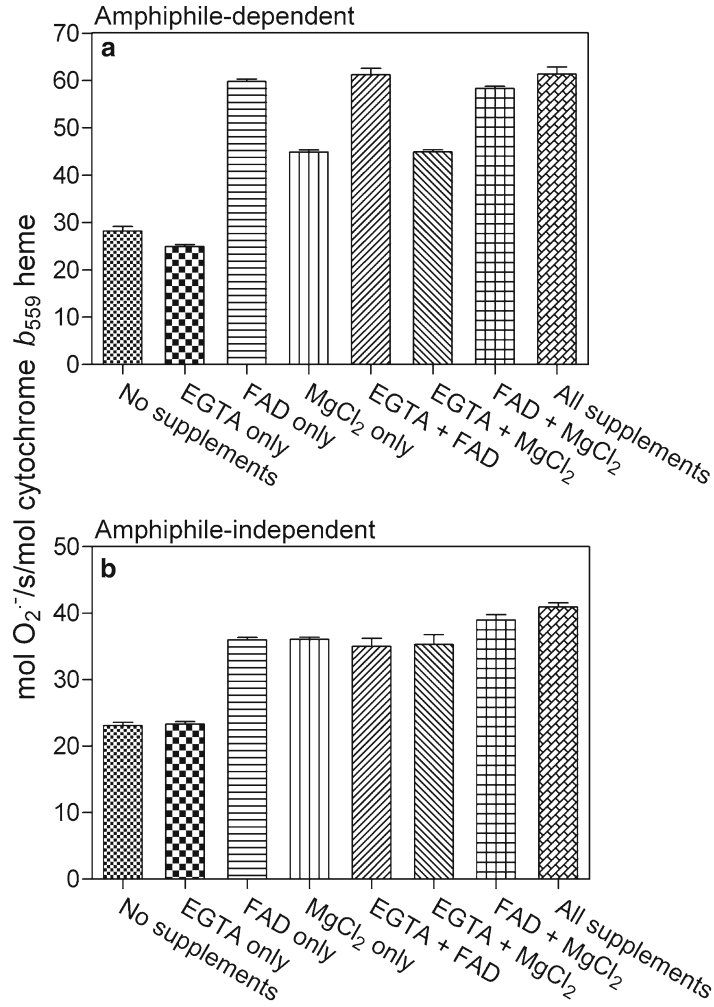

Fig. 5 Which supplements to the cell-free NADPH oxidase assay buffer are essential? Cell-free assays were performed in the canonical amphiphile-dependent system (**a**) and in the amphiphile-independent system, based on the use of prenylated Rac1 (**b**). The basic assay buffer was supplemented with 1 mM EGTA, 10 μM flavin adenine dinucleotide disodium salt, or 1 mM $MgCl_2$, or combinations of two or all three of these, as shown on the *x*-axis of panels **a** and **b**. (**a**) Amphiphile-dependent cell-free systems consisting of solubilized macrophage membrane liposomes (5 nM cytochrome b_{558} heme) and recombinant p47^{phox} (30 nM), p67^{phox} (30 nM), and non-prenylated Rac1-GMPPNP (30 nM) were incubated with 130 μM lithium dodecyl sulfate, as described. (**b**) Amphiphile-independent cell-free systems consisting of solubilized macrophage membrane liposomes (5 nM cytochrome b_{558} heme), recombinant p67^{phox} (300 nM), and recombinant Rac1-GMPPNP prenylated in vitro (300 nM*)* were incubated without amphiphile, as described. In both panels **a** and **b**, $O_2^{\cdot-}$ production was initiated by the addition of NADPH and measured by the kinetic cytochrome *c* reduction assay for 5 min. Results illustrated represent means ± SE of three experiments. Reproduced from [142] by permission of Humana Press©2007

3.6.3 "Measure for Measure": The Intricacies of Dose–Response Studies with Cytosolic Oxidase Components

1. Most cell-free oxidase activation assays follow the principle of a constant amount of membrane and variable amounts of cytosolic components. This leaves open the issue of quantitative relationships among cytosolic components (*see* **Note 47**).
2. A problem we frequently encountered when performing cell-free assays was determining the optimal methodology for relating activity turnover values to the amounts of cytosolic proteins added to a constant amount of membrane. Figure 6 summarizes the two main approaches used in our laboratory. In these experiments, the concentration of the membrane was constant. The concentrations of cytosolic components were either varied all in parallel or individually, in which case the other components were added at the maximal concentration in the range studied. Assays were run either in the amphiphile-dependent system (Fig. 6a) or in the amphiphile-independent system (Fig. 6b). In the amphiphile-dependent system, the concentration of LiDS was kept constant at 130 μM because the optimal activating concentration of LiDS did not vary with the concentration of cytosolic components within the 0–1 μM range when using purified recombinant cytosolic components.
3. It is apparent that when all components are varied in parallel, the dose–response curve has a sigmoidal shape, whereas when a single component is varied in the presence of an excess of the other component(s), the curves are hyperbolic. The highest levels of activation are seen when the concentrations of Rac1 and $p47^{phox}$ (amphiphile-dependent system) and Rac1 (amphiphile-independent system) are varied individually, in the presence of an excess of the other component(s); the lowest activities are found when $p67^{phox}$ is varied individually. The differences are particularly marked at lower concentrations of components.
4. When the purpose of performing cell-free assays is the detection of low concentrations of a cytosolic component, it is best to perform the assay in the presence of a clear excess of the other components, a situation generating hyperbolic curves (*see* **Note 48**).

3.6.4 To Exchange or to Add?

1. In the early period of the use of cell-free assays, it was reported repeatedly that the addition of GTP or non-hydrolyzable GTP analogs (GTPγS or GMPPNP) was an absolute requirement for the expression of oxidase activity. Many of these observations were made in cell-free systems consisting of membrane and total cytosol before the identification of Rac as the small GTPase involved in oxidase activation [110–113].
2. With the advent of the semi-recombinant systems, which involved the use of recombinant Rac1 or Rac2, the "habit" of

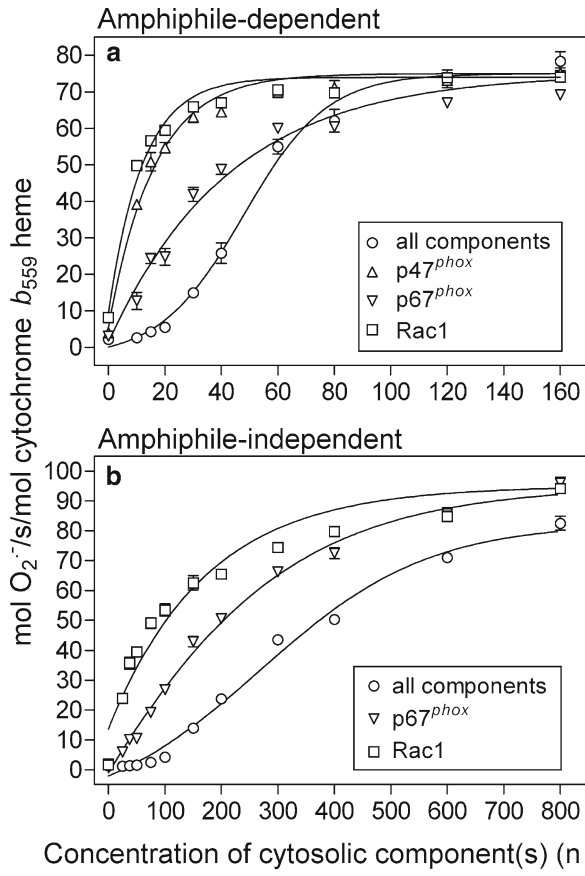

Fig. 6 The effect of concentration ratios among cytosolic components on the nature of the dose–response curves in cell-free assays. (**a**) Four types of amphiphile-dependent cell-free assays, consisting of various combinations of cytosolic components, were performed. All four consisted of solubilized macrophage membrane liposomes (5 nM cytochrome b_{558} heme), recombinant p47^{phox} (varied from 0 to 160 nM), and recombinant p67^{phox} (varied from 0 to 160 nM), and recombinant non-prenylated Rac1-GMPPNP (varied from 0 to 160 nM). The four combinations of components were: (1) All three cytosolic components were present at equal concentrations (varied from 0 to 160 nM); (2) p47^{phox} was varied from 0 to 160 nM, whereas p67^{phox} and Rac1 were both present at a concentration of 160 nM; (3) p67^{phox} was varied from 0 to 160 nM, whereas p47^{phox} and Rac1were both present at a concentration of 160 nM, and (4) Rac1 was varied from 0 to 160 nM, whereas p47^{phox} and p67^{phox} were both present at a concentration of 160 nM. In all cases, the components were incubated with 130 μM lithium dodecyl sulfate, as described. (**b**) Three types of amphiphile-independent cell-free assays, consisting of various combinations of cytosolic components, were performed. All three consisted of solubilized macrophage membrane liposomes (5 nM cytochrome b_{558} heme), recombinant p67^{phox} (from 0 to 800 nM), and recombinant Rac1-GMPPNP prenylated in vitro (from 0 to 800 nM). The three combinations of components were: (1) The two cytosolic components were present at equal concentrations (varied from 0 to 800 nM); (2) p67^{phox} was varied from 0 to 800 nM, whereas Rac1 was present at a concentration of 800 nM, and (3) Rac1 was varied from 0 to 800 nM, whereas p67^{phox} was present at a concentration of 800 nM. The components were incubated in the absence of an anionic amphiphile. In all assays, $O_2{\cdot}^-$ production was initiated by the addition of NADPH and measured by the kinetic cytochrome *c* reduction assay for 5 min. Results illustrated in both panels represent means ± SE of three experiments. Reproduced from [142] by permission of Humana Press©2007

supplementing the assay buffer with GTP analogs persisted when native Rac (Rac-GDP not exchanged to GTP) was present in the reaction. The assumed explanation for this was that added GTP analogs were bound to Rac-GDP in a nucleotide exchange reaction taking place simultaneously with oxidase assembly (*see* **Note 49**).

3. Because the concentration of Mg^{2+} in the assay buffer is prohibitive for spontaneous nucleotide exchange, the ability of prenylated Rac to take up GTP from the medium points to the intervention of a GEF. In a semi-recombinant cell-free system, GEF can originate only in the membrane but its presence, identity, and quantity are unknown parameters in the vast majority of cases and will depend on the animal species and nature of the phagocyte serving as the source for the membrane [114].
4. Another common assumption is that native Rac (Rac-GDP) is inactive in cell-free systems (however, *see* ref. 101). We have shown in the past that this is true only below a certain quantitative threshold and when this is exceeded, significant activity can be achieved. Thus, in the canonical amphiphile-dependent cell-free system, the differences in V_{max} between Rac1-GDP and Rac1-GTPγS were marked at 20 nM Rac but minimal, at 200 nM Rac [115].
5. Figure 7 summarizes studies in which the influence of the following parameters on the ability of Rac1 to support oxidase activation in cell-free systems was examined: (1) GDP vs GMPPNP-bound state; (2) supplementation of the assay buffer with GTPγS; and (3) nonprenylated versus prenylated Rac, corresponding to amphiphile-dependent and -independent assay, respectively.
6. It is apparent that in the amphiphile-dependent system, when the concentration of the cytosolic components is low (30 nM), the difference in activity between native Rac1 (Rac1-GDP) and Rac1 exchanged to GMPPNP (Rac1-GMPPNP) is pronounced (Fig. 7a). When the concentration is raised to 100 nM, the difference in activity between Rac1-GDP and Rac1-GMPPNP is much less pronounced, which is due principally to an increase in activity of Rac1-GDP (Fig. 7b). What is also seen clearly in Fig. 7a, b is that supplementation of the assay buffer with GTPγS (10 μM) has no significant enhancing effect on the activity of Rac1-GDP and does not influence the activity of Rac1-GMPPNP (*see* **Note 50**). In the amphiphile-independent cell-free system, involving the use of prenylated Rac, the difference in the ability to support oxidase activation between Rac1-GDP and Rac1-GMPPNP is marked, with practically no activity being exhibited by prenylated Rac1-GDP (Fig. 7c). The addition of GTPγS

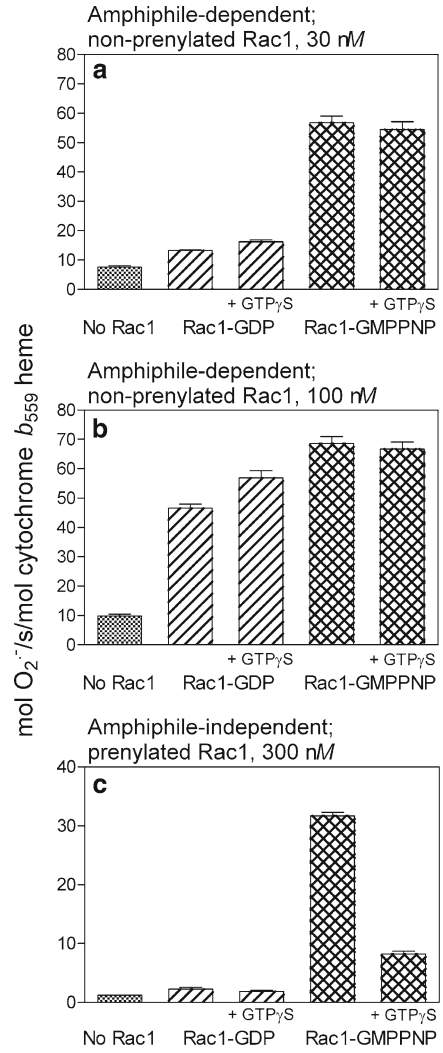

Fig. 7 Does the addition of exogenous non-hydrolyzable GTP analog (GTPγS) affect cell-free NADPH oxidase activation in the amphiphile-dependent and amphiphile-independent cell-free systems? (**a**, **b**) NADPH oxidase activity was measured in a cell-free system (±10 μM GTPγS, as indicated on the *x*-axis) consisting of solubilized macrophage membrane liposomes (5 nM cytochrome b_{558} heme), recombinant $p47^{phox}$ (30 or 100 nM) and $p67^{phox}$ (30 or 100 nM), and recombinant non-prenylated Rac1 (30 or 100 nM), either as native Rac1-GDP or as Rac1-GMPPNP. The components were incubated in the presence of 130 μM LiDS, as described. (**c**) NADPH oxidase activity was measured in a cell-free system (±10 μM GTPγS, as indicated on the *x*-axis) consisting of solubilized macrophage membrane liposomes (5 nM cytochrome b_{558} heme), recombinant $p67^{phox}$ (300 nM), and recombinant Rac1 (300 nM), either as Rac1-GDP or Rac1-GMPPNP prenylated in vitro. The components were incubated in the absence of an amphiphilic activator at room temperature. In all assays, $O_2^{\cdot-}$ production was initiated by the addition of NADPH and measured by the kinetic cytochrome *c* reduction assay for 5 min. Results illustrated in all panels represent means ± SE of three experiments. Reproduced from [142] by permission of Humana Press©2007

(10 μM) did not correct this lack of activity, in contradiction to results obtained with prenylated Rac in the presence of amphiphile [116, 117] (*see* **Note 51**).

7. Overall, we recommend that one should never rely on "in assay" nucleotide exchange, achieved by the addition of GTP analogs to the assay buffer, and always perform quantifiable nucleotide exchange on both nonprenylated and prenylated Rac, before their use in the assays. Following this advice will prevent inconsistent and poorly reproducible results, due both to the lack of conversion of Rac from the GDP- to the GTP-bound form, and to a possible inhibitory effect of free GTP.

3.6.5 Sibling Rivalry: Rac1 and Rac2

1. It is widely accepted today that the isoform of Rac relevant to oxidase function in human neutrophils is Rac2 [97]. Mouse neutrophils have similar amounts of Rac1 and Rac2, but Rac2 has the predominant role in oxidase activation [118, 119]. Human monocytes [99] and guinea pig macrophages [43, 98] use Rac1 in oxidase assembly.
2. Comparative studies of Rac1 versus Rac2 in cell-free assays have been published (*see* **Note 52**).
3. Here, we show a comparative study of the relative abilities of Rac1 and Rac2, in nonprenylated and prenylated forms and in the absence of and following exchange to GMPPNP, to activate the oxidase in the cell-free system. Nonprenylated Rac isoforms were assayed in an amphiphile-activated system whereas prenylated Rac isoforms were used in an amphiphile-independent system. As seen in Fig. 8a, contrary to the dogma, both nonprenylated Rac1-GMPPNP and Rac1-GDP are capable of activation, with V_{max} values of 89 and 83 mol $O_2^{\bullet-}$/s/mol cytochrome b_{558} heme, respectively, and EC_{50} values of 5.74 and 9.70 nM, respectively. Rac2-GMPPNP was clearly less active than Rac1-GMPPNP, as evident in the tenfold higher EC_{50} (53 nM). Rac2-GDP is, for practical purposes, inactive.
4. A similar study made with prenylated Rac1 and Rac2, in the absence of an amphiphilic activator and $p47^{phox}$, revealed that only the GMPPNP-preloaded forms of Rac1 and Rac2 are active. Again, Rac1 was more active than Rac2, as shown by the EC_{50} values of 0.13 and 0.73 μM, respectively (Fig. 8b).
5. Thus, the claim that "Rac-GTP is active; Rac-GDP is inactive" is applicable to prenylated Rac, in the absence of amphiphile and $p47^{phox}$, but is not strictly applicable to the canonical amphiphile- and $p47^{phox}$-dependent system. We believe that what determines the difference between the two situations is the presence or absence of $p47^{phox}$ (*see* **Note 53**). At the practical level, this means that, unless the cell-free assay is specifically meant to be focused on Rac2, the use of Rac1 is recommended, based on the assurance of higher oxidase activities.

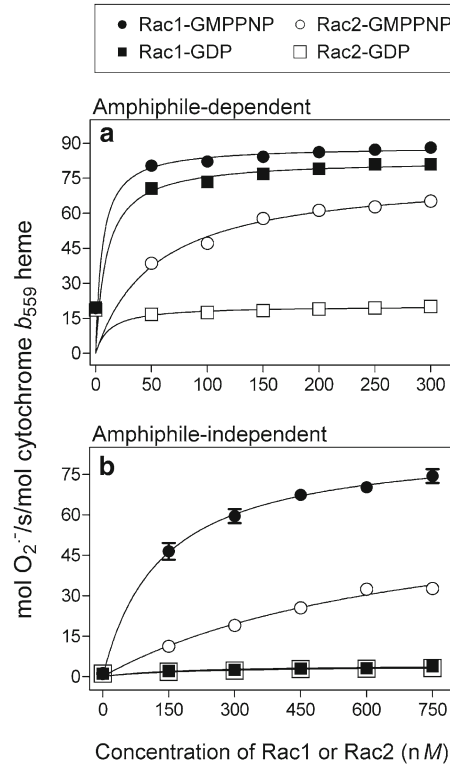

Fig. 8 Differences in the ability of Rac1 and Rac2 to support cell-free oxidase activation in relation to the nature of the bound guanine nucleotide, the absence or presence of prenylation, and the presence or absence of an amphiphilic activator. (**a**) Cell-free assays consisting of solubilized macrophage membrane liposomes (5 nM cytochrome b_{558} heme), recombinant p47^{phox} and p67^{phox} (both at a concentration of 300 nM), and recombinant non-prenylated Rac1 or Rac2, either exchanged to GMPPNP or GDP-bound (varied from 0 to 300 nM) were incubated with 130 μM LiDS, as described. (**b**) Cell-free assays consisting of solubilized macrophage membrane liposomes (5 nM cytochrome b_{558} heme), recombinant p67^{phox} (750 nM), and recombinant Rac1 or Rac2, either exchanged to GMPPNP or GDP-bound and prenylated in vitro (varied from 0 to 750 nM) were incubated in the absence of an anionic amphiphile, as described. In all assays (**a**, **b**), $O_2^{\cdot-}$ production was initiated by the addition of NADPH and measured by the kinetic cytochrome *c* reduction assay for 5 min. Results illustrated in both panels represent means ± SE of three experiments. Reproduced from [142] by permission of Humana Press©2007

3.7 Use of the Cell-Free System for Structure–Function Studies

The cell-free assay system was and continues to be invaluable as a simple and fast method to assess the oxidase activating ability of recombinant cytosolic proteins modified by mutation, truncation, deletion, chimerization, or posttranslational modification. There are uncountable examples of its application. Thus, it was used to test the effect of mutations in domains estimated to participate in functionally important protein–protein or protein–lipid

interactions, in p47^{phox} [42, 54, 120], p67^{phox} [6, 7, 42, 121], and Rac [7, 40, 42, 53, 54, 115, 122]. Testing the modified proteins in careful dose–response experiments, to allow the calculation of V_{max} and EC_{50} values, is essential. The concentration of the native (unmodified) cytosolic components, present in the assay, is also important, as shown by the finding that Rac1 mutations, which caused loss of function, were more easily detectable when the concentrations of p47^{phox} and p67^{phox} were low [115]. Finally, one should keep in mind that no in vitro method fully reproduces the environment of the whole cell. The actual concentrations of the oxidase components in the phagocyte, their compartmentalization within the cell, the presence of auxiliary components and factors missing in vitro, and the physicochemical composition of the intracellular milieu might result in an overall situation quite different from that existing in the cell-free system. This is the likely explanation for the occasions when modified oxidase components function differently in cell-free and whole cells conditions (*see* refs. 90, 91).

3.8 Use of the Cell-Free System for the Discovery of Oxidase Inhibitors

Cell-free systems are ideally suited for identifying potential oxidase inhibitors and for investigating their mechanism of action. The search for oxidase inhibitors received enormous impetus by the accumulating evidence for the involvement of nonphagocytic Noxes in the pathogenesis of a wide variety of diseases (reviewed in refs. 84, 85). So far, cell-free assays appropriate for measuring the activity of non-phagocytic Noxes are few and their use is not widespread. Thus, the cell-free assay is mostly applied to Nox2-based situations, whether in phagocytes or other cells. A central place is taken by synthetic peptide analogs of oxidase components, tested in situations in which they are expected to inhibit oxidase activation in cell-free assays (reviewed in refs. 123–125). Peptide oxidase analogs are used for two purposes: (1) as a mean of locating functional domains in individual oxidase components, and (2) to identify peptides with the potential of being used as therapeutic agents to dampen ROS production in disease situations in which excessive ROS production represents a primary or secondary pathogenic mechanism.

To achieve the first goal, arrays of overlapping peptides "covering" part of or the whole sequence of an oxidase component were tested for an effect on cell-free activation, a methodology that became known as "peptide walking." This was applied to Rac1 [126], p47^{phox} [127], p67^{phox} [92], p22^{phox} [128], and Nox2 [129]. Figure 9 illustrates the results of a typical "peptide walking" experiment, in which overlapping Nox2 DHR peptides were tested for inhibition of cell-free oxidase activation in amphiphile-dependent (Fig. 9a) and -independent (Fig. 9b) systems.

The second goal yielded rather disappointing results, with only one peptide, corresponding to residues 86–94 in the cytosol-exposed loop B of Nox2, found to inhibit oxidase activation in

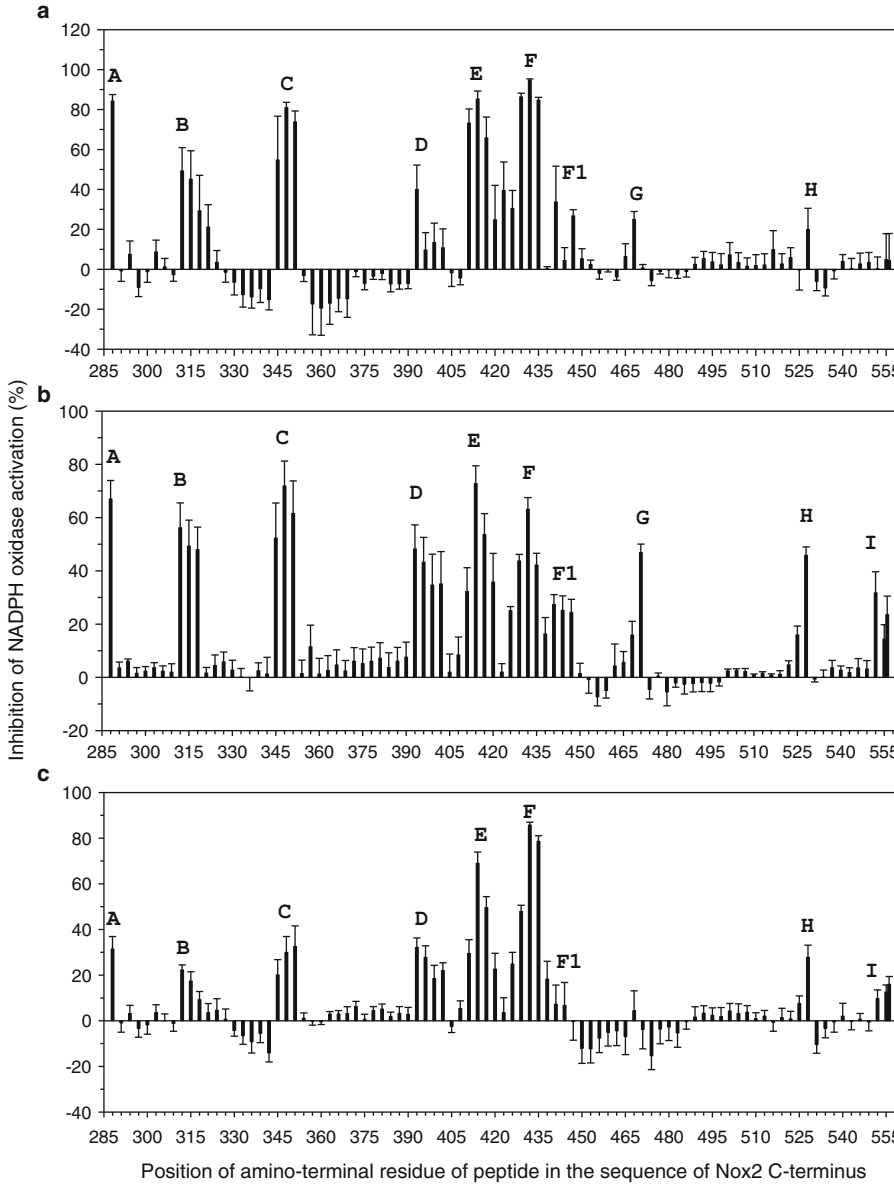

Fig. 9 Inhibition of NADPH oxidase activation by Nox2 dehydrogenase region peptides. (**a**) Inhibition in an amphiphile-dependent cell-free system. Peptides, at a concentration of 10 μM, were tested for the ability to inhibit $O_2{\cdot}^-$ production in a LiDS-activated cell-free system, consisting of solubilized macrophages membrane liposomes (equivalent to 5 nM cytochrome b_{558} heme) and recombinant p47^{phox}, p67^{phox}(1-526), and nonprenylated Rac1 Q61L, all at a concentration of 100 nM. The peptides were preincubated with the cytosolic components for 15 min before the addition of the membrane. Lithium dodecyl sulfate was then added at a concentration of 130 μM, and following incubation for further 1.5 min, $O_2{\cdot}^-$ production was initiated by addition of 238 μM NADPH. (**b**) Inhibition in an amphiphile- and p47^{phox}-independent cell-free system. Peptides were preincubated with p67^{phox}(1-526) and prenylated Rac1 Q61L, each at a concentration of 300 nM, for 15 min before the addition of the membrane. The mixtures were incubated for an additional 5 min before the addition of 240 μM NADPH. (**c**) Effect of C-terminal truncation of p67^{phox} on NADPH oxidase activation inhibition. Inhibition was measured in an amphiphile-and p47^{phox}-independent system, containing p67^{phox}(1-212) instead of p67^{phox}(1-526). All results represent means ± SEM of three experiments. *Uppercase boldface letters A–I* denote the inhibitory peptide clusters. Reproduced by permission from [129]

whole cells and organs and in an animal model, thus exhibiting a therapeutic potential [69].

We shall briefly summarize some of the critical issues to be considered when using the cell-free system for the identification of peptide or other small molecule oxidase inhibitors.

1. When assessing the significance of inhibition results, it is recommended to run peptide dose–response studies in a routine manner. These should be performed within a concentration range to enable the calculation of IC_{50} values. It is also essential that the peptide does not exert a nonspecific inhibitory effect on the actual measurement of $O_2^{\bullet-}$ production. This can be easily tested by adding the peptide to a xanthine/xanthine oxidase $O_2^{\bullet-}$-generating system.
2. Ideally, peptide inhibitors are expected to interfere with oxidase activation in the cell-free system by competing with the intact oxidase component, from which the peptide was derived, for interaction with another component of the oxidase complex. To test such an assumption, kinetic studies are required in order to demonstrate that inhibition is competitive. This was found to be the case with some peptides [100, 127] but, occasionally, what appeared as competition [130] did not withstand kinetic analysis [131].
3. Most Inhibitors active in cell-free systems are expected to interfere with the process of oxidase assembly. Such peptides inhibit only when present before the initiation of assembly and are inactive when added after the completion of assembly. Figure 10 illustrates the marked dose-dependent inhibition of amphiphile-dependent oxidase activation by a Rac1 C-terminal peptide, when added before the initiation but not after the completion of assembly. The preferential inhibition upon peptide addition before assembly is, however, not universal; some peptides and small molecule inhibitors were also found to inhibit when added after assembly, raising the possibility that they may be capable of dissociating assembled complexes [52, 129]. On rarer occasions, peptides interfere with the catalytic (redox) function of Nox2, such as by competing for the binding of cofactors or by another mechanism. To elucidate the mechanism, requires the application to the cell-free system of complex kinetic analysis (*see* ref. 129).
4. It is essential to control the sequence specificity of the inhibitory action of oxidase-analog peptides. This involves testing of scrambled and retro-peptides and unrelated peptides or small molecule compounds of similar size, charge, or hydrophobicity. Charge and hydrophobicity are important parameters in protein–protein and protein–lipid interactions and there are numerous examples of situations in which what was expected

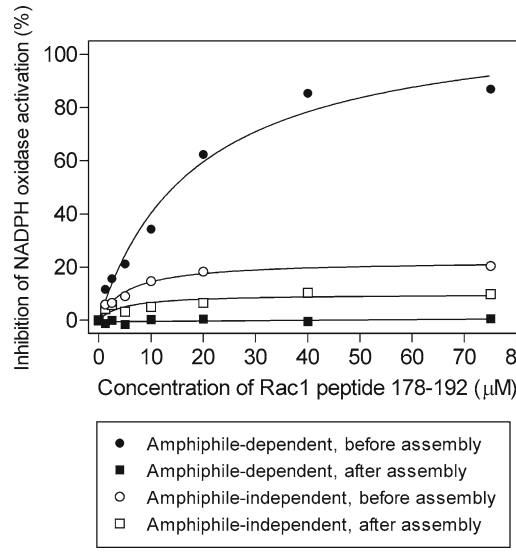

Fig. 10 Inhibition of NADPH oxidase activation in cell-free systems by a synthetic peptide, corresponding to the C-terminus of Rac1 (residues 178–192). The effect of various concentrations of the peptide (from 1.25 to 75 μM) was tested in both amphiphile-dependent and amphiphile-independent systems. The amphiphile-dependent system consisting of solubilized macrophage membrane liposomes (5 nM cytochrome b_{558} heme), recombinant p47^{phox} and p67^{phox}, and recombinant non-prenylated Rac1 Q61L mutant (all at 100 nM) was incubated with 130 μM lithium dodecyl sulfate, as described. The amphiphile-independent cell-free system consisting of solubilized macrophage membrane liposomes (5 nM cytochrome b_{558} heme), recombinant p67^{phox}, and recombinant Rac1 Q61L mutant prenylated in vitro (both at 300 nM) were incubated in the absence of an amphiphilic activator, as described. In all assays, $O_2{\cdot}^-$ production was initiated by the addition of NADPH and measured by the kinetic cytochrome *c* reduction assay for 5 min. The peptide was added either at time 0 (before assembly) or after 90 s of incubation (after assembly) but always preceding the addition of NADPH. The effect of the peptide is expressed as % inhibition of NADPH oxidase activation, with the activity in the absence of peptide being considered as 100 %. The turnover in the amphiphile-dependent system, in the absence of the peptide was 84.42 mol $O_2{\cdot}^-$/s/mol cytochrome b_{559}. In the amphiphile-independent system, the turnover in the absence of peptide was 65.01 mol $O_2{\cdot}^-$/s/mol cytochrome b_{558}. The results represent one characteristic experiment. Reproduced from [142] by permission of Humana Press©2007

to be sequence-specific inhibition by peptides, turned out to be sequence-independent (*see* refs. 52, 128, 129, 132). On the other hand, lack of sequence specificity should not be an automatic disqualifier of the inhibitory peptide for possible practical applications.

5. An important methodological consideration is the type of cell-free assay used for testing inhibitors. Thus, the amphiphile-dependent assay (with nonprenylated Rac1) is to be used when

a charge effect is involved, as illustrated by the inhibitory effect of a positively charged C-terminal Rac1 peptide; the very same peptide is inactive when tested in an amphiphile-independent assay (with prenylated Rac1), in which hydrophobic binding of Rac1 to the membrane is predominant (Fig. 10). In the latter situation, RhoGDI was found to prevent activation but was inactive when tested in the amphiphile-dependent assay (with nonprenylated Rac1) [7, 9].

6. Occasionally, peptides expected to be inhibitory on the basis of the fact they correspond to domains of previously known functional significance, were found to be inactive. Thus, peptides corresponding to the switch I region in Rac1 [126], the proline-rich region in $p22^{phox}$ [128], and the "activation domain" in $p67^{phox}$ [92], were not inhibitory in the cell-free assay.
7. Lack of effect on oxidase activation under cell-free conditions might mean that the hypothetical inhibitor acts upstream of the oxidase, most likely by interfering with phagocyte receptor-ligand interaction or with a transductional step linking the receptor to the oxidase.

3.9 "The End of the Affair"

We have been in the "cell-free business" for three decades. The message we would like to leave with you is as follows: Running cell-free assays is not only useful, simple, reproducible, and economical but, more than anything else, it is really fun. There is nothing like the feeling of taking out four proteins from the freezer and having a $O_2^{\cdot-}$ producing system (at least as good as intact phagocytes, if not better) on your desk in less than an hour. Good luck!

4 Notes

1. In addition to C20:4, oleic (C:18:1), linoleic (C18:2), and linolenic (C18:3) acids were also found to elicit $O_2^{\cdot-}$ production [21]. The cyclooxygenase product prostaglandin E_2 was inactive and the lipoxygenase product 15-hydroperoxy-5,8,11,13-eicostetraenoic acid (15-HPETE) was equal in activating ability to C20:4 [21]. A systematic study of the fatty acid specificity of cell-free oxidase activation revealed that the *trans* forms of C18:1 and C18:2 are active but long chain saturated acids (arachidic (C20:0), stearic (C18:0), and palmitic (C16:0)) are inactive [133]. Shorter chain saturated acids (lauric (C12:0), myristic (C14:0), and, to a lesser degree, palmitic (C16:0)), at high concentrations, were reported to be active [81, 83]. The complexity of the mechanism of oxidase activation is demonstrated by the recent finding that the *trans* form of C20:4 is incapable of cell-free oxidase activation (unlike the *trans* forms of C18:1 and C18:2) and acts as an inhibitor of *cis*-C20:4-induced oxidase activation [134].

2. One of the reviewers of our manuscript describing cell-free activation of the oxidase by SDS recommended rejection of the manuscript and offered the following comments: "the manuscript contains some interesting material…I express some disappointment that the authors do not approach the literature more thoroughly and attempt to relate effects seen here to those observed earlier with numerous detergents on whole cells."
3. In the "two-step" assay, the components of the oxidase are first mixed in a small volume (usually 1/10–20 of the final reaction volume) and exposed to the activating amphiphile at a concentration resulting in maximal activation. This "first-step" mixture does not contain NADPH and the $O_2^{\bullet-}$ detection reagent. After incubation for a determined time interval (leading to the assembly of the oxidase complex), the mixture is supplemented with assay buffer containing the $O_2^{\bullet-}$ detection reagent and NADPH but no amphiphile, which results in the dilution of the amphiphile to a non-activating concentration, and $O_2^{\bullet-}$ generation is measured (this second step represents the catalytic phase). The "two-step" assay is useful for testing the mechanism by which inhibitors affect oxidase activation (such as interference with assembly or competition with substrates) (*see* Subheading 3.8). Examples of its use can be found in refs. 42, 81, 106, 113).
4. The experience of our laboratory with the use of the INT reduction assay in the canonical cell-free assay is that about 80 % of the reduction is SOD-sensitive and, thus, due to reduction by $O_2^{\bullet-}$. A technical problem associated with this assay is the fact that INT precipitates SDS and LiDS, a fact also mentioned in the original description of the method [71]. INT reduction is not the choice method for the quantification of $O_2^{\bullet-}$ but is useful for measuring the spontaneous or cytosolic factors-dependent "activity" of the dehydrogenase region of Nox2 and other Noxes [74, 75].
5. The Subheadings 2 and 3 in this chapter are heavily biased toward semi-recombinant cell-free systems using membranes derived from guinea pig peritoneal exudate macrophages and human recombinant cytosolic components. The rationale behind this rather unusual combination is the ease of preparing large amounts of membranes with high cytochrome b_{558} content, excellent activity in cell-free assays, ease of solubilization, and years-long stability when kept frozen at –75 °C.
6. AEBSF was found to be an inhibitor of oxidase assembly in the cell-free assay [135], with an IC_{50} of 0.87 mM. However, the concentrations of AEBSF carried over into the assays were 250–350 times lower.

7. We have lately replaced the use of Rac1 exchanged to GMPPNP with the Rac1 mutant Q61L, which is constitutively in the GTP-bound form [103].
8. This buffer was first described by us for use in the C20:4-activated rudimentary cell-free system, based on the use of membrane and total cytosol [21] and was modified later [115].
9. A narrow bandwidth improves the sensitivity of the cytochrome *c* reduction assay. SPECTRAmax 340 has a bandwidth of 5 nm; SPECTRAmax 190 has a bandwidth of 2 nm.
10. Analysis of the cellular content of the lavage revealed it consisted of more than 90 % macrophages at 4–5 days following the injection of paraffin oil.
11. The 1 M KCl concentration is achieved by mixing 2.5 volumes of sonication buffer with 1 volume of 3.5 M KCl in 20 mM Tris–HCl, pH 7.5.
12. Washing of membranes with 1 M KCl is intended to remove loosely attached cytosolic components, with special emphasis on the removal of membrane-bound Rac. Indeed, it was reported that omission of the KCl wash step resulted in an apparent decrease in the dependence of cell-free oxidase activation on added Rac, which was due to the presence of membrane-bound Rac [117].
13. A dialysis membrane with a molecular weight cutoff of 25,000 is chosen because octyl glucoside is used for the solubilization of membranes at a concentration of 40 mM, which is well above its critical micellar concentration (CMC) of 25 mM. The micellar molecular weight of octyl glucoside is 8,000 and a large pore size membrane facilitates diffusion of the detergent from the dialysis bag to the surrounding buffer.
14. The dialysis buffer used for removing octyl glucoside and generating the membrane liposomes is identical to the solubilization buffer but contains no octyl glucoside, AEBSF, leupeptin hemisulfate, and FAD. The addition of serine protease inhibitors, especially AEBSF, to membrane preparations is avoided because of the reported likelihood of an interaction with cytochrome b_{558} [135]. FAD is omitted because it is difficult to measure the cytochrome b_{558} content accurately by sodium dithionite reduction in the presence of FAD.
15. Membrane liposomes can be kept frozen at –75 °C for long periods. We found a decrease of 1 % per year storage in the cytochrome b_{558} heme content of frozen membranes. Keeping the material in small aliquots is recommended but thawing and refreezing for up to ten times was not found to cause significant damage. When membrane liposomes are used after long periods of storage or have an uncertain data record, it is

recommended to determine the cytochrome b_{558} content again (*see* Subheading 3.1.3).

16. Routine use of solubilized membranes in the form of liposomes has the built-in advantage of providing a ready-made source of a membrane preparation which elutes as a single well-defined peak by gel filtration on a Superose12 FPLC column (in the exclusion volume). This allows the easy detection, by a variety of means, of translocation of cytosolic oxidase components to the membrane in the course of cell-free activation [9].
17. We use disposable 10 × 4 × 45 mm cuvettetes.
18. We use a Uvikon 943 double-beam spectrophotometer (Kontron Instruments), but any instrument with similar characteristics (scanning ability, narrow band-width, and data analysis (peak detection) capabilities) should be suitable.
19. Quite a number of alternative Δ extinction coefficients for calculating the cytochrome b_{558} heme concentration have been published. Most of these are centered on the 558/559 nm peak. Although this peak is more specific for cytochrome b_{558}, the fact that it is much lower than the 426/427 nm peak increases the chances of error, and we prefer to base our calculations on the 426/427 nm peak. We found no evidence for the presence of significant amounts of *b*-type cytochromes, other than b_{558}, in macrophage membranes [136].
20. The high concentration of cytochrome b_{558} heme (2 μM) might raise the question of whether freeing the solubilized membrane of octyl glucoside by dialysis is a necessary step in preparing membranes intended for the performance of cell-free assays. In these, the concentration of cytochrome b_{558} heme is 5–10 nM, and one might assume that just diluting the membrane 200- to 400-fold is sufficient for reducing the concentration of octyl glucoside well below the CMC, without a need for dialysis. It is our experience, however, that this is not the case. Solubilized membrane preparations, dialyzed free of detergent, are clearly superior in cell-free assays to preparations not subjected to dialysis.
21. It is desirable to use the same protein standard throughout in order to compare protein concentrations over long time periods. No external protein standard reflects the true protein concentration of the recombinant proteins but what is more important is to maintain the same level of "error." We use bovine gamma globulin as the standard.
22. Highly purified cytosolic components have the tendency to self-aggregate, even in the presence of 20 % glycerol. Repeated thawing–refreezing is likely to promote aggregation. Aggregated protein is inactive in cell-free assays and its presence might distort

the results when measuring protein concentration. It is, thus, highly recommended to subject frozen proteins, after thawing, to centrifugation at 12,000 × *g* at 4 °C, for 15 min, in a table top microcentrifuge accommodating 1.5 mL conical tubes. Measure protein concentration in the supernatant and keep the supernatant at 4 °C till used in the cell-free assay.

23. In the Rho GTPase folklore, it is commonly believed that GMPPNP is more resistant to the intrinsic GTPase activity than GTPγS but that the affinity for GTPγS is higher than that for GMPPNP. We are now employing exclusively GMPPNP for generating the GTP-bound form of Rac1 or Rac2.
24. Rac exchanged to GMPPNP was found, in our hands, to be stable for several weeks, and we found no reason to perform the exchange a short time before using the protein in cell-free assays. However, when larger amounts of Rac are subjected to exchange, it is wise to divide it in smaller aliquots, in order to avoid repeated thawing and freezing.
25. It is obvious that, when using this methodology, unbound GMPPNP is not removed and is present in the Rac preparations at a concentration roughly tenfold higher than that of the protein. This means that free GMPPNP is transferred to the cell-free assays, a fact which is to be taken into consideration. When removal of unbound nucleotide is desired to eliminate possible unwanted effects of free GMPPNP, the nucleotide-exchanged Rac is subjected to buffer exchange by centrifugal ultrafiltration, using 4 mL centrifugal filter units fitted with 10,000 molecular weight cutoff membranes. Three volumes of 4 mL each are filtered, using the buffer in which Rac is found, supplemented with 20 % v/v glycerol, and the sample is reconstituted to its original volume. Protein concentration is measured again, to check for some unavoidable loss in the course of ultrafiltration.
26. Prenylation can be performed after and before nucleotide exchange to a non-hydrolyzable GTP analog, but we prefer to prenylate after nucleotide exchange.
27. $ZnCl_2$ is an essential cofactor of geranylgeranyl transferase I.
28. This method can be applied to larger amounts of Rac, provided that non-prenylated Rac is sufficiently concentrated. However, the heated rotary mixer usually accommodates tubes with maximal volumes of 1.5 or 2 mL, which are also convenient for storage.
29. Two additional bands of 48 and 43 kDa are visible in the aqueous phase. These represent the α and β subunits of the enzyme geranylgeranyl transferase I.
30. This was first shown by Ligeti et al. [110] Thus, at 25 °C, full assembly was achieved after 5 min of exposure to the amphiphile

whereas, at close to 0 °C, the process took 30 min. Note, however, that at both temperatures the same level of assembly was ultimately achieved.

31. This observation was first made by Pilloud (Dagher) et al. [106] in a system composed of membrane and whole cytosol, and was thought to be related to the effect of salt on the micellar state of the anionic amphiphile. More recent work in a semi-recombinant system demonstrated that increasing ionic strength prevents binding of nonprenylated Rac1 (via its polybasic tail) to negatively charged phospholipids in the membrane [8]. No effect of ionic strength was seen on Rac2, which possesses a lesser positive charge at its C-terminus. These facts are of practical importance for the design of an optimal assay buffer and are also of relevance for the mechanism of amphiphile-independent cell-free activation of membranes enriched in anionic phospholipids [42, 51, 52].
32. If the requirements of the experiment are to add each component separately or in groupings of two, add 10 μL of each component from a 20-fold concentrated stock solution or 20 μL of a tenfold concentrated mixture of two components and 10 μL of a 20-fold concentrated stock of the third component. This will bring the total volume of the added components to 30 μL and requires the reduction of the volume of added membrane preparation to 10 μL and the proportional increase in the concentration of the membrane stock preparation to 20-fold.
33. The optimization of amphiphile concentration was first discussed in 1989 [106], a paper well worth reading even today. Because anionic amphiphiles act on both cytosolic [29] and membrane [30–32] components, optimization might be a complex issue when setting up radically new conditions and/or when non-purified components are used, some of which might bind the anionic amphiphile. It is a much simpler procedure when using purified recombinant cytosolic components.
34. Optimization of the time required for the amphiphile-dependent assembly of the oxidase complex is discussed in ref. 110. We found 90 s to be sufficient in the overwhelming majority of cases. However, it is important to point out that prolonging the time of assembly for up to 5 min might be advantageous and is, most definitely, not damaging. Thus, when in the preliminary stages of a project involving cell-free activation, exploring longer assembly times is recommended. Once the minimal time assuring full activation is found, this can be used routinely, but adding to it a "safety time supplement" is a wise move.
35. Turnovers in the amphiphile-activated cell-free system rarely exceed 100 mol $O_2^{\cdot-}$/s/mol cytochrome b_{558} heme. This corresponds to

100 pmol $O_2^{\bullet-}$/s/pmol cytochrome b_{558} heme. Thus, in each well containing 1 pmol cytochrome b_{558} heme, 100 pmol $O_2^{\bullet-}$ are produced per s, which means 6 nmol/min, and 30 nmol per 5 min. The total amount of cytochrome *c* present in the well is 40 nmol, which is sufficient for binding all the $O_2^{\bullet-}$ produced in 5 min. A total of 48 nmol NADPH are added to the well, which based on a stoichiometry of 1 mol NADPH supporting the production of 2 mol of $O_2^{\bullet-}$, is more than sufficient for the production of 30 nmol of $O_2^{\bullet-}$. When measuring high activity oxidase preparations, "bending" of the curve nevertheless occurs, in spite of apparently sufficient total amounts of NADPH and cytochrome *c* at the start of the reaction, this being due to the presence of lesser and lesser amounts of NADPH and oxidized cytochrome *c* as we approach the end of the reaction. Our group is using single sources of cytochrome *c* and NADPH as components of the assay buffer (*see* Subheading 2.1.5, **steps 1** and **2**). Because of variations in the degree of purity, the amount of water, and the proportion of oxidized and reduced material, it is wise to verify the actual amount of the two compounds present in the assay buffer. We measure the *total* concentration of cytochrome *c* by performing an absorbance wavelength scan (400–600 nm) on the native and sodium dithionite-reduced solution, determining the difference in absorbance at 550 nm between the reduced and oxidized samples and calculating the concentration by applying the extinction coefficient, $\Delta E_{550} = 21\ mM^{-1}\ cm^{-1}$ for reduced minus oxidized cytochrome *c*. The concentration of *reduced* NADPH is determined in the stock solution in H_2O by assessing the absorbance at 340 nm (the use of quartz cuvettes is required) and using the extinction coefficient, $E_{340} = 6.22\ mM^{-1}\ cm^{-1}$ [137]. In the presence of sufficient cytochrome *c*, no need was found for the addition of catalase (*see* ref. 61) to prevent reoxidation of cytochrome *c* by H_2O_2 originating in the spontaneous dismutation of $O_2^{\bullet-}$ that escaped scavenging by cytochrome *c*. However, if catalase is to be added, the assay buffer should be modified to not contain NaN_3 because of its inhibitory effect on catalase.

36. The extinction coefficient for the absorbance at 550 nm of reduced minus oxidized cytochrome *c*, as applied to a 1-cm path length, must be modified for the vertical path length of the microplate wells. This varies with the dimension and shape of the wells and the volume of the reaction mixture present in the well. Some microplate spectrophotometers (e.g., SPECTRAmax 190, Molecular Devices) have a "PathCheck" sensor, allowing the normalization of absorbance values to a 1-cm path length. This allows the use of the canonical extinction coefficient to calculate the concentration of reduced

cytochrome *c* in the well, without the need for any correction. This has only to be translated into the total amount of reduced cytochrome *c* in 210 μL, which permits the calculation of the turnover. SPECTRAmax 190 also has a wavelength bandwidth of 2 nm, which offers greater accuracy in measuring the "narrow" absorbance peak of reduced cytochrome *c* at 550 nm. With instruments not having the "PathCheck" option, the length of the vertical path length in the well must be determined by other means. Once it is known, the following equation will allow the direct calculation of nmol $O_2^{\bullet-}$ per min per well: nmol $O_2^{\bullet-}$/min/well = $\Delta mAbs_{550nm}$/min × 0.047619 × reaction volume (in mL)/path length (in cm). As an example, when then the reaction volume is 0.21 mL and the path length is found to be 0.575 cm, nmol $O_2^{\bullet-}$/min/well = $\Delta mAbs_{550\ nm}$/min × 0.047619 × 0.21/0.575 = $\Delta mAbs_{550nm}$/min × 0.017391.

37. The proper way to express results of cell-free oxidase activation assays is as turnover values. Unless there is a compelling reason for not doing so, oxidase activities should be related to the heme content of cytochrome b_{558} present in the membrane and not to cell number equivalents, total membrane protein, or the protein concentration of one or the other of the cytosolic components. The, unfortunately, common habit of expressing cell-free assay results as % change relative to a "basal" value can be thoroughly misleading in the absence of the information on the turnover corresponding to that basal value. This is critical when the effect of inhibitors on oxidase activity is expressed. Thus, a 50 % inhibition is meaningless when the basal turnover value is 2 mol $O_2^{\bullet-}$/s/mol cytochrome b_{558} heme but is potentially meaningful when the value is 80 mol $O_2^{\bullet-}$/s/mol cytochrome b_{558} heme.

38. From the advent of semi-recombinant cell-free assays and the increasing rarity of the use of whole cytosol or partially purified cytosolic fractions, the need for the SOD control has been drastically reduced. In our laboratory, in which semi-recombinant cell-free assays are performed routinely, we have not encountered a single occasion of nonspecific cytochrome *c* reduction. When a reducing agent is carried over into the reaction, cytochrome *c* reduction occurs practically at time zero and will be reflected in the absence of the typical kinetics. The presence of a cytochrome *c* reductase in the membrane preparation remains possible but is likely to be independent of the presence of the amphiphile and the cytosolic components. Of course, SOD controls should be used when cell-free assays are utilized as a diagnostic means on unpurified biologic material and in novel experimental situations. Yet another control for the specificity of cytochrome *c* reduction by $O_2^{\bullet-}$, rarely applied today, is the use of acetylated cytochrome *c* as the $O_2^{\bullet-}$ trap [61]. Acetylation

of lysine residues in cytochrome *c* decreases direct electron transfer from reductases, while maintaining the ability of $O_2^{\bullet-}$ to reduce cytochrome *c* [138].

39. The extinction coefficient for the absorbance of reduced INT at 490 nm relevant to a 1 cm path length has to be modified for the vertical path length of the microplate wells. When the microplate spectrophotometer does not have a "PathCheck" sensor, one has to know the total reaction volume per well and the length of the vertical path length. Once these are known, the following equation will allow the direct calculation of nmol INT reduced per min per well: nmol reduced INT/min/well = $\Delta mAbs_{490nm}/min \times 0.095328 \times$reaction volume (in mL)/path length (in cm). If the results are to be expressed in $O_2^{\bullet-}$ equivalents, the values are to be multiplied by 2, to account for the fact that reduction of INT is a two-electron reaction. As an example, when then the reaction volume is 0.21 mL and the path length is found to be 0.575 cm, nmol reduced INT/min/well = $\Delta mAbs_{490nm}/min \times 0.095238 \times 0.21/0.575 = \Delta mAbs_{490nm}/min \times 0.034782$ (0.069564, for $O_2^{\bullet-}$equivalent).
40. For the NADPH consumption test it is recommended to use 96-well plates for work at UV wavelengths (UV-Star plate, flat bottom, Greiner) and a microplate spectrophotometer capable to measure absorbance at 340 nm (we prefer to use the SPECTRAmax 190 (wavelength range 190–750 nm, Molecular Devices) but SPECTRAmax 340 (wavelength range 340–850 nm, Molecular Devices) is also adequate. The minimum absorbance limit of the microplate reader has to be adjusted to a negative value, to allow the recording of negative absorbance kinetics relative to the blank represented by assay buffer with NADPH. The extinction coefficient for the absorbance of reduced NADPH at 340 nm relevant to a 1 cm path length [137] has to be modified for the vertical path length of the microplate wells. When the microplate spectrophotometer does not have a "PathCheck" sensor, one has to know the total reaction volume per well and the length of the vertical path length. Once these are known, the following equation will allow the direct calculation of nmol reduced NADPH consumed per min per well using the following equation: nmol reduced NADPH consumed/min/well = $\Delta mAbs_{340nm}/min \times 0.160771 \times$ reaction volume (in mL)/path length (in cm). If the results are to be expressed in $O_2^{\bullet-}$ equivalents, the values are to be multiplied by 2, to account for the fact that one molecule of NADPH donates two electrons and yields two molecules of $O_2^{\bullet-}$. Note also that the consumption of NADPH will generate negative rate values when related to the reduced NADPH blank value. As an example, when then the reaction volume is 0.21 mL and the

path length is found to be 0.575 cm, nmol reduced NADPH consumed/min/well = $\Delta mAbs_{340nm}/min \times 0.160771 \times 0.21/0.575 = \Delta mAbs_{340nm}/min \times 0.058716$ (0.117432 for $O_2^{\bullet-}$ equivalent).

41. Dispensing 10–20 μL aliquots to the wells is best performed with electronic pipettors in the "dispensing" mode or using a Multipette. In most situations, the concentrations of $p67^{phox}$ and prenylated Rac required for reaching maximal activation, in the absence of amphiphile and $p47^{phox}$, are higher than those necessary for amphiphile-dependent activation in the presence of identical amounts of membrane.
42. In the amphiphile-independent cell-free system, we found on most occasions that prolonging the incubation to up to 5 min resulted in increased oxidase activities. This time interval should, however, not be exceeded.
43. The presence of $p47^{phox}$ is not an absolute requirement for oxidase activity to be detected in this assay, but turnover values are higher in its presence.
44. This effect was thought to be due to an elevation of the Krafft point of the fatty acids in the presence of Ca^{2+} [139].
45. These results support the recent proposal that the stability of the FAD-Nox2 bond is enhanced by anionic amphiphile-induced changes in Nox2 and by the process of assembly with the cytosolic components [140].
46. In the experiments described in Fig. 5, both non-prenylated and prenylated Rac1 were exchanged to GMPPNP and the exchange stabilized by 25 mM $MgCl_2$. Thus, it is unlikely that significant dissociation of GMPPNP from Rac can occur upon dilution of exchanged Rac preparations in assay buffer during the 90-s time interval of oxidase assembly. However, assay buffer is also used for intermediary dilution steps of recombinant cytosolic components, and it is possible that the diluted proteins are, sometimes, kept in assay buffer for longer periods of time. In the particular case of Rac, it is recommended to make such dilutions in the buffer listed, which contains 4 mM $MgCl_2$.
47. There is good evidence for equimolar and simultaneous translocation of the cytosolic components in neutrophils stimulated by two elicitors of a respiratory burst and it was also found that this translocation corresponded temporally with the generation of $O_2^{\bullet-}$ [141].
48. It is of interest that sigmoidal dose–response curves were described in the early period of the use of cell-free assays, when total cytosol was used and its amount was related to activity in the presence of a constant amount of amphiphile [105, 106].

49. This assumption was examined by Heyworth et al. [116] and Fuchs et al. [117], who showed that exchange with GTP added to the assay buffer only takes place with prenylated Rac and that preloading with GTP by Mg^{2+} chelation is required for non-prenylated Rac to work in the amphiphile-dependent cell-free assay.
50. This confirms the contention that no significant nucleotide exchange takes place on non-prenylated Rac upon addition of GTP analogs to the assay buffer [116, 117].
51. Another distinguishing feature of this system is the paradoxical inhibitory effect of added (free) GTPγS (10 μM) on oxidase activation by prenylated Rac exchanged to GMPPNP. The inhibitory effect of free GTP and GTPγS on amphiphile-independent oxidase activation was described by us in the past, but was never satisfactorily explained [52].
52. In one study, it was concluded that non-prenylated Rac1 and Rac2 were poorly active in an amphiphile-dependent cell-free assay in the absence of nucleotide exchange to GTPγS [116]. In another study, it was shown that the non-prenylated form of Rac1 exchanged to GTPγS was much superior to Rac2 exchanged to GTPγS [8]. This difference was clearly attributed to the lesser positive charge at the C-terminus of Rac2, a suggestion also supported by the inhibitory effect of increased ionic strength on the activity of Rac1, but not Rac2, and by the enhancing effect of an increase in the negative charge of the membrane on the effect of Rac1, but not Rac2 [8]. These authors also found that prenylated Rac1 and Rac2, when preloaded with GTPγS, support oxidase activation in an amphiphile-dependent system. In those studies, Rac1 was more efficient at activating the oxidase.
53. We proposed that since both $p47^{phox}$ and Rac function as Nox organizers, thereby contributing to the establishment of a more stable interaction between $p67^{phox}$ and Nox2, the presence of one organizer lessens the dependence on the other. This is expressed in the ability to activate the oxidase in the absence of $p47^{phox}$ [9, 11, 12, 53] and in a more "liberal" interpretation of the requirement for Rac to be in the GTP-bound form, when $p47^{phox}$ is present [41].

Acknowledgments

The research described in this report was supported by the Julius Friedrich Cohnheim-Minerva Center for Phagocyte Research, the Ela Kodesz Institute of Host Defense against Infectious Diseases, Israel Science Foundation Grants 428/01, 19/05, and 49/09, the

Roberts-Guthman Chair in Immunopharmacology, the Walter J. Levy Benevolent Trust, the Roberts Fund, the Milken—Lowell Fund, the Wallis Foundation, the Rubanenko Fund, and the Joseph and Shulamit Salomon Fund. It is important to point out that the cell-free system was discovered almost simultaneously by several investigators. R.A. Heyneman and R.E. Vercauteren, in Belgium, and Linda McPhail and John Curnutte, in the USA, each independently, contributed greatly to the birth of the "cell-free" paradigm. Edgar Pick would like to thank his fellow scientists, too many to name, who provided materials and invaluable advice, for making this work possible. There is no greater satisfaction than the realization of the fact that, on so many occasions, what started as collaboration (called "networking" these days) or competition, evolved into long-lasting friendship.

References

1. Nauseef WM (2007) How human neutrophils kill and degrade microbes: an integrated view. Immunol Rev 219:88–102
2. Nauseef WM (2004) Assembly of the phagocyte NADPH oxidase. Histochem Cell Biol 122:277–291
3. Quinn MT, Gauss KA (2004) Structure and regulation of the neutrophil respiratory burst oxidase: comparison with nonphagocyte oxidases. J Leukoc Biol 76:760–781
4. Groemping Y, Rittinger K (2005) Activation and assembly of the NADPH oxidase: a structural perspective. Biochem J 386:401–416
5. Sumimoto H (2008) Structure, regulation and evolution of Nox-family NADPH oxidases that produce reactive oxygen species. FEBS J 275:3249–3277
6. Han C-H, Freeman JLR, Lee T, Motalebi S, Lambeth JD (1998) Regulation of the neutrophil respiratory burst oxidase. Identification of an activation domain. J Biol Chem 273:16663–16668
7. Sarfstein R, Gorzalczany Y, Mizrahi A, Berdichevsky Y, Molshanski-Mor S, Weinbaum C, Hirshberg M, Dagher M-C, Pick E (2004) Dual role of Rac in the assembly of NADPH oxidase, tethering to the membrane and activation of $p67^{phox}$. A study based on mutagenesis of $p67^{phox}$-Rac1 chimeras. J Biol Chem 279:16007–16016
8. Kreck ML, Freeman JL, Lambeth JD (1996) Membrane association of Rac is required for high activity of the respiratory burst oxidase. Biochemistry 35:15683–15692
9. Gorzalczany Y, Sigal N, Itan M, Lotan O, Pick E (2000) Targeting of Rac1 to the phagocyte membrane is sufficient for the induction of NADPH oxidase assembly. J Biol Chem 275:40073–40081
10. Bedard K, Krause K-H (2007) The NOX family of ROS-generating NADPH oxidases: physiology and pathophysiology. Physiol Rev 87:255–313
11. Freeman JL, Lambeth JD (1996) NADPH oxidase activity is independent of $p47^{phox}$ in vitro. J Biol Chem 271:22578–22582
12. Koshkin V, Lotan O, Pick E (1996) The cytosolic component $p47^{phox}$ is not a *sine qua non* participant in the activation of NADPH oxidase but is required for optimal superoxide production. J Biol Chem 271:30326–30329
13. Cheson BD, Curnutte JT, Babior BM (1977) The oxidative killing mechanism of the neutrophil. Prog Clin Immunol 3:1–65
14. Pick E, Keisari Y (1981) Superoxide anion production and hydrogen peroxide production by chemically elicited macrophages—Induction by multiple nonphagocytic stimuli. Cell Immunol 59:301–318
15. Babior BM, Curnutte JT, McMurrich BJ (1976) The particulate superoxide-forming system from human neutrophils: properties of the system and further evidence supporting its participation in the respiratory burst. J Clin Invest 58:989–996
16. Markert M, Andrews PC, Babior BM (1984) Measurement of $O_2^{\bullet -}$ production by human neutrophils. The preparation and assay of NADPH oxidase-containing particles from human neutrophils. Methods Enzymol 105: 358–365
17. Babior BM, Kipnes RS (1977) Superoxide-forming enzyme from human neutrophils: evidence for a flavin requirement. Blood 50:517–524

18. Cross AR, Segal AW (2004) The NADPH oxidase of phagocytes—prototype of the NOX electron transport chain systems. Biochim Biophys Acta 1657:1–22
19. Bromberg Y, Pick E (1983) Unsaturated fatty acids as second messengers of superoxide generation by macrophages. Cell Immunol 79:243–252
20. Flores J, Witkum P, Sharp GWG (1976) Activation of adenylate cyclase by cholera toxin. J Clin Invest 57:450–458
21. Bromberg Y, Pick E (1984) Unsaturated fatty acids stimulate NADPH- dependent superoxide generation by cell-free system in macrophages. Cell Immunol 88:213–221
22. Heyneman RA, Vercauteren RE (1984) Activation of a NADPH oxidase from horse poymorphonuclear leukocytes in a cell-free system. J Leukoc Biol 36:751–759
23. McPhail LC, Shirley PS, Clayton CC, Snyderman R (1985) Activation of the respiratory burst enzyme from human neutrophils in a cell-free system. J Clin Invest 75:1735–1739
24. Curnutte JT (1985) Activation of human neutrophil nicotinamide adenine dinucleotide phosphate reduced (triphosphopyridine nucleotide, reduced) oxidase by arachidonic acid in a cell-free system. J Clin Invest 75:1740–1743
25. Curnutte JT, Babior BM (1987) Chronic granulomatous disease. Adv Human Genetics 16:229–297
26. Tsunawaki S, Nathan CF (1986) Release of arachidonate and reduction of oxygen. Independent metabolic bursts of the mouse peritoneal macrophage. J Biol Chem 261:11563–11570
27. Bromberg Y, Pick E (1985) Activation of NADPH-dependent superoxide production in a cell-free system by sodium dodecyl sulfate. J Biol Chem 260:13539–13545
28. Groemping Y, Lapouge K, Smerdon SJ, Rittinger K (2003) Molecular basis of phosphorylation-induced activation of the NADPH oxidase. Cell 113:343–355
29. Swain SD, Helgerson SL, Davis AR, Nelson LK, Quinn MT (1997) Analysis of activation-induced conformational changes in p47^{phox} using tryptophan fluorescence spectroscopy. J Biol Chem 272:29502–29510
30. Doussière J, Gaillard J, Vignais PV (1996) Electron transfer across the $O_2^{\bullet-}$ generating flavocytochrome of neutrophils. Evidence for transition from low-spin state to a high-spin state of the heme iron component. Biochemistry 35:13400–13410
31. Foubert TR, Burritt JB, Taylor RM, Jesaitis AJ (2002) Structural changes are induced in human neutrophil cytochrome *b* by NADPH oxidase activators, LDS, SDS and arachidonate: intermolecular resonance energy transfer between trisulfopyrenyl-wheat germ agglutinin and cytochrome b_{558}. Biochim Biophys Acta 1567:221–231
32. Taylor RM, Riesselman MH, Lord CI, Gripentrog JA, Jesaitis AJ (2012) Anionic lipid-induced conformational changes in human phagocyte flavocytochrome b precede assembly and activation of the NADPH oxidase complex. Arch Biochem Biophys 521:24–31
33. Qualliotine-Mann D, Agwu DE, Ellenburg MD, McCall CE, McPhail LC (1993) Phosphatidic acid and diacylglycerol synergize in a cell-free system for activation of NADPH oxidase from human neutrophils. J Biol Chem 268:23843–23849
34. Erickson RW, Langel-Peveri P, Traynor-Kaplan AE, Heyworth PG, Curnutte JT (1999) Activation of human neutrophil NADPH oxdase by phosphatidic acid or diacylglycerol in a cell-free system. Activity of diacylglycerol is dependent on its conversion to phosphatidic acid. J Biol Chem 274: 22243–22250
35. Tauber AI, Cox JA, Curnutte JT (1989) Activation of human neutrophil NADPH-oxidase in vitro by the catalytic fragment of protein kinase-C. Biochem Biophys Res Comm 158:884–890
36. Park J-W, Hoyal CR, El Benna J, Babior BM (1997) Kinase-dependent activation of the leukocyte NADPH oxidase in a cell-free system—Phosphorylation of membranes and p47^{phox} during oxidase activation. J Biol Chem 272:11035–11043
37. Abo A, Boyhan A, West I, Thrasher AJ, Segal AW (1992) Reconstitution of neutrophil NADPH oxidase activity in the cell-free system by four components: p67^{phox}, p47^{phox}, p21rac1, and cytochrome b_{-245}. J Biol Chem 267:16767–16770
38. Ebisu K, Nagasawa T, Watanabe K, Kakinuma K, Miyano K, Tamura M (2001) Fused p47^{phox} and p67^{phox} truncations efficiently reconstitute NADPH oxidase with higher activity than the individual components. J Biol Chem 276: 24498–24505
39. Miyano K, Ogasawara S, Han C-H, Fukuda H, Tamura M (2001) A fusion protein between Rac and p67^{phox} (1-210) reconstitutes NADPH oxidase with higher activity and stability than individual components. Biochemistry 40:14089–14097
40. Alloul N, Gorzalczany Y, Itan M, Sigal N, Pick E (2001) Activation of the superoxide-generating NADPH oxidase by chimeric proteins consisting of segments of the cytosolic

component p67^{phox} and the small GTPase Rac1. Biochemistry 40:14557–14566
41. Mizrahi A, Berdichevsky Y, Ugolev Y, Molshanski-Mor S, Nakash Y, Dahan I, Gorzalczany Y, Sarfstein R, Hirshberg M, Pick E (2006) Assembly of the phagocyte NADPH oxidase complex: chimeric constructs derived from the cytosolic components as tools for exploring structure–function relationships. J Leukoc Biol 79:881–895
42. Berdichevsky Y, Mizrahi A, Ugolev Y, Molshanski-Mor S, Pick E (2007) Tripartite chimeras comprising functional domains derived from the three cytosolic components p47^{phox}, p67^{phox} and Rac1 elicit activator-independent superoxide production by phagocyte membranes. Role of membrane lipid charge and of specific residues in the chimeras. J Biol Chem 282:22122–22139
43. Pick E, Gorzalczany Y, Engel S (1993) Role of the rac1 p21-GDP-dissociation inhibitor for *rho* heterodimer in the actvation of the superoxide-forming NADPH oxidase of macrophages. Eur J Biochem 217:441–455
44. Cross AR, Erickson RW, Curnutte JT (1999) The mechanism of activation of NADPH oxidase in the cell-free system: the activation process is primarily catalytic and not through the formation of a stoichiometric complex. Biochem J 341:251–255
45. Brown GE, Stewart MQ, Liu H, Ha V-L, Yaffe MB (2003) A novel assay system implicates PtdIns(3,4)P_2, PtdIns(3)P. and PKCδ in intracellular production of reactive oxygen species by the NADPH oxidase. Mol Cell 11: 35–47
46. Bissonnette SA, Glazier CM, Stewart MQ, Brown GE, Ellson CE, Yaffe MB (2008) Phosphatidylinositol 3-phosphate-dependent and -independent functions of p40^{phox} in activation of the neutrophil NADPH oxidase. J Biol Chem 283:2108–2119
47. Koshkin V, Pick E (1993) Generation of superoxide by purified and relipidatred cytochrome b_{559} in the absence of cytosolic activators. FEBS Lett 327:57–62
48. Koshkin V, Pick E (1994) Superoxide production by cytochrome b_{559}. Mechanism of cytosol-independent activation. FEBS Lett 338:285–289
49. Leusen JHW, Meischl C, Eppink MHM, Hilarius PM, de Boer M, Weening RS, Ahlin A, Sanders L, Goldblatt D, Skopczynska H, Bernatowska E, Palmblad J, Verhoeven AJ, van Berkel WJH, Roos D (2000) Four novel mutations in the gene encoding gp91^{phox} of human NADPH oxidase: consequences for oxidase activity. Blood 95:666–673
50. Hata K, Ito T, Takeshige K, Sumimoto H (1998) Anionic amphiphile-independent activation of the phagocyte NADPH oxidase in a cell-free system by p47^{phox} and p67^{phox}, both in C terminally truncated forms. Implications for regulatory Src himology 3 domain-mediated interactions. J Biol Chem 273:4232–4236
51. Peng G, Huang J, Boyd M, Kleinberg ME (2003) Properties of phagocyte NADPH oxidase p47^{phox} mutants with unmasked SH3 (Src homology 3) domains: full reconstitution of oxidase activity in a semi-recombinant cell-free system lacking arachidonic acid. Biochem J 373:221–229
52. Sigal N, Gorzalczany Y, Pick E (2003) Two pathways of activation of the superoxide-generating NADPH oxidase of phagocytes in vitro—Distinctive effects of inhibitors. Inflammation 27:147–159
53. Gorzalczany Y, Alloul N, Sigal N, Weinbaum C, Pick E (2002) A prenylated p67^{phox}-Rac1 chimera elicits NADPH-dependent superoxide production by phagocyte membranes in the absence of an activator and of p47^{phox}. Conversion of a pagan NADPH oxidase to monotheism. J Biol Chem 277:18605–18610
54. Mizrahi A, Berdichevsky Y, Casey PJ, Pick E (2010) A prenylated p47^{phox}-p67^{phox}-Rac1 chimera is a quintessential NADPH oxidase activator. Membrane association and functional capacity. J Biol Chem 285:25485–25499
55. Mizrahi A, Molshanski-Mor S, Weinbaum C, Zheng Y, Hirshberg M, Pick E (2005) Activation of the phagocyte NADPH oxidase by Rac guanine nucleotide exchange factors in conjunction with ATP and nucleoside diphosphate kinase. J Biol Chem 280:3802–3811
56. Pick E (2010) Editorial: When charge is in charge—"Millikan" for leukocyte biologists. J Leukoc Biol 87:537–540
57. Ugolev Y, Molshanski-Mor S, Weinbaum C, Pick E (2006) Liposomes comprising anionic but not neutral phospholipids cause dissociation of [Rac(1 or 2)-RhoGDI] complexes and support amphiphile-independent NADPH oxidase activation by such complexes. J Biol Chem 281:19204–19219
58. Ugolev Y, Berdichevsky Y, Weinbaum C, Pick E (2008) Dissociation of Rac1(GDP)-RhoGDI complexes by the cooperative action of anionic liposomes containing phosphatidylinositol 3,4,5-triphosphate, Rac guanine nucleotide exchange factor, and GTP. J Biol Chem 283(22257–22271):2008
59. DeCoursey TE, Ligeti E (2005) Regulation and termination of NADPH oxidase activity. Cell Mol Life Sci 62:2173–2193
60. van Bruggen R, Anthony E, Fernandez-Borja M, Roos D (2004) Continuous translocation of Rac2 and the NADPH oxidase component p67^{phox} during phagocytosis. J Biol Chem 279:9097–9102

61. Yamaguchi T, Kaneda M, Kakinuma K (1983) Essential requirement of magnesium ion for optimal activity of the NADPH oxidase of guinea pig polymorphonuclear leukocytes. Biochem Biophys Res Comm 115:261–267
62. Tamura M, Takeshita M, Curnutte JT, Uhlinger DJ, Lambeth JD (1992) Stabilization of human neutrophil NADPH oxidase activated in a cell-free system by cytosolic proteins and by 1-ethyl-3-(3-dimethylaminopropyl) carbodiimide. J Biol Chem 267:7529–7538
63. Knoller S, Shpungin S, Pick E (1991) The membrane-associated component of the amphiphile-activated cytosol-dependent superoxide forming NADPH oxidase of macrophages is identical to cytochrome b_{559}. J Biol Chem 266:2795–2804
64. Borregaard N, Heiple JM, Simons ER, Clark RA (1983) Subcellular localization of the *b*-cytochrome component of the human neutrophil microbicidal oxidase: translocation during activation. J Cell Biol 97:52–61
65. Lundquist H, Follin P, Khalfan L, Dahlgren C (1996) Phorbol myristate acetate-induced NADPH oxidase activity in human neutrophils: only half the story has been told. J Leukoc Biol 59:270–279
66. Clark RA, Leidal KG, Pearson DW, Nauseef WM (1987) NADPH oxidase of human neutrophils. Subcellular localization and characterization of an arachidonate-activable superoxide-generating system. J Biol Chem 262:4065–4074
67. Shpungin S, Dotan I, Abo A, Pick E (1989) Activation of the superoxide forming NADPH oxidase in a cell-free system by sodium dodecyl sulfate. Absolute lipid dependence of the solubilized enzyme. J Biol Chem 264: 9195–9203
68. Babior BM, Kipnes RS, Curnutte JT (1973) Biological defense mechanisms. The production by leukocytes of superoxide, a potential bactericidal agent. J Clin Invest 52:741–744
69. Csányi G, Cifuentes-Pagano E, Al Gouleh I, Ranayhossaini DJ, Egana L, Lopes LR, Jackson HM, Kelley EE, Pagano PJ (2011) Nox2 B-loop peptide, Nox2ds, specifically inhibits the NADPH oxidase Nox2. Free Rad Biol Med 51:1116–1125
70. Nisimoto Y, Jackson HM, Ogawa H, Kawahara T, Lambeth JD (2010) Constitutive NADPH-dependent electron transferase activity of the Nox4 dehydrogenase domain. Biochemistry 49:2433–2442
71. Cross AR, Yarchover JL, Curnutte JT (1994) The superoxide-generating system of human neutrophils possesses a novel diaphorase activity. Evidence for distinct regulation of electron flow within NADPH oxidase by $p47^{phox}$ and $p67^{phox}$. J Biol Chem 269:21448–21454
72. Han C-H, Nisimoto Y, Lee S-H, Kim ET, Lambeth JD (2001) Characterization of the flavoprotein domain of gp91*phox* which has NADPH diaphorase activity. J Biochem 129: 513–520
73. Nisimoto Y, Ogawa H, Miyano K, Tamura M (2004) Activation of the flavoprotein domain of gp91*phox* upon interaction with N-terminal p67*phox* (1-210) and the Rac complex. Biochemistry 43:9567–9575
74. Marques B, Liguori L, Paclet M-H, Villegas-Mendez A, Rothe R, Morel F, Lenormand J-L (2007) Liposome-mediated cellular delivery of active $gp91^{phox}$. PLoS ONE 2(9):e856. doi:10.1371/journal.pone.0000856
75. Nguyen MVC, Zhang L, Lhomme S, Mouz N, Lenormand J-L, Lardy B, Morel F (2012) Recombinant Nox4 cytosolic domain produced by a cell or cell-free base systems exhibits constitutive diaphorase acticvity. Biochem Biophys Res Comm 419:453–458
76. Takac I, Schroder K, Zhang L, Lardy B, Anilkumar N, Lambeth JD, Shah AJ, Morel F, Brandes RF (2011) The E-loop is involved in hydrogen peroxide formation by the NADPH oxidase Nox4. J Biol Chem 286:13304–13313
77. Zhou M, Diwu Z, Panchuk-Voloshina N, Haugland RP (1997) A stable nonfluorescent deriavative of resorufin for the fluorometric determination of trace hydrogen peroxide: applications in detecting the activity of phagocyte NADPH oxidase and other oxidases. Anal Biochem 253:162–168
78. Li Y, Zhu H, Kuppusamy P, Roubaud V, Zweier JL, Trush MA (1998) Validation of lucigenin (bis-*N*-methylacridinium) as a chemilumigenic probe for detecting superoxide anion radical production by enzymatic and cellular systems. J Biol Chem 273: 2015–2023
79. Yu L, Quinn MT, Cross AR, Dinauer MC (1998) $Gp91^{phox}$ is the heme binding subunit of the superoxide-generating NADPH oxidase. Proc Natl Acad Sci U S A 95:7993–7998
80. Sha'ag D (1989) Sodium dodecyl sulphate dependent NADPH oxidation: an alternative method for assaying NADPH-oxidase in a cell-free system. J Biochem Biophys Meth 19:121–128
81. Nishida S, Yoshida LS, Shimoyama T, Nunoi H, Kobayashi T, Tsunawaki S (2005) Fungal metabolite gliotoxin targets flavocytochrome b_{558} in the activation of the human neutrophil NADPH oxidase. Infect Immun 73:235–244
82. Pick E, Bromberg Y, Shpungin S, Gadba R (1987) Activation of the superoxide forming NADPH oxidase in a cell-free system by sodium dodecyl sulfate. Characterization of the membrane-associated component. J Biol Chem 262:16476–16483

83. Tanaka T, Makino R, Iizuka T, Ishimura Y, Kanegasaki S (1988) Activation by saturated and monounsaturated fatty acids of the O2– generating system in a cell-free preparation from neutrophils. J Biol Chem 263:13670–13676
84. Lambeth JD, Krause K-H, Clark RA (2008) NOX enzymes as novel targets for drug development. Semin Immunopathol 30:339–363
85. Jaquet V, Scapozza L, Clark RA, Krause K-H, Lambeth JD (2009) Small-molecule NOX inhibitors: ROS-generating NADPH oxidases as therapeutic targets. Antioxid Redox Signal 11:2535–2552
86. Bechtel W, Richardson R (1993) Discovering complexity: decomposition and localization as strategies in scientific research. Princeton University Press, Princeton
87. Babior BM (1984) Oxidants from phagocytes: agents of defense and destruction. Blood 64:959–966
88. Babior BM, Woodman RC (1990) Chronic granulomatous disease. Semin Hematol 27: 247–259
89. Dagher M-C, Pick E (2007) Opening the black box: lessons from cell-free systems on the phagocyte NADPH oxidase. Biochimie 89:1123–1132
90. de Mendez I, Garrett MC, Adams AC, Leto TL (1994) Role of $p67^{phox}$ SH3 domains in assembly of the NADPH oxidase system. J Biol Chem 269:16326–16332
91. Maehara Y, Miyano K, Sumimoto H (2009) Role of the first SH3 domain of $p67^{phox}$ in activation of superoxide-producing NADPH oxidases. Biochem Biophys Res Comm 379: 589–593
92. Zahavi A (2013) Elucidation of the domain(s) in the cytosolic NADPH oxidase component $p67^{phox}$ involved in binding to flavocytochrome b_{558}. *Ph.D. Thesis*, Tel Aviv University
93. Bradford MM (1976) A rapid and sensitive method for the quantitation of microgram quantities of protein utilizing the principle of protein-dye binding. Anal Biochem 72: 248–254
94. Light D, Walsh C, O'Callaghan AM, Goetzl EJ, Tauber AI (1981) Characteristics of the cofactor requirements for the superoxide-generating NADPH oxidase of human polymorphonuclear leukocytes. Biochemistry 20:1468–1476
95. Burgess RR (1991) Use of polyethyleneimine in purification of DNA-binding proteins. Meth Enzymol 208:3–10
96. Lapouge K, Groemping Y, Rittinger K (2002) Architecture of the p40-p47-$p67^{phox}$ complex in the resting state of the NADPH oxidase: a central role for $p67^{phox}$. J Biol Chem 277: 10121–10128
97. Knaus UG, Heyworth PG, Kinsella BT, Curnutte JT, Bokoch GM (1992) Purification and characterization of Rac2. A cytosolic GTP-binding protein that regulates human neutrophil NADPH oxidase. J Biol Chem 267:23575–23582
98. Abo A, Pick E, Hall A, Totty N, Teahan CG, Segal AW (1991) Activation of the NADPH oxidase involves the small GTP-binding protein p21 rac 1. Nature 353:668–670
99. Zhao X, Carnevale KA, Cathcart MK (2003) Human monocytes use Rac1, not Rac2, in the NADPH oxidase complex. J Biol Chem 278:40788–40792
100. Kreck ML, Uhlinger DJ, Tyagi SR, Inge KL, Lambeth JD (1994) Participation of the small molecular weight GTP-binding protein Rac1 in cell-free activation and assembly of the respiratory burst oxidase. Inhibition by a carboxyl-terminal Rac peptide. J Biol Chem 269:4161–4168
101. Bromberg Y, Shani E, Joseph G, Gorzalczany Y, Sperling O, Pick E (1994) The GDP-bound form of the small G protein rac1 p21 is a potent activator of the superoxide forming NADPH oxidase of macrophages. J Biol Chem 269:7055–7058
102. Sigal N, Gorzalczany Y, Sarfstein R, Weinbaum C, Zheng Y, Pick E (2003) The guanine nucleotide exchange factor Trio activates the phagocyte NADPH oxidase in the absence of GDP to GTP exchange on Rac. "The emperor's new clothes". J Biol Chem 278:4854–4861
103. Xu X, Wang Y, Barry DC, Chanock SJ, Bokoch GM (1997) Guanine nucleotide binding properties of Rac2 mutant proteins and analysis of the responsiveness to guanine nucleotide dissociation stimulator. Biochemistry 36:626–632
104. Bordier C (1981) Phase separation of integral membrane proteins in Triton X-114 solution. J Biol Chem 256:1604–1607
105. Babior BM, Kuver R, Curnutte JT (1988) Kinetics of activation of the respiratory burst oxidase in a fully soluble system from human neutrophils. J Biol Chem 23:1713–1718
106. Pilloud Dagher M-C, Doussiere J, Vignais PV (1989) Parameters of activation of the membrane-bound $O_2^{\bullet-}$-generating oxidase from neutrophils in a cell-free system. Biochem Biophys Res Comm 159:783–790
107. Cross AR, Erickson RW, Curnutte JT (1999) Simultaneous presence of $p47^{phox}$ and flavocytochrome b_{245} are required for activation of NADPH oxidase by anionic amphiphiles. Evidence for an intermediate state of oxidase activation. J Biol Chem 274:15519–15525
108. Pick E, Mizel D (1981) Rapid microassays for the measurement of superoxide and hydrogen

peroxide production by macrophages in culture using an automatic enzyme immunoassay reader. J Immunol Methods 46:211–226
109. Pick E (1986) Methods for studying the oxidative metabolism of macrophages. Microassays for $O_2^{\bullet-}$ and H_2O_2 production and NBT reduction using an enzyme immunoassay microplate reader. Meth Enzymol 132:407–421
110. Ligeti E, Doussiere J, Vignais PV (1988) Activation of the $O_2^{\bullet-}$-generating oxidase in plasma membrane from bovine polymorphonuclear neutrophils by arachidonic acid, a cytosolic factor of protein nature, and nonhydrolyzable analogues of GTP. Biochemistry 27:193–200
111. Seifert R, Rosenthal W, Schultz G (1986) Guanine nucleotides stimulate NADPH oxidase in membranes of human neutrophils. FEBS Lett 105:161–165
112. Gabig TG, English D, Akard LP, Schell MJ (1987) Regulation of neutrophil NADPH oxidase activation in a cell-free system by guanine nucleotides and fluoride. Evidence for participation of a pertussis and cholera toxin-insensitive G protein. J Biol Chem 262: 1685–1690
113. Aharoni I, Pick E (1990) Activation of the superoxide-generating NADPH oxidase of macrophages by sodium dodecyl sulfate in a soluble cell-free system. Evidence for involvement of a G protein. J Leukoc Biol 48: 107–115
114. Lawson CD, Donald S, Anderson KE, Patton DT, Welch HCE (2011) P-Rex1 and Vav1 cooperate in the regulation of formyl-methionyl-leucyl-phenylalanine-dependent neutrophil responses. J Immunol 186: 1467–1476
115. Toporik A, Gorzalczany Y, Hirshberg M, Pick E, Lotan O (1998) Mutational analysis of novel effector domains in Rac1 involved in the activation of nicotinamide adenine dinucleotide phosphate (reduced) oxidase. Biochemistry 37:7147–7156
116. Heyworth PG, Knaus UG, Xu X, Uhlinger DJ, Conroy L, Bokoch GM, Curnutte JT (1993) Requirement for posttranslational processing of Rac GTP-binding proteins for activation of human neutrophil NADPH oxidase. Mol Biol Cell 4:261–269
117. Fuchs A, Dagher M-C, Jouan A, Vignais PV (1994) Activation of the $O_2^{\bullet-}$-generating NADPH oxidase in a semi-recombinant cell-free system. Assessment of the function of Rac in the activation process. Eur J Biochem 226: 587–595
118. Li S, Yamauchi A, Marchal CC, Molitoris JK, Quiliam LA, Dinauer MC (2002) Chemoattractant-stimulated Rac activation in wild-type and Rac2-deficient murine neutrophils: preferential activation of Rac2 and Rac2 gene dosage on neutrophil functions. J Immunol 169:5043–5051
119. Glogauer M, Marchal CC, Zhu F, Worku A, Clausen B, Foerster I, Marks P, Downey GP, Dinauer MC, Kwiatkowski DJ (2003) Rac1 deletion in mouse neutrophils has selective effects on neutrophil functions. J Immunol 170:5652–5657
120. Sumimoto H, Hata K, Mizuki K, Ito T, Kage Y, Sakaki Y, Fukumaki Y, Nakamura M, Takeshige K (1996) Assembly and activation of the phagocyte NADPH oxidase. Specific interaction of the N-terminal src homology 3 domain of $p47^{phox}$ with $p22^{phox}$ is required for activation of the NADPH oxidase. Proc Natl Acad Sci U S A 271:22152–22158
121. Maehara Y, Miyano K, Yuzawa S, Akimoto R, Takeya R, Sumimoto H (2010) A conserved region between the TPR and activations domains of $p67^{phox}$ participates in activation of the phagocyte NADPH oxidase. J Biol Chem 285:31435–31445
122. Kwong CH, Adams AG, Leto TL (1995) Characterization of the effector-specifying domain of Rac involved in NADPH oxidase activation. J Biol Chem 270:19868–19872
123. El-Benna J, Dang PM-C, Périanin A (2010) Peptide-based inhibitors of the phagocyte NADPH oxidase. Biochem Pharmacol 80: 778–785
124. Dahan I, Pick E (2012) Strategies for identifying synthetic peptides to act as inhibitors of NADPH oxidases, or "All that you did and did not want to know about Nox inhibitory peptides". Cell Mol Life Sci 69:2283–2305
125. El-Benna J, Dang PM-C, Périanin A (2012) Towards specific NADPH oxidase inhibition by small synthetic peptides. Cell Mol Life Sci 69:2307–2314
126. Joseph G, Pick E (1995) "Peptide walking" is a novel method of mapping functional domains in proteins. Its application to the Rac1-dependent activation of NADPH oxidase. J Biol Chem 270:29079–29082
127. Morozov I, Lotan O, Joseph G, Gorzalczany Y, Pick E (1998) Mapping of functional domains in $p47^{phox}$ in volved in the activation of NADPH oxidase by "peptide walking". J Biol Chem 273:153435–15444
128. Dahan I, Issaeva I, Gorzalczany Y, Sigal N, Hirschberg M, Pick E (2002) Mapping of functional domains in the $p22^{phox}$ subunit of flavocytochrome b_{559} participating in the assembly of the NADPH oxidase complex by "peptide walking". J Biol Chem 277:8421–8432
129. Dahan I, Molshanski-Mor S, Pick E (2012) Inhibition of NADPH oxidase activation by

peptides mapping within the dehydrogenase region of Nox2—A "peptide walking" study. J Leuk Biol 91:501–515
130. Rotrosen D, Kleinberg ME, Nunoi H, Leto T, Gallin JI, Malech HL (1990) Evidence for a functional cytoplasmic domain of phagocyte oxidase cytochrome b_{558}. J Biol Chem 265:8745–8750
131. Uhlinger DJ, Tyagi SR, Lambeth JD (1995) On the mechanism of inhibition of the neutrophil respiratory burst oxidase by a peptide from the C-terminus of the large subunit of cytochrome b_{558}. Biochemistry 34:524–527
132. Joseph G, Gorzalczany Y, Koshkin V, Pick E (1994) Inhibition of NADPH oxidase activation by synthetic peptides mapping within the carboxy-terminal domain of small GTP-binding proteins. Lack of amino acid sequence specificity and importance of the polybasic motif. J Biol Chem 269:29024–29031
133. Seifert R, Schultz G (1987) Fatty acid-induced activation of NADPH oxidase in plasma membranes of human neutrophils depends on neutrophil cytosol and is potentiated by stable guanine nucleotides. Eur J Biochem 162:563–569
134. Souabni H, Thoma V, Bizouarn T, Chatgilialoglu C, Siafaka-Kapadai A, Baciou L, Ferreri C, Houée-Levin C, Ostuni MA (2012) t*rans* arachidonic acid isomers inhibit NADPH-oxidase activity by direct interaction with enzyme components. Biochim Biophys Acta 1818:2314–2324
135. Diatchuk V, Lotan O, Koshkin V, Wikstroem P, Pick E (1997) Inhibition of NADPH oxidase activation by 4-(2-aminoethyl)-benzenesulfonyl fluoride and related compounds. J Biol Chem 272:13292–13301
136. Pick E, Gadba R (1988) Certain lymphoid cells contain the membrane-associated component of the phagocyte-specific NADPH oxidase. J Immunol 140:1611–1617
137. Horecker BL, Kornberg A (1948) The extinction coefficients of the reduced band of pyridine nucleotides. J Biol Chem 175: 385–390
138. Azzi A, Montecucco C, Richter C (1975) The use of acetylated ferricytochrome *c* for the detection of superoxide radicals produced in biological membranes. Biochem Biophys Res Comm 65:597–603
139. Yamaguchi T, Kaneda M, Kakinuma K (1986) Effect of saturated and unsaturated fatty acids on the oxidative metabolism of human neutrophils. The role of calcium ion in the extracellular medium. Biochim Biophys Acta 861:440–446
140. Hashida S, Yuzawa S, Suzuki NN, Fujioka Y, Takikawa T, Sumimoto H, Inagaki F, Fujii H (2004) Binding of FAD to cytochrome b_{558} is facilitated during activation of the phagocyte NADPH oxidase, leading to superoxide production. J Biol Chem 279:26378–26386
141. Quinn MT, Evans T, Loetterle LR, Jesaitis AJ, Bokoch GM (1993) Translocation of Rac correlates with NADPH oxidase activation. Evidence for equimolar translocation of oxidase components. J Biol Chem 268: 20983–20987
142. Molshanski-Mor S, Mizrahi A, Ugolev Y, Dahan I, Berdichevsky Y, Pick E (2007) Cell-free assays. The reductionist approach to the study of NADPH oxidase assembly, or "All you wanted to know about cell-free assays but did not dare to ask". Methods Mol Biol 412:385–428

Chapter 23

Assessment of Priming of the Human Neutrophil Respiratory Burst

Margarita Hurtado-Nedelec, Karama Makni-Maalej, Marie-Anne Gougerot-Pocidalo, Pham My-Chan Dang, and Jamel El-Benna

Abstract

Neutrophils play an essential role in host defense against microbial pathogens and in the inflammatory reaction. Upon activation, neutrophils produce reactive oxygen species (ROS) such as superoxide anion ($O_2^{\cdot-}$), hydrogen peroxide (H_2O_2), and hypochlorous acid (HOCl), a process referred to as the respiratory burst. The enzyme responsible for this process is called the NADPH oxidase or respiratory burst oxidase. This multicomponent enzyme system is composed of two transmembrane proteins (p22phox and gp91phox/NOX2, which form the cytochrome b_{558}), three cytosolic proteins (p47phox, p67phox, p40phox), and a GTPase (Rac1 or Rac2), which assemble at membrane sites upon cell activation. The NADPH oxidase is in a resting state in circulating neutrophils, and its activation can be induced by a large number of soluble and particulate agents such as the formylated peptide, formyl-methionyl-leucyl-phenylalanine (fMLF). This activation can be enhanced or "primed" by pro-inflammatory cytokines, LPS and other agents. Priming is a "double-edged sword" process as it contributes to a rapid and efficient elimination of the pathogens but can also induce the generation of large quantities of toxic ROS that can damage surrounding tissues and participate to inflammation. In this chapter, we describe the techniques used to measure priming of the NADPH oxidase in human neutrophils.

Key words Neutrophils, NADPH oxidase, Priming, Respiratory burst, NOX2, ROS

1 Introduction

Neutrophils play a key role in host defense against invading pathogens [1, 2]. In response to a variety of agents, they release large quantities of superoxide anion ($O_2^{\cdot-}$) and other ROS in a process known as the respiratory burst. Neutrophil production of $O_2^{\cdot-}$ is dependent on the activation of the NADPH oxidase, a multicomponent enzyme system that catalyzes the NADPH-dependent reduction of oxygen to $O_2^{\cdot-}$ [3–5]. In resting cells, the NADPH oxidase is inactive and its components are distributed between the cytosol and the membranes. When cells are activated, the cytosolic

Mark T. Quinn and Frank R. DeLeo (eds.), *Neutrophil Methods and Protocols*, Methods in Molecular Biology, vol. 1124,
DOI 10.1007/978-1-62703-845-4_23,

components (p47phox, p67phox, p40phox, and Rac2) migrate to the membranes, where they associate with the membrane-bound component comprised of p22phox and gp91phox (flavocytochrome b_{558}, NOX2) to assemble the catalytically active oxidase [6, 7]. The phosphorylation of p47phox on several serines plays a pivotal role in oxidase activation in intact cells [8–12]. As the oxidants produced by the NADPH oxidase are highly toxic, not only for infectious agents but also for the neighboring host tissues, tight regulation of the enzyme complex is necessary to control ROS production.

Neutrophil $O_2^{\cdot-}$ production can be potentiated by prior exposure to "priming" agents such as the pro-inflammatory cytokines GM-CSF, TNFα, and IL-8 [13–18] and the TLR agonists LPS and CL097 [19, 20]. These cytokines inherently induce a very weak oxidative response by neutrophils, but they strongly enhance neutrophil release of ROS upon exposure to a secondary stimulus such as the bacterial *N*-formyl peptide, *N*-formyl-methionyl-leucyl-phenylalanine (fMLF). This process is believed to play a key role in efficient pathogen elimination; however, as mentioned earlier, excessive ROS production can induce tissue injury, which participates to inflammatory diseases [17, 21–25]. In this chapter, we describe the techniques used to measure cytokine-induced priming of neutrophil ROS production. The first technique uses whole blood and flow cytometry, thus avoiding neutrophil isolation and manipulation; the second technique uses sterile neutrophil isolation by a one-step gradient centrifugation and luminol-amplified chemiluminescence for the measurement of ROS production.

2 Materials

2.1 Reagents

1. TNFα: 10 μg/mL in phosphate-buffered saline (PBS), 0.05 % human serum albumin. Aliquot and store at −70 °C.
2. GM-CSF: 10 μg/mL in PBS, 0.05 % human serum albumin. Aliquot and store at −70 °C.
3. IL-8: 50 μg/mL in PBS, 0.05 % human serum albumin. Aliquot and store at −70 °C.
4. *N*-formyl-methionyl-leucyl-phenylalanine (fMLF): 10 mM in sterile DMSO. Aliquot and store at −20 °C. Prepare working solutions in PBS prior to use and keep on ice.
5. Cytochrome c from bovine heart: 20 mg/mL in PBS, prepare fresh.
6. Superoxide dismutase (SOD): 30,000 Units/mL in PBS. Aliquot and store at −70 °C.
7. Luminol: 100 mM in DMSO, store at −20 °C.
8. Hydroethidine (HE) stock solution: 15 mg/mL in acetonitrile. Store at −20 °C. Prepare working solutions in PBS immediately prior to use.

2.2 Buffers and Solutions

1. Sterile PBS.
2. Sterile Hanks balanced-salt solution containing Ca^{2+}, Mg^{2+}, and D-glucose (HBSS).
3. PolymorphPrep: 13.8 g of sodium diatrizoate, 100 mL of injection grade sterile water. To this add 8 g of Dextran T500 and filter-sterilize. Store the solution at 4 °C for up to 4 weeks (*see* **Note 1**).
4. FACS lysing solution (Becton Dickinson).

3 Methods

3.1 Priming of ROS Production as Measured by Flow Cytometry Without Neutrophil Isolation

Superoxide anion production is measured with a flow cytometric assay derived from the HE oxidation technique [26]. HE diffuses into cells, and during the PMN oxidative burst, non-fluorescent intracellular HE is oxidized by $O_2^{\cdot-}$ to the highly fluorescent ethidium (E+), which is trapped in the nucleus by intercalation into DNA (*see* **Note 2**).

1. Samples (500 µL) from whole blood, collected onto preservative-free lithium heparinate (10 U/mL), are pre-incubated for 15 min with HE (1,500 ng/mL) in a water bath with gentle horizontal shaking at 37 °C.
2. Incubate the samples with a priming agent such as TNFα or GM-CSF (20 ng/mL) diluted in PBS or with PBS alone for 30 min at 37 °C.
3. Add fMLF diluted in PBS (10^{-6} M final concentration) or PBS alone for 5 min at 37 °C.
4. After stimulation, lyse 100 µL samples with 2 mL FACS lysing solution (Becton Dickinson, Immunocytometry Systems, San Jose, CA) for 10 min.
5. After one wash (400×*g*, 5 min), fix white cells in 1 % paraformaldehyde–PBS (500 µL). Keep the fixed samples on ice until use for flow cytometry on the same day.
6. Flow cytometry analysis is performed here with a FACS CantoII (BD Biosciences, Immunocytometry Systems, San Jose, CA). Forward and side scatter are used to identify the neutrophil population and to gate out other cells and debris.
7. Assess purity of the gated cells using a conjugated anti-CD15 antibody (BD Biosciences). Monitor orange fluorescence of E+ between 549 and 601 nm.
8. Acquire 5,000 events per sample, with constant photomultiplicator gain. Use the mean fluorescence intensity to quantify the cell response. An example of a typical result obtained using this protocol is shown in Fig. 1.

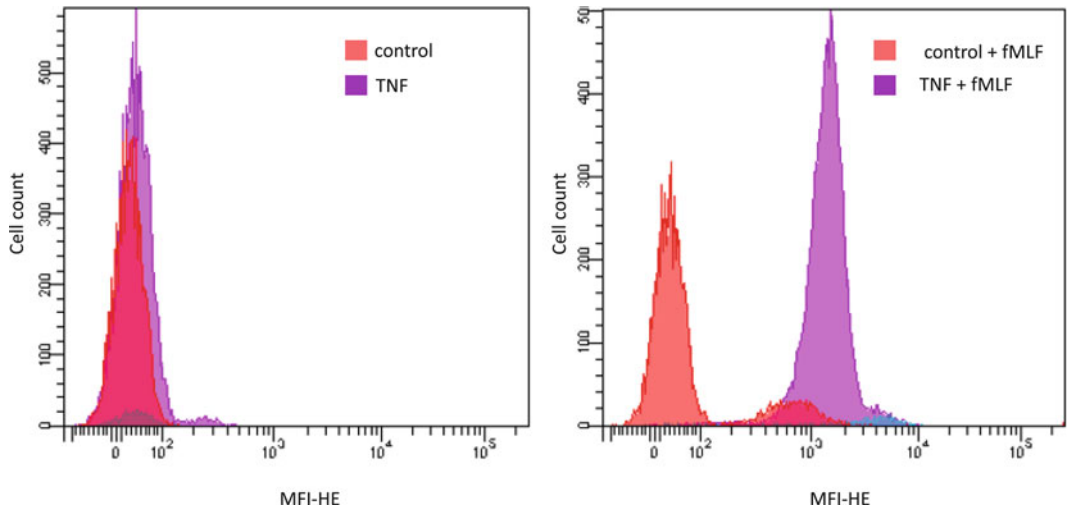

Fig. 1 TNFα induces priming of fMLF-stimulated $O_2^{\cdot-}$ production by neutrophils, as measured by flow cytometry. Human blood was incubated with PBS (control) or 20 ng/mL of TNFα in the presence of hydroethidine (HE) for 30 min at 37 °C, then stimulated with 1 μM of fMLF. Red cells were lysed and leukocytes were fixed. Cells were analyzed by flow cytometry for ethidium fluorescence after gating the neutrophil population using an anti-CD15 antibody. MFI-HE (Mean Fluorescence Intensity-Hydroethydine)

3.2 Isolation of Human Neutrophils by the Polymorphprep Technique

Neutrophils prepared by means of a one-step centrifugation using this protocol respond to priming agents better than neutrophils isolated by other techniques (*see* **Note 3**).

1. Gently layer blood (2 volumes) on PolymorphPrep (1 volume) (*see* **Note 4**).
2. Centrifuge the tubes at 500 × *g* for 30 min in a swinging rotor at 22 °C with gentle braking.
3. After centrifugation, two leukocyte bands should be visible. The top first band contains the mononuclear cells (lymphocytes and monocytes), and the second band contains the neutrophils. The erythrocytes are in the pellet.
4. Discard the upper layer of mononuclear cells by aspiration.
5. Collect the neutrophils using a disposable sterile plastic pipette.
6. Resuspend cells in five- to tenfold volume of sterile PBS and collect by centrifugation at 400 × *g* for 10 min at 22 °C.
7. If necessary, lyse the erythrocytes by gently dispersing the pellet containing neutrophils and contaminating erythrocytes. Add 12 mL of ice-cold sterile 0.2 % NaCl for 30 s to remove contaminating erythrocytes by hypotonic lysis, mix gently and restore isotonicity by adding 12 mL of 1.6 % NaCl (*see* **Note 5**).
8. Centrifuge the tubes at 400 × *g* for 8 min at 4 °C. Aspirate the red supernatant and resuspend the neutrophil pellet in an adequate volume of PBS, depending on the total amount of blood used.

9. Count the cells by diluting in trypan blue (1/100) and using a hemocytometer (*see* **Note 6**). Adjust to the desired concentration with HBSS.

3.3 Priming of ROS Production as Measured by Luminol-Amplified Chemiluminescence

1. Suspend neutrophils (5×10^5) in 0.5 mL HBSS in different tubes.
2. Add luminol (10 μM) and place the tubes at 37 °C in the thermostated chamber of the luminometer.
3. After 5 min, add either 20 ng/mL TNFα, 20 ng/mL GM-CSF, or 50 ng/mL IL-8 to the cells and measure chemiluminescence during 20 min.
4. Add fMLF (10^{-7} M) to the control tube without cytokines and to the tubes with cytokines and record chemiluminescence. An example of a result obtained using this protocol is shown in Fig. 2.

3.4 Priming of Superoxide Production as Measured by the Cytochrome c Reduction Assay

Priming can also be measured by using the classical cytochrome c reduction assay

1. Suspend neutrophils (1×10^6) in 1 mL HBSS in different cuvettes.
2. Control cuvettes contain neutrophils (1×10^6) in 1 mL HBSS + 5 U of SOD.
3. Add cytochrome c (1 mg/mL final concentration) to each cuvette and place at 37 °C in the thermostated chamber of a spectrophotometer.
4. After 5 min, add cytokines and measure basal absorbance at 550 nm during 20 min.
5. Add fMLF (10^{-7} M) to the control tube and to the tubes with cytokines and record absorbance at 550 nm.

4 Notes

1. All solutions used for cell preparation and cell manipulation, such as the PolymorphPrep solution, are prepared with injection grade sterile water. A ready-made PolymorphPrep can be purchased from companies such as Axis-Shield.
2. Other fluorescent probes, such as 2′,7′-dichlorofluorescin-diacetate (DCFH-DA, Eastman Kodak, Rochester, NY), can be used to study ROS production by neutrophils in whole blood in order to minimize cell activation during the isolation procedure. However, DCFH is mainly oxidized by H_2O_2, and thus does not measure $O_2^{\cdot-}$ production per se. By contrast, $O_2^{\cdot-}$ preferentially oxidizes HE (as with cytochrome c) [26, 27].

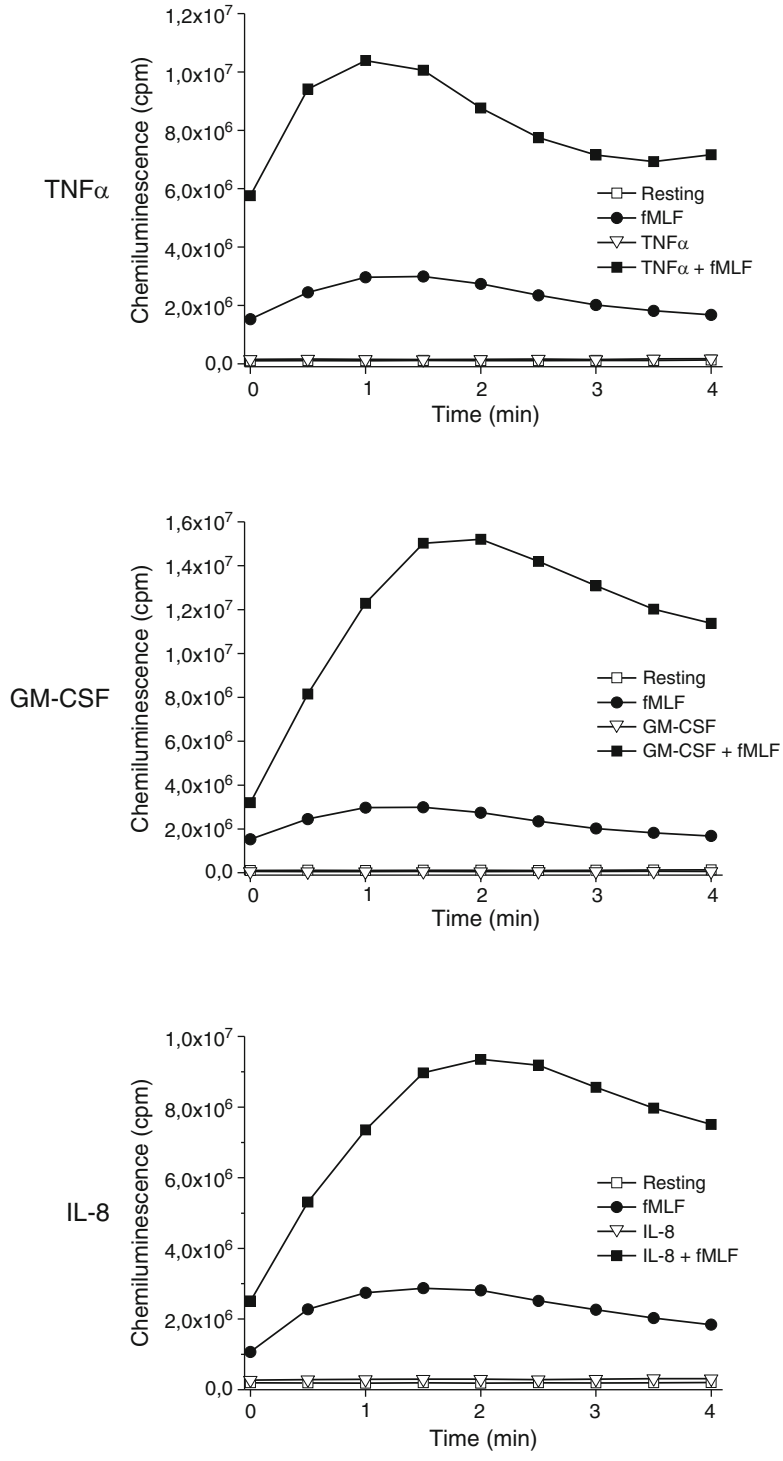

Fig. 2 TNFα, GM-CSF, and IL-8 induce priming of fMLF-stimulated ROS production by neutrophils as measured by luminol-amplified chemiluminescence. Human neutrophils (1×10^6/mL) were resuspended in Hanks buffer containing 10 μM luminol, incubated with either 20 ng/mL of TNFα, 20 ng/mL of GM-CSF, or 50 ng/mL of IL-8 for 20 min, stimulated with fMLF (10^{-7} M), and ROS production was measured by chemiluminescence

3. Other isolation techniques, such as Dextran/Ficoll, can be used, but the best priming result is obtained by a rapid one-step isolation technique. Some commercial Ficoll preparation may contain LPS, which also primes the PMN.
4. When layering the blood on PolymorphPrep, pay particular attention not to mix the two media.
5. With some donors, the contamination of neutrophils by erythrocytes is greater, requiring hypotonic lysis.
6. Other techniques can be used for counting.

Acknowledgments

This work was supported by grants from INSERM, CNRS, University Paris7, the Labex Inflammex and VLM.

References

1. Nauseef WM (2007) How human neutrophils kill and degrade microbes: an integrated view. Immunol Rev 219:88–102
2. El-Benna J, Dang PM, Gougerot-Pocidalo MA, Elbim C (2005) Phagocyte NADPH oxidase: a multicomponent enzyme essential for host defenses. Arch Immunol Ther Exp (Warsz) 3:199–206
3. Babior BM (1999) NADPH oxidase: an update. Blood 93:1464–1476
4. Chanock SJ, El Benna J, Smith RM, Babior BM (1994) The respiratory burst oxidase. J Biol Chem 269:24519–24522
5. Groemping Y, Rittinger K (2005) Activation and assembly of the NADPH oxidase: a structural perspective. Biochem J 386:401–416
6. DeLeo FR, Quinn MT (1996) Assembly of the phagocyte NADPH oxidase: molecular interaction of oxidase proteins. J Leukoc Biol 60: 677–691
7. Quinn MT, Gauss KA (2004) Structure and regulation of the neutrophil respiratory burst oxidase: comparison with nonphagocyte oxidases. J Leukoc Biol 76:760–781
8. El-Benna J, Dang PMC, Gougerot-Pocidalo MA, Marie JC, Braut-Boucher F (2009) p47phox, the phagocyte NADPH oxidase/NOX2 organizer: structure, phosphorylation and implication in diseases. Exp Mol Med 41: 217–225
9. El-Benna J, Faust LP, Babior BM (1994) The phosphorylation of the respiratory burst oxidase component p47phox during neutrophil activation. Phosphorylation of sites recognized by protein kinase C and by proline-directed kinases. J Biol Chem 269:23431–23436
10. El Benna J, Faust LP, Johnson JL, Babior BM (1996) Phosphorylation of the respiratory burst oxidase subunit p47phox as determined by two-dimensional phosphopeptide mapping. Phosphorylation by protein kinase C, protein kinase A, and a mitogen-activated protein kinase. J Biol Chem 271:6374–6378
11. Faust LR, el Benna J, Babior BM, Chanock SJ (1995) The phosphorylation targets of p47phox, a subunit of the respiratory burst oxidase. Functions of the individual target serines as evaluated by site-directed mutagenesis. J Clin Invest 96:1499–1505
12. Belambri SA, Hurtado-Nedelec M, Senator A, Makni-Maalej K, Fay M, Gougerot-Pocidalo MA, Marie JC, Dang PM, El-Benna J (2012) Phosphorylation of p47phox is required for receptor-mediated NADPH oxidase/NOX2 activation in Epstein-Barr virus-transformed human B lymphocytes. Am J Blood Res 2: 187–193
13. El-Benna J, Dang PMC, Gougerot-Pocidalo MA (2008) Priming of the neutrophil NADPH oxidase activation: role of p47phox phosphorylation and NOX2 mobilization to the plasma membrane. Semin Immunopathol 30:279–289
14. Sheppard FR, Kelher MR, Moore EE, McLaughlin NJ, Banerjee A, Silliman CC (2005) Structural organization of the neutrophil NADPH oxidase: phosphorylation and translocation during priming and activation. J Leukoc Biol 78:1025–1042
15. Hallett MB, Lloyds DL (1995) Neutrophil priming: the cellular signals that say 'amber' but not 'green'. immunol. Immunol Today 16: 264–268

16. Dewas C, Dang PM, Gougerot-Pocidalo MA, El-Benna J (2003) TNF-alpha induces phosphorylation of p47(phox) in human neutrophils: partial phosphorylation of p47phox is a common event of priming of human neutrophils by TNF-alpha and granulocyte–macrophage colony-stimulating factor. J Immunol 171: 4392–4398
17. Dang PMC, Stensballe A, Boussetta T, Raad H, Dewas C, Kroviarski Y, Hayem G, Jensen ON, Gougerot-Pocidalo MA, El-Benna J (2006) A specific p47phox-serine phosphorylated by convergent MAPKs mediates neutrophil NADPH oxidase priming at inflammatory sites. J Clin Invest 116:2033–2043
18. Boussetta T, Gougerot-Pocidalo MA, Hayem G, Ciappelloni S, Raad H, Arabi Derkawi R, Bournier O, Kroviarski Y, Zhou XZ, Malter JS, Lu PK, Bartegi A, Dang PM, El-Benna J (2010) The prolyl isomerase Pin1 acts as a novel molecular switch for TNF-alpha-induced priming of the NADPH oxidase in human neutrophils. Blood 116:5795–5802
19. DeLeo FR, Renee J, McCormick S, Nakamura M, Apicella M, Weiss JP, Nauseef WM (1998) Neutrophils exposed to bacterial lipopolysaccharide upregulate NADPH oxidase assembly. J Clin Invest 101:455–463
20. Makni-Maalej K, Boussetta T, Hurtado-Nedelec M, Belambri SA, Gougerot-Pocidalo MA, El-Benna J (2012) The TLR7/8 agonist CL097 primes N-formyl-methionyl-leucyl-phenylalanine-stimulated NADPH oxidase activation in human neutrophils: critical role of p47phox phosphorylation and the proline isomerase Pin1. J Immunol 189: 4657–4665
21. Linas SL, Whittenburg D, Parsons PE, Repine JE (1992) Mild renal ischemia activates primed neutrophils to cause acute renal failure. Kidney Int 42:610–616
22. Chollet-Martin S, Montravers P, Gibert C, Elbim C, Desmonts JM, Fagon JY, Gougerot-Pocidalo MA (1992) Subpopulation of hyperresponsive polymorphonuclear neutrophils in patients with adult respiratory distress syndrome. Role of cytokine production. Am Rev Respir Dis 146:990–996
23. Nurcombe HL, Bucknall RC, Edwards SW (1991) Neutrophils isolated from the synovial fluid of patients with rheumatoid arthritis: priming and activation in vivo. Ann Rheum Dis 50:147–153
24. Jacobi J, Sela S, Cohen HI, Chezar J, Kristal B (2006) Priming of polymorphonuclear leukocytes: a culprit in the initiation of endothelial cell injury. Am J Physiol Heart Circ Physiol 290:H2051–H2058
25. Sela S, Shurtz-Swirski R, Cohen-Mazor M, Mazor R, Chezar J, Shapiro G, Hassan K, Shkolnik G, Geron R, Kristal B (2005) Primed peripheral polymorphonuclear leukocyte: a culprit underlying chronic low-grade inflammation and systemic oxidative stress in chronic kidney disease. J Am Soc Nephrol 16:2431–2438
26. Rothe G, Valet G (1990) Flow cytometric analysis of respiratory burst activity in phagocytes with hydroethidine and 2′,7′-dichlorofluorescin. J Leukoc Biol 47:440–448
27. Bass DA, Parce JW, Dechatelet LR, Szejda P, Seeds MC, Thomas M (1983) Flow cytometric studies of oxidative product formation by neutrophils: a graded response to membrane stimulation. J Immunol 130:1910–1917

Chapter 24

Affinity Purification and Reconstitution of Human Phagocyte Flavocytochrome b for Detection of Conformational Dynamics in the Membrane

Marcia Riesselman and Algirdas J. Jesaitis

Abstract

Human flavocytochrome b (Cyt b) is the core electron transferase of the NADPH oxidase in phagocytes and a number of other cell types. The oxidase complex generates superoxide, initiating production of a cascade of reactive oxygen species critical for the killing of infectious agents. Many fundamental questions still remain concerning its structural dynamics and electron transfer mechanisms. In particular, Cyt b structure/function correlates in the membrane have been relatively unstudied. In order to facilitate the direct analysis of Cyt b structural dynamics in the membrane, the following method provides rapid and efficient procedures for the affinity purification of Cyt b from isolated neutrophil membrane fractions and its functional reconstitution in purified lipid preparations. The protocol presented here contains some new optimized procedures that will facilitate Cyt b isolation and reconstitution. Additional methods are presented that facilitate examination of conformational dynamics of the membrane reconstituted purified Cyt b by fluorescence resonance energy transfer (FRET) as measured by steady-state and lifetime fluorescence techniques.

Key words Phagocyte, Reactive oxygen species, Flavocytochrome b, Immunoaffinity purification, Reconstitution, Membrane conformational dynamics, Fluorescence lifetime analysis

1 Introduction

Neutrophils, monocytes, and macrophages migrate to sites of infection and tissue injury in response to inflammatory stimuli. Upon arrival they release large amounts of the oxidant precursor, superoxide anion, by activation of the multiprotein NADPH oxidase complex [1, 2]. The core electron transferase of the oxidase, flavocytochrome b (Cyt b), is a heterodimeric, integral membrane protein [3, 4] composed of a heavily glycosylated 570 residue large subunit (gp91^{phox}; Nox2) and a 195 residue small subunit (p22^{phox}) [5, 6]. Since Cyt b is currently isolated from whole human blood in limited quantities, our group has refined the rapid, single-step

Mark T. Quinn and Frank R. DeLeo (eds.), *Neutrophil Methods and Protocols*, Methods in Molecular Biology, vol. 1124,
DOI 10.1007/978-1-62703-845-4_24,

purification of Cyt b from neutrophil membranes using a monoclonal antibody (mAb CS9) that binds the $p22^{phox}$ subunit [7, 8] as well as the more traditional heparin affinity chromatography method [3]. Both methods involve detergent solubilization of neutrophil membranes. Following specific binding of Cyt b to the mAb CS9 affinity matrix, high-yield elution of Cyt b is achieved by the addition of an epitope-mimicking peptide, Ac–AEARKKPSEEEAA–$CONH_2$, derived by phage-display analysis of mAb CS9 [8, 9]. This immunoaffinity procedure reproducibly results in final Cyt b yields of ~20–50 % producing a Cyt b sample of about 2–4 μM that can be concentrated to relatively high levels for reconstitution into lipid mixtures of defined composition.

With appropriate fluorescence donor/acceptor pairs, fluorescence resonance energy transfer (FRET) methods provide a highly sensitive assay for measuring both distance and conformational changes in biological molecules within the range of approximately 10–100 Å [10, 11]. We have examined activation-induced conformational changes of Cyt b in detergent extracts using fluorescently labeled Cyt b-specific mAbs. Distances and distance changes from the mAb fluorophores (donors) are measured by heme acceptor fluorescence quenching which varies as the inverse sixth power of distance when brought into close proximity to the Cyt b heme prosthetic groups. This quenching is manifested as a reduction in the fluorescence intensity and lifetime of the fluorescence donor chromophore. The steady-state fluorescence quenching and lifetime methods described here provide a sensitive and rigorous way to monitor antibody binding and characterize lipid-induced conformational changes in immunoaffinity-purified Cyt b reconstituted into liposomes of defined lipid composition [12].

2 Materials

2.1 MAb CS9 Affinity Purification Matrix

1. Antibody binding matrix: Protein G-Sepharose or GammaBind Plus-Sepharose (GE Healthcare Biosciences).
2. Hybridoma culture supernatant containing the $p22^{phox}$-specific mAb CS9: generated in-house by standard hybridoma culture technology and stored at 4 °C. CS9 is also commercially available (Immuquest, North Yorkshire, UK; Santa Cruz Biotechnology, Santa Cruz, CA; and United States Biological, Swampscott, MA).
3. 250 mL polypropylene centrifuge tubes.
4. Disposable 5″ polystyrene chromatography columns (Evergreen Scientific).
5. Phosphate-buffered saline (PBS): 10 mM sodium phosphate (pH 7.4), 150 mM NaCl.

6. Cyanogen Bromide-activated Sepharose 4B (GE Healthcare Biosciences).
7. 0.5 M Acetic acid, pH 3.
8. 100 mM HCl.
9. Bicarbonate buffer: 100 mM $NaHCO_3$.
10. 500 mM NaCl.
11. 100 mM Trizma.
12. Ultracentrifuge.
13. Centricon concentrator with YM-50 (50,000 MW cutoff filters, Millipore).
14. Dialysis tubing or cassettes: MW cutoff 12–14,000.

2.2 Heparin and Immunoaffinity Cyt b Purification

1. Human neutrophil membrane fractions: prepared as previously described [3] and store at −70 °C prior to use.
2. 5 M NaCl stock in dH_2O, stored at room temperature.
3. 15-mL glass homogenizer.
4. Relax Buffer: 10 mM HEPES (pH 7.4), 100 mM KCl, 10 mM NaCl, 1 mM EDTA.
5. Octyl β-D-glucopyranoside (OG): prepare in dH_2O as a 20 % stock (w/v) at 20 °C and store at −20 °C. Store for no more than a month at 4 °C.
6. 200 mM PMSF in ethanol, store at 4 °C.
7. Mammalian protease inhibitor cocktail (Sigma): purchase as a 1,000-fold concentrated stock in DMSO, store at −20 °C.
8. 100 mM Dithiothreitol: prepare fresh in dH_2O.
9. Column buffer: 10 mM HEPES (pH 7.4), 1.2 % OG.
10. Sonicator and/or dounce homogenizer for membrane dispersion.
11. CS9 elution peptide (Ac–AEARKKPSEEEAA–$CONH_2$, Macromolecular Resources; Fort Collins, CO): store lyophilized at −20 °C.
12. Spectrophotometer with quartz microcuvettes.
13. Heparin Sepharose 6 Fast Flow (GE Healthcare Biosciences): for heparin affinity purification of Cyt b.
14. Heparin-sepharose column buffer: 10 mM HEPES (pH 7.4), 1.2 % OG.

2.3 Concentration and Desalting of Cyt b

1. Econo-Pac 10 DG desalting columns (30 × 10 mL; BioRad) equilibrated in Relax buffer containing 1.2 % OG at 4 °C.

2.4 Reconstitution of Cyt b

1. 10 mg/mL phosphatidylcholine: 99 % phosphatidylcholine (Sigma) in $CHCl_3$, store at −20 °C. Briefly cover lipid stocks with argon prior to storage in order to minimize oxidation.

2. 80 % glycerol in dH_2O.
3. Membrane dialysis buffer: 50 mM K_2HPO_4 (pH 7.3), 150 mM NaCl, 1 mM EGTA, 1 mM $MgCl_2$, 20 % glycerol (w/v).

2.5 Cascade Blue Labeling of mAbs

1. Cascade Blue (CCB): 10 mg/mL of cascade blue acetyl azide (Life Technologies/Molecular Probes): in methanol, store dessicated at −20 °C.
2. GammaBind Plus-Sepharose (GE Healthcare Biosciences).
3. Labeling reaction quenching buffer: 1 M Tris, pH 7.4.
4. Econo-Pac 10 DG desalting columns equilibrated in PBS at room temperature.

2.6 FRET Analysis

1. Cylindrical, UV-transparent microcuvettes (Sienco, Fargelanda, Sweden) with micro stir bar. The cuvette holders were manufactured in-house.
2. 10:0 Phosphatidic acid (Avanti): 30 μM in $CHCl_3$, store at −20 °C. Briefly cover lipid stocks with argon prior to storage in order to minimize oxidation.
3. Irrelevant IgG_1 mAb that does not cross-react with other antigens. For these studies anti-rhodopsin mAb K16 was used.
4. Polyethersulfone syringe filters (0.2 μM).
5. Ultracentrifugation for small volume samples (e.g., Beckman TLA-100 and TLA-100.2 rotor).
6. Photon Technologies International Quantamaster® system capable of real-time steady-state fluorescence emission spectroscopy and Timemaster® system capable of fluorescence lifetime spectroscopy were used for the described measurements (Photon Technologies International, Birmingham, NJ).

2.7 Formation of the Reconstituted Cyt b-CS9:CCB Complex for Fluorescence Lifetime Analysis

1. HPLC.
2. Superdex 200 10/300 GL size-exclusion HPLC column.
3. Dulbecco's phosphate-buffered saline (DPBS).
4. Gel filtration markers (e.g., BioRad).
5. Empty phosphatidyl choline membrane vesicles prepared as described in Subheading 3.4 but substituting heparin column elution buffer in place of the Cyt b eluate.

3 Methods

The following methods outline the preparation of purified, detergent-solubilized Cyt b reconstituted into phospholipid vesicles for analysis of conformational changes in membrane bound Cyt b by FRET. Several modifications to the original protocol for

heparin [3] or immunoaffinity purification of Cyt b [7] that result in improved preparations are described, including (1) washing of the affinity matrix in a column (rather than batch) format; (2) elution of Cyt b at detergent concentrations near the critical micelle concentration; (3) concentration of eluted Cyt b samples using a 50 kDa cutoff membrane to minimize the simultaneous concentration of detergent; and (4) the rapid removal of elution peptide and/or buffer exchange on a desalting column. Either affinity purification procedure can be readily conducted in a single day and generates ample material for conducting extensive resonance energy transfer measurements.

3.1 Preparation of the CS9 mAb Affinity Matrix

1. Prior to the Cyt b purification, purify CS9 with two passes of 1 L hybridoma culture supernatant over 1 mL of GammaBind Plus-Sepharose in fritted plastic columns with gravity flow.
2. Wash columns with PBS until A_{280} is at background level.
3. Elute twice with 5 mL of 0.5 M acetic acid (pH 3), and neutralize immediately with Tris base.
4. Measure absorbance, pool, and centrifuge at 100,000 × *g* for 20 min.
5. Concentrate the pool to approximately 2.5–3.5 mg/mL, dialyze extensively against PBS with 0.02 % NaN_3, and store at −70 °C.
6. Resuspend 0.3 g dried CNBr-activated Sepharose in 10 mL of 1 mM HCl, allow to swell (1 mL), wash extensively with 1 mM cold HCl, followed by washing and equilibration with 100 mM $NaHCO_3$, 500 mM NaCl.
7. Dilute 2 mg of CS9 mAb to 7.5 mL in bicarbonate buffer and measure A_{280}.
8. Add CS9 mAb to the CNBr-activated Sepharose beads and rotate end-over-end to mix for 30 min at room temperature. Place in a disposable columns.
9. Collect flow-through fractions and measure A_{280} to confirm that the mAb has coupled to the beads.
10. Wash column with 5 volumes of bicarbonate buffer.
11. Block the unreacted column sites with 10 mL of 100 mM Tris, 500 mM NaCl for 1 h at room temperature. Coupling should be quantitative by analysis of flow-through fractions.
12. Wash beads and equilibrate in PBS. 1.5 mL of beads (50 % slurry) are used for immunoaffinity purification of 5×10^9 cell equivalents of membrane or neutrophil extract (*see* below).

3.2 Immunoaffinity Purification of Cyt b

1. Thaw 10 mL of neutrophil membranes (~5×10^9 cell equivalents), homogenize, sonicate, and bring the solution to 1 M NaCl by the addition of 5 M NaCl stock.
2. Centrifuge the mixture at 114,000 × *g* for 30 min at 4 °C.

3. Homogenize the resulting membrane pellet in 9 mL of Relax buffer supplemented with 0.1 mM DTT, 2 mM PMSF, and 1 μL/mL mammalian protease inhibitor cocktail. Following the 1 M NaCl wash, membrane fractions can vary in the ease with which they are dispersed. To increase Cyt b extraction efficiency, this homogenization step should be carried out until the membranes appear optimally dispersed.
4. Add the 20 % OG to achieve a final concentration of 1.2 %.
5. Homogenize the extract and then briefly sonicate (3 × 5 s, setting 3).
6. Rotate the extract at 4 °C for 40 min.
7. Centrifuge the membrane extract at 114,000 × *g* for 30 min at 4 °C.
8. Collect the supernatant and analyze by absorption spectroscopy (200–700 nm). The Cyt b content is determined using $\varepsilon_{414} = 131{,}000\ M^{-1}\ cm^{-1}$ for the heme Soret band with the assumption of two heme prosthetic groups per Cyt b heterodimer.
9. Add the membrane extract to 1.5 mL of the CS9 affinity matrix equilibrated in Relax, buffer/1.2 % OG. Rotate for 1 h at 4 °C.
10. Pour the above slurry into a disposable column and analyze the flow-through fraction by absorption spectroscopy to assess binding of Cyt b to the affinity matrix.
11. Wash the packed beads with Relax buffer/1.2 % OG until the absorption spectrum (200–700 nm) is at baseline.
12. Elute the CS9 affinity matrix with 1.2 % OG containing 200 μM elution peptide (Ac–AEARKKPSEEEAA–$CONH_2$).
13. Collect 0.5–1 mL fractions allowing the affinity matrix to soak in the peptide elution buffer for 5–10 min between collections. Cyt b should elute within 1–4 mL.
14. Assess the yield by absorbance spectrophotometry and by immunoblot analysis of $p22^{phox}$ (*see* **Note 1**).
15. For removal of elution peptide, pass the concentrated Cyt b sample over an Econo-Pac 10 DG desalting column at 4 °C. Collect 0.5 mL fractions and analyze for Cyt b content by absorption spectroscopy.
16. Following desalting and pooling of fractions, concentrate Cyt b (*see* **Note 2**) as desired and store at 4 °C prior to resonance energy transfer measurements. Yield per 5×10^9 cell equivalents of starting membranes is about 160 μg or 1.9 nmol in about 1 mL (*see* **Notes 3–5**).

3.3 Heparin Affinity Purification of Cyt b

1. Thaw 10 mL of neutrophil membranes (~5×10^9 cell equivalents), homogenize, sonicate, and bring the solution to 1 M NaCl by the addition of 5 M NaCl stock.
2. Centrifuge the mixture at 114,000 × *g* for 30 min at 4 °C.

3. Resuspend the resulting membrane pellet by homogenization in 9 mL of Relax buffer supplemented with 0.1 mM DTT, 2 mM PMSF, and 1 μL/mL of mammalian protease inhibitor cocktail. Following the 1 M NaCl wash, membrane fractions can vary in the ease with which they are dispersed. To increase Cyt b extraction efficiency this homogenization step should be carried out until the membranes appear optimally dispersed.
4. Add the 20 % OG to achieve a final concentration of 1.2 %.
5. Homogenize the extract and then briefly sonicate (3 × 5 s, setting 3).
6. Rotate the extract at 4 °C for 40 min.
7. Centrifuge the membrane extract at 114,000 × *g* for 30 min at 4 °C.
8. Collect the supernatant and analyze by absorption spectroscopy (200–700 nm). Cyt b content is determined using $\varepsilon_{414} = 131{,}000\ M^{-1}\ cm^{-1}$ for the heme Soret band with the assumption of two heme prosthetic groups per Cyt b.
9. Dilute the OG membrane extract into 70 mL of column buffer supplemented with 0.1 mM DTT and 1 μL/mL of mammalian protease inhibitor cocktail.
10. Add the diluted extract to 2 mL (packed volume) of the Heparin-sepharose affinity matrix pre-equilibrated in column buffer. Mix by rotator for 1 h at 4 °C.
11. Transfer the heparin bead slurry to a disposable column.
12. Collect and analyze the flow-through fraction by absorption spectroscopy to assess binding of Cyt b to the affinity matrix.
13. Wash the packed beads with column buffer until the flow-through absorbance (200–700 nm) is at baseline.
14. Elute Cyt b in column buffer containing 800 mM NaCl. Collect 500 μL fractions, place on ice, and analyze the Cyt b content by absorbance spectroscopy.
15. Pool desired elution fractions. A typical yield of Cyt b in 1.5–2 mL of heparin eluate is 2–3 nmol.
16. If necessary, concentrate Cyt b to about 1.5 μM in a Centricon-50 concentrator (*see* **Note 2**). Confirm by the absorption spectrum of the filtrate that the Cyt b is retained.

3.4 Reconstitution of Cyt b in Phosphatidylcholine Membrane Vesicles by Dialysis

1. Prepare 2 mg/mL phosphatidylcholine solubilized in OG as follows:
   (a) Dry 200 μL of the phosphatidylcholine stock in a glass tube under a stream of argon while vortexing.
   (b) To the dried lipid, add 1 mL of 1.2 % OG in membrane dialysis buffer.
   (c) Solubilize the lipid by vortexing and sonication (setting 2, two 3 s bursts).

2. Combine OG-solubilized phosphatidylcholine (final concentration of 400 μg/mL), 20 % glycerol (from an 80 % stock), and heparin (or CS9) eluate containing ~1.5–1.7 μM Cyt b (3:1:1 by volume, heparin eluate:solubilized lipid:glycerol stock). The final concentration of Cyt b will be ~1 μM.
3. Analyze Cyt b content of the mixture by absorbance spectroscopy to determine the actual concentration of Cyt b for use in experimental quantitation of activity.
4. Incubate the mixture for 20 min on ice.
5. Dialyze mixture against 1 L of membrane dialysis buffer over night at 4 °C.
6. Collect the retentate and confirm retention of Cyt b (along with scattering consistent with incorporation of the protein into phospholipid vesicles) by absorbance spectroscopy.
7. Store aliquots at −70 °C.

3.5 Cascade Blue Labeling of Cyt b-Specific mAbs

1. Purify monoclonal antibody CS9 on GammaBind-Sepharose as previously described above and by Lord et al. [7]. This preparation can be stored at 4 °C in PBS, 0.02 % NaN_3.
2. For labeling, add a 40-fold molar excess of CCB to the cleared and filtered (0.2 μm) antibody (0.5 mg of mAb CS9 in 400 μL PBS) and rotate this mixture for 1.5 h at room temperature. Cover the microfuge tube with aluminum foil to protect the reaction from light.
3. Terminate the labeling reaction by adding Tris–HCl buffer (pH 7.5) to a final concentration of 75 mM. Rotate the mixture at room temperature for 10 min.
4. Remove free dye by passing mixture through an Econo-Pac 10 DG desalting column (equilibrated in PBS at room temperature). Detect eluted antibody by absorption spectroscopy.
5. Pool the labeled, desalted mAb and optionally, concentrate the pool to approximately 250 μL.
6. Purify the labeled antibody by HPLC gel filtration (e.g., Agilent ZORBAX GF-250 9.4×250 mm column) in DPBS containing 0.02 % NaN_3.
7. Collect the immunoglobulin peak with CCB absorbance spectrum and store at 4 °C in the dark (*see* **Note 6**).
8. For determination of antibody labeling stoichiometry, quantify protein and CCB by absorbance spectroscopy using $\varepsilon_{280} = 216{,}580\ M^{-1}\ cm^{-1}$ for CS9 and $\varepsilon_{400} = 31{,}400\ M^{-1}\ cm^{-1}$ for CCB.

3.6 Steady-State FRET Analysis

1. Perform steady-state fluorescence measurements in continuously stirred, cylindrical UV-transparent microcuvettes at room temperature with the excitation monochromator set at

376 nm and the emission monochromator set at 418 nm. Set the slit width for both monochromators at 2 nm, corresponding to 4 and 8 nm band pass for the excitation and emission monochromators, respectively.

2. Prepare FRET mixture by diluting CCB-labeled CS9 mAb (21 nM mAb final) and an irrelevant IgG_1 mAb (e.g., anti-rhodopsin mAb K16, produced in-house; 100 μg/mL final) into PBS. Filter and keep on ice. The irrelevant IgG_1 is included in the FRET mixture to minimize any potential nonspecific antibody binding to the proteoliposomes and glass cuvettes.
3. Prior to fluorescence measurements, sonicate reconstituted Cyt b phosphatidylcholine membranes and clear by centrifugation at $14{,}000 \times g$ for 2 min at room temperature.
4. Add the cleared membrane sample to the FRET mixture to achieve a final concentration of 20–30 nM Cyt b (40–60 % saturation).
5. Monitor CCB fluorescence of the labeled antibody until a stable steady-state emission is observed.
6. Various agents (e.g., lipids, amphiphiles, peptides) can then be added directly to the micro-cuvette and fluorescence emission monitored until a steady state is achieved. In our studies, a relaxation of fluorescence quenching (not attributable to a direct effect of lipids on antibody fluorescence emission, dissociation of the CCB-mAb:Cyt b complex, or perturbation of Cyt b heme prosthetic groups) has been taken as a measure of conformational changes in Cyt b.
7. Important controls include measurement of fluorescence from the CS9-CCB-labeled mAb in the presence of empty phosphatidylcholine vesicles to assess the effects of the added agents on the mAb fluorescence alone. Additionally, size-exclusion chromatography (see below) can be used to show that mAb CS9 and reconstituted Cyt b have not dissociated.

3.7 Formation of the Cyt b-CS9:CCB Complex for Fluorescence Lifetime Analysis

1. Mix dialyzed membranes and labeled mAb to achieve 150 nM Cyt b and 100 nM CS9:CCB in DPBS supplemented with 100 mg/mL irrelevant IgG_1 mAb carrier (e.g., mAb K16) and 0.02 % NaN_3.
2. Incubate the mixture at room temperature for 30 min.
3. To separate unbound label from the phosphatidylcholine membrane Cyt b-bound CS9:CCB complex, elute 250 μL of the mixture through a Superdex 200 10/300 GL size-exclusion column (presaturated by a series of empty phosphatidylcholine vesicle injections) with DPBS/0.02 % NaN_3 mobile phase at 0.7 mL/min.
4. Collect 1 min fractions, monitoring absorbance and fluorescence ($\lambda_{ex} = 376$ nm, $\lambda_{em} = 420$ nm).

5. Combine the two peak protein fractions that have CCB fluorescence to obtain the Cyt b-CS9:CCB proteoliposome complex, which is used for fluorescence lifetime analysis. The peak will elute in advance of the 670 kDa gel filtration marker (void volume).

3.8 Fluorescence Decay Measurements and Lifetime Analysis

1. Monitor the fluorescence emission of samples in a stirred cuvette at room temperature.
2. Various agents (lipids and epitope-mimicking peptides) can be added to assess the effects on the membrane reconstituted Cyt b-CS9:CCB complex. For example, we collected emission data on the complex before and after adding 30 μM 10:0 phosphatidic acid, then 200 μM of the complex disrupting epitope peptide, stirring each for 15–30 min (*see* Fig. 1 and ref. 12).

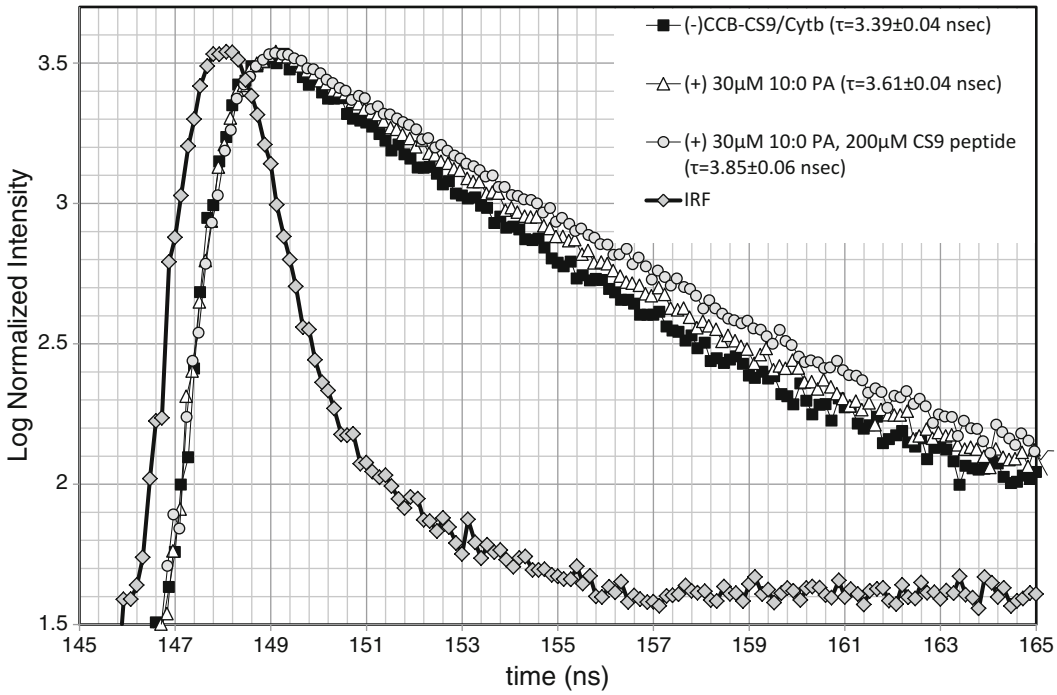

Fig. 1 Fluorescence lifetime analysis of free CCB-CS9 and bound to Cyt b. Complexes of Cyt b and CCB-CS9 were purified by size-exclusion liquid chromatography. The dependence of fluorescence lifetime of the untreated complex (filled squares; -■-) was compared to that exposed to 30 μM 10:0 PA (open triangles; -Δ-) and to 30 μM 10:0 PA plus antibody-releasing 200 μM epitope-mimicking peptide, Ac–AEARKKPSEEEAA–NH_2 (open circles; -○-). The log fluorescence intensity (normalized to a value of 3,500) is plotted as a function of time in the nanosecond range as shown. As a reference, the excitation pulse is shown as the instrument response time (open diamonds; -◇-;IRF) intensity of scattered light from a sample where $\lambda_{ex} = \lambda_{em} = 376$ nm. For comparison, the linear regions of the intensity rises were superimposed to facilitate comparison of the data. The change in lifetime suggests that Cyt b heme acceptor and the CCB donor reorient or move away from one another upon interaction with 10:0 PA

3. Each fluorescence decay curve collected is the average of five acquisitions fluorescence lifetime spectrophotometer (excitation 376 nm). Emission photons are measured by a voltage delay gated photomultiplier (420 nm).
4. Normalize and average four decay curves acquired from each sample.
5. Use Felix32 software or comparable software for lifetime analysis (*see* below).

3.9 Lifetime Analysis

1. The fluorescence lifetime analysis of reconstituted Cyt b-CS9: CCB complexes is accomplished by using Felix32 or comparable software, which generates fluorescence transients such as are shown in Fig. 1. The purpose of the measurement is to get a measure of the FRET efficiency, *E*, which can be derived from the expression:

$$E = 1 - \left(\tau_{D+A} / \tau_{D} \right)$$

where τ_{D+A} is the lifetime in the presence of the donor and acceptor; and τ_{D} is the lifetime in the presence of only the donor.

2. The theoretical distance between the single donor-single acceptor model case is shown graphically in Fig. 2 (*see* **Note 7**). A full description of these results can be found in Taylor et al. [12].

3.10 Steady-State FRET Analysis

1. An example of how the dynamics of conformational change may be related to NADPH oxidase activity is shown in Fig. 3.
2. In this series of experiments, FRET [12] is measured by steady-state relaxation of quenching, and NADPH oxidase activity is measured by the superoxide-dismutase-inhibitable, NADPH-dependent reduction of cytochrome c. Both activities are graphed as a function of the concentration of 10:0 phosphatidic acid added to the system to initiate oxidase activity.
3. Clearly Cyt b conformational change precedes NADPH oxidase activation in 10:0 PA sensitivity and it is almost half maximal prior to the appearance of any 10:0 PA dependent NADPH oxidase activity. We interpret this result to suggest that 10:0 PA provides a membrane environment that may be required for Cyt b to achieve a conformation permissible for superoxide production. Since this activity takes place in the membrane, it examines another potential mechanism of cellular control for this important redox activity.
4. In separate experiments, we have found that NADPH oxidase activity and the *magnitude* of the Cyt b conformational change induced by phosphatidic acid depends very strongly on the amounts of negatively charged lipids in the reconstitution mixture (unpublished data), supporting the potential regulatory role of negatively charged lipids on Cyt b activity.

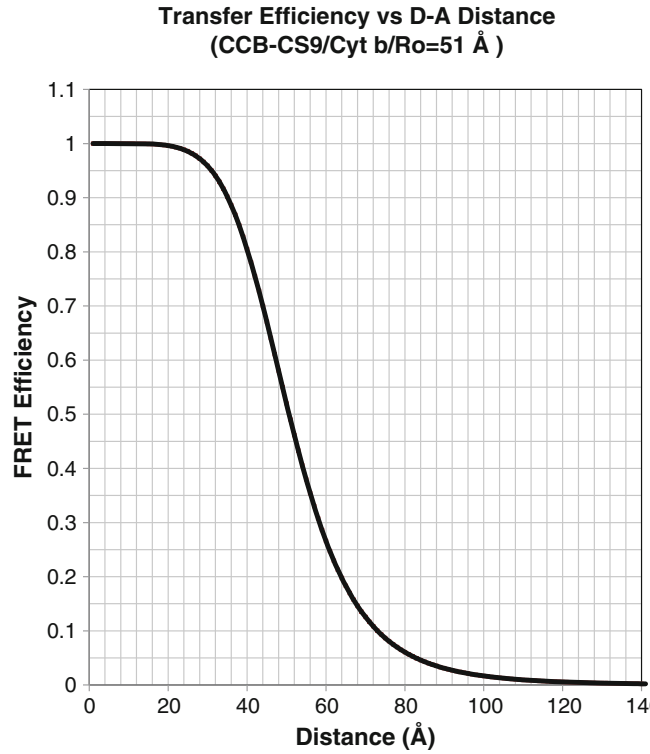

Fig. 2 Distance estimates for the CCB/Heme Donor/Acceptor pair. Förtser spectroscopic ruler for measuring IgG-conjugated Cascade Blue donor to heme acceptor distances. The relationship between fluorescent resonance energy transfer (FRET) efficiency (*E*) and donor↔acceptor distance as measured by fluorescence quenching or fluorescence lifetime analysis is shown graphically. This model system assumes a single donor (CCB) interacting with a single heme acceptor. The calculated 50 % transfer efficiency distance, R_0, is 51 Å. *See* ref. 12

4 Notes

1. Following peptide elution from the affinity matrix, mAb CS9 is occasionally observed as a minor contaminant of the Cyt b preparations (as confirmed by Western blot analysis and MALDI peptide mass mapping). To remove any contaminating CS9 immunoglobulin from this preparation, a size-exclusion chromatography step can be used to separate the immunoglobulin from the detergent-bound Cyt b.
2. Concentration of purified Cyt b samples in the 50 kDa cutoff membrane proves critical for control of final OG levels as free OG micelles have been shown to pass through the membrane and not concentrate with purified protein–detergent complex.
3. Recent studies have also indicated efficient elution of Cyt b from the affinity matrix at room temperature.

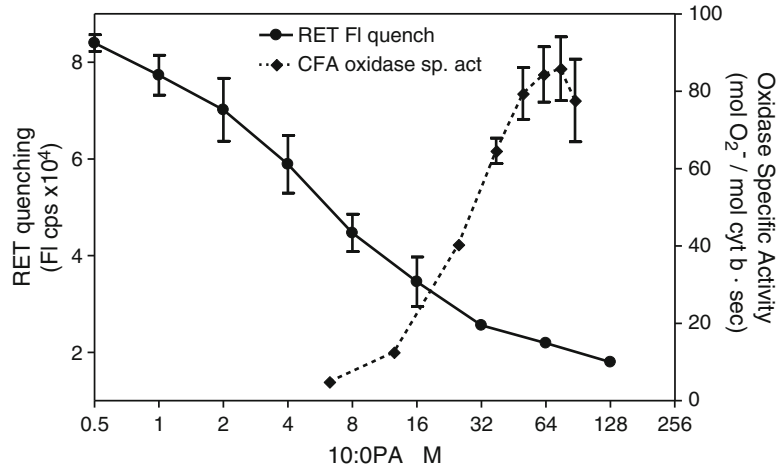

Fig. 3 Comparison of FRET and maximal superoxide production rates as a function of concentration of 10:0 PA. CCB-CS9 steady-state fluorescence quenching by Cyt b was determined following formation of the CCB-mAb:Cyt b complexes as described in the text and the reaction mixtures were treated with 10:0 PA to assess lipid-induced conformational changes in Cyt b. The average maximum fluorescence quenching in fluorescence quenching observed when the CCB-CS9:Cyt b complex was treated with 10 μM addition of 10:0 PA (averages of two sets of three replicates) was plotted as a function of 10:0 PA concentration (filled circles; -●-; fluorescence units on left ordinate). The right ordinate is scaled to display the maximal rates of superoxide production (filled diamonds; -◆-), expressed as mol superoxide produced per mole Cyt b per sec or turnover with the units per second measured and similarly plotted as a function of the final 10:0 PA concentration. The data for quenching was fit by nonlinear regression analysis to a two site hyperbolic binding curve using GraphPad Prism version 3.03. Recalculated from ref. 12

4. The absorbance spectrum of detergent-solubilized Cyt b is indistinguishable from the original material following a single freeze/thaw cycle. This suggests OG-solubilized Cyt b to maintain structural and functional integrity following storage at –20 °C with 20 % glycerol.
5. Following the Cyt b purification, the protein G-Sepharose beads can be regenerated for use in multiple preparations by washing with 2–3 bed volumes of cleaning 1 M acetic acid, pH 2.5, followed by re-equilibration with 2–3 bed volumes of binding buffer. For longer periods of storage, GammaBind G-Sepharose should be kept at 4–8 °C in a bacteriostatic solution such as 20 % ethanol. The affinity matrix cannot be frozen after washing with PBS. Storage at 4 °C after 0.5 M acetic acid (pH 3.0) elution and washing in PBS is possible, if the slurry is supplemented with 0.02 % NaN_3.
6. RET studies have also been successfully conducted using other Cyt b-specific mAbs such as mAb 44.1, NS1, and 7D5 labeled

with either Cascade Blue acetyl azide or AlexaFluor 350 succinimidyl ester.

7. Gross distance approximation (mAb epitope to Cyt b hemes) is possible as long as conclusions are qualified by uncertainties arising from donor–donor transfer and heme reorientation. Mass spectrometry analysis of tryptic digests of CCB-labeled mAb analogous to that performed for proof of principle on cytochrome c labeled with CCB [13], reduces uncertainties as to CCB conjugation loci on mAbs.

References

1. Nauseef WM (2007) How human neutrophils kill and degrade microbes: an integrated view. Immunol Rev 219:88–102
2. Sumimoto H (2008) Structure, regulation and evolution of Nox-family NADPH oxidases that produce reactive oxygen species. FEBS J 275: 3249–3277
3. Parkos CA, Allen RA, Cochrane CG, Jesaitis AJ (1987) Purified cytochrome b from human granulocyte plasma membrane is composed of two polypeptides with relative molecular weights of 91,000 and 22,000. J Clin Invest 80:732–742
4. Parkos CA, Allen RA, Cochrane CG, Jesaitis AJ (1988) The quaternary structure of the plasma membrane b-type cytochrome of human granulocytes. Biochim Biophys Acta 932:71–83
5. Parkos CA, Dinauer MC, Walker LE, Allen RA, Jesaitis AJ, Orkin SH (1988) Primary structure and unique expression of the 22-kilodalton light chain of human neutrophil cytochrome b. Proc Natl Acad Sci U S A 85: 3319–3323
6. Vignais PV (2002) The superoxide-generating NADPH oxidase: structural aspects and activation mechanism. Cell Mol Life Sci 59: 1428–1459
7. Lord CI, Riesselman MH, Gripentrog JM, Burritt JB, Jesaitis AJ, Taylor RM (2008) Single-step immunoaffinity purification and functional reconstitution of human phagocyte flavocytochrome b. J Immunol Methods 329: 201–207
8. Taylor RM, Burritt JB, Baniulis D, Foubert TR, Lord CI, Dinauer MC, Parkos CA, Jesaitis AJ (2004) Site-specific inhibitors of NADPH oxidase activity and structural probes of flavocytochrome b: characterization of six monoclonal antibodies to the p22phox subunit. J Immunol 173:7349–7357
9. Burritt JB, Quinn MT, Jutila MA, Bond CW, Jesaitis AJ (1995) Topological mapping of neutrophil cytochrome b epitopes with phage- display libraries. J Biol Chem 270: 16974–16980
10. dos Remedios CG, Moens PD (1995) Fluorescence resonance energy transfer spectroscopy is a reliable "ruler" for measuring structural changes in proteins. Dispelling the problem of the unknown orientation factor. J Struct Biol 115:175–185
11. Heyduk T (2002) Measuring protein conformational changes by FRET/LRET. Curr Opin Biotechnol 13:292–296
12. Taylor RM, Riesselman MH, Lord CI, Gripentrog JM, Jesaitis AJ (2012) Anionic lipid-induced conformational changes in human phagocyte flavocytochrome b precede assembly and activation of the NADPH oxidase complex. Arch Biochem Biophys 521: 24–31
13. Taylor RM, Lin B, Foubert TR, Burritt JB, Sunner J, Jesaitis AJ (2002) Cascade blue as a donor for resonance energy transfer studies of heme-containing proteins. Anal Biochem 302: 19–27

Chapter 25

Evaluation of p47phox Phosphorylation in Human Neutrophils Using Phospho-Specific Antibodies

Sahra Amel Belambri, Pham My-Chan Dang, and Jamel El-Benna

Abstract

Superoxide anions production by neutrophils plays a key role in host defense against pathogens and in inflammation. The enzyme responsible for this process is called the NADPH oxidase. It is a multicomponent enzyme comprised of a membrane-bound flavocytochrome b_{558} and several cytosolic proteins (p47phox, p67phox, p40phox, and p21rac1/2). The phosphorylation of p47phox is essential for the activation of the complex in intact cells. Until recently, analysis of the phosphorylation of p47phox in neutrophils required radioactive labeling, which implied the use of high amount of radioactive (^{32}P)-orthophosphoric acid, high number of cells, and protein recovery by immunoprecipitation. In this study, we describe a radioactive-free technique to analyze the phosphorylation of p47phox in cell lysates, based on the use of phospho-specific antibodies, SDS-polyacrylamide gel electrophoresis (SDS-PAGE), and Western blotting. This technique could be used to quickly and easily study the phosphorylation of p47phox under different conditions, such as testing the effects of pharmacological agents in this process or assessing the activation status of neutrophils in situ.

Key words Neutrophils, p47phox-phosphorylation, NADPH oxidase, NOX2, Phospho-specific antibodies

1 Introduction

Professional phagocytes, such as neutrophils, monocytes, and macrophages, undergo a respiratory burst in response to infectious agents or inflammatory mediators. This process generates high amount of superoxide anion and other reactive oxygen species (ROS) [1, 2]. The enzyme system responsible for superoxide anion production in phagocytic cells is the multicomponent enzyme, NADPH oxidase [3–5]. This complex includes the membrane-bound cytochrome b_{558} (composed of p22phox and gp91phox) and several cytosolic proteins (p47phox, p67phox, p40phox, and Rac1/2) [3–5]. In resting cells, the components are separated between cytosol and membranes, with p47phox in the cytosol as a non-phosphorylated inactive form. Upon activation of the NADPH oxidase in neutrophils stimulated by formyl-Met-Leu-Phe (fMLF)

Mark T. Quinn and Frank R. DeLeo (eds.), *Neutrophil Methods and Protocols*, Methods in Molecular Biology, vol. 1124,
DOI 10.1007/978-1-62703-845-4_25,

peptide or phobol myristate acetate (PMA), the cytosolic components translocate to the membrane to form a catalytically active oxidase complex [6, 7]. Phosphorylation of p47phox on serines localized between amino acid 303 and Ser379 is required for NADPH oxidase assembly and activation [8–12]. Activation of the NADPH oxidase in neutrophils can be enhanced by proinflammatory agents in a process called priming [13, 14]. In contrast to activating agents, priming agents such as the proinflammatory cytokines TNFα and GM-CSF and the TLR agonist LPS, induce partial p47phox phosphorylation on one serine, namely Ser345 [15–17]. Phosphorylated Ser345 was shown to be a critical docking site for the proline isomerase Pin1, which induces p47phox conformational changes and facilitates p47phox phosphorylation by other protein kinases on other sites [18, 19]. Thus, the state of phosphorylation of p47phox reflects the state of neutrophil activation.

In the past, analysis of p47phox phosphorylation is required tedious and time-consuming manipulations, such as the use of high amounts of radioactive (^{32}P)-orthophosphoric acid, labeling of a large number of cells, immunoprecipitation of p47phox, and phosphopeptide mapping analysis, all of which demanding specialized expertise [20]. In this chapter, we describe a nonradioactive protocol based on the use of phospho-specific antibodies, allowing for quick and easy assessment of the p47phox phosphorylation status. Briefly, neutrophils are treated with agonists, lysed in a hot fortified Laemmli sample Buffer, proteins are separated by sodium dodecyl sulfate-polyacrylamide gel electrophoresis (SDS-PAGE) and transferred to membranes, which are then probed with phospho-p47phox antibodies by immunoblotting.

2 Materials

2.1 Reagents

1. Phorbol myristate acetate (PMA): 1 mg/mL in sterile DMSO. Aliquot and store at −70 °C.
2. TNFα: 10 μg/mL in phosphate-buffered saline (PBS), 0.05 % human serum albumin. Aliquot and store at −70 °C.
3. GM-CSF: 10 μg/mL in PBS, 0.05 % human serum albumin. Aliquot and store at −70 °C.
4. Diisopropylfluorophosphate (DFP): 5.4 M solution, as purchased.
5. Leupeptin: 10 mg/mL in PBS, store at −20 °C.
6. Aprotonin: 10 mg/mL in PBS, store at −20 °C.
7. Pepstatin: 10 mg/mL in DMSO, store at −20 °C.
8. Calyculin A: 100 μM in PBS. Aliquot and store at −20 °C.
9. Antibodies directed against phospho-Ser345-p47phox and phospho-Ser328-p47phox. Production is described elsewhere [16, 18] (*see* **Note 1**).

10. Peroxidase-conjugated goat anti-rabbit antibody: aliquot and store at –20 °C.
11. Reagents for SDS-PAGE and Western blotting [20, 21].

2.2 Buffers and Solutions

1. Dextran T500, 2 %: 10 g of Dextran T500, 500 mL of 0.9 % NaCl. Filter-sterilize and store at 4 °C for up to 4 weeks (*see* **Note 2**).
2. Sterile PBS.
3. Hanks buffered-salt solution containing Ca^{2+}, Mg^{2+}, and D-glucose (HBSS).
4. Modified Laemmli sample buffer, 5× [21]: 312.5 mM Tris–HCl (pH 6.8), 15 % SDS, 20 % beta-mercaptoethanol, 45 % glycerol, 5 mM Na_3VO_4, 2.5 mmol/L p-NPP, 10 mM NaF, 50 nM Calyculin A, 2.5 mM EDTA, 2.5 mM EGTA, 20 μg/mL leupeptin, 20 μg/mL pepstatin, 20 μg/mL aprotinin. Stored at –20 °C for up to 6 months (*see* **Note 3**).
5. Transfer buffer: 50 mM Tris base, 95 mM glycine, 0.08 % SDS, 20 % methanol (*see* **Note** 4).
6. Tris-buffered saline/Tween 20 (TBST) buffer: 25 mM Tris–HCl (pH 7.5), 150 mM NaCl, 0.05 % Tween 20.

3 Methods

3.1 Isolation of Human Neutrophils

Venous blood from healthy adult volunteers is collected into citrate as the anticoagulant. Neutrophils are isolated by Dextran sedimentation and Ficoll density gradient centrifugation:

1. To 1 volume of whole blood (up to 400 mL can be used in some experiments), add 1 volume of 2 % Dextran T500 solution. Gently mix by inverting the tubes several times and allow to sediment at room temperature for 20–30 min.
2. Collect the upper layer into 50-mL centrifuge tubes, and discard the red cell phase. Centrifuge at 400 × *g* for 8 min at room temperature (*see* **Note 5**).
3. After centrifugation, the pellets contain the leukocytes and contaminating erythrocytes. Remove the supernatant and resuspend each pellet in 5 mL of PBS, pool several pellets, gently layer on Ficoll (2 volumes of cells/1 volume of Ficoll), and centrifuge at 400 × *g* for 30 min at 22 °C (*see* **Note 6**).
4. Discard the upper layers and mononuclear cells, which are at the interface of the buffer and Ficoll.
5. Disperse the pellet containing neutrophils and contaminating erythrocytes. Remove contaminating erythrocytes by hypotonic lysis by adding 12 mL of ice-cold sterile 0.2 % NaCl for 30 s while mixing gently, and restore isotonicity by adding 12 mL of 1.6 % NaCl (*see* **Note** 7).

6. Centrifuge the tubes at 400 × *g* for 8 min at 4 °C. Remove the red supernatant containing the lysed erythrocytes and resuspend the neutrophil pellet in 5–10 mL of PBS (*see* **Note 8**).
7. Count the cells by diluting in trypan blue (1/100) and using a hemocytometer (*see* **Note 9**).

3.2 Diisopropyl Fluorophosphate Treatment

Diisopropyl fluorophosphate (DFP) protects proteins from degradation by inhibiting neutrophil serine proteases [22]. DFP is extremely toxic; thus, appropriate safety precaution must be used, such as handling it only in a fume hood, and wearing gloves and lab coats. All tips and other materials contaminated with DFP must be discarded in a 1 N NaOH-containing waste container placed under the hood (*see* **Note 10**).

1. Resuspend cells at 5–10 × 10^7 cells/mL in PBS buffer.
2. Add DFP (2.7 mM) by diluting the stock solution (5.4 M) to 1/2,000 and incubate for 15 min at 4 °C.
3. Add 10 volumes of PBS buffer, centrifuge at 400 × *g* and 4 °C, discard the supernatant in 1 N NaOH, and resuspend the neutrophil pellet in Hanks buffer.

3.3 Stimulation of Neutrophils, Lysis, and Protein Denaturation

1. For stimulation, adjust the cells to 1.5 × 10^7 cells in 0.4 mL of HBSS and preincubate at 37 °C for 10 min prior to adding either TNFα (20 ng/mL) for 20 min, GM-CSF (20 ng/mL) for 20 min, or PMA (200 ng/mL) for 8 min.
2. Stop the reaction by adding 100 μL of hot 5× modified Laemmli sample buffer (*see* **Note 11**). This procedure also allows instant lysis of neutrophils.
3. In some experiments the reaction was stopped by adding 5 mL ice-cold PBS or 1 mL of 10 % trichloroacetic acid (TCA) and centrifugation.
4. Incubate the samples for 2 min in boiling water (100 °C) for complete denaturation.
5. Sonicate viscous samples twice for 5 s each to break up DNA, centrifuge at 2,000 × *g* for 8 min, and store at −70 °C until use (*see* **Note 12**).

3.4 Electrophoresis and Western Blotting

The denatured proteins are subjected to SDS-polyacrylamide gel electrophoresis (SDS-PAGE) in 10 % polyacrylamide gels, using standard techniques [20, 21]. The separated proteins are then electro-transferred to nitrocellulose membranes [23] using the transfer buffer described above.

1. Incubate the membranes in TBST/5 % Blotto-milk for 30 min at room temperature on a rotating shaker to block any nonspecific protein binding sites.

2. Add the antibodies: anti-phospho-Ser345-p47phox (1:10,000), anti-phospho-Ser328-p47phox, or anti-p47phox (1/5,000 dilution) in TBST buffer/1 % Blotto-milk and incubate for 1 h at room temperature (*see* **Note 13**).
3. Wash three times with TBST buffer for 10 min each wash.
4. Add a peroxidase-labeled goat anti-rabbit antibody (1/10,000 dilution), and incubate for 1 h at room temperature.
5. Wash three times with TBST for 10 min each wash.
6. Develop with the Luminol reagent (*see* **Note 14**).
7. Representative results obtained with this protocol are shown in Fig. 1 for the anti-phosphoSer345 antibody and in Fig. 2 for the anti-phosphoSer28 antibody.

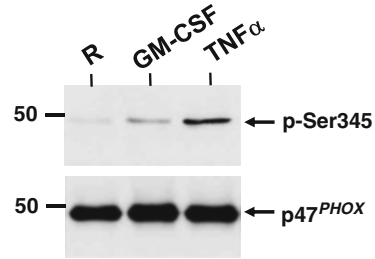

Fig. 1 Representative immunoblot showing p47phox phosphorylation on Ser 345 in human neutrophils treated by TNFα and GM-CSF. Human neutrophils (15×10^6/400 μL) were incubated with TNFα or GM-CSF for 20 min and the reaction was stopped by denaturation with 100 μL hot modified Laemmli sample buffer. Homogenates were subjected to SDS-PAGE and Western blotting using anti-phospho-Ser-345-p47phox and anti-p47phox antibodies

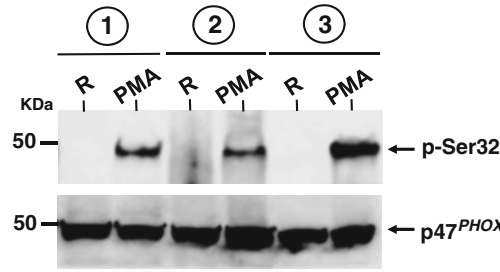

Fig. 2 Representative immunoblot showing a comparison of the different protocols used to stop the p47phox phosphorylation reaction in human neutrophils. Human neutrophils (15×10^6/400 μL) were incubated with PMA (200 ng/mL) for 10 min and the reaction was stopped by: (1) ice-cold PBS, centrifugation, followed by denaturation or (2) trichloroacetic acid (10 %) precipitation followed by denaturation or (3) addition of 100 μL hot modified Laemmli sample buffer, as described above. Homogenates were subjected to SDS-PAGE and Western blotting using the anti-phospho-Ser328-p47phox and the anti-p47phox antibodies

4 Notes

1. The antibodies were produced by private companies. Several companies offer to synthesize the peptide, couple it to a carrier, produce the antibody in rabbits, and purify.
2. All solutions used for cell preparation and cell manipulation, such as the Dextran solution, are prepared with sterile water or sterile 0.9 % NaCl for injection.
3. Calyculin A is a powerful phosphatase 1/2A inhibitor. It is added to the buffer just before use from a 100 μM stock solution.
4. Solutions used for SDS-PAGE and Western Blots are prepared in very pure water (resistivity: 18.2 MΩ cm).
5. This centrifugation step is used to concentrate the cells, and thus to use less Ficoll. If a small volume of blood is used, the supernatant can be layered directly on Ficoll.
6. It is important to use sterile PBS in order to avoid cell activation. When layering the cells on Ficoll, avoid mixing the two phases. The interface between the cell suspension and the Ficoll layer must be clearly visible.
7. Never vortex the cells, and lyse the erythrocytes only after having dispersed the pellet, as the cells will otherwise aggregate.
8. If 400 mL blood is used, cells are resuspended in 10 mL PBS. In general, for each 100 mL blood, 2.5 mL PBS is used to resuspend the cells.
9. Other techniques can be used for counting.
10. Other serine proteases inhibitors have been used, but DFP continues to be favored despite its toxicity, as it yields the best results.
11. Next to the water bath at 37 °C, prepare boiling water in a beaker on a hot plate to immediately stop the reaction.
12. Phosphorylated proteins are stable for months under these conditions.
13. Antibodies can be also incubated overnight at 4 °C if more convenient.
14. Do not use amplified chemiluminescence reagents.

Acknowledgments

This work was supported by grants from INSERM, CNRS, University Paris7, the Labex Inflammex, and the association Vaincre la mucoviscidose (VLM).

References

1. Nauseef WM (2007) How human neutrophils kill and degrade microbes: an integrated view. Immunol Rev 219:88–102
2. El-Benna J, Dang PM, Gougerot-Pocidalo MA, Elbim C (2005) Phagocyte NADPH oxidase: a multicomponent enzyme essential for host defenses. Arch Immunol Ther Exp (Warsz) 3:199–206
3. Babior BM (1999) NADPH oxidase: an update. Blood 93:1464–1476
4. Chanock SJ, El Benna J, Smith RM, Babior BM (1994) The respiratory burst oxidase. J Biol Chem 269:24519–24522
5. Groemping Y, Rittinger K (2005) Activation and assembly of the NADPH oxidase: a structural perspective. Biochem J 386:401–416
6. DeLeo FR, Quinn MT (1996) Assembly of the phagocyte NADPH oxidase: molecular interaction of oxidase proteins. J Leukoc Biol 60:677–691
7. Quinn MT, Gauss KA (2004) Structure and regulation of the neutrophil respiratory burst oxidase: comparison with nonphagocyte oxidases. J Leukoc Biol 76:760–781
8. El-Benna J, Dang PMC, Gougerot-Pocidalo MA, Marie JC, Braut-Boucher F (2009) p47phox, the phagocyte NADPH oxidase/NOX2 organizer: structure, phosphorylation and implication in diseases. Exp Mol Med 41:217–225
9. El-Benna J, Faust LP, Babior BM (1994) The phosphorylation of the respiratory burst oxidase component p47phox during neutrophil activation. Phosphorylation of sites recognized by protein kinase C and by proline-directed kinases. J Biol Chem 269:23431–23436
10. El Benna J, Faust LP, Johnson JL, Babior BM (1996) Phosphorylation of the respiratory burst oxidase subunit p47phox as determined by two-dimensional phosphopeptide mapping. Phosphorylation by protein kinase C, protein kinase A, and a mitogen-activated protein kinase. J Biol Chem 271:6374–6378
11. Faust LR, el Benna J, Babior BM, Chanock SJ (1995) The phosphorylation targets of p47phox, a subunit of the respiratory burst oxidase. Functions of the individual target serines as evaluated by site-directed mutagenesis. J Clin Invest 96:1499–1505
12. Belambri SA, Hurtado-Nedelec M, Senator A, Makni-Maalej K, Fay M, Gougerot-Pocidalo MA, Marie JC, Dang PM, El-Benna J (2012) Phosphorylation of p47phox is required for receptor-mediated NADPH oxidase/NOX2 activation in Epstein-Barr virus-transformed human B lymphocytes. Am J Blood Res 2: 187–193
13. El-Benna J, Dang PMC, Gougerot-Pocidalo MA (2008) Priming of the neutrophil NADPH oxidase activation: role of p47phox phosphorylation and NOX2 mobilization to the plasma membrane. Semin Immunopathol 30:279–289
14. Sheppard FR, Kelher MR, Moore EE, McLaughlin NJ, Banerjee A, Silliman CC (2005) Structural organization of the neutrophil NADPH oxidase: phosphorylation and translocation during priming and activation. J Leukoc Biol 78:1025–1042
15. Dewas C, Dang PM, Gougerot-Pocidalo MA, El-Benna J (2003) TNF-alpha induces phosphorylation of p47(phox) in human neutrophils: partial phosphorylation of p47phox is a common event of priming of human neutrophils by TNF-alpha and granulocyte-macrophage colony-stimulating factor. J Immunol 171:4392–4398
16. Dang PMC, Stensballe A, Boussetta T, Raad H, Dewas C, Kroviarski Y, Hayem G, Jensen ON, Gougerot-Pocidalo MA, El-Benna J (2006) A specific p47phox-serine phosphorylated by convergent MAPKs mediates neutrophil NADPH oxidase priming at inflammatory sites. J Clin Invest 116:2033–2043
17. DeLeo FR, Renee J, McCormick S, Nakamura M, Apicella M, Weiss JP, Nauseef WM (1998) Neutrophils exposed to bacterial lipopolysaccharide upregulate NADPH oxidase assembly. J Clin Invest 101:455–463
18. Boussetta T, Gougerot-Pocidalo MA, Hayem G, Ciappelloni S, Raad H, Arabi Derkawi R, Bournier O, Kroviarski Y, Zhou XZ, Malter JS, Lu PK, Bartegi A, Dang PM, El-Benna J (2010) The prolyl isomerase Pin1 acts as a novel molecular switch for TNF-alpha-induced priming of the NADPH oxidase in human neutrophils. Blood 116:5795–5802
19. Makni-Maalej K, Boussetta T, Hurtado-Nedelec M, Belambri SA, Gougerot-Pocidalo MA, El-Benna J (2012) The TLR7/8 agonist CL097 primes N-formyl-methionyl-leucyl-phenylalanine-stimulated NADPH oxidase activation in human neutrophils: critical role of p47phox phosphorylation and the proline isomerase Pin1. J Immunol 189:4657–4665
20. El-Benna J, Dang PM (2007) Analysis of protein phosphorylation in human neutrophils. Methods Mol Biol 412:85–96
21. Laemmli UK (1970) Cleavage of structural proteins during the assembly of the head of bacteriophage T4. Nature 227:680–685
22. Amrein PC, Stossel TP (1980) Prevention of degradation of human polymorphonuclear leukocyte proteins by diisopropylfluorophosphate. Blood 56:442–447
23. Towbin H, Staehlin T, Gordon J (1979) Electrophoretic transfer of proteins from polyacrylamide gels to nitrocellulose sheets: procedure and some applications. Proc Natl Acad Sci U S A 76:4350–4354

Part VII

Analysis of Neutrophil Gene Expression and Transcription Factors

Chapter 26

Genome-Scale Transcript Analyses with Human Neutrophils

Scott D. Kobayashi, Daniel E. Sturdevant, and Frank R. DeLeo

Abstract

Transcriptome analyses of single- and multicellular organisms have changed fundamental understanding of biological and pathological processes across multiple scientific disciplines. Over the past decade, studies of polymorphonuclear leukocyte (PMN or neutrophil) gene expression on a global scale have provided new insight into the molecular processes that promote resolution of infections in humans. Herein we present methods to analyze gene expression in human neutrophils using Affymetrix oligonucleotide microarrays, which include isolation of high-quality RNA, generation and labeling of cRNA, and GeneChip hybridization and scanning. Notably, the procedures utilize commercially available reagents and materials and thus represent a standardized approach for evaluating PMN transcript levels.

Key words Neutrophil, Microarray, Gene expression, Affymetrix, Transcript, Phagocyte, Polymorphonuclear leukocytes

1 Introduction

Mature polymorphonuclear leukocytes (PMNs, granulocytes, or neutrophils) are fully equipped to destroy invading microorganisms, and inhibitors of transcription and translation fail to have an immediate effect on phagocytosis and microbicidal capacity [1–4]. As such, it was widely presumed that new gene transcription played no significant role in neutrophil function. However, extended incubation with actinomycin D (≥1 h), an inhibitor of RNA synthesis, significantly reduces granulocyte phagocytosis, superoxide production, and bactericidal activity [1–4], suggesting that new gene transcription is important for maintaining PMN function.

Methods for measuring gene expression in human granulocytes have existed for at least 40 years. In 1966, Cline first reported that phagocytosis increases RNA synthesis in human granulocytes [4, 5], and subsequent studies by Jack and Fearon showed that peripheral blood neutrophils constitutively synthesize a limited repertoire of mRNA transcripts and proteins [6]. These early studies used

Mark T. Quinn and Frank R. DeLeo (eds.), *Neutrophil Methods and Protocols*, Methods in Molecular Biology, vol. 1124,
DOI 10.1007/978-1-62703-845-4_26,

radiolabel-based techniques, such as incorporation of H^3-uridine or C^{14}-orotic acid into RNA, to estimate overall increases in transcript levels [5, 6]. Northern blotting has also been a widely used method for evaluating neutrophil mRNA levels [7, 8]. Inasmuch as these methods are suited to evaluate a limited number of transcripts or provide an indication of general RNA synthesis, they are not appropriate for genome-wide analyses of transcript levels. More recently, studies by Itoh et al. and Subrahmanyam et al. investigated patterns of gene expression in neutrophils by sequencing of 3′-directed cDNA libraries or cDNA display, respectively [9, 10]. Such studies were the first to use global approaches to investigate neutrophil gene expression. The work by Itoh et al. and Subrahmanyam et al. provided a segue into current PMN transcriptome analyses, which almost exclusively use microarray-based approaches [11–22]. Importantly, the microarray-based work has significantly enhanced our understanding of neutrophil biology and function. For example, studies of the PMN transcriptome during phagocytosis provided new insight into the role of PMNs in the resolution of inflammation and infection [23, 24].

In this chapter, we provide a method for analyzing human PMN gene expression with Affymetrix oligonucleotide microarrays, arguably the most universal platform for microarray-based research in human tissues. With the exception of human neutrophils, all of the materials are commercially available. Therefore, the method described in the following pages produces results that can be compared readily to those generated by other laboratories using the same methodology.

2 Materials

2.1 Isolation of Neutrophils and Analysis of Purity

1. Ficoll-Paque^{PLUS} (GE Healthcare).
2. Injection- or irrigation-grade water.
3. Dulbecco's phosphate-buffered saline (DPBS), pH 7.2.
4. Injection- or irrigation-grade 0.9 % NaCl solution (w/v).
5. 3 % Dextran solution (w/v): 150 mL of 20 % Dextran Solution (Sigma; 500,000 MW), 850 mL of injection- or irrigation-grade 0.9 % NaCl solution, 1.35 g NaCl. Filter-sterilize using a 0.2-μm bottle-top filter, and test for endotoxin.
6. 1.7 % NaCl solution (w/v): 17 g of RNase-free NaCl in final volume of 1 L of injection- or irrigation-grade water. Filter-sterilize using a 0.2-μm bottle-top filter, and test for endotoxin.

2.2 Purification of RNA from Neutrophils

1. RPMI 1640 medium.
2. Buffered RPMI 1640 medium: 5 mL of sterile, endotoxin-tested 1 M HEPES in a new 500 mL bottle of RPMI 1640 medium.

3. 12-well flat-bottom non-pyrogenic polystyrene cell culture plates.
4. Aerosol-resistant micropipette tips: RNase-free and non-pyrogenic.
5. 1.7 mL microcentrifuge tubes: RNase-free, nonstick.
6. RNeasy mini kit (Qiagen, Valencia, CA).
7. 14.5 M 2-mercaptoethanol (2-ME).
8. QiaShredder columns (Qiagen).
9. Diethylpyrocarbonate (DEPC)-treated or nuclease-free H_2O.

2.3 Determination of RNA Quantity

1. Quant-iT RiboGreen RNA Assay (Molecular Probes).
2. 96-well black microtiter plates.

2.4 Analysis of RNA Quality

1. RNA 6000 Nano LabChip (Agilent Technologies).
2. RNA 6000 Ladder (Ambion).

2.5 Generation of Labeled cRNA

1. Affymetrix GeneChip one-cycle target labeling and control reagents kit (Affymetrix) (*see* **Note 1**).
2. 1 M Tris–acetate solution: 121.14 g Trizma base in nuclease-free H_2O, adjust pH to 8.1 with glacial acetic acid.
3. 5× cRNA fragmentation buffer: 4.0 mL 1 M Tris–acetate solution, 0.64 g MgOAc, and 0.98 g KOAc. Make up to a final volume of 20 mL with nuclease-free H_2O. Filter-sterilize and store at room temperature.

2.6 Hybridization of cRNA to Affymetrix GeneChips

1. Control oligo B2, 3 nM (Affymetrix).
2. Amber microcentrifuge tubes.
3. Tough-Spots label dots (Diversified Biotech).
4. 5 M NaCl solution: RNase- and DNase-free.
5. 20× SSPE: 3 M NaCl, 0.2 M NaH_2PO_4, 0.02 M ethylenediamene tetraacetic acid (EDTA).
6. ImmunoPure Streptavidin (Pierce).
7. Herring sperm DNA.
8. 0.5 M EDTA disodium salt solution.
9. Goat immunoglobulin (Ig)G, reagent grade.
10. Biotinylated goat anti-streptavidin antibody.
11. 12× MES stock solution: 64.61 g MES hydrate, 193.3 g MES sodium salt, 800 mL nuclease-free water. Adjust volume to 1 L; the solution pH should fall between 6.5 and 6.7. Filter-sterilize, and store shielded from light at 2–8 °C.
12. Wash buffer A (non-stringent): 6× SSPE (from 20× stock), 0.01 % Tween-20 (v/v). Filter-sterilize, and store at room temperature.

13. Wash buffer B (stringent): 100 mM MES, 0.1 M [Na+], 0.01 % Tween-20. This buffer is prepared from 12× MES, 5 M NaCl, and 10 % Tween-20 stocks; passed through a 0.2 μm filter; and stored at room temperature.
14. 2× hybridization buffer: 200 mM MES, 2 M [Na+], 40 mM EDTA, 0.02 % Tween-20. Use 12× MES, 5 M NaCl, 0.5 M EDTA, and 10 % Tween-20 stocks to prepare this solution. The solution is stored between 2 and 8 °C and shielded from light.
15. 2× stain buffer: 200 mM MES, 2 M [Na+], 0.1 % Tween-20. Solution is prepared from 12× MES, 5 M NaCl, and 10 % Tween-20 stocks; passed through a 0.2 μm filter; and stored shielded from light between 2 and 8 °C.
16. Steptavidin–phycoerythrin (SAPE) solution: Prepare fresh by mixing 1× MES (from 2× stock), 2 mg/mL bovine serum albumin (BSA), and 10 μg/mL SAPE (from 1 mg/mL stock prepared in DPBS).
17. Antibody solution: Prepare fresh by mixing 1× MES (from 2× stock), 2 mg/mL BSA (from 50 mg/mL stock), 0.1 mg/mL goat IgG (10 mg/mL stock prepared in 150 mM NaCl), and 5 μg/mL biotinylated anti-streptavidin antibody (0.5 mg/mL stock).
18. Hybridization cocktail: Hybridization reaction (single-probe array; 200 μL/array) contains 1× hybridization buffer (2× stock), 50 pM B2 control oligo (3 nM stock), 0.1 mg/mL herring sperm DNA (10 mg/mL stock), 0.5 mg/mL BSA (50 mg/mL stock), 7.8 % dimethylsulfoxide (DMSO) (100 % stock), 15 μg fragmented and labeled cRNA, 20× spike-in.

2.7 GeneChip Processing, Scanning, and Conversion of Image Files

1. Affymetrix GeneChip Scanner 3000, enabled for high-resolution scanning.
2. Affymetrix GeneChip Command Console (AGCC) including AGCC Portal, AGCC Viewer, Data Exchange Console, AGCC Scan Control, AGCC Fluidic Control, and Expression Console.

3 Methods

3.1 Isolation of Neutrophils

1. Human PMNs can be isolated using Hypaque-Ficoll gradient separation described by Nauseef [25] or Siemsen et al. [26]. The factors most critical for transcriptome analyses are high purity of PMN preparations, i.e., ≤1 % contaminating mononuclear cells (typically lymphocytes and monocytes), and that cells are not primed or activated. Techniques used to assess cell purity and viability are described previously [25, 26].

3.2 Purification of RNA from Neutrophils

1. PMN assays (e.g., phagocytosis) are routinely performed in 12-well tissue culture plates containing 10^7 PMNs/well.
2. Lyse PMNs directly in the wells by adding 600 µL RLT + 2-ME (143 mM final) per 10^7 PMNs (*see* **Note 2**). Lysate should be pipetted to ensure complete lysis of PMN and to provide maximum protection to RNA. When performing time course experiments, lysate can be stored at –20 or –80 °C to facilitate sample processing.
3. Homogenize lysate by passage over QIAshredder column and centrifuge (30,000 × *g*) in a microcentrifuge for 2 min.
4. Add 600 µL of 70 % ethanol and mix by pipetting. Load one-half of lysate onto a Qiagen RNeasy column and centrifuge for 15 s (30,000 × *g*). Decant flow-through, and repeat with second half of lysate.
5. Place column in a new collection tube, and add 500 µL of buffer RPE. Spin for 15 s in microcentrifuge (30,000 × *g*), decant flow-through, and repeat.
6. Place the column in a new collection tube and centrifuge for 2 min (30,000 × *g*) to remove any residual wash. Place the column in a new RNase-free elution tube.
7. Elute RNA by addition of 50 µL of DEPC-treated H_2O (70 °C), allow to sit for 1 min, and then centrifuge (30,000 × *g*) for 1 min. Repeat a second time for maximum elution of RNA, and pool the two eluates (100 µL total).
8. Second purification of RNA is critical for complete cDNA synthesis (*see* **Note 3**). To the 100 µL of RNA eluate, add 350 µL of RLT + 2-ME (143 mM final).
9. Add 250 µL of 100 % ethanol, and mix by pipetting. Apply mixture to a new RNeasy column and spin (30,000 × *g*) for 15 s.
10. Decant flow-through, and add 500 µL of RPE. Spin for 15 s (30,000 × *g*), decant flow-through, and repeat.
11. Place column in a new tube and spin for 1 min at the maximum rpm to remove residual wash.
12. Place the column in an elution tube, add 50 µL of DEPC-treated H_2O (70 °C), allow to sit for 1 min, and centrifuge (30,000 × *g*) for 1 min.
13. Repeat a second time for maximum elution of RNA. Store RNA at –80 ° C. The expected yield of total RNA prepared by this method is approximately 2.0–5.0 µg.

3.3 Determination of RNA Quantity

1. RNA quantity can be measured either by absorbance at 260 nm or by fluorescence. The following protocol assumes the use of a microplate spectrofluorometer (e.g., Molecular Devices Gemini XPS) and the Molecular Probes Quant-iT RiboGreen

RNA Assay. The excitation maximum for RiboGreen bound to RNA is 500 nm and the emission maximum is 525 nm (*see* **Note 4**).

2. Prepare a 2× working stock of RiboGreen using a 1:200 dilution of the manufacturer's supplied stock and use at a concentration of 1× per assay.
3. Each microtiter plate should contain two blank wells (1× RiboGreen) and a serial dilution of control rRNA (supplied).
4. Each assay should contain 1 μL of PMN total RNA, 1× RiboGreen, and 1× TE buffer. The expected final concentration of total RNA as prepared above (from 10^7 PMNs) is ~20 μg/mL (0.02 μg/mL in the assay). Thus, the final concentration of the rRNA for the standard curve in the RiboGreen assay should cover a range from 0 to 1 μg/mL.
5. Incubate for 2–5 min at room temperature and protected from light.
6. Scan the plate using a microplate reader.
7. Calculate the concentration of PMN total RNA by extrapolating from the standard rRNA curve (*see* **Note 5**).

3.4 Analysis of RNA Quality

1. Isolation of high-quality RNA is essential for microarray analysis. RNA integrity of low-yield samples can be assessed on microfluidics-based automated electrophoresis systems (Fig. 1). The following protocol assumes the use of an Agilent 2100 Bioanalyzer (Agilent Technologies) or a similar device and the RNA 6000 Nano LabChip (Agilent).
2. Mix the gel–dye mix by centrifuging 400 μL RNA gel matrix through the supplied spin filter at 1,500 × *g* for 10 min. Store at 4 °C, and it must be used within 4 weeks.
3. To make the working stock of gel matrix–dye reagent, add 2 μL of RNA dye concentrate to 130 μL of the filtered gel mix and thoroughly vortex. Store the remaining gel–dye mix protected from light at 4 °C and use within 1 week.
4. Place a new chip on the priming station, and load 9 μL prepared gel–dye mix into the well labeled "G" (third row, black circle). Close the priming station, and depress plunger until it engages with the clip. After 30 s, release the clip and check the back of the chip for air bubbles.
5. Add 9 μL prepared gel–dye mix to the remaining two "G" wells (rows 1 and 2, no circle). Load 5 μL of the supplied marker buffer to the ladder well and all 12 sample wells. Add 1 μL heat-denatured (95 °C, 5 min) RNA 6000 ladder to the ladder well, and load 1 μL of purified PMN RNA to each sample well.

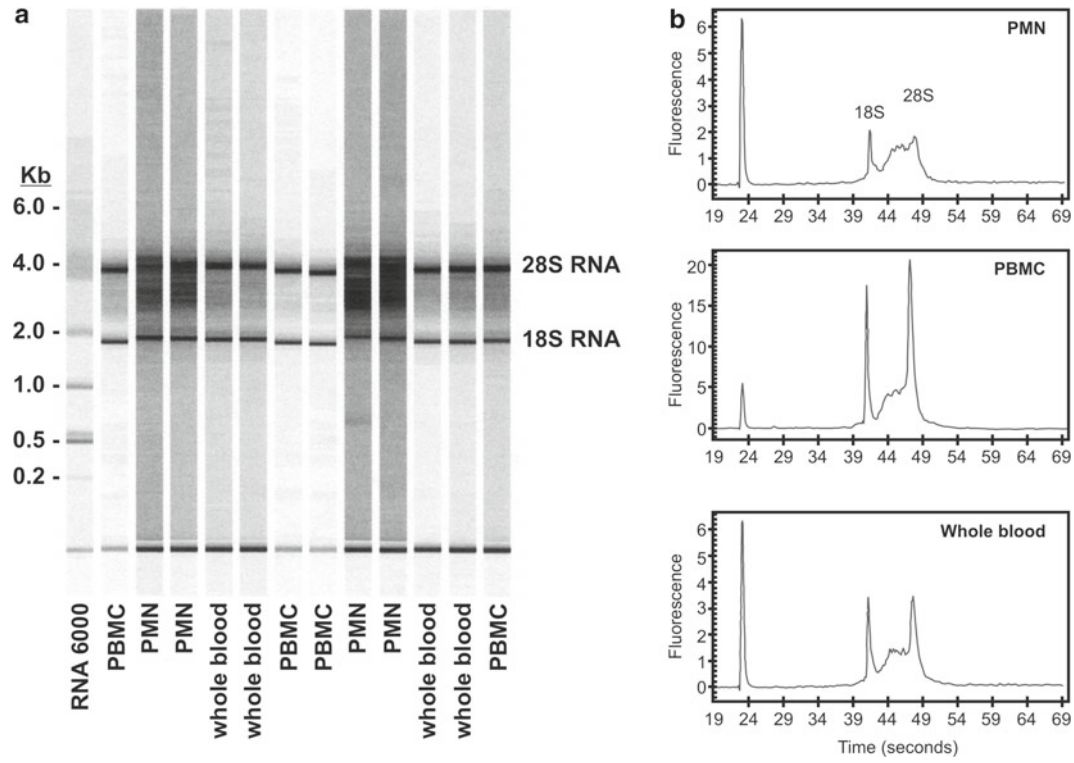

Fig. 1 Analysis of RNA quality using a microfluidics-based automated electrophoresis system. **(a)** 1 μL of total RNA (typically 20–30 ng) purified from whole blood, peripheral blood mononuclear cells (PBMC), or polymorphonuclear neutrophils (PMN) was evaluated with an Agilent 2100 Bioanalyzer. RNA 6000 indicates an RNA 6000 Ladder (Ambion) comprising 6 transcripts of varied size as shown. **(b)** Histograms of representative RNA samples. Reproduced from ref. 27 by permission of Humana Press©2007

6. Place the loaded chip into the adapter in the supplied vortexer, and mix for 1 min. The chip must be run within 5 min.
7. Read using the integrated eukaryotic total RNA algorithm. RNA integrity is assessed by the appearance of two well-defined peaks denoting the 18S and 28S rRNA subunits (approx 2:1 ratio) (Fig. 1).

3.5 Generation of Labeled cRNA

1. Reduce the volume of PMN total RNA to 8 μL in a centrifugal vacuum concentrator, or alternatively desiccate and suspend in 8 μL of RNase-free water.
2. Perform cDNA synthesis, cleanup, and cRNA labeling with the GeneChip one-cycle target labeling and control reagent kit (*see* **Note 6**).
3. Prepare poly-A RNA spike-in controls, which consist of four *Bacillus subtilis* genes (*lys*, *phe*, *thr*, and *dap*) that are absent from eukaryotic samples and are used to monitor the labeling efficiency

of target RNA, using a final spike-in control concentration based on the amount of total PMN RNA (~1–2 μg).

4. Prepare three serial dilutions from the Affymetrix poly-A control stock. For the first dilution, add 2 μL poly-A control stock to 38 μL of poly-A control dilution buffer (1:20). The second and third dilutions are prepared at 1:50 into dilution buffer. Use 2 μL of the final dilution in each cDNA synthesis reaction.
5. For first-strand cDNA synthesis primer hybridization, add 2 μL T7-Oligo (dT) primer (50 μM), 8 μL total PMN RNA, and 2 μL diluted poly-A controls to a 0.5-mL RNase-free tube, and incubate the reaction for 10 min at 70 °C and cool to 4 °C.
6. For first-strand cDNA synthesis, add 2 μL DTT (0.1 M), 4 μL 5× first-strand cDNA synthesis buffer, and 1 μL dNTP (10 mM) and incubate for 2 min at 42 °C.
7. Add 1 μL SuperScript III RT and incubate at 42 °C for 60 min.
8. For second-strand cDNA synthesis, add to each tube from the first-strand cDNA reaction 130 μL master mix (91 μL DEPC-treated H_2O, 30 μL second-strand buffer, 3 μL dNTPs [10 mM], 1 μL DNA ligase [10 U/μL], 4 μL DNA polymerase I [10 U/μL], and 1 μL RNase H [2 U/μL]), and incubate the reactions at 16 °C for 2 h.
9. Add 2 μL T4 DNA polymerase to each reaction and incubate at 16 °C for 15 min.
10. Stop the reaction by addition of 10 μL 0.5 M EDTA, pH 8.0.
11. For purification of cDNA and sample cleanup, add 600 μL of cDNA binding buffer to the double-stranded cDNA reaction mix and vortex for 3 s, and apply 500 μL of the sample to the cDNA cleanup spin column (save the remaining sample).
12. Centrifuge for 1 min at 8,000×*g*, and discard the flow-through.
13. Reload the spin column with the remaining sample and centrifuge for 1 min at 8,000×*g*.
14. Discard the flow-through and collection tube.
15. Transfer the spin column to a new 2-mL collection tube, and add 750 μL of the cDNA wash buffer to the spin column.
16. Centrifuge for 1 min at 8,000×*g*, and discard the flow-through.
17. Cut the cap off of the spin column (label the side of the column) and centrifuge for 5 min at >25,000×*g*. Discard the flow-through and the collection tube.
18. Transfer the spin column to a new collection tube, and add 14 μL of cDNA elution buffer directly onto the spin column membrane.

19. Incubate for 1 min at room temperature and centrifuge for 1 min at >25,000 × *g*. The expected volume of cDNA following cleanup is 12 μL.
20. For synthesis of labeled cRNA by in vitro transcription (IVT) labeling, the entire 12 μL of cDNA (from 10^7 PMNs) is used in the labeling reaction. Prepare a master mix containing 4 μL 10× IVT labeling buffer, 12 μL IVT labeling NTP mix, 8 μL RNase-free water, and 4 μL IVT labeling enzyme mix per reaction.
21. Add 28 μL of the IVT master mix to 12 μL cDNA in 0.5-mL PCR tubes, and incubate the reaction at 37 °C for 16 h. Store labeled cRNA at −70 °C or proceed to cleanup.
22. Use the sample cleanup described above for cleanup of labeled cRNA. Add 60 μL of RNase-free water to the IVT reaction and mix by vortexing for 3 s.
23. Add 350 μL IVT cRNA binding buffer to the sample and vortex for 3 min.
24. Add 250 μL 100 % ethanol and mix well by pipetting.
25. Apply the sample to the IVT cRNA cleanup spin column and centrifuge for 15 s at 8,000 × *g*. Discard the flow-through and collection tube.
26. Transfer the spin column to a new collection tube, and pipe 500 μL IVT cRNA wash buffer onto the column. Centrifuge for 15 s at 8,000 × *g*, and discard flow-through.
27. Pipet 500 μL 80 % (v/v) ethanol onto the spin column, centrifuge for 15 s at 8,000 × *g*, and discard flow-through.
28. Cut the cap off of the spin column (label the side of the column) and centrifuge for 5 min at >25,000 × *g*. Transfer the spin column to a new collection tube, and pipe 11 μL of RNase-free water directly onto the spin column membrane. Centrifuge for 1 min at >25,000 × *g* to elute.
29. Pipet 10 μL of RNase-free water directly onto the spin column membrane and centrifuge for 1 min at >25,000 × *g*. Store cRNA at −70 °C.
30. Determine cRNA quantity as described above for total RNA under Subheading 3.3 (by use of RiboGreen). However, the expected yield of cRNA generated from the IVT reaction is tenfold the starting amount of total RNA. Therefore, the cRNA sample should be diluted tenfold in order to fall within the linear range of the rRNA standard curve.
31. *Optional*: Labeled cRNA samples can be analyzed with an Agilent 2100 Bioanalyzer as described under Subheading 3.4. A typical signature for PMN cRNA is a broad smear of rather than distinct bands (Fig. 2).

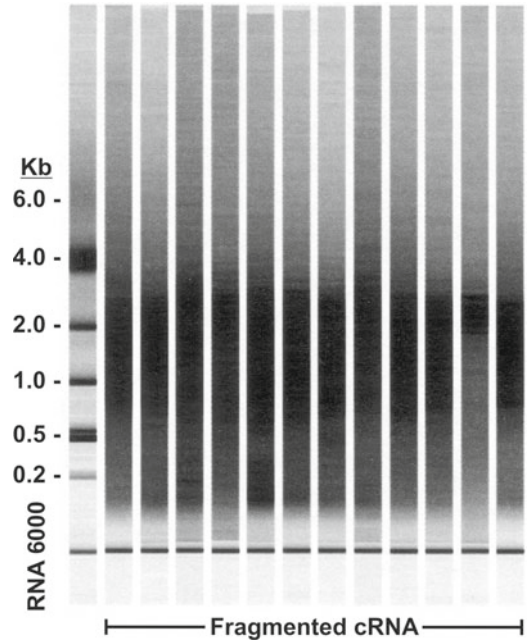

Fig. 2 Analysis of labeled polymorphonuclear neutrophil cRNA using an Agilent 2100 Bioanalyzer. Reproduced from ref. 27 by permission of Humana Press©2007

32. Fragmentation of target cRNA prior to hybridization is necessary for optimal assay sensitivity. For fragmentation, desiccate cRNA in a centrifugal vacuum concentrator and suspend to 1 μg/μL in RNase-free water.
33. Add 8 μL of 5× fragmentation buffer and 17 μL of RNase-free water to 15 μL of cRNA. The cRNA is fragmented by incubation at 94 °C for 35 min followed by cooling on ice.

3.6 Hybridization of cRNA to Affymetrix GeneChips

1. The following protocol is designed for the analysis of human PMN RNA transcripts on Affymetrix 49 format (standard) arrays such as the U133 Plus 2.0.
2. Remove chips from 4 °C storage and acclimate to room temperature (≥ 60 min) prior to hybridization.
3. Remove reagents from cold storage and thaw at room temperature. Set heat blocks to 65 and 99 °C. Set the hybridization oven to 45 °C.
4. Place the 20× eukaryotic hybridization control tube into the 65 °C heat block for 5 min.
5. Mix the hybridization cocktail for each chip, by using 15 μg of cRNA mix with 5 μL of control oligonucleotide B2 at 3 nM, 15 μL of 20× eukaryotic hybridization controls that have been

heated to 65 °C for 5 min, 3 μL of herring sperm (10 mg/mL), 3 μL of BSA (50 mg/mL), 150 μL of 2× hybridization buffer, 30 μL of DMSO, and 54 μL RNase-free water for a final volume of 300 μL.

6. Incubate the hybridization cocktail at 99 °C for 5 min.
7. Place the chips on the bench so that the back is facing up, insert a 200-μL pipette tip into one of the septa, and fill the chip with 200 μL of 1× hybridization buffer through the remaining septum.
8. Incubate the filled chips in the 45 °C hybridization oven for 10 min at 60 rpm.
9. The hybridization cocktail is incubated at 45 °C for 5 min and centrifuged for 5 min at maximum rpm.
10. Remove the chips from the hybridization oven, and place a 200-μL pipette tip in one of the septa. Then using the other septum, remove the 1× buffer and add 200 μL of the appropriate hybridization cocktail.
11. Place the chips back into the 45 °C hybridization oven for 16 h at 60 rpm.

3.7 GeneChip Processing, Scanning, and Conversion of Image Files

The following protocol requires the use of an Affymetrix GeneChip Scanner 3000, enabled for high-resolution scanning and the Affymetrix GeneChip Command Console (AGCC) software package.

1. It is important to process the Affymetrix GeneChips directly following hybridization. The preparation of staining and washing reagents and the priming of the Affymetrix workstation must occur prior to completion of the hybridization step.
2. Turn on the fluidics station and verify that tubing is appropriately connected to wash bottles A and B, water, and waste.
3. Turn on the scanning workstation, and start the AGCC Fluidics Control.
4. Select and prime the workstation(s) intended for use.
5. For each chip, using an amber tube, mix 600 μL of 2× stain buffer, 48 μL BSA (50 mg/mL), 12 μL SAPE (1 mg/mL), and 540 μL of distilled water. This is the SAPE solution mix.
6. Remove 600 μL of the SAPE solution and place into another amber tube.
7. For each chip, using a clear tube, mix 300 μL of 2× stain buffer, 24 μL BSA (50 mg/mL), 6 μL goat IgG stock (10 mg/mL), 3.6 μL biotinylated antibody (0.5 mg/mL), and 266.4 μL of distilled water. This is the antibody solution mix.
8. Remove the chips from the hybridization oven, and place a 200-μL pipette tip into one of the septa. Remove the hybridization

cocktail and place into the appropriate sample tube. These samples can be run on other chips at a later date. Store at –70 °C.

9. Fill the chip with 250 μL of wash buffer A without air bubbles. If processing more chips than allowed in the fluidics station, the remaining filled chips can be stored for up to 4 h at 4 °C.
10. In the AGCC Portal, select samples and register all samples to be run using the preferred method of single, quick, or batch.
11. Once all samples are registered, they can be viewed in AGCC Portal, Data, folder, or project view.
12. In the AGCC Fluidics Control, select the appropriate protocol for each module and station and select run.
13. Place the appropriate chip into the fluidics modules, and place the SAPE solution mix tubes into sample holder positions 1 and 3 for each module.
14. Place the antibody solution mix tube into sample holder position 2 for each module.
15. The protocol should take approximately 90 min to finish. Once the fluidics station displays "remove cartridge" take the chip out and inspect for air bubbles. If any are present place back into fluidics module and let it refill. If there are still bubbles then the chip must be filled manually with wash buffer A.
16. Place a tough spot over each septum of the chips to be scanned.
17. Gently wipe the glass of the chip with a kimwipe in one direction. Do not change direction or the paraffin at the edges may coat the glass, making scanning difficult.
18. Scanning: The scanning protocol is written using the autoloader. If an autoloader is not present, the protocol must be altered to accommodate single-chip scanning.
19. Press the start button on the scanner.
20. Open the AGCC Scan Control, and verify that the connection between the scanner and workstation is complete.
21. Allow scanner to warm up for 10 min.
22. Place chips into the autoloader starting with position one.
23. In the AGCC Scan Control select the "start scan" icon, and while the chip is being scanned, the AGCC Viewer can be started to visualize previously scanned chips.
24. A successful scan will create the *.DAT, *.jpg, *.audit, and *.CEL files with verification of grid alignment of the *.DAT, and correct *.CEL file creation is possible by using the AGCC viewer. Third-party software can be used to analyze these files, and Expression Console can be used to create the *.CHP files.

4 Notes

1. The one-cycle target labeling kit contains reagents for cDNA synthesis, IVT labeling, sample cleanup, and control reagents. Reagents are provided for 30 reactions.
2. Do not exceed 10^7 PMNs per Qiagen RNA mini-column. Numbers in excess do not increase RNA quantity and effectively reduce purity of final RNA. Larger quantities of total RNA can be obtained by pooling multiple preparations or, alternatively, using larger RNA purification columns.
3. The second purification of PMN total RNA on RNeasy columns is essential for obtaining high-quality RNA. Omission of this step may lead to incomplete cDNA synthesis and subsequent poor (5′:3′) ratios of labeled target cRNA.
4. The optimal excitation and emission spectra of the RiboGreen fluorophore should be empirically determined on the fluorometer to ensure that sample readings remain in the detection range.
5. Residual DNA from the PMN total RNA preparations will contribute to the overall signal obtained in the RiboGreen assay. We have found that the levels of contaminating DNA present in the RNA samples do not affect the overall yield of labeled target cRNA. The concentration of cRNA will also be obtained in the determination of RNA quality (Subheading 3.4) and can be used to verify the RiboGreen results.
6. Unless stated otherwise, the incubation steps for all cDNA and target labeling reactions are performed in a thermocycler.

Acknowledgments

This work was supported by the Intramural Research Program of the National Institutes of Allergy and Infectious Diseases, NIH.

References

1. Kasprisin DO, Harris MB (1977) The role of RNA metabolism in polymorphonuclear leukocyte phagocytosis. J Lab Clin Med 90: 118–124
2. Chang FY, Shaio MF (1990) In vitro effect of actinomycin D on human neutrophil function. Microbiol Immunol 34:311–321
3. Kasprisin DO, Harris MB (1978) The role of protein synthesis in polymorphonuclear leukocyte phagocytosis II. Exp Hematol 6:585–589
4. Cline MJ (1966) Phagocytosis and synthesis of ribonucleic acid in human granulocytes. Nature 212:1431–1433
5. Cline MJ (2002) Ribonucleic acid biosynthesis in human leukocytes effects of phagocytosis on RNA metabolism. Blood 28:188–200
6. Jack RM, Fearon DT (1988) Selective synthesis of mRNA and proteins by human peripheral blood neutrophils. J Immunol 140: 4286–4293
7. Newburger PE, Dai Q, Whitney C (1991) *In vitro* regulation of human phagocyte cytochrome *b* heavy and light chain gene expression by bacterial lipopolysaccharide and recombinant human cytokines. J Biol Chem 266: 16171–16177

8. Newburger PE, Ezekowitz C, Whitney J et al (1988) Induction of phagocyte cytochrome b heavy chain gene expression by interferon gamma. Proc Natl Acad Sci U S A 85: 5215–5219
9. Itoh K, Okubo K, Utiyama H et al (1998) Expression profile of active genes in granulocytes. Blood 92:1432–1441
10. Subrahmanyam YVBK, Yamaga S, Prashar Y et al (2001) RNA expression patterns change dramatically in human neutrophils exposed to bacteria. Blood 97:2457–2468
11. Borjesson DL, Kobayashi SD, Whitney AR et al (2005) Insights into pathogen immune evasion mechanisms: *Anaplasma phagocytophilum* fails to induce an apoptosis differentiation program in human neutrophils. J Immunol 174:6364–6372
12. Kobayashi SD, Voyich JM, Buhl CL et al (2002) Global changes in gene expression by human polymorphonuclear leukocytes during receptor-mediated phagocytosis: cell fate is regulated at the level of gene expression. Proc Natl Acad Sci U S A 99:6901–6906
13. Kobayashi SD, Voyich JM, Somerville GA et al (2003) An apoptosis-differentiation program in human polymorphonuclear leukocytes facilitates resolution of inflammation. J Leukoc Biol 73:315–322
14. Kobayashi SD, Voyich JM, Braughton KR, DeLeo FR (2003) Down-regulation of proinflammatory capacity during apoptosis in human polymorphonuclear leukocytes. J Immunol 170:3357–3368
15. Kobayashi SD, Braughton KR, Whitney AR et al (2003) Bacterial pathogens modulate an apoptosis differentiation program in human neutrophils. Proc Natl Acad Sci U S A 100:10948–10953
16. Kobayashi SD, Voyich JM, Braughton KR et al (2004) Gene expression profiling provides insight into the pathophysiology of chronic granulomatous disease. J Immunol 172: 636–643
17. Kobayashi SD, Voyich JM, Whitney AR, DeLeo FR (2005) Spontaneous neutrophil apoptosis and regulation of cell survival by granulocyte macrophage-colony stimulating factor. J Leukoc Biol 78:1408–1418
18. Fessler MB, Malcolm KC, Duncan MW, Worthen GS (2002) Lipopolysaccharide stimulation of the human neutrophil - an analysis of changes in gene transcription and protein expression by oligonucleotide microarrays and proteomics. Chest 121:75S–76S
19. Theilgaard-Mönch K, Knudsen S, Follin P, Borregaard N (2004) The transcriptional activation program of human neutrophils in skin lesions supports their important role in wound healing. J Immunol 172:7684–7693
20. Tsukahara Y, Lian Z, Zhang XQ et al (2003) Gene expression in human neutrophils during activation and priming by bacterial lipopolysaccharide. J Cell Biochem 89:848–861
21. Kluger Y, Tuck DP, Chang JT et al (2004) Lineage specificity of gene expression patterns. Proc Natl Acad Sci U S A 101:6508–6513
22. Zhang XQ, Kluger Y, Nakayama Y et al (2004) Gene expression in mature neutrophils: early responses to inflammatory stimuli. J Leukoc Biol 75:358–372
23. Kobayashi SD, DeLeo FR (2004) An apoptosis differentiation programme in human polymorphonuclear leucocytes. Biochem Soc Trans 32:474–476
24. DeLeo FR (2004) Modulation of phagocyte apoptosis by bacterial pathogens. Apoptosis 9:399–413
25. Nauseef WM (2007) Isolation of human neutrophils from venous blood. Methods Mol Biol 412:15–20
26. Siemsen DW, Schepetkin IA, Kirpotina LN et al (2007) Neutrophil isolation from nonhuman species. Methods Mol Biol 412:21–34
27. Kobayashi SD, Sturdevant DE, DeLeo FR (2007) Genome-scale transcript analysis in human neutrophils. Methods Mol Biol 412:441–454

Chapter 27

Fast and Accurate Quantitative Analysis of Cytokine Gene Expression in Human Neutrophils

Nicola Tamassia, Marco A. Cassatella, and Flavia Bazzoni

Abstract

Polymorphonuclear neutrophils, traditionally viewed as short-lived effector cells, are nowadays regarded as important components of effector and regulatory circuits in the innate and adaptive immune systems. Most of the physiological functions of neutrophils as crucial players in the host immune response, able not only to act in the early phases of acute inflammation but also to condition the progression of the inflammatory reaction and the subsequent initiation of the specific immune response, rely on their capacity to produce and release a number of proinflammatory and immunoregulatory cytokines. This fact has reevaluated the importance, role, and physiological and pathological significance of neutrophils in the pathogenesis of inflammatory, infectious, autoimmune, and neoplastic diseases and has identified neutrophils as an important potential target for selective pharmacological intervention to both promote and restrain inflammation. In this context, understanding the mechanisms of modulation of neutrophil-derived cytokines and chemokines represents a critical step toward a better understanding of how neutrophils may influence pathophysiological processes in vivo. Herein, we describe and discuss an updated version of the methods that we have developed to rapidly and precisely characterize the pattern of cytokine expression in in vitro-activated human neutrophils. The validation of the reverse transcription quantitative real-time PCR assay as a suitable strategy for an accurate, sensitive, reliable, and *bona fide* analysis of cytokine gene expression in human neutrophils overcomes several problems strictly specific to neutrophils and offers an important tool, in the neutrophil research area, to test many experimental conditions for gene expression analysis.

Key words Neutrophils, RT-qPCR, Cytokines, SYBR Green, Gene expression

1 Introduction

Neutrophils constitute a first line of defense against pathogens by virtue of their ability to release a set of preformed cytotoxic enzymes and generate reactive oxygen-derived species. Neutrophils can also produce, upon appropriate stimulation in vitro and in vivo, a variety of proteins, including cytokines, chemotactic molecules, and other mediators that are involved in various effector functions [1]. This latter function is currently the subject of a new wave of enthusiastic research, in that it shows that neutrophils may also act as key regulators of the in vivo cross talk between immune,

Mark T. Quinn and Frank R. DeLeo (eds.), *Neutrophil Methods and Protocols*, Methods in Molecular Biology, vol. 1124,
DOI 10.1007/978-1-62703-845-4_27,

endothelial, stromal, and parenchymal cells. For a fairly exhaustive description of experimental conditions leading to the production of individual cytokines by neutrophils, as well as the molecular regulation and potential biological relevance of this process, the reader is referred to recent reviews [1].

There is an increasing interest in the identification and molecular characterization of protein/cytokine expression and production by neutrophils. In most studies aimed at characterizing neutrophil-derived proteins, granulocytes are isolated from fresh blood or buffy coats, suspended in culture medium containing up to 10 % serum, and then cultured at 37 °C in a 5 % CO_2 humidified atmosphere. Other investigators suspend neutrophils in serum-free medium or in buffered solutions containing various concentrations of serum or bovine serum albumin. Although this is appropriate for short-term incubations, it is not recommended for experiments requiring several hours in culture, such as the determination of neutrophil gene expression or protein release. In our studies, highly purified neutrophil populations are routinely suspended at no more than 10^7 cells/mL in medium containing 10 % low-endotoxin fetal bovine serum (FBS). Under these conditions, granulocytes can be cultured in tissue culture plasticware for up to 44 h if appropriate neutrophil survival factor(s) is (are) added to the cultures.

Cytokine synthesis and/or release by polymorphonuclear neutrophils (PMN) can be measured in cell-free supernatants (or in cell pellets) by using different methods, such as enzyme-linked immunosorbent assay (ELISA), radioimmunoassay (RIA), immunoprecipitation after metabolic labeling, bioassays, and also intracellular staining followed by flow cytometry and immunohistochemistry. Because the induction of cytokine production and release by neutrophils are usually preceded by an increased accumulation of the related mRNA transcripts, a number of molecular biology techniques, such as Northern blotting, ribonuclease protection assays (RPA), reverse-transcription (RT)-PCR, in situ hybridization, microarray analysis, and RNA-Seq, can be also performed.

Northern blots and RPA have the advantage of making differences in cytokine mRNA expression quantitatively measurable, but the very low RNA content of neutrophils (average 1 μg/10^7 cells) represents a limiting factor in the analysis of gene expression modulation when many experimental conditions are tested. The development of reverse transcription quantitative real-time PCR (RT-qPCR) has revolutionized the measurement of gene expression, because it requires less RNA template than other methods of gene expression analysis and allows a reliable quantification of RT-PCR products. RT-qPCR assays are more sensitive than RPA [2] and dot blot [3] and can even detect a single copy of a specific transcript [4]. This feature represents a notable advantage, in that the expression of several (up to 10) cytokine/chemokine genes can

be analyzed in RT-qPCR starting from as little as 0.1 μg of total RNA (Fig. 1). For its accuracy, RT-qPCR is also the method of choice for the validation of microarray [5] (Fig. 1) or RNA-Seq [6] results. On the other hand, because of its extremely high sensitivity, RT-qPCR can easily amplify cytokine mRNA from a few (<0.5 %) contaminating monocytes, lymphocytes, or eosinophils. This represents a major concern, because peripheral blood mononuclear cells (PBMCs) possess 10–20 times more RNA per cell than neutrophils, so that a contamination of only 1 % PBMCs can translate into an up to 20 % of contamination at the RNA level. Recently a novel neutrophil purification procedure based on negative immunoselection with magnetic beads (EasySep neutrophil enrichment kit, StemCell Technologies), that allow to achieve very high level of purity (>99.5 %), has been developed [7]. The use of this procedure is therefore crucial to generate uncontroversial evidence that cytokine mRNA expression can be directly attributed to neutrophils, excluding the potential contribution of PBMCs or even eosinophils. Based on reports from our group [8–10] as well as from other laboratories [11, 12], the absence of detectable IFNβ, IL-10, or IL-6 mRNA in lipopolysaccharide (LPS)-stimulated neutrophils represents a good control of neutrophil purity (Fig. 2). In addition, correct methodological analysis and detailed investigation of the pattern of cytokine gene expression by neutrophils in vitro represent the required and important steps.

In this chapter, we describe validated methods currently used in our laboratory for the optimal application of the RT-qPCR strategy in the analysis of human neutrophil cytokine gene expression. There are several types of detection chemistry available for the quantitative real-time PCR (qPCR) assay (DNA-binding dyes, hybridization probes, hydrolysis probes, molecular beacons, scorpions, etc.). Among the two most commonly used (SYBR Green and TaqMan probes), we describe here the SYBR Green-based assay. SYBR Green is a fluorescent DNA intercalator dye that binds to double-stranded PCR products that accumulate during cycling. With well-designed primers, SYBR Green produces results with the sensitivity and range of quantification comparable to those obtained with TaqMan, making this strategy very flexible and less expensive as compared to other chemistries. Finally, and most importantly, the data obtained by this RT-qPCR strategy have been validated by comparable results obtained with other methods for gene expression analysis (Fig. 1).

2 Materials

2.1 Miscellaneous

1. Cell culture medium: RPMI-1640 medium supplemented with 10 % low-endotoxin FBS (endotoxin content must be lower than 5–10 pg/mL, certified by the company or verified by a *Limulus Amebocyte* Lysate [LAL] assay).

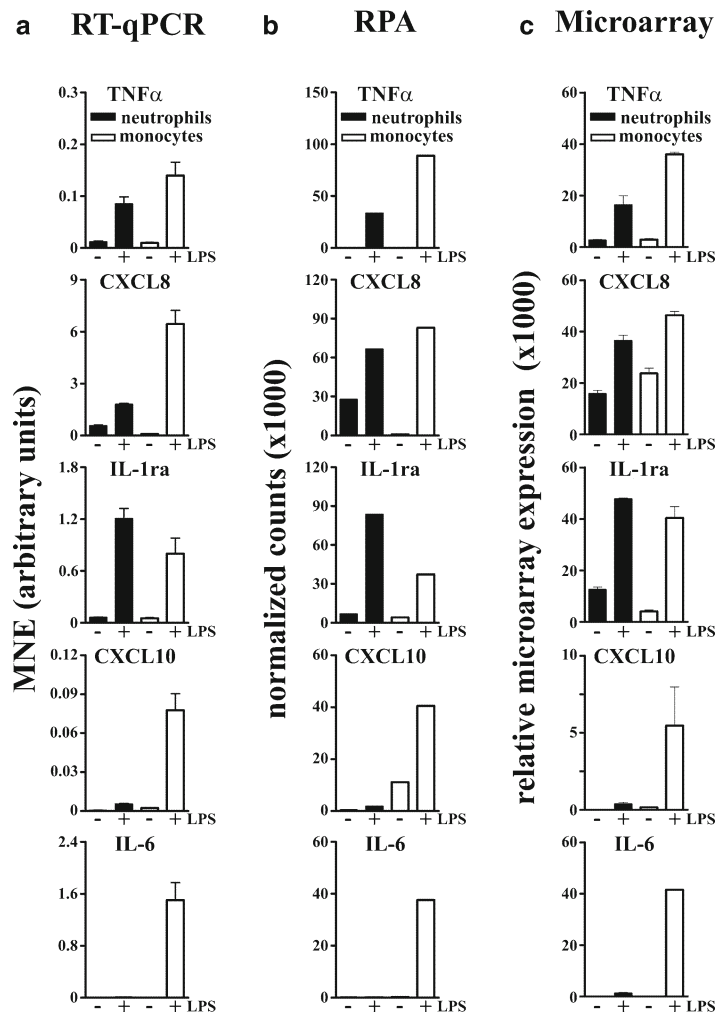

Fig. 1 Quantitative analysis of cytokine gene expression in activated neutrophils and monocytes performed in RT-qPCR (**a**), ribonuclease protection assay (RPA) (**b**), and microarray (**c**). Neutrophils and autologous monocytes were cultured with 100 ng/mL ultrapure LPS. After 4 h, total RNA was extracted and analyzed for TNF-α, CXCL8, IL-1ra, CXCL10, and IL-6 mRNA accumulation. (**a**) 1 μg RNA/condition was processed by RT-qPCR (described in this chapter). Expression levels of cytokine mRNAs are reported as mean normalized expression (MNE), calculated after GAPDH normalization (*see* **Note 15**). (**b**) 5 μg of total RNA/sample were processed by RPA assay, using a custom kit (Pharmingen) and according to the manufacturer's protocol. Radioactive signals were quantified with InstantImager (Packard Instruments) and plotted after GAPDH normalization. (**c**) 10 μg of total RNA/sample were processed and analyzed by NimbleGen oligonucleotide microarray (Roche) according to the manufacturer's protocol. Data are reported as mean relative microarray expression ($n = 3$) after quantile normalization. Graphs demonstrate that these three techniques produce similar quantitative results

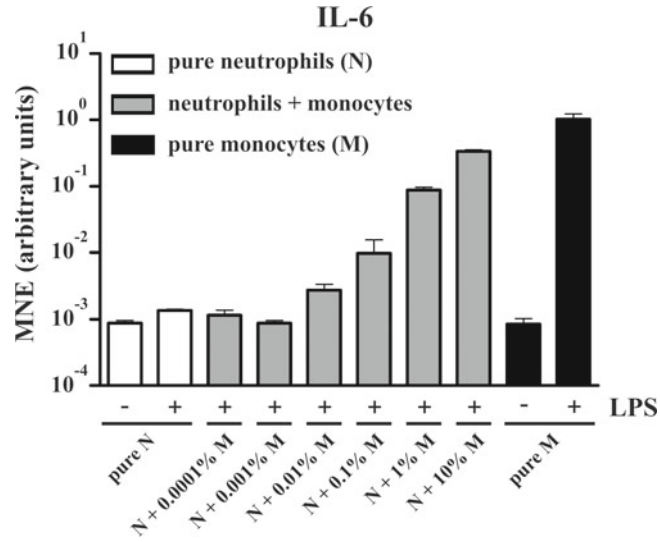

Fig. 2 The presence of few contaminating monocytes in LPS-treated neutrophils can lead to a considerable IL-6 mRNA induction. Neutrophils (N), purified by negative immunomagnetic selection; monocytes (M), purified by CD14-positive immunomagnetic selection; or neutrophils to which were added increasing percentages of monocytes (ranging from 0.0001 to 10 %) were treated or not with 100 ng/mL ultrapure LPS for 2 h. Total RNA was then extracted, and levels of IL-6 transcript were analyzed by RT-qPCR, as described in this chapter. Gene expression is depicted as MNE units, calculated after GAPDH normalization (*see* **Note 15**)

2. Agonists: Ultrapure LPS, extracted by successive enzymatic hydrolysis steps and purified by the phenol–TEA–DOC extraction (commercially available from different sources).
3. All plasticware utilized to work with RNA (pipet tips, polypropylene tubes, syringes, 20-G needles) must be RNase-free, autoclaved, and kept in a separate dedicated area. All disposable plastics utilized for RT and qPCR, including pipet tips or tubes, must be certified for the absence of DNA contamination, RNase, DNase, or other PCR inhibitors and kept in a dedicated area.
4. Whenever indicated, use sterile, pyrogen- and RNase-free H_2O approved for clinical use. One-milliliter aliquots are prepared and used for RNA, cDNA, and qPCR.
5. 70 % (v/v) ethanol: Dilute ethanol in RNase-free H_2O, and use it for RNA manipulation only.

2.2 Total RNA Purification

1. RNeasy mini kit (Qiagen): Contains RNeasy mini spin columns, RLT buffer (lysis buffer) (supplement with 143 mM β-mercaptoethanol immediately before use), RW1 buffer (first washing buffer), and RPE buffer (second washing buffer) (dilute with 4 vol of 96–100 % ethanol immediately before use) (*see* **Note 1**).

2. RNase-Free DNase Set (Qiagen): Contains RNase-free water; DNase I, which must be dissolved in 550 µL of RNase-free water, aliquoted, and stored at –20 °C (*see* **Note 2**); RDD buffer for on-column DNA digestion (stored at 4 °C); and DNase I incubation mix, which must be prepared by adding 10 µL of a DNase I stock solution to 70 µL of RDD buffer (*see* **Note 1**).

2.3 RNA Quantification

1. RiboGreen RNA Quantification Kit (Molecular Probes): Contains RiboGreen RNA quantification reagent (store at –20 °C protected from the light); 20× TE (200 mM Tris–HCl, 20 mM ethylenediamine tetraacetic acid [EDTA], pH 7.5), which must be stored at 4 °C and diluted to 1× with RNase-free water before use; ribosomal RNA standard (2 µg/mL), which must be stored at 4 °C or –20 °C for short- or long-term periods, respectively (*see* **Note 1**).
2. Black, 96-well microplates optimized for fluorescence readings.
3. Fluorescence microplate reader equipped with approx 480-nm excitation and approx 520-nm emission filters (e.g., VICTOR^3 Multilabel Counter, Perkin Elmer).

2.4 RNA Reverse Transcription

1. Reverse Transcriptase: Superscript™ III Reverse Transcriptase (200 U/µL), supplied with 5× First-Strand Buffer and 0.1 M dithiothreitol (DTT) (Life Technologies). Store all reagents at –20 °C.
2. Recombinant Ribonuclease Inhibitor: RNaseOUT™ Recombinant enzyme (acidic protein) from Life Technologies. Store at –20 °C.
3. Keep Superscript III and RNaseOUT in a refrigerated bench cooler (–20 °C) when performing reactions.
4. 10 mM dNTP mix: Aliquot and store at –20 °C.
5. Random primers: Dilute at 100 ng/µL with RNase-free H_2O. Aliquot and store at –20 °C.

2.5 Quantitative Real-Time PCR

1. Thermocycler for qPCR: The protocol described here is optimized for the ViiA™ 7 real-time PCR system, including the ViiA™ 7 software (Life Technologies) (*see* **Note 3**).
2. SYBR Green qPCR master mix (2× concentrated solution; e.g., Fast SYBR Green Master Mix [Life Technologies]): Store at –20 °C protected from light. Once thawed, store master mix at 4 °C. This solution contains all necessary reagents to perform a qPCR (i.e., appropriate buffer, dNTPs, SYBR Green I dye, ROX™ dye passive reference, and AmpliTaq® Fast DNA Polymerase), except primers (*see* **Note 4**).
3. Forward and reverse primers: Dissolve in RNase-free H_2O at a final concentration of 100 µM. Dilute primers at the working concentration of 20 µM. Aliquot and store at –20 °C.

4. 96- or 384-well microplates for fast qPCR equipped with optical adhesive film suitable for a thermocycler. All plastics must be stored in a clean place to avoid any possible contamination by external DNA.

3 Methods

3.1 Total RNA Purification

The extraction of total RNA from neutrophils can be performed by different methods. However, depending on the method chosen, the quantity and/or the quality of the RNA extracted from neutrophils may greatly differ. It is essential for the RNA used in RT-qPCR not to be degraded, to contain as little contaminating salts as possible, and to be free of genomic DNA. For RT-qPCR, small quantities of total RNA are required (from 1 ng to 1 μg), unlike other methodologies, including the Northern blotting or RPA, which need at least 5–10 μg of RNA for each condition. Thus, the low yield of RNA usually purified from neutrophils does not represent a limiting factor for this technique.

RNA purification methods that rely on selective RNA binding properties of silica gel-based membranes are, in our opinion, the best because they are fast and reliable, allow rapid and simultaneous processing of many samples at once, and do not need a phenol/chloroform extraction step. If one desires to obtain 1 μg of total RNA per sample (which is the optimum RNA amount that can be used for RT-qPCR studies), the optimal starting cell number is 10^7 neutrophils/condition, given that 10^6 neutrophils contain approx 0.1 μg of total RNA. 10^7 cells correspond to the maximum number of cells per sample that can be processed by an RNeasy mini kit (*see* **Note 5**). We process and purify our samples exactly as described in the "spin protocol for animal cells" reported in the RNeasy mini kit instruction manual. The protocol is detailed, comprehensive, and easy to follow, so that no detailed explanation needs to be given herein. The volumes used to resuspend cells in the initial steps of the procedures are specified as follows.

1. Resuspend purified neutrophils at 5×10^6 cells/mL in RPMI supplemented with 10 % low-endotoxin FBS (*see* **Note 6**).
2. Plate 10^7 cells in a six-well tissue culture plate (2 mL/well), stimulate as appropriate, and incubate at 37 °C in a 5 % CO_2 atmosphere for the desired time.
3. Collect neutrophils into 2-mL tubes and pellet at $300 \times g$ for 5 min.
4. Carefully remove culture supernatants, and loosen cell pellets thoroughly by flicking the tube several times.
5. Resuspend pellets in 600 μL of RLT buffer and vortex (*see* **Note 7**).

6. Homogenize lysates by passing them through a 20-G needle fitted to a syringe at least five times or until the solution becomes less dense. At this stage, lysates can be further processed or stored at −70 °C for several months without any change in RNA integrity (*see* **Note 8**).
7. We do not perform the optional **step 6** of the RNeasy mini kit protocol because we perform the on-column DNase digestion (*see* **Note 9**). Instead, the optional **step 9** of the RNeasy mini kit protocol is performed. Otherwise, there are no further changes to the procedures described in the manual supplied with the kit.
8. Elute RNA from the column with 30 μL of RNase-free water. The expected RNA yield is approx 0.1 μg per 10^6 neutrophils.
9. RNA can be quickly concentrated up to 12 μL using vacuum concentrator system. From this step onward, RNA must be kept on ice or stored at −20 to −70 °C.

3.2 RNA Quantification

RNA quantification is a crucial step for optimal RT-qPCR results, and we recommend performing the RT reaction with equivalent amounts of RNA from each sample. This limits differences in RT efficiency among the samples and favors subsequent normalization of RT-qPCR results. If extracting RNA from less than 3×10^6 human neutrophils we do not recommend absorbance-based quantification because is not precise for detecting low target concentrations even with new-generation spectrophotometers like nanodrop (Thermo Scientific). The use of more sensitive methods, such as staining of nucleic acid with fluorescent dyes, overcomes this problem. We routinely use the RiboGreen RNA quantification reagent that consists of an ultrasensitive fluorescent nucleic acid stain. This reagent detects as little as 1 ng/mL of RNA in solution. The following method is adapted from the instructions included in the RiboGreen RNA quantification kit (*see* **Note 1**).

1. Prepare a standard curve by diluting the standard RNA solution (provided with the kit and usually corresponding to 2 μg/mL) with TE.
2. Prepare 1,000, 500, 50, and 20 ng/mL standards and blanks in duplicate. Pipet 100 μL of the prepared dilutions into 96-well black microtiter plates.
3. Dilute RNA samples directly into the microtiter plates by adding 1 μL of RNA sample to 99 μL of TE. Make one or more replicates.
4. Dilute (200-fold) the RiboGreen reagent with TE, and add 100 μL of the diluted RiboGreen reagent to each well.
5. Gently shake the plate, and incubate it in the dark for 5 min.
6. Measure the fluorescence in each well with a fluorescence microtiter plate reader (excitation ~480 nm, emission ~520 nm) (*see* **Note 10**).

7. Subtract the blank signal from the fluorescence value of each sample, and generate a standard curve of fluorescence vs. RNA concentration.
8. Determine the RNA concentration of the various samples by linear regression using the standard curve as reference.

3.3 RNA Reverse Transcription

RT is carried out with SuperScript III Reverse Transcriptase following the protocol included in the manual for this enzyme (*see* **Notes 1** and **11**).

1. For each sample, prepare the following RNA/primer mix directly in a 0.2-mL tube (keep samples on ice) (*see* **Note 12**): from 1 to 0.1 μg of total RNA, 1 μL of random primers from 100 ng/μL stock, and 1 μL of dNTP mix from 10 mM stock. Make up to 14 μL final volume with RNase-free H_2O.
2. Prepare identical samples for controls that will not receive reverse transcriptase (–RT) (*see* **Note 13**).
3. Centrifuge the tubes briefly (quick-spin).
4. For optimal RNA/random primer denaturation, incubate samples at 65 °C for 5 min in a preset thermocycler.
5. Prepare RT reaction master mix. For each reaction add 4 μL of 5× first-strand buffer, 1 μL of DTT from 0.1 M stock, 0.5 μL RNaseOUT from 40 U/μL stock, and 0.5 μL of SuperScript III from 200 U/μL stock. Prepare a volume of master mix greater than what is necessary. For the –RT controls, prepare the RT reaction master mix in the same manner, but omit SuperScript III.
6. At the end of the denaturation step, pause the thermocycler, put tubes on ice for at least 1 min and add 6 μL of RT reaction master mix to each tube. Mix by pipetting, and, if bubbles form, perform a quick-spin with the tubes.
7. For RNA/random primer annealing incubate tubes at 25 °C for 5 min and then at 42 °C for 1 h for RT. Subsequently heat-inactivate the reactions at 95 °C for 5 min.
8. At this stage, samples are single-strand cDNA and can be stored at –20 °C or immediately used as template for amplification in PCR.

3.4 Quantitative Real-Time PCR

The following qPCR procedure is adjusted for use of Fast SYBR Green Master Mix as qPCR master mix in combination with a ViiA™ 7 thermocycler (*see* **Notes 3** and **4**). The use of qPCR instruments and reagents enabled for fast PCR protocol allows a significant overall reduction of the reaction time from the typical 90–120 min to less than 40 min. For normalization strategy, in addition to the target genes, we always quantify also endogenous reference genes. Thermocycling conditions are constant for all assays.

1. Edit the following program in the real-time thermocyler:
   (a) Step 1: 95 °C for 20 s (initial denaturation) (*see* **Note 4**).
   (b) Step 2: 95 °C for 1 s (denaturation); 60 °C for 20 s (annealing/extension); fluorescence read. Repeat for 45 cycles. An extension step is not required, because all of the PCR products are 50–250 bp.
   (c) Step 3: Melting curve, set the final sample heating from 60 to 90 °C and have the fluorescence reading recorded every 0.5 °C (*see* **Note 14**).
2. Prepare qPCR master mixes based upon the number of genes to be analyzed. Each sample must be tested in triplicate, and negative controls must be included. For every experiment the analysis of the expression of at least two reference genes must be always performed for accurate normalization (*see* **Note 15**).
3. For a 10 μL reaction, use the following components for each well or tube (*see* **Note 16**): 5 μL of 2× Fast SYBR Green Master Mix, 0.1 μL of forward primer from 20 μM stock, 0.1 μL of reverse primer from 20 μM stock, 1.8 μL of autoclaved H_2O (7 μL final volume).
4. Dilute all cDNA samples to be analyzed to a concentration of 1 ng/μL (*see* **Notes 17** and **18**).
5. Aliquot sequentially 7 μL of qPCR master mix and 3 μL of sample or H_2O (for the "no-template" control) or –RT (for the negative control) into each well or tube. This step must be carried out very rapidly, as SYBR Green is light sensitive.
6. Carefully close the wells, with optical adhesive film, using the appropriate sealer, paying great attention not to touch or scratch the upper part of the film.
7. Briefly centrifuge the plate or the tubes, and then start the reaction in the real-time thermocycler.
8. Optional: Remove the plate or the tubes from the thermocycler after the qPCR is finished. Separate 5 μL of each sample by electrophoresis on a 2 % agarose gel to check for quality of PCR products. If the reaction proceeded correctly, a single amplified product of the expected length should be visible in the gel.
9. At the end of the reaction, check the melting curve analysis to verify whether abnormal amplification plots or any bimodal dissociation curves are present (*see* **Note 14** and Fig. 3a).
10. At the end of the run, the ViiA 7 system software returns raw data [fluorescence value (ΔRn: normalized reporter value) of each sample for each real-time PCR cycle] that must be analyzed.

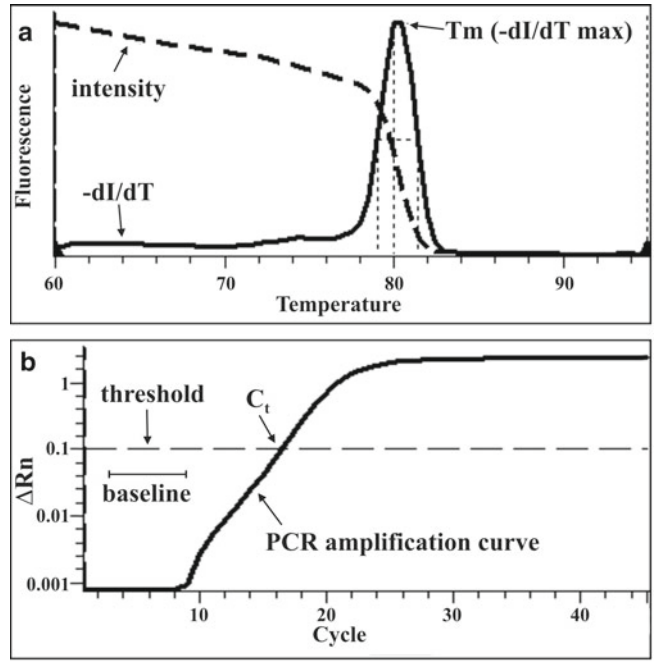

Fig. 3 Melting and PCR amplification curves as shown by the ViiA 7 system software. (**a**) The melting curve is plotted as fluorescence intensity (*dot line*) or as first derivative (–d*I*/d*T*) (*solid line*) of the PCR product as function of temperature. The melting temperature (*T*m) of the PCR product is defined as the temperature at which –d*I*/d*T* reach the maximum value. (**b**) PCR amplification curve. The fluorescence intensity (ΔRn) is plotted as a function of cycle number. The baseline, threshold, and threshold cycle are indicated (reproduced from Tamassia et al. [19] with permission from Humana Press)

3.5 Analysis of Real-Time PCR Data

ViiA7 software calculates the RT-qPCR results using the ΔΔCt method [13]. This method does not correct RT-qPCR data for amplification efficiency of the reaction that is an important consideration when performing relative quantification. To overcome this problem, we calculate by LinRegPCR software [14] the average amplification efficiency for each gene analyzed (including reference genes) from each single sample. Subsequently we calculate the RT-qPCR results using the Q-Gene software application [15] that will give back the expression level of the gene of interest relative to an endogenous reference gene mRNA. A detailed description is referred in each software manual or original article [14, 15].

1. Set the baseline on the analysis settings of ViiA 7 system software. The initial cycles of PCR where there is little fluorescence signal are termed "baseline" and should be eliminated (Fig. 3b). The baseline should be wide enough to eliminate background but should not overlap with the area in which the amplification signal begins to rise above background (*see* **Note 19**).

2. Set the threshold on the analysis settings of ViiA 7 system software. The threshold is an arbitrary fluorescence value that must intercept the PCR amplification curve in the exponential phase of the reaction (*see* **Note 20** and Fig. 3b).
3. From the ViiA 7 system software export amplification data and results data of the qPCR run.
4. Calculate the efficiency of qPCR reaction for each gene assayed using amplification data. There are several methods of calculating amplification efficiency on raw data collected during PCR. We routinely calculate the amplification efficiency with LinRegPCR software [14]. The program uses linear regression analysis to find the best-fit straight line through the PCR data set. From this line, PCR efficiency of each individual sample is calculated. The amplification efficiency value that we take for each gene is the average of the single efficiencies calculated with LinRegPCR (*see* **Note 21**).
5. From the results data export threshold cycle (Ct) values to the Q-Gene Excel datasheet. The cycle at which the fluorescence signal from the reaction crosses the threshold line is defined as the Ct. Once the threshold line is set, the real-time software automatically generates a Ct value for each sample. The Ct is a reliable indicator of the initial copy number of each amplified cDNA.
6. Perform the final quantification with Q-Gene software (*see* **Note 22**). Insert the following values in the Q-Gene Excel datasheet: (1) the Ct s generated for each sample, both for the target gene and for the reference gene by the real-time thermocycler software; (2) the calculated amplification efficiency for the gene of interest and for the reference gene; and (3) the calculation procedure 2, corresponding to equation 3 described by Muller and coauthors [15].
7. The Q-Gene software calculates the mean normalized expression (MNE) with standard errors for each sample, corrected for amplification efficiencies. Examples of the results that can be obtained are shown in Figs. 1 and 2.

4 Notes

1. See accompanying instruction manual for further details.
2. Once thawed, reconstituted DNase I is stable for up to 6 weeks at 4 °C. Do not refreeze the aliquots after thawing. Never vortex DNase I, because this enzyme is ultrasensitive to physical denaturation.
3. If qPCR thermocyclers from other suppliers are going to be used, appropriate modifications to our protocol should be

preliminarily determined (for instance, the reaction volumes, the PCR reaction settings, usage of reference dyes in the master mix, and so forth).

4. Many qPCR master mix solutions are commercially available. If using qPCR master mix purchased from a different company, we suggest carefully reviewing the accompanying product insert. Changes in the reaction preparation and/or in the PCR reaction (for instance, the initial denaturation step or the annealing/elongation step) may vary, as the length of the denaturation step depends on the polymerase included in the master mix.
5. Among the commercially available kits, we have experimentally verified that the "RNeasy mini kit" works well, because it facilitates purification of high-quality RNA (not degraded, salt- and genomic DNA-free), whose integrity and purity are easily assessed by denaturing agarose gel electrophoresis or, in case of very low amount of material, by Agilent 2100 Bioanalyzer. In addition, this kit permits the use of an on-column DNase digestion step, thereby avoiding potential DNase carryover.
6. We strongly recommend working with highly pure neutrophil preparations obtained by negative immunoselection with magnetic beads (EasySep neutrophil enrichment kit, StemCell Technologies). Preparation purity can be rapidly checked by flow cytometry for the high CD66b surface expression of neutrophil. Using this procedure contamination by eosinophils, which were co-purified with the conventional density gradient sedimentation method (varying from 1 to 8 % depending on the donor), is excluded. The same is also true for mononuclear leukocytes (monocytes and lymphocytes) whose presence, as low as 1 %, may greatly influence the results attributed to neutrophils. Most importantly, the presence of as little as 0.01 % contaminating monocytes, likely generating false-positive results, in the neutrophil culture can be revealed by the analysis of cytokines such as IL-6 (Fig. 2), IFNβ, and/or IL-10 (not shown) expression.
7. Some neutrophil agonists, such as LPS, other Toll-like receptor (TLR) ligands, or tumor necrosis factor (TNF)-α, cause strong cell adherence to the culture vessel, especially within the first 2 h of incubation. In this case, we suggest removing culture medium and adding RLT buffer directly into the well.
8. The quality of the cDNA template depends on the integrity of the RNA. All possible precautions must be taken in order to maintain an RNase-free environment when handling/manipulating RNA. Hands and dust particles may carry common sources of RNase contamination, such as bacteria and molds. Always wear gloves and change them frequently. Because RNases are less active at cold temperature, we suggest keeping samples chilled on ice, especially following RNA extraction.

9. DNA digestion is a necessary step in all cases in which contaminating genomic DNA can interfere with subsequent applications. The RNeasy kit offers the optional step of "on-column" DNase treatment, which we always perform. If a different kit for RNA purification is used, genomic DNA should be removed by a DNase digestion step following RNA isolation. To avoid the risk of a possible DNase carryover, which could be detrimental for the subsequent cDNA synthesis step, we recommend performing phenol–chloroform treatment of all RNA samples after DNase treatment.
10. The excitation maximum for RiboGreen reagent bound to RNA is ~500 nm and the emission maximum is ~525 nm.
11. Because even a small amount of contaminants can greatly impact results of the assay, use of molecular biology-grade water, RNase/DNase/nucleic acid-free tubes, aerosol-barrier pipet tips, and dedicated pipettors of all types (i.e., pipettors used only for RNA or PCR applications, which are kept out of areas used for plasmid or genomic DNA work) is strongly recommended for all steps. The use of a small PCR hood may be very helpful to avoid PCR contamination. If a hood is not available, perform PCR in a dedicated space, possibly at distance from the thermocycler or spaces in which the electrophoresis equipment are located.
12. We suggest processing all samples from each experiment at the same time, starting from the same amount of RNA for each sample. This reduces differences in the quality and quantity of cDNAs obtained and increases the reliability of the final RT-qPCR results. If RNA recovery is low following the RNA purification step, RT can be performed with <1 μg of RNA without major problems. However, we suggest that the RT reaction be performed with ≥0.1 μg of RNA.
13. Because most of the primers we use in RT-qPCR span an exon junction, the –RT control is not needed for every sample. We usually perform –RT controls only for new primer pairs and occasionally on random samples.
14. Specificity of the qPCR reaction can be confirmed by melting curve analysis, where the presence of different PCR products is reflected in the number of first-derivative melting peaks. The melting curve analysis is set as final step of the qPCR program by gradually heating the qPCR product (from 60 to 95 °C) and recording the fluorescence value every 0.5 °C. As the temperature increases from 60 to 95 °C, the final double-strand PCR product is denatured, intercalating SYBR Green is released, and the fluorescence intensity is decreased (*see* Fig. 3a). The fluorescence intensity vs. temperature plotted as first derivative ($-dI/dT$) generates the melting curve. The presence of more than one peak indicates that more than one PCR product has been

formed and that the PCR reaction is not specific. The negative control, containing PCR primers but no template, could give rise to a peak in the melting curve that usually has a low Tm and is formed in the last PCR cycles. This peak is usually representative of primer dimer formation.

15. Normalization to an endogenous reference gene or genes is the preferred method to more accurately quantify the expression levels of a given mRNA. To select a stable reference gene it is very important to avoid acquisition of biologically irrelevant data. Unfortunately it is very hard to identify a single reference gene stable in all the possible experimental conditions that can be tested; therefore, the best approach that we have found is to always measure two–three reference genes and use the more stable one for normalization. The genes that we commonly test are glyceraldehyde 3-phosphate dehydrogenase (GAPDH), ribosomal protein L32 (RPL32), peptidylprolyl isomerase B (PPIB), and β2-microglobulin (B2M).
16. Primer designing is a crucial step for performance of qPCR. Primers should be designed according to standard PCR guidelines. A good primer (1) is 19–24 bases in length; (2) preferably has a base composition of 50–60 % in G+C; (3) preferably has a primer ending at the 3′-end that is a G or a C, or CG or GC: this prevents "breathing" of ends and increases efficiency of priming; (4) has no runs of three or more Cs or Gs at the 3′-end of primers, which may promote mispriming at G- or C-rich sequences (because of stability of annealing) and should be avoided; (5) has 3′-ends that are not complementary (i.e., base pair), as otherwise primer dimers will be synthesized preferentially to any other product; and (6) has no primer self-complementarity (ability to form 2° structures such as hairpins). To optimize efficiency, the product of qPCR must be approx 80–250 bp. Melting temperature (Tm) of the primers should be 60–64 °C; it is important that all the primers function at the same annealing temperature, thereby allowing analysis of different targets in the same plate. When designing primers for RT-qPCR, we suggest identifying at least one primer that overlaps an exon–exon boundary in order to prevent the amplification of genomic DNA. Alternatively, the two primers should anneal to two different exons on each side of an intron. A public database for the selection of primer sequences suitable for RT-qPCR, RTPrimerDB, is available at the following website: http://medgen.ugent.be/rtprimerdb/index.php [16]. Our primers are designed with the PerlPrimer software [17], which is free at http://perlprimer.sourceforge.net. The specificity of the identified primers can be computationally tested by Primer-BLAST [18]. This software tool permits to identify all the possible PCR products that can be formed, on the whole transcriptome, using different primer pairs. If potential erroneous

amplicons are detected using the Primer-BLAST default parameters, different primer pairs should be designed.

17. It is possible to use 1 pg to 100 ng of cDNA in a qPCR reaction, and the amount available will likely depend on the quantity of total RNA isolated from neutrophils. We experimentally determined that 3 ng of cDNA is an optimal amount and permits quantification of low- and high-expression transcripts.
18. Note that there is a risk for pipetting errors associated with manipulating very small vol (<2 μL) that could cause differential input of template.
19. For most of the cytokine genes, baseline can be set at cycle range 3–15. For low-expression genes this value should be extended to 3–20.
20. In our conditions, the threshold is usually set at a fluorescence value (ΔRn) of 0.1 for all the genes. Because plate variation introduced during the PCR run is minimal in the current generation of real-time PCR cyclers, the ViiA7 software enables the analysis of different genes on different plates, a feature especially useful when many genes are analyzed using the same samples.
21. Amplification efficiency of the reaction is an important consideration when performing relative quantification. An efficiency value of 2 means that the PCR product doubles during every cycle within the exponential phase of the reaction. However, many PCR reactions do not have ideal amplification efficiencies, and calculation without an appropriate correction factor may overestimate starting concentration. We use as amplification efficiency for each gene analyzed (including reference genes) the average of amplification efficiencies calculated by LinRegPCR [14] for each single sample. Data input and output are through an Excel spreadsheet. The LinRegPCR software is freely available at http://LinRegPCR.nl.
22. Q-Gene is an Excel-based software available free for download at http://www.gene-quantification.de/download.html#qgene [15].

Acknowledgments

This work was supported by grants from the Ministero dell'Istruzione, dell'Università e della Ricerca (2009MFXE7L_001 and 200999KRFW_004), Associazione Italiana per la Ricerca sul Cancro (AIRC, IG-11782), Fondazione Cassa di Risparmio di Verona, Vicenza, Belluno e Ancona, and the University of Verona (a Joint Project_2010 grant). N.T. is recipient of an FIRC Fellowship.

References

1. Mantovani A, Cassatella MA, Costantini C et al (2011) Neutrophils in the activation and regulation of innate and adaptive immunity. Nat Rev Immunol 11:519–531
2. Wang T, Brown MJ (1999) mRNA quantification by real time TaqMan polymerase chain reaction: validation and comparison with RNase protection. Anal Biochem 269:198–201
3. Malinen E, Kassinen A, Rinttila T et al (2003) Comparison of real-time PCR with SYBR Green I or 5'-nuclease assays and dot-blot hybridization with rDNA-targeted oligonucleotide probes in quantification of selected faecal bacteria. Microbiology 149:269–277
4. Palmer S, Wiegand AP, Maldarelli F et al (2003) New real-time reverse transcriptase-initiated PCR assay with single-copy sensitivity for human immunodeficiency virus type 1 RNA in plasma. J Clin Microbiol 41:4531–4536
5. Arikawa E, Sun Y, Wang J et al (2008) Cross-platform comparison of SYBR Green real-time PCR with TaqMan PCR, microarrays and other gene expression measurement technologies evaluated in the MicroArray Quality Control (MAQC) study. BMC Genomics 9:328
6. Nagalakshmi U, Wang Z, Waern K et al (2008) The transcriptional landscape of the yeast genome defined by RNA sequencing. Science 320:1344–1349
7. Pelletier M, Maggi L, Micheletti A et al (2010) Evidence for a cross-talk between human neutrophils and Th17 cells. Blood 115:335–343
8. Bazzoni F, Cassatella MA, Laudanna C et al (1991) Phagocytosis of opsonized yeast induces tumor necrosis factor-alpha mRNA accumulation and protein release by human polymorphonuclear leukocytes. J Leukoc Biol 50:223–228
9. Tamassia N, Le Moigne V, Calzetti F et al (2007) The MyD88-independent pathway is not mobilized in human neutrophils stimulated via TLR4. J Immunol 178:7344–7356
10. Davey MS, Tamassia N, Rossato M et al (2011) Failure to detect production of IL-10 by activated human neutrophils. Nat Immunol 12:1017–1018, author reply 1018–1020
11. Wang P, Wu P, Anthes JC et al (1994) Interleukin-10 inhibits interleukin-8 production in human neutrophils. Blood 83: 2678–2683
12. Reglier H, Arce-Vicioso M, Fay M et al (1998) Lack of IL-10 and IL-13 production by human polymorphonuclear neutrophils. Cytokine 10:192–198
13. Livak KJ, Schmittgen TD (2001) Analysis of relative gene expression data using real-time quantitative PCR and the 2(–Delta Delta C(T)) Method. Methods 25:402–408
14. Ruijter JM, Ramakers C, Hoogaars WM et al (2009) Amplification efficiency: linking baseline and bias in the analysis of quantitative PCR data. Nucleic Acids Res 37:e45
15. Muller PY, Janovjak H, Miserez AR et al (2002) Processing of gene expression data generated by quantitative real-time RT-PCR. Biotechniques 32: 1372–1374, 1376, 1378–1379
16. Lefever S, Vandesompele J, Speleman F et al (2009) RTPrimerDB: the portal for real-time PCR primers and probes. Nucleic Acids Res 37:D942–D945
17. Marshall OJ (2004) PerlPrimer: cross-platform, graphical primer design for standard, bisulphite and real-time PCR. Bioinformatics 20:2471–2472
18. Ye J, Coulouris G, Zaretskaya I et al (2012) Primer-BLAST: a tool to design target-specific primers for polymerase chain reaction. BMC Bioinformatics 13:134
19. Tamassia N, Cassatella MA, Bazzoni F (2007) Fast and accurate quantitative analysis of cytokine gene expression in human neutrophils by reverse transcription real-time PCR. Methods Mol Biol 412:455–471

Chapter 28

High-Purity Neutrophil Isolation from Human Peripheral Blood and Saliva for Transcriptome Analysis

Flavia S. Lakschevitz and Michael Glogauer

Abstract

The oral cavity is a source of readily available neutrophils and can be used as a model to better understand the role of neutrophils in chronic inflammatory diseases such as rheumatoid arthritis, bronchitis, periodontitis, and inflammatory bowel disease. In this chapter we describe reproducible methods to obtain highly purified neutrophil samples from blood and saliva in humans to enable cell analysis using whole-genome microarrays.

Key words Saliva, Oral neutrophils, Transcriptome analysis, Microarray

1 Introduction

Microarray technology, which exploits the preferential binding of complementary single-stranded nucleic acid sequence to a large set of oligonucleotide probes, enables monitoring of gene expression in pathological processes in tissues and cells from diverse phenotypes or physiological states [1]. Our understanding of neutrophil biology has significantly progressed through the use of genome-wide approaches to study the role of neutrophils in inflammation [2], tumor sites [3], and many inflammatory diseases [4].

Neutrophils are the predominant immune cell population in the oral cavity [5, 6]. This gives us an opportunity to not only monitor the progression of oral diseases associated with neutrophil deficiencies such as periodontal diseases but also understand the innate immune system as a whole [6]. The oral neutrophil transcriptome can be a powerful screening tool for studying tissue-specific neutrophil phenotypes and can be used as a model to better understand chronic inflammatory disease such as periodontitis, rheumatoid arthritis, bronchitis, and inflammatory bowel disease (IBD) [7–9].

Mark T. Quinn and Frank R. DeLeo (eds.), *Neutrophil Methods and Protocols*, Methods in Molecular Biology, vol. 1124,
DOI 10.1007/978-1-62703-845-4_28,

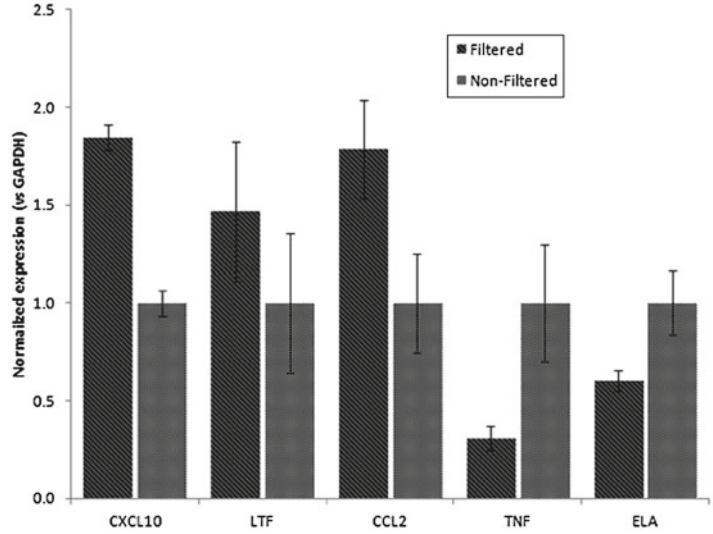

Fig. 1 Oral neutrophil purification is required for accurate transcriptome analysis. To confirm expression levels of neutrophil-associated genes, five genes were amplified from oral rinse before and after filtration by qRT-PCR. Levels of GAPDH mRNA were measured to normalize selected mRNA. Results are expressed as fold change vs. non-filtered expression used as internal control. The values are shown as means ± SEM of three independent experiments performed in triplicate

Obtaining a highly pure homogenous cell population is the key element of many study designs, especially when dealing with more sensitive molecular biology techniques [10–12]. Contamination with unwanted cells can result in difficult-to-interpret and erroneous results [11]. Although numerous neutrophil isolation methods are currently available they fail to provide a combination of purity, viability, and truly resting cells [13]. In a previous study from our group, we demonstrated the need to use highly pure neutrophil samples for transcriptome analysis since expression of genes from contaminating cells such as epithelial cells can lead to erroneous data [6] (Fig. 1).

In this chapter, we describe methods to obtain neutrophils from peripheral blood and from saliva in humans. Additionally, we describe simple methods to assess the quality of neutrophil isolates including a purity assay and a viability assay. Finally we describe our method of choice for total RNA isolation and cRNA labeling for microarray analysis.

2 Materials

2.1 Blood Cell Separation

1. 10 mL sterile syringe.
2. 20-G sterile needle.
3. Sodium citrate buffer: 37.9 mg/mL sodium citrate in sodium phosphate buffer.

4. 1-Step Polymorphs (Accurate Chemical & Scientific Corp, Westbury, NY, USA): Store at room temperature and keep from exposure to light.
5. Phosphate-buffered saline (PBS) without Ca^{2+} and Mg^{2+}.
6. Pharm Lyse buffer (BD Biosciences).
7. 15-mL polypropylene conical tubes.
8. Cooled centrifuge with releasable brake.
9. 1.5-mL Eppendorf tubes.

2.2 Oral Cavity Cell Separation

1. 0.9 % irrigation-grade sodium chloride solution.
2. 50- and 15-mL polypropylene conical tubes.
3. Sterile cell strainer: 40 μm nylon mesh.
4. 20 and 11 μm nylon filters.
5. Swinnex 25 filter holders (Millipore Corporation, Billerica, MA, USA).
6. 20 mL sterile syringe.
7. 1.5-mL Eppendorf tubes.

2.3 Negative Magnetic Purification

1. Fetal bovine serum (FBS).
2. Dipotassium ethylenediaminetetraacetic acid (K_2EDTA).
3. Easysep magnet (Stemcell Technologies, Vancouver, BC, Canada).
4. EasySep Human Neutrophil Enrichment Kit (Stemcell Technologies, Vancouver, BC, Canada).
5. Easysep buffer: PBS, 2 % FBS, 1 mM EDTA.
6. 5-mL polystyrene round-bottom tubes.

2.4 Cell Count, Purity Check, and Cell Viability Test

1. Cell counter: Z1 Coulter counter (Coulter Electronics, Brea, CA, USA).
2. Trypan blue solution.
3. Diff-Quick Stain Set.
4. Cytospin centrifuge.
5. Acridine orange.

2.5 Extraction of Total RNA

1. RNaseZap® (Ambion by Life Technologies, Houston, TX, USA).
2. 1.5 mL pre-sterilized, nuclease-free Eppendorf tubes.
3. 1–10 μL, 10–100 μL, and 100–1,000 μL pre-sterilized, nucleases-free pipette tips.
4. Phenol:chloroform: 5:1 mixture.
5. 100 % ethanol: ACS reagent grade or equivalent.

6. mirVana miRNA Isolation Kit (Ambion by Life Technologies, Houston, TX, USA).
7. DNA-free™ Kit (Ambion by Life Technologies, Houston, TX, USA).

2.6 Analysis of RNA Quality

1. 1–10 μL pre-sterilized, nucleases-free pipette tips.
2. TE buffer: 100 mM Tris (pH 7.4), 10 mM EDTA (pH 8.0).
3. Microvolume spectrophotometer (e.g., Nanodrop ND-1000).
4. Access to a microfluidics-based automated electrophoresis systems for RNA quality control and quantification (e.g., Agilent 2100 Bioanalyzer).

2.7 Generation of Labeled cRNA

1. Illumina® TotalPrep™ RNA Amplification Kit (Ambion).
2. Thermocycler.
3. Vacuum centrifuge concentrator.
4. Illumina Human-12 v2 Expression BeadChip (Illumina, San Diego, CA, USA).
5. Access to a microarray core facility for hybridization of the samples to Illumina microarrays.

3 Methods

3.1 Neutrophil Isolation from Human Blood

Peripheral blood neutrophils are obtained from volunteers, whose informed consent is ensured in accordance with the relevant institutional review board. Perform all procedures aseptically in a sterile environment.

1. Collect 10 mL of blood with a 10 mL syringe using a 20-G needle, according to standard protocols (*see* **Note 1**).
2. After collection, transfer to a 15-mL falcon tube with sodium citrate (1:10) (*see* **Note 2**).
3. In two 15-mL tubes, add 5 mL of 1-step polymorphs to each tube and carefully layer 5 mL of the blood on the top of each.
4. Centrifuge at 450 × *g* for 35–40 min in a swinging bucket rotor at 20 °C without brake (*see* **Note 3**).
5. After centrifugation two clearly visible bands will form. The upper band will consist of mononuclear cells (monocytes, lymphocytes, and basophils) and a lower band of granulocytes (comprising neutrophils and eosinophils). A red cell pellet will accumulate in the bottom of the tube. Carefully aspirate off the plasma and mononuclear layer to avoid contamination between the cell populations (*see* **Note 4**).
6. Collect the lower band of PMNs into a new 15-mL falcon tube with a disposable plastic Pasteur pipette.

7. Wash collected cells by adding 10 mL of PBS and centrifuge at 400 × *g* for 5 min at room temperature.
8. Discard the supernatant.
9. Excessive red blood cell contamination of the desired granulocyte layer can be removed by adding 1 mL of 1× Pharm Lyse buffer. Incubate on ice for 3 min, and centrifuge at 400 × *g* for 5 min at room temperature (*see* **Note 5**).
10. Discard supernatant, and resuspend the cells in 1 mL of cold PBS.
11. Count the cells (see below). Check for purity with Diff-Quick staining (see below) or by flow cytometry and viability by the trypan blue exclusion test (see below) or any other available method.
12. Isolated neutrophils from peripheral blood should contain less than 2 % contaminating cells and display at least 98 % viability. If purity of samples is bellow that mark, further purification is required and can be achieved by negative magnetic selection (see below). Otherwise, transfer to a 1.5-mL endonuclease-free Eppendorf tube, and start total RNA isolation protocol (see below).

3.2 Neutrophil Isolation from Human Oral Cavity

The low yield of neutrophils from saliva and its rapid degradation plays a major role in the challenges of the technique described here. However, reducing the time between collection and isolation and performing all steps on ice can overcome these problems. The same ethics procedure should be followed for salivary sample collection.

1. Ask patients to swish with 5 mL of sterile 0.9 % NaCl solution for 30 s and expectorate into a sterile 50-mL conical tube that is placed on ice.
2. Repeat these procedure five times, and wait 3 min between each rinse (*see* **Note 6**).
3. Mount 20 and 10 μm nylon filters in a Swinnex 25 filter holder.
4. Connect each set of filter/filter holder to a 20 mL syringe, and discard the plunger. Place it on the top of a 15-mL falcon tube. Keep it on ice.
5. Sequentially filter cells through a series of filters. Start with a 40 μm sterile cell strainer on the top of a 50-mL falcon tube to remove debris, and then use 20 and 10 μm nylon filters without plunging to allow separation of neutrophils from epithelial cells and monocytes (*see* **Note 7** and Fig. 2).
6. Centrifuge the effluent containing the neutrophils at 500 × *g* for 10 min at 4 °C.
7. Remove the supernatant, and suspend the pellet in 1 mL of cold PBS.

Fig. 2 Purification of oral neutrophils. 20-mL syringes are connected to a set of filter/Swinnex 25 filter holder. Rinsed samples are loaded into the syringes without plunging it. The purified neutrophils are collected in the falcon tubes below

8. Count the cells (see below). Check for purity with Diff-Quick staining (see below) or by flow cytometry and viability by the trypan blue exclusion test (see below) or any other available method.
9. Isolated neutrophils from saliva usually contain less than 1 % contaminating cells and display at least 80 % viability. If purity of samples is bellow that mark, further purification is required and can be achieved by negative magnetic selection (see below). Otherwise, transfer to a 1.5-mL endonuclease-free Eppendorf tube, and start total RNA isolation protocol (see below).

3.3 Negative Magnetic Purification

1. In a 5-mL polystyrene tube, resuspend previous isolated cells in 500 μL of Easysep buffer. Adjust cell concentration to 5×10^6 cells/mL (*see* **Note 8**).
2. Add 25 μL of EasySep Human Neutrophil Enrichment Cocktail (50 μL/mL cells). Mix well, and incubate at 4 °C for 10 min.
3. Mix Easysep nanoparticles by pipetting gently 2–3 times. *Do not vortex.*
4. Add 50 μL of nanoparticles (100 μL/mL cells). Mix well, and incubate at 4 °C for 10 min.
5. Bring the cell suspension to a total volume of 2.5 mL by adding Easysep buffer. Mix cells by pipetting gently 2–3 times.
6. Place the tube (without cap) into the magnet.
7. Set aside for 5 min.

8. In one continuous motion, invert the magnet and tube, pouring into a new 5 mL tube, and leave for 2–3 s. *Do not shake the tube*.
9. Remove the empty tube from the EasySep magnet, and place the new tube containing the supernatant into the magnet.
10. Set aside for 5 min.
11. In one continuous motion invert the magnet and tube, pouring into a new 5-mL tube, and leave for 2–3 s. *Do not shake the tube*.
12. The negatively selected and enriched cells in the new tube are now ready for use.
13. Count the cells (see below). Check for purity with Diff-Quick staining (see below) or by flow cytometry and viability by the trypan blue exclusion test (see below) or any other available method.

3.4 Cell Count, Purity Check, and Cell Viability Test

An accurate cell count can be obtained using an automatic particle counter or by manual counting with a hemocytometer. To simplify this step we use a Z1 Coulter Particle Counter.

1. Add 19.5 mL of isotonic solution in a cell-counting vial.
2. Mix samples well, and then add 475 μL of PBS and 25 μL of sample to the cell counter vial.
3. Place vial on the stage, select concentration, and start count.
4. Repeat each count at least twice for accuracy. Average the results and multiply by 20 (dilution factor). This will give the number of cells per mL of diluted solution.
5. To calculate the total number of cells in the original cell suspension, multiply the results obtained by the total volume of cell suspension.

3.4.1 Diff-Quick Staining for Purity Check

Visual inspection is our method of choice to determine cell purity. We use Diff-Quick, a commercial name for the Romanowsky stain, as our standard method. Diff-Quick is designed to incorporate cytoplasmic (pink) staining with nuclear (blue) staining and fixation as a single step for smears and thin films of tissue.

1. Prepare the cytospins by spinning 100 μL of cell suspension in assembled cytocentrifuge chambers using a cytospin centrifuge for 5 min at $60 \times g$ with a medium acceleration. This method allows the cells to be deposited on a defined area of a glass slide and allows absorption of any excess fluid into the chamber's filter card.
2. Air-dry the cell smears.
3. Once dry, start the staining procedure by fixing cells in the Diff-Quick fixative for 30 s.

4. Drain excess fixative, and immediately immerse slide in Diff-Quick solution II for 30 s.
5. Drain excess, and immediately immerse slide in Diff-Quick solution I for 30 s.
6. Wash slide in distilled water to remove excess stain.
7. Rapidly dehydrate by dipping slide in 100 % ethanol.
8. Clear and mount. Place slides on the stage of a microscope, and focus on the cells.
9. Isolated neutrophils should contain less than 2 % contaminating cells.

3.4.2 Trypan Blue Exclusion Test of Cell Viability

This test is used to determine the number of viable cells present in a sample. Basically, live cells possess intact cell membranes that "exclude" certain dyes, such as trypan blue, while dead cells will allow the dye to penetrate into the cytoplasm. A viable cell will have a clear cytoplasm, whereas a nonviable cell will have a blue cytoplasm.

1. Mix 10 μL of trypan blue and 10 μL of cell suspension in an Eppendorf tube.
2. Allow mixture to incubate for 3 min at room temperature. Cells should be counted within 3–5 min of mixing with trypan blue, as longer incubation periods will lead to cell death and reduced viability counts.
3. Apply 10 μL of trypan blue/cell mixture to a hemocytometer.
4. Place the hemocytometer on the stage of a microscope, and focus on the cells.
5. Count the unstained (viable) and stained (nonviable) cells separately in the hemocytometer.
6. To quantify cell number with hemocytometer, dilute 1 μL of acridine orange (1 mg/mL) into 100 μL of the final cell suspension. Incubate at room temperature for 15 min in the dark.
7. Pipette 10 μL to the hemocytometer chamber, and count the cells contained in the 25 squares inside the double lines in the center of the hemocytometer. Count neutrophils that are easily identified by their characteristic multilobed nuclei.
8. Divide the number of neutrophils counted by 25 to obtain average per square, and then multiply by 5×10^6. To obtain the final cell counts, multiply the results obtained by the total volume of cell suspension.

3.5 RNA Isolation from Cells with mirVana

When processing the samples, we recommend the use of certified nuclease-free filtered tubes and tips to avoid contaminations with exogenous nucleases. Surfaces and instruments should be treated with an RNase removal fluid (e.g., RNase Zap). If possible, use a dedicated workspace to all RNA-related work or hood.

1. Pellet cells and remove all the remaining PBS from samples.
2. Add 600 µL of lysis/binding solution and vortex until you have a homogenous lysate.
3. Add 60 µL of homogenate additive, vortex for 1 min, and incubate on ice for 10 min.
4. Add 600 µL of acid-phenol:chloroform to the sample, shake vigorously for approximately 15 s, vortex for 1 min, and centrifuge for 5 min (*see* **Note 9**).
5. Carefully remove the colorless aqueous (upper) phase containing the RNA, and transfer it to a new 1.5-mL Eppendorf tube using a pipette with a 1 mL filtered tip.
6. Add 750 µL 100 % ethanol.
7. Pipette 700 µL into a filter cartridge/collection tube, spin for 15 s, and discard the flow-thru. Repeat with the remaining sample.
8. Add 700 µL of wash solution 1 to the filter, spin for 10 s, and discard the flow-thru.
9. Add 500 µL of wash solution 2/3, spin for 10 s, and discard the flow-thru.
10. Add another 500 µL wash solution 2/3, spin for 2 min, and discard the flow-thru.
11. Transfer column to new collection tube and spin for an additional minute to remove trace amounts of wash solution.
12. Transfer filter to a new nuclease-free collection tube.
13. Add 40 µL of preheated at 95 °C elution solution and spin for 30 s.
14. Proceed with DNase removal treatment (Subheading 3.5.1), and finalize with RNA quality and quantity check (Subheading 3.5.2) before the cRNA labeling step.

3.5.1 DNase Treatment

1. Add 4 µL of 10× DNase I buffer and 1 µL of rDNase I to 40 µL of fresh isolated RNA and mix gently. *Do not vortex.*
2. Incubate at 37 °C for 30 min.
3. Vortex DNase inactivation reagent for 30 s, and add 5 µL to the sample. Mix well.
4. Incubate for 2 min at room temperature, and mix occasionally.
5. Centrifuge at 10,000 × *g* for 1.5 min, and transfer to a new RNAse/DNase-free tube.

3.5.2 RNA Quality Check

1. Initial quality and quantity check of total RNA can be done with a microvolume spectrophotometer by using 1.5 µL of total RNA to measure the concentration.
2. Use sterilized nuclease-free water or TE buffer as the blank.

3. The A_{260}/A_{230} ratio should be between 1.8 and 2.2. The samples can then be stored at −80 °C, if needed.
4. Check degradation of total RNA before labeling by submitting samples to a facility that has a bioanalyzer (*see* **Note 10**).

3.6 Generation of Labeled cRNA

1. Prepare wash buffer by adding 24 mL of 100 % ethanol to the bottle labeled Wash Buffer. Mix well.
2. Prepare reverse transcription master mix in a nuclease-free tube at room temperature by mixing (for a single reaction) 1 μL of T7 Oligo(dT) primer, 4 μL of dNTP mix, 2 μL of 10× first-strand buffer, 1 μL of ArrayScript, and 1 μL of RNase inhibitor. Mix well, centrifuge briefly (~5 s) to collect the reverse transcription master mix at the bottom of the tube, and place on ice until use.
3. On ice, prepare a second-strand master mix in a nuclease-free tube by mixing in the order listed (for a single reaction): 63 μL of nuclease-free water, 10 μL of 10× second-strand buffer, 4 μL of dNTP mix, 2 μL of DNA polymerase, and 1 μL of RNase H. Mix well, centrifuge briefly (~5 s) to collect the second-strand master mix at the bottom of the tube, and place on ice until use.
4. At room temperature, prepare the IVT master mix by adding the following reagents to a nuclease-free microcentrifuge tube (for a single 25 μL reaction): 2.5 μL of T7 10× reaction buffer, 2.5 μL of T7 enzyme mix, and 2.5 μL of biotin–NTP mix. Mix well, centrifuge briefly (~5 s) to collect the IVT master mix at the bottom of the tube, and place on ice until use.

3.6.1 Reverse Transcription to Synthesize First-Strand cDNA

1. Reduce the volume of PMN total RNA (50–500 ng) to 11 μL in a centrifugal vacuum concentrator.
2. Add 9 μL of reverse transcription master mix to each RNA sample. Mix thoroughly by pipetting up and down 2–3 times, and centrifuge briefly to collect the reaction in the bottom of the tube.
3. Place the samples in the thermal cycler, and incubate reactions for 2 h at 42 °C.
4. Place on ice immediately after thermal cycler run (*see* **Note 11**).

3.6.2 Second-Strand cDNA Synthesis

1. Add 80 μL of second-strand master mix to each sample. Mix thoroughly by pipetting up and down 2–3 times, and centrifuge briefly to collect the reaction in the bottom of the tube.
2. Place the samples in the thermal cycler, and incubate reactions for 2 h at 16 °C (*see* **Note 12**).
3. Place on ice immediately after thermal cycler run (*see* **Note 13**).

3.6.3 cDNA Purification

1. Preheat a minimum of 20 μL per sample of nuclease-free water to 55 °C (*see* **Note 14**).
2. Add 250 μL of cDNA binding buffer to each sample, and mix thoroughly by pipetting up and down 2–3 times.
3. Centrifuge briefly to collect the reaction in the bottom of the tube (*see* **Note 15**). Proceed quickly to the next step.
4. Using cDNA filter cartridge/washing tube provided in the kit, pipette the cDNA sample/cDNA binding buffer that you previously prepared onto the cDNA filter cartridge.
5. Centrifuge for 1 min at 10,000 × *g*.
6. Discard the flow-thru, and replace the cDNA filter cartridge in the wash tube.
7. Add 500 μL wash buffer to each cDNA filter cartridge.
8. Centrifuge for 1 min at 10,000 × *g*.
9. Discard the flow-thru, and spin the cDNA filter cartridge for an additional minute to remove trace amounts of wash buffer.
10. Transfer cDNA filter cartridge to a cDNA elution tube.
11. Apply 20 μL of preheated nuclease-free water (55 °C) to the center of the filter in the cDNA filter cartridge.
12. Leave at room temperature for 2 min, and then centrifuge for 1 min at 10,000 × *g*.
13. The double-stranded cDNA will now be in the elute (~17.5 μL).

3.6.4 In Vitro Transcription to Synthesize cRNA

1. Transfer each cDNA sample (~17.5 μL) to a nuclease-free PCR tube.
2. Add 7.5 μL of IVT master mix that you have previously prepared to each cDNA sample.
3. Mix thoroughly by pipetting up and down 2–3 times, and centrifuge briefly to collect the reaction mixture in the bottom of the tube.
4. Place the samples in the thermal cycler, and incubate reactions for 14 h at 37 °C (*see* **Note 16**).
5. Stop the reaction by adding 75 μL of nuclease-free water to each cRNA sample to bring the final volume to 100 μL. Mix thoroughly by gentle vortexing.

3.6.5 cRNA Purification

1. Before beginning the cRNA purification, preheat a minimum of 200 μL of nuclease-free water to 55 °C.
2. For each sample, place a cRNA filter cartridge into a cRNA collection tube and set aside for later use.
3. Check to make sure that each IVT reaction was brought to 100 μL with nuclease-free water.

4. Add 350 μL of cRNA binding buffer to each cRNA sample. Proceed to the next step immediately.
5. Add 250 μL of 100 % ethanol to each cRNA sample, and mix by pipetting the mixture up and down three times. *Do NOT vortex, and do NOT centrifuge*. Proceed immediately to the next step.
6. Pipette each sample mixture in the cRNA filter cartridge. Centrifuge for 1 min at 10,000 × *g*. Continue until the mixture has passed through the filter. Discard the flow-thru, and replace the cRNA filter cartridge back into the cRNA collection tube.
7. Apply 650 μL of wash buffer to each cRNA filter cartridge. Centrifuge for 1 min at 10,000 × *g* or until all the wash buffer is through the filter.
8. Discard the flow-thru, and spin the cRNA filter cartridge for an additional 1 min to remove trace amounts of wash buffer. Transfer filter cartridge(s) to a fresh cRNA collection tube.
9. Add 200 μL of nuclease-free water (preheated to 55 °C). Incubate the samples in a 55 °C heat block for 10 min.
10. Centrifuge for 2 min at 10,000 × *g*. The cRNA will now be in the cRNA collection tube in 200 μL of nuclease-free water.

3.6.6 Positive Control Reaction

Always use a control sample to make sure that the kit is working properly. RNA consisting of 1 mg/mL HeLa cell total RNA is provided.

1. Dilute the control RNA 1:10 by adding 1 μL of control RNA to 9 μL nuclease-free water.
2. Use 2 μL of the diluted control RNA (200 ng) in an Illumina RNA amplification reaction. Add 9 μL of nuclease-free water to bring control RNA to a final volume of 11 μL.
3. Continue with the procedure described under Subheading 3.6.1 as for your study samples.
4. The positive control reaction should produce ≥5 μg of cRNA, and the average size of the cRNA should be ≥1 kb.

3.6.7 Assessing cRNA Yield by UV Absorbance

1. The concentration of a cRNA solution can be determined by measuring its absorbance at 260 nm using a microvolume spectrophotometer by using 1.5 μL cRNA to measure the concentration.
2. Use sterilized nuclease-free water or TE buffer as the blank. The A_{260}/A_{230} ratio should be between 1.8 and 2.2. The samples can then be stored at −80 °C.
3. At this point, you can submit your samples to a microarray core facility for cRNA quality check using a bioanalyzer and hybridization of the samples to Illumina microarrays (*see* **Notes 17** and **18**).

4 Notes

1. For best results blood should be used within 2 h of drawing from the donor. If not possible keep blood at room temperature until isolation procedure. On average, neutrophil isolation procedure takes 2–3 h to finalize. At the latest time point RNA degradation is frequently observed.
2. Our anticoagulant of choice is sodium citrate. Alternately, K_2EDTA or tripotassium ethylenediaminetetraacetic acid (K_3EDTA) can be used. Heparin-based anticoagulant should be avoided.
3. The high osmolality of one-step polymorph causes the loss of water from erythrocytes, but it only happens effectively at 18–20 °C. Thus, the temperature of the blood sample and the medium should be kept in that range during all procedures.
4. This is a critical step to avoid contamination with monocytic cells. Using a vacuum aspirator, aspirate the whole content of the plasma and the upper monocytic band, and also partially aspirate the one-step polymorph layer immediately bellow the monocytic band. Under homeostatic conditions, eosinophils constitute 0–3 % of peripheral blood nucleated cells in healthy individuals. If a high percentage of eosinophil contamination occurs a second purification step is mandatory.
5. Alternatively, a hypotonic shock lysis can be performed by adding 1 mL of chilled double-distilled H_2O and immediately add 10 mL of PBS to stop the reaction.
6. From oral samples of healthy subjects, the maximum number of neutrophils obtainable are in a range of $0.5–1.5 \times 10^6$ PMNs, and from 10 mL of blood we isolate an average of $8 \pm 1.5 \times 10^6$ neutrophils. Neutrophil repopulation in the oral cavity requires a minimum of 3 min to be achieved, so a 3-min interval between each rinse is critical for a good yield.
7. Neutrophils are usually 9–16 μm in diameter; monocytes vary considerably, ranging in size from 12 to 30 μm in diameter. Thus, a passive filtration system is required to avoid contamination with monocytes from salivary samples.
8. According to the manufacturer's instructions [14], the use of less than 5×10^7 cells per separation may result in suboptimal performance. Unfortunately, it is virtually impossible to achieve such a high yield from oral samples. We were able to obtain high-purity samples from 5×10^6 cells but with a final yield of $0.8–1 \times 10^6$ cells. Such low yield will impact the quality of total RNA obtained after extraction.

9. From this point on, all centrifugation can be carried out at room temperature at 10,000 × *g*, unless otherwise stated.
10. We recommend to routinely control the quality of total RNA, cRNA, and fragmented cRNA using an Agilent Bioanalyzer. Although this procedure can be time consuming, RNA quality is critical for a reliable analysis. Use RNA with RIN of seven to ten.
11. A calibrated thermal cycler with a temperature-adjustable heated lid is recommended for the greatest temperature control and stability during Illumina TotalPrep RNA Amplification reaction incubations. Allow the thermal cycler to equilibrate to the required temperature before placing the tubes in the block for incubation. A high temperature may inhibit the reaction, and low temperature may cause condensation.
12. It is important to cool the thermal cycler block to 16 °C before adding the reaction tubes because subjecting the reactions to temperatures >16 °C will compromise cRNA yield. If the lid temperature cannot be adjusted to match the 16 °C block temperature, cover the reactions with the heated lid turned off.
13. Alternatively, you can immediately freeze reactions at –20 °C. Do not leave the reactions on ice for more than 1 h.
14. Preheat the nuclease-free water to a maximum of 55 °C; temperatures above 58 °C can partially denature the cDNA, compromising final cRNA yield.
15. Check the cDNA binding buffer for precipitation before using. If a precipitate is visible, redissolve it by warming the solution to 37 °C for up to 10 min and vortexing vigorously. Cool to room temperature before use.
16. The recommended IVT reaction incubation time is based on the amount of input RNA used in the amplification reaction: ranging from 4 to 14 h. For input RNA of 100–500 ng, IVT incubation should be 4–14 h. For input RNA <100 ng, IVT incubation should be 14 h. Neutrophils usually have low RNA content; thus, 14-h incubation is necessary.
17. Use dry ice to transport cRNA to a core microarray facility to avoid thaw and freeze that will affect the quality of cRNA.
18. Illumina offers two options of expression arrays. Human Expression BeadChip that targets over 47,000 probe sets can be used for low-abundance RNA samples (50–500 ng of input RNA), while the Whole-Genome DASL HT with over 29,000 transcripts is useful for low-abundance and partially degraded human RNA samples (10–100 ng input RNA). Both assays allow us to obtain accurate gene expression data; depending on the final quality and quantity of the RNA samples one might opt for one assay over the other.

Acknowledgments

This work was funded by The Canadian Institutes of Health Research (CIHR, Ottawa, ON) and the Alpha Omega Foundation of Canada (Toronto, ON). FL is supported by CIHR Training Fellowship, TGF-53877, and the Harron scholarship (Faculty of Dentistry, University of Toronto).

References

1. Kobayashi SD, Sturdevant DE, Deleo FR (2007) Genome-scale transcript analyses in human neutrophils. Methods Mol Biol 412: 441–453
2. Kobayashi SD (2005) Spontaneous neutrophil apoptosis and regulation of cell survival by granulocyte macrophage-colony stimulating factor. J Leukoc Biol 78:1408–1418
3. Fridlender ZG, Sun J, Mishalian I et al (2012) Transcriptomic analysis comparing tumor-associated neutrophils with granulocytic myeloid-derived suppressor cells and normal neutrophils. PLoS One 7:e31524
4. Reynier F, Pachot A, Paye M et al (2010) Specific gene expression signature associated with development of autoimmune type-I diabetes using whole-blood microarray analysis. Genes Immun 11:269–278
5. Dos-Santos MC, Matos-Gomes N, Makimoto FH et al (2009) Cell phenotyping in saliva of individuals under psychological stress. Cell Immunol 260:39–43
6. Lakschevitz FS, Aboodi GM, Glogauer M (2013) Oral neutrophils display a site-specific phenotype characterized by expression of T-cell receptors. J Periodontol 84:1493–1503. doi:10.1902/jop.2012.120477
7. Cascão R, Rosário HS, Souto-Carneiro MM, Fonseca JE (2010) Neutrophils in rheumatoid arthritis: more than simple final effectors. Autoimmun Rev 9:531–535
8. Farooq SM, Stillie R, Svensson M et al (2009) Therapeutic effect of blocking CXCR2 on neutrophil recruitment and dextran sodium sulfate-induced colitis. J Pharmacol Exp Ther 329: 123–129
9. Baines KJ, Simpson JL, Scott RJ, Gibson PG (2009) Immune responses of airway neutrophils are impaired in asthma. Exp Lung Res 35:554–569
10. Pelletier M et al (2010) Evidence for a cross-talk between human neutrophils and Th17 cells. Blood 115:335–343
11. Davey MS, Tamassia N, Rossato M et al (2011) Failure to detect production of IL-10 by activated human neutrophils. Nature Immunol 12:1017–1018
12. Zhang X, Ding L, Sandford AJ (2005) Selection of reference genes for gene expression studies in human neutrophils by real-time PCR. BMC Mol Biol 6:4
13. Watson F, Robinson JJ, Edwards SW (1992) Neutrophil function in whole blood and after purification: changes in receptor expression, oxidase activity and responsiveness to cytokines. Biosci Rep 12:123–133
14. http://www.stemcell.com/~/media/Technical%20Resources/4/E/7/1/B/29125_IS_1_0_0.ashx
15. http://www.illumina.com/applications/detail/gene_expression_analysis/transcriptome_analysis.ilmn

Chapter 29

Detection of Intact Transcription Factors in Human Neutrophils

Patrick P. McDonald and Richard D. Ye

Abstract

The crucial contribution of neutrophils to innate immunity extends well beyond their traditional role as professional phagocytes. Indeed, it is now well established that neutrophils generate a plethora of inflammatory cytokines and chemokines that are profoundly involved in the onset and evolution of the inflammatory reaction. Several recent studies have also shown that neutrophils can represent an important source of inflammatory cytokines in a number of pathophysiological settings. The inflammatory cytokines produced by neutrophils are generally encoded by immediate-early response genes, which in turn depend on the activation of transcription factors such as those belonging to the nuclear factor-kappa B and signal transducers and activators of transcription families. We have shown in the past that such factors are expressed and inducible in neutrophils stimulated by physiological agonists. However, the detection of *intact* (i.e., undegraded) transcription factors in neutrophils requires special precautions and an alternative protocol due to the huge amounts of endogenous proteases present in these cells. This protocol is the focus of this chapter.

Key words Transcription factors, NF-κB, STAT, Nuclear extracts, Electrophoresis mobility shift assay, Granulocytes

1 Introduction

Neutrophils are the most abundant circulating leukocytes and play a crucial role in innate immunity. They are usually the first cells to infiltrate inflamed tissues, where they exert a series of antimicrobial responses culminating in the elimination or the inactivation of the infectious agent. In addition to their traditional role as professional phagocytes, neutrophils also express a plethora of genes in response to pro-inflammatory cytokines and bacterial products such as LPS and *N*-formyl peptides [1–5]. Examples include cytokines such as TNFα, IL-1, and IL-12; chemokines such as IL-8/CXCL8, Mip-1α/CCL3, Mip-1β/CCL4, MIG/CXCL9, IP-10/CXCL10, and I-TAC/CXCL11; and receptors such as MHCII and the high-affinity receptor for IgG, FcγRI/CD64. A common characteristic of these molecules (aside from

Mark T. Quinn and Frank R. DeLeo (eds.), *Neutrophil Methods and Protocols*, Methods in Molecular Biology, vol. 1124,
DOI 10.1007/978-1-62703-845-4_29,

their pivotal implication in the inflammatory reaction) is that they are encoded by immediate-early response genes, which are under the control of the nuclear factor-kappa B (NF-κB) and/or signal transducers and activators of transcription (STAT) factors. We have previously shown that the same stimulatory conditions allowing for the expression of the aforementioned mediators and receptors also lead to the activation of the NF-κB or the STAT transcription factors in neutrophils [6–11].

Both NF-κB and STAT factors are normally sequestered in the cytoplasm and are mobilized to the nucleus upon cell activation, where they can bind to their cognate sequences on the promoter region of target genes, and thereby initiate or enhance gene transcription (for recent reviews, *see* refs. 12–15). The activation of NF-κB is a highly regulated process, which usually involves the engagement of cell surface receptors, thereby generating various intracellular signals that eventually converge on the κB kinase (IKK) complex. This results in the phosphorylation and activation of IKK subunits, which can in turn phosphorylate the inhibitor protein IκB-α, thereby targeting it for ubiquitin-dependent degradation. The proteolysis of IκB-α, which is coupled to NF-κB dimers in the cytoplasm of resting cells, unmasks nuclear localization sequences on NF-κB subunits that allow the NF-κB complexes to translocate to the nucleus. By comparison, the STAT proteins are latent cytoplasmic proteins that are rapidly recruited to SH2 domains within the cytoplasmic tail of cytokine receptors upon cell stimulation, where they become tyrosine-phosphorylated by Janus kinases (JAK). Tyrosine-phosphorylated STAT proteins can then dimerize into various DNA-binding configurations, forming homo- or heterodimers, and translocate to the nucleus.

The detection of nuclear transcription factors involves cell disruption followed by the preparation of nuclear extracts, which are then incubated with an excess of radiolabeled oligonucleotide probe that contains the cognate DNA-binding sequence for a given factor. The resulting mixtures are then migrated on native gels to separate transcription factor complexes bound to labeled probe from unbound probe. Conventional protocols typically achieve cell lysis by solubilizing the cytoplasmic membrane with nonionic detergents [16] or sometimes by repeated freeze–thaw cycles or homogenization. In neutrophils, however, these approaches are problematic because of the huge quantities of proteolytic enzymes that are present in neutrophil cytoplasmic granules. Indeed, repeated freeze–thaw cycles break open the protease-rich neutrophil granules [17, 18]. We have shown that detergent lysis similarly results in the solubilization of granule-bound proteases, resulting in partially degraded NF-κB or STAT complexes and individual constituent proteins, even in the presence of an elaborate cocktail of protease inhibitors [8]. Accordingly, transcription factor complexes that are detected following neutrophil disruption by conventional procedures almost

invariably migrate faster than authentic complexes and no longer react with certain antibodies (extensively reviewed in ref. 19). In contrast, nitrogen cavitation represents a gentle, yet efficient, way to disrupt human neutrophils while preserving the integrity of intracellular organelles such as granules and nuclei [17]. We have adapted this technique to the preparation of neutrophil nuclear extracts, and this approach consistently yields *intact* (i.e., undegraded) NF-κB and STAT complexes [6, 8, 10]. Our cavitation-based protocol is the focus of this chapter.

2 Materials

2.1 Neutrophils

Peripheral blood neutrophils are obtained from healthy volunteers, whose informed consent is ensured in accordance with the relevant institutional review board. Neutrophils must be prepared under endotoxin-free conditions to avoid inadvertent activation during isolation. The isolation procedure we use [20] is one of the many variations of the original Boyum protocol [21]. Details on neutrophil isolation can be found in Chapter 2 of this volume. Regardless of the exact variation, isolated neutrophils should contain less than 1 % contaminating mononuclear cells and display at least 98 % viability.

2.2 Buffers

1. Hank's balanced salt solution (HBSS).
2. Krebs-Ringer phosphate buffer containing dextrose (KRPD).
3. Relaxation buffer: 10 mM PIPES, pH 7.30, 30 mM NaCl, 3.5 mM $MgCl_2$, 0.5 mM EGTA, 0.5 mM EDTA, and 1 mM DTT. Relaxation buffer is supplemented with an anti-protease cocktail (1 mM DFP, 1 mM AEBSF, 1 mM PMSF, and 10 μg/mL each of aprotinin, leupeptin, and pepstatin A, final concentrations) and phosphatase inhibitors (10 mM NaF, 1 mM Na_3VO_4, 10 mM $Na_4P_2O_7$). This buffer is designed for the generation of nuclear extracts from cavitated neutrophils (*see* **Note 1**).
4. Nuclear extraction buffer: Relaxation buffer, 10 % (v/v) glycerol, anti-protease cocktail. Phosphatase inhibitors may also be used, with the exception of Na_3VO_4, which interferes with protein quantitation by the Bradford method [22].
5. Binding buffer: 20 mM Tris base, pH 7.50, 50 mM KCl, 1 mM EDTA, 1 mM DTT, 300 μg/mL μg acetylated BSA, 50 μg/mL poly (dI-dC), 0.1 % NP-40 (v/v), and 5 % glycerol (v/v). This is the buffer in which transcription factors present in nuclear extracts are allowed to interact with labeled DNA probes (*see* **Note 2**).

2.3 Nitrogen Cavitation Vessel

A cell disruption bomb of any model can be used. We favor Model 4635 (Parr Instrument Company, Moline, IL, USA), custom fitted with four discharge valves, as this makes it possible to process many samples simultaneously.

2.4 Electrophoretic Mobility Shift Assay

1. For NF-κB binding, use any double-stranded oligonucleotide probe containing a consensus NF-κB sequence. In this chapter, we use an oligonucleotide containing tandemly repeated NF-κB sites (capitalized) identical to those of the HIV promoter (5′-gatca GGGACTTTCC gctg GGGACTTTCC-3′).
2. For the binding of STAT proteins, use various commercially available double-stranded oligonucleotide probes, depending on the nature of the STAT complex. In this chapter, we use an oligonucleotide probe corresponding to the gamma response region (GRR) of the CD64 promoter (5′-CTT TTC TGG GAA ATA CAT CTC AAA TCC TTG AAA CAT GCT-3′), which can bind STAT1-, STAT3-, and STAT5-containing complexes.
3. [γ-32P]ATP with specific activity of at least 3,000 Ci/mmol for probe labeling.
4. Sephadex G-50 spin columns for the separation of labeled oligonucleotide probe from unincorporated [γ-32P] ATP, used according to the manufacturer's instructions.

2.5 Native Polyacrylamide Gel Electrophoresis

1. TBE buffer: 89 mM Tris, 89 mM boric acid, 0.2 mM EDTA, pH 8.30. Use the same batch of TBE buffer for gel preparation and subsequent electrophoresis. A 5× TBE stock can be made and stored at RT (*see* also **Note 3**).
2. Non-denaturing polyacrylamide gel preparation: Using a 25:1 mixture of acrylamide:bis acrylamide ensures that large protein complexes migrate through the gel without undue hindrance. Although 5 % gels are generally used, varying the total acrylamide content of the gels can yield better resolution. Use a freshly prepared ammonium persulfate solution to ensure optimal polymerization. Always let the gels completely polymerize (at least 1.5 h) to ensure the best possible resolution. Finally, it is advisable to use a gel size of 16×14 cm (w×h), as it allows for better sample separation than mini-gels. A gel thickness of 1–1.5 mm works well.

3 Methods

Neutrophil stimulation with several physiological agonists results in a greatly enhanced detection of nuclear NF-κB-binding complexes in electrophoretic mobility shift assay (EMSA) and in the onset of nuclear STAT-containing DNA-binding activities (reviewed in ref. 19).

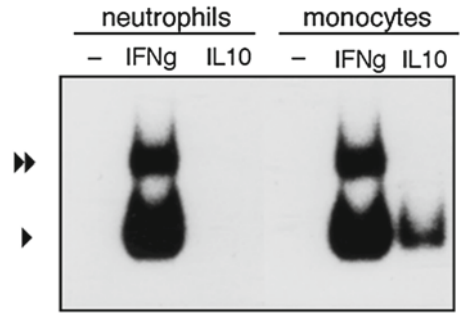

Fig. 1 Induction of STAT1 multimers in neutrophils and monocytes. Human neutrophils and autologous monocytes were stimulated with 100 U/mL IFNγ, 1,000 U/mL IL-10, or diluent control for 15 min at 37 °C. Cells were cavitated, and nuclear extracts were prepared and analyzed in EMSA using a GRR probe. The *single arrowhead* represents STAT1 dimers, and the *double arrowheads* represent STAT1 tetramers, as previously reported [10]. Reproduced from ref. 25 by permission of Humana Press © 2007

However, the detection of intact (i.e., unproteolyzed) transcription factors in neutrophils requires an alternative protocol that we developed, which is based on nitrogen cavitation of the cells. This protocol consistently yields NF-κB and STAT complexes that are indistinguishable from those isolated from other cell types, such as human monocytes or Jurkat cells [8] (*see* also Fig. 1 for STAT multimers and Figs. 3 and 4 for NF-κB dimers). In the case of STAT complexes, conventional detergent-based methods additionally produce artifacts such as the detection of a constitutive DNA binding in nuclear extracts from resting neutrophils [8, 23], which are not observed when the neutrophils are cavitated instead [8] (*see* also Fig. 1). The above considerations make it clear that nitrogen cavitation offers unmatched advantages for the preparation of neutrophil nuclear extracts. Because few granules are ever broken, protease inhibitors can effectively neutralize the small quantities of proteases which may be released during preparation (as opposed to the huge amounts released using conventional approaches).

Over the years, several refinements have been made to the procedure that we originally described [6, 8], which we have incorporated in the following protocol. Because crucial aspects of the protocol are the disruption of neutrophils and preparation of nuclear extracts, we will mainly focus on these aspects. The subsequent EMSA analysis is essentially the same for neutrophil nuclear extracts as for extracts originating from other cell types.

3.1 Preparation of Neutrophil Nuclei

1. Stimulate neutrophils either in suspension or plated in tissue culture-treated plasticware and then stimulated (both approaches will yield a comparable outcome).
2. Use at least 3×10^7 cells per experimental condition to offset the loss of material due to the significant void volume of the cavitation device (*see* **Note 4**).

3. For suspension cells, a maximum concentration of 10^7 cells/mL is recommended. Keep the cells in suspension by gentle swirling at 2–3-min intervals (or with constant swirling in an orbital water bath) during the stimulation period.
4. For plated cells, neutrophils can be cultured in large tissue culture-treated petri dishes in an incubator. Cell density is less important, but care must be taken so that neutrophils do not stack on each other when they sediment to the bottom of the dish.
5. For suspension or plated cells, add an equal volume of ice-cold buffer to stop the incubation [the same buffer used for cell incubations, such as HBSS, KRPD, or culture medium containing 2 mM DFP and phosphatase inhibitors (10 mM NaF, 1 mM Na_3VO_4, 10 mM $Na_4P_2O_7$).
6. For plated neutrophils, collect cells by gentle resuspension using a pipette fitted with a 1 mL tip that has been cut at the end to minimize turbulence.
7. Centrifuge collected cells ($300 \times g$, 5 min, 4 °C) and resuspend in ice-cold relaxation buffer supplemented with protease and phosphatase inhibitors in 100×16 mm round-bottom polypropylene centrifuge tubes. The final cell concentration should be 2×10^7/mL or less (Fig. 2, middle panel) to ensure total cell lysis.
8. Place samples into a nitrogen bomb containing crushed ice. This keeps the samples cold and also helps position the four tubes into the four-outlet bomb (*see* **Note 4**).
9. Place a small magnetic stir bar in each tube, and place the nitrogen bomb itself a magnetic stirrer to prevent cells from aggregating during the cavitation process (*see* **Note 5**).

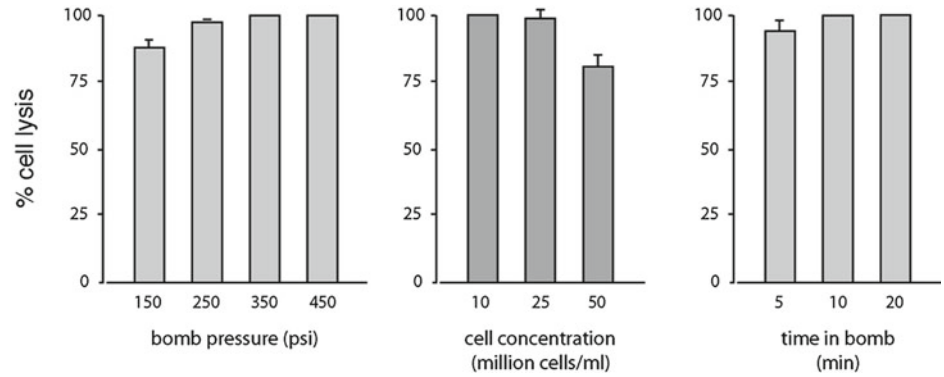

Fig. 2 Nitrogen cavitation setups for human neutrophils. *Left panel*, neutrophils (10^7/mL) were cavitated at the indicated pressures for 10 min. *Middle panel*, neutrophils were cavitated (350 psi, 10 min) at the indicated cell concentrations. *Right panel*, neutrophils (10^7/mL) were cavitated at 350 psi for the indicated times. Mean ± s.e.m. of at least three independent experiments. Reproduced from ref. 25 by permission of Humana Press © 2007

10. Pressurize samples with N_2 (350 psi) for 10 min at 4 °C (*see* **Note 6** and Fig. 2).
11. Collect each sample by inserting the bomb's outlet tube halfway into a 15 mL conical polypropylene centrifuge tube and carefully opening the discharge valve.
12. Collect cavitate dropwise into the tube, as opposed to releasing the sample all at once. This step requires some practice, because it must be performed correctly and swiftly to avoid leaving the last sample for too long in the bomb (*see* **Note 7**).
13. Place tubes on ice immediately after each cavitate is collected.
14. Centrifuge the cavitate (1,500 × *g*, 4 °C, 10 min) to pellet the nuclei.
15. Collect the resulting supernatants and recentrifuge under the same conditions to pellet the remaining nuclei.
16. Combine the nuclear pellets, wash once with 500 µL relaxation buffer, and use immediately for preparation of nuclear extracts (*see* **Note 8**).

3.2 Preparation of Nuclear Extracts

1. Gently resuspend nuclear pellets in nuclear extraction buffer using a 100 µL pipette tip that has been cut at the end to avoid breaking the fragile nuclei during pipetting. We found that using a volume (in µL) that is 1.5 times the number of million cell-equivalents in the nuclear pellet works best.
2. Add NaCl from a concentrated NaCl solution (made in relaxation buffer) to yield a final concentration of 400 mM (*see* **Notes 9–11**).
3. Immediately mix samples by flicking the Eppendorf tubes a few times.
4. Perform nuclear extraction on wet ice for 20 min, with occasional flicking of the tubes (*see* **Note 12**).
5. Pellet samples in a microfuge (top speed, 10 min, 4 °C).
6. Set aside a small volume of the resulting supernatants (the nuclear extracts) for protein content determination, and immediately snap-freeze the extracts in liquid nitrogen.
7. Store frozen extracts at –80 °C (*see* **Note 13**). Nuclear extracts prepared in this manner should contain 1–1.5 µg/µL of protein.

3.3 Radiolabeling of Oligonucleotide Probe

1. End label annealed oligonucleotide probes with either T4 polynucleotide kinase or Klenow fragment according to the supplier's instructions.
2. Proper labeling generates probes with at least 2×10^6 cpm/pmol probe (corrected for the reference date of the radiolabel).
3. A labeled probe has a useful life of about 4 weeks, although using freshly labeled probe obviously reduces the autoradiography exposure times.

3.4 Binding Reaction

The basic protocol for nuclear extract binding to a labeled probe is described first. This is followed by variations in which competition binding or antibody binding is also involved.

1. For each sample, mix 2–5 μg of the nuclear extract proteins with 10 μL of binding buffer by gentle flicking of the Eppendorf tubes (*see* **Note 14**).
2. Adjust the final volume to 15 μL.
3. Incubate the samples at room temperature for 10 min.
4. Add approximately 20 fmol of ^{32}P-labeled oligonucleotide probe (30,000–50,000 cpm) in a volume of 2 μL, and incubate the reaction mixture for an additional 10 min at room temperature.
5. Immediately load the samples on native polyacrylamide gels.

3.5 Confirming of Specificity

To confirm the specificity of the interaction between the DNA-binding complexes and the DNA sequence of interest, the following competition experiments can be performed.

1. Allow the nuclear extracts to interact with unlabeled competitor probes for 10 min at room temperature in binding buffer.
2. Add labeled probe and incubate for another 10 min at room temperature.
3. For best results, add increasing amounts of unlabeled oligonucleotide probe to the binding mix (typically, 10×, 25×, and 50× excess cold probe) to compete with the radiolabeled probe for binding to the transcription factor. Any specific binding should be displaced using 10× or 25× cold probe (as shown for neutrophil NF-κB DNA-binding activities in Fig. 3).
4. As a negative control, perform the same competition experiments using an oligonucleotide with a mutated binding site for the transcription factor of interest, which should only displace nonspecific complexes (as shown in Fig. 3).

3.6 Identification of DNA-Binding Complex Constituents

To directly identify the constituents of a specific DNA-binding complex, antibodies raised against potential candidates can be included in the binding mix.

1. Allow the nuclear extracts to interact with one or more antibodies (about 2 μg each) for 20 min at room temperature in binding buffer.
2. Add labeled probe, and incubate for another 10 min at room temperature.
3. As a negative control, use isotype-matched control antibodies at the same concentration (*see* **Note 15**).
4. Binding of antibody to its target protein will increase the size of the DNA–protein complex, resulting in further retardation

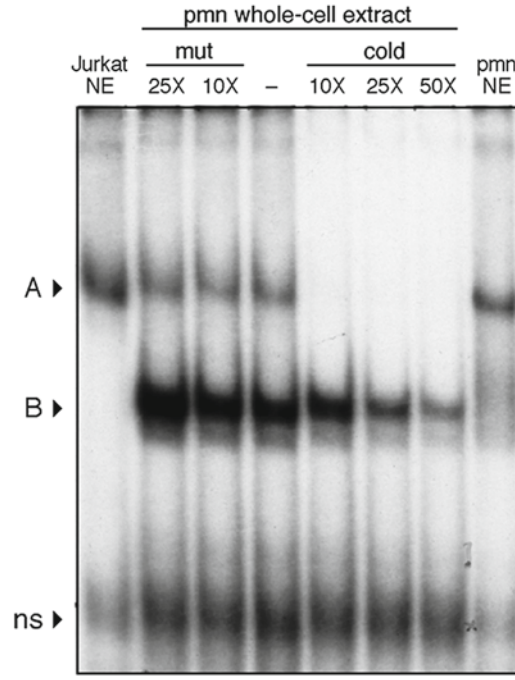

Fig. 3 Human neutrophils were stimulated for 10 min with 100 U/mL TNFα, and whole-cell extracts were prepared by supplementing raw cavitates with glycerol and NaCl (10 % v/v and 400 mM final concentrations, respectively) and incubating on ice for 20 min, prior to centrifugation. Extracts were then incubated in binding buffer in the absence ("–") or the presence of increasing concentrations of either unlabeled NF-κB probe ("cold") or of a mutated NF-κB probe ("mut") in which the consensus sequence was changed to 5′-AATACTTTCC (the mutated nucleotides are underlined), prior to addition of labeled NF-κB probe and subsequent EMSA analysis. For comparison, a nuclear extract from the same neutrophil preparation was loaded in the last lane ("pmn NE"), and a nuclear extract from TNF-activated Jurkat cells ("Jurkat NE") was loaded in the first lane as a positive control. "A" denotes the specific, inducible NF-κB complex; "B" denotes a constitutive complex showing some specificity which is present in whole-cell extracts (but mostly absent from the corresponding nuclear extracts); "ns" denotes a constitutive nonspecific complex. Reproduced from ref. 25 by permission of Humana Press © 2007

of its gel mobility or "supershift" (as shown in Figs. 4 and 5 for neutrophil NF-κB and STAT DNA-binding activities, respectively).

5. Sometimes, the antibody used binds at, or near to, a transcription factor's DNA-binding domain. In this particular case, the labeled DNA probe can no longer interact with the resulting DNA-binding complex, and there will consequently be no observable supershift, but rather a disappearance of the band (as shown in Fig. 4, lane 3).

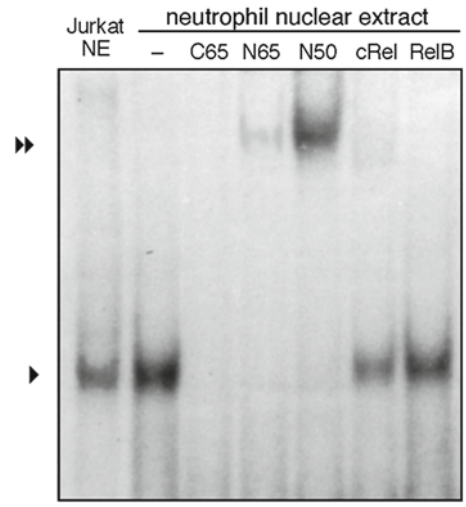

Fig. 4 Human neutrophils were stimulated for 10 min with 100 ng/mL LPS, and nuclear extracts were incubated in binding buffer in the absence ("–") or the presence of antibodies directed at a C-terminal sequence within RelA that abuts the Rel homology domain ("C65"), the N-terminus of RelA ("N65"), the N-terminus of p50 ("N50"), the C-terminus of c-Rel ("cRel"), or the N-terminus of RelB ("RelB"), prior to addition of labeled NF-κB probe and subsequent EMSA analysis. A nuclear extract from TNF-activated Jurkat cells ("Jurkat NE") was loaded in the first lane as a positive control. The *single arrowhead* denotes the specific, inducible NF-κB complex; *double arrowheads* indicate the supershifted complexes. Reproduced from ref. 25 by permission of Humana Press © 2007

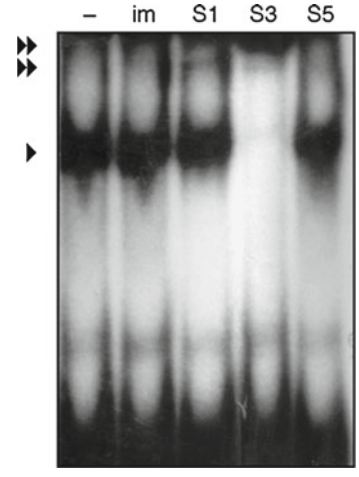

Fig. 5 Human neutrophils were stimulated for 10 min with 1,000 U/mL G-CSF, and nuclear extracts were incubated in binding buffer in the absence ("–") or the presence of antibodies directed at STAT1 ("S1"), STAT3 ("S3"), STAT5 ("S5"), or an isotype-matched control Ab ("im"), prior to the addition of labeled GRR probe and subsequent EMSA analysis. The *single arrowhead* denotes the specific, inducible GRR complex; *double arrowheads* indicate the supershifted complexes. Reproduced from ref. 25 by permission of Humana Press © 2007

3.7 Sample Analysis by Polyacrylamide Gel Electrophoresis and Autoradiography

1. Pre-run the native gels made in TBE or in an alternative buffer (*see* **Note 3**) for 90 min at 10 V/cm. This ensures a completely isocratic buffer system for optimal migration.
2. Load the samples immediately after the binding reaction. Also load 10 μL xylene cyanol (0.1 % w/v in binding buffer) in the first and last lanes of the gel as a tracking dye.
3. Run the gels at 12–14 V/cm for an additional 2–3 h. The total run time depends on how far the tracking dye has migrated. Empirically determine what distance corresponds to the optimal migration of the transcription factor complexes under study.
4. Transfer the gels to Whatman DE-81 paper and heat dry under vacuum in a gel dryer for 60 min or until the gels are completely dry.
5. Expose the dried gels to autoradiographic film at −80 °C with intensifying screens. Alternatively, gels can be exposed to PhosphorScreens (GE Healthcare) at RT prior to being read on a STORM 860 PhosphorImager (Molecular Devices).

4 Notes

1. Our relaxation buffer formulation represents a modification of the original relaxation buffer described by Borregaard [17], which among other things contained too much salt, resulting in the extraction of nuclear proteins during cell disruption. Our formulation overcomes this limitation. We no longer include the protease inhibitors, phosphoramidon, and bestatin, because they do not alter the degradation of NF-κB or STAT complexes by purified neutrophil granule proteases.
2. This formulation gives very consistent results with either NF-κB or STAT transcription factors. For other factors, various parameters may need to be changed, such as the amounts of DTT, acetylated BSA, and poly(dI-dC); the presence of $MgCl_2$; and so forth.
3. TGE buffer (50 mM Tris–HCl, pH 7.5, 380 mM glycine, 2 mM EDTA, pH 8.0) may be used instead of TBE. Again, use the same buffer for gel preparation and electrophoresis. Because of the high ionic strength of this buffer, the concentration of carrier DNA may be reduced.
4. The device we use for nitrogen cavitation is a Model 4635 Cell Disruption Bomb fitted with four outlets (*see* Subheading 2.3). The length of each dip tube used for sample collection is about 12 cm, with a diameter of 1 mm. This translates into a void volume of about 0.5 mL, which makes it difficult to work with small volumes without incurring a significant loss of cavitated sample. A smaller cell disruption device (Model 4639) is also

available from the same company, featuring nearly no void volume, but it does not allow custom fitting of additional discharge valves for the simultaneous fractionation of multiple samples.

5. Small magnetic stir bars ("fleas") can be bought from Sigma-Aldrich (cat # Z11, 884-2).
6. As shown in Fig. 2, neutrophils are efficiently lysed over a wide pressure range. However, it must be pointed out that although 450 psi achieves total cell lysis, the resulting nuclear extracts usually contain fewer DNA-binding transcription factor complexes. Thus, cavitating between 250 and 350 psi is recommended. Figure 2 also shows that a cavitation time of 10 min is sufficient to achieve total cell lysis; 5 min also yields good results, albeit with significant variability.
7. One can practice using distilled water instead of a cell suspension. The entire step should not last more than 10 min for the collection of four samples. It is also sometimes necessary to inject more nitrogen into the bomb, if the pressure goes down to 250 psi after collecting 2–3 samples.
8. No further purification of the nuclei is required, as the current protocol does not yield any unbroken cells that would otherwise co-sediment with the nuclei. Nuclei thus prepared are free from cytoplasmic contamination [6, 24].
9. The final NaCl concentration must not exceed 500–600 mM, as nuclear lysis is likely to occur.
10. We found that adding NaCl after the nuclear pellets have been resuspended (instead of including it in the nuclear extraction buffer, as with conventional protocols) improves the yield of extracted transcription factors significantly.
11. We observed that our modified relaxation buffer, unlike the original formulation, results in the association of about 10–15 % of the granules with the nuclei (as determined by the presence of myeloperoxidase and lactoferrin). These granules are still intact, as evidenced by the consistent lack of transcription factor degradation achieved using our protocol. By comparison, resuspension of nuclear pellets in the presence of high NaCl in the nuclear extraction buffer results in some degradation of the NF-κB and STAT proteins. This possibly reflects the impossibility of adding enough protease inhibitors to neutralize the large quantities of proteases released in a very small volume as the nuclear-bound granules break, presumably during resuspension of the nuclei.
12. Nuclei should not be allowed to extract for longer times, as significant nuclear lysis already occurs at 30 min.
13. Simply placing the samples at −80 °C results in a noticeable loss of activity, and this loss increases after each subsequent

freeze–thaw cycle. By contrast, snap-freezing almost completely prevents this loss.

14. The volume of nuclear extract in the binding mix must not exceed 5 μL or the NaCl concentration will be too high, resulting in unpalatable smearing on the gels. If the samples are too dilute, they can be reconcentrated and desalted using spin columns with an MW cutoff of about 100 kDa, such as the Microcon-100 (Millipore).
15. The signal can sometimes be a little stronger with the control antibody. This has been observed in many studies and is considered normal.

Acknowledgments

This work was supported by grants to PPMcD from the Canadian Institutes for Health Research and the Arthritis Foundation of Canada and to RDY from the National Institutes of Health. PPMcD is a scholar from the Fonds de la recherche en santé du Québec (FRSQ).

References

1. Cassatella MA (1999) Neutrophil-derived proteins: selling cytokines by the pound. Adv Immunol 73:369–509
2. Scapini P, Lapinet-Vera JA, Gasperini S, Calzetti F, Bazzoni F, Cassatella MA (2000) The neutrophil as a cellular source of chemokines. Immunol Rev 177:195–203
3. Ellis TN, Beaman BL (2004) Interferon-gamma activation of polymorphonuclear neutrophil function. Immunology 112:2–12
4. Galligan C, Yoshimura T (2003) Phenotypic and functional changes of cytokine-activated neutrophils. Chem Immunol Allergy 83: 24–44
5. Cheng SS, Kunkel SL (2003) The evolving role of the neutrophil in chemokine networks. Chem Immunol Allergy 83:81–94
6. McDonald PP, Bald A, Cassatella MA (1997) Activation of the NF-κB pathway by inflammatory stimuli in human neutrophils. Blood 89: 3421–3433
7. Bovolenta C, Gasperini S, Cassatella MA (1996) Granulocyte colony-stimulating factor induces the binding of STAT1 and STAT3 to the IFNγ response region within the promoter of the FcγRI/CD64 gene in human neutrophils. FEBS Lett 386:239–242
8. McDonald PP, Bovolenta C, Cassatella MA (1998) Activation of distinct transcription factors in neutrophils by bacterial LPS, interferon-γ, and GM-CSF and the necessity to overcome the action of endogenous proteases. Biochemistry 37:13165–13173
9. McDonald PP, Cassatella MA (1997) Activation of transcription factor NF-kB by phagocytic stimuli in human neutrophils. FEBS Lett 412: 583–586
10. Bovolenta C, Gasperini S, McDonald PP, Cassatella MA (1998) High affinity receptor for IgG (FcγRI/CD64) gene and STAT protein binding to the IFNγ response region (GRR) are regulated differentially in human neutrophils and monocytes by IL-10. J Immunol 160:911–919
11. McDonald PP, Russo MP, Ferrini S, Cassatella MA (1998) Interleukin-15 induces NF-κB activation and IL-8 production in human neutrophils. Blood 92:4828–4835
12. Hayden MS, Ghosh S (2012) NF-κB, the first quarter-century: remarkable progress and outstanding questions. Genes Dev 26:203–234
13. Gilmore TD, Wolenski FS (2012) NF-κB: where did it come from and why? Immunol Rev 246:14–35

14. Stark GR, Darnell JE Jr (2012) The JAK-STAT pathway at twenty. Immunity 36:503–514
15. Kiu H, Nicholson SE (2012) Biology and significance of the JAK/STAT signalling pathways. Growth Factors 30:88–106
16. Dignam JD, Lebovitz RM, Roeder RG (1983) Accurate transcription initiation by RNA polymerase II in a soluble extract from isolated mammalian nuclei. Nucleic Acids Res 11: 1475–1489
17. Borregaard N, Heiple JM, Simons ER, Clark RA (1983) Subcellular localization of the b-cytochrome component of the human neutrophil microbicidal oxidase: translocation during activation. J Cell Biol 97:52–61
18. Nachman R, Hirsch JG, Baggiolini M (1972) Studies on isolated membranes of azurophil and specific granules from rabbit polymorphonuclear leukocytes. J Cell Biol 54:133–140
19. McDonald PP (2004) Transcriptional regulation in neutrophils: teaching old cells new tricks. Adv Immunol 82:1–48
20. Cloutier A, Ear T, Borissevitch O, Larivee P, McDonald PP (2003) Inflammatory cytokine expression is independent of the c-Jun N-terminal kinase/AP-1 signaling cascade in human neutrophils. J Immunol 171:3751–3761
21. Boyum A (1968) Isolation of mononuclear cells and granulocytes from human blood. Scand J Clin Lab Invest Suppl 97:77–89
22. Bradford MM (1976) A rapid and sensitive method for the quantitation of microgram quantities of protein utilizing the principle of protein-dye binding. Anal Biochem 72: 248–254
23. Epling-Burnette PK, Zhong B, Bai F, Jiang K, Bailey RD, Garcia R, Jove R, Djeu JY, Loughran TP Jr, Wei S (2001) Cooperative regulation of Mcl-1 by Janus kinase/STAT and phosphatidylinositol 3-kinase contribute to granulocyte-macrophage colony-stimulating factor-delayed apoptosis in human neutrophils. J Immunol 166:7486–7495
24. Ear T, Cloutier A, McDonald PP (2005) Constitutive nuclear expression of the IκB kinase complex and its activation in human neutrophils. J Immunol 175:1834–1842
25. McDonald PP, Ye RD (2007) Detection of intact transcription factors in human neutrophils. Methods Mol Biol 412:473–486

Part VIII

Neutrophil Defects and Diagnosis

Chapter 30

Disorders of Neutrophil Function: *An Overview*

Mary C. Dinauer

Abstract

Primary disorders of neutrophil function result from impairment in neutrophil responses that are critical for host defense. This chapter summarizes inherited disorders of neutrophils that cause defects in neutrophil adhesion, migration, and oxidative killing. These include the leukocyte adhesion deficiencies, actin defects, and other disorders of chemotaxis, hyperimmunoglobulin E syndrome, Chédiak–Higashi syndrome, neutrophil-specific granule deficiency, chronic granulomatous disease, and myeloperoxidase deficiency. Diagnostic tests and treatment approaches are also summarized for each neutrophil disorder.

Key words *Aspergillus* species, Chédiak–Higashi syndrome, Chronic granulomatous disease, Hyperimmunoglobulin E, Leukocyte adhesion deficiency, Myeloperoxidase, NADPH oxidase, Neutrophil granule, *Staphylococcus aureus*

1 Introduction

This chapter provides a brief overview of disorders of neutrophil function. Neutrophils play an essential role in the initial response to invading bacteria and fungi; thus, patients with defects in neutrophil function typically present in infancy or childhood with recurrent and/or difficult-to-treat bacterial infections [1–4]. Infections typically involve the skin, mucosa, gums, lung, or draining lymph nodes or cause deep tissue abscesses. The microorganisms causing these infections are often unusual or opportunistic pathogens. Many of the disorders have characteristic clinical and microbiological features that are related to the specific nature of the defect in neutrophil function. Note that congenital disorders affecting neutrophil function represent at most 20 % of reported primary immune deficiencies. Thus, patients with suspected disorders of host defense should also be screened for defects in antibody production, T cell function, and complement system. Figure 1 summarizes key steps in the response of neutrophils to invading microbes, which include initial adhesion to the endothelium, subsequent migration toward a site of infection, ingestion of the pathogen, and pathogen killing

Mark T. Quinn and Frank R. DeLeo (eds.), *Neutrophil Methods and Protocols*, Methods in Molecular Biology, vol. 1124,
DOI 10.1007/978-1-62703-845-4_30,

via oxidative metabolites, proteases, and other toxic peptides in neutrophil granules. Disorders of neutrophil function can affect one or more of these pathways (Fig. 1).

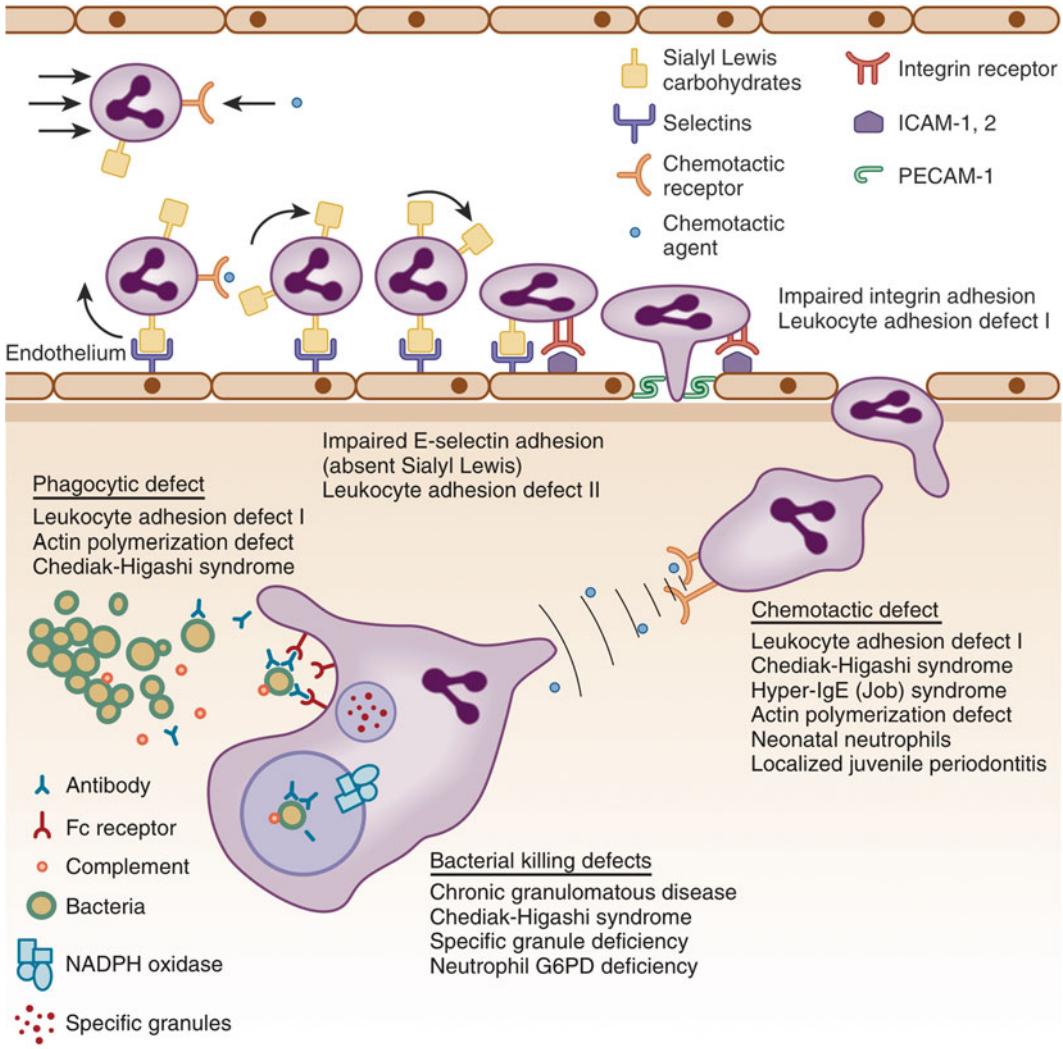

Fig. 1 Steps in the response of circulating neutrophils to infection or inflammation. The adhesion molecule E selectin is upregulated on endothelial cells in response to inflammatory mediators (IL-1, endotoxin, and TNF-α). Neutrophils interact with E-selectins on endothelial cells through sialyl Lewis carbohydrates, resulting in rolling attachment and margination. Chemoattractants, such as IL-8, upregulate neutrophil β2 integrins, which, in turn, mediate tight adhesion to ICAM-1 and PECAM-1 on endothelial cells. Activated neutrophils detect small changes in the chemoattractant gradient, which causes them to move toward the site of tissue infection. Neutrophils phagocytose bacteria opsonized by antibody and complement. Both oxidative and non-oxidative antimicrobial mechanisms mediate bacterial killing. Disorders of phagocyte function associated with each of these steps are listed (reprinted from *Hematology: Basic Principles and Practice*, 6th edition, Mary C. Dinauer and Thomas D. Coates, *Disorders of Phagocyte Function*, Chapter 48, Pages 655–673, Copyright Elsevier, 2012, with permission)

In the diagnostic work-up of a patient with bacterial and fungal infections, a clinician must decide whether a complete evaluation of neutrophil function is warranted. Four key aspects of the patient history with infections should be considered in reaching this decision, namely, frequency, severity, and location of infections and the identity of the causal infectious agent. The presence of unusual features should trigger consideration of a neutrophil disorder. The patient's age and other medical conditions should also be taken into account. For example, one might suspect neutrophil dysfunction if an infectious agent that commonly affects children is observed in an older patient. Distinctive clinical findings can provide helpful guidelines in determining which patients merit further testing and which tests are appropriate. A family history can also provide useful clues.

2 Disorders of Adhesion and Chemotaxis

The ability of neutrophils to adhere to the endothelium, tissue matrix, and invading microbes is essential for their migration from the bloodstream to sites of infection, where they eliminate pathogens. Interactions between cell surface glycoproteins expressed on neutrophils and endothelial cells are fundamental to this process. The initial steps of adhesion require expression of E selectins on the surface of endothelial cells, which bind to fucosylated proteins on leukocytes. The next step involves induction and activation of cell surface integrins on leukocytes, which mediate tight adhesion between neutrophils and endothelial cells. Subsequent migration from capillaries into tissues uses additional cell surface receptors. Defects in these interactions and/or chemotaxis impair recruitment of neutrophils into sites of infection or inflammation, often with relative neutrophilia in peripheral blood yet poor formation of pus.

2.1 Leukocyte Adhesion Deficiency Type I

Leukocyte adhesion deficiency type I (LAD I) is an autosomal recessive disorder characterized by deficiency of three leukocyte glycoproteins that are members of the integrin superfamily of cell surface adhesion molecules (Table 1) and has been reported in hundreds of patients [1, 4–6]. This disorder results from autosomal recessive genetic defects in CD18, the common chain of the β_2 integrin family, which is required for stable expression of three distinct β_2 integrins: CD11a/CD18 (LFA-1; lymphocyte function antigen), CD11b/CD18 (Mac-1), and CD11c/CD18 (p150,95). In LAD I, mutations in the common CD18 chain typically eliminate expression of these three leukocyte glycoprotein complexes. β_2 integrins interact with ICAM-1 proteins expressed on endothelial cells, which are upregulated in response to inflammatory cytokines. Thus, neutrophil adhesion to the endothelium is severely defective

Table 1
Leukocyte adhesion deficiency

	Genetic defect	Clinical presentation	Diagnosis
LAD I	*ITGB2*; encodes CD18 subunit of β_2 integrins, resulting in impaired adhesion, chemotaxis, and neutrophil activation	Skin infection, soft tissue abscesses, delayed separation of umbilical cord and omphalitis, periodontal disease	Flow cytometry for CD11b/CD18 (Mac1)
LAD II	*SLC35C1*; encodes GDP-fucose transporter 1, resulting in impaired expression of fucosylated proteins, including SLeX ligand for selectins	Similar infections to LAD I but not as severe; developmental delay, short stature	Flow cytometry for leukocyte CD15s (SLeX) Bombay (hh) phenotype in red blood cell typing
LAD III	*FERMT3*; encodes kindlin-3, resulting in defective integrin activation and impaired leukocyte and platelet adhesion	Similar to LAD I; also bleeding tendency	Functional assays for neutrophil and platelet adhesion

in LAD I. In addition, Mac-1 is the major receptor for the opsonic complement fragment C3bi, an important trigger for phagocytosis of complement-opsonized microbes. Mac-1 also mediates binding to fibrinogen. Finally, binding to Mac-1 provides an important co-stimulatory signal for activating other pathways important for adhesion, degranulation, and activation of reactive oxidant production [7]. Because of the multiple defects in adhesion-related functions, LAD I patients develop recurrent bacterial and fungal infections, typically with *Staphylococcus aureus* or gram-negative enteric microbes. Characteristic clinical features include frequent skin and periodontal infections, delayed separation of the umbilical cord and omphalitis, and deep tissue abscesses. Neutrophilia with paucity of neutrophils at inflamed or infected sites is characteristic.

Mutations in the CD18 gene in patients with LAD I are heterogeneous. Typically, cell surface expression of the CD11/CD18 heterodimers is absent, although variants with low-level expression have been described; the latter phenotype is associated with reduced severity of disease.

Diagnosis of LAD I is straightforward and can be made by flow cytometry of peripheral blood leukocytes, most often with a monoclonal antibody directed to the CD11b/CD18 heterodimer, Mac-1. Patients with LAD I also have diminished neutrophil migration in vivo. This can be studied with the Rebuck skin window; however, this test is no longer used for diagnostic purposes due to the availability of flow cytometric methods.

Because of the severity of infectious complications, allogeneic hematopoietic stem cell (HSC) transplantation is generally recommended for patients with severe LAD I [1, 4]. Patients with partial expression of LAD I have a longer life expectancy without HSC transplantation but require good supportive care including prophylactic antibiotics and scrupulous dental hygiene. Nevertheless, morbidity from periodontal disease, bacterial infection, and delayed healing are still problematic.

2.2 Leukocyte Adhesion Deficiency Types II and III

Two other autosomal recessive forms of leukocyte adhesion deficiency associated with distinct clinical and genetic defects have been described in a small number of patients (Table 1) [4, 5]. Leukocyte adhesion deficiency type II (LAD II) is very rare (fewer than ten patients) and caused by mutations in the membrane transporter for fucose, leading to loss of expression of fucosylated glycans on the cell surface. This disorder is also known as congenital disorder of glycosylation type IIc (CDG-IIc). Fucosylated proteins, such as sialyl Lewis X (CD15s), are ligands for endothelial selectins and are important for the early phases of adhesion to endothelial cells. Patients with LAD II also have leukocytosis and form pus poorly, although infections tend to be less severe in LAD II patients compared to LAD I patients. In addition, LAD II patients have severe mental retardation and short stature, and the absence of fucosylated proteins on the surface of red blood cells results in the Bombay (hh) red cell phenotype. LAD II is readily diagnosed by flow cytometry for expression of leukocyte CD15s. Prolonged therapy with oral fucose has been beneficial in some but not all LAD II patients.

Leukocyte adhesion deficiency type III (LAD III) has been described in about 20 patients to date [4, 5]. LAD III is characterized by defects in the activation of multiple classes of integrins downstream of G-protein-coupled receptors due to mutations in kindlin-3, a hematopoietic protein that regulates integrin activation. The phenotype of this disorder is similar to LAD I but is also associated with defects in integrin-mediated platelet aggregation and excessive bleeding similar to Glanzmann thrombasthenia. The diagnosis of LAD III should be considered in patients with the clinical features of LAD I but normal expression of β_2 integrins. Defective platelet aggregation can be evaluated using readily available clinical laboratory blood tests. Evaluation of leukocyte adhesion in such patients requires specialized functional assays that are usually carried out in research laboratories.

2.3 Defect in Adhesion and Chemotaxis Due to Mutation in Rac2 GTPase

A dominant-negative mutation in the Rac2 GTPase was described in an infant with impaired neutrophil adhesion and motility, along with decreased NADPH oxidase activation and degranulation in response to chemoattractants [8, 9]. Symptoms similar to LAD I developed in the first months of life. Leukocyte β_2 integrin expression was normal, and the phenotype presumably results from

interference by the mutant Rac2 in Rac-regulated signaling pathways. This patient successfully underwent HSC transplantation. A similar patient with severe, recurrent skin and tissue abscesses, normal leukocyte β_2 integrin expression, and similar neutrophil function defects in response to chemoattractants died in infancy without determination of the genetic defect [10].

2.4 Other Genetic Disorders of Chemotaxis

Several rare human diseases characterized primarily by prominent defects in neutrophil chemotaxis have been described. In general, the neutrophils in these patients exhibit normal adhesive properties. Patients typically present with recurrent, severe skin and soft tissue infections in infancy. One patient exhibited markedly abnormal polymerization of neutrophil actin and higher than normal expression of an actin-binding protein [11, 12]. A young female patient is reported to have a heterozygous point mutation in β-actin and impaired binding to actin-regulatory proteins [13]. The phenotype of this patient includes recurrent infections, mental retardation, and photosensitivity.

Localized juvenile periodontitis (LJP) is a rare disorder of unknown etiology that presents in children and adolescents as chronic and recurrent periodontal infections and severe alveolar bone loss [14, 15]. This disorder is heterogeneous and is associated with defective neutrophil chemotaxis in vitro. Some cases are sporadic, but others appear to be familial and thus may be linked to genetic defects. Children or teenagers who present with periodontal disease should be carefully evaluated for neutropenia or disorders of neutrophil function, since these are frequently associated with periodontal disease. LJP is diagnosed by its characteristic clinical features, the absence of non-periodontal infections, normal neutrophil counts and morphology, normal expression of β_2 integrins, and normal oxidative burst.

Hyperimmunoglobulin E (hyper-IgE or HIES) syndrome is characterized by elevated serum levels of IgE (i.e., ≥2,000 IU-mL) and recurrent *Staphylococcal* infections of the skin and lung, pneumatoceles, chronic dermatitis, and skeletal and dental abnormalities [16–18]. Patients with this syndrome have variable and often profound defects in neutrophil chemotaxis, which are independent of fluctuations in serum IgE. Localized *Staphylococcal* infections are indolent and lack the usual characteristics of inflammation ("cold" abscesses). Chronic candidiasis of the mucosal surface and nail beds, hyperextensible joints, and scoliosis are also frequently observed, and delay or failure to shed the primary teeth is not uncommon. Many patients have coarse facial features by early adolescence. Inherited or sporadic autosomal dominant mutations in *STAT3* account for the majority of cases of HIES. STAT3 is a Janus kinase (JAK)-activated transcription factor utilized downstream of many cytokines and growth factors. HIES-associated mutations in

STAT3 involve DNA- or protein-binding domains, resulting in interference with the function of wild-type STAT3. Rare forms of HIES result from autosomal recessive mutations in either *DOCK8* or *TYK2*, which encode proteins regulating leukocyte signaling, and are additionally associated with profound lymphocyte function defects. The relationship between the immunologic abnormalities, neutrophil chemotactic defects, and other features of HIES is only now emerging. STAT3-dependent responses to both pro-inflammatory and anti-inflammatory cytokines are altered. Differentiation of T helper type 17 (Th17) lymphocytes, which are important for control of Candida, are impaired. High serum IgE levels may reflect a T-lymphocyte imbalance, which causes abnormally high production of IgE. Diagnostically, the hallmark laboratory finding in hyper-IgE syndrome is the marked elevation of serum IgE, especially in children or young adults. DNA testing should be used to confirm the diagnosis of HIES. Antibiotic prophylaxis for Staphylococcal infection is beneficial in patients with hyper-IgE syndrome. Atopic dermatitis is the major differential diagnosis, as it can also be associated with eosinophilia and elevated serum IgE.

2.5 Non-inherited Disorders of Neutrophil Chemotaxis

A chemotactic abnormality, detected by in vitro assay, has been reported in neonatal neutrophils [19, 20]. This abnormality may be due in part to defects in cellular adhesion and impaired mobilization and activation of intracellular adhesion proteins at the cell surface. Reduced neutrophil chemotaxis has also been described in burn victims and in patients with bacterial sepsis or diabetes. However, the chemotactic defects in these settings are variable, and their contribution to associated infectious complications is uncertain.

3 Disorders of Ingestion and Degranulation

Following phagocytosis, neutrophil granules fuse with phagosome membranes and release proteases, enzymes, and antibacterial proteins into the phagosome lumen. This process greatly facilitates microbial killing. In LAD I patients, C3bi-opsonized microbes fail to be ingested, because CD11b/CD18 (Mac-1), the receptor for C3bi, is not expressed. This receptor also provides an important co-stimulatory signal for Fcγ receptor-mediated phagocytosis. Deficiency of opsonization with complement is seen in serum complement deficiencies, and primary B cell deficiencies, such as Bruton's agammaglobulinemia, result in defective opsonization with specific immunoglobulins. Thus, these patients can present with recurrent infections with pyogenic bacteria, such as *S. aureus*, *Pneumococci*, and *H. influenzae*. In contrast, primary neutrophil

defects causing disorders of ingestion and/or degranulation are very rare. Two such genetic disorders affecting neutrophil granules have been described (see below), both of which are associated with increased frequency of bacterial infections.

3.1 Chédiak–Higashi Syndrome

Chédiak–Higashi syndrome is a rare autosomal recessive disorder associated with widespread defects in granule morphogenesis and multi-organ pathology, including ineffective granulopoiesis, moderate neutropenia, and delayed and incomplete degranulation [21–23]. Neutrophils from patients with Chédiak–Higashi syndrome have giant peroxidase-positive granules that appear to be a coalescence of azurophilic and specific granules. The giant granules are often more prominent in bone marrow neutrophils than in peripheral blood neutrophils. Giant granules are also seen in lymphocytes and natural killer cells from patients with Chédiak–Higashi syndrome. Patients with Chédiak–Higashi syndrome experience frequent *S. aureus* infections in lung and skin and develop gingivitis and periodontitis. Patients also have partial oculocutaneous albinism, a mild tendency to bleed and neuropathies. These manifestations are all related to abnormal granule morphogenesis. Chédiak–Higashi syndrome is caused by mutations in *CHS1*, which encodes a large protein thought to regulate lysosomal and granule trafficking. Supportive care with prophylactic antibiotics is a mainstay of treatment. Of importance, Chédiak–Higashi syndrome is a cause of inherited hemophagocytic histiocytosis (HLH), which results from the granule defects in natural killer cells and other lymphocytes and can be precipitated by viral infections including Epstein–Barr virus [23]. The majority of Chédiak–Higashi syndrome patients that survive childhood develop this HLH. In this phase of the disease, which was often referred to as the "accelerated phase," patients experience fever, lymphadenopathy, lymphohistiocytic infiltration, and progressive pancytopenia, which is fatal unless treated with allogeneic HSC transplantation.

3.2 Neutrophil-Specific Granule Deficiency

Neutrophil-specific granule deficiency (SGD) is a very rare disorder characterized by the absence of specific or secondary granules in developing neutrophils [24, 25]. Neutrophils from SGD patients also typically have morphologically abnormal bilobed nuclei. SGD neutrophils are markedly deficient in many important microbicidal granule proteins, including lactoferrin and the defensins. SGD neutrophils also demonstrate relatively severe chemotactic defects, which are thought to result from a decrease in the pool of intracellular leukocyte adhesion molecules normally mobilized to the cell surface in response to inflammatory stimuli. SGD patients present with recurrent and difficult-to-treat bacterial and fungal infections, primarily involving the skin and lungs. *S. aureus*, enteric gram-negative bacteria, *P. aeruginosa*, and *Candida albicans* are

the major pathogens. This disorder appears to be inherited in an autosomal recessive manor. The molecular defect responsible for some cases of SGD involves the myeloid transcription factor C/EBPε [25, 26]. C/EBPε plays an important role as a gene-specific transcriptional regulator during late promyelocyte and early myelocyte development. The diagnosis of SGD is made if microscopic examination of neutrophils reveals the absence of specific granules. The diagnosis can be confirmed by assessing expression of granule-specific proteins (i.e., lactoferrin or gelatinase) by staining or other assays. Treatment of SGD is supportive, with prophylactic antibiotics and prompt and prolonged treatment of infections.

4 Disorders of Oxidative Metabolism

Reactive oxygen species play an important role in killing microbial pathogens. The major source of reactive oxygen species is the phagocyte respiratory burst pathway, which is activated in response to phagocytosis or soluble inflammatory stimuli. The initial reaction in this pathway is catalyzed by an NADPH oxidase, which is found in plasma and phagosome membranes of neutrophils, monocytes/macrophages, and eosinophils. NADPH oxidase produces the superoxide free radical by catalyzing the transfer of electrons from NADPH to molecular oxygen. Superoxide is converted to hydrogen peroxide and, in the presence of neutrophil myeloperoxidase, HOCl, in addition to numerous other microbicidal oxidants that synergize with granule proteins to kill microbes in the neutrophil phagosome. Thus, patients lacking key steps in the respiratory burst pathway are deficient in microbial killing and develop recurrent and severe infections. These infections typically involve microorganisms for which oxidant-mediated killing is particularly critical for effective host defense.

4.1 Chronic Granulomatous Disease

Chronic granulomatous disease (CGD) is a group of inherited disorders caused by defects in the phagocyte NADPH oxidase complex. Genetic defects in four critical subunits of NADPH oxidase cause CGD, and these mutations lead to complete or, less frequently, partial loss of NADPH oxidase activity [1, 27–35]. The estimated incidence of CGD is approximately 1 in 200,000 live births, and it is the most common clinically significant inherited disorder of neutrophil function. Because respiratory burst oxidants are an important component of microbial killing mechanisms, CGD patients suffer recurrent, often life-threatening bacterial and fungal infections. An additional and distinctive hallmark of CGD is the formation of inflammatory granulomas and other inflammatory complications.

Table 2
Genetic defects in NADPH oxidase subunits in chronic granulomatous disease

Subunit	Inheritance	Gene locus and affected gene	Function	Mutations	Frequency in CGD
gp91^{phox} (NOX2)	X	Xp21.1 *CYBB*	Integral membrane glycoprotein; contains flavoprotein domain and heme groups for electron transport	Heterogeneous, most with absent flavocytochrome b_{558}	~70 %
gp22^{phox}	AR	16p24 *CYBA*	Integral membrane protein, flavocytochrome subunit; contains docking site for p47^{phox}	Heterogeneous, most with absent flavocyto-chrome b_{558}	~5 %
p47^{phox}	AR	7q11.23 *NCF1*	Cytosolic protein, activated by phosphorylation, mediates translocation of p67^{phox} to flavocytochrome b_{558}	Majority with GT deletion in exon 2; absent expression of p47^{phox}	~25 %
p67^{phox}	AR	1q25 *NCF2*	Cytosolic protein, activates electron transport after translocation	Heterogeneous, most with absent expression of p67^{phox}	~5 %
p40^{phox}	AR	22q13.1 *NCF4*	Cytosolic protein, regulates phagosome membrane NADPH oxidase through binding to phosphatidylinositol 3-phosphate	A single patient described to date, with a missense and a frameshift mutation	1 patient

Five polypeptide subunits are essential for NADPH oxidase function, and mutations in the corresponding genes are responsible for the different genetic subgroups of CGD (Table 2). These NADPH subunits are referred to by their apparent molecular mass (kDa) and the designation *phox* (phagocyte oxidase). Approximately 70 % of CGD cases result from X-linked recessive defects in the gene encoding the gp91^{phox} subunit of flavocytochrome b_{558}, a membrane heterodimer that is the redox center of NADPH oxidase. This subunit contains both flavoprotein- and heme-binding domains and is also sometimes referred to as NOX2 (NOX, NADPH oxidase; 2, referring to its number in a series of homologous flavocytochromes) [36]. An uncommon autosomal recessive form of CGD is associated with mutations in the gene encoding p22^{phox}, which mediates translocation of two regulatory subunits of

NADPH oxidase, $p47^{phox}$ and $p67^{phox}$. Mutations in genes encoding $p47^{phox}$, $p67^{phox}$, or $p40^{phox}$ are affected in three other autosomal recessive subgroups of CGD. $p47^{phox}$ binds $p22^{phox}$ and acts as an adapter protein for recruitment and positioning of the $p67^{phox}$ subunit, which contains an activation domain that stimulates electron transport through flavocytochrome *b*. A single patient with defects in the gene encoding $p40^{phox}$ has been reported [30]. This subunit plays a selective role in stimulating NADPH oxidase activity on phagosome membranes via a domain that binds to the membrane lipid phosphatidylinositol 3-phosphate. Mutations in the genes encoding the flavocytochrome *b* subunits and $p67^{phox}$ are heterogeneous and cause deficient expression of the affected subunit. In patients with $p47^{phox}$ mutations, a deletion of a GT dinucleotide at the start of exon 2 in the $p47^{phox}$ gene is frequently seen, which results from recombination with a closely linked pseudogene. This deletion causes a frameshift and premature stop codon that terminates translation of the $p47^{phox}$ mRNA transcript [37].

NADPH oxidase activity also requires activated Rac, which binds to and activates $p67^{phox}$. As described above, a dominant-negative mutation in the Rac2 GTPase has been reported, which inhibits NADPH oxidase activity in response to certain agonists. However, the clinical phenotype resembled leukocyte adhesion deficiency rather than CGD, reflecting the important role for Rac2 in regulating the neutrophil cytoskeleton, adhesion, and motility.

Patients with CGD typically present in infancy or early childhood with recurrent infections involving the skin, lung, and draining lymph nodes; liver abscesses and osteomyelitis also develop due to hematogenous spread of microorganisms [1]. *S. aureus* is the most common microbe involved, but CGD patients are also prone to infection by opportunistic pathogens such as *Burkholderia cepacia*, *Serratia marcescens*, *Aspergillus* species, and *Nocardia*. Many of these organisms express catalase, which removes microbe-generated hydrogen peroxide and thus inhibits ROS-mediated killing in the phagosomes of CGD cells. The lymph nodes, liver, and spleen of CGD patients can become enlarged. CGD patients can also develop chronic inflammatory granulomas, which are a hallmark of this subgroup of neutrophil disorders. Chronic inflammatory granulomas can obstruct the gastric outlet or the urinary tract or cause granulomatous colitis and the symptoms of inflammatory bowel disease. These chronic inflammatory complications are thought to reflect an important role for superoxide in down-regulating the inflammatory response. Patients with X-linked CGD or autosomal recessive CGD involving the $p22^{phox}$ or $p67^{phox}$ subunits have a more severe clinical course than individuals with $p47^{phox}$-deficient CGD [32]. In the latter subgroup, very low levels of superoxide activity are often still detectable [38], which may explain the typically milder clinical course. Polymorphisms in oxygen-independent antimicrobial defense mechanisms or other

components of the innate immune response are also thought to modify the severity of CGD in some patients [39].

The diagnosis of CGD is made by measuring respiratory burst activity in neutrophils. The nitroblue tetrazolium test (NBT) using peripheral blood neutrophils is the classic method, in which the soluble yellow dye NBT is reduced by activated neutrophils, forming insoluble dark purple formazan deposits. However, a flow cytometry assay, based on oxidation of dihydrorhodamine 123 (DHR) by activated neutrophils, is increasingly replacing the NBT test for diagnosis in clinical laboratories [38, 40]. Both the NBT and DHR tests identify two populations of neutrophils in female carriers of X-linked CGD. Neutrophils that lack functional $p47^{phox}$ can make a small amount of superoxide, and therefore NBT and DHR assays can be weakly positive in this form of CGD. Chemiluminescence-based assays for respiratory burst activity are also occasionally used for clinical diagnosis. Family history and carrier testing will frequently discriminate between X-linked and autosomal recessive forms of CGD. However, approximately 10 % of patients with X-linked CGD carry new mutations. Molecular genetic testing is commercially available for all five subgroups of CGD and is recommended unless the subgroup is known based on prior family testing.

All forms of CGD are treated similarly. Prophylactic trimethoprim-sulfamethoxazole (or dicloxacillin in sulfa-allergic patients) as antibiotic prophylaxis is a mainstay of treatment. Recent studies show that daily itraconazole reduces the incidence of *Aspergillus* infections, a serious complication of CGD [41]. Thus, prophylactic itraconazole is now recommended for routine use. Prophylactic interferon gamma, which is thought to enhance non-oxidative phagocyte functions, is also recommended for routine use, based on reports that it substantially decreases infectious complications in CGD patients [42, 43]. With optimal medical management, including aggressive treatment of acute infections, the mortality for CGD is now estimated to be approximately 2 % per patient per year [43]. Allogeneic HSC transplantation has also been used to treat CGD [31]. Despite improved success rates and reduced complications of graft-versus-host disease and other transplant-associated toxicities, use of this procedure remains an individualized decision. Gene replacement therapy targeted at HSC is currently under development [44].

4.2 Myeloperoxidase Deficiency

Myeloperoxidase (MPO) deficiency is the most common inherited disorder of phagocytes, with complete deficiency occurring in approximately 1 in 4,000 individuals [45]. However, MPO deficiency is rarely associated with clinical symptoms. MPO is inherited in an autosomal recessive manner and is caused by mutations in the MPO gene on chromosome 17. Mutations in the MPO gene are frequently point mutations that cause defective

posttranslational processing of the MPO precursor protein. Deficiency in myeloperoxidase inhibits formation of hypochlorous acid from chloride and hydrogen peroxide. There is a remarkable lack of clinical symptoms in most individuals with MPO deficiency, despite in vitro defects in the ability to kill *C. albicans* and *Aspergillus fumigatus* hyphae. Bacterial killing in vitro is also slower than normal. Nevertheless, patients with MPO deficiency rarely develop symptoms unless they also suffer from diabetes mellitus, which leads to disseminated candidiasis and other fungal infections. Diagnosis of MPO deficiency is straightforward using histochemical analysis of peroxidase activity. Because patients with MPO deficiency are typically asymptomatic, no prophylactic antibiotics are prescribed. Individuals with MPO deficiency and diabetes are usually treated aggressively to prevent fungal infections.

4.3 Neutrophil Glucose-6-Phosphate Dehydrogenase Deficiency

NADPH, the primary substrate for the superoxide-generating NADPH oxidase, is generated by the first two reactions of the hexose monophosphate shunt pathway, catalyzed by glucose-6-phosphate dehydrogenase (G6PD) and 6-phosphogluconate dehydrogenase (6PGD). The leukocyte and erythrocyte G6PD are encoded by the same gene. However, the only symptom of vast majority of individuals with inherited G6PD deficiency is red cell hemolysis triggered by oxidative stress [46]. Most G6PD mutations cause a gradual decay in G6PD, which has little or no impact in short-lived neutrophils; in contrast, longer lived erythrocytes are severely affected by loss of G6PD activity. Even most of the more unstable G6PD variants that cause chronic non-spherocytic hemolytic anemia even in the absence of oxidative stress do not result in critically low levels of NADPH in neutrophils. A few rare G6PD mutations lead to extremely low levels of G6PD in both neutrophils and erythrocytes, resulting in chronic, severe hemolytic anemia and CGD-like symptoms; these combined features clearly distinguish this very rare form of NADPH oxidase deficiency from CGD.

References

1. Dinauer MC, Coates TD (2012) Disorders of phagocyte function. In: Hoffman (ed) Hematology: basic principles and practice. Elsevier, Philadelphia, Pa, pp 655–673
2. Lekstrom-Himes JA, Gallin JI (2000) Immunodeficiency diseases caused by defects in phagocytes. N Engl J Med 343: 1703–1714
3. Dale DC et al (2008) The phagocytes: neutrophils and monocytes. Blood 112:935–945
4. Bouma G et al (2010) Recent advances in the understanding of genetic defects of neutrophil number and function. Br J Haematol 151:312–326
5. Hanna S, Etzioni A (2012) Leukocyte adhesion deficiencies. Ann N Y Acad Sci 1250:50–55
6. van de Vijver E et al (2012) Hematologically important mutations: leukocyte adhesion deficiency (first update). Blood Cells Mol Dis 48:53–61
7. Schymeinsky J et al (2007) Neutrophil activation via beta2 integrins (CD11/CD18): molecular mechanisms and clinical implications. Thromb Haemost 98:262–273

8. Ambruso DR et al (2000) Human neutrophil immunodeficiency syndrome is associated with an inhibitory Rac2 mutation. Proc Natl Acad Sci USA 97:4654–4659
9. Williams DA et al (2000) Dominant negative mutation of the hematopoietic-specific Rho GTPase, Rac2, is associated with a human phagocyte immunodeficiency. Blood 96:1646–1654
10. Roos D et al (1993) A novel syndrome of severe neutrophil dysfunction: unresponsiveness confined to chemotaxin-induced functions. Blood 81:2735–2743
11. Coates TD et al (1991) An inherited defect of neutrophil motility and microfilamentous cytoskeleton associated with abnormalities in 47-Kd and 89-Kd proteins. Blood 78: 1338–1346
12. Howard T et al (1994) The 47-kD protein increased in neutrophil actin dysfunction with 47- and 89-kD protein abnormalities is lymphocyte-specific protein. Blood 83: 231–241
13. Nunoi H et al (1999) A heterozygous mutation of beta-actin associated with neutrophil dysfunction and recurrent infection. Proc Natl Acad Sci USA 96:8693–8698
14. Van Dyke TE, Vaikuntam J (1994) Neutrophil function and dysfunction in periodontal disease. Curr Opin Periodontol 28:19–27
15. Oh TJ et al (2002) Periodontal diseases in the child and adolescent. J Clin Periodontol 29:400–410
16. Grimbacher B et al (1999) Hyper-IgE syndrome with recurrent infections: an autosomal dominant multisystem disorder. N Engl J Med 340:692–702
17. Sowerwine KJ et al (2012) Hyper-IgE syndrome update. Ann N Y Acad Sci 1250:25–32
18. Zhang Q, Su HC (2011) Hyperimmunoglobulin E syndromes in pediatrics. Curr Opin Pediatr 23:653–658
19. Koenig JM, Yoder MC (2004) Neonatal neutrophils: the good, the bad, and the ugly. Clin Perinatol 31:39–51
20. Hill HR (1987) Biochemical, structural, and functional abnormalities of polymorphonuclear leukocytes in the neonate. Pediatr Res 22:375–382
21. Kaplan J et al (2008) Chediak-Higashi syndrome. Curr Opin Hematol 15:22–29
22. Introne WJ et al (2010) Chediak-Higashi syndrome. In: Pagon RA, Bird TD, Dolan CR, Stephens K, Adam MP (eds) GeneReviews. University of Washington, Seattle, WA
23. Janka GE (2012) Familial and acquired hemophagocytic lymphohistiocytosis. Annu Rev Med 63:233–246
24. Gallin JI (1985) Neutrophil specific granule deficiency. Annu Rev Med 36:263–274
25. Gombart AF, Koeffler HP (2002) Neutrophil specific granule deficiency and mutations in the gene encoding transcription factor C/EBP(epsilon). Curr Opin Hematol 9:36–42
26. Lekstrom-Himes JA et al (1999) Neutrophil-specific granule deficiency results from a novel mutation with loss of function of the transcription factor CCAAT/enhancer binding protein epsilon. J Exp Med 189:1847–1852
27. Dinauer MC (2005) Chronic granulomatous disease and other disorders of phagocyte function. Hematology Am Soc Hematol Educ Program 2005:89–95
28. Seger RA (2008) Modern management of chronic granulomatous disease. Br J Haematol 140:255–266
29. Schappi MG et al (2008) Hyperinflammation in chronic granulomatous disease and anti-inflammatory role of the phagocyte NADPH oxidase. Semin Immunopathol 30:255–271
30. Matute JD et al (2009) A new genetic subgroup of chronic granulomatous disease with autosomal recessive mutations in p40 phox and selective defects in neutrophil NADPH oxidase activity. Blood 114:3309–3315
31. Kang EM et al (2011) Chronic granulomatous disease: overview and hematopoietic stem cell transplantation. J Allergy Clin Immunol 127:1319–1326
32. Kuhns DB et al (2010) Residual NADPH oxidase and survival in chronic granulomatous disease. N Engl J Med 363:2600–2610
33. Roos D et al (2010) Hematologically important mutations: the autosomal recessive forms of chronic granulomatous disease (second update). Blood Cells Mol Dis 44:291–299
34. Roos D et al (2010) Hematologically important mutations: X-linked chronic granulomatous disease (third update). Blood Cells Mol Dis 45:246–265
35. Bustamante J et al (2011) Germline CYBB mutations that selectively affect macrophages in kindreds with X-linked predisposition to tuberculous mycobacterial disease. Nat Immunol 12:213–221
36. Al Ghouleh I et al (2011) Oxidases and peroxidases in cardiovascular and lung disease: new concepts in reactive oxygen species signaling. Free Radic Biol Med 51:1271–1288

37. Roesler J et al (2000) Recombination events between the p47-phox gene and its highly homologous pseudogenes are the main cause of autosomal recessive chronic granulomatous disease. Blood 95:2150–2156
38. Vowells SJ et al (1996) Genotype-dependent variability in flow cytometric evaluation of reduced nicotinamide adenine dinucleotide phosphate oxidase function in patients with chronic granulomatous disease. J Pediatr 128:104–107
39. Foster CB et al (1998) Host defense molecule polymorphisms influence the risk for immune-mediated complications in chronic granulomatous disease. J Clin Invest 102: 2146–2155
40. Vowells SJ et al (1995) Flow cytometric analysis of the granulocyte respiratory burst: a comparison study of fluorescent probes. J Immunol Methods 178:89–97
41. Gallin JI et al (2003) Itraconazole to prevent fungal infections in chronic granulomatous disease. N Engl J Med 348:2416–2422
42. Marciano BE et al (2004) Long-term interferon-gamma therapy for patients with chronic granulomatous disease. Clin Infect Dis 39:692–699
43. The International Chronic Granulomatous Disease Cooperative Study Group (1991) A controlled trial of interferon gamma to prevent infection in chronic granulomatous disease. N Engl J Med 324:509–516
44. Grez M et al (2011) Gene therapy of chronic granulomatous disease: the engraftment dilemma. Mol Ther 19:28–35
45. Klebanoff SJ et al (2013) Myeloperoxidase: a front-line defender against phagocytosed microorganisms. J Leukoc Biol 93:185–198
46. Beutler E (1994) G6PD deficiency. Blood 84:3613–3636

Chapter 31

Diagnostic Assays for Chronic Granulomatous Disease and Other Neutrophil Disorders

Houda Zghal Elloumi and Steven M. Holland

Abstract

Inasmuch as neutrophils are the primary cellular defense against bacterial and fungal infections, disorders that affect these white cells typically predispose individuals to severe and recurrent infections. Therefore, diagnosis of such disorders is an important first step in directing long-term treatment/care for the patient. Herein, we describe methods to identify chronic granulomatous disease, leukocyte adhesion deficiency, and neutropenia. The assays are relatively simple to perform and cost effective and can be performed with equipment available in most laboratories.

Key words Chronic granulomatous disease (CGD), Chemiluminescence, Leukocyte adhesion deficiency (LAD), Neutropenia, Nitroblue tetrazolium, Reactive oxygen species, Superoxide

1 Introduction

Neutrophils play a key role in protecting the body, utilizing a wide array of oxygen-dependent and oxygen-independent microbicidal weapons to destroy and remove infectious agents [1]. Oxygen-dependent mechanisms involve the production of reactive oxygen species (ROS), which can be microbicidal [2], while oxygen-independent mechanisms include most other neutrophil functions, such as chemotaxis, phagocytosis, degranulation, and release of lytic enzymes and bactericidal peptides [3]. Thus, it is important to consider and evaluate various neutrophil functions when patients present from recurrent and/or hard-to-treat bacterial and fungal infections [4].

The importance of neutrophil ROS production is exemplified by chronic granulomatous disease (CGD), a disorder first described in 1957 [5]. CGD is characterized by recurrent, life-threatening bacterial and fungal infections and tissue granuloma formation. CGD is caused by mutation in any of the five components of the NADPH oxidase, formed by proteins of the *ph*agocyte *ox*idase

Mark T. Quinn and Frank R. DeLeo (eds.), *Neutrophil Methods and Protocols*, Methods in Molecular Biology, vol. 1124,
DOI 10.1007/978-1-62703-845-4_31,

complex (gp91^{phox}, p22^{phox}, p47^{phox}, p67^{phox}, p40^{phox}), and is diagnosed by analysis of neutrophil function using one of several assays that measure the capability of neutrophils to produce superoxide anion, hydrogen peroxide, or bleach. As detailed in this chapter, neutrophil ROS production can be measured spectrophotometrically by ferricytochrome c reduction, microscopically using nitroblue tetrazolium reduction, with a flow cytometer, and by other methods based on chemiluminescence or electron-spin resonance. Kinetics of O_2^- production can also be followed by ferricytochrome c reduction or chemiluminescence assays. Immunoblotting is typically used to determine which gene of the NADPH oxidase complex (i.e., gp91^{phox}, p47^{phox}, p22^{phox}, p67^{phox}, or p40^{phox}) is defective [6]. Genomic or complementary DNA (cDNA) sequencing is then used to specify mutations. Since protein-positive mutations exist in each gene, immunoblotting alone is a good, but not infallible, guide for identifying the affected gene.

Leukocyte adhesion deficiency (LAD) is caused by defects in cellular adhesion and function. LAD-1 is an autosomal recessive disorder resulting from mutations in the gene encoding CD18 (*ITGB2*), the common β subunit for all the β_2 integrins [7]. CD18 associates with CD11a to form LFA-1, with CD11b to form Mac-1, and with CD11c to form p150,95. β_2 integrins are expressed as inactive adhesion receptors that undergo conversion to their active form with stimulation to mediate leukocyte motility and adhesion. We describe diagnostic assays to measure β_2 integrin expression, cell adhesion, and chemotaxis.

Neutropenia is characterized by reduction of the absolute neutrophil count (ANC) below 1,500 neutrophils/mm^3 [8]. Cyclic and severe congenital neutropenias are characterized by early maturation arrest of myelopoiesis [9], and mutations in the gene encoding neutrophil elastase have been associated with both forms [10]. Neutropenia in peripheral blood can be associated with retention of mature neutrophils in bone marrow, as in the case of the autosomal dominant WHIM syndrome (warts, hypogammaglobulinemia, immunodeficiency, myelokathexis), which is due to heterozygous mutations of the chemokine receptor CXCR4 [11, 12]. Neutropenia can also be autoimmune due to the formation of autoantibodies against a variety of neutrophil antigens (HNA). These autoantibodies can be detected in patient serum by the granulocyte immunofluorescence test (GIFT) [13].

2 Materials

2.1 Diagnostic Assays for Chronic Granulomatous Disease

1. Phorbol 12-myristate 13-acetate (PMA) solution: 1 mg/mL PMA stock solution in dimethyl sulfoxide (DMSO). Aliquot and store at –20 °C.
2. Dulbecco's modified Eagle's medium (DMEM).

3. Phosphate-buffered saline (PBS), pH 7.2.
4. HBSS–: Hank's balanced salt solution (HBSS) without Ca^{2+}, Mg^{2+}, and phenol red.
5. HBSS+: HBSS with Ca^{2+} and Mg^{2+}.
6. RPMI 1640 media.
7. 1 % safranin O solution or Giemsa stain.
8. Nitroblue tetrazolium (NBT) solution: 100 mg/mL NBT in 70 % dimethylformamide (v/v).
9. 2 M Potassium hydroxide (KOH) solution: 56 g of KOH in sterile H_2O (500 mL final volume).
10. Superoxide dismutase (SOD): 400 μg/mL stock solution in PBS or HBSS–. Aliquot and store at –20 °C.
11. 2-(4-iodophenyl)-3-(2,4-disulfophenyl)-5-2H-tetrazolium, monosodium salt (WST-1; Dojindo Laboratories): 10 mM stock solution in PBS or HBSS–. Protect from light.
12. Horse heart ferricytochrome c: 1 mM stock solution in PBS or HBSS–. Aliquot and store at –20 °C.
13. Catalase: 1 mg/mL stock solution in PBS or HBSS–. Aliquot and store at –20 °C.
14. Lucigenin (Molecular Probes): 250 μM stock solution in PBS.
15. Incubation buffer: RPMI 1640, 10 mM HEPES, pH 7.4, 10 % fetal calf serum.
16. Lysis buffer: 829 mg ammonium chloride, 100 mg potassium bicarbonate, and 3.7 mg EDTA in 100 mL of distilled H_2O.
17. Flow buffer: 500 mL of HBSS–, 0.5 g of albumin (human fraction V), 1 mL of 0.5 M EDTA.
18. Dihydrorhodamine-123 (DHR) solution: 1 M DHR in DMSO. For experiments, make a working stock by diluting 10 μL of the stock solution in 990 μL PBS for a final concentration of 1 mM.
19. 2′,7′-dichlorofluorescein 3′,6′-diacetate (DCFH-DA): 1 M DCFH-DA in DMSO. For experiments, make a working stock by diluting 10 μL of the stock solution in 490 μL PBS for a final concentration of 2 mM.
20. 12- and 24-well tissue culture plates.
21. 5-(diethoxyphosphoryl)-5-methyl-1-pyrroline *N*-oxide (DEPMPO).

2.2 Diagnostic Assays for Leukocyte Adhesion Deficiency

1. PBS, pH 7.2.
2. Bovine serum albumin (BSA), fraction V.
3. FACS buffer: PBS containing 3 % BSA (w/v) and 0.1 % w/v sodium azide.
4. 2,7-bis-(2-carboxyethyl)-5-(and-6)-carboxyfluorescein, acetoxymethyl ester fluorescent dye (BCECF, Molecular Probes).

5. Polycarbonate-permeable transwell filters with 5 μm pore size and a surface area of 0.33 cm^2 (Costar).
6. Polystyrene round-bottom tubes.
7. Anti-CD18 monoclonal antibody: Can be selected from a variety of sources and can be unlabeled or conjugated directly with fluorochrome.
8. Mouse IgG or IgM.
9. Fluorophore-conjugated secondary antibody: Can be selected from a variety of sources (*see* **Note 1**).
10. Adhesion buffer: RPMI 1640, 10 mM HEPES, pH 7.4, 10 % fetal calf serum (v/v).
11. $MgCl_2$/EDTA solution: 100 mM $MgCl_2$ and 20 mM EGTA in PBS.
12. $MnCl_2$ solution: 10 mM $MnCl_2$ in PBS.

2.3 Diagnostic Assays for Neutropenia

1. Vacutainer tubes containing EDTA (Becton-Dickinson).
2. PBS, pH 7.2.
3. PBS–EDTA buffer: PBS, 0.1 mM EDTA, 0.02 % sodium azide.
4. Paraformaldehyde (PFA) solution: 1 % PFA (v/v) in PBS.
5. Fluorescein isothiocyanate (FITC)-conjugated anti-human IgG antibody F(ab′)2 specific for IgG or IgM.
6. Anti-FcγRIII (CD16) monoclonal antibody.
7. Lysis buffer: PBS, 1 % Triton X-100, 3 % BSA, protease inhibitors (2 mM phenylmethylsulfonyl fluoride, 5 mM EDTA, 0.2 μg/mL soybean trypsin inhibitor).
8. Goat anti-mouse IgG.
9. Horseradish peroxidase (HRP)-conjugated goat anti-human IgG.
10. HRP substrate.
11. Microtiter plate reader (e.g., Molecular Devices SpectraMax).

3 Methods

3.1 Diagnostic Assays for CGD

3.1.1 Nitroblue Tetrazolium Assay

The NBT assay relies on the accumulation of blue-black formazan precipitate. The membrane-permeable, water-soluble, yellow NBT is reduced to blue-black formazan by O_2^-, which is generated upon activation of phagocytes, typically by phorbol myristate acetate (PMA) (Fig. 1) [14]. PMA activates NADPH oxidase by enhancing protein kinase C (PKC) and thus stimulates production of ROS. This assay is easily read by light microscopy, allowing the recognition of individual cells that have reduced NBT.

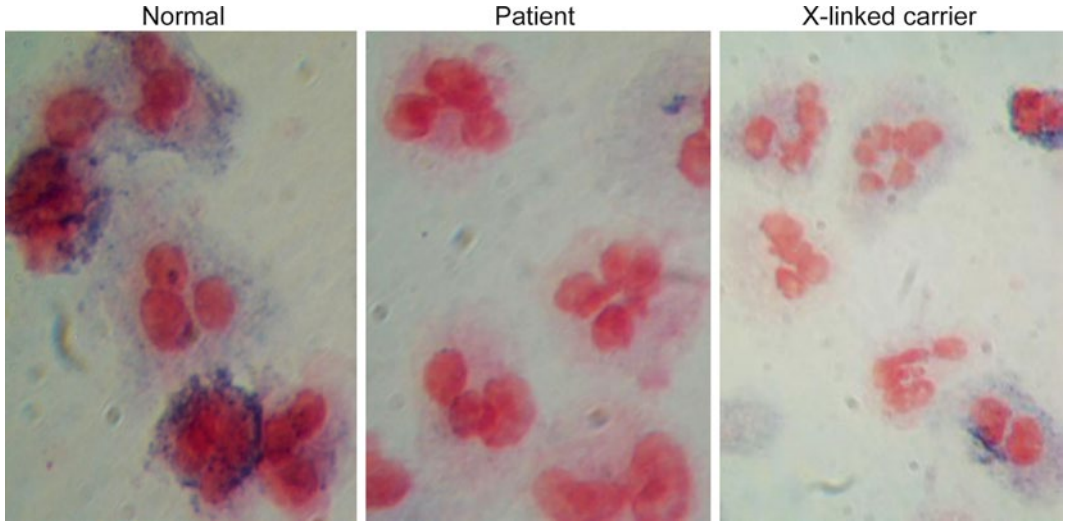

Fig. 1 NBT assay. Following PMA stimulation, reduction of yellow nitroblue tetrazolium (NBT) to *blue-black* formazan occurred in the healthy control cells (*left*) but is completely absent in cells from an X-linked CGD patient (*center*). The mother of the patient is a carrier of the mutation and has both NBT-positive and -negative cell populations (*right*). Reproduced from ref. 50 with permission from Humana Press © 2007

More than 95 % of normal neutrophils will reduce NBT, showing orange nuclei with clumps of blue-black precipitate in the cytoplasm. CGD cells have no or greatly diminished NBT reduction. Mothers of patients with X-linked CGD typically show mosaicism of peripheral blood neutrophil NBT reduction, since X-inactivation is thought to occur randomly in hematopoietic precursors (lyonization). This mosaic pattern can range from 0.001 to 97 % of neutrophils, although the range of NBT reduction for cells from most carriers is spread across the spectrum. At the extremes of lyonization, X-linked carriers may be indistinguishable from CGD patients or normal individuals, respectively. The X-linked form of CGD is the most common (about 65 % of cases). Thus, analysis of the mother's blood at the time of her son's NBT test can identify disease, and if the mother is a carrier, strongly suggest X-linked inheritance (*see* **Note 2**).

1. Isolate neutrophils from peripheral blood of a patient and a healthy control individual as described elsewhere in this book (e.g., Chapter 2).
2. Place glass cover slips in a 12-well tissue culture plate.
3. Aliquot cells into the wells at 5×10^5 neutrophils per well in 400 μL of DMEM.
4. Allow cells to adhere to the cover slips for 1 h at 37 °C.
5. Add 100 μL of NBT solution to each well.
6. Add 1 μL of PMA stock (200 ng/mL final) or buffer (unstimulated control) to the wells, and incubate plate for 20 min at 37 °C.

7. Wash the cells twice with warm (37 °C) PBS.
8. Allow the cover slips to air-dry.
9. Fix the cells with methanol and counterstain with 1 % safranin O solution. Alternatively, stain with Giemsa stain for 15 min. Wash and air-dry cover slips.
10. View cover slips under microscope to determine the percentage of cells containing blue-black formazan particles.
11. Express results as the number of neutrophils with reduced NBT/total number of neutrophils counted.
12. This assay can also be performed on regular microscope slides.

3.1.2 Modified Colorimetric NBT Assay

The NBT test is semiquantitative and does not precisely reflect the amount of O_2^- produced. A new colorimetric assay is more sensitive, quantitative, and can detect even small amounts of O_2^- production. This assay dissolves cells after stimulation allowing for plate-based absorbance measurements to reflect the amount of NBT reduced by neutrophils [15].

1. Isolate neutrophils from peripheral blood as described elsewhere in this book (e.g., Chapter 2).
2. Aliquot cells into the wells of a 24-well plate at 1×10^5 neutrophils per well in 400 μL of DMEM.
3. Add 100 μL of NBT solution to each well.
4. Add 1 μL of PMA stock (200 ng/mL final) or buffer (unstimulated control) to the wells, and incubate plate for 30 min at 37 °C.
5. Wash the cells twice with warm (37 °C) PBS. It is critical to remove extracellular NBT.
6. Fix cells with methanol, and air-dry plates.
7. Add 120 μL of KOH solution per well to solubilize the cell membranes.
8. Dissolve the blue formazan deposited inside the cells by adding 140 μL of DMSO per well and gently shaking for 10 min at room temperature.
9. Transfer the dissolved NBT solution to a 96-well plate, and measure the absorbance at 620 nm with a microtiter plate reader.
10. Compare absorbance at 620 nm between the NBT + PMA and NBT – PMA conditions to quantify O_2– production in each cell sample.

3.1.3 WST-1 Assay

In recent years, newer tetrazolium salt derivatives have been developed to measure O_2^- production. For example, the sulfonated tetrazolium salt, 2-(4-iodophenyl)-3-(2,4-disulfophenyl)-5-2H-tetrazolium, monosodium salt (WST-1), can be used for diagnostic

measurement of O_2^- [16–18]. WST-1 is efficiently reduced by O_2^- to a stable, water-soluble formazan with high molar absorptivity. In addition, WST-1 generates a twofold greater increase in absorbance than ferricytochrome c [16]. SOD is added to control samples to demonstrate specificity for O_2^- [17]. The methods described are based on previously reported microtiter plate-based WST-1 assay systems [16, 18].

1. Isolate neutrophils from peripheral blood as described elsewhere in this book (e.g., Chapter 2).
2. Resuspend neutrophils at 1×10^6 cells/mL in HBSS+ containing glucose (2 mg/mL).
3. Aliquot 100 µL of cells into wells of a 96-well microtiter plate (*see* **Note 3**).
4. Add 4 µL of WST-1 stock solution (500 µM final) and 4 µL of catalase stock solution (20 µg/mL final), with or without 10 µL SOD stock (20 µg/mL final).
5. Add 81 µL of HBSS+ for a final volume of 199 µL.
6. Equilibrate samples for 3 min at 37 °C in the microplate reader, and monitor baseline absorbance at 450 nm.
7. Add 1 µL of PMA stock (200 ng/mL final) or buffer (unstimulated control) to the wells, and monitor absorbance at 450 nm for 20 min at 37 °C (*see* **Note 4**).
8. Calculate O_2^- equivalents using the molar extinction coefficient for WST-1 (37.0×10^3 M^{-1} cm^{-1} at 450 nm).
9. Calculate specific O_2^- generation by subtracting signal obtained with SOD from that obtained without SOD for each pair of samples.

3.1.4 Ferricytochrome c Reduction

Specific detection of O_2– production can be monitored by measuring the SOD-inhibitable reduction of ferricytochrome c to ferrocytochrome c, as shown in Eq. 1:

$$Fe^{3+} - \text{cyt c} + O_2^- \rightarrow 3Fe^{2+} - \text{cyt c} + O_2 \qquad (1)$$

This spectrophotometric reaction is monitored at 550 nm, since ferricytochrome c and ferrocytochrome c have different extinction coefficients (0.89×10^4 M/cm and 2.99×10^4 M/cm, respectively). Reduction of cytochrome c is not absolutely specific for O_2^- and can also be caused by other cellular reductants, such as ascorbate and glutathione; thus, SOD must be added to control samples to demonstrate specific generation of O_2^- [17]. The ferricytochrome c assay has been readily adapted to a microtiter plate format [19] (*see* **Note 5**).

1. Isolate neutrophils from peripheral blood as described elsewhere in this book (e.g., Chapter 2).

2. Resuspend neutrophils at 1×10^6 cells/mL in HBSS+ containing glucose (2 mg/mL).
3. Aliquot 100 μL of cells into wells of a 96-well microtiter plate (*see* **Note 3**).
4. Add 16 μL of ferricytochrome c stock (80 μM final) and 4 μL of catalase stock solution (20 μg/mL final), with or without 10 μL SOD stock (20 μg/mL final).
5. Add 69 μL of HBSS+ for a final volume of 199 μL.
6. Equilibrate samples for 3 min at 37 °C in the microplate reader, and monitor baseline absorbance at 550 nm.
7. Add 1 μL of PMA stock (200 ng/mL final) or buffer (unstimulated control) to the wells, and monitor absorbance at 450 nm for 20 min at 37 °C (*see* **Note 4**).
8. Calculate O_2^- equivalents using the molar extinction coefficient for ferrocytochrome c (21.1×10^3 M^{-1} cm^{-1} at 550 nm).
9. Calculate specific O_2^- generation by subtracting the signal obtained with SOD from that obtained without SOD for each pair of samples.

3.1.5 Chemiluminescence Assays

Reaction with O_2^- can cause a variety of reagents to luminesce, and these reagents can provide higher sensitivity and analysis of both intracellular and extracellular O_2^- [20–22]. Among the most commonly used chemiluminescent reagents for detection of O_2^- are lucigenin (bis-*N*-methylacridinium nitrite), luminol, isoluminol, and L-012 [20–22]. One of the problems with chemiluminescence detection systems has been the presence of artifacts due to redox cycling of the detection reagents (e.g., lucigenin) and lack of specificity for distinct radical species (O_2^-, H_2O_2, OH^-, etc.) [21, 23]. More recently, improved chemiluminescence-based reagents have emerged, such as Diogenes (National Diagnostics) that has been shown to be a O_2^--specific chemiluminescence reagent, with 10^6 greater response to O_2^- versus H_2O_2 [24].

Lucigenin

1. Isolate neutrophils from peripheral blood as described elsewhere in this book (e.g., Chapter 2).
2. Resuspend neutrophils at 5×10^5 cells in 480 μL of incubation buffer in plastic tubes.
3. Add 10 μL of lucigenin stock solution (50 μM final) with or without 10 μL SOD stock (20 μg/mL final).
4. Add 1 μL of PMA stock (200 ng/mL final) or buffer (unstimulated control) to the tubes, and monitor chemiluminescence with a luminometer at 30-s intervals for 5 min (*see* **Note 6**).
5. Subtract the signal obtained with SOD from that obtained without SOD for each pair of samples.

Luminol

1. Isolate neutrophils from peripheral blood as described elsewhere in this book (e.g., Chapter 2).
2. Resuspend neutrophils at 1×10^6 cells/mL in HBSS+ containing glucose (2 mg/mL).
3. Aliquot 100 µL of cells into wells of a 96-well black microtiter plate (*see* **Note 3**).
4. Add 10 µL of luminol stock (500 µM final) with or without 10 µL SOD stock (20 µg/mL final).
5. Add 90 µL of HBSS+ for a final volume of 200 µL.
6. Equilibrate samples for 3 min at 37 °C in the luminescence microplate reader to monitor baseline luminescence.
7. Add 1 µL of PMA stock (200 ng/mL final) or buffer (unstimulated control) to the wells, and monitor luminescence for 15 min at 37 °C (*see* **Note 4**).
8. Subtract the signal obtained with SOD from that obtained without SOD for each pair of samples.

L-012 Chemiluminescence Assay for Whole Blood

1. Collect blood from patients and healthy donors in vacutainer tubes.
2. Dilute blood 1:10 in HBSS, and aliquot 180 µL of this diluted blood into wells of a 96-well black microtiter plate.
3. Add 10 µL L-012 stock (200 µM final) with or without 10 µL SOD stock (20 µg/mL final).
4. Equilibrate samples for 3 min at 37 °C in the luminescence microplate reader to monitor baseline luminescence.
5. Add 1 µL of PMA stock (200 ng/mL final) or buffer (unstimulated control) to the wells, and monitor luminescence for 15 min at 37 °C (*see* **Note 4**).
6. Subtract the signal obtained with SOD from that obtained without SOD for each pair of samples.

3.1.6 Flow Cytometry

Flow cytofluorometric assays using dyes sensitive to the generation of ROS are more sensitive and rapid and are replacing NBT and chemiluminescence methods [25]. The first flow cytometry-based assay reported by Bass et al. [26] required granulocyte isolation prior to adding the dye DCFH-DA, which is highly sensitive for measuring H_2O_2 [27]. DCFH-DA is a small nonpolar, nonfluorescent molecule that is able to diffuse into cells, where it is stable for a few hours. After entering the cell, DCFH-DA is hydrolyzed by nonspecific intracellular esterases to liberate the polar molecule 2′,7′-dichlorofluorescein (DCFH). Upon reaction with ROS, DCFH is converted to the highly fluorescent DCFH, which is measured after excitation by blue light (488 nm). The resulting fluorescence is linearly related to the activity of the respiratory burst.

However, other molecules, such as nitric oxide (NO), have been shown to excite DCFH. DCFH can also be auto-oxidized, resulting in a spontaneous increase in fluorescence following light exposure [28]. For these reasons, newer fluorescence probes specific for the generation of different ROS species have been developed. For example, DHR freely enters the cell and, after oxidation by ROS to rhodamine-123 (RHO), emits a bright fluorescent signal exclusively localized inside the cell [29]. DHR can be used with as little as 0.2 mL of whole blood and shows the greatest fluorescent intensity and separation of fluorescent signals between CGD and normal granulocytes (Fig. 2) [25].

DCFH and DHR can react with various ROS, including O_2^-, H_2O_2, and NO. In order to minimize the artifactual activation of cells prior to testing, Alvarez-Larran and colleagues [30] developed a method using whole blood, DHR, and the fluorescent dye DRAQ-5 (BioStatus). The latter stains nucleated cells, avoiding the erythrocyte lysis and wash steps, thus reducing neutrophil depletion. However, the lysis method may lead to significantly higher DHR values, with a higher PMA activation index.

1. Obtain freshly drawn, heparin-anticoagulated whole blood from patients and control.
2. Incubate 150 μL of blood in a propylene tube with 2 mL of pre-warmed (37 °C) lysis buffer.

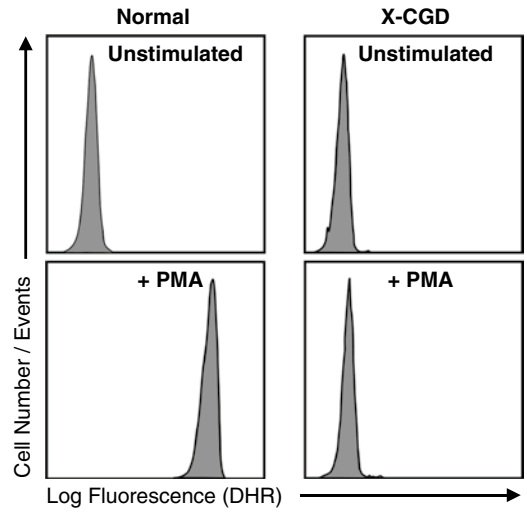

Fig. 2 DHR assay. In the *top panels* are DHR histograms from unstimulated cells from both a healthy control and a patient with X-linked CGD. The *lower panels* show DHR oxidation after PMA stimulation. Whereas the normal shows shift of the peak to the right, the X-CGD patient shows no shift with stimulation, corresponding to a lack of superoxide production. Reproduced from ref. 50 with permission from Humana Press © 2007

3. Mix tubes by inversion, and let stand for 5 min at room temperature.
4. Centrifuge tubes at 800 × *g* for 5 min at room temperature to pellet the leukocytes. Discard the supernatant, and blot tubes dry.
5. Wash the cell pellet with flow buffer and centrifuge again (800 × *g* for 5 min).
6. Add 400 µL flow buffer and mix gently to resuspend the pellet.
7. Add 5 µL of catalase solution to each tube.
8. Add 2 µL of DHR stock (5 µM final) or DCFH-DA stock (10 µM final), and incubate tubes at 37 °C in a shaking water bath for 5 min. Keep tubes covered with foil.
9. Add 1 µL of PMA stock (200 ng/mL final) or suspension buffer (unstimulated control) to the tubes and incubate for 15 min at 37 °C in a shaking water bath. Keep tubes covered with foil.
10. Immediately analyze cells by flow cytometry. In the granulocyte gate, collect non-fluorescent measurements (forward and side scatter) as well as 585 nm fluorescence for 10,000 events.
11. Compare healthy subjects and patients on the basis of the stimulation index (SI), which represents the fold increase in signal (mean channel fluorescence of stimulated neutrophils/mean channel fluorescence of unstimulated neutrophils) (*see* **Note 7**).

3.1.7 Electron Spin Resonance

O_2^- formation can be measured by electron paramagnetic resonance (EPR) spectroscopy, one of the most sensitive and quantitative methods [31, 32]. The most widely used spin trap for the detection of O_2^- is 5,5-dimethyl-1-pyrroline-*N*-oxide (DMPO) [31]. However, the O_2^- adduct DMPO-OOH is unstable, with a half-life of less than 1 min, and further decomposes to form DMPO-OH. A new spin trap, 5-(diethoxyphosphoryl)-5-methyl-1-pyrroline-*N*-oxide (DEPMPO), is reported to have improved properties for O_2^- detection, with a good efficiency for trapping O_2^- [32] (*see* **Note 8**).

1. Isolate neutrophils from peripheral blood as described elsewhere in this book (e.g., Chapter 2).
2. Resuspend neutrophils at 4×10^6 cells/mL in PBS containing glucose (2 mg/mL) and aliquot into plastic or polypropylene test tubes (400 µL/tube).
3. Add 2 µL of PMA stock (200 ng/mL final) or 40 µL of opsonized zymosan (1 mg/mL final). As an unstimulated control add buffer to the tubes (*see* **Note 4**).
4. Add DEPMPO at a final concentration of 10 mM.

5. Incubate the reaction mixture at 37 °C in a shaking water bath for 15 min.
6. Transfer to a capillary or a quartz flat cell and measure with an EPR spectrometer (e.g., Magnettech Miniscope or Bruker ER 300).

3.1.8 Prenatal Diagnosis

Prenatal diagnosis of CGD can be performed by measuring NADPH oxidase activity in cells from fetal blood [33]. NBT staining can be performed on blood samples obtained from fetal placental vessel puncture [34] or from cultured amniotic fibroblasts [35], and luminol-enhanced chemiluminescence has been adapted for prenatal diagnosis of CGD [35] (*see* **Note 9**).

3.2 Diagnostic Assays for LAD-1

The diagnosis of LAD-1 is typically made by flow cytometric analysis of neutrophils for the expression of CD18-containing molecules. The clinical phenotype reflects the level of β_2 integrins expressed. Those individuals with 1–10 % of normal CD18 expression have a milder course than those with <1 % expression. Neutrophils from heterozygotes have 40–60 % expression of β2 integrins and are clinically normal [36]. Many antibodies are currently available for flow cytometry. For example, CD18 monoclonal antibodies L130 (BD Biosciences) and MEM-48 (Abcam) work well for measuring cell surface β_2 integrin expression by flow cytometry (*see* **Note 10**).

3.2.1 Flow Cytometry

1. Isolate neutrophils from peripheral blood as described elsewhere in this book (e.g., Chapter 2).
2. Resuspend neutrophils at 1×10^6 cells/mL in FACS buffer and aliquot into polystyrene round-bottom tubes (50 μL/tube).
3. Add desired primary antibody (0.1–10 μg/mL) and incubate for 30 min at room temperature. Set up a parallel control labeling reaction using an isotype-matched immunoglobulin (e.g., mouse IgG).
4. Centrifuge cells ($400 \times g$ for 5 min) and wash three times with FACS buffer.
5. Resuspend cell pellet in ice-cold FACS buffer.
6. Dilute the fluorochrome-labeled secondary antibody in FACS buffer at the optimal dilution (according to the manufacturer's instructions), and then resuspend the cells in this solution (*see* **Note 1**).
7. Incubate for at least 30 min on ice. Cover tubes with foil. This incubation must be done in the dark.
8. Wash the cells three times as in **step 4**. Resuspend final pellet in 200 μL FACS buffer.
9. The cells are now ready for analysis. Keep the cells on ice until analysis.
10. Analyze by flow cytometry. Perform a parallel control labeling using control isotype- and species-matched antibody.

3.2.2 Cell Adhesion Assay

The β2 cytoplasmic tail interacts with a number of actin-binding proteins through which the adhesion properties of LFA-1 and Mac-1 are regulated. LFA-1-mediated adhesion can therefore be assayed on the immobilized ligand, intracellular adhesion molecule I (ICAM-1). The integrins bind divalent cations such as Mg^{2+} or Mn^{2+} in order to function. Specificity of adhesion can be tested by running the assay in the presence of a function-blocking antibody [37].

Loading Neutrophils with BCECF

1. Isolate neutrophils from peripheral blood as described elsewhere in this book (e.g., Chapter 2).
2. Resuspend neutrophils at 1×10^5 cells/mL in adhesion buffer (*see* **Note 3**).
3. Add 3.0 mM BCECF and incubate for 20 min at 37 °C.
4. Wash labeled cells once and resuspend at 1×10^5 cells/mL in adhesion buffer.

Analysis of LFA-1 Adhesion to ICAM-1

1. Coat wells of a microtiter plate with 100 μL/well of goat anti-human IgG at 5 μg/mL in 50 mM sodium bicarbonate buffer for 16–20 h at 4 °C.
2. Block nonspecific binding sites with PBS containing 0.5 % (w/v) BSA for 30 min at 37 °C.
3. Coat each well with 50 μL of the soluble recombinant form of human ICAM1/Fc chimera (R&D systems), used at a final concentration of 1 μg/mL in PBS containing 0.1 % BSA (w/v).
4. Incubate plate for 2 h at room temperature.
5. Load 200 μL of neutrophils (2×10^4 cells) into each well of the ligand-coated plates and incubate for 30 min at 37 °C in 5 % CO_2 incubator.
6. Add 10 μL of $MgCl_2$/EGTA solution to activate LFA-1-mediated adhesion and incubate for 5 min at 37 °C.
7. Wash the plate three times, and then measure bound cell fluorescence using a fluorescence plate reader.

Analysis of Mac-1-Mediated Adhesion

1. Coat wells of a microtiter plate with 100 μL/well of 50 μg/mL BSA in 50 mM sodium bicarbonate buffer for 24 h at 4 °C.
2. Block nonspecific binding with 150 μL/well of 0.2 % (w/v) polyvinylpyrrolidone in PBS for 30 min at 37 °C.
3. Wash coated plates twice with adhesion buffer.
4. Load 200 μL of neutrophils (2×10^4 cells) into each well of the ligand-coated plates and incubate for 30 min at 37 °C and 5 % CO_2.
5. Add 10 μL of $MnCl_2$ solution to activate Mac-1-mediated adhesion and incubate for 5 min at 37 °C.
6. Wash the plate three times with wash buffer, and measure bound cell fluorescence using a fluorescence microtiter plate reader.

3.2.3 Neutrophil Transmigration Assay

1. Isolate neutrophils from peripheral blood as described elsewhere in the book (e.g., Chapter 2) (*see* **Note 11**).
2. Resuspend neutrophils at 1×10^7 cells/mL in HBSS+.
3. Set up transwell plates with 0.5 mL of HBSS+ in the lower chamber.
4. Aliquot 150 μL of cell suspension into the upper chamber of the transwell.
5. Initiate transmigration by adding chemoattractants (e.g., 0.1 μM fMLP, 0.4 μg/mL IL-8, or 0.1 μM LTB4) into the lower chamber.
6. Cover and incubate the plate for 2 h at 37 °C and 5 % CO_2.
7. Quantify neutrophil migration into the lower chamber by counting cells or solubilizing cells with 1 % Triton X-100 in order to do a colorimetric assay for myeloperoxidase (MPO) (*see* **Note 12**).
8. Time-course assays can be performed by moving the transwell to a fresh well every 30 min. The same concentration of chemoattractant is used in the lower well (*see* **Note 3**).

3.3 Diagnostic Assays for Neutropenia

3.3.1 Granulocyte Immunofluorescence Test Using Flow Cytometry

This method, originally described by Verheugt in 1977 [38], detects antibodies against neutrophil surface antigens. Flow cytometric analysis using a panel of donor neutrophils to consistently quantify neutrophil-associated antibodies has allowed testing of patient serum samples against a panel of normal donor neutrophils already typed for the antigens HNA-1a, -1b, -1c, -2a, and -5a [39].

1. Collect blood from normal donors in vacutainer tubes.
2. Isolate neutrophils from peripheral blood as described elsewhere in this book (e.g., Chapter 2).
3. Wash cells twice in 2 mL of PBS–EDTA, centrifuging the cells between each wash at $300 \times g$ for 5 min.
4. Resuspend the pellets in 200 μL of PFA solution and incubate for 5 min at 22° to fix the cells.
5. Wash fixed cells with PBS–EDTA. Centrifugation at $300 \times g$ for 5 min between washes.
6. Store serum or EDTA-anticoagulated plasma from neutropenic patients. A negative control serum is also included in the study.
7. Incubate donor neutrophils with patient serum or control serum in polystyrene test tubes for 30 min at 20–22 °C.
8. Wash the cells three times with PBS–EDTA, as in **step 5**.
9. Add 100 μL of FITC-labeled anti-human IgG or anti-human IgM antiserum and incubate for 30 min at 4 °C.
10. Centrifuge the tubes at $300 \times g$ for 5 min, discard the supernatant, and wash once with 3 mL of PBS–EDTA.

11. Resuspend cells in 0.5 mL of PBS–EDTA.
12. Measure antibody binding by flow cytometry, and grade the results from – to +++ on the basis of the fluorescence intensity.
13. The ratio of the mean fluorescence channel of each sample to that of control serum is expressed as relative fluorescence intensity (RFI) [39, 40].
14. Report increased binding of IgG or IgM over the normal control sera.

3.3.2 Monoclonal Antibody Immobilization of Granulocyte Antigens Assay

Neutrophil antigens can be targets for autoimmune attack. This assay detects neutrophil targets of autoantibodies by allowing binding of antibodies to antigen and then detecting these after incubation with an anti-human antibody bound to an ELISA plate.

1. Collect blood from normal donors in vacutainer tubes.
2. Isolate neutrophils from peripheral blood as described elsewhere in this book (e.g., Chapter 2). Resuspend at 5×10^6 cells/mL in PBS/EDTA buffer.
3. Incubate 20 μL of cell suspension (10^6 cells) with 60 μL of serum for 1 h at room temperature.
4. Wash fixed cells three times with PBS–EDTA. Centrifuge at $300 \times g$ for 5 min between washes.
5. Resuspend cells in PBS/BSA containing anti-FcγRIII (CD16) monoclonal antibody to block Fc receptors and incubate for 1 h at room temperature.
6. Wash the cells two times with PBS–EDTA, as in **step 4**.
7. Add 200 μL of lysis buffer and incubate for 30 min at 4 °C to lyse the cells.
8. Add cell lysates to wells of a microtiter plate coated with goat anti-mouse IgG to capture neutrophil antigen–serum antibody complexes.
9. Incubate overnight at 4 °C, and wash the wells with PBS/EDTA.
10. Add 100 μL of horseradish peroxidase-labeled goat anti-human IgG, and incubate for 2 h at 4 °C.
11. Wash plate with PBS/EDTA, and add HRP substrate.
12. Read the plate at 405 nm with a microtiter plate reader to quantify the HRP signal.
13. Use sera with known HNA-1a and HNA-1b specificity and sera from AB-positive controls as positive and negative assay controls, respectively.
14. Results for a patient's serum are considered positive if the mean optical density (OD) value obtained is ≥ to twice the mean OD obtained with the normal serum control [38].

4 Notes

1. Primary antibodies can often be purchased directly conjugated to the desired fluorophore. If a directly conjugated antibody is used, then the secondary antibody is not required.
2. The NBT assay has numerous limitations. For example, neutrophils from CGD patients, such as some protein-positive gp91^{phox}-deficient patients and many of those with p47^{phox} deficiency, may exhibit some residual O_2^- production and reduce small amounts of NBT. This makes differentiation from normal individuals difficult. In addition, since the NBT test is based on visual inspection of a limited number of cells, it is not ideal for X-linked carrier screening. Finally, drugs such as D-penicillamine can act as O_2^--generating sources when oxidized and reduce NBT.
3. The number of cells per well can be adjusted to achieve the desired signal strength.
4. PMA concentration should be adjusted empirically to achieve maximal responses.
5. Any SOD-independent ferricytochrome c reduction can be minimized by reducing the concentration of ferricytochrome c without losing signal. O_2^- does not effectively cross biological membranes; thus, the ferricytochrome c assay is not useful for measurement of ROS generated inside cells. If measurement of intracellular O_2^- is desired, other detection reagents are utilized (i.e., chemiluminescent and fluorescent dyes) (see other chapters in this book).
6. This assay is easily adapted to a microtiter plate format if a luminescence microtiter plate reader is available.
7. PMA-stimulated DHR oxidation yields between 50- and 200-fold greater mean channel fluorescence than in unstimulated cells. In contrast, CGD neutrophils usually show less than tenfold augmentation of DHR oxidation by PMA. X-linked carriers show two distinct populations of neutrophils, those which oxidize normally in the presence of PMA and those which do not [41]. False-positive results on the DHR test are seen in MPO deficiency, whereas the NBT and ferricytochrome c reduction give the expected results.
8. In the presence of O_2^-, DEPMPO is transformed into DEPMPO-OOH with no significant decomposition to DEPMPO-OH [32]. When neutrophils are stimulated by PMA or zymosan in the presence of DEPMPO, the major signal observed is the O_2^- adduct DEPMPO-OOH, with a small amount of DEPMPO-OH (less than 8 % at 20 min). In the absence of stimulant, no signal is observed. The ESR signal is completely inhibited by SOD, whereas catalase has no effect on either DEPMPO-OOH or DEPMPO-OH.

9. Prenatal diagnosis can also be accomplished by restriction fragment length polymorphism (RFLP) [42]. Where available, identification of specific mutations is preferred [43]. Genomic DNA from chorionic villi can be analyzed by sequence analysis [44].
10. Other neutrophil disorders are also characterized by an impaired chemotaxis, such as Chediak–Higashi syndrome (CHS) and specific granule deficiency (SGD). CHS is a rare autosomal recessive disorder characterized by severe immune deficiency with neutropenia [45]. CHS neutrophils contain giant granules that are easily appreciated under the light microscope. In SGD, another rare congenital disorder, neutrophils show abnormalities in nuclear morphology with an atypical bilobed nuclei and lack expression of secondary and tertiary granule proteins. The diagnosis of SGD can be made by electron microscopy as well as by measuring lactoferrin and/or defensins [46]. Commercial ELISA kits are available.
11. It is critical to use freshly isolated PMN, and avoid any treatment inducing cell priming. Activation of PMN dramatically affects their chemotactic transmigration [47].
12. An alternative method for quantification of transmigrated cells is to use a colorimetric lactate dehydrogenase (LDH) assay (e.g., CytoTox 96 Non-Radioactive Cytotoxicity Assay; Promega). The LDH measurements can then be converted to absolute cell numbers by comparison of the values to standard curves created by aliquoting a range of control cell standards into wells containing no transwell inserts and processing identically to the sample wells with inserts [48].

References

1. Witko-Sarsat P, Rieu B, Descamps-Latscha PL, Halbwachs-Mecarelli L (2000) Neutrophils: molecules, functions and pathophysiological aspects. Lab Invest 80:617–653
2. Rigby KM, DeLeo FR (2012) Neutrophils in innate host defense against Staphylococcus aureus infections. Semin Immunopathol 34: 237–259
3. Cederlund A, Gudmundsson GH, Agerberth B (2011) Antimicrobial peptides important in innate immunity. FEBS J 278:3942–3951
4. Rosenzweig SD, Holland SM (2011) Recent insights into the pathobiology of innate immune deficiencies. Curr Allergy Asthma Rep 11:369–377
5. Berendes H, Bridges RA, Good RA (1957) A fatal granulomatous disease of childhood: the clinical study of a new syndrome. Minn Med 40:309–312
6. Levy R, Rotrosen D, Nagauker O, Leto T, Malech H (1990) Induction of the respiratory burst in HL-60 cells, correlation of function and protein expression. J Immunol 145: 2595–2601
7. Hanna S, Etzioni A (2012) Leukocyte adhesion deficiencies. Ann N Y Acad Sci 1250: 50–55
8. Boztug K, Klein C (2011) Genetic etiologies of severe congenital neutropenia. Curr Opin Pediatr 23:21–26
9. Kostman R (1975) Infantile genetic agranulocytosis. A review with presentation of ten new cases. Acta Paediatr Scand 64:362–368
10. Horwitz M, Benson KF, Person RE, Aprikyan AG, Dale DC (1999) Mutations in ELA2 encoding neutrophil elastase, define a 21-day biological clock in cyclic haematopoiesis. Nat Genet 23:433–436
11. Zuelzer WW (1964) "Myelokathexis": a new form of chronic granulocytopenia. N Engl J Med 270:699–704
12. Hernandez PA, Gorlin RJ, Lukens JN, Taniuchi S, Bohinjec J, Francois F, Klotman ME, Diaz GA (2003) Mutations in the chemokine receptor

gene CXCR4 are associated with WHIM syndrome, a combined immunodeficiency disease. Nat Genet 34:70–74
13. Stroncek DF, Skubitz KM, McCullough J (1990) Biochemical nature of the neutrophil-specific antigen NB1. Blood 75:744–755
14. Baehner RL, Boxer LA, Davis J (1976) The biochemical basis of nitroblue tetrazolium reduction in normal human and chronic granulomatous disease polymorphonuclear leukocytes. Blood 48:309–313
15. Choi HS, Kim JW, Cha YN, Kim C (2006) A quantitative nitroblue tetrazolium assay for determining intracellular superoxide anion production in phagocytic cells. J Immunoass Immunochem 27:31–44
16. Tan AS, Berridge MV (2000) Superoxide produced by activated neutrophils efficiently reduces the tetrazolium salt, WST-1 to produce a soluble formazan: a simple colorimetric assay for measuring respiratory burst activation and for screening anti-inflammatory agents. J Immunol Methods 238:59–68
17. Tarpey MM, Wink DA, Grisham MB (2004) Methods for detection of reactive metabolites of oxygen and nitrogen: in vitro and in vivo considerations. Am J Physiol Regul Integr Comp Physiol 286:R431–R444
18. Peskin AV, Winterbourn CC (2000) A microtiter plate assay for superoxide dismutase using a water-soluble tetrazolium salt (WST-1). Clin Chim Acta 293:157–166
19. Björquist P, Palmer M, Ek B (1994) Measurement of superoxide anion production using maximal rate of cytochrome (III) C reduction in phorbol ester stimulated neutrophils, immobilised to microtiter plates. Biochem Pharmacol 48: 1967–1972
20. Liu L, Dahlgren C, Elwing H, Lundqvist H (1996) A simple chemiluminescence assay for the determination of reactive oxygen species produced by human neutrophils. J Immunol Methods 192:173–178
21. Hasegawa H, Suzuki K, Nakaji S, Sugawara K (1997) Analysis and assessment of the capacity of neutrophils to produce reactive oxygen species in a 96-well microplate format using lucigenin- and luminol-dependent chemiluminescence. J Immunol Methods 210:1–10
22. Kielland A, Blom T, Nandakumar KS, Holmdahl R, Blomhoff R, Carlsen H (2009) In vivo imaging of reactive oxygen and nitrogen species in inflammation using the luminescent probe L-012. Free Radic Biol Med 47:760–766
23. Skatchkov MP, Sperling D, Hink U, Mülsch A, Harrison DG, Sindermann I, Meinertz T, Münzel T (1999) Validation of lucigenin as a chemiluminescent probe to monitor vascular superoxide as well as basal vascular nitric oxide production. Biochem Biophys Res Commun 254:319–324
24. Stielow C, Catar RA, Muller G, Wingler K, Scheurer P, Schmidt HH, Morawietz H (2006) Novel Nox inhibitor of oxLDL-induced reactive oxygen species formation in human endothelial cells. Biochem Biophys Res Commun 344:200–205
25. Vowells SJ, Sekhsaria S, Malech HL, Shalit M, Fleisher TA (1995) Flow cytometric analysis of the granulocyte respiratory burst: a comparison study of fluorescent probes. J Immunol Methods 178:89–97
26. Bass DA, Parce W, Dechatelet LR, Szejda P, Seeds MC, Thomas M (1983) Flow cytometry studies of oxidative product formation by neutrophils: a graded response to membrane stimulation. J Immunol 130:1910–1917
27. Keston AS, Brandt R (1965) The fluorometric analysis of ultramicro quantities of hydrogen peroxide. Anal Biochem 11:1–5
28. Hempel SL, Buettner GR, O'Malley YQ, Wessels DA, Flaherty DM (1999) Dihydrofluorescein diacetate is superior for detecting intracellular oxidants: comparison with 2′,7′-dichlorodihydrofluorescein diacetate, 5(and 6)-carboxy-2′, 7′-dichlorodihydrofluorescein diacetate, and dihydrorhodamine 123. Free Radic Biol Med 27:146–159
29. Emmendörffer A, Nakamura M, Rothe G, Spiekermann K, Lohmann Matthes ML, Roesler J (1994) Evaluation of flow cytometric methods for the diagnosis of chronic granulomatous disease variants under routine laboratory conditions. Cytometry 18:147–155
30. Alvarez-Larran A, Toll T, Rives S, Estella J (2005) Assessment of neutrophil activation in whole blood by flow cytometry. Clin Lab Haematol 27:41–46
31. Pou S, Rosen GM, Bntigan BE, Cohen MS (1989) Intracellular spintrapping of oxygen centered radicals generated by human neutrophils. Biochim Biophys Acta 991:459–464
32. Roubaud V, Sankarapandi S, Kuppusamy P, Tordo P, Zweier JL (1997) Quantitative measurement of superoxide generation using the spin trap 5-(diethoxyphosphoryl)-5-methyl-1-pyrroline *N*-oxide. Anal Biochem 247: 404–411
33. Leiding JW, Holland SM (2012) Chronic granulomatous disease. In: Pagon RA, Bird TD, Dolan CR, Stephens K, Adam MP (eds) GeneReviews™ [internet]. University of Washington, Seattle, Seattle, WA, 1993–2013
34. Newburger PE, Cohen HJ, Rothchild SB, Hobbins JC, Malawista SE, Mahoney MJ (1979) Prenatal diagnosis of chronic granulomatous disease. N Engl J Med 300:178–181

35. Matthay KK, Golbus MS, Wara DW, Mentzer WC (1984) Prenatal diagnosis of chronic granulomatous disease. Am J Med Genet 17: 731–739
36. Anderson DC, Schmalsteig FC, Finegold MJ, Hughes BJ, Rothlein R, Miller LJ et al (1985) The severe and moderate phenotypes of heritable Mac-1, LFA-1 deficiency: their quantitative definition and relation to leukocyte dysfunction and clinical features. J Infect Dis 152:669–689
37. Tan SM, Hyland RH, Al-shamkhani A, Douglass WA, Shaw JM, Law SK (2000) Effect of integrin beta 2 subunit truncations on LFA-1 (CD11a/CD18) and Mac-1 (CD11b/CD18) assembly, surface expression, and function. J Immunol 165:2574–2581
38. Verheugt FW, Von dem Borne AE, Decary F, Engelfriet CP (1977) The detection of granulocyte alloantibodies with an indirect immunofluorescence test. Br J Haematol 36: 533–544
39. Curtis BR, Reno C, Aster RH (2005) Neonatal alloimmune neutropenia attributed to maternal immunoglobulin G antibodies against the neutrophil alloantigen HNA-1c (SH): a report of five cases. Transfusion 45:1308–1313
40. Wikman A, Olsson I, Shanwellt A, Lundahl J (2001) Detection by flow cytometry of antibodies against surface and intracellular granulocyte antigens. Scand J Clin Lab Invest 61: 307–316
41. Vowells SJ, Fleisher TA, Sekhsaria S, Alling DW, Maguire TE, Malech HL (1996) Genotype-dependent variability in flow cytometric evaluation of reduced nicotinamide adenine dinucleotide phosphate oxidase function in patients with chronic granulomatous disease. J Pediatr 128:104–107
42. Lindlöf M, Kere J, Ristola M, Repo H, Leirisalo-Repo M, van Koskull H, Ammala P, De la Chapelle A (1987) Prenatal diagnosis of X-linked granulomatous disease using restriction fragment length polymorphism analysis. Genomics 1:87–92
43. Heyworth PG, Curnutte JT (2006) Molecular diagnosis of chronic granulomatous disease. In: Detrick B, Hamilton RG, Folds JD (eds) Manual of molecular and clinical laboratory immunology, 7th edn. ASM press, Washington, DC, pp 262–271
44. Chien SC, Lee CN, Hung CC, Tsao PN, Su YN, Hsieh FJ (2003) Rapid prenatal diagnosis of X-linked chronic granulomatous disease using a denaturing high performance liquid chromatography (DHPLC) system. Prenat Diagn 23:1092–1096
45. Kaplan J, De Domenico I, Ward DM (2008) Chediak-Higashi syndrome. Curr Opin Hematol 15:22–29
46. Tamura A, Agematsu K, Mori T, Kawai H, Kuratsuji T, Shimane M, Tani K, Asano S, Komiyama A (1994) A marked decrease in defensin mRNA in the only case of congenital neutrophil-specific granule deficiency reported in Japan. Int J Hematol 59:137–142
47. Zen K, Reaves TA, Soto I, Liu Y (2006) Response to genistein: assaying the activation status and chemotaxis efficacy of isolated neutrophils. J Immunol Methods 309:86–98
48. Hanson AJ, Quinn MT (2002) Effect of fibrin sealant composition on human neutrophil chemotaxis. J Biomed Mater Res 61:474–481
49. Mauch L, Lun A, O'Gorman MRG, Harris JS, Schulze I, Zychlinsky A, Fuchs T, Oelschlagel U, Brenner S, Kutter D, Rosen-Wolff A, Roesler J (2007) Chronic granulomatous disease (CGD) and complete myeloperoxidase deficiency both yield strongly reduced dihydrorhodamine 123 test signals but Can Be easily discerned in routine testing for CGD. Clinical Chem 53(5):890–896
50. Elloumi HZ, Holland SM (2007) Diagnostic assays for chronic granulomatous disease and other neutrophil disorders. Methods Mol Biol 412:505–523

Chapter 32

Diagnostic Assays for Myeloperoxidase and Myeloperoxidase Deficiency

William M. Nauseef

Abstract

Neutrophils (PMN) represent the dominant cell in the acute response to microbial infection and can contribute to some of the tissue damage that accompanies sterile inflammation. Effective antimicrobial activity in neutrophil phagosomes reflects the combined action of soluble agents in plasma with PMN-derived reactive oxygen species and granule proteins, including the azurophilic granule protein myeloperoxidase (MPO). The inhibition or the absence of the MPO–H_2O_2–halide system results in marked reduction in PMN killing of a variety of microbes, implicating its relative prominence in the hierarchy of PMN antimicrobial systems. Although the most profound clinical defects are manifested in patients lacking the capacity to generate reactive oxygen species, as seen in chronic granulomatous disease, an inherited deficiency of MPO can also increase the frequency or the severity of clinical infections.

Like related peroxidases expressed in animals, MPO can catalyze both one- and two-electron oxidations, thereby mediating peroxidation and halogenation, respectively. The presence of each activity can be assessed in inflammatory fluids or by stimulated PMN. Furthermore, histochemical staining provides an assessment of functional MPO in tissue or within PMN, and immunoblotting of isolated PMN for MPO can provide additional insight into the molecular basis of the observed absence of functional enzyme.

Key words Peroxidase, Myeloperoxidase, Eosinophil peroxidase, Azurophilic granules

1 Introduction

Restricted to PMN and monocytes, myeloperoxidase (MPO) is present in high concentrations in the azurophilic granules of PMN, thereby endowing pus with its characteristic yellow–green color (Fig. 1). As noted elsewhere in this volume, optimal microbicidal action of human PMN relies on the integrated activity of reactive oxygen species generated by the NADPH oxidase and of an array of granule proteins delivered to the phagosome during phagosome–granule fusion. Granule contents include proteins that exert direct antimicrobial activity, such as bactericidal permeability-increasing protein, as well as proteases such as elastase and cathepsins, which

Mark T. Quinn and Frank R. DeLeo (eds.), *Neutrophil Methods and Protocols*, Methods in Molecular Biology, vol. 1124,
DOI 10.1007/978-1-62703-845-4_32, © Springer Science+Business Media, LLC 2014

Fig. 1 Comparison of PMN from PMN from healthy subjects (normal) and those with MPO deficiency (MPO deficient). Primary human PMN were isolated from venous blood using a published protocol [14]

indirectly contribute to the killing and degradation of ingested microbes. Like other members of the family of animal peroxidases, which includes eosinophil peroxidase (EPO), lactoperoxidase (LPO), and thyroid peroxidase (TPO), MPO can catalyze halogenation reactions and thereby halogenate targets. However, MPO has the unique capacity to oxidize Cl^- to Cl^+ at physiologic pH, thereby generating HOCl, a potent microbicidal agent.

Thus the MPO–H_2O_2–chloride system represents a major contributor to antimicrobial activity in the PMN phagosome [1, 2], and defects in any component of the system compromise innate host defense. The profound morbidity and mortality associated with defects in H_2O_2 generation that define chronic granulomatous disease (CGD) have been described elsewhere in this book. In contrast to the dramatic clinical consequences of CGD, the phenotype of inherited MPO deficiency is much less severe, with the most severe infections being disseminated or visceral candidiasis, particularly in patients with concomitant diabetes mellitus [3]. The different morbidities associated with CGD and MPO deficiency may reflect, in part, the fact that H_2O_2 alone is microbicidal, although its activity is augmented ~50-fold by MPO. However, the antimicrobial activities of normal and MPO-deficient PMN are incompletely understood [1, 2].

Given the cellular distribution of MPO and its contribution to PMN antimicrobial activity, a need to measure MPO activity commonly arises in two different settings. Since PMN represent the main cellular source of MPO, with much less in monocytes, investigators often assay tissue or inflammatory fluids for its presence as a surrogate marker of acute inflammation. In addition, an assay of MPO is part of the evaluation of patients with unexplained infections with *Candida* species or with frequent infections that suggest PMN dysfunction. In the latter setting, assessing both enzymatically and immunochemically MPO in PMN provides important complementary information, as the combined data will distinguish the absence of protein from the presence of enzymatically inactive MPO. The contribution of MPO to assays employed to assess NADPH oxidase activity, such as oxidation of dihydrorhodamine, needs to be kept in mind when interpreting results, as complete MPO deficiency will resemble CGD [4].

The fundamental chemistry in all peroxidase (PX) assays is summarized in the following reactions and one-electron oxidation of AH by Compound I:

$$\mathrm{PX} + \mathrm{H_2O_2} \rightarrow \text{Compound I}$$

$$\text{Compound I} + \mathrm{AH} \rightarrow \mathrm{A^+} + \text{Compound II}$$

where AH is a substrate that is chromogenic when oxidized. The substrate may be a histochemical dye (e.g., diaminobenzidine or benzidine dihydrochloride), thereby staining in situ the cellular compartment in which the peroxidase resides, or a soluble chromagen (e.g., tetramethylbenzidine, *o*-dianisidine, or guaiacol), thus providing a spectrophotometric means to quantitate activity. Although peroxidase assays are sensitive, they do not distinguish among the peroxidases that might be present in biological situations (e.g., MPO, EPO, LPO).

As noted earlier, the animal peroxidases can catalyze the two-electron oxidation of halides and the pseudohalide thiocyanate to generate the corresponding hypohalous acids. Uniquely, MPO can catalyze the oxidation of chloride and generation of HOCl:

$$\mathrm{MPO} + \mathrm{H_2O_2} \rightarrow \text{Compound I}$$

$$\text{Compound I} + \mathrm{H^+} + \mathrm{Cl^-} \rightarrow \mathrm{MPO} + \mathrm{HOCl}$$

Chlorination, as a measure of HOCl production, provides a quantitative assay specific for the activity of MPO. Several methods for measuring MPO-mediated chlorination have been published (review refs. 5, 6), but a recently published method based on the oxidation of taurine monochloramine by iodide is extremely sensitive and easy to use [7]. Oxidation of the substrate, 3,3′,5,5′-tetramethylbenzidine (TMB) by hypoiodous acid yields a blue product that can be quantitated spectrophotometrically.

Immunoblotting of isolated leukocytes allows identification of the MPO protein, independent of its enzymatic activity, and thus

makes it possible to identify missense mutations that compromise function but not the synthesis of the protein. Collectively, these approaches provide the investigator with tools to determine the presence of MPO in biological samples and to evaluate individuals for MPO deficiency, assessing the presence and subcellular location of MPO as well as its enzymatic activity.

2 Materials

2.1 Histochemical Staining

1. Fixative: 5 mL of 37 % formaldehyde, 45 mL of absolute ethanol, prepare fresh each time.
2. Staining solution: Combine in the following order: 150 μg of benzidine dihydrochloride in 50 mL of 30 % ethanol (*see* **Note 1**), 0.5 mL of 3.8 % (w/v) $ZnSO_4$, 500 μg sodium acetate, 35 μL of 30 % H_2O_2, 750 μL of 1.0 N NaOH, and 100 μg of safranin O (*see* **Note 2**). Once filtered, this solution can be stored at room temperature for up to 6 months.
3. Counterstain: 500 μg cresyl violet acetate, 50 mL H_2O. Use if desired.

2.2 Spectrophotometric Quantitation of Peroxidase Activity

1. Peroxidase activity can be quantified in tissue extracts, biological fluids, secretions from stimulated PMN, or lysates of PMN (*see* **Note 3**).
   (a) Isolated PMN lysates: Pellet cells and resuspend in phosphate-buffered saline containing 0.2 % Triton X-100, with frequent but careful pipetting to insure disruption of the azurophilic granules (*see* **Note 4**).
   (b) Stimulated PMN supernatant: Suspend 2×10^6 PMN in 200 μL buffer for treatment with buffer alone or agonist (e.g., 100 ng/mL phorbol myristate acetate, 1 μM fMLF). After rotating for 15 min at 37 °C, pellet PMN ($500 \times g$ 5 min at 4 °C) and collect supernatant.
2. Assay buffer: 50 mM sodium acetate, pH 5.4 (*see* **Note 5**).
3. TMB stock: 17.5 mM TMB in DMF.
4. Substrate: Dilute TMB stock in assay buffer to a final concentration of 1.4 mM TMB, bring to 37 °C before use.
5. Stop solution: 0.2 M acetic acid, keep on ice.
6. Catalase solution: 377 μg/mL catalase in PBS, keep at room temperature.
7. Diluted sample of a peroxidase as a positive control (*see* **Note 6**).
8. Reaction initiator: Dilute reagent-grade H_2O_2 (8.8 M) to 30 mM H_2O_2 in assay buffer (*see* **Note 7**).

2.3 Spectrophotometric Quantitation of Chlorination

1. Freeze–thaw buffer: PBS without Ca^{2+} or Mg^{2+}, 0.3 % hexadecyltrimethylammonium bromide (CTAB), 1 % protease inhibitor cocktail.
2. Relaxation buffer: 100 mM KCl, 3 mM NaCl, 1 mM adenosine triphosphate-Na_2, 3.5 mM $MgCl_2$, 10 mM PIPES, pH 7.3.
3. To evaluate the chlorination activity of cell-associated MPO, it is best to use a granule-enriched pellet from cytoplasm rather than a PMN lysate (*see* **Note 8**).
   (a) Pretreat intact PMN with 2 mM diisopropylfluorophosphate (DFP), resuspend in relaxation buffer in the presence of 1 % protease inhibitor cocktail, and disrupt by sonication (*see* **Note 9**).
   (b) Centrifuge at low speed (228 × *g*, 10 min, room temperature) to remove unbroken cells and nuclei.
   (c) Centrifuge at high speed (10,800 × *g*, 20 min, 4 °C) to recover the granule-rich pellet.
   (d) Resuspend the pellet in freeze–thaw buffer, and subject the mixture to three cycles of freeze-thawing in a methanol–dry ice bath. With each thaw, vigorously pipette 15 times to optimally disrupt the granules.
   (e) Centrifuge the suspension (50,000 × *g*, 10 min, 4 °C) to yield solubilized granule proteins in the supernatant (*see* **Note 10**).
4. 5 mM taurine in PBS.
5. 20 mM TMB in DMF.
6. 100 mM NaI.
7. 50 mM glycine-HCl buffer, pH 2.0.
8. 100 μM H_2O_2.
9. 10 nM MPO.
10. 800 μg/mL catalase.
11. 500 μM HOCl (*see* **Note 11**).
12. TMB-developing reagent: 2 mM TMB, 100 μM NaI, 10 % DMF in 400 mM acetate buffer, pH 5.4.

2.4 Immunoblotting for MPO-Related Proteins

1. Pellet isolated cells or prepare cell lysates for solubilization in sample buffer for SDS-polyacrylamide gel electrophoresis (PAGE).
2. SDS-PAGE sample buffer: 2.3 % SDS in 62 mM Tris–HCl (pH 6.8), 5 % (v/v) β-mercaptoethanol, 5 % glycerol. Heat samples to 100 °C for 3 min to denature and solubilize proteins and cool before loading the gel for electrophoresis.
3. Transfer buffer: 0.025 M Tris base, 0.192 M glycine, 20 % methanol.

3 Methods

3.1 Histochemical Staining

1. Either peripheral blood smear or a sample of isolated cells can be examined. In the latter case, dilute the PMN suspension to 5×10^5 PMN/mL in phosphate-buffered saline or media and centrifuge 100 μL at 500 RPM (Cytospin 2, Shandon Corporation) to pellet PMN (5×10^4) onto the slide.
2. Flood the slide with fixative and incubate at room temperature for 1 min.
3. Remove fixative by washing for 15–30 s with running tap water. Shake off excess water.
4. Immerse the slide in staining solution for 30 s.
5. Wash the slide in doubly distilled water for 5–10 s.
6. Counterstain (optional) for 1 min and then rinse off with tap water.
7. Allow the slide to air-dry (*see* **Note 12**).

3.2 Spectrophotometric Quantitation of Peroxidase Activity

1. Perform assay in 37 °C water bath and use 5-mL polypropylene tubes. Always include a blank tube and perform positive control and experimental samples in triplicate.
2. Mix TMB in assay buffer with buffer alone (blank) or sample. Add 7.5 μL of H_2O_2. The total volume of the reaction will be 750 μL.
3. Incubate for 3 min in 37 °C water bath.
4. Vortex tubes and immediately place in ice bath.
5. Add 2.7 mL of ice-cold 0.2 M acetic acid and 20 μL of catalase (final of 2.2 μg/mL catalase).
6. Dilute samples 1:5 or 1:10 in 0.2 M acetic acid and read absorbance at 655 nm (*see* **Note 13**).
7. Add 10 μL of the sample, mix quickly, return the cuvette to the sample compartment, and record absorbance at 460 nm (*see* **Note 6**).

3.3 Spectrophotometric Quantitation of Chlorinating Activity

1. Establish HOCl standard curve by mixing taurine/PBS and varied amounts (0–50 μM) of HOCl in a 96-well clear microtiter plate.
2. Add TMB-developing reagent and read at 650 nm (Fig.2).
3. If desired, an MPO standard curve can be generated as well, using known concentrations of MPO (0–2.0 nM). Mix taurine/PBS, known amounts of MPO, and H_2O_2 in a 96-well microtiter plate and incubate at room temperature for 30 min.
4. Stop the reaction by adding 10 μL catalase and incubating at room temperature for 5 min.

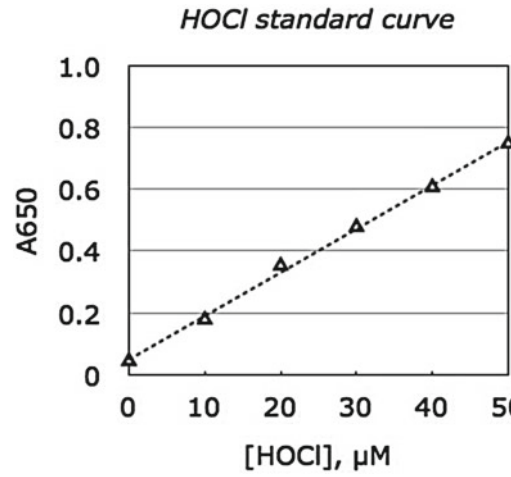

Fig. 2 Standard curve for chlorination by HOCl. A standard curve for absorbance at 650 nm for varied concentrations of reagent HOCl allows conversion of the spectrophotometric results to corresponding amounts of HOCl generated by samples

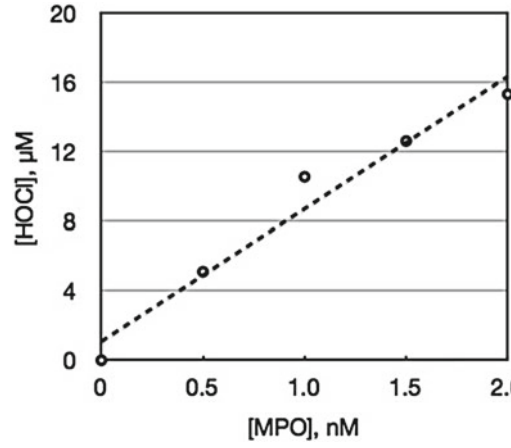

Fig. 3 Standard curve for chlorination by purified MPO. Using the amounts of HOCl generated by samples, the standard curve allows conversion to the concentration of enzymatically active MPO in samples

5. Add TMB-developing reagent, mix with pipettor, and incubate at room temperature for 5 min. Read at 650 nm (Fig. 3).
6. For solubilized samples, add taurine/PBS and H_2O_2 and incubate at room temperature for 30 min.
7. Stop reaction by adding 10 μL catalase and incubating at room temperature for 5 min.
8. Add TMB-developing reagent, mix with pipettor, and incubate at room temperature for 5 min. Read at 650 nm.
9. Using the standard curve for A_{650} vs. [HOCl], calculate the amount of HOCl produced by the sample.

10. For studies of intact PMN, suspend PMN in taurine/PBS and stimulate with PMA at 37 °C for 30 min.
11. Stop reaction by adding catalase and place on ice for 5 min.
12. Pellet PMN and collect supernatant.
13. Pipette 200 μL of supernatant into a clear 96-well microtiter plate.
14. Add TMB-developing reagent, mix with pipettor, and incubate at room temperature for 5 min before reading at 650 nm.

3.4 Immunoblotting for MPO-Related Proteins

1. Separate proteins by SDS-PAGE.
2. Immunoblot using standard conditions. Make sure to prepare transfer buffer and cool to 4 °C before use. In the case of electroblotting for MPO-related proteins, transfer for 140–150 V-h (e.g., 70 V × 2 h).
3. Block and process in standard fashion (*see* **Note 14**).

4 Notes

1. Benzidine dihydrochloride is a carcinogen and thus must be handled carefully.
2. A precipitate will form once the $ZnSO_4$ is added, but the subsequent addition of NaOH will clear the solution. The addition of $ZnSO_4$ stabilizes the oxidized benzidine dihydrochloride.
3. Keep in mind that Compound I of MPO generated in the presence of H_2O_2 will attack all vulnerable targets in solution, not exclusively the reporter substrate employed to detect peroxidase activity. Consequently, estimates of MPO content in biological fluids based on measurements of peroxidase activity may underestimate the amount of MPO present.
4. The peroxidase-containing granules must be disrupted either by solubilization of isolated cells in 0.2 % Triton X-100 in Tris-buffered saline (TBS) (pH 7.5) or by sonication of the cells suspended in TBS or PBS. Freeze-thawing of granules will promote their lysis and can be performed in addition.
5. The oxidation of TMB is optimal at pH 5.4. If alternative substrates are used, modifications of the buffer pH may be needed.
6. As the assay is not specific for MPO but measures the activity of any peroxidase, horseradish peroxidase will be fine.
7. Concentrations of H_2O_2 can be determined spectrophotometrically; the extinction coefficient is 43.6 M^{-1} cm^{-1} at 240 nm.
8. Use PBS as the buffer for chlorination reactions, as the amino groups in Tris and HEPES buffers will scavenge HOCl.

In addition, biological fluids contain many substrates that are vulnerable to attack by HOCl.

9. DFP is a potent neurotoxin and extreme care must be used when handling it. We use a Misonix XL-2000 sonicator (maximum 100 W) on a setting of 7.5 (full scale 0–20) for 10 s with the sample on ice. If a nitrogen bomb is available, it is preferred to perform nitrogen cavitation to disrupt PMN, as granules remain intact better after cavitation than after sonication.
10. The use of CTAB improves recovery of MPO from granules but also inhibits the chlorination assay. A final concentration of 0.03 and 0.3 % CTAB inhibits chlorination by 30 and 70 %, respectively.
11. Concentrations of HOCl can be determined spectrophotometrically; the extinction coefficient is 350 M^{-1} cm^{-1} at 292 nm.
12. Peroxidases are normally packaged in intracellular granules in PMN, monocytes, and eosinophils. In PMN and monocytes, the MPO-containing azurophilic granules will appear blue, with faint blue staining of the surrounding cytoplasm. Although lymphocytes, basophils, erythrocytes, and platelets do not stain, the granules in eosinophils are intensely stained, reflecting the presence of EPO. An important strength of including histochemical examination of peripheral blood or isolated leukocytes in assessment of an individual's MPO status rests on the ability to identify the cellular source of peroxidase activity detected by an enzymatic assay (e.g., *o*-dianisidine). In guinea pigs, eosinophils possess tenfold more peroxidase than do the MPO-containing heterophils [8], and the specific peroxidase activity, expressed on the basis of cell number, is higher for eosinophils [9]. The same is true for humans, as human eosinophils contain 15 μg EPO/10^6 cells [10] (19.5 pmol/10^6 cells), whereas PMN possess ~7.25 pmol/10^6 cells (based on spectroscopic determinations in our lab). Thus very little eosinophil contamination in a cell lysate can contribute to significant peroxidase activity and obfuscate the detection of partial MPO deficiency as highlighted several years ago [11]. In addition, eosinophils have normal peroxidase activity in inherited MPO deficiency (Fig. 4).
13. In this assay (with a 1:5 dilution), 7 pmol yields a change in absorbance of 0.338 ± 0.015 ($n = 16$).
14. Under reducing conditions, the 59- and 13.5-kDa heavy and light subunits, respectively, are detected as separate immunoreactive bands. In addition, there may be immunoreactive proteins at ~90 kDa and at 39 kDa. The former represents apoproMPO and proMPO, two precursors synthesized in the endoplasmic reticulum and destined for proteolytic processing into the subunits of mature MPO [12]. The 39-kDa species is the product of autolytic cleavage of the heavy subunit [13].

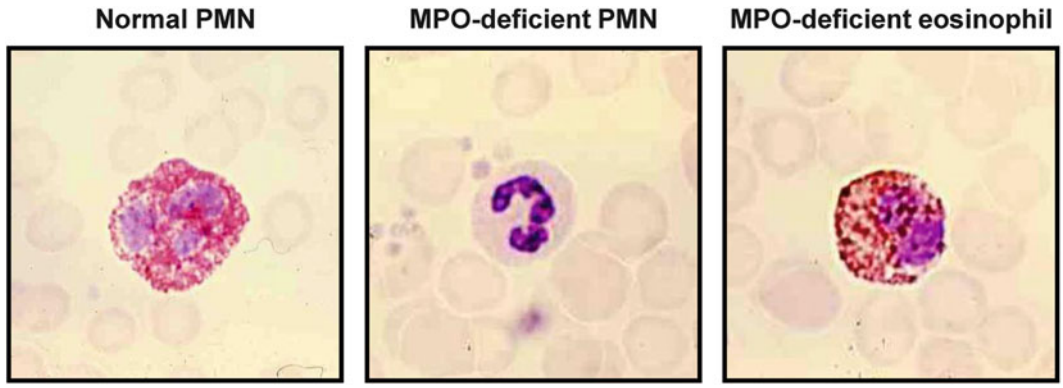

Fig. 4 Peroxidase activity in PMN from a healthy subject (normal PMN) or an individual with MPO deficiency (as indicated). Panel at far right indicates normal peroxidase activity in an eosinophil isolated from an individual with MPO deficiency. Histochemical staining was performed as described in Subheading 3.1

References

1. Klebanoff SJ, Kettle AJ, Rosen H et al (2013) Myeloperoxidase: a front-line defender against phagocytosed microorganisms. J Leukoc Biol 93:185–198
2. Hurst JK (2012) What really happens in the neutrophil phagosome? Free Radic Biol Med 53:508–520
3. Dinauer MC, Nauseef WM, Newburger PE (2001) Inherited disorders of phagocyte killing. In: Scriver CR, Beaudet al, Valle D et al (eds) The metabolic and molecular bases of inherited diseases, vol 8. McGraw-Hill Companies, New York, pp 4857–4887
4. Mauch L, Lun A, O'Gorman MRG et al (2007) Chronic granulomatous disease (CGD) and complete myeloperoxidase deficiency both yield strongly reduced dihydrorhodamine 123 test signals but can be easily discerned in routine testing for CGD. Clin Chem 53:890–896
5. Kettle AJ, Winterbourn CC (1994) Assays for the chlorination activity of myeloperoxidase. Methods Enzymol 233:502–512
6. Kettle AJ (1999) Detection of 3-chlorotyrosine in proteins exposed to neutrophil oxidants. Methods Enzymol 300:111–120
7. Dypbukt JM, Bishop C, Brooks WM et al (2005) A sensitive and selective assay for chloramine production by myeloperoxidase. Free Radic Biol Med 39:1468–1477
8. Mage MM, Evans WH, Himmelhoch SR et al (1971) Immunological identification and quantification of guinea pig heterophil and eosinophil peroxidases. J Reticuloendothel Soc 9:201–208
9. Fabian I, Aronson M (1975) Deamination of histamine by peroxidase of neutrophils and eosinophils. J Reticuloendothel Soc 17: 141–145
10. Carlson MG, Peterson CG, Venge P (1985) Human eosinophil peroxidase: purification and characterization. J Immunol 134:1875–1879
11. Dri P, Cramer R, Soranzo MR et al (1982) New approaches to the detection of myeloperoxidase deficiency. Blood 60:323–327
12. Hansson M, Olsson I, Nauseef WM (2006) Biosynthesis, processing, and sorting of human myeloperoxidase. Arch Biochem Biophys 445: 214–224
13. Taylor KL, Pohl J, Kinkade JM Jr (1992) Unique autolytic cleavage of human myeloperoxidase. J Biol Chem 267:25282–25288

INDEX

Mark T. Quinn and Frank R. DeLeo (eds.), *Neutrophil Methods and Protocols*, Methods in Molecular Biology, vol. 1124,
DOI 10.1007/978-1-62703-845-4, © Springer Science+Business Media, LLC 2014

D

E

F

G

H

I

J

K

L

M

N

O

P

R

S

T

Z